Discovery of *S*-Adamantyl Group Directed Site-Selective Acylation and Its Applications in the Streamlined Assembly of Oligosaccharides

By

Stephanie Blaszczyk

A dissertation submitted in partial fulfillment of

the requirements for the degree of

Doctor of Philosophy

in

Chemistry

at the

University of Wisconsin – Madison

2020

Date of final oral examination: 06/05/2020

The dissertation is approved by the following members of the Final Oral Committee:
Weiping Tang, Professor, School of Pharmacy & Department of Chemistry
Jennifer Golden, Assistant Professor, School of Pharmacy & Department of Chemistry
Sandro Mecozzi, Professor, School of Pharmacy & Department of Chemistry
Ying Ge, Professor, Cell and Regenerative Biology & Department of Chemistry

Discovery of *S*-Adamantyl Group Directed Site-Selective Acylation and Its Applications in the Streamlined Assembly of Oligosaccharides

Stephanie Blaszczyk

Under the supervision of Professor Weiping Tang

at the University of Wisconsin – Madison

ABSTRACT

While most people are familiar with carbohydrates from a nutritional standpoint, they're often unaware that carbohydrates play important roles in many biological processes. Because of their significance to the human body, a number of carbohydrate-based drugs and vaccines are currently being tested in clinical trials or have already been approved by regulatory agencies such as the FDA.

Carbohydrates are structurally diverse macromolecules and challenging synthetic targets. Chemists' inability to efficiently synthesize structurally complex carbohydrates hinders biologists' ability to probe how structural differences in carbohydrates affect their biological functions. As one of the major classes of biopolymers, carbohydrates pose extra synthetic burdens compared to their protein and nucleic acid counterparts. One of the major issues is that each carbohydrate building block represents a densely functionalized molecule bearing multiple hydroxyl groups with similar reactivities.

Differentiating and modifying one of these hydroxyl groups without affecting the others – known as site-selective functionalization – is a long-standing problem in

carbohydrate chemistry. The lack of a general and efficient method for the stereoselective formation of glycosidic bonds has also plagued chemists for decades. During the past three years, my research has focused on developing new ways to perform site-selective functionalization or stereoselectively form glycosidic bonds in a reliable and predictable manner.

Numerous methods have been developed for the differentiation of *cis*-1,2-diols in carbohydrates. Site-selective functionalization of the prevalent *trans*-1,2-diols, however, is much less developed and more challenging. Our group previously reported the ability to site-selectively acylate *trans*-1,2-diols in *O*-glycosides using chiral benzotetramisole (BTM) catalysts. Knowing that *O*-glycosides and *S*-glycosides are isoelectronic, we speculated that we could selectively functionalize *S*-glycosides with this protocol as well. *S*-glycosides are synthetically accessible, benchtop stable, chemically orthogonal building blocks that can be easily activated for glycosylation and used to assemble biologically relevant oligosaccharides.

To our surprise, experimental results indicated that a sterically encumbered thioether substituent – the adamantyl group – was the best director of site-selectivity. Density Functional Theory calculations indicated that the site-selective acylation of *S*-glycosides results from dispersion interactions between the adamantyl substituent and the pi system of the cationic acylated catalyst. This mechanism is entirely different from what we originally envisioned and previously published.

This methodology significantly streamlines oligosaccharide synthesis, and now chemists *and* biologists can easily synthesize structurally complex carbohydrates for research and drug development purposes.

Acknowledgements

My route back to graduate school was non-traditional at best, but I attribute a fair portion of my success to the perspective that I gained taking the "scenic route back to 1101 University Avenue," which is what I titled the personal essay when I applied to the University of Wisconsin–Madison Department of Chemistry PhD program.

If I approach acknowledgements somewhat chronologically, then it only makes sense I have to start from the beginning – with my mom and dad. The two of them have always stressed the importance of education, and they went above and beyond to provide my sister and I with an exceptional childhood education that laid the groundwork for our success in college and beyond. They also encouraged us to try every sport or extracurricular activity available, which taught me how to be a productive member of a group – something that's been essential considering how much collaboration is in science. When I was finishing my undergraduate education, my parents were the ones who got up with Emma in the middle of the night so I could get some sleep. They were the ones who would entertain her and take her on day trips so I could study on the weekend, and even to this day they take her to school and often have sleepovers with her so I can finish my doctorate. Without their love, support, and guidance, none of this would have been possible.

To my daughter Emma, I know that our lives haven't always been the easiest, and you have often got the short end of the stick because I've been in school most of your life. I hope you understand the importance of following your dreams – against all odds. I wanted to be a role model for you and show you that anything was possible. I've often been asked how I managed to handle graduate school with a child, and the answer is that

you made it easy to come home; I couldn't wait to see you after a long day in lab. Regardless of if I got good or bad results that day, I knew I could count on you for hugs, kisses, and snuggles. I know I missed a lot of good mornings and good nights, but I'm so excited to be home all of the time with you as you near your teenage years.

To James, you were the biggest part of making my PhD possible. You are undoubtedly the rock of this family, and Emma and I will always be grateful for that. Just as I've been in school most of Emma's life, I've been in school almost the entire time we have known each other. Your patience, encouragement, love, understanding, kindness, and mantra "One day at a time, just keep swimming" was what made the last four years possible. I love you 788.

To Professor Helen Blackwell and Professor Tehshik Yoon, I owe both of you an immense thank you. Having both of you for my organic chemistry professors in 2011 is what turned me from a History major to a Chemistry major and eventually led me back to Madison for graduate school.

To my coworkers at Geneva Laboratories – Dr. Daigneault, Nestor, Kelly, Keishah, and Eric – I loved my time with all of you. Geneva was my first "real" industry job, and I couldn't have asked for a better group to work with.

However, graduate school wouldn't have even been on my radar if Dr. Jim Smoot, my supervisor at Tate & Lyle, had not been candid and said there's no real future for you at this company without a PhD. Jim, Dr. Mark Beltz, and Dr. Penny Patton gave me first taste of what industrial research and development looked like, and I will always be grateful that Jim allowed me to write whenever there was an opportunity.

To Linda Fanis, thank you for writing a letter of recommendation to get me into UW. It wasn't until the last year that someone shared with me how much thought you put into that letter to give me a fighting chance at being accepted to Madison.

To Dr. Arrietta Clauss, I'll never forget my "visit" weekend in 2016. When we were chatting on that Saturday, and you mentioned that there were a lot of people rooting for me – that's exactly what I needed because I honestly had no idea what I was getting myself into. Our chats throughout the first semester of graduation school sincerely helped remind me the importance of chasing my dreams and being a role model for Emma, even if it was different from the norm.

To Professor Steve Burke, I'll never forget how motivated I felt after I talked to you at the visit weekend also. We were chatting Friday night at the poster session, and I told you about my history and some of my concerns about starting graduate school. You reassured me that people like me were wanted, and I'll always be thankful for that memory. Although my time in lab with you was short, I was honored to have you as one of my mentors through this journey.

To Professor Clark Landis, thank you for also being one of my early mentors. It was obvious from day one that you were truly interested in "teaching" us to communicate our science, and I've always valued those lessons.

To the Landis group, especially Dr. Floriana Fiorta, thank you for your help those first few months when I felt like I knew absolutely nothing. Having done minimal academic research prior to graduate school, I was lucky to have a great teacher and patient person in my corner during those early days in lab.

To my entire organic path cohort from 2016, I will always have a special place in my heart for you. When James and I got married and you all made the trip down to Illinois for the wedding, and I could not have been happier to see all of your smiling faces! I also owe more than a few of you a big thanks for letting me borrow your sofa on those random nights I had to stay in Madison. This journey has had ups and downs for all of us, but we are almost finished!

To Jessica Roberts, we never did have to flip a table for any reason, and I'm so happy about that ☺ Thank you for all of the nights you let me crash on your couch, the Starbucks runs, the late night NMR sessions, and for being one of my bridesmaids. Without you, there's no doubt my first-year would have been even more challenging.

To Professor Lt. Col. Victor Jaffett, I have an immense amount of respect for everything you've done for this country and for me. Believe it or not, if it wasn't for you, I would have left graduate school my first semester. There were many little chats we had in the Burke Lab that ended up keeping me in Madison despite the hardships we faced. I was so happy we both ended up in the School of Pharmacy! I usually keep my perspective pretty well, but when I would lose it you always helped bring it back.

To Tatum Lyles Flick, I have no doubt that my life would not be where it is if it weren't for you. When I reached out about starting to do science writing, you let me jump right in with you. You've been one of the most instructive people in my life, and I couldn't be happier to know and work with you.

To Tom Koetting, my editor at the Milwaukee Journal Sentinal for my 2019 AAAS Mass Media Fellowship, thank you for one of the best professional experiences of my life.

I thought I had a handle on science communication but spending time at the Sentinal taught me that science communication is so much more than just spewing facts!

To Ahna Skop, I knew the moment I left your office for the first time that my life would never be the same. Our instant bond and passion for science outreach have led us to a wonderful friendship already, and I cannot wait to see how our future endeavors benefit the lives of young people interested in STEM careers for years to come. I'm so thankful that one tweet brought us together, and I look forward to hundreds more memories with you.

I'd like to thank all of the Tang Lab members that I've had the pleasure to work with over the years – too many to count in fact – but I want to give some a special mention.

To Dr. Dan Glazier, thank you for being the welcoming senior grad student when I had to choose a new research lab. You were always willing to answer questions and made the Tang Lab feel like home, before it even was home. I learned so many lab things from you like running a column, changing pump oil, and a whole bunch of random safety facts. You really did know a little about everything.

To Chris Simmons, you were undoubtedly a source of humor for the lab and the kindest individual in the group. I'm so happy for you and Amanda!

To Professor Changgui Zhao, I'm not the only one who feels this way, but we all felt better when you were in lab. You were such a knowledgeable, patient mentor, and we knew we could always count on you to answer our questions. Having you physically present in lab was almost like our insurance that if anything went wrong, things would be alright because you would know exactly what to do when we messed up an extraction, thought we lost our product, etc.

To Dr. Peng Wen, your immense carbohydrate knowledge, willingness to answer even the most silly of questions, and fun personality made the last two years wonderful. In a way, I always feel like you've had to clean up my shortfalls, but I've learned so much from you that I'll always be grateful you came to UW.

To Kerry Smith, you lit up the office from the day you joined, and I'm so glad that so many of my fun memories have you in them, and I look forward to more in the future.

To Bethany McCarthy, it was wonderful to finally have another female in the office when you came to our group. Emma and I loved our trip to Notre Dame with you, and we know you will do great things!

To the Chemistry Biology Interface cohort and Professor Blackwell and Cara Jenkins, thank you for the opportunity to explore more than just chemistry.

To my mentoring committee – Professor Jennifer Golden, Professor Sandro Mecozzi, and Professor Ying Ge – thank you for the support during the past four years. I know my PhD was somewhat unconventional, especially considering all of the technical writing and scientific writing I did, but I truly feel like that's where my strengths are and where I can make the most impact in the world.

Most of all, I want to give my research advisor Professor Weiping Tang my most sincere gratitude. From the moment we first met in your office, I knew the Tang lab could be a special place for me. You have supported my career ambitions from day one, and that will always be one of my fondest memories. Your willingness to let me be so heavily involved in community outreach, mentoring, science writing for the general public, and technical writing was really what made my PhD so special to me. The opportunities you provide us to engage with the broader scientific community through attending

conferences, organizing conferences, and being part of things such as the NIH Glycoscience consortium meetings are the exposures we need to develop into critical thinkers and independent scientists. A million "thank yous" will never be enough. I'm forever grateful that I was able to call the Tang Lab my home, and I hope to keep my relationship with this group long after I graduate.

Table of Contents

Chapter 1

Recent Advances in Site-Selective Functionalization of Carbohydrates Mediated by Organocatalysts

Part of this chapter was taken from the following published article.

Recent advances in site-selective functionalization of carbohydrates mediated by organocatalysts. Blaszczyk, S.A.; Homan, T.; Tang, W. *Carbohydr. Res.* **2019**, *471*, 64-77.

1.1 Introduction

As one of the four macromolecules of life, carbohydrates have a vital role in a multitude of biological processes, including cellular communication, disease progression, and metabolism. Carbohydrate scaffolds can be found in commercially available therapeutics and vaccines in various stages of pharmaceutical development.[1] The evolving methods for carbohydrate synthesis continue to influence the drug discovery landscape.[2] Considering the widespread roles that carbohydrates play in daily life, scientists constantly seek to learn more about their structure-function relationships and how they influence natural systems. At the end of the day, further progress towards understanding the role of carbohydrates in the body is often limited by synthetic success, or lack thereof.

One of the most challenging aspects of working with carbohydrates results from their physical structures. While there are less than a dozen mammalian monosaccharides, the different types of isomers and anomers all present their own challenges in terms of synthesis. Furthermore, the existence of multiple hydroxyl groups in similar environments makes the site-selective functionalization of carbohydrates even more daunting. These challenges, coupled with the possibility to link monosaccharides in a linear or branched manner at multiple attachment points, makes the production of a relatively small oligosaccharide quite the formidable task.

Other macromolecules, such as proteins, nucleic acids, and lipids, have less varied structures and more general synthetic routes, which has led to successful automation platforms for the quick, efficient syntheses of these molecules. While automation in carbohydrate chemical synthesis is becoming more common thanks to efforts from

synthetic [3-5] and chemoenzymatic groups,[6] challenges still remain for accessing diverse monosaccharide building blocks and oligosaccharides. For example, it is difficult to perform reliable large-scale chemical syntheses of carbohydrates, obtain carbohydrates in homogenous forms, and site-selectively functionalize carbohydrates. With these issues at hand, the importance of innovation in regard to synthetic methodology cannot be understated. From an environmental impact point of view, continually increasing reaction efficiency in terms of step counts and reagents via catalysis remains attractive and is the subject of this review chapter.

1.2 Scope of this review chapter

A brief review chapter, such as this, cannot possibly cover all pertinent publications related to the site-selective functionalization of carbohydrates. A comprehensive review of methods for the regioselective acylation, alkylation, silylation, and glycosylation of monosaccharides was published in 2016.[7] The goal of this review chapter is to provide a more targeted update focusing on recent advances in organocatalytic reactions that highlights new angles and perspectives taken since 2015. Site-selective chemical methods prior to this date have been previously covered[8-10] as have enzymatic methods.[11-13] his review is organized by the different types of organocatalysts, including achiral catalysts, chiral nucleophilic bases, chiral N-heterocyclic carbenes, and chiral phosphoric acids, with an emphasis on the catalytic nature in each case as appropriate. Looking ahead to the future of the field and the need for untraditional approaches to longstanding problems, recent publications in boron chemistry will also be presented. Much of the work presented here comes from research groups that are not solely devoted to carbohydrate chemistry, and it is encouraging to see how various new ideas and

strategies were introduced to the field of carbohydrate research from chemists with varied expertise. The intent of this review chapter is to provide the reader with the resources to obtain a strong understanding of current trends in organocatalysis for the site-selective functionalization of carbohydrates so they have a better idea of where this field is heading in the future.

1.3 Achiral catalysts

The initial catalysts to be covered are achiral catalysts, *N,N*-diisopropylethylamine (DIPEA) and 4-dimethylaminopyridine (DMAP), and their use in site-selective transformations. Dong and Ren recently reported the self-catalyzed site-selective acylation of methyl pyranosides using a catalytic amount DIPEA in the presence of an anhydride to functionalize the C3 and/or C6 hydroxyl of various monosaccharides (**Scheme 1-1**).[14]

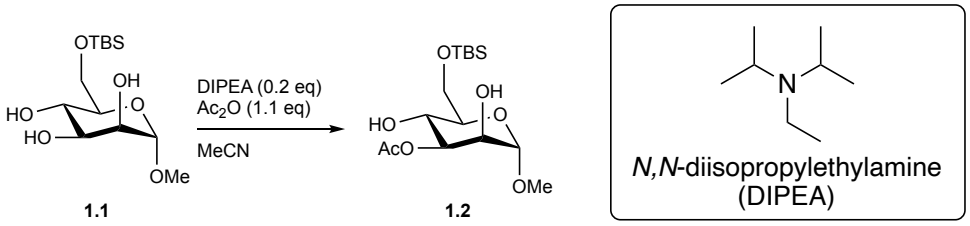

Scheme 1-1 Overview of Dong and Ren's use of DIPEA and an anhydride to self-catalyze a site-selective acylation of methyl pyranosides

Initial studies using methyl 6-*O*-(*tert*-butyldimethylsilyloxy)-α-D-mannopyranoside **1.1** were carried out in the presence of DIPEA, acetic anhydride, and an anticipated required metal catalyst, $Fe(dibm)_3$, which afforded the C3-acylated product **1.2** in 92% yield. Further studies with different metal catalysts, all produced the C3-acylated product

leading the authors to conclude that the metal catalyst was not involved in the reaction. This hypothesis was supported when the same result was obtained in the absence of any metal catalyst, which enhanced the method's appeal since one less reagent is needed. Bases other than DIPEA were examined, but lower yields and poor selectivity resulted. Overall, DIPEA exhibited the best combination of steric hindrance and base strength compared with other amines or K_2CO_3. The use of AcCl as the acylating reagent resulted in poor yield and selectivity, and anhydrides were shown to be the superior acylating reagent. Furthermore, the reaction with Ac_2O in the absence of DIPEA yielded less than 10% of the acylated product indicating the necessity of the DIPEA.

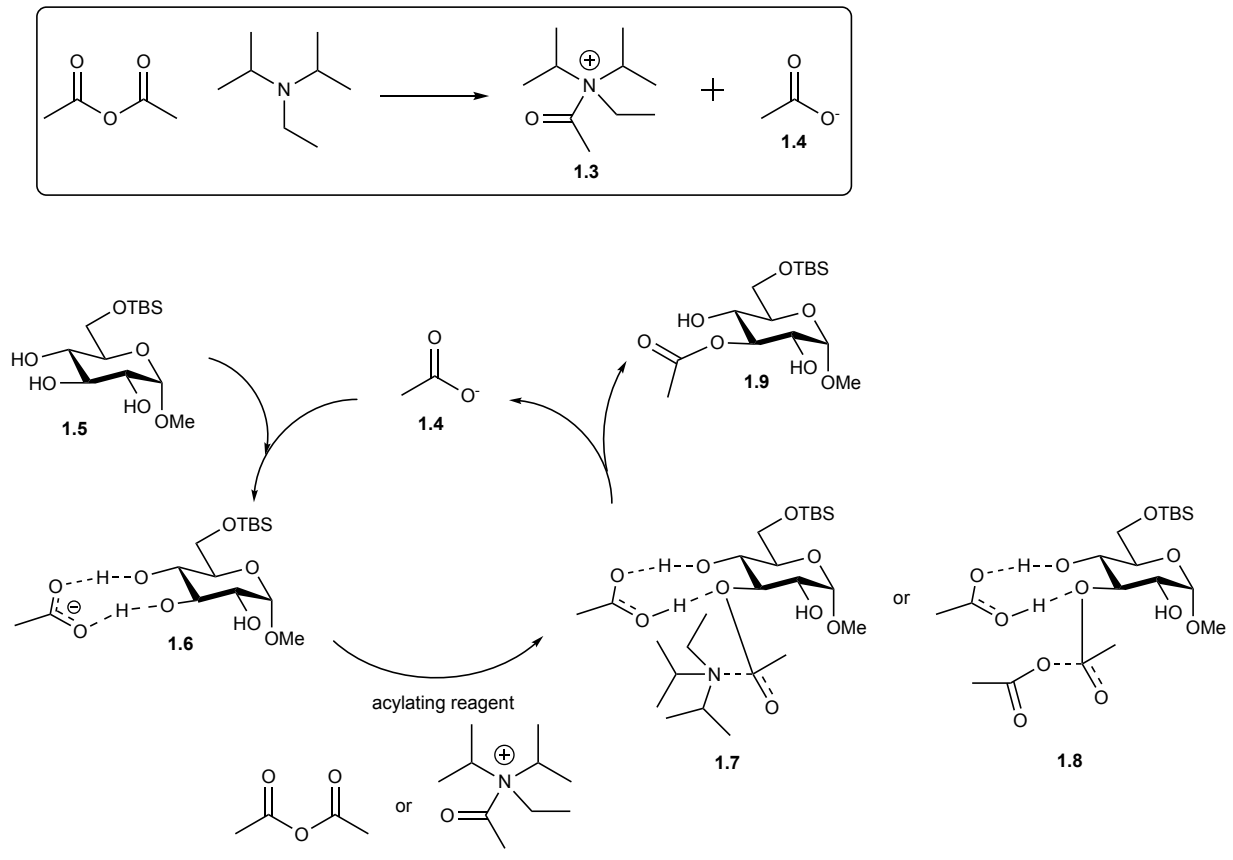

Scheme 1-2 Dong and Ren's proposed DIPEA-triggered, self-catalyzed acylation mechanism

The authors' proposed catalytic cycle is shown in **Scheme 1-2**. The cycle begins with the reaction of DIPEA with acetic anhydride to form acylammonium ion **1.3** and release carboxylate ion **1.4**. The mechanism is based on the fact that the carboxylate ion forms dual hydrogen bonds with a 1,2-diol such **1.5**, as shown in **1.6**. These hydrogen bonds activate the alcohol groups for acylation (either by way of **1.7** or **1.8**) and result in the formation of **1.9**, which frees DIPEA to react with another equivalent of anhydride. The catalytic cycle was investigated using variable temperature NMR and by examining the change in chemical shift of the hydroxyl protons in a 1,2-diol. In the presence of a carboxylate ion, the hydroxyl protons shifted approximately 0.3 ppm downfield while in the presence of DIPEA alone, there is essentially no change in chemical shift. Following the reaction by NMR, there is approximately a 0.2 ppm downfield shift after 20 minutes. This data, along with the fact that reactions using AcCl instead of Ac_2O resulted in poor yields and selectivity, strongly supports the formation of a dual hydrogen bonded complex with the diol. In conjunction with an achiral catalyst and anhydride, the authors have developed an operationally simple protocol for an organic amine self-catalyzed, site-selective acylation of manno-, gluco- and galactopyranosides that supplements other protocols currently in use.

There are a number of methods for the site-selective acylation of the equatorial hydroxyl groups in *cis*-1,2-diols, yet methods for functionalizing the axial hydroxyl group remain sparse. In 2016 Schmidt published a method for the selective acylation of the axial hydroxyl group in *cis*-1,2-diols in appropriately protected pyranosides using benzoyl cyanide (BzCN) in the presence of a catalytic amount of DMAP (**Scheme 1-3**).[15]

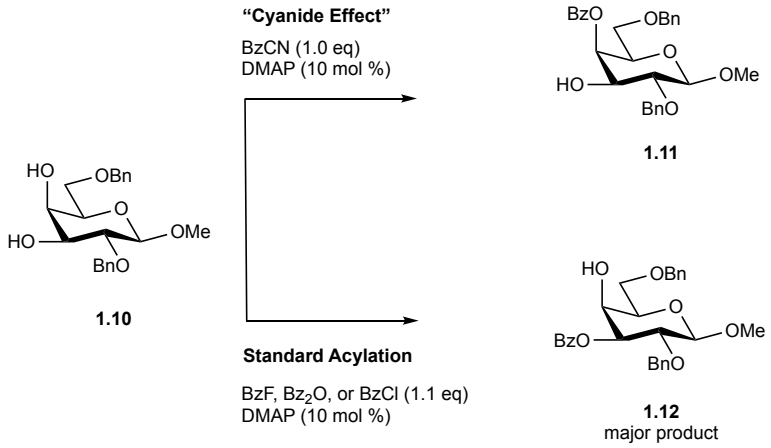

Scheme 1-3 Schmidt's use of benzoyl cyanide to acylate the axial hydroxyl group in *cis*-1,2-diols.

Specifically, methoxyphenyl 2,6-di-*O*-benzyl-β-D-galactopyranoside **1.10** yielded only the axial C4-benzoylated product **1.11** in 90% yield. Conversely, using Bz_2O, BzCl, or BzF as the acylating agent produced the C3-benzoylated isomer **1.12** as the major or exclusive product. The authors put forth the "cyanide effect" as the source of site-selectivity with BzCN (**Scheme 1-4**).

By using BzCN in conjunction with DMAP, cationic adduct **1.13** is formed leaving the negatively charged cyanide ion as a counterion. The cyanide ion is relatively basic compared to other counterions, such as chloride or carboxylate, which increases the rate of reaction and allows acylation to occur at lower temperatures. The cyanide ion is also sterically small and capable of forming hydrogen bonds with hydroxyl groups at either its carbon or nitrogen atom. Cyanide's base strength and size, in conjunction with the greater acidity of the C4-OH versus the C3-OH in galactopyranosides, provides the environment for cyanide to preferentially hydrogen bond to the C4-OH activating it for acylation relative to the C3-OH at low temperatures. Furthermore, the activation of the axial C4-OH hydroxyl group by cyanide is strong enough to cause this secondary C4-OH

group to react faster than the primary C6-OH group with a 2-*O*-benzyl galactopyranoside substrate.

The method was then tested on a series of protected galactopyranosides to determine if either sterics or electronics would influence the site of functionalization. The authors increased the steric bulk of the protecting group at the C6-OH (TBDPS) and the electron withdrawing ability of the protecting groups at the C2-OH and C6-OH (Bz and Ac), but in each case the axial C4-OH was selectively benzoylated (using BzCN, 84 – 92% isolated yields) or acetylated (using AcCN, 77 - 87% isolated yields).

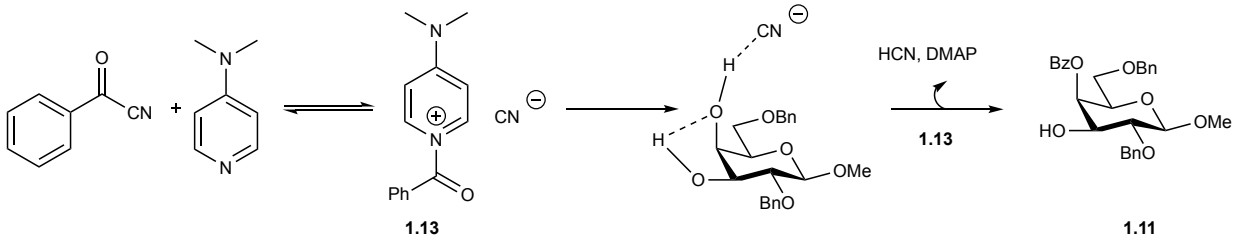

Scheme 1-4 Schmidt's proposed "cyanide effect" to acylate the axial hydroxyl group in *cis*-1,2-diols.

Computational studies were completed using allyl 4,6-*O*-benzylidene-α-D-mannopyranoside as the model compound to examine the energies of the intermediates formed when the cyanide ion hydrogen bonds to the axial C2-OH and the equatorial C3-OH. Results indicated that when the carbon atom of the cyanide ion was involved in hydrogen bonding with the designated hydroxyl group, the resulting structure was more stable than if the nitrogen atom of the cyanide ion was involved. The hydrogen bonded structure with the cyanide carbon associated with the more acidic axial C2-OH was 1.0 kcal/mol lower in energy than when the cyanide carbon was associated with the equatorial C3-OH. The deprotonation of the more acidic C2-OH by the cyanide ion is facilitated and

stabilized by intramolecular hydrogen bonding from the C3-OH to form a five-membered ring, thus leading to the activation of the C2-OH towards acylation relative to the C3-OH. Studies using fluoride rather than cyanide as the counter ion/base showed the fluoride ion hydrogen bonded to both hydroxyl groups to be the most stable structure. With no clear preference for C2-OH coordination/deprotonation, the C3-OH acylated product results from the preferred reaction pathway. The "cyanide effect" provides an avenue for the selective acylation of the axial hydroxyl group of *cis*-1-2-diols via reagent control. The reaction of BzCN with a catalytic amount of DMAP complements the use of other acylating reagents (Bz_2O, BzF) in affording selective acylation at either the axial or equatorial hydroxyl groups in *cis*-1,2-diols

Schmidt and Peng later extended their 2016 work by reporting the direct formation of 3-*O*-α-galacto- and fucopyranosides in a single pot benzoylation with either a 6-*O*-protected or unprotected pyranoside as the starting compound and using a catalytic amount of DMAP in conjunction with DIPEA (**Scheme 1-5**).[15] Initial studies were carried out on methyl 6-*O*-*tert*-butyldiphenylsilyl-α-D-galactopyranoside **1.14** to examine the relative reactivities of the C2, C3, and C4 hydroxyl groups under various acylation reaction conditions with the goal of leaving the C3-OH unfunctionalized. Theoretically, the equatorial C2-OH, being adjacent to the axial anomeric alkoxy group, should be functionalized quickly with BzCN due to the "alkoxy mediated diol effect". Additionally, previous studies demonstrated the kinetic selectivity of the C4-OH to be functionalized over the C3-OH due to the "cyanide effect", thus leaving the C3-OH unprotected. The authors determined that benzoylation of the 6-*O*-protected galactopyranoside did in fact produce the 2,4-di-*O*-benzoyl-α-D-galactopyranoside product **1.15** in 60% yield.

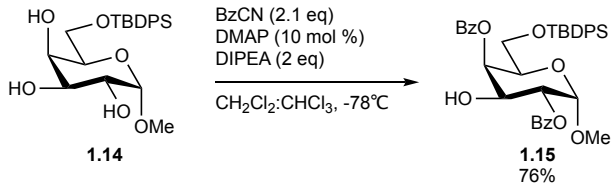

Scheme 1-5 Schmidt and Peng's one-pot synthesis of unprotected C3-OH monosaccharides via site-selective acylation

Since undesired mono- and dibenzoylated products contributed to the modest 60% yield of **1.15**, attempts to increase the selectivity of the reaction and enhance the yield were carried out using different amines as catalysts. However, each produced a lower yield and poorer selectivity. Changes in solvent composition did not improve selectivity either. The addition of a chloroform mixture (CH_2Cl_2:$CHCl_3$, 1:3) or chloroform alone, however, did improve the yield of the desired product to 70% and 69%, respectively. The use of 2.0 equivalents of DIPEA to neutralize the acid formed in the reaction also increased the selectivity. Optimized reaction conditions yielded **1.15** in 76% yield. The method was examined on a series of α-galactopyranosides where the C6-OH protecting group and anomeric group varied while the C2, C3, and C4 hydroxyl groups remained unprotected (**Scheme 1-6**). All of the glycosides studied yielded the 2,4-*di*-O-benzoyl-α-D-galactopyranosides products in 70 – 76% yields.

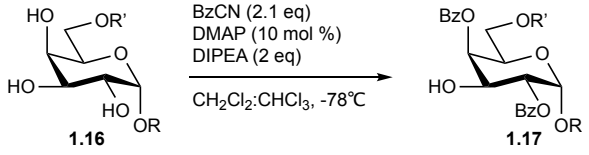

R = Me, p-OMePh, p-NO_2Ph, H; R' = TBDPS, Tr, Bn, Bz

Scheme 1-6 Scope of Schmidt and Peng's one-pot synthesis of unprotected C3-OH monosaccharides via site-selective acylation

1.4 Chiral nucleophilic bases

As a small molecule organocatalyst, benzotetramisole (BTM, **1.18** and **1.19**) has emerged as a promising catalyst for the site-selective acylation of carbohydrates. Although originally developed by Birman for the kinetic resolution of alcohols,[16, 17] in 2017 we in the Tang group used the commercially-available paired chiral BTM catalysts to differentiate the prevalent *trans*-1,2-diol motif in various pyranoses (**Scheme 1-7**).[18] The results of this work will be discussed more in detail in Chapter 2.

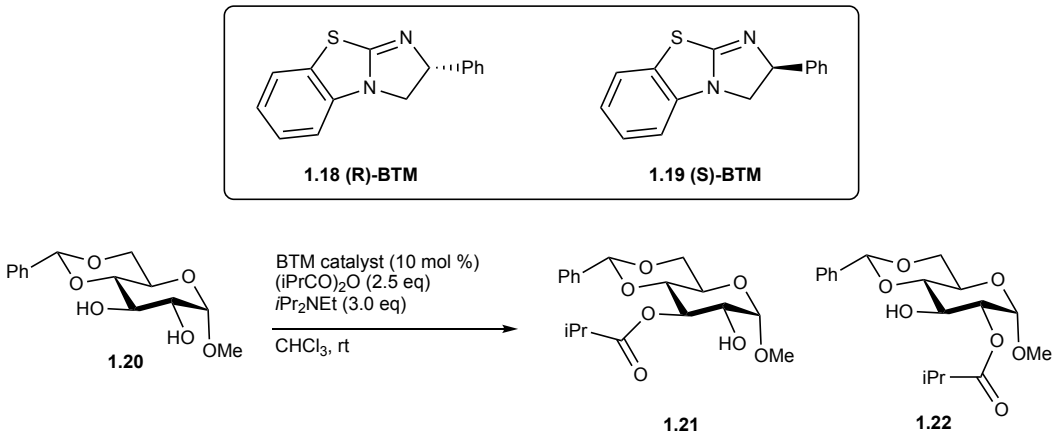

Scheme 1-7 Tang's use of chiral benzotetramisole (BTM) catalysts to differentiate *trans*-1,2-diols for site-selective acylation

The proposed mechanism for cation-lone pair directed acylation (**Scheme 1-8**) and a partial substrate scope (**Scheme 1-9**) shown below will also be addressed in Chapter 2.

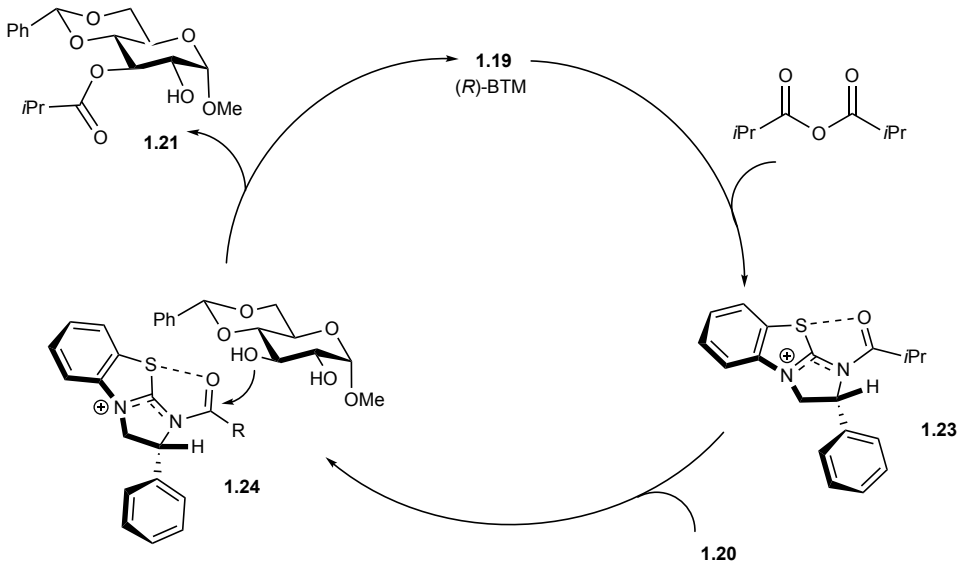

Scheme 1-8 Working model for Tang's use of chiral benzotetramisole catalysts to differentiate *trans*-1,2-diols for acylation

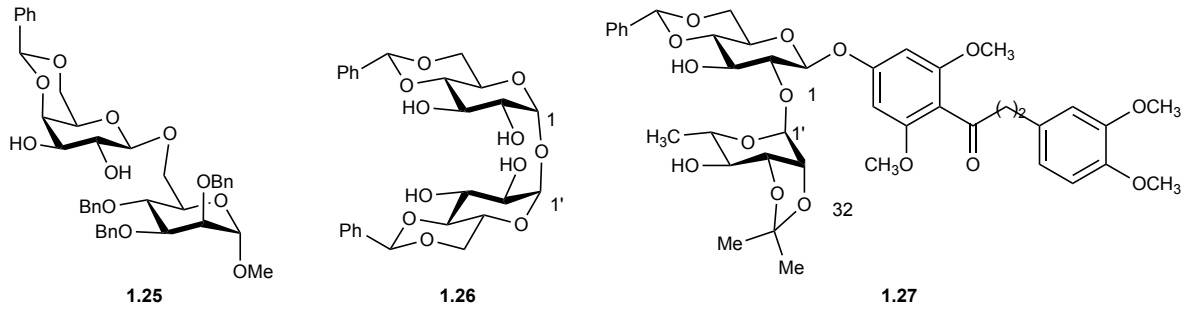

Scheme 1-9 Selected examples of site-selective acylation of *trans*-1,2-diols using cation-lone pair directed acylation

In 2017, Kawabata reported the C4-acylation of β-glucopyranosides with a chiral pyrrolidinopyridine (PPy) catalyst and an acid chloride in the presence of a carboxylic acid and base (**Scheme 1-10**).[19] Both catalyst loading and reaction times were substantially decreased from previously published results leading to a significantly increased catalytic efficiency for this process.[20] The authors previously used anhydrides to site-selectively acylate the C4-hydroxyl, but the reaction times ranged from 12-24 hours depending on

the anhydride and amount of catalyst used. In contrast, the most recent work using an acid chloride and carboxylic acid takes less than an hour in most cases, regardless of the amount of catalyst used.

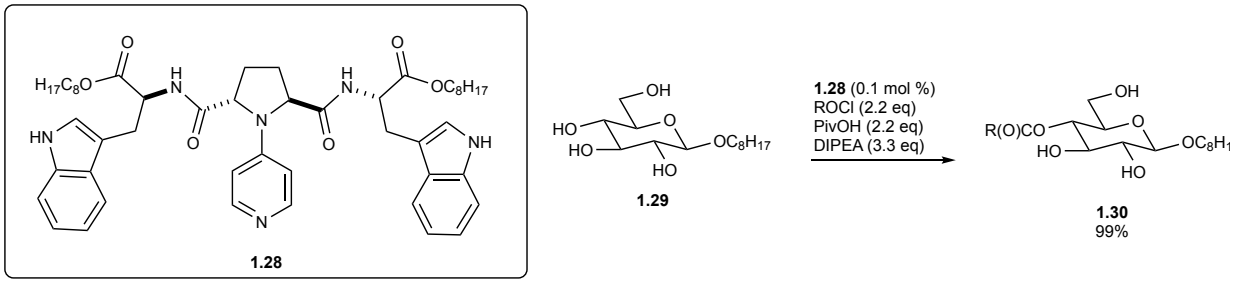

Scheme 1-10 Kawabata's use of *in-situ* counter anion exchange to promote quick site-selective acylation

To begin their work, the authors used PPy catalyst **1.28** and an acid chloride or anhydride to study the formation of acylpyridinium salts and their subsequent reaction with 1-phenyl-2,2-dimethylethanol to produce the acylated product. Results showed the formation of the acylpyridinium salts was fast and complete with the acid chlorides, while the anhydrides showed lower conversions into the desired acylpyridinium salt. However, when *in situ* counter anion exchange provided the acylpyridinium carboxylates, these species were 800-1300 times more active than the corresponding acylpyridinium chlorides in the acylation of 1-phenyl-2,2-dimethylethanol. This significant increase in activity then led the authors to try their system with a carbohydrate substrate. The anticipated result was realized in the acylation of octyl β-D-glucopyranoside **1.29** to selectively produce the octyl C4-acyl glucopyranoside **1.30** (C4-acylation:C3-acylation ratio 98:2) in 99% yield in just five minutes using 0.1 mol % catalyst and isobutyryl

chloride. Almost identical results were achieved in 25 minutes with 0.02 mol% catalyst (C4-acylation:C3-acylation ratio 96:4, 96% yield). The reaction with benzoyl chloride and 0.1 mol % catalyst led to an 87% yield of monobenzoylation products in 15 minutes with high site-selectivity (C4-benzoylation: C3-benzoylation:C6-benzoylation, 95:4:1). Reducing the catalyst loading to 0.02 mol% maintained site-selectivity but required a 12-hour reaction time to give a 76% yield of monobenzoylated products (C4-benzoylation:C3-benzoylation, 95:5).

The first step of the catalytic cycle is the reaction between chiral catalyst **1.28** and the acid chloride to form the acylpyridinium chloride **1.31** (**Scheme 1-11**). Next, an *in situ* counter anion exchange occurs to form the more reactive acylpyridinium carboxylate **1.32**, which results in an increased acylation rate. The carboxylate ion, being both a stronger base than chloride and being able to coordinate to the C2-hydrogen of the acylpyridinium ion and a carbohydrate hydroxyl group via hydrogen bonds, promotes the reactivity of the acylpyridinium ion in the following acylation step of the catalytic cycle. Introduction of **1.33** and subsequent acyl group delivery, depicted in **1.34**, then leads to formation of product **1.35** and regeneration of the catalytic species.

Prior to this paper, Kawabata achieved selective C4-acylation using 1 or 10 mol % catalyst with 1.1 equivalents of acylating agent and 1.5 equivalents of collidine over a 12-24 hour period. The performance of PPy catalyst **1.28** is significantly increased by generating the acylpyridinium ion with an acid chloride in the presence of a carboxylate ion. The current procedure matches C4-OH selectivity and yield while significantly reducing both reaction time and catalyst loading (0.02 or 0.1 mol%). Thus, the identity of

the counter anion is the key to achieving high catalytic activity within this system while retaining the same chiral catalyst used previously.

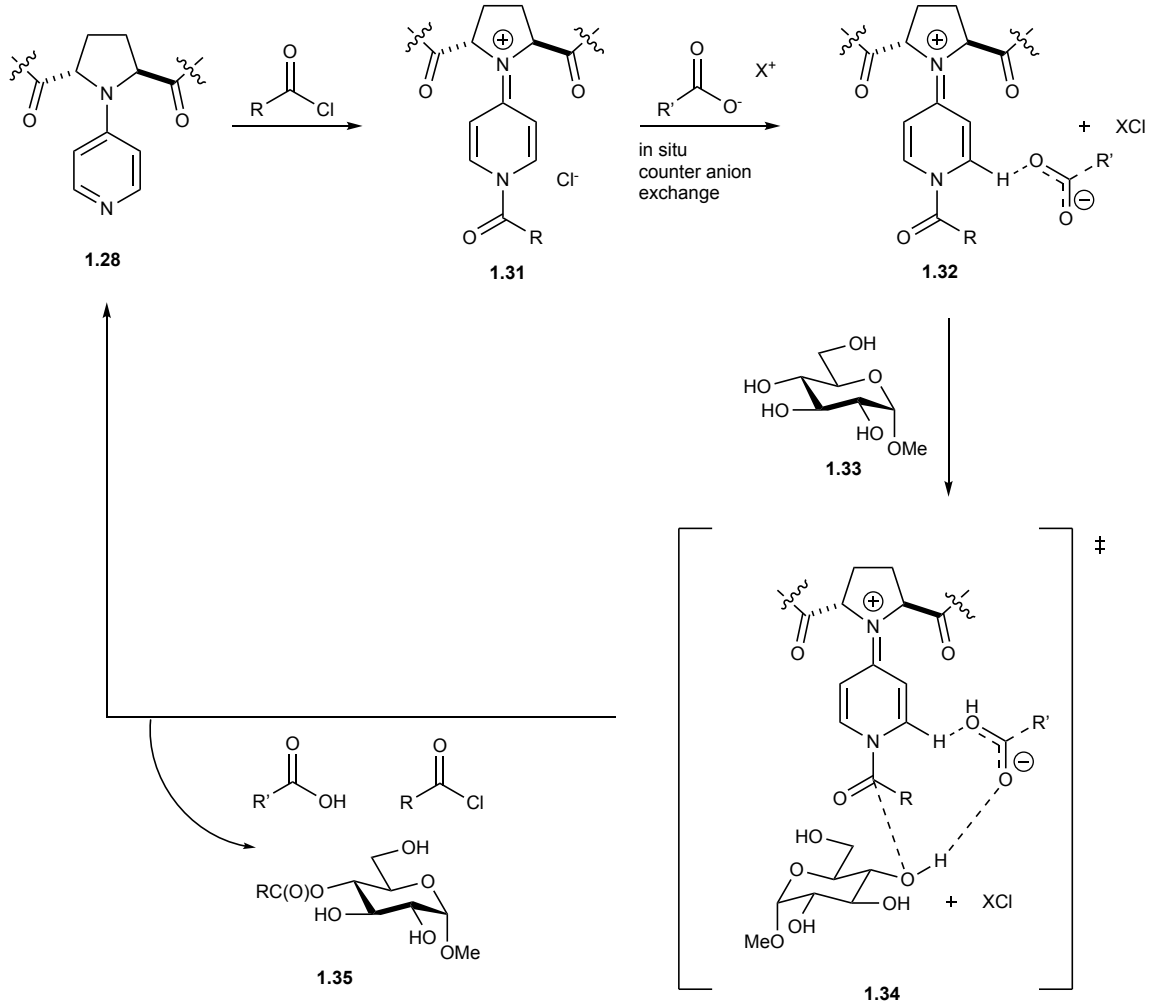

Scheme 1-11 Mechanism of Kawabata's *in-situ* counter anion exchange to promote quick site-selective acylation

Continuing the prevalent trend of using peptide catalysts for site-selective functionalization,[21] in 2016 Kirsch and co-workers reported an instance where DMAP-based small molecular peptides were synthesized using click chemistry to tether DMAP to a peptide side chain.[22] DMAP, being one of the most well-studied acylation catalysts, was the catalytically active unit, while the peptide unit influenced the site-selective

outcome. Using solid-phase peptide synthesis, a variety of peptide scaffolds were synthesized to form a library of DMAP-based catalysts.

Upon screening the catalyst library, the authors determined that the peptide catalyst **1.36** was superior, and substrate **1.37** could undergo C2-acylation to form product **1.38** with excellent site-selectivity (96%) and yield (91%) (**Scheme 1-12**). When DMAP was used to determine intrinsic reactivity, only 51% of the C2-acylated product was formed, along with 18% of the C3-acylated product and 31% bisacylated product, which made the peptide catalyst's result even more impressive. Overall, catalyst **1.36** provided improvement in terms of site-selectivity, however, the fact that peptide catalysts are highly substrate-specific still remains as the major limitation. Different peptide catalysts must be screened for different monosaccharide substrates or even the same monosaccharide with different protecting groups. When looking to functionalize a specific target compound with multiple hydroxyl groups there is often a need for substrate-specific catalysts, and peptide catalysts can provide a solution.

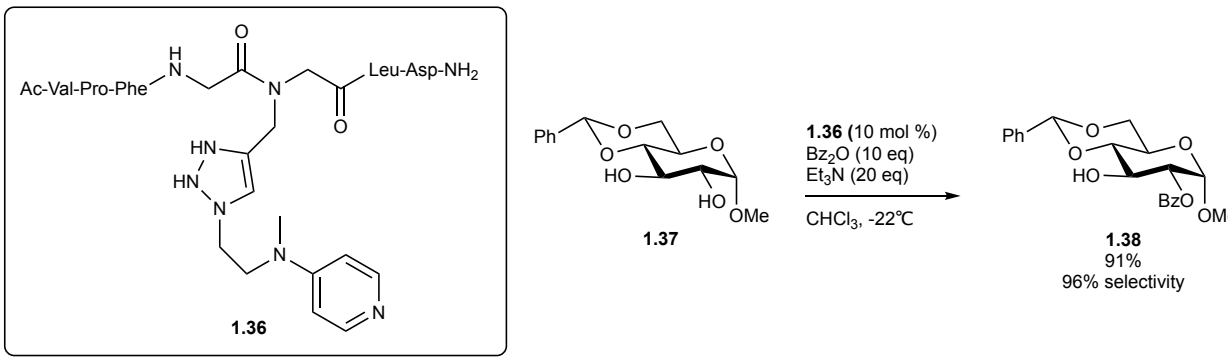

Scheme 1-12 Kirsch's use of a DMAP-based amino acid catalyst for site-selective acylation

As a follow up to their initial peptide catalysis work, in 2017 Kirsch discovered that increased site-selectivity and an easier purification process could be achieved when they attached the peptide catalysts to solid supports.[23] By attaching the DMAP-peptide unit to

a Boc-glycine Merrifield resin, the catalytic units could be made via automated synthesis. Additionally, the solid-supported catalysts also provided a simplified purification procedure of the product from the reaction mixture, and the recovery of the catalysts for additional future use is also possible. The authors questioned whether the resin alone was the reason for site-selectivity, but upon screening catalysts with subtle variations in the peptide sequence, they determined that catalyst structure undoubtedly influenced reaction selectivity. Their eventual conclusion was that the solid-supported catalysts made of resin could influence substrate-specificity via diffusion and polarity effects. Although different catalysts were still required for different substrates, the addition of the solid-supported catalysts allowed the entire process to be more cost-effective than their previous protocol.

This work is limited by the fact that the authors did not rationally design the peptide structures. Instead, the amino acid sequence was randomly selected. Perhaps future studies will subject rationally designed peptide structures to the above conditions and allow for greater insight into how various catalysts contribute to site-selectivity. This work is just one of many harnessing the power of peptides in recent years, and undoubtedly more catalysts of this type or similar strategies will be seen in the future.

1.5 Chiral N-heterocyclic carbenes

In recent years the Sundén and Studer groups have taken a different approach to site-selective functionalization by employing the use of N-hetereocyclic carbenes (NHCs). In 2016 the Sundén group used dialkylimidazolium-based ionic liquids to generate the NHCs, and since ionic liquids are generally considered to be safe and recyclable solvents,[24] their methods embrace the intentions of the current green chemistry

movement while also providing an example of the innovation that will keep carbohdrate chemistry moving forward.

Since sterics often affect reactivity patterns, Sundén envisioned that sterically encumbered ionic liquid-derived acylazolium compounds could be used to site-selectively functionalize carbohydrates by discriminating against the incoming polyol nucleophile in a regioselective fashion, thereby directing the nucleophile to a desired hydroxyl group.[25]

Using ionic liquid 1-ethyl-3-methylimidazolium acetate (EMIMAc) **1.39**, DBU, cinnamaldehyde **1.41**, and a chalcone **1.42**, the first step towards product formation is the construction of the acylazolium compound **1.43**, which occurs in a highly disastereoselective manner as a 1:1 ratio of the two *anti*-diastereomers was formed (**Scheme 1-13**). Using this IL-derived NHC complex can assist in dissolving polar substrates, such as **1.40**, and subsequent attack by the primary hydroxyl on the acylazolium complex leads to functionalization of the primary alcohol **1.44** in each case. Alternatively, the authors discovered that using non-ionic liquid derived NHC complexes were unsuccessful in forming the desired product.

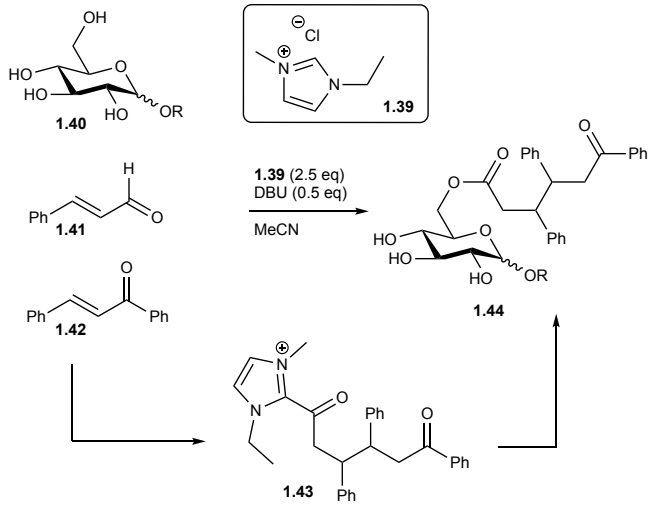

Scheme 1-13 Sundén's use of ionic liquids to promote a NHC-catalyzed site-selective functionalization

DFT calculations rationalize the greather than 20:1 preference for functionalization of the primary hydroxyl in **1.40** over any possible secondary hydroxyls by considering the conformation of the intermediate in conjunction with solvation effects. When the C6-OH attacks the acylazolium complex, the intermediate forms a rather compact structure. This conformation minimizes contact between the hydrophobic regions of the molecule and the polar acetonitrile solvent while simultaneously exposing the imidazolium and carbohydrate backbone to the solvent. Conversely, when the authors performed calculations that used the C4-OH attacking the acylazolium complex, a more elongated intermediate formed to relieve steric stress at the expense of losing stabilization due to solvation. Overall, the most stable intermediate formed by C6-OH attack was favored by 6 kJ/mol over the most stable intermediate formed by C4-OH attack, which is in agreement with experimental results.

Products resulting from this method could be isolated without column chromatography, and although an excess of the ionic liquid **1.39** was used, the authors consistently recycled the ionic liquid and used it in further runs without sacrificing yields. Additionally, the reactions were shown to be successful on the gram scale, able to be run in one-pot, and amenable to various aromatic substituents on the chalcone, making this method a promising approach to introduce large functional groups to the primary hydroxyl.

Also in 2016, Studer and co-workers employed chiral NHCs for the site-selective acylation of diols and triols in various carbohydrates.[26] Since the actual acylating reagent in oxidative NHC catalysis is an acylazolium ion formed from an aldehyde, modifying the original aldehyde or the actual NHC allows for a fair amount of flexibility in terms of tuning

reagents. Substrate **1.46** when reacted with **1.47**, **1.49**, and chiral NHC catalyst **(*S*)-1.45**, yielded the C2-acylated product **1.48** in 85% yield with 89% site-selectivity (**Scheme 1-14**). Because their previous work[27, 28] indicated that a second equivalent of the free NHC catalyst was required in the acylation step, the authors expected a nonlinear effect on the site-selectivity of the reaction. Upon screening different ratios of **(*S*)-1.45** and **(*R*)-1.45**, they did observe this non-linear trend and found that when the ratio between **(*S*)-** and **(*R*)-1.45** was 3:1, 99% site-selectivity for product **1.48** was obtained. These results indicated that a cooperative process was involved in this reaction. During the acylating step, one enantiomer of the catalyst was part of acylating reagent, while the other enantiomer of the catalyst likely activated the alcohol for acylation through hydrogen bonding. Compound **1.49** was used as a two-electron-oxidant to oxidize key Breslow intermediate **1.51** through radical cation **1.52** and radical **1.53** intermediates, resulting in **1.48** and **1.50**.

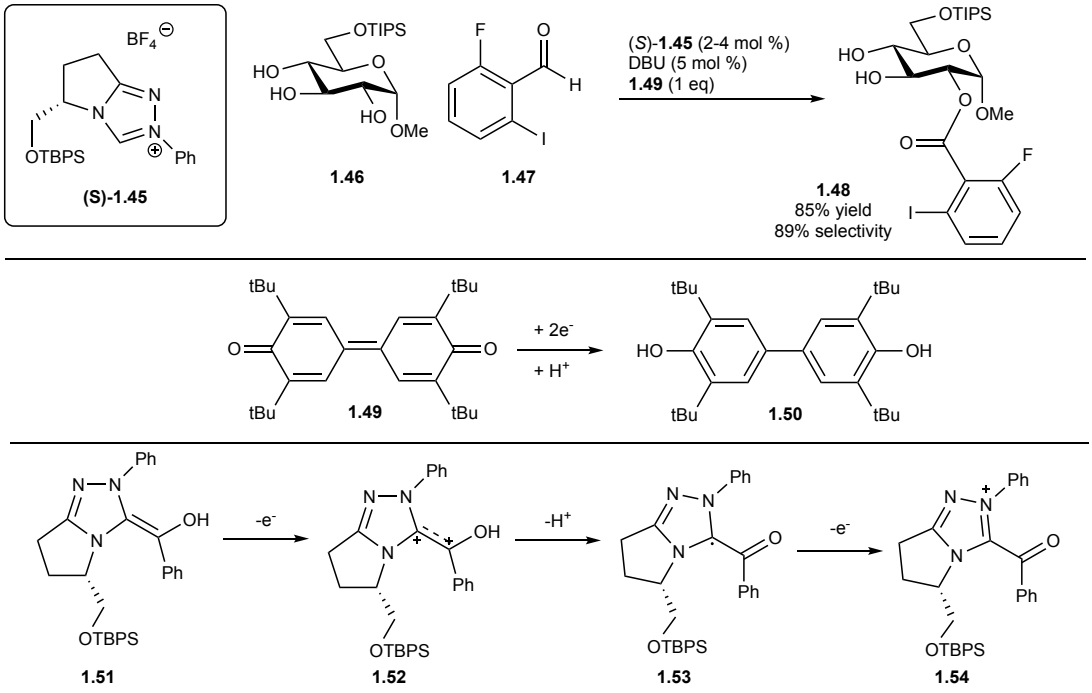

Scheme 1-14 Studer's use of oxidative NHC catalysis for site-selective acylation

1.6 Chiral phosphoric acids

While most of the material presented thus far has focused on the site-selective functionalizaton of carbohydrates, the site-selective glycosylation of carbohydrates is equally important. The ability to complete a late-stage glycosylation of a complex molecule, natural product, or polyol with multiple free hydroxyl groups without additional protection and deprotection steps is essential for synthetic chemists. In these situations, site-selective glycosylations are highly valuable, and methods to accomplish the desired result are imperative. To this end, chiral phosphoric acids have recently been used to increase the site- and stereoselectivity in glycosylations.[29, 30]

Just as peptide catalysts are used to discriminate substrates, chiral catalysts can be used to discriminate glycosyl donors by changing their surrounding environments. The Nagorny group has been one team to tackle site-selective glycosylations, and their strategy of choice is to employ a chiral phosphoric acid to functionalize complex polyols, such as oleandomycin-derived macrolactones.[31] To demonstrate the ability of chiral catalysts to promote the site-selective glycosylation of complex molecules, Nagorny chose triol, 6-deoxyerythronolide B (6-dEB), as the target molecule for his teams's work (**Scheme 1-15**). Not only were the authors able to functionalize all three hydroxyl groups individually, but they also completed the mechanistic studies to explain the selectivity.

After control experiments were done to determine the intrinsic reactivity of the C3, C5, and C11 hydroxyl groups, the authors determined that BINOL based **(*S*)-1.55** was superior at promoting the glycosylation at C5 leading to **1.60** (**1.60**:**1.61** 99:1, 98% yield). Structurally similar catalyst **(*R*)-1.56** was able to provide a majority of C3- glycosylated product, but there was definitely the opportunity for selectivity gains and yield

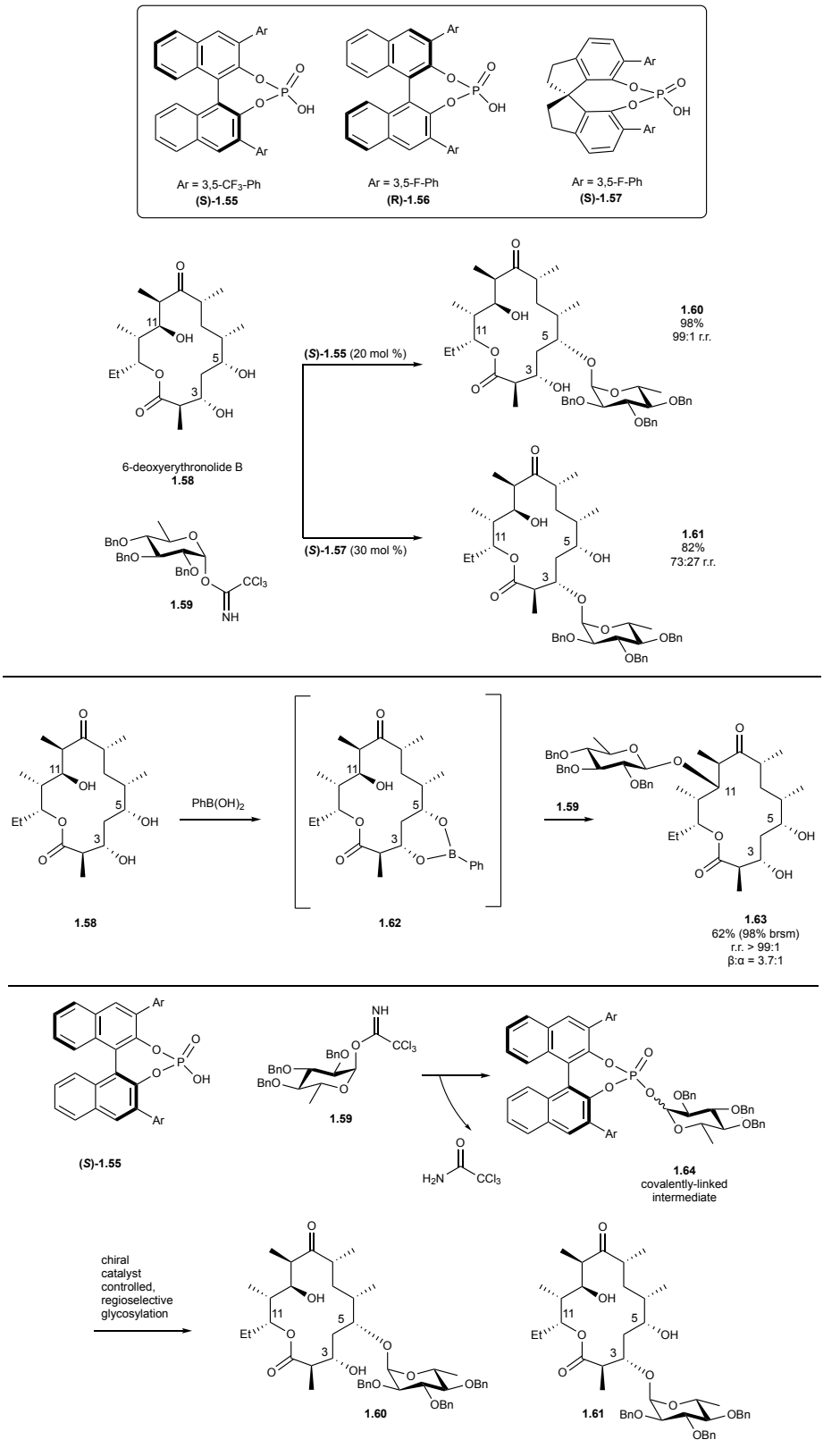

Scheme 1-15 Nagorny's use of chiral phosphoric acids to site-selectively glycosylate 6-deoxy-erythronolide B

improvement. By screening SPINOL-based catalysts, which boast a less flexible backbone, the authors were able to obtain the C3-glycosylated product **1.61** in 82% yield with a 73:27 ratio of **1.61**:**1.60** using **(*S*)-1.57**. With 2 of the 3 hydroxyl groups able to be differentiated, the authors began to tackle the functionalization of the C11 hydroxyl group. Having 1,3-*syn* hydroxyl groups at C3 and C5 led the authors to hypothesize the formation of a transient cyclic boronic ester protecting group **1.62**, followed by glycosylation at the C11 hydroxyl and subsequent removal of the boronic ester. While this type of protecting group strategy has gained attention recently, its potential for success on a complex molecule was unknown. The authors' plan was successful, and the C11-glycosylated product **1.63** was obtained in 62% yield (99:1 r.r., 3.7:1 β:α).

To further rationalize observed glycosylation selectivities, the authors ran computational experiments on a simplified model system. Their data suggested that covalently linked anomeric phosphates **1.64** were the reactive intermediates instead of traditional oxocarbenium ion pairs. Since these results were not consistent with results from similar systems, the authors sought experimental evidence to support the computations, which they obtained via NMR studies. The authors intend to perform additional mechanistic investigations to determine the origin of the observed selectivities. While this review has primarily focused on chiral organocatalysts promoting the site-selective functionalization of monosaccharides, Nagorny has shown that chiral organocatalysts can be employed for the site-selective glycosylation of complex chiral polyols in lieu of enzymatic approaches.

Recognizing the inherent potential of chiral phosphoric acids, in 2017 the Galan group reported the use of a chiral phosphoric acid in conjunction with a thiourea catalyst

to promote the stereoselective formation of deoxyglycosides from glycals.[32] Galan previously used thiourea catalysts to prepare 2-deoxygalactosides, but long reaction times and a limited substrate scope prompted the development of a more successful method.[33] Using thiourea catalyst **1.65,** the authors determined that it had a significant effect on the reaction rate and yield, while chiral phosphoric acid **1.66** was the predominant species affecting the stereoselectivity of the reaction (**Scheme 1-16**). Furthermore, the absence of **1.66** resulted only in starting material, reinforcing the synergistic nature of both catalysts. Using **1.68** as a model substrate, the reaction was shown to proceed fairly quickly (<6 hours) to yield the desired products in good yield and greater than 30:1 α:β selectivity while also tolerating acetal, ether, ester, and carbamate protecting groups. Since the scope of the glycosyl donor in the authors' previous work was limited, they now turned to various galactals, glucals, and rhamnals with diverse protecting groups to investigate the generality of their method. The authors were pleased to find that using a model secondary acceptor **1.67** resulted in good yields and greather than 30:1 α:β selectivity in a majority of cases.

Using deuterated galactal **1.68**, the authors employed NMR spectroscopy and analyzed proton shifts leading to the formation of **1.69**, in which the newly formed bonds are *cis* to each other, indicating that the C-H and C-O bond forming events occur in a *syn*-diastereoselective fashion. Thus, the authors propose that a hydrogen-bond-mediated complex **1.70** forms from the association of **1.65** and **1.66**. The phosphoric acid proton from **1.70** then adds to the more accessible face of the deuterated enol ether to form a transient oxocarbenium intermediate **1.71**. **1.71** is then trapped by the corresponding nucleophile, in this case **1.67**, and subsequently activated by the phosphate intermediate

generated *in situ* to form **1.69**. With this cycle in mind, the authors rationalize why the chirality of the phosphoric acid affects the stereoselectivity of the glycosylation. The authors synthesized various disaccharides, glycosyl-amino acids, and glycoconjugates using their cooperative Brønsted-acid/thiourea synergistic catalysis system for direct glycosylation and hope to apply it to other important glycosides in the future. Their method was amenable to a host of glycosyl donors and various nucleophile acceptors while leading to a high degree of selectivity for α-anomers of each product.

1.7 Stoichiometric boronic esters as temporary protecting groups or activating groups

To this point, this chapter has focused on recent examples of organocatalysts that have been used for site-selective reactions. Boron is typically considered a metalloid, a type of chemical element with properties between metals and nonmetals. Taylor's group has developed a series of reactions using boron-based catalysts for the site-selective functionalization of carbohydrates by forming cyclic boronic ester intermediates.[34] This section will focus on the Taylor group's work since 2015 and related work from others, most of which actually employ stoichiometric amount of boronic acids. Although the boron reagents are not catalytic, the ability to recover them prompted their inclusion in this this chapter, especially as we continue to develop nontraditional methods for site-selective reactions.

In 2017, the Taylor group made two key contributions regarding the use of boronic esters as activating and protecting groups for carbohydrate functionalization. In the first,

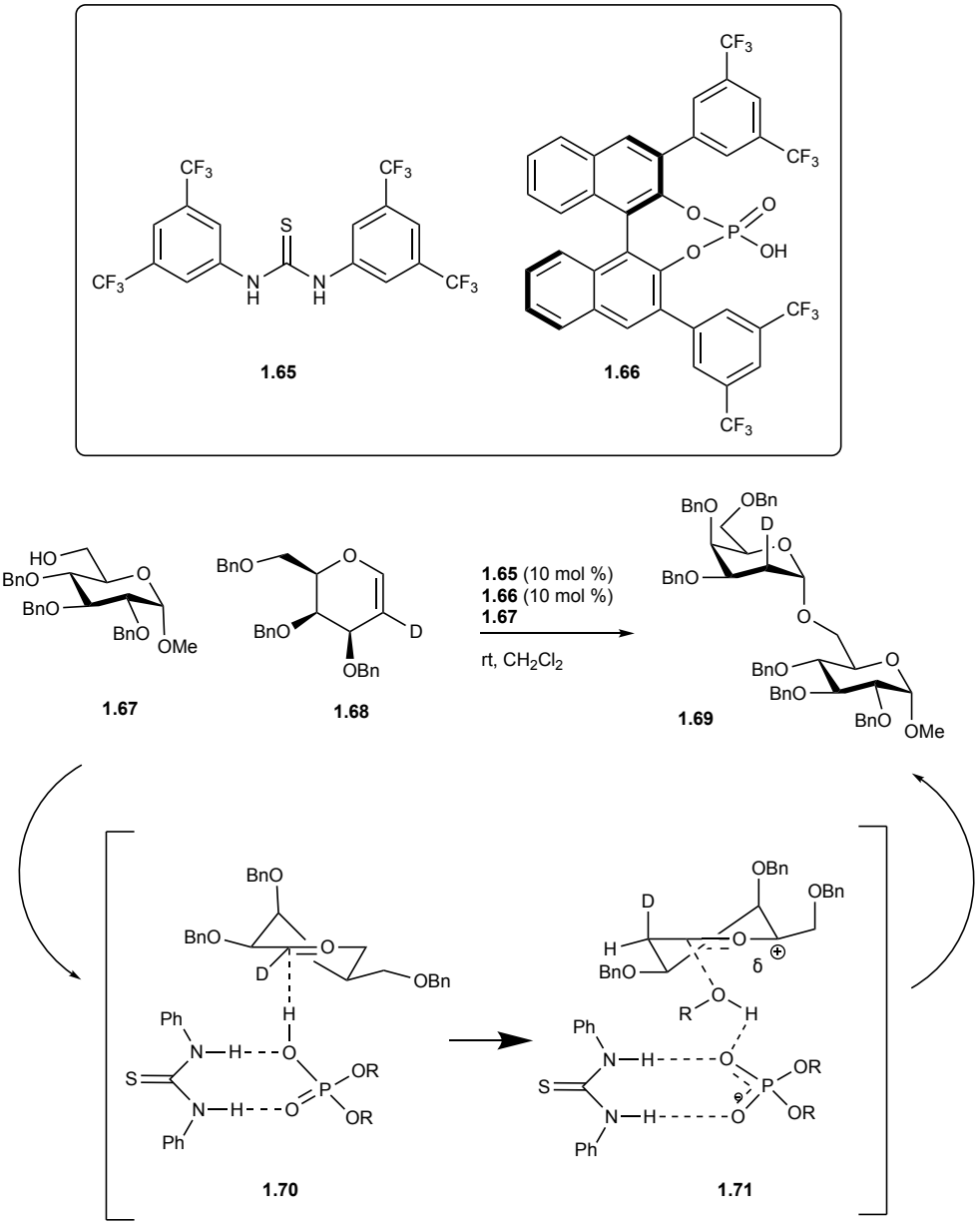

Scheme 1-16 Galan's synergistic catalysis using thiourea and a chiral phosphoric acid to promote stereoselective glycosylation

phenylboronic acids were used as protective intermediates for *cis*-1,2- or *cis*-1,3-diols to site-selectively install a variety of functional groups, including acyl groups, silyl ethers, and *para*-methoxybenzyl (PMB) ethers to furanoside and pyranoside substrates.[35]

Using methyl α-D-glucopyranoside **1.72** as a model substrate, the authors aimed to acylate a variety of monosaccharides and then recover the boronic acid **1.74**, in addition to the desired product **1.75**. Using a simple three step sequence: protection with phenylboronic acid, acylation, and deprotection, the authors were able to generate the cyclic boronic ester and form the acylated product (**Scheme 1-17**).

The utility of the boronic acid hinges upon the formation of the cyclic boronic ester that temporarily masks the C4 and C6 hydroxyl groups. Once functionalization of the C2 and C3 hydroxyl groups is complete, facile removal of the boronic ester allows for any remaining transformations to be completed. While protection and acylation proceeded as expected, hydrolysis of the boronic ester, however, proved more challenging than anticipated. After screening various hydrolysis methods with little success, Taylor envisioned that using Hall's "phase-switching" method[36] could alleviate the deprotection issue by using a liquid-liquid extraction method. This method was successful for producing bisacylated compound **1.75** in 80% yield while also allowing recovering 77% of the phenylboronic acid **1.74** used. The authors used this three-step sequence for the synthesis of a variety of mono- and bisacylated products and were able to scale up the procedure leading to isolation of products on the gram scale.

Likewise, Taylor has been able to use boronic acids to promote the site-selective *O*-arylation of carbohydrates by way of a copper (II) mediated process.[37] *O*-arylation of carbohydrates is a difficult feat on its own, and the authors' success completing *O*-arylation site-selectively is even more impressive. The authors started with methyl α-L-rhamnopyranoside **1.79** and treated it with an arylboronic acid to form the canonical organoboron complex **1.80**. Traditionally, acylation, silylation, or some other

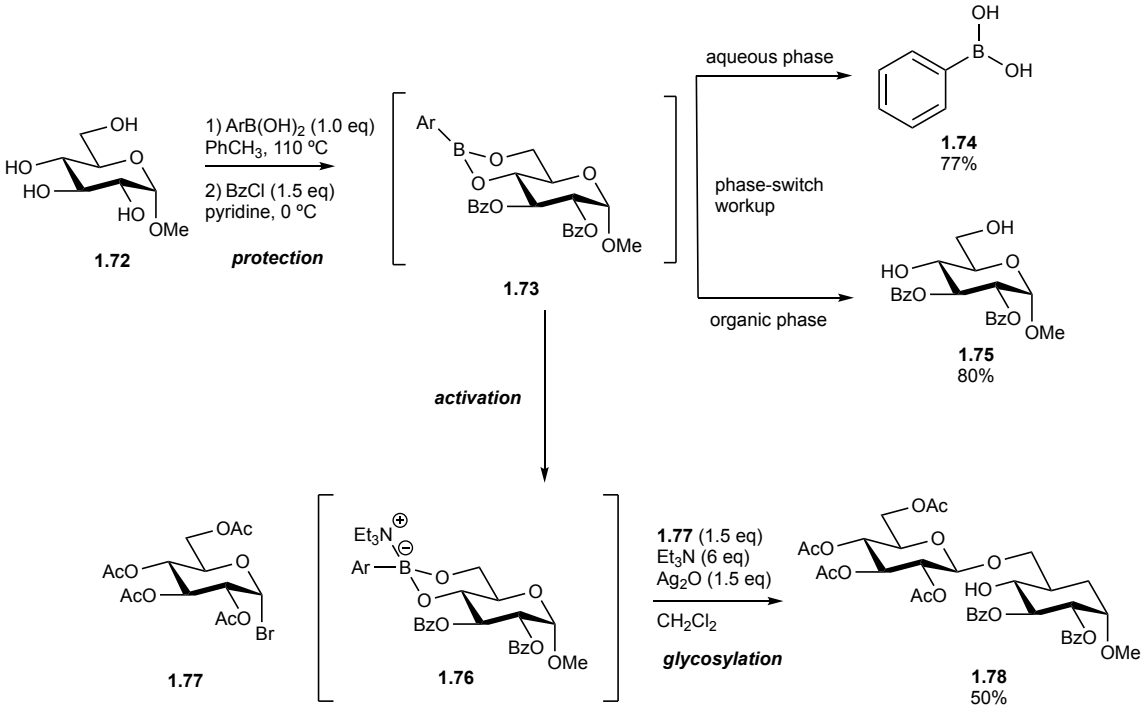

Scheme 1-17 Taylor's use of boronic acid esters as transient protecting groups and activators for site-selective glycosylation

functionalization occurs at this point, but in this case, the addition of $Cu(OAc)_2$ directly leads to formation of the C4-monoarylated product **1.83** in 72% yield with greater than 20:1 site-selectivity (**Scheme 1-18**). The site-selective outcome is in accordance with previous experimental observations where the boronic acid ester is formed with the *cis*-diols and the remaining free hydroxyl group is functionalized. Aside from being the transient protecting group, competition experiments also indicated that the boronic acid ester may facilitate quicker arylation of the free hydroxyl group. In an effort to better understand the reaction results, the authors set out to determine the mechanism of the reaction, and they used DFT calculations to help explain the origin of the accelerating effect of boronic ester. Computational results indicate a Lewis acid-base interaction between the cyclic boronic ester and the acetate ligand in **1.81** and subsequent formation

of the copper alkoxide in **1.82** may be responsible for the previously mentioned accelerating effect, but additional mechanistic studies are needed to conclude this definitively. This method not only boasted a large substrate scope of various furanosides, pyranosides, and glucals, but also allowed for the installation of many substituted aryl ethers. Overall, using copper (II) acetate, Taylor was able to demonstrate that site-selective carbohydrate *O*-arylation is possible, and the resulting products can be used in applications with widespread implications in the synthetic and therapeutic arenas.

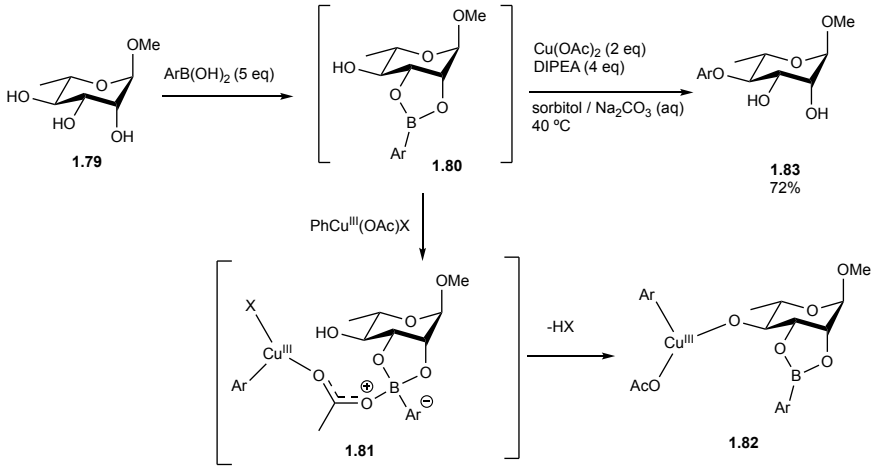

Scheme 1-18 Taylor's use of boronic acid esters to promote copper (II) mediated *O*-arylation of carbohydrates

While Taylor has worked extensively with phenylboronic acids for site-selective functionalization of carbohydrates, the Makino group has also employed phenylboronic acids, albeit for site-selective sulfation in a similar sequence. Considering the importance of sulfated carbohydrates in biological events and pharmaceuticals agents, it should come as no surprise that novel methods for the site-selective sulfation of carbohydrates have come out of the pipeline. Makino's new sulfation method, which boasts tin-free conditions and the use of unprotected substrates, permitted the authors to use phenylboronic acid alongside a 2,2,2-trichloroethyl-protected (TCE) sulfurylimidazolium salt **1.86** to

successfully perform sulfation in a one-pot protocol.[38] Traditionally, sulfur trioxide-amine complexes are used as sulfating reagents, but conversion and purification issues often ensue. Using the TCE-protected sulfurylimidazolium salt alleviates the traditional issues while allowing for further functionalization of the sulfated carbohydrates. Additionally, one would expect that unprotected carbohydrates would have poor solubility in organic solvents, but the presence of the cyclic boronic ester actually increases the solubility of these compounds to allow reactions to proceed smoothly in various organic solvents. In a given monosaccharide, such as methyl α-L-fucopyranoside **1.84**, the boronic ester **1.85** is formed, addition of **1.86** and 1,2-dimethylimidazole (1,2-dMeIm) yields **1.87**, and subsequent deprotection with pinacol yields monosulfated product **1.88** in 93% yield (**Scheme 1-19**).

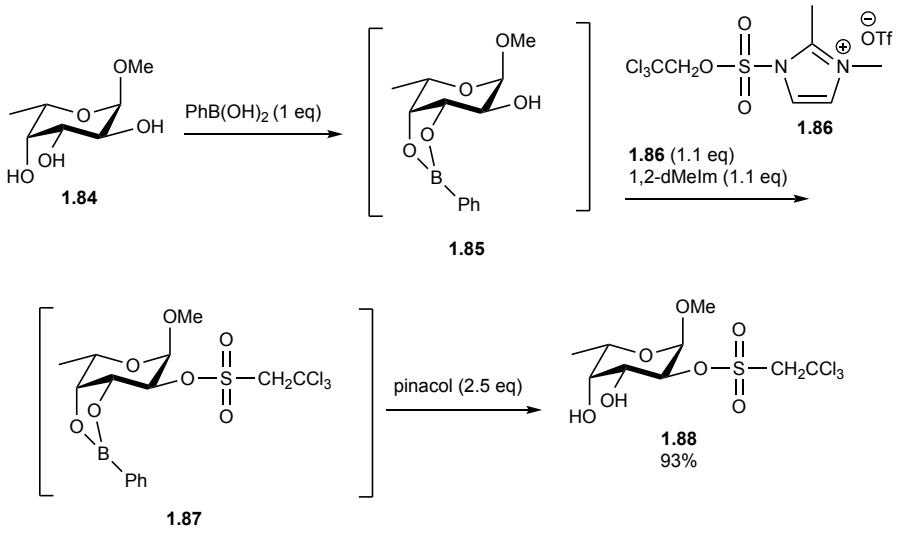

Scheme 1-19 Makino's use of boronic acid esters for site-selective sulfation

Obviously, if only one free hydroxyl group remains in a carbohydrate species, it will clearly be the site of sulfation. In the case of glucose and galactose, however, two free

hydroxyl groups remain at C2 and C3 after protection with a boronic ester. It has been observed that glucose is sulfated exclusively at the C2 hydroxyl, while galactose is sulfated at the C3 hydroxyl. The reason for this revolves around steric considerations and the necessity for adequate space around the reaction site. When two free hydroxyls remain unprotected, sulfation will preferentially occur at the equatorial hydroxyl group whose adjacent neighbor is oriented axially, which provides the increased space. Using this protocol Makino was able to site-selectively perform sulfation on a variety of unprotected monosaccharides and more complex molecules like D-trehalose. Disulfated compounds could also be obtained by simple scaling up the appropriate reagents. In the future, the authors hope to apply this methodology to the synthesis of more complicated sulfoglycolipids. However, for the time being, their sulfation method employing phenylboronic acid as a temporary protecting group is a step away from excessive manipulations in the past and a step towards a more efficient process.

As most of the previous work covered the functionalization of groups with *cis*-1,2-diols, a knowledge gap remains of how to efficiently site-selectively functionalize glucose. In an attempt to realize this need, Moitessier uses arylboronic acids in conjunction with DMAP and an acylating reagent to site-selectively functionalize methyl-α-D-glucopyranoside **1.72** and extends the method to include its galactose and mannose counterparts (**Scheme 1-20**).[39] After some extensive optimizations, experimental results showed that phenylboronic acid was the superior boronic acid. Trace amounts of water were detrimental to the reaction so the authors used a Dean-Stark apparatus to avoid moisture in the reactions. Overall, smaller electrophiles, such as acetic anhydride, led to a majority of the C3-acylated product **1.93**, while larger electrophiles, such as pivaloyl

chloride and benzoyl chloride preferentially formed the C2-acylated product **1.92**. Furthermore, the authors demonstrated the viability of this method to be successful on the gram scale while completing all of the necessary reactions in one-pot, which adds to the green and efficient nature of the method.

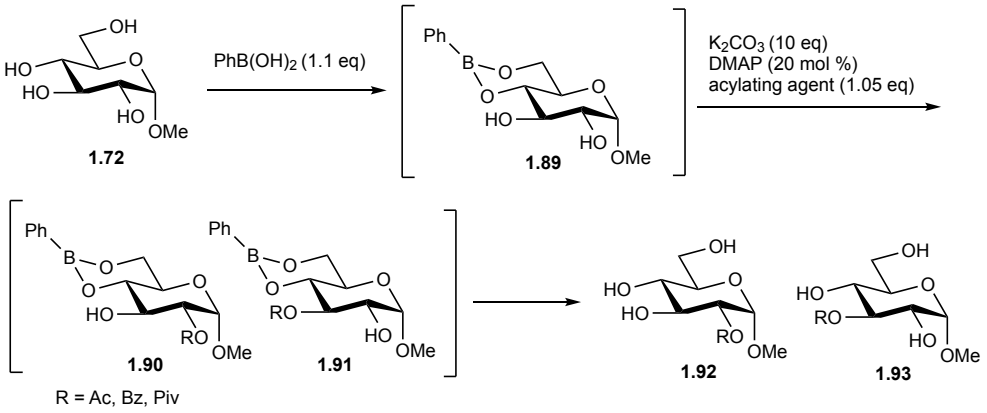

Scheme 1-20 Moitessier's use of boronic acid esters to site-selectively acylation unprotected carbohydrates

On one occasion in 2016 the O'Doherty group used a combination of boron and palladium catalysts to promote glycosylations necessary to synthesize the mezzettiasides, a family of natural products consisting of partially acetylated rhamnose monosaccharide units.[40] Prior to this study, the authors noticed that different acetylation patterns with cleistriosides and cleistetrosides significantly affected their biological activity,[41] and they decided that a natural continuation of that work was to access the mezzettiasides. As the O'Doherty group has a history using the *de novo* asymmetric approach to synthesize natural products, including those with carbohydrate motifs, they continued with the *de novo* strategy in this work while incorporating a dual B-/Pd-catalyzed glycosylation using the popular boron reagent, 2-aminoethyl diphenylborinate **1.96**, developed by Taylor.[42] After condition optimization, the authors were able to obtain

a 6:1 ratio of C3:C2 isomers in a 77% yield. O'Doherty surmises that the anionic character of the borinate complex **1.96** makes it a suitable coupling partner for the cationic Pd-π-allyl complex shown in **1.97**. Furthermore, they observed that smaller ester groups on the C4 position led to even better regioselectivity in the glycosylation.

Overall, the innovation of this dual catalysis strategy and its iterative use allowed for the first synthesis of all 10 members of the mezzettiaside family of natural products and structure-activity studies that came as a result of this synthetic strategy discovered previously unknown antibacterial activities of the mezzettiasides.[43] O'Doherty's use of chemical methods to answer biological questions is exactly the type of critical thinking needed as researchers work on more significant challenges at the chemistry-biology interface.

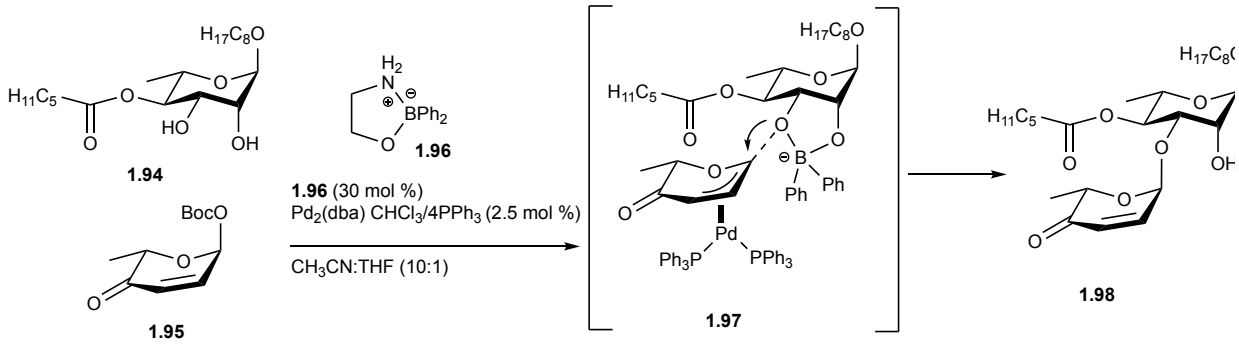

Scheme 1-21 O'Doherty use of boron and palladium catalysts to promote glycosylations necessary to synthesize the mezzettiasides

1.8 Conclusion

The highly varied structures of carbohydrates make developing universal methods for their modification a formidable challenge, and until this challenge is met, the site-selective functionalization of carbohydrates will remain an active area of research. Many

of the chemists working on the site-selective carbohydrate functionalization come from varied backgrounds far outside the carbohydrate chemistry field, and their unique experiences and skill sets will be instrumental in addressing current carbohydrate problems from different angles. Furthermore, while this chapter has focused on chemical methods utilizing organocatalysts, nature remains the ultimate synthetic chemist. Thus, enzymatic and chemoenzymatic methods constitute complementary strategies to promote site-selective transformations. While many of the modifications presented here focused on acylation or alkylation, site-selective sulfation, phosphorylation, and glycosylation will be important to address in the future as well. The subset of mammalian monosaccharides is relatively small, yet immenses challenges result when trying to modify this limited group of molecules. As the field becomes more competent in manipulating mammalian monosaccharides, scientists will likely turn an eye towards the synthesis and funtionalization of bacterial and/or rare sugars. With hundreds of monosaccharides comprising these groups, the need for site-selective methods will continue and be greater than ever.

1.9 References

1. Wang, H. Y.; Blaszczyk, S. A.; Xiao, G.; Tang, W., Chiral reagents in glycosylation and modification of carbohydrates. *Chem. Soc. Rev.* **2018,** *47* (3), 681-701.

2. Seeberger, P. H.; Werz, D. B., Automated synthesis of oligosaccharides as a basis for drug discovery. *Nat. Rev. Drug Discov.* **2005,** *4* (9), 751-63.

3. Hsu, C. H.; Hung, S. C.; Wu, C. Y.; Wong, C. H., Toward automated oligosaccharide synthesis. *Angew. Chem. Int. Ed.* **2011,** *50* (50), 11872-923.

4. Panza, M.; Pistorio, S. G.; Stine, K. J.; Demchenko, A. V., Automated chemical oligosaccharide synthesis: Novel approach to traditional challenges. *Chem. Rev.* **2018,** *118* (17), 8105-8150.

5. Seeberger, P. H., Automated oligosaccharide synthesis. *Chem. Soc. Rev.* **2008,** *37* (1), 19-28.

6. Wen, L.; Edmunds, G.; Gibbons, C.; Zhang, J.; Gadi, M. R.; Zhu, H.; Fang, J.; Liu, X.; Kong, Y.; Wang, P. G., Toward automated enzymatic synthesis of oligosaccharides. *Chem. Rev.* **2018,** *118* (17), 8151-8187.

7. Lawandi, J.; Rocheleau, S.; Moitessier, N., Regioselective acylation, alkylation, silylation and glycosylation of monosaccharides. *Tetrahedron* **2016,** *72* (41), 6283-6319.

8. Taylor, M. S., Catalyst-controlled, regioselective reactions of carbohydrate derivatives. *Top. Curr. Chem.* **2016,** *372*, 125-55.

9. Williams, R.; Galan, M. C., Recent advances in organocatalytic glycosylations. *Eur. J. Org. Chem.* **2017,** *2017* (42), 6247-6264.

10. Song, W.; Zheng, N., Chiral catalyst-directed site-selective functionalization of hydroxyl groups in carbohydrates. *J. Carbohydr. Chem.* **2017,** *36* (4-6), 143-161.

11. Baba, A.; Yoshioka, T., Complementary and synergistic roles in enzyme-catalyzed regioselective and complete hydrolytic deprotection of o-acetylated beta-d-glucopyranosides of n-arylacetohydroxamic acids. *J. Org. Chem.* **2012,** *77* (4), 1675-84.

12. Gridley, J. J.; Hacking, A. J.; Osborn, H. M. I.; Spackman, D. G., Regioselective lipase-catalysed acylation of 4,6-o-benzylidene-α- and-β-d-pyranoside derivatives displaying a range of anomeric substituents. *Tetrahedron* **1998,** *54*, 14925-14946.

13. Mastihubova, M.; Mastihuba, V., Donor specificity and regioselectivity in lipolase mediated acylations of methyl alpha-d-glucopyranoside by vinyl esters of phenolic acids and their analogues. *Bioorg. Med. Chem. Lett.* **2013,** *23* (19), 5389-92.

14. Ren, B.; Gan, L.; Zhang, L.; Yan, N.; Dong, H., Diisopropylethylamine-triggered, highly efficient, self-catalyzed regioselective acylation of carbohydrates and diols. *Org. Biomol. Chem.* **2018,** *16* (31), 5591-5597.

15. Li, T.; Li, T.; Cui, T.; Sun, Y.; Wang, F.; Cao, H.; Schmidt, R. R.; Peng, P., Regioselective one-pot benzoylation of triol and tetraol arrays in carbohydrates. *Org. Lett.* **2018,** *20* (13), 3862-3865.

16. Birman, V. B.; Li, X., Benzotetramisole- a remarkably enantioselective acyl transfer catalyst. *Org. Lett.* **2006,** *8*, 1351-1354.

17. Birman, V. B.; Uffman, E. W.; Jiang, H.; Li, X.; Kilbane, C. J., 2,3-dihydroimidazo[1,2-a]pyridines- a new class of enantioselective acyl transfer catalysts and their use in kinetic resolution of alcohols. *J. Am. Chem. Soc.* **2004,** *126*, 12226-12227.

18. Xiao, G.; Cintron-Rosado, G. A.; Glazier, D. A.; Xi, B. M.; Liu, C.; Liu, P.; Tang, W., Catalytic site-selective acylation of carbohydrates directed by cation-n interaction. *J. Am. Chem. Soc.* **2017,** *139* (12), 4346-4349.

19. Yanagi, M.; Imayoshi, A.; Ueda, Y.; Furuta, T.; Kawabata, T., Carboxylate anions accelerate pyrrolidinopyridine (ppy)-catalyzed acylation: Catalytic site-selective acylation of a carbohydrate by in situ counteranion exchange. *Org. Lett.* **2017,** *19* (12), 3099-3102.

20. Kawabata, T.; Muramatsu, W.; Nishio, T.; Shibata, T.; Schedel, H., A catalytic one-step process for the chemo- and regioselective acylation of monosaccharides. *J. Am. Chem. Soc.* **2007,** *129*, 12890-12895.

21. Giuliano, M. W.; Miller, S. J., Site-selective reactions with peptide-based catalysts. *Top. Curr. Chem.* **2016,** *372*, 157-201.

22. Huber, F.; Kirsch, S. F., Site-selective acylations with tailor-made catalysts. *Chem. Eur. J.* **2016,** *22* (17), 5914-8.

23. Tong, M. L.; Huber, F.; Taghuo Kaptouom, E. S.; Cellnik, T.; Kirsch, S. F., Enhanced site-selectivity in acylation reactions with substrate-optimized catalysts on solid supports. *Chem. Commun.* **2017,** *53* (21), 3086-3089.

24. Welton, T., Ionic liquids: A brief history. *Biophys. Rev.* **2018,** *10* (3), 691-706.

25. Axelsson, A.; Ta, L.; Sundén, H., Direct highly regioselective functionalization of carbohydrates: A three-component reaction combining the dissolving and catalytic efficiency of ionic liquids. *Eur. J. Org. Chem.* **2016,** *2016* (20), 3339-3343.

26. Cramer, D. L.; Bera, S.; Studer, A., Exploring cooperative effects in oxidative nhc catalysis: Regioselective acylation of carbohydrates. *Chemistry* **2016,** *22* (22), 7403-7.

27. Samanta, R. C.; De Sarkar, S.; Fröhlich, R.; Grimme, S.; Studer, A., N-heterocyclic carbene (nhc) catalyzed chemoselective acylation of alcohols in the presence of amines with various acylating reagents. *Chem. Sci.* **2013,** *4* (5).

28. Sarkar, S. D.; Grimme, S.; Studer, A., Nhc catalyzed oxidations of aldehydes to esters- chemoselective acylation of alcohols in presence of amines. *J. Am. Chem. Soc.* **2010,** *132*, 1190-1191.

29. Cox, D. J.; Smith, M. D.; Fairbanks, A. J., Glycosylation catalyzed by a chiral brønsted acid. *Org. Lett.* **2010,** *12* (7), 1452-1455.

30. Liu, D.; Sarrafpour, S.; Guo, W.; Goulart, B.; Bennett, C. S., Matched/mismatched interactions in chiral brønsted acid-catalyzed glycosylation reactions with 2-deoxy-sugar trichloroacetimidate donors. *J. Carbohydr. Chem.* **2014,** *33* (7-8), 423-434.

31. Tay, J. H.; Arguelles, A. J.; DeMars, M. D., 2nd; Zimmerman, P. M.; Sherman, D. H.; Nagorny, P., Regiodivergent glycosylations of 6-deoxy-erythronolide b and oleandomycin-derived macrolactones enabled by chiral acid catalysis. *J. Am. Chem. Soc.* **2017,** *139* (25), 8570-8578.

32. Palo-Nieto, C.; Sau, A.; Williams, R.; Galan, M. C., Cooperative bronsted acid-type organocatalysis for the stereoselective synthesis of deoxyglycosides. *J. Org. Chem.* **2017,** *82* (1), 407-414.

33. Balmond, E. I.; Coe, D. M.; Galan, M. C.; McGarrigle, E. M., Alpha-selective organocatalytic synthesis of 2-deoxygalactosides. *Angew. Chem. Int. Ed.* **2012,** *51* (36), 9152-5.

34. Taylor, M. S., Catalysis based on reversible covalent interactions of organoboron compounds. *Acc. Chem. Res.* **2015,** *48* (2), 295-305.

35. Mancini, R. S.; Lee, J. B.; Taylor, M. S., Boronic esters as protective groups in carbohydrate chemistry: Processes for acylation, silylation and alkylation of glycoside-derived boronates. *Org. Biomol. Chem.* **2016,** *15* (1), 132-143.

36. Mothana, S.; Grassot, J. M.; Hall, D. G., Multistep phase-switch synthesis by using liquid-liquid partitioning of boronic acids: Productive tags with an expanded repertoire of compatible reactions. *Angew. Chem. Int. Ed.* **2010,** *49* (16), 2883-7.

37. Dimakos, V.; Garrett, G. E.; Taylor, M. S., Site-selective, copper-mediated o-arylation of carbohydrate derivatives. *J. Am. Chem. Soc.* **2017,** *139* (43), 15515-15521.

38. Fukuhara, K.; Shimada, N.; Nishino, T.; Kaji, E.; Makino, K., Regioselective, tin-free sulfation of unprotected hexopyranosides by using phenylboronic acid. *Eur. J. Org. Chem.* **2016,** *2016* (5), 902-905.

39. Rocheleau, S.; Pottel, J.; Huskić, I.; Moitessier, N., Highly regioselective monoacylation of unprotected glucopyranoside using transient directing-protecting groups. *Eur. J. Org. Chem.* **2017,** *2017* (3), 646-656.

40. Bajaj, S. O.; Sharif, E. U.; Akhmedov, N. G.; O'Doherty, G. A., De novo asymmetric synthesis of the mezzettiaside family of natural products via the iterative use of a dual b-/pd-catalyzed glycosylation. *Chem. Sci.* **2014,** *5* (6), 2230-2234.

41. Wu, B.; Li, M.; O'Doherty, G. A., Synthesis of several cleistriosides and cleistetrosides natural products via a divergent de novo asymmetric approach. *Org. Lett.* **2010,** *12* (23), 5466-5469.

42. Lee, D.; Taylor, M. S., Borinic acid-catalyzed regioselective acylation of carbohydrate derivatives. *J. Am. Chem. Soc.* **2011,** *133* (11), 3724-7.

43. Bajaj, S. O.; Shi, P.; Beuning, P. J.; O'Doherty, G. A., Structure activity relationship study of mezzettiasides natural products and their four new disaccharide analogues for anticancer/antibacterial activity. *Medchemcomm* **2014,** *5* (8), 1138-1142.

Chapter 2

Stereo- and Site-Selective Acylation in Carbohydrate Synthesis

2.1 Abstract

The prevalent roles of carbohydrates in physiological and pathological processes have necessitated that chemists investigate and expedite their chemical synthesis so that glycobiologists can better elucidate carbohydrate function. Two major knowledge gaps in carbohydrate chemistry are site-selective functionalization and stereoselective functionalization of the anomeric hydroxyl group. This chapter will detail how the Tang group has developed stereo- and site-selective acylation methods to improve the stereoselectivity and efficiency for the synthesis of complex carbohydrates. We have used both transition-metal catalysts and chiral organocatalysts to control the traditionally challenging stereoselective transformations, finding chiral benzotetramisole (BTM) organocatalysts particularly useful. The utility of BTM catalysts was further extended from stereoselective acylation of the anomeric hydroxyl group to site-selective acylation of carbohydrate hydroxyl groups. Recently, we also employed isoquinolinic and picolinic esters for the preparation of glycosides and glycosyl halides under mild conditions. We hope these methods will allow glycobiologists to better understand the roles of carbohydrates in human health and diseases, and we challenge current members of the field to be creative and think outside of their wheelhouse to address the two problems that consistently plague carbohydrate chemists – site-selective functionalization and stereoselective glycosylation.

2.2 Introduction

The prevalent roles of carbohydrates in physiological and pathological processes have necessitated that chemists investigate and expedite their chemical synthesis so that glycobiologists can better elucidate carbohydrate function.[1-3] However, compared to other classes of biopolymers, carbohydrates pose significantly more synthetic burdens than their protein and nucleic acid counterparts, which are produced through templated biosynthetic pathways or automated chemical synthesis platforms. One of the major issues associated with carbohydrate synthesis is the fact that each carbohydrate building block is usually a densely functionalized molecule bearing multiple hydroxyl groups. These hydroxyls have similar reactivities so modifying one hydroxyl while leaving the others unchanged is difficult – a process known as site-selective functionalization. In fact, site-selective functionalization has been termed a "Holy Grail" in chemistry.[4-6] Another significant knowledge gap in carbohydrate chemistry is a general and efficient method for stereoselective functionalization of the anomeric hydroxyl group.

This chapter will detail how we in the Tang group have developed stereo- and site-selective acylation methods to improve the stereoselectivity and efficiency for the synthesis of complex carbohydrates. To expedite the synthesis of rare sugars and carbohydrate analogs, we have frequently drawn upon the Achmatowicz rearrangement[7] to form dihydropyranone intermediates. Our group took advantage of the equilibrium between two lactol stereoisomers to preferentially acylate one stereoisomer via a dynamic kinetic process. We have used both transition-metal catalysts and chiral organocatalysts to control the traditionally challenging stereoselective transformations, finding chiral benzotetramisole (BTM) organocatalysts particularly useful. The utility of BTM catalysts

was further extended from stereoselective acylation of the anomeric hydroxyl group to the site-selective acylation of carbohydrate hydroxyl groups. Recently, we also employed isoquinolinic and picolinic esters for the preparation of glycosides and glycosyl halides under mild conditions. An overview of the reactions covered in this review can be found in **Scheme 2-1**. We hope the reader will enjoy the story behind how our lab used the seemingly simple acylation reaction to solve some of the challenging problems in carbohydrate chemistry, and we hope other researchers will employ these methods to continue making advances in glycoscience.

2.3 Dynamic kinetic transformations mediated by transition metal catalysts prompt our carbohydrate research

The first work that we will delve into is our stereoselective iridium-catalyzed dynamic kinetic internal transfer hydrogenation.[8] In 2015 we reported this research, which was one of our initial publications in the area of carbohydrate chemistry, and believe it or not, these findings were actually serendipitous. While trying to develop stereoselective allylic alkylation reactions using allylic alcohol **2-2** as the substrate and different nucleophiles, we noticed an unexpected spot on the TLC plate. Rather than ignoring this

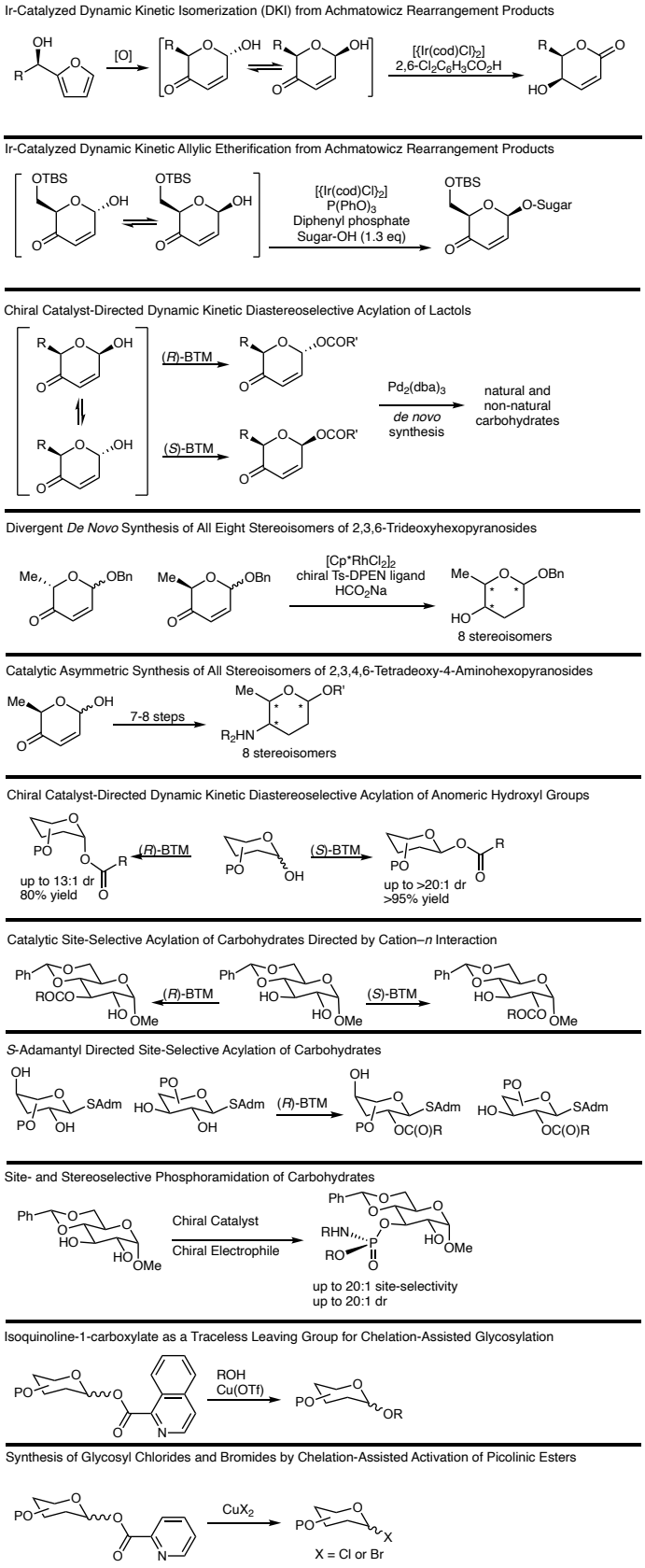

Scheme 2-1 Summary of the reactions covered in this chapter

by-product and moving forward, we purified the reaction mixture and isolated this unexpected spot. We later determined that the spot corresponded to an isomerization product that occurred when trying to optimize the originally studied allylic alkylation reaction. We found this isomerization process interesting because we started with a 3:1 ratio of ***cis*-2-2**:***trans*-2-2**, but after optimization we were able to boost that ratio to favor the *cis* isomer by >20:1.

Our investigation into the isomerization pathway began with the preparation of starting material **2-1** by an asymmetric reduction of 2-acylfuran and subsequent Achmatowicz rearrangement of alcohol **2-1** to form dihydropyranones **2-2**, which existed as a mixture of epimers. These dihydropyranones could then undergo internal redox isomerizations and result in the stereoselective synthesis of lactone **2-3**, the *cis* isomer, as the major product (**Scheme 2-2**).

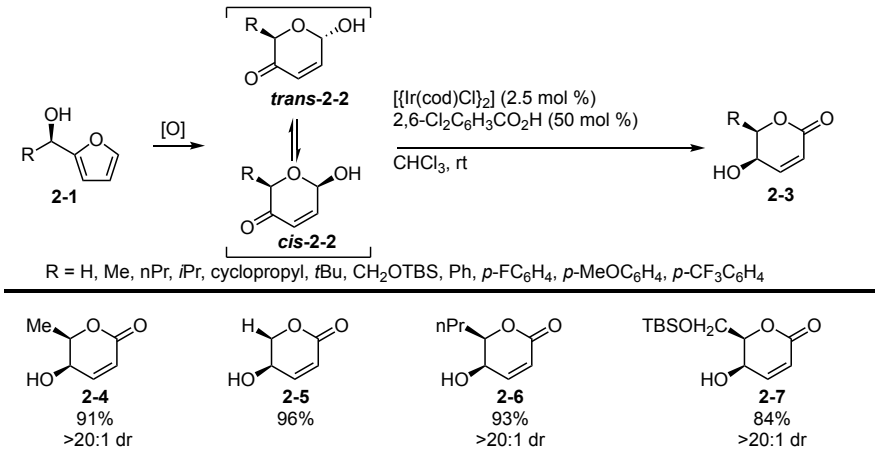

Scheme 2-2 Overview of the iridium(I)-catalyzed dynamic kinetic stereoselective isomerization (top) and partial substrate scope (bottom)

Though we knew an isomerization occurred from **2-2** to **2-3**, we still had to optimize the reaction. After screening various transition metal catalysts, we observed that only

iridium-based catalysts provided the desired product. Further optimization prompted some interesting insights. When we subjected a 3:1 ratio of ***cis*-2-2:*trans*-2-2,** where R = Me, to the reaction with only the iridium catalyst, we obtained **2-4** but only in a 3:1 ratio favoring the *cis* product. This result suggested that the metal catalyst plays no role in the equilibration between the dihydropyranones. However, as we screened various Brønsted acids in an attempt to accelerate the rate of equilibration between ***cis*-2-2** and ***trans*-2-2**, we noticed the diastereoselectivity of the products began to more heavily favor the *cis* product. In the end, we found that using 2,6-dichlorobenzoic acid as a co-catalyst provided the *cis* isomer in a >20:1 ratio. As we move forward in this review, we will see how a carboxylic acid additive biases the reaction to improve the diastereoselectivity.

The isomerization from **2-2** to **2-3** worked well when R = various alkyl and silyl ether groups. Aryl groups also worked regardless of the presence of electron-donating or electron-withdrawing substituents. When a *gem*-dimethyl group, as seen in **2-9**, was used in the isomerization reaction, the product **2-10** can undergo methylation, reduction, and dihydroxylation to complete the *de novo* formal synthesis of the carbohydrate noviose (**Scheme 2-3**).[9]

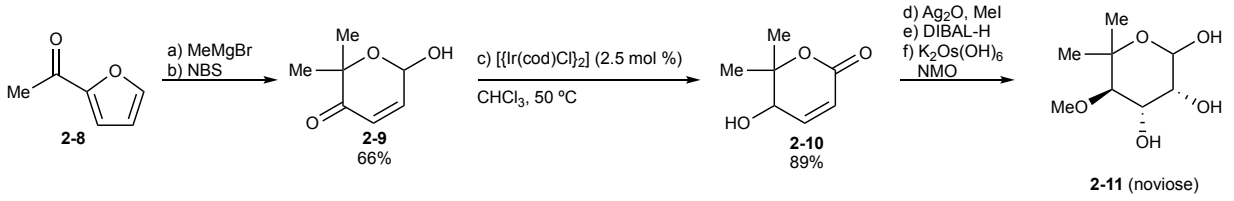

Scheme 2-3 Formal synthesis of the carbohydrate noviose

As an added advantage, the stereochemical configuration maintained high fidelity through the isomerization even in gram scale reactions (**2-14**, 0.95 g, 98% ee). Using **2-14** as a key intermediate, this method yielded L-rhodinose and allowed for the formal synthesis

of numerous deoxy sugars (**Scheme 2-4**), of which intermediates **2-14** and **2-16** have been converted into amino sugar derivatives.[10] Other groups have used this isomerization reaction to complete the total synthesis of the natural product angiopteralactone B,[11] (+)/(-)-*cis*-osmundalactone,[12] and phosdiecin A.[13]

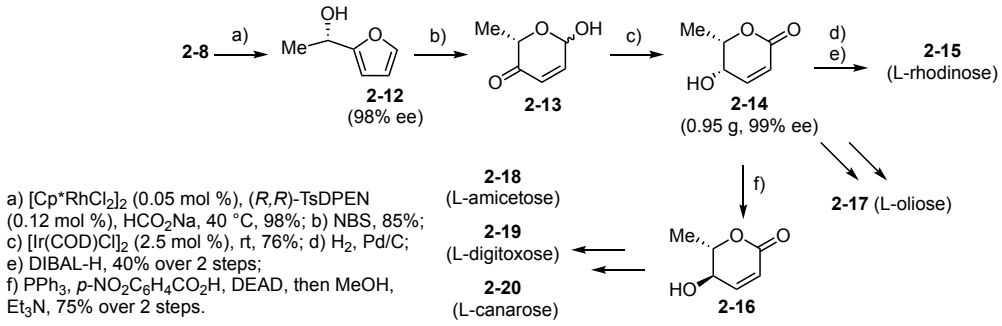

Scheme 2-4 Formal synthesis of deoxy sugars using the iridium-catalyzed isomerization to obtain necessary intermediates

When we originally started the iridium-catalyzed work, we were devising efficient methods to access allylic alkylation products directly from allylic alcohols derived from Achmatowicz rearrangement and different nucleophiles. We did not try any alcohol nucleophiles because we thought it would be difficult to differentiate the allylic alcohol substrate, which itself is also an alcohol, and the external alcohol nucleophile. We previously discussed the detour of finding and publishing the isomerization reaction, which was performed best using chloroform as the solvent. The commercially available chloroform is stabilized by either amylene or ethanol. When we accidentally used chloroform stabilized by ethanol, we obtained a mixture of isomerization product and allylic etherification product derived from nucleophilic attack of ethanol to the metal-π-allyl. We subsequently began investigating the allylic etherification reaction using different

alcohols as the nucleophiles and chloroform stabilized by amylene. However, isomerization was the dominant pathway under most conditions. Finally in 2017, we reported that the addition of a triphenyl phosphite ligand can suppress the isomerization pathway and promote the allylic etherification pathway (**Scheme 2-5**).[14]

In optimizing the allylic etherification reaction, we started with a 3:1 ratio of ***cis*-2-21**:***trans*-2-21** and used benzyl alcohol as the nucleophile to obtain the desired product **2-22** (**Scheme 2-5**, top). We found that phosphine ligands resulted in no reaction, but phosphite ligands suppressed the isomerization reaction we previously reported, with triphenyl phosphite being superior. We also knew from our previous work that Brønsted acids could influence the degree of diastereoselectivity. After screening different Brønsted acid additives, we determined that diphenyl phosphate provided the best dr (10:1 for ***cis*-2-22**/***trans*-2-22**).

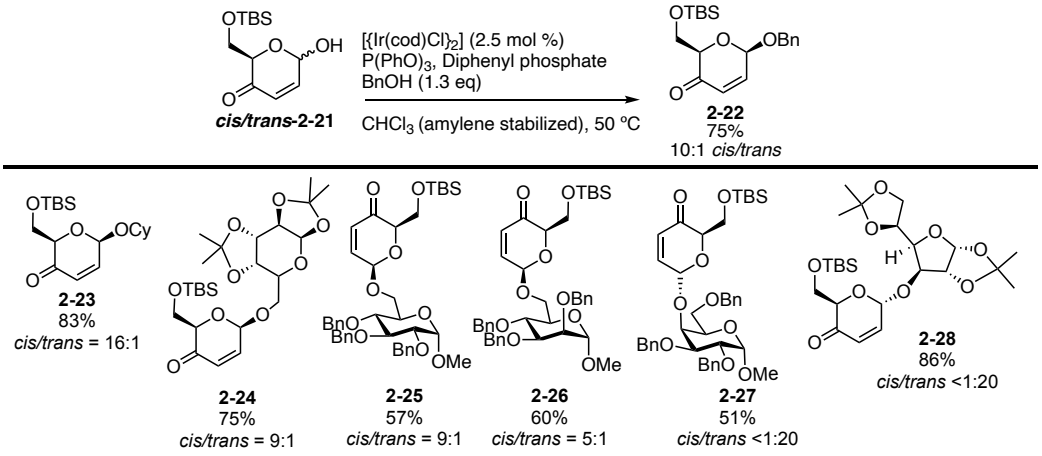

Scheme 2-5 Optimized conditions (top) and selected products (bottom) for the iridium-catalyzed dynamic kinetic stereoselective allylic etherification

It's interesting to note just how much the acid additive and solvent choice can affect the iridium-catalyzed isomerization and allylic etherification. With the isomerization, 2,6-dichorobenzoic acid was the best for maximizing the yield and diastereoselectivity, but in

the allylic etherification, the same acid additive resulted in no reaction or a poor yield (41%).

Furthermore, even though diphenyl phosphate was sufficient for maximizing the diastereoselectivity in the etherification reaction, solvent choice could negate any gains made by the addition of the appropriate acid. For example, using triphenyl phosphite and diphenyl phosphate gave a 10:1 dr favoring ***cis*-2-22** over ***trans*-2-22** using chloroform, but no diastereoselectivity resulted when the same reaction was run in dichloromethane.

Following optimization, we explored the scope of the reaction, which was tolerant of primary alcohols, secondary alcohols, and even tertiary alcohols (**Scheme 2-5**, bottom). Glycosyl acceptors with primary and secondary hydroxyls were also successful in this reaction. Sterically less encumbered acceptors tended to promote the formation of the *cis*-isomers or β-anomers as the major product, and sterically bulky acceptors tended to promote the formation of the *trans*-isomers or α-anomers as the major product.

Because the same starting materials were used for the iridium-catalyzed dynamic kinetic isomerization and allylic etherification,[8] the proposed mechanisms for both are shown in **Scheme 2-6**. In both cases, there's a rapid acid-catalyzed epimerization of the hemiacetals ***cis*-2-2** and ***trans*-2-2** where the equilibrium favors ***cis*-2-2**. For the isomerization we propose that the dehydrogenation of ***cis*-2-2** and ***trans*-2-2** forms iridium-hydride species **2-29** and **2-30**. The stereoselective iridium-catalyzed transfer hydrogenation then leads to **2-3** and **2-31**. When an acid co-catalyst is absent from the reaction, the product ratio of **2-3**: **2-31** is approximately 3:1, which is similar to the ratio of ***cis*-2-2** and ***trans*-2-2** at equilibrium. This observation suggests that when an acid is

absent, the rate of internal transfer hydrogenation is faster than the equilibration of the two hemiacetals.

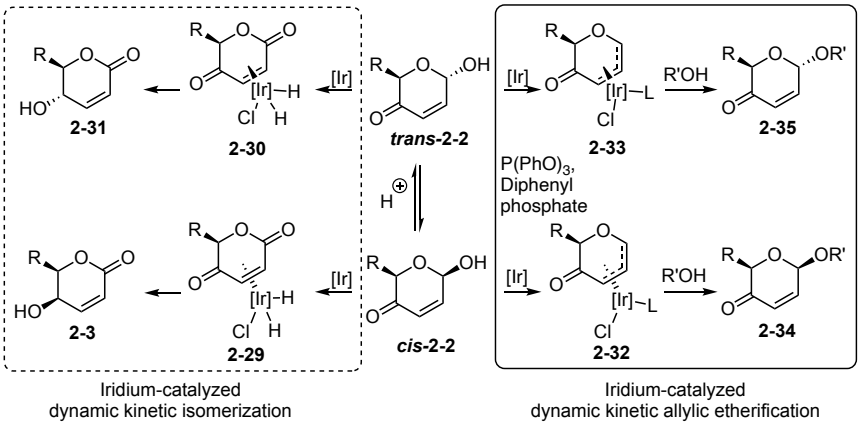

Scheme 2-6 Proposed mechanism for the iridium-catalyzed dynamic kinetic isomerization (dotted lines) and the iridium-catalyzed dynamic kinetic stereoselective allylic etherification (solid line)

To avoid the formation of **2-29** and **2-30**, triphenyl phosphite was added to promote formation of the iridium-π-allyl species **2-32** and **2-33**. When sterically unencumbered nucleophiles are used, the iridium complex will approach the alkene from the side opposite to the R group to minimize steric interactions. This leads to intermediate **2-32** and results in product **2-34**. However, when sterically demanding nucleophiles are present, the reaction proceeds through intermediate **2-33** to avoid steric interactions between the alcohol nucleophile and the R-group. This results in product **2-35**, which has opposite diastereoselectivity compared to **2-34**. These trends can be seen when observing the product distribution ratios for the various nucleophiles in the bottom of Scheme 5.

2.4 Continuation of the dynamic kinetic transformations using chiral organocatalysts for carbohydrate synthesis

Although our iridium-catalyzed dynamic allylic etherification provides the glycosylation products directly from allylic alcohol **2-21**, it should be noted that the glycosyl donor was mostly limited to substrates with the -OTBS protecting group at the C6 position and the diastereoselectivity often varies depending on the glycosyl acceptor. The O'Doherty group has used a wide range of glycosyl donors and glycosyl acceptors for the palladium-catalyzed stereospecific glycosylation reactions,[15, 16] but the issue of developing efficient and diastereoselective methods to prepare allylic carbonates or allylic esters from the allylic alcohol remains. Building upon our previous success using dynamic kinetic stereoselective transformations with lactols, we speculated that we could use chiral organocatalysts to improve the diastereoselectivity for the formation of anomeric esters, which has been a significant bottleneck in *de novo* carbohydrate synthesis. We envisioned that we could improve the diastereoselectivity of anomeric acylation of ***cis*-2-2** and ***trans*-2-2** by either reinforcing or overriding the intrinsic diastereoselectivity through a chiral catalyst-directed dynamic kinetic diastereoselective acylation (DKDA), shown in **Scheme 2-7**.[17]

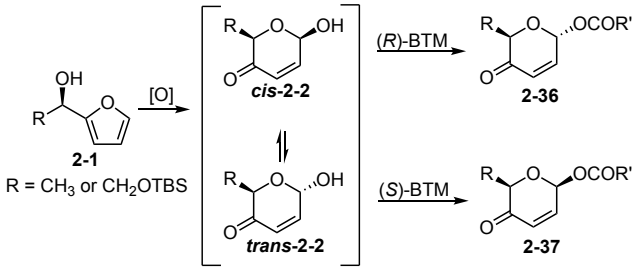

Scheme 2-7 Overview of the dynamic kinetic diastereoselective acylation (DKDA) of lactols

Our initial condition optimization used chiral lactol **2-13**, prepared enantioselectively in two steps, and commercially available chiral organocatalyst (*S*)-levamisole **2-38**.We screened various anhydrides and were pleased to see that the acetic anhydride led to **2-39** in quantitative yield with a diastereomeric ratio of 8:1 favoring the *trans* isomer. Furthermore, more hindered anhydrides increased this ratio, an observation which paralleled those of Birman.[18, 19] Using isobutyric anhydride, we were able to obtain **2-40** in great yield with 15:1 dr, also favoring the *trans* isomer (**Scheme 2-8**). Unfortunately, only (*S*)-levamisole is commercially available, and the synthesis of (*R*)-levamisole is not trivial.

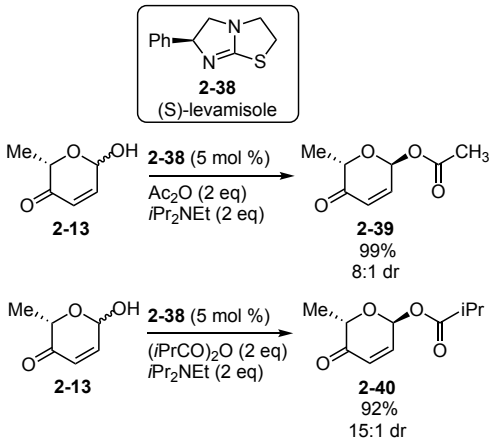

Scheme 2-8 Screening of anhydrides for the DKDA of lactols using (*S*)-levamisole

Inspired by Birman's use of BTM catalysts[18, 19] **2-41** and **2-42**, of which both enantiomers are commercially available, and Shiina's mixed anhydride method,[20-22] we decided to investigate the feasibility of acylating **2-43** with BTM catalysts, pivalic anhydride, and a readily available carboxylic acid to obtain the desired product in both matched and mismatched scenarios (**Scheme 2-9**). Using the BTM catalysts and the

mixed anhydride method, we were able to improve the diastereoselectivity of the both matched and mismatched reactions.

We were then able to use **2-44** and **2-45** in a palladium-catalyzed glycosidation to synthesize the corresponding benzyl ethers **2-46** and **2-47**. This two-step strategy of using DKDA developed by us and Pd-catalyzed glycosidation pioneered by O'Doherty[23] afforded us complete stereochemical control of the anomeric position and allowed us to easily achieve a starting point for the *de novo* synthesis of many natural and non-natural carbohydrates. Later in the review, we will demonstrate how the diastereoselective acylation of lactols guided our way further into synthetic methodology development for carbohydrate synthesis. Our lactol acylation work was published concurrently with a research group from Bristol-Myers Squibb (BMS) who reported a similar transformation using **2-38**.[24]

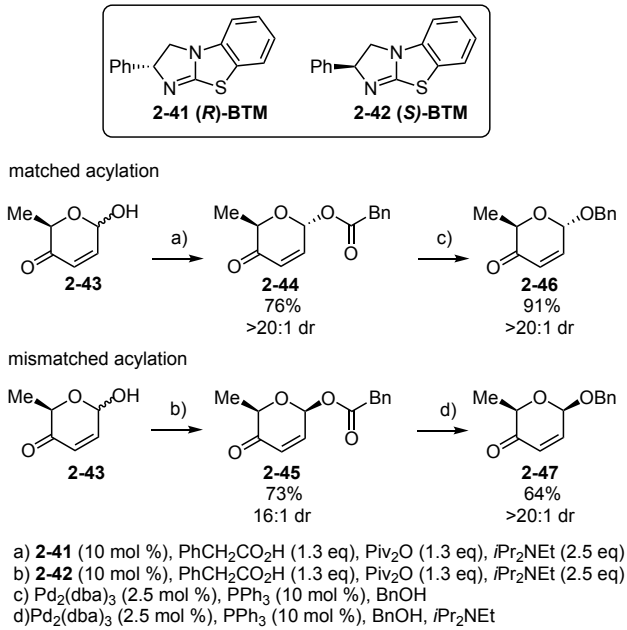

Scheme 2-9 Results of using Birman's benzotetramisole catalysts and Shiino's mixed anhydride method for the DKDA of lactols and results from palladium-catalyzed glycosidation

Since the early days of Emil Fisher, synthetic chemists have lacked a systematic way to access all stereoisomers of particular monosaccharides, and this knowledge gap still remains. However, continuing with our use of reagent control, we exploited a chiral catalyst-based divergent strategy to access all eight stereoisomers of 2,3,6-trideoxyhexopyranosides, which includes the rhodinopyranosides and amicetopyranosides.[25]

From work already presented in this review, we've repeatedly used the Achmatowicz rearrangement to convert inexpensive feedstock furan **2-8** to valuable dihydropyranone intermediates **2-13**, and we've also taken advantage of O'Doherty's palladium-catalyzed glycosidation to prepare anomeric ethers **2-48** and **2-49** through Pd-π-allyl intermediates (**Scheme 2-10**). We will discuss the details for the formation of the carbonate or ester intermediates from key intermediate **2-13** later to have a better comparison.

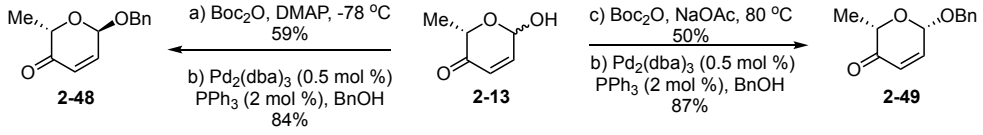

Scheme 2-10 Preparation of key intermediates **2-48** and **2-49** for the synthesis of all eight stereoisomers of 2,3,6-trideoxyhexopyranosides

In 2015, as we were thinking about ways to access the 2,3,6-trideoxyhexopyranoside stereoisomers, our literature review indicated that there was no known way to go directly from **2-48**/**2-49** to **2-53** - **52-6** (**Scheme 2-11**). We hypothesized that we could complete a chiral catalyst-controlled tandem reduction to obtain the eight 2,3,6-trideoxyhexopyranoside stereoisomers. Because the reduction of **2-48** and **2-49** with an achiral Ts-ethylenediamine ligand **2-50** showed low intrinsic diastereoselectivity,

we were further convinced that a chiral catalyst strategy with chiral ligands **2-51** and **2-52** could be successful.

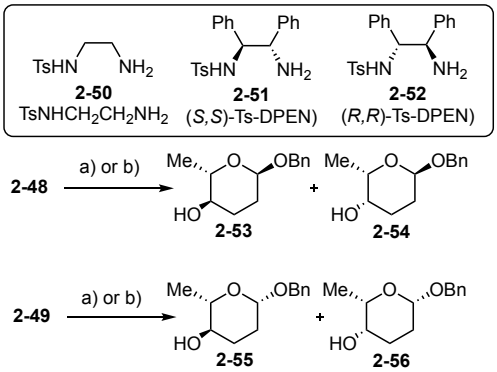

a) Low intrinsic diastereoselectivity with achiral ligand **50**; $[Cp^*RhCl_2]_2$ (0.5 mol %), $TsNHCH_2CH_2NH_2$ **2-50** (1.2 mol %), HCO_2Na, 40 °C
b) Complete stereoselectivity with chiral ligands **2-51** or **2-52**; $[Cp^*RhCl_2]_2$ (0.5 mol %), **2-51** or **2-52** (1.2 mol %), HCO_2Na, 40 °C

Scheme 2-11 Preparation of four 2,3,6-trideoxyhexopyranoside stereoisomers. When achiral ligand **2-50** was used, low intrinsic diastereoselectivity was observed. When chiral ligand **2-51** or **2-52** was used (depending on the desired product), complete stereoselectivity was observed.

We were pleased that our hypothesis was correct. Depending on the choice of substrate (**2-48**, **2-49, 2-57**, **2-58**) and chiral ligand (**2-51**, **2-52**), we were able to use rhodium-catalysis to obtain eight single stereoisomers (**Scheme 2-12**). In each case, hydroxyl groups with (*S*) configurations resulted from using the (*S*,*S*)-Ts-DPEN ligand, and hydroxyl groups with (*R*) configurations resulted from using the (*R*,*R*)-Ts-DPEN ligand. This work demonstrated that the absolute or relative stereochemistry of the enone starting materials (**2-48**, **2-49, 2-57**, **2-58**) had no effect on the stereochemistry of the final product.

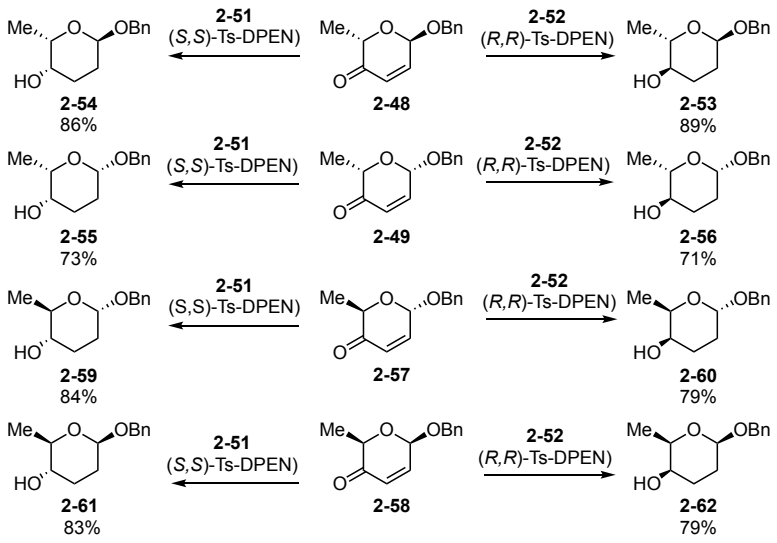

Scheme 2-12 Divergent *de novo* synthesis of all eight stereoisomers of 2,3,6-trideoxyhexopyranosides using a chiral catalyst-controlled reduction. Conditions: $[Cp^*RhCl_2]_2$ (0.5 mol %), ligand **51** / **52** (1.2 mol %), HCO_2Na, 40 °C

Mechanistic studies using the standard reaction conditions except a reduced amount of sodium formate resulted in 50% of unreacted starting material **2-49**, 40% of alcohol **52-5**, and 10% of ketone **2-63**, based on NMR analysis of the crude product mixture (**Scheme 2-13**). Considering no allylic alcohol **2-64** was observed, this suggests that the 1,4-reduction of enone starting material **2-49** is significantly faster than the 1,2-reduction of **2-49**.

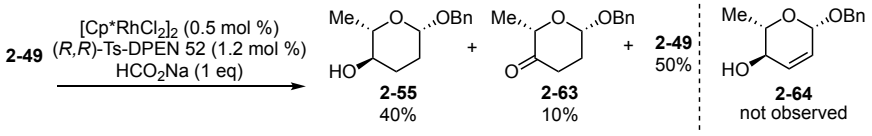

Scheme 2-13 Product distribution resulting from the reduction of enone **2-49** as a way to investigate the mechanism of the chiral catalyst-controlled reduction

Using a sequence of palladium-catalyzed glycosidation and a divergent chiral catalyst-controlled reduction, we synthesized all eight stereoisomers of the 2,3,6-

trideoxyhexopyranosides. We also demonstrated the utility of this method by synthesizing both isomers of narbosine B **2-65** and **2-66** while also making tetrasaccharide **2-67** (**Scheme 2-14**).

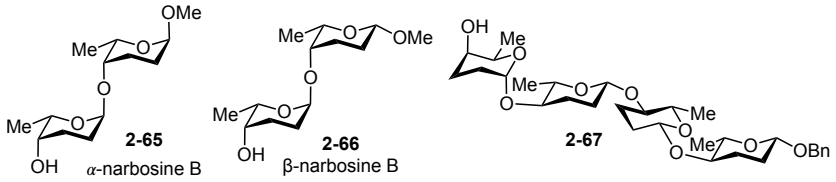

Scheme 2-14 Selected bioactive natural products and saccharides made using a Pd-catalyzed glycosidation and divergent chiral catalyst-directed tandem reduction

While our previous divergent synthesis was useful, we published an update to this method in 2018.[26] The products in **Scheme 2-12** originally proceeded through carbonate intermediates **2-68** and **2-69**, which suffered from poor stereoselectivity (no greater than roughly 3:1) in the transformation from **2-13** (**Scheme 2-15**). We thought our previously published dynamic kinetic stereoselective acylation of lactols using chiral benzotetramisole catalysts[17] could be used instead to prepare **2-53** - **2-56** and their respective enantiomers. But in this case, the desired products would go through a completely stereoselective acylation to yield intermediates **2-71** and **2-72** and their enantiomers using benzotetramisole catalysts. Using the new method shown in the bottom of Scheme 15, we were able to access the enone starting materials **2-48**, **2-49**, **2-57**, and **2-58** needed to access all of the 2,3,6-trideoxyhexopyranosides stereoisomers shown in **Scheme 2-12**.

With a more efficient synthesis in hand for the production of 2,3,6-trideoxyhexopyranosides, we looked to produce their corresponding deoxyamino sugars. through a Mitsunibu reaction to introduce the azido group and a subsequent reduction

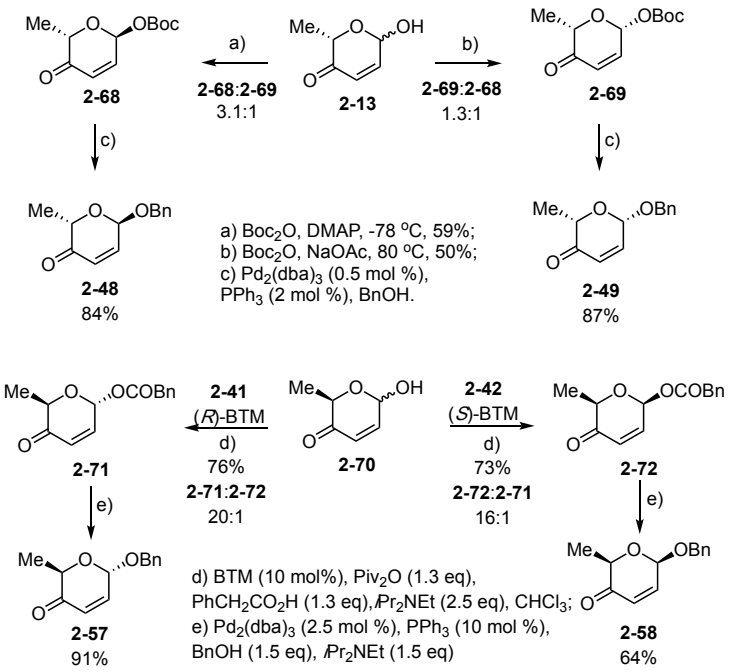

Scheme 2-15 Comparison of old and new methods to access enone intermediates to obtain all stereoisomers of 2,3,6-trideoxyhexopyranosides

(**Scheme 2-16**). Deoxyaminosugars are commonly part of natural products, including anthracyclines, macrolides, and aminoglycoside.[27] Continuing with the theme of the work in this review, reagent control is the key to achieving the stereodivergent synthesis of the deoxy- and deoxyaminosugars presented here.

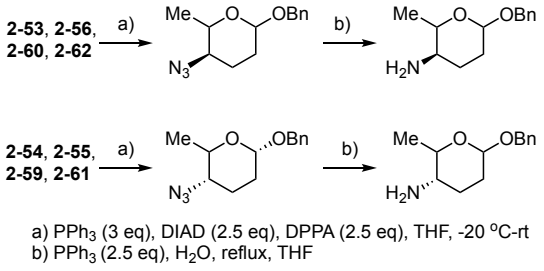

Scheme 2-16 Synthesis of all possible 2,3,4,6-tetradeoxy-4-aminopyranosides

Although some time had passed since we published our work on the DKDA of allylic lactols, we did not pay too much attention to the detailed mechanism of this

reaction. We always thought a cation-π interaction between the cationic acylated-BTM catalyst and the π system of the substrates was the driving force for the high selectivity. This was what Houk and Birman proposed for the BTM catalyzed kinetic resolution of benzylic, allylic, and propargylic secondary alcohols,[28] which states the enantioselectivity in these reactions results from interactions between the cationic acylated-BTM catalyst and the π system of the substrates. We also had a π system in our allylic lactol substrates, and we thought our reaction should just follow the same mechanism.

However, there was a flaw in this logic because the π system in our substrates, such as **2-43**, was an enone. and the electron-withdrawing carbonyl group makes the alkene π system electron-deficient. Thus, it would be difficult for our π component to interact with the cationic acylated-catalyst through the cation-π interaction. But we did not realize this until later when we figured out the actual interaction that governed the selectivity. As discussed later, we had some very interesting results for the BTM-catalyzed site-selective acylation of α-glucosides, but we could not rationalize the results we observed. We then had to come back to the BTM-catalyzed stereoselective acylation reaction and ask ourselves if we really understand this reaction that we had we already published.

One day out of nowhere, in the midst of our ponderings, we took out our molecular modeling kit. We used the kit to build the structures for both (*R*)-BTM and substrate **2-73** to try to predict the reaction outcome based on a cation-π interaction. The model predicted **2-74**, but our experimental results indicated that **2-75** was the major product (**Scheme 2-17**)!

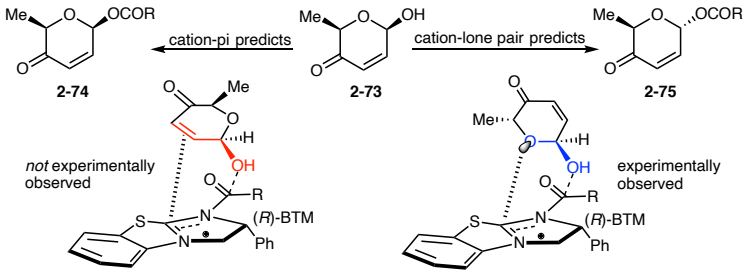

Scheme 2-17 Models comparing the acylation product of **2-73** via a cation-π interaction or a cation-n interaction

To get the experimentally observed product **2-75**, we had to place the ring oxygen instead of the alkene on the top of the π–system of the acylated BTM catalyst. It appears that if there is cation-lone pair or cation-n interaction between the lone pair of the oxygen atom on the pyranose ring, we can then predict the correct reaction outcome. One way to evaluate this hypothesis was to try a monosaccharide substrate, where we eliminate the enone moiety, which was previously thought to be the directing group, but retain the pyranose ring. With a monosaccharide substrate we could test whether or not it was actually the ring oxygen that dictated the reaction outcome.

In 2017 we demonstrated that our DKDA method could be applied to saturated pyranosides.[29] This was a significant step forward in the realm of carbohydrate synthesis because until this work, chemists lacked a general, catalyst-controlled method for the stereoselective acylation of anomeric hydroxyl groups (**Scheme 2-18**).

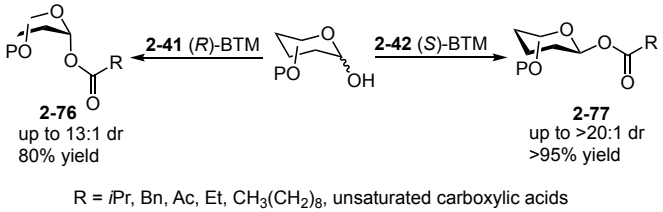

Scheme 2-18 Overview of the BTM-catalyzed dynamic kinetic diastereoselective acylation of anomeric hydroxyl groups

We screened commercially available chiral catalysts for the DKDA of glucose derivative **2-78** (**Scheme 2-19**). We determined that (*S*)-tetramisole **2-38** and (*S*)-BTM **2-42** were the best catalysts for producing the β-anomer as the major product while (*R*)-BTM **2-41** provided the α-anomer as the major product. Although using the anhydride method with isobutyric anhydride for the catalyst screening worked well enough, favoring a 1:13 ratio of **2-79**: **2-80,** we once again turned to Shiina's mixed anhydride method. And again, the mixed anhydride method, which used isobutyric acid and pivalic anhydride, proved superior and increased the ratio of **2-79**: **2-80** to <1:20 with (*S*)-BTM.

The mixed anhydride method also allows for a greater variety of anomeric esters to be formed because it uses many readily available carboxylic acids. The mixed anhydride method worked great in conjunction with (*S*)-BTM and phenylacetic acid to make β-anomer **2-82**, but the results for formation of the α-anomer **2-81** left room for improvement since the ratio of **2-81**: **2-82** was only 7:1. To increase the selectivity for the α-anomer we examined BTM catalysts with varying steric and electronic properties, but (*R*)-BTM remained the best option. Solvent screening showed that chloroform, which was used in our previous acylation work, was still our best option.

A variety of carboxylic acids were amenable to this reaction, including acetic acid, long alkyl chain carboxylic acids, and unsaturated acids. The β-anomers were consistently obtained with high selectivity, and the selectivity for the α-anomer ranged from 6:1 to 8:1. The scope of carbohydrates for this method is also shown in **Scheme 2-20**. When an achiral catalyst, DMAP **2-83**, was used for this reaction, the intrinsic selectivity was generally low. But we were able to show that chiral catalysts could

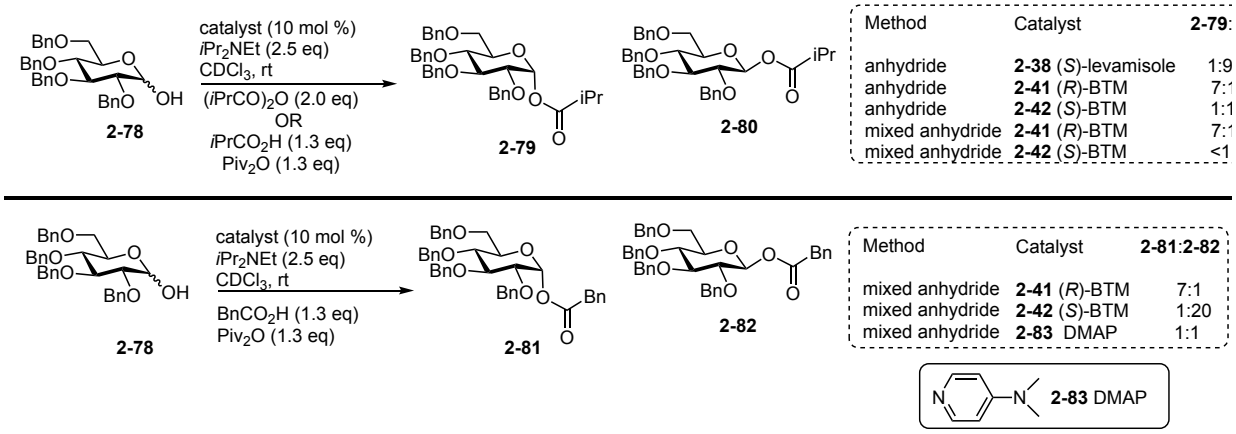

Scheme 2-19 Screening of catalysts and conditions for the BTM-catalyzed dynamic kinetic diastereoselective acylation of anomeric hydroxyl groups

enhance or even override the intrinsic selectivity in the case of β-mannoside **2-84c** and β-xyloside **2-84d**. We also showed that the α- or β-acylsugars **2-85** and **2-86** formed via this method exhibited different reactivity to the same reduction protocol. In fact, only **2-85** can undergo controlled reduction to form **2-87**.

The diastereoselective anomeric hydroxyl acylation is another example of how we have used chiral catalysts to solve longstanding problems in carbohydrate synthesis. Furthermore, since carbohydrates are prevalent in natural products and pharmaceuticals, the ability to predictably functionalize the anomeric position is essential for downstream transformations. The stereoselectivity we observed for these carbohydrate substrates without any π-system in the ring are consistent with the cation-n interaction model proposed in Scheme 18. A more rigorous analysis of the cation-n interaction with the support of computational chemistry is illustrated later.

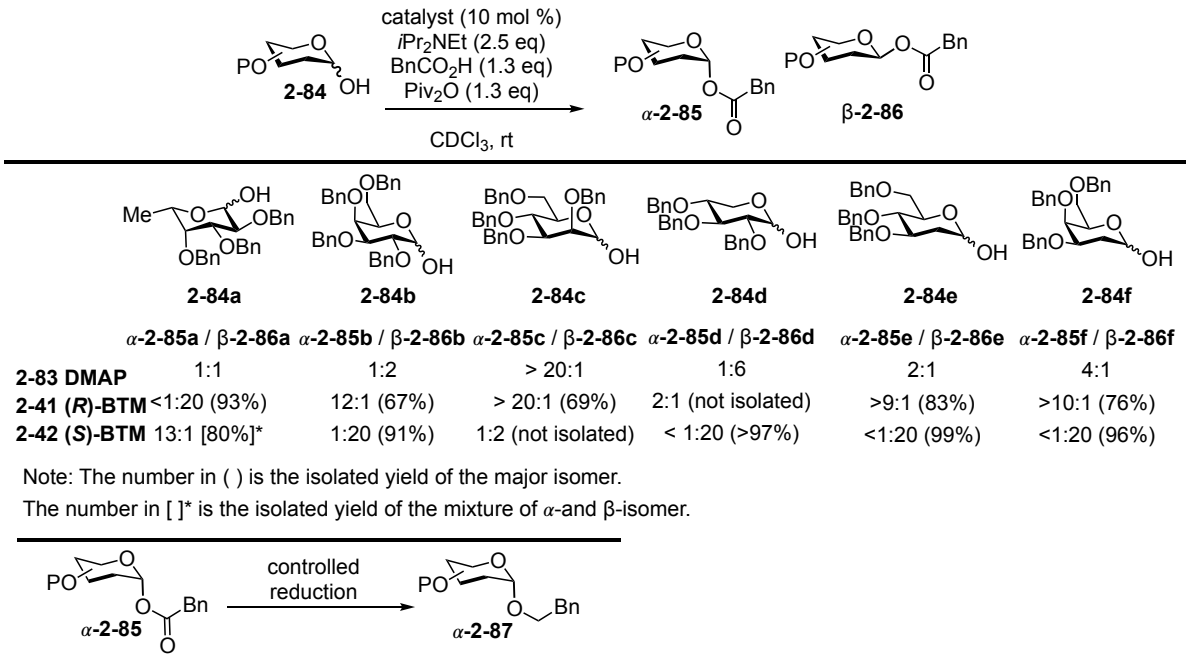

Scheme 2-20 Scope of carbohydrates for the BTM-catalyzed dynamic kinetic diastereoselective acylation of anomeric hydroxyl groups

Our work with carbohydrates, however, was far from over. In fact, the rest of this review will focus on how acylation reactions may provide some solutions for two major problems in carbohydrate chemistry – the site-selective functionalization of carbohydrates and the glycosylation reaction.

2.5 Using the same chiral organocatalysts for site-selective acylation

While working on the BTM-catalyzed stereoselective acylation of anomeric hydroxyl group, we started wondering if there were other reactions where we could use the BTM catalysts. As discussed earlier, site-selective functionalization of carbohydrates is essential for the efficient synthesis of carbohydrate building blocks. Historically, most research efforts have focused on differentiating *cis*-diols in carbohdyrates.[30, 31] This

differentiation is possible because the intrinsic reactivity of axial and equatorial hydroxyl groups in *cis*-diol is different and this difference can be further amplified by chelation with metals.[30-33] *Trans*-diols are much harder to site-selectively functionalize because both hydroxyl groups are on the equatorial positions.

We once again relied on reagent control, employing paired chiral BTM catalysts, to differentiate *trans*-diols in *O*-glycosides and more complicated substrates through a cation-lone pair interaction discussed before.[34]

We first used (*R*)-BTM **2-41** and isobutyric anhydride to functionalize commercially available α-glycoside **2-88**. We obtained C3-acylated product **2-89** in 92% yield with greater than 20:1 selectivity (**Scheme 2-21**). Interestingly, when we used (*S*)-BTM **2-42** as the catalyst, the major product was the C2-acylated glucoside **2-90**, which was obtained in 94% yield and favored in 17:1 ratio over **2-89**. The site-selectivity of this method is even more impressive considering that there was no intrinsic selectivity when achiral DMAP **2-83** was used as the catalyst.

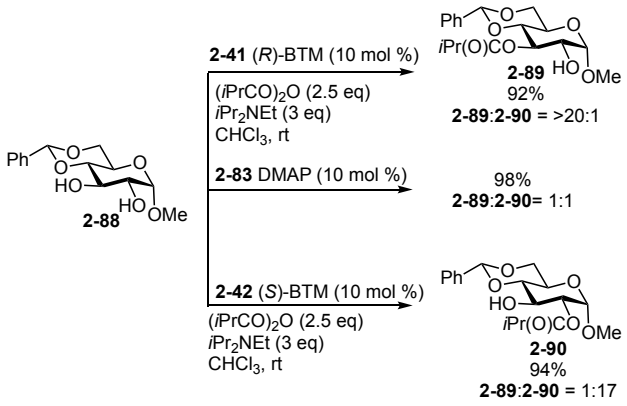

Scheme 2-21 Paired chiral BTM catalyzed site-selective functionalization of hydroxyl groups in a monosaccharide

We had the above nearly perfect site-selective acylation result right after we published the stereoselective acylation method in 2015. However, when we applied the same condition on β-glucoside, no site-selectivity was observed using either the (*R*)- or (*S*)-BTM catalyst. We thought this reaction was limited to α-glycosides and then tried α-galactoside. Again, neither the (*R*)- nor (*S*)-BTM catalyst provided any site-selectivity. We stuck with one substrate, the α-glucoside, for a long time without being able to extend the scope of reaction. We realized that we need to understand the mechanism of the reaction and the source of the site-selectivity in order to make any progress. However, we could not rationalize it using any known interactions reported for chiral organocatalysts. We started going back to our previously reported stereoselective acylation to examine if it was really directed by the cation-π interaction. As discussed before, a cation-π interaction does not lead the observed stereoisomer, and we recognized that the cation-n interaction was the controlling factor for stereoselectivity. We asked ourselves does the same type of cation-n interaction govern the site-selective acylation of α-glucoside **2-88**? After playing with the molecular modeling kit for a while with chiral BTM-catalysts, α-glucoside, β-glucoside, and α-galactoside we realized that all of the results we obtained, whether positive or negative, make perfect sense if we introduce the cation-n interaction to the system.

The left side of **Scheme 2-22** shows the catalytic cycle for (*R*)-BTM-catalyzed selective acylation of the C3-OH group, which is facilitated by the lone pair on the C4-oxygen. A cation was generated after the acylation of the BTM catalyst to form active catalyst **2-91**. The acyl group remained in the same plane as the heterocycle due to the non-bonding interaction between the oxygen and sulfur. The C3-OH group attacks the

carbonyl in **2-92** from the top face of the heterocycle to avoid steric clash with the phenyl group located on the bottom of the ring. This will place the lone pair on the equatorial C4-oxygen pointing towards the cationic (*R*)-BTM catalyst for the acylation of C3-OH group as shown in the bottom half of the scheme.

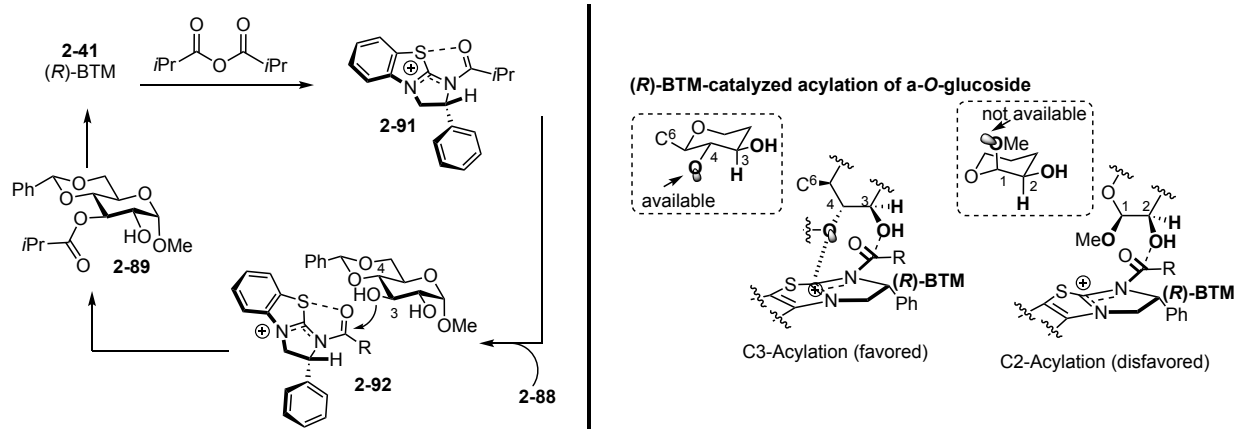

Scheme 2-22 Mechanism for the site-selective acylation of *trans*-1,2-diols in α-glucoside

On the other hand, the lone pair on the axial C2-oxygen, which locates on the top face of the heterocycle, points away from the cationic catalyst for the acylation of the C2-OH group. The (*R*)-BTM catalyst-mediated acylation of C3-OH group is therefore favored, while the acylation of C2-OH group is disfavored. This rationalized why selective acylation of C3-OH group was observed for α-glucoside, when the (*R*)-BTM catalyst was employed. This is summarized in **Ia** and **Ib** (**Scheme 2-23A**) using the arrow to indicate how the lone pair in the right direction can or cannot facilitate the acylation of the corresponding OH group. When the (*S*)-BTM catalyst was employed for the acylation of α-glucoside, the axial anomeric methoxy group can create steric clash with the catalyst and disable the cation-n interaction between the lone pair on the C2-oxygen and the cationic catalyst (**Ic**, **Scheme 2-23B**). Selective C2-OH acylation was observed as shown **Id** (Scheme 2B).

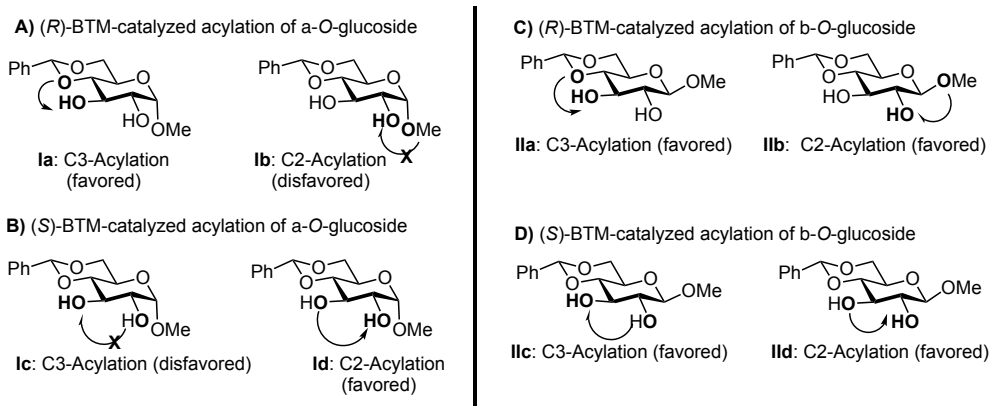

Scheme 2-23 Predictive models for the site-selective acylation of *trans*-1,2-diols

The disfavored situation in **Ib** and **Ic** are due to the axial anomeric OMe group. In the case of β-glucoside, all four situations (**IIa-IId**, **Scheme 2-23C/D**) are favored. This explains why no selectivity was observed for β-glucoside using either enantiomer of the catalyst. Density-functional theory (DFT) calculations also supported the cation-n interaction-directed site-selectivity and our proposed model. Using this model, we are able to predict what substrates can or cannot undergo selective acylation using which catalyst. Indeed, we observed high selectivity for all substrates that were predicted to be selective and low selectivity for all substrates that were predicted to be unselective.

We were able to functionalize a broad range of *trans*-1,2-diols in common sugars including glucosides, galactosides, mannosides, rhamnosides, and also xylosides. This strategy could even be extended to more complex substrates, including trehalose derivative **2-93** and disaccharide **2-96**, which has two hydroxyl group in two different monosaccharides (**Scheme 2-24**).

Overall, our theoretical predictions were consistently correct and corroborated by experimental evidence. We could now systematically and predictably achieve the site-selective acylation of *trans*-diols in carbohydrates.

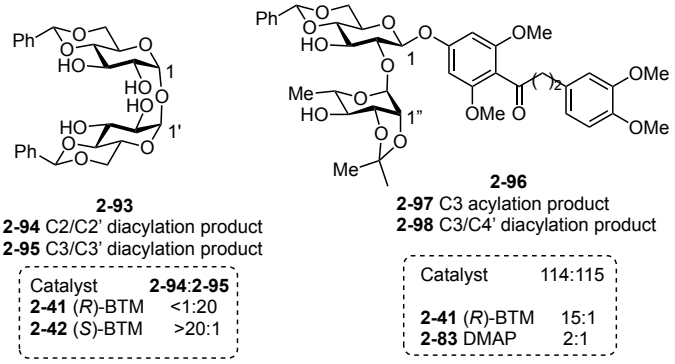

Scheme 2-24 Site-selectivity for complex substrates

When we were considering how to extend the scope of the cation-lone pair directed acylation of *O*-glycosides, we wondered if we could similarly acylate *S*-glycosides with *trans*-diols through the same interaction because they're isoelectronic with *O*-glycosides. In 2019 we reported that we could indeed use *S*-glycosides to direct site-selective acylation of *trans*-diols.[35] This work will be reported in depth in Chapter 3.

Now with our ability to site-selectively acylate *trans*-1,2-diols, we wondered if we could successfully execute other types of site-selective functionalization. We chose site-selective phosphoramidation as our next target because phosphoramidated carbohydrates have found use in prodrugs[36] and have been studied as anti-tumor agents.[37] While the site- selective acylation of *O*- and *S*- glycosides was relatively straightforward, successful phosphoramidation would pose more of a challenge. Since phosphoramidates are chiral at the phosphorous center, a high degree of both site- and stereoselectivity would have to be obtained in order for our method to be widely useful.

Bicycloimidazole-based catalysts have been used for the dynamic kinetic resolution of phosphorous centers[38] and to install phosphoramidates on primary alcohols

of nucleotides,[39] so we reasoned these catalysts would be a good place to start. In 2019, after screening multiple chiral catalysts and chiral electrophiles, we reported that bicycloimidazole-based catalyst **2-100** and (*D*)-alanine derived chiral electrophile **2-101** could be used to achieve the site-selective phosphoramidation of α-glucosides and β-galactosides (**Scheme 2-25**).[40] A dynamic kinetic. resolution at the phosphorus center contributes to the stereoselectivity of the reaction. Then, the high stereoselectivity promotes the high site-selectivity. Aside from using chiral catalysts to direct site-selective acylation and phosphoramidation, we've also had success using anomeric esters and copper salts to promote stereoselective glycosylation reactions under very mild conditions.

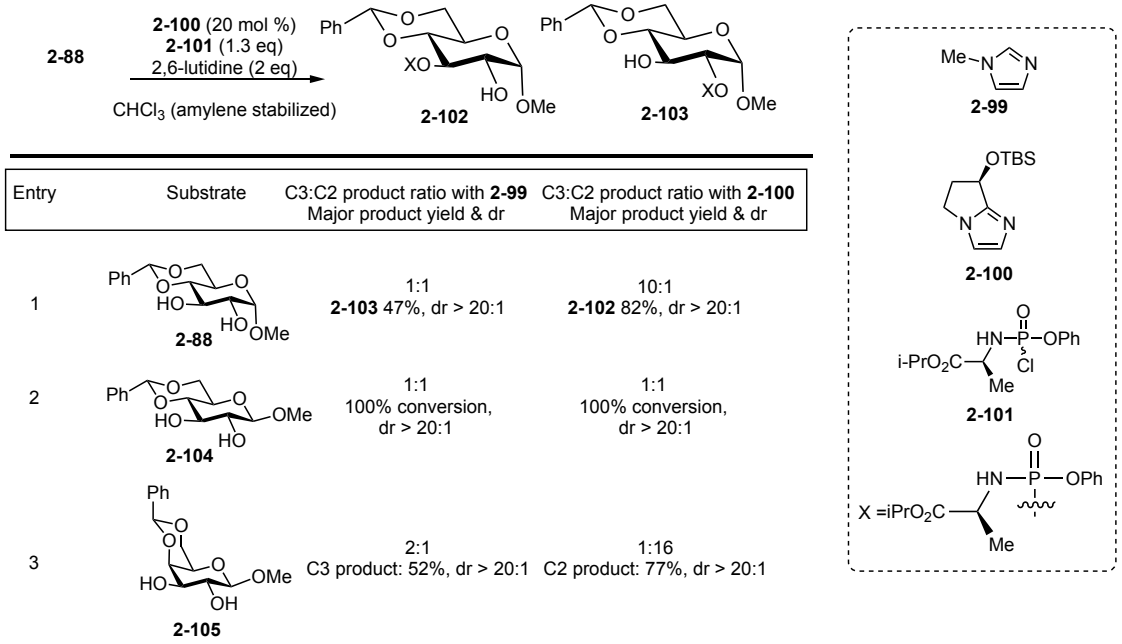

Entry	Substrate	C3:C2 product ratio with **2-99** Major product yield & dr	C3:C2 product ratio with **2-100** Major product yield & dr
1	**2-88**	1:1 **2-103** 47%, dr > 20:1	10:1 **2-102** 82%, dr > 20:1
2	**2-104**	1:1 100% conversion, dr > 20:1	1:1 100% conversion, dr > 20:1
3	**2-105**	2:1 C3 product: 52%, dr > 20:1	1:16 C2 product: 77%, dr > 20:1

Scheme 2-25 Site-selective phosphoramidation of carbohydrates using a chiral catalyst and chiral electrophile (top) and partial substrate scope (bottom)

2.6 Glycosylation under one of the mildest conditions using an ester as the leaving group

Traditionally, stereoselective glycosylations rely on strong Lewis acids, Brønsted acids, or reactive electrophiles to proceed efficiently. However, glycosyl donors that can be easily activated under mild and neutral conditions are extremely attractive. In 2017, we reported that isoquinoline-1-carboxylate was a glycosyl donor that could do just that (**Scheme 2-26**).

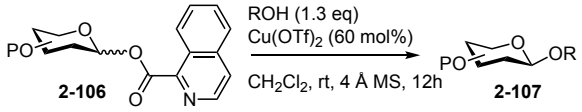

Scheme 2-26 Isoquinoline-1-carboxylate as a traceless leaving group for chelation-assisted glycosylation

We knew of reports where transition metals[41, 42] could activate anomeric ester donors for glycosylation (donors with remote alkynes), but these cases all require purification post-reaction. Our thought was to improve upon these methods by having the carboxylate precipitate out of the solution after the reaction, thereby rendering it a traceless leaving group.[41-44]

We first used $Cu(OTf)_2$ to examine anomeric picolinic esters as the glycosyl donor, but we observed significant amounts of transesterification products. We reasoned that a bulkier substituent on the 3-position of the picolinic ester could help prevent nucleophilic attack of the acceptor on the carbonyl carbon, which would minimize the transesterification product.

We identified isoquinoline-1-carboxylic acid as the most inexpensive (e.g. $80/100 g from Ark Pharm, Inc.) yet sterically encumbered reagent with a bulky 3-substituent. The

isoquinolinic esters were easily prepared, and they provided the desired products using 60 mol % $Cu(OTf)_2$. We also completed a competition experiment between anomeric picolinic and isoquinolinic esters to determine their relative reactivity and determined that the isoquinolinic ester was far more reactive. Additionally, this ester was benchtop stable for months at room temperature. Our new anomeric ester worked well as the glycosyl donor when present within a variety of monosaccharides and with both primary and secondary alcohols as acceptors of varying complexities (**Scheme 2-27**). Because our isoquinolinic ester activated by copper was orthogonal to the anomeric ester activated by gold, reported by Yu,[41, 42] we used these complementary approaches to complete an iterative synthesis of tetrasaccharide **2-108**.

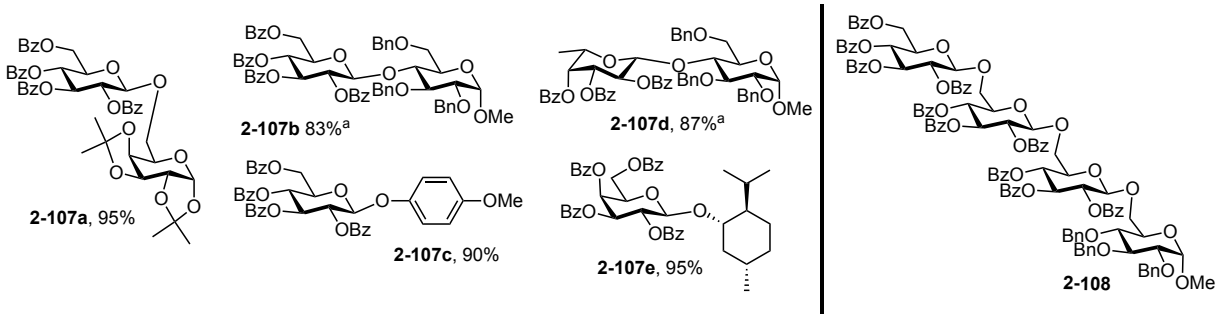

Scheme 2-27 Partial substrate scope using isoquiniline-1-carboxylate as a traceless leaving group (left) and tetrasaccharide synthesized (right)

Even though picolinic esters didn't work well for glycosylation reactions, in 2020 we reported that they could be used to make glycosyl chlorides and glycosyl bromide under mild and neutral conditions, just like our previous isoquinolinic esters.[45] Picolinic esters are stable glycosyl donors that are activated by nontoxic copper (II) salts under mild conditions.[46, 47] As we screened copper (II) sources for the activation of isoquinolinic esters in our previous work, we observed that glycosyl chlorides were produced instead

of the desired *O*-glycoside product. As an added advantage, the glycosyl chloride was produced under mild enough conditions that historically acid-labile protecting groups could be present on the substrate.

The substrate scope for this work was rather large, therefore only a small portion is shown in **Scheme 2-28**. All benzylated sugars led to the α-isomer as the major product in high yield, and this configuration was achieved independent of the anomeric picolinic ester's stereochemistry, which suggests the involvement of an oxocarbenium intermediate. In most cases, the crude glycosyl halide product could be used for further derivatization without purification. When electron-withdrawing protecting groups were present on the starting materials, the reactions required longer reaction times and an increased amount of $CuCl_2$, but they still produced the glycosyl chlorides in good yield. However, starting materials with *gluco*-configurations resulted in β-isomers as the major product, such as in **2-118**, which indicates that C2 neighboring group participation is the major contributor to anomeric stereoselectivity.

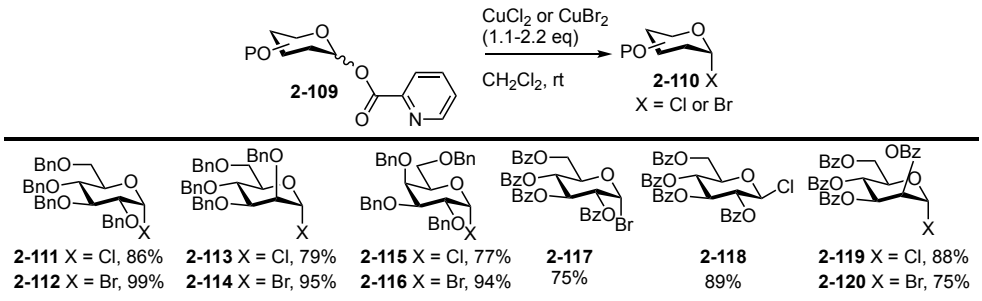

Scheme 2-28 Synthesis of glycosyl chlorides and glycosyl bromides via chelation assisted activation of picolinic esters (top) and partial substrate scope (bottom)

Glycosyl bromides could also be accessed easily using $CuBr_2$, but regardless of the presence of armed/disarmed protecting groups on the starting materials, only α-glycosyl bromides were produced. These results are logical considered that the bromide

ion is a better leaving group compared to the chloride ion, and the high reactivity of β-glycosyl bromides. Unfortunately, we were unable to produce glycosyl fluorides or iodides in the same manner, using copper (II) fluoride and copper (I) iodide respectively. We were however, able to demonstrate the utility of this method by synthesizing two disaccharides from glycosyl bromides, including **2-107a** and **2-121** (**Scheme 2-29**).

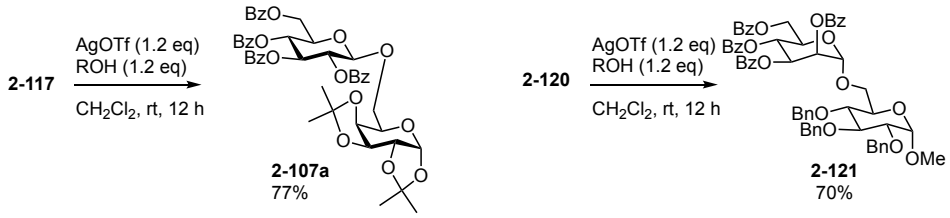

Scheme 2-29 Glycosyl bromide donors for the synthesis of disaccharides

2.7 Conclusion

In order for glycobiologists to better understand the roles of carbohydrates in human health and diseases, chemists are tasked with finding new methods to expediate the synthesis of carbohydrates. This task will require current members of the field to be creative and think outside of their wheelhouse to address the two problems that consistently plague carbohydrate chemists – site-selective functionalization and stereoselective glycosylation. We hope this review has been informative and shown the reader how our group has approached carbohydrate synthesis, and we look forward to the new approaches in the future.

2.8 References

1. Bertozzi, C. R.; Kiessling, L. L., Chemical glycobiology. *Science* **2001,** *291* (5512), 2537-2364.

2. Stallforth, P.; Lepenies, B.; Adibekian, A.; Seeberger, P. H., 2009 claude s. Hudson award in carbohydrate chemistry. Carbohydrates: A frontier in medicinal chemistry. *J. Med. Chem.* **2009,** *52* (18), 5561-77.

3. Ernst, B.; Magnani, J. L., From carbohydrate leads to glycomimetic drugs. *Nat. Rev. Drug Discov.* **2009,** *8* (8), 661-77.

4. Hartwig, J. F., Catalyst-controlled site-selective bond activation. *Acc. Chem. Res.* **2017,** *50*, 549-555.

5. Toste, F. D.; Sigman, M. S.; Miller, S. J., Pursuit of non-covalent interactions for strategic site-selective catalysis. *Acc. Chem. Res.* **2017,** *50*, 609-615.

6. Blaszczyk, S. A.; Tang, W., Addressing the challenge of carbohydrate site selectivity by synergistic catalysis. *Chem* **2017,** *3* (5), 722-723.

7. Achmatowicz, O.; Bukowski, P.; Szechner, B.; Zwierzchowska, Z.; Zamojski, A., Synthesis of methyl 2,3-dideoxy-dl-alk-2-enopyranosides from furan compounds : A general approach to the total synthesis of monosaccharides. *Tetrahedron* **1971,** *27* (10), 1973-1996.

8. Wang, H. Y.; Yang, K.; Bennett, S. R.; Guo, S. R.; Tang, W., Iridium-catalyzed dynamic kinetic isomerization: Expedient synthesis of carbohydrates from achmatowicz rearrangement products. *Angew. Chem. Int. Ed.* **2015,** *54* (30), 8756-9.

9. Schmidt, B.; Hauke, S., Metathesis-based de novo synthesis of noviose. *Eur. J. Org. Chem.* **2014,** *2014* (9), 1951-1960.

10. Matsushima, Y.; Kino, J., Synthesis of n -bz-protected d -daunosamine and d -ristosamine by silica gel promoted intramolecular conjugate addition of trichloroacetimidates obtained from osmundalactone and its epimer. *Eur. J. Org. Chem.* **2010,** *2010* (11), 2206-2211.

11. Thomson, M. I.; Nichol, G. S.; Lawrence, A. L., Total synthesis of (-)-angiopterlactone b. *Org. Lett.* **2017,** *19* (9), 2199-2201.

12. Blume, F.; Liu, Y.-C.; Thiel, D.; Deska, J., Chemoenzymatic total synthesis of (+)- & (−)-cis-osmundalactone. *J. Mol. Catal. B Enzym.* **2016,** *134*, 280-284.

13. Della-Felice, F.; Sarotti, A. M.; Krische, M. J.; Pilli, R. A., Total synthesis and structural validation of phosdiecin a via asymmetric alcohol-mediated carbonyl reductive coupling. *J. Am. Chem. Soc.* **2019,** *141* (35), 13778-13782.

14. Zhu, Z.; Wang, H.-Y.; Simmons, C.; Tseng, P.-S.; Qiu, X.; Zhang, Y.; Duan, X.; Yang, J.-K.; Tang, W., Iridium-catalyzed dynamic kinetic stereoselective allylic etherification of achmatowicz rearrangement products. *Adv. Synth. Catal.* **2018,** *360* (3), 595-599.

15. Babu, R. S.; Zhou, M.; O'Doherty, G. A., De novo synthesis of oligosaccharides using a palladium-catalyzed glycosylation reaction. *J. Am. Chem. Soc.* **2004,** *126*, 3428-3429.

16. Babu, R. S.; O'Doherty, G. A., A palladium-catalyzed glycosylation reaction: The de novo synthesis of natural and unnatural glycosides. *J. Am. Chem. Soc.* **2003,** *125*, 12406-12407.

17. Wang, H. Y.; Yang, K.; Yin, D.; Liu, C.; Glazier, D. A.; Tang, W., Chiral catalyst-directed dynamic kinetic diastereoselective acylation of lactols for de novo synthesis of carbohydrate. *Org. Lett.* **2015,** *17* (21), 5272-5.

18. Birman, V. B.; Li, X., Benzotetramisole- a remarkably enantioselective acyl transfer catalyst. *Org. Lett.* **2006,** *8*, 1351-1354.

19. Li, X.; Jiang, H.; Uffman, E. W.; Guo, L.; Zhang, Y.; Yang, X.; Birman, V. B., Kinetic resolution of secondary alcohols using amidine-based catalysts. *J. Org. Chem* **2012,** *77* (4), 1722-1737.

20. Nakata, K.; Gotoh, K.; Ono, K.; Futami, K.; Shiina, I., Kinetic resolution of racemic 2-hydroxy-γ-butyrolactones by asymmetric esterification using diphenylacetic acid with pivalic anhydride and a chiral acyl-transfer catalyst. *Org. Lett.* **2013,** *15* (6), 1170-1173.

21. Shiina, I.; Nakata, K.; Ono, K.; Onda, Y.; Itagaki, M., Kinetic resolution of racemic α-arylalkanoic acids with achiral alcohols via the asymmetric esterification using carboxylic anhydrides and acyl-transfer catalysts. *J. Am. Chem. Soc.* **2010,** *132* (33), 11629-11641.

22. Shiina, I.; Nakata, N., The first asymmetric esterification of free carboxylic acids with racemic alcohols using benzoic anhydrides and tetramisole derivatives: An application to the kinetic resolution of secondary benzylic alcohols. *Tetrahedron Lett.* **2007,** *48* (47), 8314—8317.

23. Babu, R. S.; Qian, C.; Kang, S.-W.; Zhou, M.; O'Doherty, G. A., De novo asymmetric synthesis of all-d-, all-l-, and d-/l-oligosaccharides using atom-less protecting groups. *J. Am. Chem. Soc.* **2012,** *134* (29), 11952-11955.

24. Ortiz, A.; Benkovics, T.; Beutner, G. L.; Shi, Z.; Bultman, M.; Nye, J.; Sfouggatakis, C.; Kronenthal, D. R., Scalable synthesis of the potent hiv inhibitor bms-986001 by non-enzymatic dynamic kinetic asymmetric transformation (dykat). *Angew. Chem. Int. Ed.* **2015,** *54*, 7185-7188.

25. Song, W.; Zhao, Y.; Lynch, J. C.; Kim, H.; Tang, W., Divergent de novo synthesis of all eight stereoisomers of 2,3,6-trideoxyhexopyranosides and their oligomers. *Chem. Commun.* **2015,** *51* (98), 17475-8.

26. Zhu, Z.; Glazier, D. A.; Yang, D.; Tang, W., Catalytic asymmetric synthesis of all possible stereoisomers of 2,3,4,6-tetradeoxy-4-aminohexopyranosides. *Adv. Synth. Catal.* **2018,** *360* (11), 2211-2215.

27. Elshahawi, S. I.; Shaaban, K. A.; Kharel, M. K.; Thorson, J. S., A comprehensive review of glycosylated bacterial natural product. *Chem. Soc. Rev.* **2015,** *44* (21), 7591-7697.

28. Li, X.; Liu, P.; Houk, K. N.; Birman, V. B., Origin of enantioselectivity in cf3−pip-catalyzed kinetic resolution of secondary benzylic alcohols. *J. Am. Chem. Soc.* **2008,** *130*, 13836-13837.

29. Wang, H. Y.; Simmons, C. J.; Zhang, Y.; Smits, A. M.; Balzer, P. G.; Wang, S.; Tang, W., Chiral catalyst-directed dynamic kinetic diastereoselective acylation of anomeric hydroxyl groups and a controlled reduction of the glycosyl ester products. *Org. Lett.* **2017,** *19* (3), 508-511.

30. Wang, H. Y.; Blaszczyk, S. A.; Xiao, G.; Tang, W., Chiral reagents in glycosylation and modification of carbohydrates. *Chem. Soc. Rev.* **2018,** *47* (3), 681-701.

31. Lawandi, J.; Rocheleau, S.; Moitessier, N., Regioselective acylation, alkylation, silylation and glycosylation of monosaccharides. *Tetrahedron* **2016,** *72* (41), 6283-6319.

32. Ueda, Y.; Kawabata, T., Topics in current chemistry. Kawabata, T., Ed. Springer International Publishing AG: Gewerbestrasse, 2016; Vol. 372, p 203.

33. Giuliano, M. W.; Miller, S. J., Topics in current chemistry. Kawabata, T., Ed. Springer International Publishing AG: Gewerbestrasse, 2016; Vol. 372, p 157.

34. Xiao, G.; Cintron-Rosado, G. A.; Glazier, D. A.; Xi, B. M.; Liu, C.; Liu, P.; Tang, W., Catalytic site-selective acylation of carbohydrates directed by cation-n interaction. *J. Am. Chem. Soc.* **2017,** *139* (12), 4346-4349.

35. Blaszczyk, S. A.; Xiao, G.; Wen, P.; Hao, H.; Wu, J.; Wang, B.; Carattino, F.; Li, Z.; Glazier, D. A.; McCarty, B. J.; Liu, P.; Tang, W., S-adamantyl group directed site-selective acylation: Applications in streamlined assembly of oligosaccharides. *Angew. Chem. Int. Ed.* **2019,** *58* (28), 9542-9546.

36. Alanazi, A. S.; James, E.; Mehellou, Y., The protide prodrug technology: Where next? *ACS Med. Chem. Lett.tetre* **2019,** *10* (1), 2-5.

37. Dai, Q.; Chen, R., Synthesis of novel phosphonopeptide derivatives and their biological activity. *Heteroatom Chemistry* **1997,** *8* (3), 279-282.

38. Liu, S.; Zhang, Z.; Xie, F.; Butt, N. A.; Sun, L.; Zhang, W., First catalytic enantioselective synthesis of p-stereogenic phosphoramides via kinetic resolution promoted by a chiral bicyclic imidazole nucleophilic catalyst. *Tetrahedron: Asymmetry* **2012,** *23* (5), 329-332.

39. DiRocco, D. A.; Ji, Y.; Sherer, E. C.; Klapars, A.; Reibarkh, M.; Dropinski, J.; Mathew, R.; Maligres, P.; Hyde, A. M.; Limanto, J.; Brunskill, A.; Ruck, R. T.;

Campeau, L.-C.; Davies, I. W., A multifunctional catalyst that stereoselectively assembles prodrugs. *Science* **2017,** *356* (6336), 426-430.

40. Glazier, D. A.; Schroeder, J. M.; Blaszczyk, S. A.; Tang, W., Site- and stereoselective phosphoramidation of carbohydrates using a chiral catalyst and a chiral electrophile. *Adv. Synth. Catal.* **2019,** *361* (16), 3729-3732.

41. Zhu, Y.; Yu, B., Characterization of the isochromen-4-yl-gold(i) intermediate in the gold(i)-catalyzed glycosidation of glycosyl ortho-alkynylbenzoates and enhancement of the catalytic efficiency thereof. *Angew. Chem. Int. Ed.* **2011,** *50* (36), 8329-32.

42. Tang, Y.; Li, J.; Zhu, Y.; Li, Y.; Yu, B., Mechanistic insights into the gold(i)-catalyzed activation of glycosyl ortho-alkynylbenzoates for glycosidation. *J. Am. Chem. Soc.* **2013,** *135* (49), 18396-405.

43. Koppolu, S. R.; Niddana, R.; Balamurugan, R., Gold-catalysed glycosylation reaction using an easily accessible leaving group. *Org. Biomol. Chem.* **2015,** *13* (18), 5094-7.

44. Mishra, B.; Neralkar, M.; Hotha, S., Stable alkynyl glycosyl carbonates: Catalytic anomeric activation and synthesis of a tridecasaccharide reminiscent of mycobacterium tuberculosis cell wall lipoarabinomannan. *Angew. Chem. Int. Ed.l* **2016,** *55* (27), 7786-91.

45. Wen, P.; Simmons, C. J.; Ma, Z. X.; Blaszczyk, S. A.; Balzer, P. G.; Ye, W.; Duan, X.; Wang, H. Y.; Yin, D.; Stevens, C. M.; Tang, W., Synthesis of glycosyl chlorides and bromides by chelation assisted activation of picolinic esters under mild neutral conditions. *Org. Lett.* **2020,** *22* (4), 1495-1498.

46. Koide, K.; Ohno, M.; Kobayashi, S., *Tetrahedron Lett.* **1991,** *32*, 7065−7068.

47. Furukawa, H.; Koide, K.; Takao, K.-i.; Kobayashi, S., *Chem. Pharm. Bull.* **1998,** *46*, 1244−1247.

Chapter 3

Discovery of *S*-Adamantyl Group Directed Site-Selective Acylation and Its Applications in the Synthesis of Oligosaccharides

Part of this chapter was taken from the following published articles.

S-Adamantyl group directed site-selective acylation and its applications in the streamlined assembly of oligosaccharides. Blaszczyk, S.A.; Xiao, G.; Wen, P.; Hao, H.; Wu, J.; Wang, B.; Carattino, F.; Li, Z.; Glazier, D. A.; McCarty, B. J.; Liu, P.; Tang, W. *Angew. Chem. Int. Ed.* **2019**, *58*, 9542-9546.

Chiral reagents in glycosylation and modification of carbohydrates. Wang, H.-Y.; Blaszczyk, S. A.; Xiao, G.; Tang. W. *Chem. Soc. Rev.* **2018**, *47*, 681-701.

3.1 Abstract

Carbohydrates are structurally diverse, synthetically challenging molecules with vital biological roles. Chemists' inability to efficiently synthesize carbohydrates hinders biologists' ability to probe how their structural differences affect biological function. Thus, the site-selective functionalization of carbohydrates is an active area of research. We previously reported that a cation-lone pair interaction can direct site-selective acylation in *O*-glycoside *trans*-1,2-diols using a chiral catalyst. We speculated that we could selectively functionalize *S*-glycosides via a similar interaction. Surprisingly, the sterically encumbered adamantyl group directed site-selective acylation at the C2 position of *S*-glycosides through dispersion interactions between the adamantyl C-H bonds and the π-system of the cationic acylated catalyst, which may have broad implications in many other chemical reactions. Because of their stability, chemical orthogonality, and ease of activation for glycosylation, the site-selective acylation of *S*-glycosides streamlines oligosaccharide synthesis and will have wide applications in complex carbohydrate synthesis.

3.2 Introduction

While most people are familiar with carbohydrates from a nutritional standpoint, they're often unaware that they play significant roles in almost all biological processes, including inflammation and infection, growth and development, cell signaling/molecular recognition events,[1] tumor formation, and cancer metastasis.[2-4] Carbohydrates also influence structural conformation and protein folding in the endoplasmic reticulum[5] and facilitate virus-host cell interactions.[6] Protein glycosylation is a ubiquitous post-translational modification (PTM) in eukaryotes, and research suggests that more than 50% of proteins found in nature are glycosylated.[7]

Carbohydrate scaffolds are found in common prescription drugs, such as zanamivir, acarbose, and heparin (**Scheme 3-1**).[8] Because of their significance to the human body, a number of carbohydrate-based drugs and vaccines are currently being tested in clinical trials or have already been approved by regulatory agencies such as the FDA. Additionally, some vaccines contain sucrose and lactose as stabilizers.[9]

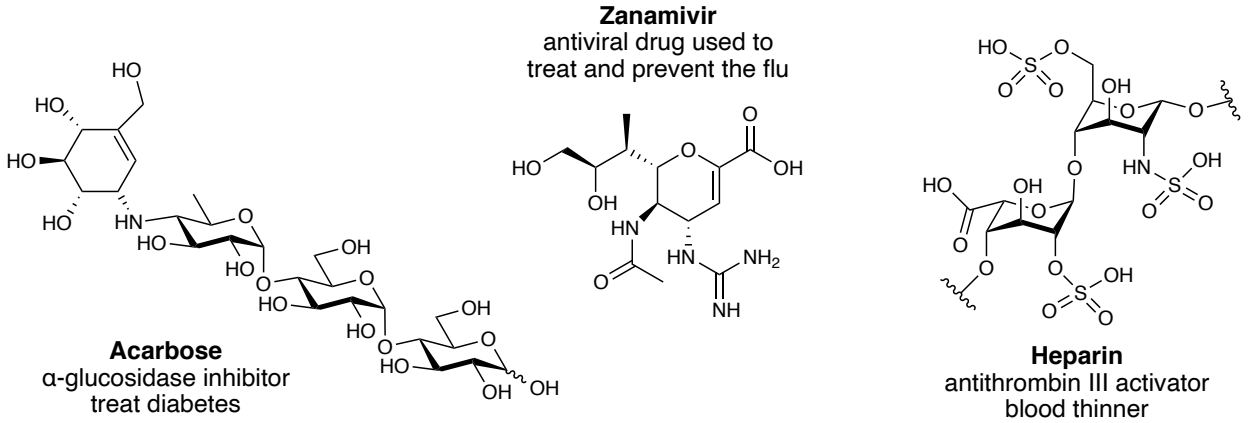

Scheme 3-1 Examples of carbohydrate scaffolds found in prescription drugs

Although carbohydrate research has been ongoing since the seminal work by Emil Fisher in the early twentieth century, carbohydrate research has lagged behind that of other biological molecules, such as lipids, proteins, and nucleic acids. However, just because carbohydrates are less well studied doesn't mean that they're any less important. Glycobiologists seek to lessen the knowledge gaps in carbohydrate chemistry, many of which can be attributed to the vast structural diversity of carbohydrates and their lack of homogenous form. For example, two amino acids and two nucleotides can have two different linear combinations. Additionally, nucleotides and proteins are synthesized through reliably templated biosynthetic pathways.[10] Two monosaccharides, however, can have a total of 20 different linear combinations, which results from the attachment of different hydroxyl groups as well as alpha and beta anomers (**Scheme 3-2**).[8] Biologically relevant carbohydrates can often be isolated from natural sources, but the work is tedious. Reliable separation can also be challenging, as seen with the heparin sulfate incident, where oversulfated chondroitin sulfate (OSCS) contaminated the desired heparin that was administered to patients and resulted in over 100 deaths.[11]

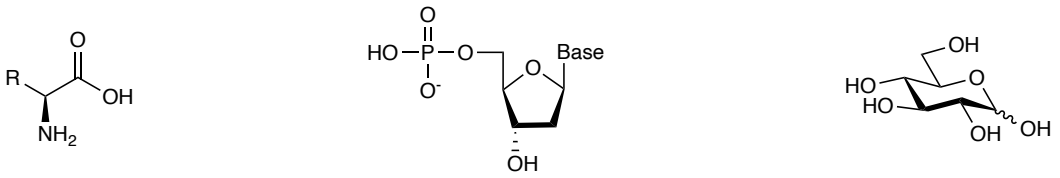

Amino acid
linear combination of
two different amino acids: **2**

Nucleotide
linear combination of
two different nucleotides: **2**

Monosaccharide
linear combination of
two different monosaccharides: **20**

Scheme 3-2 Combinatorial complexity of two amino acids or two nucleotides compared to two monosaccharides

Carbohydrate research is essential because, according to the National Research Council, "glycans are responsible for the pathophysiology of every major disease".[12] As such, researchers constantly seek to better understand how structural differences influence their biological functions. Because of their structural complexity, carbohydrates are synthetically challenging targets. Our inability as chemists to efficiently synthesize carbohydrates then hinders both chemists' and biologists' ability to probe how structural differences affect their biological functions.

A preeminent goal of carbohydrate chemistry is to develop site-selective functionalization methods for the synthesis of carbohydrate building blocks and complex glycans. Site-selective functionalization of molecules with the same type of functional groups has traditionally been of the most difficult transformations to realize, often being referred to as the “Holy Grail” (**Scheme 3-3**).[13-15] It is not surprising that the same functional groups have nearly identical chemical properties and reactivities under a certain set of conditions, and this makes it difficult to manipulate one functional group and not the other. Considering that monosaccharides can have up to five similar yet distinct hydroxyl groups, distinguishing one from the other is imperative. To aid in this matter, one can use nearby hydroxyl groups that provide steric and electronic handles and use specifically designed reagents or catalysts to amplify the different reactivity of individual hydroxyl groups.[16] Though many groups have made progress towards site-selective functionalization of the hydroxyls in carbohydrates, general and efficient methods remain elusive yet highly desirable.

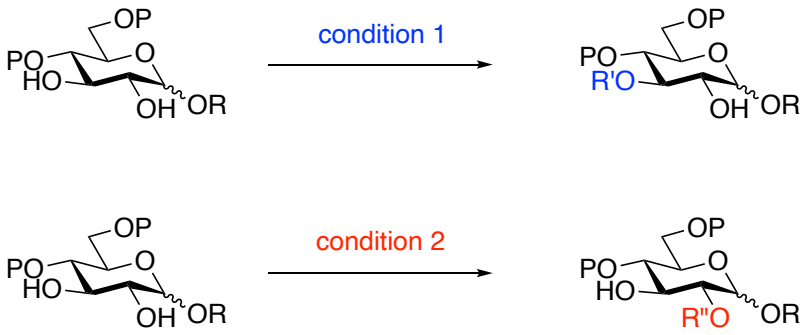

Scheme 3-3 Overview of site-selective functionalization of *trans*-1,2-diols, one of the main problems to be solved in carbohydrate chemistry

In many cases, 1,2- and 1,3-diols need to be differentiated within a given monosaccharide. Historically, site-selective methods have targeted *cis*-1,2-diols[8, 17-19] because of the inherent reactivity differences between equatorial and axial hydroxyl groups and the ability to amplify this reactivity difference by chelation with metals, such as boron,[20-25] tin,[26, 27] and iron.[28, 29] Conversely, the intrinsic selectivity can be overridden using achiral[30] and chiral[31] catalysts. Peptide catalysts can also be used to differentiate hydroxyl groups, but this method often lacks generality.[32-35] While significant progress has been made in respect to *cis*-1,2-diols, the site-selective functionalization of prevalent *trans*-1,2-diols is much less developed and more challenging.[8, 17-19, 36, 37]

3.3 History of *trans*-1,2-diol differentiation in the Tang Lab

For the past few years, our group has made efforts toward differentiating *trans*-1,2-diols, but our breakthrough in this area of carbohydrate chemistry didn't come until after we had used commercially available, paired chiral benzotetramisole (BTM) catalysts for a few years prior. Initially, our group used BTM catalysts for the stereoselective acylation

of lactols bearing an allylic alcohol.[38] We originally thought that the stereoselective acylation was governed by a cation-π interaction between the cationic acylated-BTM catalyst and the π system of the allylic alcohol substrates, which was what Houk and Birman proposed for the BTM catalyzed kinetic resolution of secondary alcohols.[39] We then decided to use BTM catalysts for the site-selective acylation of α-glucosides, such as **3.1**, and we observed nearly perfect site-selectivity and great yields with both (*R*)- and (*S*)-BTM catalysts (**Scheme 3-4**).

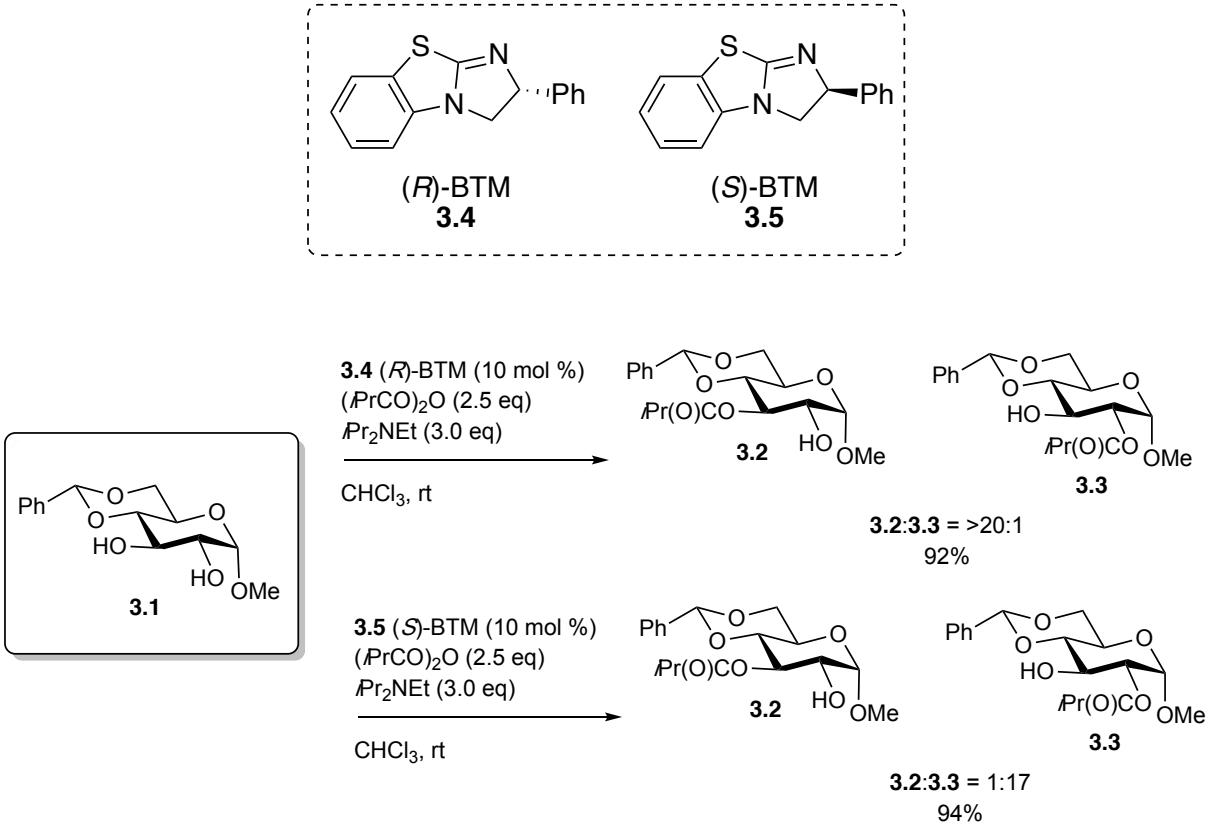

Scheme 3-4 Site-selective acylation results when BTM catalysts were used to functionalize α-glucosides

However, when we applied the same conditions to β-glucoside **3.6**, no site-selectivity was observed using either catalyst. We thought this reaction was limited to α-

glycosides and then tried α-galactoside **3.9**. Again, neither the (*R*)- nor (*S*)-BTM catalyst provided any site-selectivity (**Scheme 3-5**). We were stuck with these results for a long time and concluded that we would have to understand the mechanism of the reaction if we wanted to make further progress with site-selective acylation.

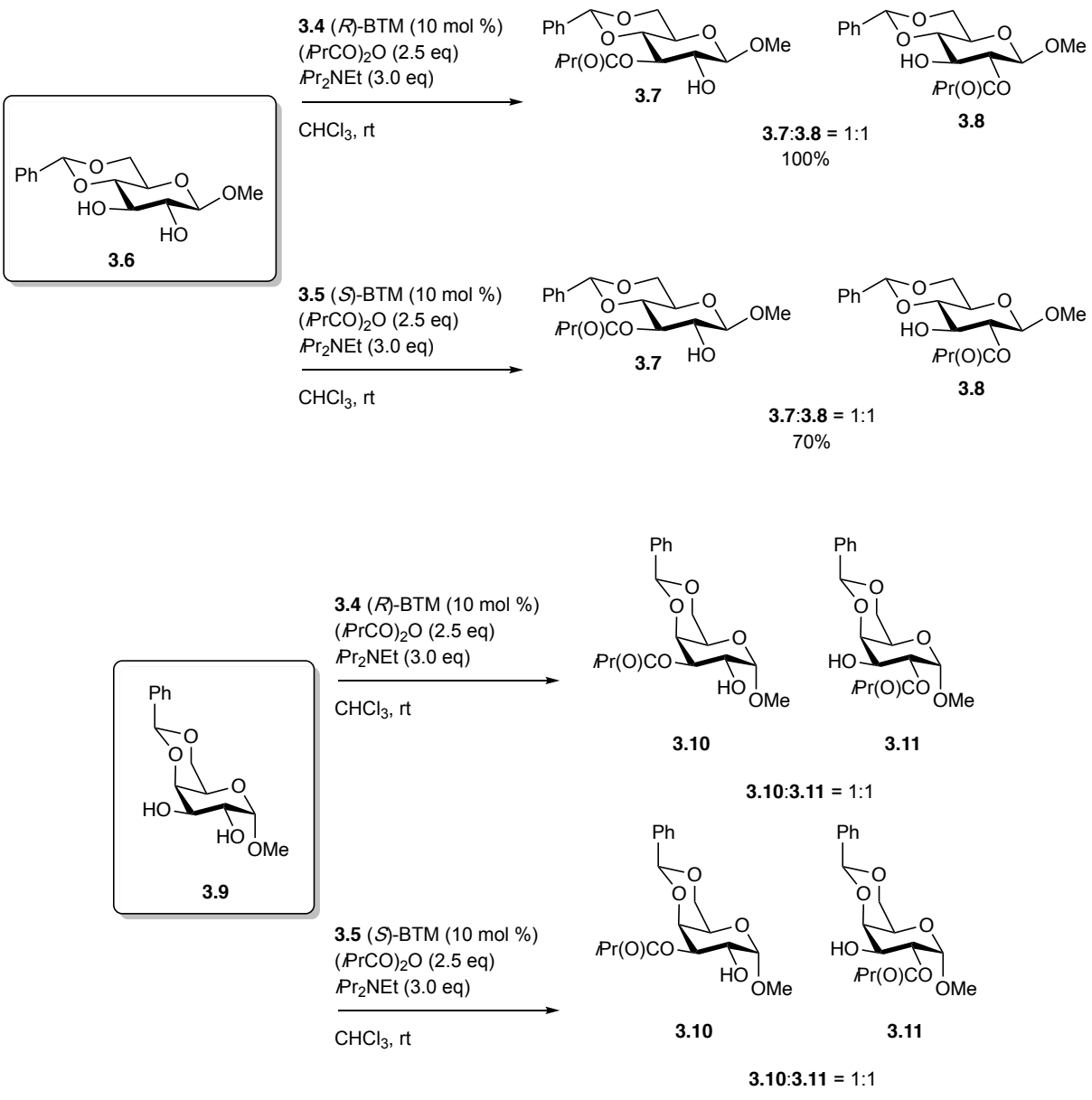

Scheme 3-5 No site-selectivity was obtained when BTM catalysts were used to acylate β-glucosides and α-galactosides

However, we could not rationalize the results we observed for α-glucoside **3.1**, β-glucoside **3.6**, and α-galactoside **3.9** using any known interactions reported for chiral catalysts. As discussed in Chapter 2, we then went back to a simpler system – the stereoselective acylation of lactols bearing an allylic alcohol – and realized that the cation-π interaction between the cationic acylated-BTM catalyst and the π system of our allylic alcohol substrates led to the stereoisomer we did not observe. We then recognized that the cation-lone pair interaction governs the stereoselectivity for the acylation of lactols bearing an allylic alcohol. If we assume that a cation-lone pair interaction was at play for the site-selective acylation, then all of the results in **Scheme 3-4** made perfect sense. Density functional theory (DFT) calculations were performed by our collaborator Peng Liu and his student Gabriel Cintron Rosado at the University of Pittsburgh. They determined that cation-lone pair interactions stabilize the transition state of the acylation and allow for site-selective functionalization, and we published this work in 2017.[40] Additional information about the cation-lone pair directed acylation can be found in Chapter 2.

3.4 Site-selective acylation of *S*-glycosides

While considering how to extend the scope of this cation-lone pair site-selective acylation, our attention was drawn to the fact that *O*-glycosides and *S*-glycosides are isoelectronic. We hypothesized that we could acylate *trans*-1,2-diols within *S*-glycosides in a similar manner (**Scheme 3-6**). Should our hypothesis be correct, we would be able to site-selectively functionalize an additional subset of carbohydrates and significantly streamline the synthesis of oligosaccharides.

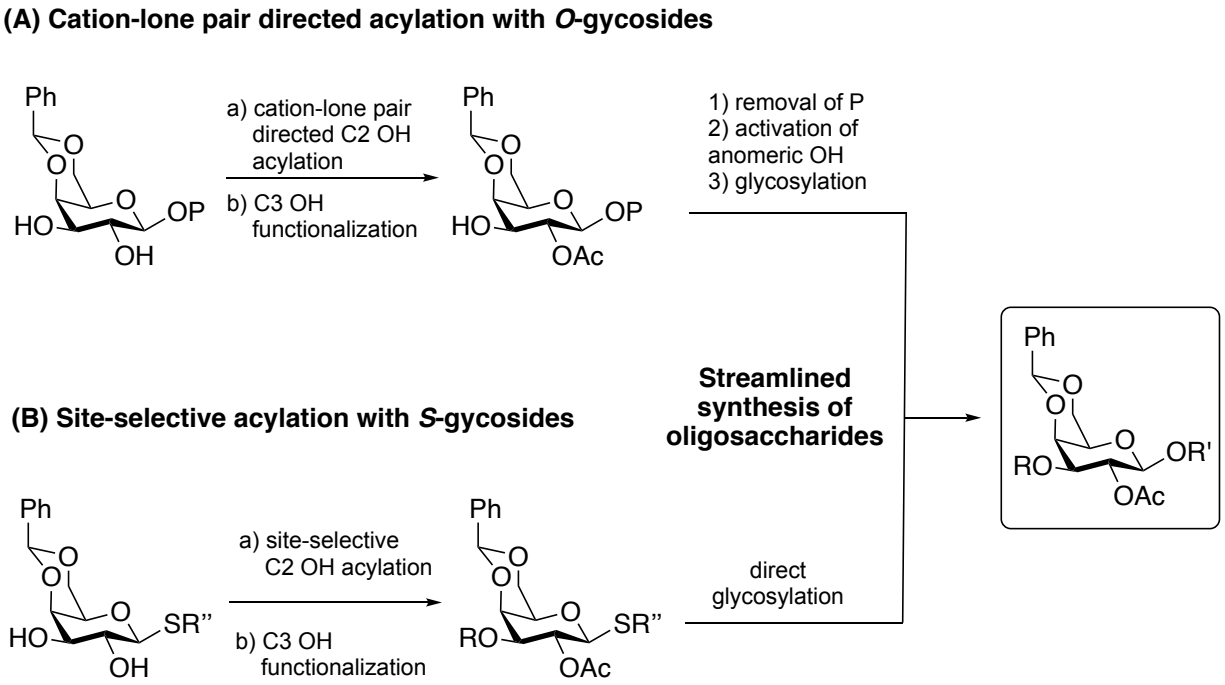

Scheme 3-6 Comparison of site-selective acylation using *O*- and *S*-glycosides

S-glycosides have found widespread use in oligosaccharide synthesis. They are easy to make, stable to various protecting group manipulations, orthogonal to many other glycosyl donors, and easily converted into other glycosyl donors, such as glycosyl halides.[41, 42] This chapter reports our development of a site-selective acylation method for *S*-glycosides,[43] which will further add to their synthetic utility. Surprisingly, we found that the sterically demanding *S*-adamantyl group was the best directing group for C2 OH acylation. DFT calculations indicated that dispersion interactions between the adamantyl C-H bonds and the electron-deficient π-system of the cationic acylated catalyst directed the site-selectivity in *S*-glycosides.

3.5 Results and Discussion

3.5.1 Determining a *S*-glycoside to direct site-selective acylation

To determine a suitable directing group for site-selective acylation, we synthesized *S*-glycosides **3.12a-e** with different thioalkyl or thioaryl substituents. We then used these *S*-glycosides in our previously reported site-selective acylation protocol[40] in the presence of chiral (*R*)-BTM catalysts (**Table 3-7**). Intrinsic site-selectivity was measured by using 4-dimethylaminopyridine (DMAP) as an achiral catalyst in the site-selective acylation protocol. In our previous studies, the lone pair on the anomeric oxygen of β-*O*-galactoside interacts with the cationic π-system of the acylated (*R*)-BTM catalyst to direct the C2-acylation for β-*O*-galactoside. We expected a similar type of interaction between the lone pair of the anomeric sulfur and (*R*)-BTM catalyst for β-*S*-galactosides **3.12a-e**. Initial thioglycoside donors with ethyl and phenyl thioalkyl substituents only led to minimal selectivity enhancements, as determined by ^{1}H NMR spectroscopy of the crude reaction mixture (entries 1 and 2). To increase the electron-donating ability of the *S*-glycoside, we synthesized a donor with a *para*-methoxyphenyl substituent (entry 3). While this donor could override the intrinsic selectivity, the selectivity gains were modest. To our surprise, the bulky *tert*-butyl group showed a significant increase in selectivity, increasing the C2:C3 acylated product ratio to 11:1 (entry 4). With an inclination that sterically more encumbered substituents may be the best directing groups, we synthesized adamantyl 4,6-*O*-benzylidene-1-thio-β-D-galactopyranoside **3.12e**. We were pleased to observe >20:1 selectivity for the C2-acylated product **3.13e** and to identify *S*-adamantyl (*S*-Adm) as the superior directing group for site-selective acylation and future oligosaccharide

synthesis. This was one of the first reactions I run during my first year in the Tang group and the unexpected discovery I made for the *S*-Adm directed site-selective acylation became the topic of my thesis.

Table 3-7 Screening of *S*-glycoside substituents to determine the best directing group for site-selective acylation

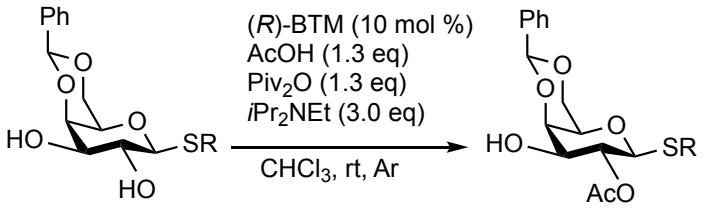

Entry	Substrate	R	(*R*)-BTM C2/C3/C2+C3	DMAP C2/C3/C2+C3
1	**3.12a**	ethyl	5:1:0.6	2:2:1
2	**3.12b**	phenyl	4:1:0.6	2:1:1
3	**3.12c**	*p*-methoxyphenyl	5:1:0.5	1:2.5:1
4	**3.12d**	*tert*-butyl	11:1	1:1
5	**3.12e**	adamantyl	>20:1:1	3:1:1

3.5.2 Determining what factors contributed to C2 selectivity

In our previous studies with *O*-glycosides, the stabilizing interactions between the oxygen lone pair and the positively charged π-system of the acylated catalyst were identified as the dominant factor that controlled the site-selectivity. If this lone-pair/π interaction indeed directed the acylation of *S*-glycosides, then we would expect the ethyl and phenyl substituents on the sulfur (**3.12a** and **3.12b**) to be superior for C2-acylation due to the steric accessibility of the lone pairs on sulfur. The fact that the sterically

encumbered adamantyl substituent (**3.12e**) led to the best result was inconsistent with this site-selectivity model.

We performed DFT calculations to understand what factors contributed to the high C2-selectivity with adamantyl-substituted *S*-glycoside **3.12e**. Because the site-selectivity of the reaction is determined in the acyl transfer from the acylated (*R*)-BTM catalyst to the *S*-glycoside, we calculated the possible isomers of the acylation transition states with **3.12e** at the ωB97XD/6-311++G(d,p)//M06-2X/6-31G(d)/SMD level of theory. The most stable C2- and C3-acylation transition states (**C2-TS** and **C3-TS**) are shown in **Figure 3-8**. The C2-acylation transition state (**C2-TS**) is 3.5 kcal/mol lower in energy than the C3-acylation transition state (**C3-TS**), which is consistent with the high experimentally observed C2-selectivity. The lone pair/π interactions are relatively weak in both the C2- and C3-acylation transition states. In **C2-TS**, the vertical distance between the sulfur atom and the BTM π system (*d*4 = 3.86 Å) is too long for an effective stabilizing interaction. In **C3-TS**, the C4-oxygen atom on the axial position is not placed above the BTM catalyst. Instead, C-H/π interactions between the adamantyl group and the BTM π system and π/π interactions between the benzylidene protecting group and the BTM are observed in **C2-TS** and **C3-TS**, respectively. To investigate the relative strength of the C-H/π and π/π interactions, we computed the dispersion energy ($\Delta E_{\text{dispersion}}$) between the *S*-glycoside substrate and the BTM catalyst in the transition states, which are shown in **Figure 3-8** (see section **3.6.4** for more details). The calculations indicated a substantial amount of dispersion interactions in **C2-TS** due to contributions from multiple C-H/π interactions (d1-d3 ≈ 2.4~2.6 Å, **Figure 3-8**). On the other hand, the substrate-catalyst dispersion interaction in **C3-TS** is 3.7 kcal/mol weaker. These results suggest the greater stability of

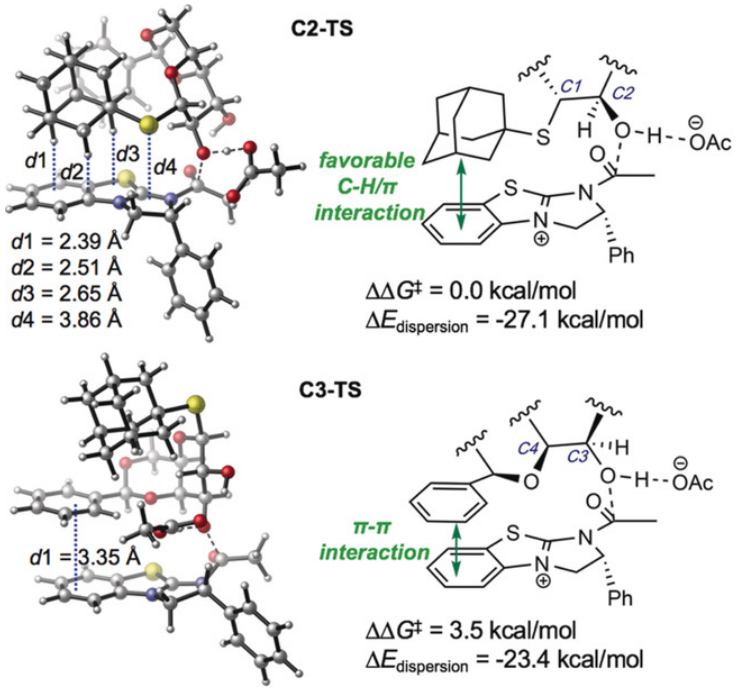

Figure 3-8 Most stable transition states of the C2-/C3-acylation of *S*-glycoside **3.12e**

the C2-acylation transition state (**C2-TS**) is largely due to the more favorable C-H/π interactions between the *S*-adamantyl group and the BTM π-system. Since the bulky adamantyl group is effectively locked into the *exo*-syn conformation by the *exo*-anomeric effect[44] and multiple C-H bonds from adamantly are available for the C-H-π interactions, it was not surprising that we saw much higher C2-selectivity for the adamantyl group than other groups.

3.5.3 Comparing the relative strength of a cation-lone pair interaction versus dispersion interactions

We were then interested in determining the relative strength of the cation-lone pair interaction (as previously reported) versus the dispersion interactions (this work). We used β-*S*-glucoside **3.14** as a substrate capable of both a cation-lone pair interaction between the benzylidene C4 oxygen atom and the (*R*)-BTM catalyst and dispersion interactions between the adamantyl group and the (*R*)-BTM catalyst (**Table 3-9**). We

previously observed a 1:1 ratio of C2/C3 acylation products for the corresponding β-*O*-glucoside using the (*R*)-BTM catalyst, suggesting that the anomeric oxygen lone pair and the C4-oxygen lone pair have the similar ability to interact with the (*R*)-BTM catalyst. We determined the cation-lone pair interaction outcompetes the dispersion interactions, though not by much, leading the C3-acylated product **3.15** to be slightly favored in comparison to the C2-acylated product **3.16** (**Scheme 3-9**). However, by inserting a *para*-nitrobenzylidene protecting group in **3.17**, the C2-acylation product **3.19** is slightly favored over **3.18** because the nitro group electronically decreases the ability of the benzylidene C4 oxygen atom lone pair to interact with the cationic catalyst. We thus concluded that the relative strength of the cation-lone pair interactions is similar to dispersion interactions.

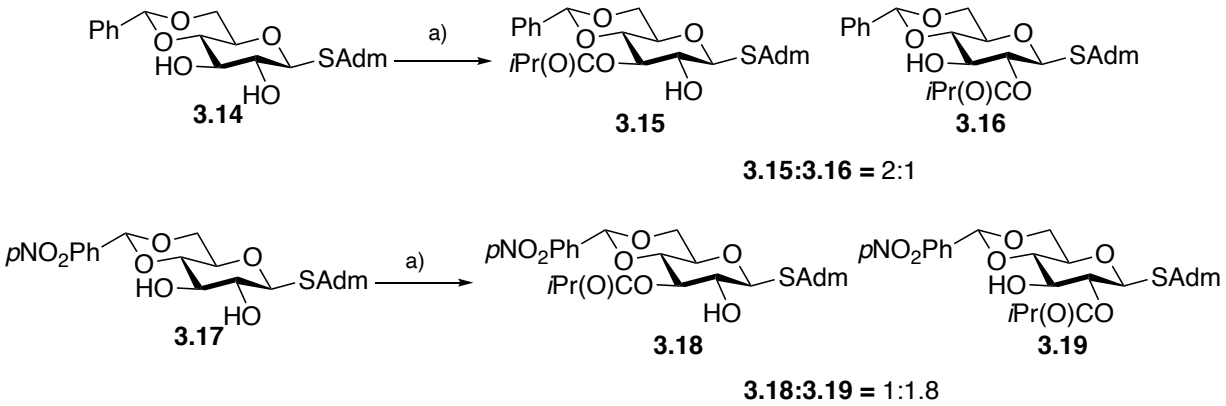

a) (*R*)-BTM **3.4** (10 mol %), isobutyric anhydride (2.5 eq), *i*Pr$_2$NEt (3.0 eq), $CHCl_3$, rt, Ar.

Scheme 3-9 Comparison of the relative strength of a cation-lone interaction versus dispersion interactions

3.5.4 Substrate scope

After having a better understanding of the origin of the selectivity, we proceeded to examine the scope of this method (**Table 3-10**). Using the mixed anhydride method,[45-47] various acyl groups can be introduced to final products **3.13e-i,** depending on the choice

of the carboxylic acid (entries 1-5). The magnitude of site-selectivity was >20:1 for acylation at the C2 hydroxyl of *S*-galactoside **3.12e**, in most cases, by employing the (*R*)-BTM catalyst, and isolated yields ranged from 81-95%. This method showed a tolerance for carboxylic acids of varying complexities, from acetic acid to those bearing alkene, alkyne, and ketone functionalities, which will be useful for further transformations.

β-*S*-Glucosides that featured a 4,6-*O*-benzylidene protecting group (e.g. **3.14** and **3.17**) did not show any selectivity for the acylation of the C2 OH group, due to the competing cation-lone pair interaction,[40] which facilitates acylation of the C3 OH group as previously discussed. We envisioned that applying an electron-withdrawing protecting group on the C4 OH would disable the cation-lone pair interaction between the C4 oxygen lone pair and the cationic acylated catalyst. Indeed, selective C2 OH acylation was observed for β-*S*-glucosides **3.20**, **3.22**, and **3.24**, with acetyl, benzoyl, and silyl protecting groups on the C4 and C6 OH groups (entries 6-8). The C2-selective acylation can be further extended to disaccharide **3.26** (entry 9).

In all of the above β-*S*-glucosides, low site-selectivity was observed when (*S*)-BTM catalyst was employed as the catalyst. This is what one would predict with our previously proposed model[40] because the lone pair on the C2-oxygen or C3-oxygen can interact with the cationic acylated catalyst when the C3 or C2 OH undergoes acylation, respectively.

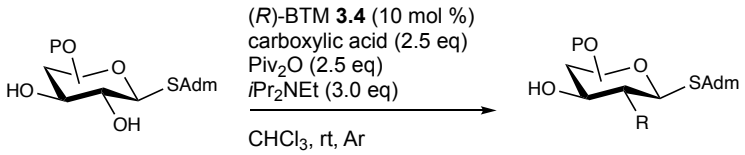

Entry	Substrate	Product	Yield	C2:C3:C2+C3
1	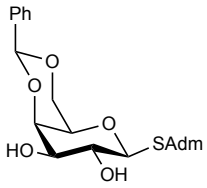 **3.12e**	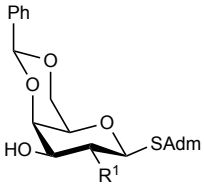 **3.13e** R^1 = OAc		>20:1
2		**3.13f** R^1 = OLev	88%	11:1 (1.5:1:0)
3		**3.13g** R^1 = 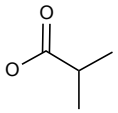	95%	>20:1
4		**3.13h** R^1 = 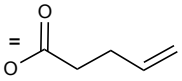	81%	10:1
5		**3.13i** R^1 = 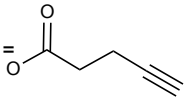	91%	>20:1
6	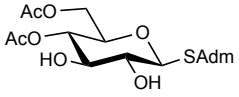 **3.20**	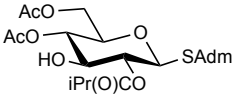 **3.21**	90%	>20:1:1 (5:1:1)
7	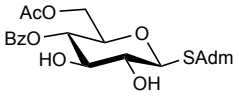 **3.22**	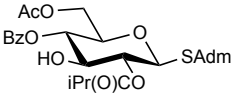 **3.23**	86%	>20:1:1 (2:1:2)
8	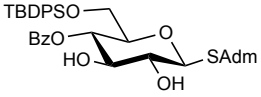 **3.24**	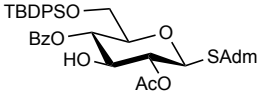 **3.25**	89%	>20:1:1 (1.5:1:1)
9	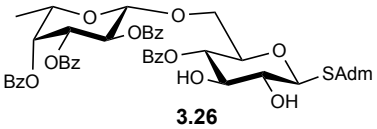 **3.26**	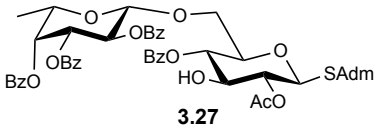 **3.27**	92%	>20:1:1 (2:1:1)

Table 3-10 Substrate scope for the site-selective acylation of *trans*-1,2-diols

We next examined the site-selectivity for the acylation of C2,C4-1,3-diols in galactoside **3.28**, arabinopyranoside **3.30**, and fucopyranoside **3.32** (**Table 3-11**, entries 1-3). In all cases, the C2 OH group was selectively acylated using a chiral BTM catalyst. Notably, (*S*)-BTM catalyst was needed for L-fucose **3.32**, while all other carbohydrates have D-configuration and require the (*R*)-BTM catalyst. Selective acylation of the C2 OH group was also observed in the presence of achiral DMAP catalyst, which reflects the intrinsically more reactive nature of the equatorial OH group over the axial OH group in these cases. However, the much higher selectivity observed using the (*R*)-BTM catalyst, except L-fucose **3.32**, indicates that the dispersion interactions between the acylated catalyst and the *S*Adm group is a significant contributor to the site-selectivity. We were pleased to find that good site-selectivity was observed for triol **3.34** and tetraol **3.36** (entries 4 and 5). No site-selectivity was observed using DMAP as the catalyst (see SI for details), but when using (*R*)-BTM as the catalyst, the C2 acylated product **3.35** was favored over the C2+C3 bisacylated compound in a 4.3:1 ratio. When tetraol **3.34** with a free primary hydroxyl group was subjected to the procedure, a ratio of 7:1 was observed for the formation of C2+C6 bisacylated product and C2 OH monoacylated product, suggesting that C2 OH was acylated first in the presence of the chiral catalyst.

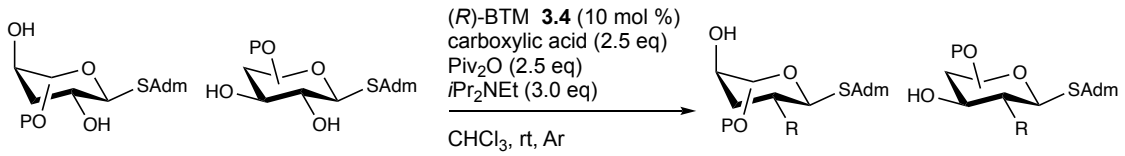

Entry	Substrate	Product	Yield	C2:C3/4:C2+C3/4[a]
1	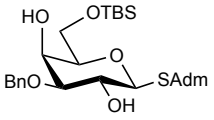 **3.28**	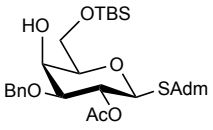 **3.29**	92%	>20:1 (7.3:0:1)
2	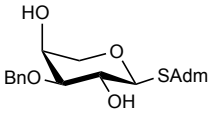 **3.30**	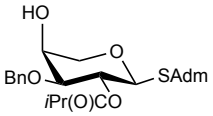 **3.31**	82%	>20:1 (4.7:1:1.2)
3	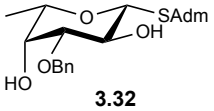 **3.32**	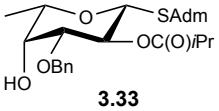 **3.33**	83%	>20:1[b] (5.4:1:1.4)
4	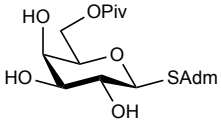 **3.34**	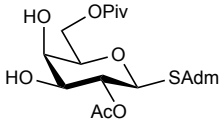 **3.35**	64%	4.3:1
5	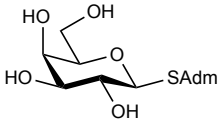 **3.36**	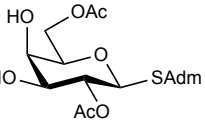 **3.37**	56%	*n.d.*

[a] C2/C3 or C2/C3/ C2+C3 for C2,C3-diols; C2/C4 or C2/C4/C2+C4 for C2,C4-diols. The values within parentheses are the ratios obtained when DMAP (10 mol %) was used as a catalyst.
[b] (*S*)-BTM was used as a catalyst for l-sugar.

Table 3-11 Substrate scope for the site-selective acylation of 1,3-diols and minimally protected monosaccharides

3.5.5 C2 acyl group promoted formation of β-glycosidic bonds

After successful development of the site-selective acylation method for *S*-glycosides, we envisioned that the acylated products could be readily activated and used as glycosyl donors for glycosylation. *S*-glycosides have been widely used for oligosaccharide

synthesis because they are easily synthesized, benchtop stable, orthogonal to many other glycosyl donors, and easily activated for glycosylation.[41, 42] Unfortunately, many of the thiols used to make *S*-glycosides result in pervasive and unpleasant odors. 1-Adamantanethiol, however, is a solid, odorless thiol, making it attractive for the synthesis of *S*-glycosides.[48] Furthermore, adamantyl-substituted *S*-glycosides avoid unwanted aglycon transfer reactions observed between trichloroimidate glycosyl donors and thioglycoside acceptors,[49] and they are more reactive than common thioglycoside donors, including *S*-phenyl.[50, 51] Thus, adamantyl-substituted *S*-glycosides can not only direct site-selective acylation, but they are also preferred glycosyl donors to make complex glycans.

Using adamantyl-substituted *S*-glycosides with a C2-acyl group provided an inherent driving force for the formation of a β-glycosidic bond via neighboring group participation. C2 acyl product **3.13g** was protected at C3 with a benzoyl group to provide **3.38** as our model glycosyl donor (**Table 3-12**). In four of the six glycosylations, only the β-anomer was obtained, and the other two glycosylations still produced the β-anomer as the major product. These results demonstrate the ability of *S*-glycosides to serve as glycosyl donors for glycosyl acceptors of varying complexity and preferentially form β-glycosidic bonds.

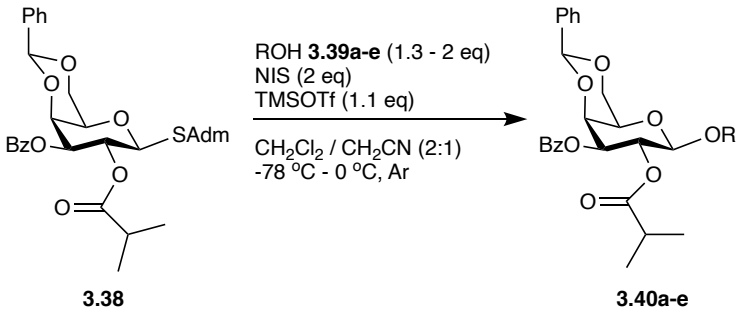

3.38 **3.40a-e**

Entry	ROH **3.39**	Yield	Ratio β:α
1	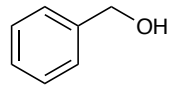 **3.39a**	81%	β only
2	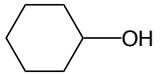 **3.39b**	51%	β only
3	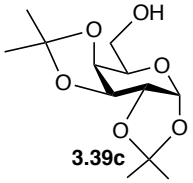 **3.39c**	58%	β only

Entry	ROH **3.37**	Yield	Ratio β:α
4	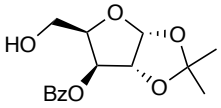 **3.39d**	β 58% α 9%	6.5 : 1
5	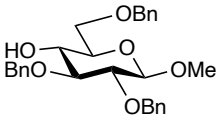 **3.39e**	73%	β only
6	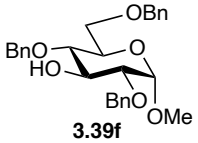 **3.39f**	β 62% α 13%	5.3 : 1

Table 3-12 Demonstration of ability of S-glycoside to promote b-glycosidic bond formation by the presence of a C2 acyl group

3.5.6 Streamlined synthesis of an oligosaccharide

We next evaluated the site-selective acylation method's ability to streamline the assembly of oligosaccharides. The presence of particular glycolipids can stimulate natural killer T cells to release cytokines, which then trigger proinflammatory and immunomodulatory responses.[52, 53] One glycolipid of particular importance is isoglobotrihexosylceramide **3.41**, which has been shown to be an antigen for natural killer T cells.[54] Our site-selective acylation protocol provides a streamlined method to obtain the protected trisaccharide core **3.42** of isoglobotrihexosylceramide (**Figure 3-13**).

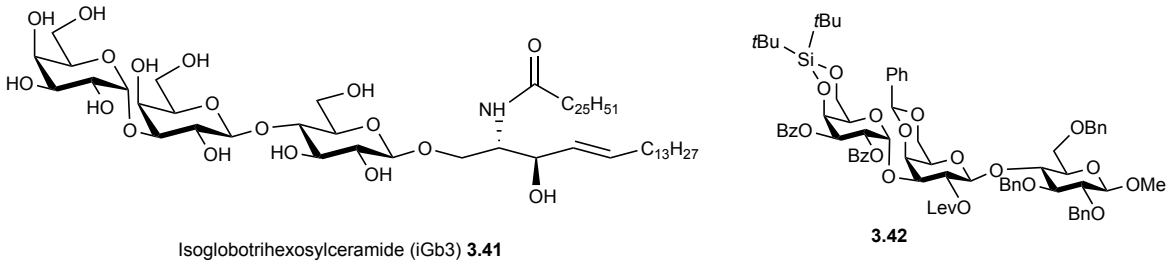

Figure 3-13 Glycolipid isoglobotrihexosylceramide and the protected carbohydrate backbone of isoglobotrihexosylceramide

Without site-selective acylation, we estimate that the chemical synthesis of the protected core of isoglobotrihexosylceramide would take a minimum of 7 steps. This includes tedious protection and deprotection steps to go from **3.43** to access the middle galactoside building block **3.44** and late stage anomeric position manipulations to prepare **3.46** for the final glycosylation with **3.45** (**Scheme 3-14**).

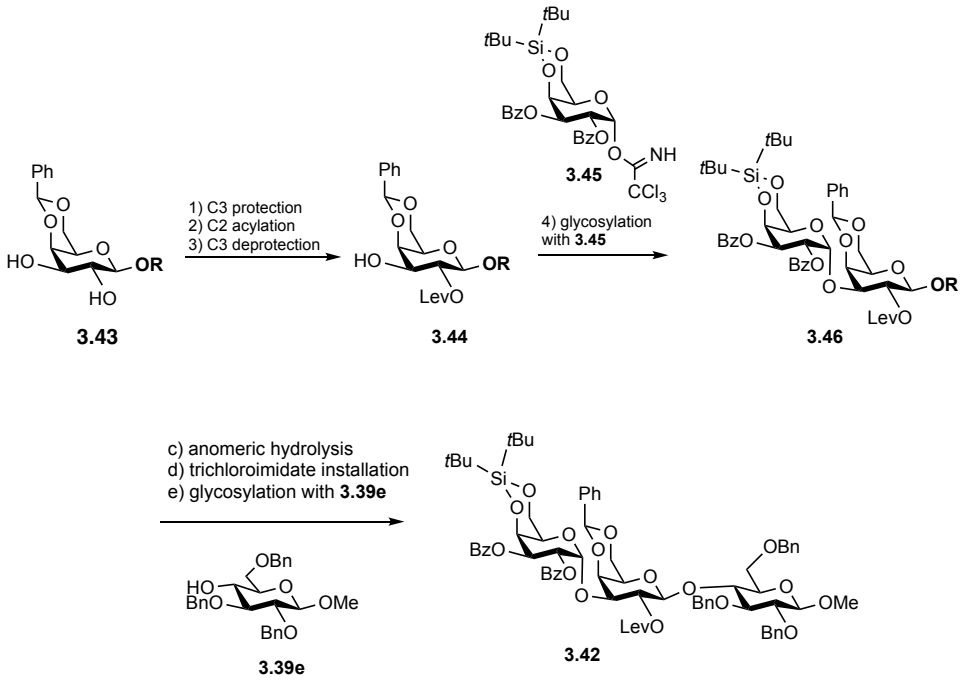

Scheme 3-14 Oligosaccharide synthesis without site-selective acylation

Our cation– lone pair directed acylation can selectively acylate the C2 hydroxy group of *O*-glycoside **3.47**. Unfortunately, the cation–lone pair directed methodology still required late-stage anomeric position manipulations to go from **3.49** to **3.50** (**Scheme 3-14**).

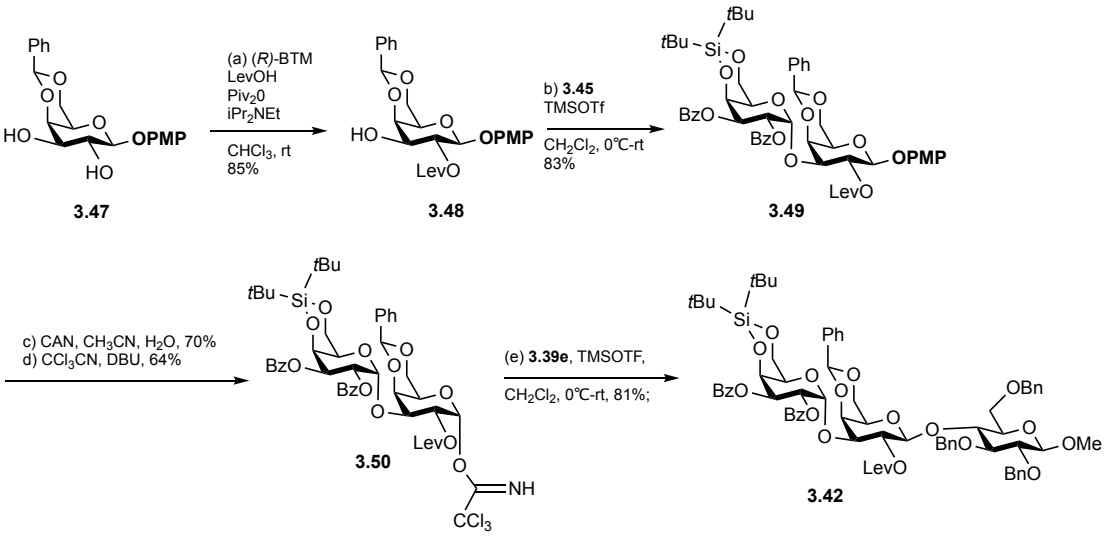

Scheme 3-14 Oligosaccharide synthesis using cation-lone pair directed site-selective acylation of *O*-glycosides to access **3.42**

Our S-adamantyl-directed acylation can also selectively acylate the C2 hydroxy group of **3.12e** in high selectivity. The advantage of using *S*-glycoside **3.12e** is the elimination of late-stage hydrolysis and installation of an anomeric leaving group (i.e. **3.49** to **3.50**), meaning we can directly glycosylate **3.51** to yield the same product **3.42**. We thus shortened the synthesis of **3.42** from five steps to three steps. We anticipate that this sequence of site-selective acylation and direct glycosylation can be used to construct oligosaccharides with various linkages.

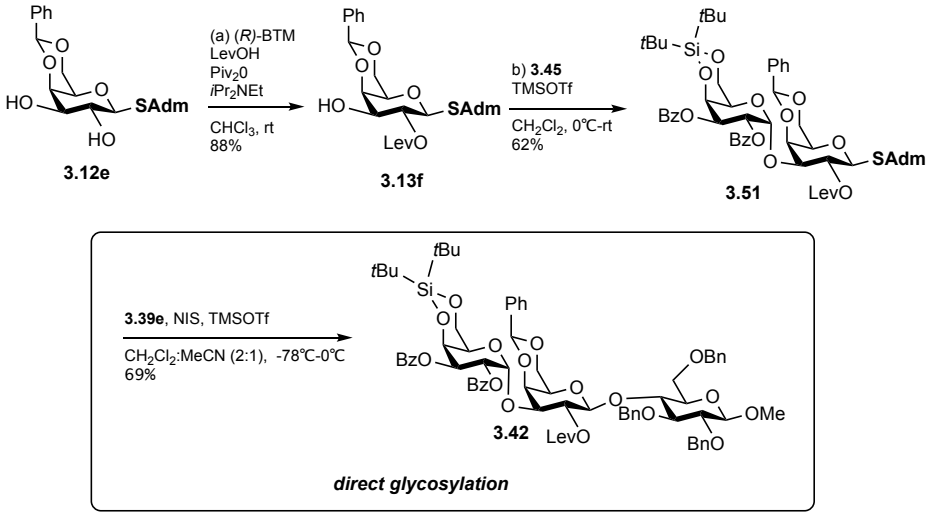

Scheme 3-15 Oligosaccharide synthesis using *S*-adamantyl directed site-selective acylation to access **3.42**

3.6 Conclusion

Using chiral catalysts and the adamantyl directing group, we have developed a site-selective acylation protocol for 1,2- trans-diols, 1,3-diols, triol, and even tetraol in various *S*-glycosides. DFT calculations indicated that dispersion interactions between the C-H bonds of the adamantyl group and the π system of the cationic acylated catalyst are the major contributor to the high degree of site selectivity. This dispersion-interaction-directed selectivity may have broad implications in many other chemical reactions. The *S*-adamantyl group directed C2-OH-selective acylation method eliminates tedious protection and deprotection steps often needed for site-selective functionalization and results in a stable, chemically orthogonal, readily activated glycosyl donor. The utility of the method was demonstrated in the streamlined synthesis of oligosaccharides. We

anticipate this method will find applications for the synthesis of many more complex carbohydrates.

3.7 Experimental Section

3.7.1 General remarks

All solvents were dried prior to use, all glassware was oven-dried, and all reactions were completed under an argon atmosphere, unless noted otherwise. Thin layer chromatography was performed using pre-coated silica gel plates. Flash column chromatography was performed using a TeleDyne ISCO CombiFlash system and the reported solvent systems. Infrared spectra (IR) were obtained on a Bruker Equinox 55 Spectrophotometer. ^{1}H and ^{13}C nuclear magnetic resonance spectra (NMR) were obtained on a Bruker Avance 400 MHz spectrometer recorded in ppm (δ) downfield of TMS (δ = 0) in $CDCl_3$ unless noted otherwise. Signal splitting patterns were described as singlet (s), doublet (d), triplet (t), quartet (q), quintet (quint), or multiplet (m), with coupling constants (*J*) in hertz. High resolution mass spectra (HRMS) were performed by Analytical Instrument Center at the School of Pharmacy or Department of Chemistry on an Electron Spray Injection (ESI) mass spectrometer. (RT = room temperature.)

3.7.2 General procedures

General procedure A for thioglycosylation of acetylated sugars with 1-adamantanethiol

To an oven-dried round-bottom (RB) flask equipped with a magnetic stir bar, commercially available acetylated sugars (1.0 equiv) and 1-adamantanethiol (1.4 equiv) were added and dissolved in dry CH_2Cl_2 to reach a reaction concentration of 0.2 M. The RB was then flushed with Argon, capped, and placed in a 0°C ice bath, allowing the contents of the RB flask to cool for ~20 minutes. Next, BF_3-OEt_2 (1.2 equiv, 48%) was added to the RB. The reaction mixture was stirred at 0°C until reaction completion (generally less than 2.5 hours). Note: Produced beta anomers will undergo anomerization to the alpha anomer if subjected to the reaction conditions for too long. As such, regularly checking the reaction for completion or near-completion is essential to avoid significant loss of product to anomerization. The reaction was quenched with sat. aq. $NaHCO_3$ and extracted with CH_2Cl_2. The combined organic layers were dried with Na_2SO_4, filtered, concentrated *in vacuo*, and purified by column chromatography.

General procedure B for the deacetylation of adamantyl 1-thio-β-D-pyranosides

To an oven-dried RB equipped with a magnetic stir bar, the acetylated adamantyl 1-thio-β-D-pyranoside (1.0 equiv) was dissolved in dry MeOH to a reaction concentration of 0.3 M, and solid NaOMe (0.1 equiv) was added. The RB was flushed with Argon, capped, and stirred at room temperature. Upon reaction completion, the reaction mixture was quenched with Amberlite CG-120 acidic resin to pH neutral. Filtration and subsequent

concentration *in vacuo* provided the crude material, which was carried forward without further purification.

General procedure C for the 4,6-*O*-benzylidene protection of unprotected adamantyl 1-thio-β-D-pyranosides

To an oven-dried RB equipped with a magnetic stir bar, the previously mentioned deacetylated adamantyl 1-thio-β-D-pyranoside (1.0 equiv, product from general procedure B) was suspended in dry MeCN to a reaction concentration of 0.3 M. Benzaldehyde dimethyl acetal (2.0 equiv) and (*S*)-(+)-10-camphorsulfonic acid (CSA) (0.2 equiv) were added sequentially to the RB, and the RB was flushed with Argon and capped with a septum. The RB was then placed in an 80°C oil bath and allowed to stir until reaction completion. The reaction was quenched with Et_3N to pH neutral. The quenched reaction mixture was then concentrated *in vacuo*, and the crude product was purified via column chromatography.

General procedure D for the site-selective acylation of thioglycosides using the anhydride method (isobutyric anhydride) and (*R*)-BTM or (*S*)-BTM:

To an oven-dried vial equipped with a magnetic stir bar, differentially protected adamantyl 1-thio-β-D-pyranoside diol substrates (1.0 equiv) were dissolved in dry amylene-stabilized chloroform (dried with 4 Å molecular sieves prior to use) to a reaction concentration of 0.1 M. (*R*)-BTM *or* (*S*)-BTM (10 mol %) and *N*,*N*-diisopropylethylamine (aka Hünig's base, DIPEA, iPr_2NEt) (3.0 equiv) were added sequentially, followed by dropwise addition of isobutyric anhydride (2.5 equiv). The reaction mixture was stirred at room temperature until reaction completion. 1 mL of methanol per 0.1 mmol of substrate was added to

quench the reaction. After the quenched reaction mixture had stirred for 10 min, 3 mL of saturated ammonium chloride was added per 0.1 mmol of substrate. The aqueous phase was extracted with CH_2Cl_2 (3×5 mL). The combined organic layers were dried over Na_2SO_4, filtered and concentrated *in vacuo*. The crude material was purified by column chromatography (hexane:ethyl acetate).

General procedure E for the site-selective acylation of thioglycosides using the *mixed* anhydride method (pivalic anhydride and carboxylic acid) and (*R*)-BTM or (*S*)-BTM:

To an oven-dried vial equipped with a magnetic stir bar, differentially protected adamantyl 1-thio-β-D-pyranoside diol substrates (1.0 equiv) were dissolved in dry amylene-stabilized chloroform (dried with 4 Å molecular sieves prior to use) to a reaction concentration of 0.1 M. (*R*)-BTM *or* (*S*)-BTM (10 mol %), *N*,*N*-diisopropylethylamine (aka Hünig's base, DIPEA, *i*Pr_2NEt) (3.0 equiv), and carboxylic acid (2.5 equiv) were added sequentially, followed by dropwise addition of pivalic anhydride (2.5 equiv). The reaction mixture was stirred at room temperature until reaction completion. 1 mL of methanol per 0.1 mmol of substrate was added to quench the reaction. After the quenched reaction mixture had stirred for 10 min, 3 mL of saturated ammonium chloride was added per 0.1 mmol of substrate. The aqueous phase was extracted with CH_2Cl_2 (3×5 mL). The combined organic layers were dried over Na_2SO_4, filtered and concentrated *in vacuo*. The crude material was purified by column chromatography (hexane:ethyl acetate).

General procedure F for benzylation of pyranosides with a C3 equatorial hydroxyl group

To an oven dried vial equipped with a magnetic stir bar, C2, C3, C4 triol adamantyl 1-thio-β-D-pyranoside substrates (1.0 equiv) were dissolved in MeCN to a reaction concentration of 0.3 M. Then, Ag_2O (0.6 equiv), TBAB (0.1 equiv), $Fe(dibm)_3$ (0.1 equiv), and BnBr (1.5 equiv) were added sequentially. The vial was flushed with Argon, capped with a septum, and stirred in a 40°C oil bath overnight. Upon reaction completion, the crude reaction mixture was directed purified via column chromatography.

3.7.3 Characterization Data

Preparation of **3.1** – **3.11** was done according to literature procedures.[40]

Preparation of **3.12a** was done according to literature procedures.[55]

Preparation of **3.12b-d** was done according general procedure A, except the appropriate thiol nucleophile was used instead of 1-adamantanethiol.

Preparation of **adamantyl 4,6-*O*-benzylidene-1-thio-β-D-galactopyranoside (3.12e)**

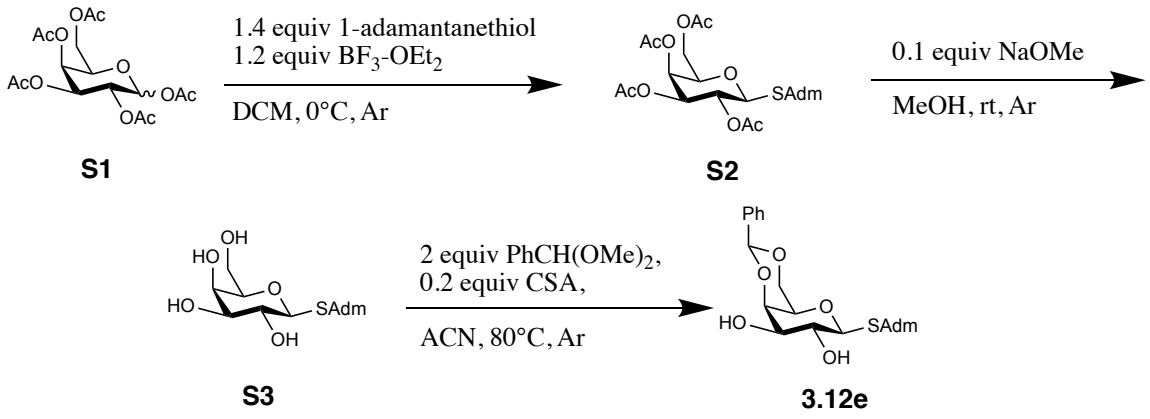

Following general procedure A, commercially available **S1** (2.0g, 5.12 mmol), 1-adamantanethiol (1222 mg, 1.4 equiv, 7.26 mmol), dry CH_2Cl_2 (10 mL), and BF_3-OEt_2 (1.45 mL, 1.2 equiv, 5.64 mmol) were used to produce **S2** as a white foam (2.19 g, 86%). The experimental NMR spectra matched those provided in the literature.[49]

3.12e was produced following general procedures B and C. General procedure B used **S2** (2.19 g, 4.4 mmol), dry MeOH (14 mL), and solid NaOMe (23.8 mg, 0.44 mmol). General procedure C used some of the tetra-ol intermediate **S3** (890 mg, 2.69 mmol), dry MeCN (9 mL), benzaldehyde dimethyl acetal (807 µL, 2 equiv, 5.38 mmol), and (*S*)-(+)-

10-camphorsulfonic acid (CSA) (125 mg, 0.2 equiv, 0.54 mmol). Product **3.12e** was obtained as an amorphous solid (850 mg, 76%).

^{1}H NMR (400 MHz, $CDCl_3$) δ 7.47 (dd, *J* = 6.5, 2.9 Hz, 2H), 7.37–7.30 (m, 3H), 5.50 (s, 1H), 4.48 (d, *J* = 9.0 Hz, 1H), 4.29 (d, *J* = 12.5 Hz, 1H), 4.22 (d, *J* = 2.5 Hz, 1H), 4.00 (dd, *J* = 12.5, 1.6 Hz, 1H), 3.60 - 3.70 (m, 2H), 3.48 (s, 1H), 2.68 (d, *J* = 7.0 Hz, 1H), 2.58 (s, 1H), 2.09 – 1.94 (m, 6H), 1.89 (d, *J* = 12.0 Hz, 3H), 1.75 – 1.62 (m, 6H).

^{13}C NMR (101 MHz, $CDCl_3$) δ 137.7, 129.4, 128.3 (2C), 126.7 (2C), 101.6, 82.4, 75.7, 74.0, 70.2, 69.9, 69.6, 46.7, 44.3 (3C), 36.3 (3C), 29.9 (3C).

IR (neat) v: 3412, 2964, 2905, 2850, 2360, 2335, 1721, 1692, 1630, 1451, 1364, 1260, 1164, 1099, 1028, 816, 756, 698.

HRMS (ESI) m/z calculated for $C_{23}H_{30}O_5SNa$ $(M+Na)^+$ 441.1712, found 441.1691.

Preparation of **adamantyl 4,6-*O*-benzylidene-1-thio-β-D-glucopyranoside (3.14)**

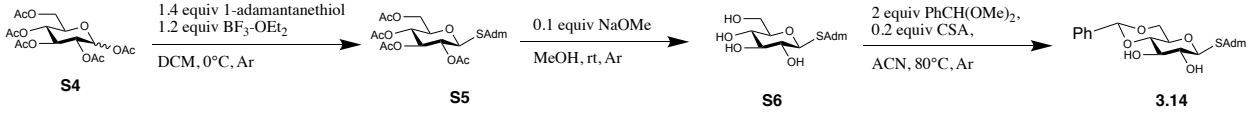

Using commercially available **S4** (2.0 g, 1.0 equiv, 5.12 mmol), 1-adamantanethiol (1222 mg, 1.4 equiv, 7.26 mmol), dry CH_2Cl_2 (10mL), and BF_3-OEt_2 (1.45 mL, 1.2 equiv, 5.64 mmol), **S5** (2.19 g, 86%, white foam) was produced following general procedure A. The experimental NMR spectra matched those provided in the literature.[44] Using **S5** (2.19 g), NaOMe (23.8 mg), and MeOH (11 mL), **S6** (1055 mg, 73%, white solid) was produced following general procedure B and was carried forward for benzylidene protection without further purification.

In an oven-dried RB, **S6** (0.5 g, 1.51 mmol, 1 equiv.) was dissolved in MeCN (10 mL). Then, benzaldehyde dimethyl acetal (0.273 mL, 1.82 mmol, 1.2 equiv) and (*S*)-(+)-10-camphorsulfonic acid (CSA) (70 mg, 0.302 mmol, 0.2 equiv) were added sequentially. The reaction mixture was stirred at 80 ºC for 2 hours. Then, the reaction was cooled down to room temperature and quenched with Et_3N to pH neutral. The reaction contents were transferred to a separatory funnel, followed by the addition of water and ethyl acetate. Upon extraction, the combined organic phase was washed with water, followed by brine. The organic layers were dried over Na_2SO_4, filtered and concentrated *in vacuo*. The crude material was purified by column chromatography (hexane:ethyl acetate – 5:1 to 3:1 to 4:3) to provide **3.14** (338 mg, 53%) as a white foam. NMR spectral data for **3.14** was in accordance with the literature.[44]

---

adamantyl 4,6-*O*-benzylidene-3-*O*-isobutyryl-1-thio-β-D-glucopyranoside (3.15)

adamantyl 4,6-*O*-benzylidene-2-*O*-isobutyryl-1-thio-β-D-glucopyranoside (3.16)

Following general procedure D, **3.14** (50 mg, 0.119 mmol, 1 equiv), dry amylene-stabilized chloroform (1 mL, dried with 4 A molecular sieves prior to use), (*R*)-BTM (3 mg, 0.012 mmol, 0.1 equiv), *i*Pr_2NEt (0.063 mL, 0.358 mmol, 3.0 equiv) and isobutyric anhydride (0.051 mL, 0.30 mmol, 2.5 equiv) were used. Products **3.16** (20 mg) and **3.15** (36 mg) were both obtained as a light-yellow foam with a total yield of 97%. (**3.16/3.15**: 1/1.8)

adamantyl 4,6-*O*-benzylidene-3-*O*-isobutyryl-1-thio-β-D-glucopyranoside (3.15)

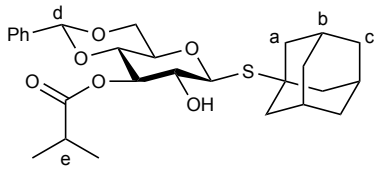

^{1}H NMR (400 MHz, $CDCl_3$) δ 7.41 (d, 2H, *J* = 8.8 Hz, 2×H-Ar), 7.35-7.33 (m, 3H, 3×H-Ar), 5.50 (s, 1H, H-d), 5.28 (t, 1H, *J* = 9.2 Hz, H-3), 4.69 (d, 1H, *J* = 9.3 Hz, H-1), 4.33 (dd, 1H, *J* = 10.5, 4.5 Hz, H-6), 3.77 (t, 1H, *J* = 10.0 Hz, H-6), 3.66 (t, 1H, *J* = 9.3 Hz, H-4), 3.60 (m, 1H, H-5), 3.50 (t, 1H, *J* = 9.2 Hz, H-2), 2.60 (m, 1H, H-e), 2.08 (m, 3H, 3×H-b), 1.97 (m, 3H, 3×H-c), 1.88 (m, 3H, 3×H-c), 1.71 (m, 6H, 6×H-a), 1.20-1.16 (m, 6H, 2×CH_3)

^{13}C NMR ($CDCl_3$, 101 MHz): δ176.9 ($CH(CH_3)_2\underline{C}O$), 148.4 (C^{quat}), 143.5 ($C^{tert.}$), 127.4 (2C) (2×$C^{tert.}$), 123.6 (2C) (2×C^{tert}), 99.9 (C-d), 83.4 (C-1), 78.8 (C-4), 73.9 (C-3), 72.0 (C-2), 70.5 (C-5), 68.9 (C-6), 47.2 (S-$\underline{C}$), 44.3(3C) (3×C-c), 36.1(3C) (3×C-a), 34.2 (C-e), 29.9(3C) (3×C-b), 19.2 (CH_3), 19.0 (CH_3)

IR (neat) v: 3497, 2975, 2907, 2851, 23560, 1739, 1469, 1265, 1190, 1155, 1073, 1041, 981, 734, 698

HRMS (ESI): Calculated for $C_{27}H_{36}O_6SNa$ $(M+Na)^+$: 511.2124; Found: 511.2116

adamantyl 4,6-*O*-benzylidene-2-*O*-isobutyryl-1-thio-β-D-glucopyranoside (3.16)

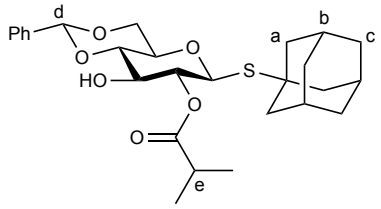

^{1}H NMR (400 MHz, $CDCl_3$) δ 7.49-7.47 (m, 2H, 2×H-Ar), 7.39-7.36 (m, 3H, 3×H-Ar), 5.54 (s, 1H, H-d), 4.88 (t, 1H, *J* = 9.4 Hz, H-2), 4.76 (d, 1H, *J* = 9.8 Hz, H-1), 4.32 (dd, 1H, *J* = 10.5, 4.9 Hz, H-6), 3.92 (t, 1H, *J* = 9.0 Hz, H-3), 3.79 (t, 1H, *J* = 10.5 Hz, H-6), 3.60 (t, 1H, *J* = 9.4 Hz, H-4), 3.52 (m, 1H, H-5), 2.60 (m, 1H, H-e), 2.06 (m, 3H, 3×H-b), 1.93 (m, 3H, 3×H-c), 1.84 (m, 3H, 3×H-c), 1.70 (m, 6H, 6×H-a), 1.24-1.20 (m, 6H, 2×CH_3)

^{13}C NMR ($CDCl_3$, 101 MHz): δ176.2 ($CH(CH_3)_2\underline{C}O$), 137.0 ($C^{quat.}$), 129.3 ($C^{tert.}$), 128.4 (2C) (2×$C^{tert.}$), 126.3 (2C) (2×C^{tert}), 101.9 (C-d), 80.8 (C-4), 80.5 (C-1), 73.9 (C-3), 72.3 (C-2), 70.0 (C-5), 68.7 (C-6), 46.4 (S-$\underline{C}$), 44.1(3C) (3×C-c), 36.1(3C) (3×C-a), 34.1 (C-e), 29.8(3C) (3×C-b), 19.1 (CH_3), 18.9 (CH_3)

IR (neat) v: 3449, 2920, 2851, 2360, 1739, 1454, 1385, 1246, 1152, 1093, 1042, 994, 735, 698

HRMS (ESI): Calculated for $C_{27}H_{36}O_6SNa$ $(M+Na)^+$: 511.2124; Found: 511.2111

Preparation of **adamantyl 4,6-*O*-(4-nitrophenyl)methylene-1-thio-β-D-glucopyranoside (3.17)**

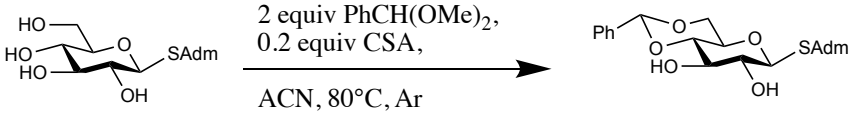

S7 **3.17**

In an oven-dried RB, **S7** (0.5 g, 1.51 mmol, 1 equiv) was dissolved in dioxane (10 mL). 4-nitrobenzaldehyde (274 mg, 1.82 mmol, 1.2 equiv) was added, followed by the addition of concentrated sulfuric acid (0.5 mL). The reaction mixture was stirred at room

temperature for 3 hours. Then, it was poured into sat. aq. $NaHCO_3$ to neutralize the acid. The reaction contents were transferred to a separatory funnel, followed by the addition of water and ethyl acetate. Upon extraction, the combined organic phase was washed with water, followed by brine. The organic layer was dried over Na_2SO_4, filtered and concentrated *in vacuo*. The crude material was purified by column chromatography (CH_2Cl_2/MeOH : 99/1 to 98/2) to provide **3.17** (338 mg, 53%) as a yellow foam.

^{1}H NMR (400 MHz, $CDCl_3$) δ 8.23 (d, 2H, *J* = 8.8 Hz, 2×H-Ar), 7.68 (d, 2H, *J* = 8.7 Hz, 2×H-Ar), 5.63 (s, 1H, H-d), 4.64 (d, 1H, *J* = 9.9 Hz, H-1), 4.35 (dd, 1H, *J*= 10.5, 4.8 Hz, H-6), 3.88 (t, 1H, *J* = 8.6 Hz, H-3), 3.79 (t, 1H, H-6), 3.63 (t, 1H, *J* = 9.2 Hz, H-4), 3.55 (m, 1H, H-5), 3.42 (t, 1H, *J* = 9.1 Hz, H-2), 2.72 (d, 1H, *J* = 1.7 Hz, OH), 2.53 (d, 1H, *J* = 1.5 Hz, OH), 2.09 (m, 3H, 3×H-b), 1.98 (m, 3H, 3×H-c), 1.94 -1.82 (m, 3H, 3×H-c), 1.70 (m, 6H, 6×H-a).

^{13}C NMR ($CDCl_3$, 101 MHz): δ 148.6, 143.5, 127.7(2C) (2×$C^{tert.}$), 123.7(2C) (2×C^{tert}), 100.4 (C-d), 82.8 (C-4), 80.5 (C-1), 74.6 (C-3), 73.5 (C-2), 70.3 (C-5), 68.9 (C-6), 47.1 (S-C), 44.3 (3C) (3×C-c), 36.2 (3C) (3×C-a), 29.9(3C) (3×C-b).

IR (neat) v: 3455, 2970, 2907, 2851, 1738, 1524, 1349, 1300, 1228, 1102, 1077, 1040, 855, 735, 702

HRMS (ESP): Calculated for $C_{23}H_{29}NO_7SNa$ $(M+Na)^+$: 486.1557; Found: 486.1550

---

adamantyl 4,6-*O*-(4-nitrophenyl)methylene-3-*O*-isobutyryl-1-thio-β-D-glucopyranoside (3.18)

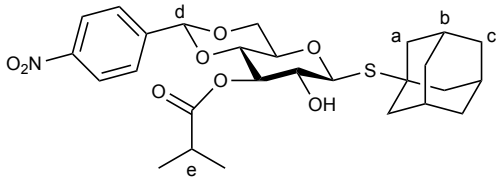

^{1}H NMR (400 MHz, $CDCl_3$) δ 8.20 (d, 2H, *J* = 8.8 Hz, 2×H-Ar), 7.59 (d, 2H, *J* = 8.8 Hz, 2×H-Ar), 5.56 (s, 1H, H-d), 5.29 (t, 1H, *J* = 9.2 Hz, H-3), 4.69 (d, 1H, *J* = 9.9 Hz, H-1), 4.36 (dd, 1H, *J*= 10.7, 5.0 Hz, H-6), 3.79 (t, 1H, *J* = 9.9 Hz, H-6), 3.67 (t, 1H, *J* = 9.5 Hz, H-4), 3.60 (m, 1H, H-5), 3.51 (t, 1H, *J* = 9.5 Hz, H-2), 2.61 (m, 1H, H-e), 2.08 (m, 3H, 3×H-b), 1.97 (m, 3H, 3×H-c), 1.87 (m, 3H, 3×H-c), 1.70 (m, 6H, 6×H-a), 1.17-1.15 (m, 6H, 2×CH_3)

^{13}C NMR ($CDCl_3$, 101 MHz): δ176.9 ($CH(CH_3)_2\underline{C}O$), 148.4, 143.5, 127.3 (2C) (2×$C^{tert.}$), 123.6 (2C) (2×C^{tert}), 99.8 (C-d), 83.4 (C-1), 78.8 (C-4), 73.9 (C-3), 71.2 (C-2), 70.5 (C-5), 68.9 (C-6), 47.19 (S-$\underline{C}$), 44.3 (3C) (3×C-c), 36.1 (3C) (3×C-a), 34.2 (C-e), 29.90(3C) (3×C-b), 19.2 (CH_3), 19.0 (CH_3)

IR (neat) v: 3462, 2970, 2917, 2851, 1738, 1524, 1349, 1229, 1203, 1076, 1015, 854, 834, 734, 701

HRMS (ESI): Calculated for $C_{27}H_{35}NO_8SNa$ $(M+Na)^+$: 556.1975; Found: 556.1968

Following general procedure D, **3.17** (50 mg, 0.108 mmol, 1 equiv), dry amylene-stabilized chloroform (1 mL, dried with 4 Å molecular sieves prior to use), (*R*)-BTM (2.72 mg, 0.011 mmol, 0.1 equiv), *i*Pr_2NEt (0.056 mL, 0.323 mmol, 3.0 equiv) and isobutyric anhydride (0.046 mL, 0.27 mmol, 2.5 equiv) were used. Products **3.19** (30 mg) and **3.18** (16 mg) were both obtained as a light-yellow foam with a total yield of 83%. (**3.19**/**3.18**: 2/1)

adamantyl 4,6-*O*-(4-nitrophenyl)methylene-2-*O*-isobutyryl-1-thio-β-D-glucopyranoside (3.19)

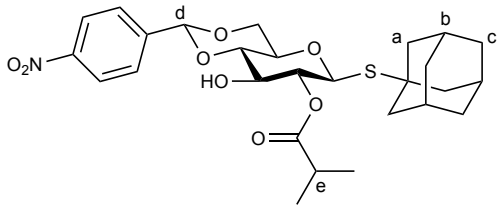

^{1}H NMR (400 MHz, $CDCl_3$) δ 8.23 (d, 2H, *J* = 8.4 Hz, 2×H-Ar), 7.68 (d, 2H, *J* = 8.5 Hz, 2×H-Ar), 5.63 (s, 1H, H-d), 4.86 (t, 1H, *J* = 9.5 Hz, H-2), 4.76 (d, 1H, *J*= 10.0 Hz, H-1), 4.35 (dd, 1H, *J*= 10.7, 5.1 Hz, H-6), 3.94 (t, 1H, *J* = 9.0 Hz, H-3), 3.81 (t, 1H, *J*= 10.7 Hz, H-6), 3.64 (t, 1H, *J* = 9.4 Hz, H-4), 3.53 (m, 1H, H-5), 2.61 (m, 1H, H-e), 2.05 (m, 3H, 3×H-b), 1.94 (m, 3H, 3×H-c), 1.84 (m, 3H, 3×H-c), 1.70 (m, 6H, 6×H-a), 1.26-1.19 (m, 6H, 2×CH_3)

^{13}C NMR ($CDCl_3$, 101 MHz): δ176.6 ($CH(CH_3)_2\underline{C}O$), 148.5, 143.5, 127.6 (2C) (2×$C^{tert.}$), 123.6 (2C) (2×C^{tert}), 100.3 (C-d), 81.0 (C-4), 80.6 (C-1), 74.0 (C-3), 72.7 (C-2), 69.9 (C-5), 68.9 (C-6), 46.6 (S-$\underline{C}$), 44.3 (3C) (3×C-c), 36.2 (3C) (3×C-a), 34.2 (C-e), 29.88(3C) (3×C-b), 19.2 (CH_3), 19.0 (CH_3)

IR (neat) v: 3457, 2970, 2908, 2851, 1738, 1524, 1348, 1216, 1152, 1092, 854, 834, 734, 701

HRMS (ESI): Calculated for $C_{27}H_{36}NO_8S$ $(M+Na)^+$: 534.2156; Found: 534.2129

Preparation of **adamantyl 4,6-*O*-benzylidene-1-thio-β-D-galactopyranoside (3.12e)**

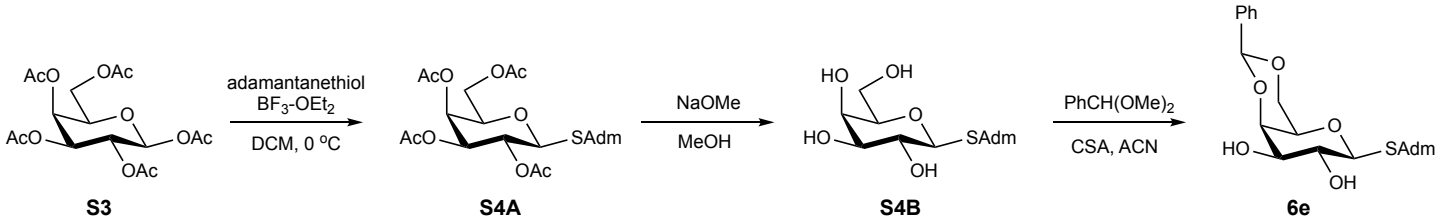

Following general procedure A, commercially available **S3** (2.0g, 5.12 mmol), 1-adamantanethiol (1222 mg, 1.4 equiv, 7.26 mmol), dry CH_2Cl_2 (10 mL), and BF_3-OEt_2 (1.45 mL, 1.2 equiv, 5.64 mmol) were used to produce **S4A** as a white foam (2.19 g, 86%). The experimental NMR spectra matched those provided in the literature.[49]

6e was produced following general procedures B and C. General procedure B used **S4A** (2.19 g, 4.4 mmol), dry MeOH (14 mL), and solid NaOMe (23.8 mg, 0.44 mmol). General procedure C used some of the tetra-ol intermediate **S4B** (890 mg, 2.69 mmol), dry MeCN (9 mL), benzaldehyde dimethyl acetal (807 µL, 2 equiv, 5.38 mmol), and (*S*)-(+)-10-camphorsulfonic acid (CSA) (125 mg, 0.2 equiv, 0.54 mmol). Product **6e** was obtained as an amorphous solid (850 mg, 76%).

^{1}H NMR (400 MHz, $CDCl_3$) δ 7.47 (dd, *J* = 6.5, 2.9 Hz, 2H), 7.37–7.30 (m, 3H), 5.50 (s, 1H), 4.48 (d, *J* = 9.0 Hz, 1H), 4.29 (d, *J* = 12.5 Hz, 1H), 4.22 (d, *J* = 2.5 Hz, 1H), 4.00 (dd, *J* = 12.5, 1.6 Hz, 1H), 3.60 - 3.70 (m, 2H), 3.48 (s, 1H), 2.68 (d, *J* = 7.0 Hz, 1H), 2.58 (s, 1H), 2.09 – 1.94 (m, 6H), 1.89 (d, *J* = 12.0 Hz, 3H), 1.75 – 1.62 (m, 6H).

^{13}C NMR (101 MHz, $CDCl_3$) δ 137.7, 129.4, 128.3 (2C), 126.7 (2C), 101.6, 82.4, 75.7, 74.0, 70.2, 69.9, 69.6, 46.7, 44.3 (3C), 36.3 (3C), 29.9 (3C).

IR (neat) v: 3412, 2964, 2905, 2850, 2360, 2335, 1721, 1692, 1630, 1451, 1364, 1260, 1164, 1099, 1028, 816, 756, 698.

HRMS (ESI) m/z calculated for $C_{23}H_{30}O_5SNa$ $(M+Na)^+$ 441.1712, found 441.1691.

---

adamantyl 2-*O*-acetyl-4,6-*O*-benzylidene-1-thio-β-D-galactopyranoside (3.13e)

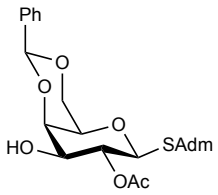

According to general procedure E, **3.12e** (37 mg, 0.09 mmol), (*R*)-BTM (2.3 mg, 10 mol %, 0.009 mmol), *i*Pr_2NEt (29 μL, 3.0 equiv, 0.18 mmol), AcOH (7 μL, 0.12 mmol), Piv_2O (20 μL, 0.12 mmol) and $CHCl_3$ (1 mL) were used. The product **3.13e** was isolated by column chromatography on silica gel (hexane:ethyl acetate - 1:1) as a colorless foam (37 mg, 90%).

^{1}H NMR (400 MHz, $CDCl_3$) δ 7.49 (dd, *J* = 6.4, 2.7 Hz, 2H), 7.44 – 7.29 (m, 3H), 5.51 (s, 1H), 5.01 (t, *J* = 9.7 Hz, 1H), 4.57 (d, *J* = 10.0 Hz, 1H), 4.30 (d, *J* = 12.4 Hz, 1H), 4.23 (d, *J* = 3.6 Hz, 1H), 4.01 (d, *J* = 12.4 Hz, 1H), 3.73 (d, *J* = 6.6 Hz, 1H), 3.48 (s, 1H), 2.09 (s, 3H), 2.06 – 1.82 (m, 9H), 1.73 – 1.62 (m, 6H).

^{13}C NMR (101 MHz, $CDCl_3$) δ 170.5, 137.5, 129.5, 128.4 (2C), 126.7 (2C), 101.8, 79.9, 75.9, 72.8, 70.9, 69.8, 69.4, 46.3, 44.1 (3C), 36.3 (3C), 29.9 (3C), 21.4.

IR (neat) v: 3456, 2962, 2918, 2850, 2364, 2335, 1735, 1693, 1452, 1370, 1234, 1138, 1099, 1062, 1043, 816, 758, 698.

HRMS (ESI) m/z calculated for $C_{25}H_{32}O_6SNa$ $(M+Na)^+$ 483.1817, found 483.1802.

---

adamantyl 4,6-*O*-benzylidene-2-*O*-4-oxopentanoyl-1-thio-β-D-galactopyranoside (3.13f)

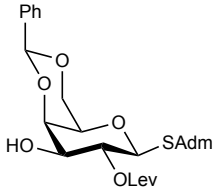

According to general procedure E, **3.12e** (42 mg, 0.1 mmol), (*R*)-BTM (2.5 mg, 0.01 mmol), *i*Pr_2NEt (50 μL, 3.0 equiv, 0.3 mmol), LevOH (26 μL, 2.5 equiv, 0.25 mmol), Piv_2O (43 μL, 2.5 equiv, 0.25 mmol) and $CHCl_3$ (1 mL) were used. The product **3.13f** was isolated by column chromatography on silica gel (hexane:ethyl acetate - 3:1) as a colorless foam (42 mg, 88%).

^{1}H NMR (400 MHz, $CDCl_3$) δ 7.54 – 7.42 (m, 2H), 7.41 – 7.27 (m, 3H), 5.50 (s, 1H), 5.02 (t, *J* = 9.7 Hz, 1H), 4.58 (d, *J* = 10.1 Hz, 1H), 4.21 – 4.31 (m, 2H), 4.00 (d, *J* = 12.2 Hz, 1H), 3.74 (dd, *J* = 9.4, 3.6 Hz, 1H), 3.47 (s, 1H), 2.72 – 2.80 (m, 2H), 2.58 - 2.64 (m, 2H), 2.14 (s, 3H), 2.06 – 1.81 (m, 9H), 1.75 – 1.60 (m, 6H).

^{13}C NMR (101 MHz, $CDCl_3$) δ 206.9, 172.3, 137.5, 129.4, 128.3 (2C), 126.7 (2C), 101.6, 79.8, 75.8, 72.7, 71.1, 69.7, 69.4, 46.3, 44.1 (3C), 38.3, 36.3 (3C), 30.0, 29.9 (3C), 28.4.

IR (neat) v: 3422, 2965, 2918, 2851, 2359, 2342, 1738, 1719, 1628, 1451, 1366, 1260, 1161, 1099, 1041, 817, 754, 698.

HRMS (ESI) m/z calculated for $C_{28}H_{36}O_7SNa$ $(M+Na)^+$ 539.2079, found 539.2068.

---

adamantyl 4,6-*O*-benzylidene-2-*O*-isobutyryl-1-thio-β-D-galactopyranoside (3.13g)

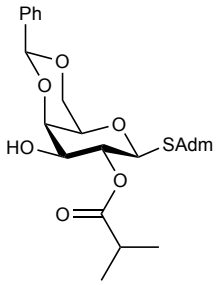

According to general procedure D, **3.12e** (621 mg, 1.48 mmol), (*R*)-BTM (37.8 mg, 0.15 mmol), *i*Pr$_2$NEt (775 μL, 3.0 equiv, 4.45 mmol), isobutyric anhydride (492 μL, 2.0 equiv, 2.96 mmol), and $CHCl_3$ (14.7 mL) were used. The product **3.13g** was isolated by column chromatography on silica gel (hexane:ethyl acetate - 3:1) as a colorless foam (633 mg, 87%).

^{1}H NMR (400 MHz, Chloroform-*d*) δ 7.54 – 7.47 (m, 2H), 7.39 – 7.33 (m, 3H), 5.53 (s, 1H), 5.05 (t, *J* = 9.7 Hz, 1H), 4.64 (d, *J* = 10.0 Hz, 1H), 4.31 (dd, *J* = 12.5, 1.5 Hz, 1H), 4.25 (d, *J* = 3.8 Hz, 1H), 4.03 (dd, *J* = 12.5, 1.9 Hz, 1H), 3.76 (dd, *J* = 9.4, 3.9 Hz, 1H), 3.50 (d, *J* = 1.9 Hz, 1H), 2.59 (hept, *J* = 7.0 Hz, 1H), 2.09 – 2.01 (m, 3H), 2.02 – 1.93 (m, 3H), 1.91 – 1.82 (m, 3H), 1.69 (d, *J* = 3.6 Hz, 6H), 1.22 (d, *J* = 7.3 Hz, 3H), 1.19 (d, *J* = 7.1 Hz, 3H).

^{13}C NMR (101 MHz, $CDCl_3$) δ 176.4, 137.4, 129.3, 128.2 (2C), 126.6 (2C), 101.5, 79.9, 75.8, 72.8, 70.2, 69.6, 69.3, 46.2, 44.1 (3C), 36.2 (3C), 34.1, 29.8 (3C), 19.1, 18.9.

IR (neat) v: 2980, 2903, 2852, 1741, 1455, 1399, 1365, 1242, 1300, 1244, 1188, 1157, 1093, 1079, 1054, 1043, 1027.

HRMS (ESI) m/z calculated for $C_{27}H_{36}O_6SNa$ $(M+Na)^+$ 511.2125, found 511.2113.

---

adamantyl 4,6-*O*-benzylidene-2-*O*-4-pentenoyl-1-thio-β-D-galactopyranoside (3.13h)

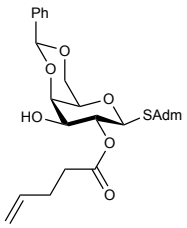

According to general procedure E, **3.12e** (42 mg, 0.1 mmol), (*R*)-BTM (2.5 mg, 10 mol %, 0.01 mmol), *i*Pr_2NEt (50 μL, 3.0 equiv, 0.3 mmol), 4-pentenoic acid (26 μL, 2.5 equiv, 0.25 mmol), Piv_2O (43 μL, 2.5 equiv, 0.25 mmol) and $CHCl_3$ (1 mL) were used. The product **3.13h** was isolated by column chromatography on silica gel (hexane:ethyl acetate - 2:1) as a colorless foam (41 mg, 81%).

^{1}H NMR (400 MHz, $CDCl_3$) δ 7.48 (dd, *J* = 6.4, 2.8 Hz, 2H), 7.45 – 7.30 (m, 3H), 5.93 – 5.78 (m, 1H), 5.51 (s, 1H), 5.14 – 4.93 (m, 3H), 4.59 (d, *J* = 10.1 Hz, 1H), 4.29 (d, *J* = 12.4 Hz, 1H), 4.23 (d, *J* = 3.7 Hz, 1H), 4.05 – 3.97 (m, 1H), 3.73 (dd, *J* = 9.4, 3.7 Hz, 1H), 3.48 (s, 1H), 2.47 – 2.35 (m, 5H), 2.07 – 1.81 (m, 9H), 1.73 – 1.62 (m, 6H).

^{13}C NMR (101 MHz, $CDCl_3$) δ 172.5, 137.5, 137.0, 129.4, 128.3 (2C), 126.7 (2C), 115.6, 101.7, 79.9, 75.9, 72.8, 70.8, 69.7, 69.4, 46.3, 44.2 (3C), 36.3 (3C), 33.8, 29.9 (3C), 28.9.

IR (neat) v: 3432, 2971, 2906, 2851, 2358, 2336, 1736, 1452, 1400, 1341, 1248, 1166, 1100, 1059, 999, 817, 758, 698.

HRMS (ESI) m/z calculated for $C_{28}H_{36}O_6SNa$ $(M+Na)^+$ 523.2130, found 523.2107.

---

adamantyl 4,6-*O*-benzylidene-2-*O*-4-pentynoyl-1-thio-β-D-galactopyranoside (3.13i)

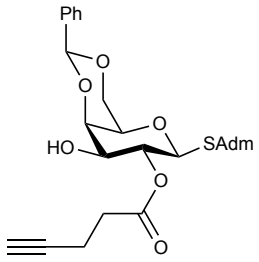

According to general procedure E, **3.12e** (42 mg, 0.1 mmol), (*R*)-BTM (2.5 mg, 10 mol%, 0.01 mmol), *i*Pr_2NEt (50 μL, 3.0 equiv, 0.3 mmol), 4-pentynoic acid (25 mg, 2.5 equiv, 0.25 mmol), Piv_2O (43 μL, 2.5 equiv, 0.25 mmol) and $CHCl_3$ (1 mL) were used. The product **3.13i** was isolated by column chromatography on silica gel (hexane:ethyl acetate – 2:1) as a colorless foam (45 mg, 91%).

^{1}H NMR (400 MHz, $CDCl_3$) δ 7.48 (m, 2H), 7.38 – 7.30 (m, 3H), 5.50 (s, 1H), 5.04 (t, *J* = 9.7 Hz, 1H), 4.58 (d, *J* = 10.1 Hz, 1H), 4.29 (dd, *J* = 12.4, 1.0 Hz, 1H), 4.23 (d, *J* = 3.6 Hz, 1H), 4.00 (dd, *J* = 12.5, 1.6 Hz, 1H), 3.74 (d, *J* = 6.7 Hz, 1H), 3.48 (s, 1H), 2.63-2.49 (m, 5H), 2.03-1.82 (m, 10H), 1.75 – 1.62 (m, 6H).

^{13}C NMR (101 MHz, $CDCl_3$) δ 171.2, 137.5, 129.4, 128.3 (2C), 126.7 (2C), 101.7, 82.7, 79.8, 75.8, 72.7, 71.1, 69.7, 69.4, 69.2, 46.3, 44.1 (3C), 36.3 (3C), 33.6, 29.9 (3C), 14.4.

IR (neat) v: 3440, 3307, 2966, 2906, 2850, 2363, 2335, 1740, 1451, 1401, 1370, 1259, 1165, 1098, 1042, 996, 899, 865, 816, 757, 698.

HRMS (ESI) m/z calculated for $C_{28}H_{34}O_6SNa$ $(M+Na)^+$ 521.1974, found 521.1973.

Preparation of thioglycosides **3.20**, **3.22**, **3.24** and **3.26**

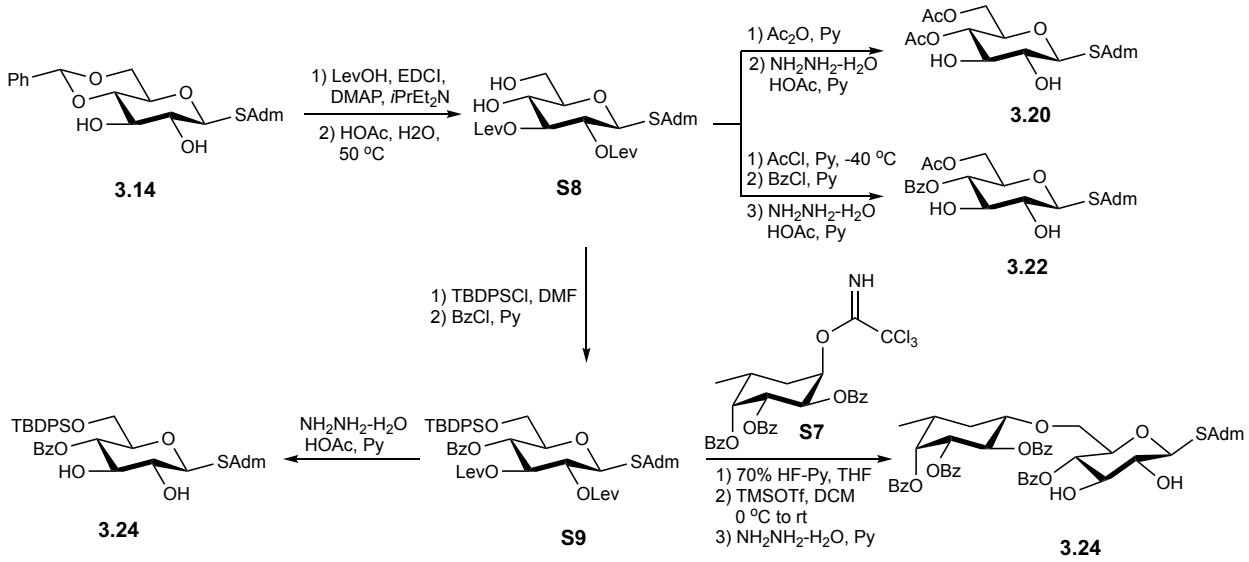

---

adamantyl 4,6-di-*O*-acetyl-1-thio-β-D-glucopyranoside (3.20)

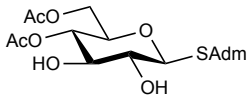

Diol **3.14**[1] (1.18 g, 2.82 mmol), LevOH (1.2 mL, 11.3 mmol), DMAP (138 mg, 1.13 mmol) and *i*Pr_2NEt (2.8 mL, 16.9 mmol) were dissolved in dry CH_2Cl_2 (10 mL), and then EDCI (2.2 g, 11.3 mmol) was added. After stirring overnight at room temperature, the reaction mixture was diluted with CH_2Cl_2, washed with water and brine, and dried over anhydrous Na_2SO_4. Filtration, concentration *in vacuo* and purification via column chromatography on silica gel (hexane:ethyl acetate - 1/1) afforded the intermediate (1.39 g, 80%).

The above intermediate (1.39 g, 2.26 mmol) was dissolved in HOAc (8 mL) and H_2O (2 mL). After stirring at 50 ^oC for 11 hours, the reaction mixture was cooled to room temperature and concentrated *in vacuo*. The crude residue was purified by column chromatography on silica gel (hexane:ethyl acetate - 1/1 to 0/1) to provide the diol **S8** (988 mg, 83%).

Diol **S8** (200 mg, 0.38 mmol) was dissolved in dry pyridine (1 mL). Ac_2O (0.11 mL, 1.14 mmol) was added. After stirring overnight at room temperature, the reaction mixture was quenched with methanol (0.3 mL) and concentrated in vacuo. The residue was purified by column chromatography on silica gel (hexane:ethyl acetate - 1/2) to provide the intermediate (199 mg, 86%).

The above intermediate (183 mg, 0.3 mmol) was dissolved in dry CH_2Cl_2 (3 mL). The reaction mixture was cooled to 0 ^oC. AcOH (1.3 mL) and pyridine (1.9 mL) were added, followed by the addition of NH_2NH_2-H_2O (0.12 mL, 2.4 mmol). After stirring for 5 hours, the reaction mixture was quenched with acetone (1 mL) and concentrated in vacuo. The residue was purified by silica gel column chromatography (hexane:ethyl acetate - 1/3) to afford the product **3.20** (82 mg, 66%) as a colorless foam.

^{1}H NMR (500 MHz, $CDCl_3$): δ 4.85 (t, *J* = 9.5 Hz, 1H), 4.48 (d, *J* = 9.5 Hz, 1H), 4.16-4.04 (m, 2H), 3.67-3.61 (m, 2H), 3.35 (t, *J* = 9.0 Hz, 1H), 2.07 (s, 3H), 2.00 (s, 3H), 2.00-1.84 (m, 9 H), 1.66-1.63 (m, 6H).

^{13}C NMR (126 MHz, $CDCl_3$) δ 170.9, 170.6, 82.0, 76.1, 75.6, 73.0, 70.5, 63.1, 46.8, 44.2 (3C), 36.2 (3C), 29.9 (3C), 21.0, 20.8.

IR (neat) v 3420, 2906, 2850, 1743, 1450, 1371, 1240, 1091, 1031, 756.

HRMS (ESI) m/z calculated for $C_{20}H_{30}O_7SNa$ $(M+Na)^+$ 437.1610, found 437.1589.

---

adamantyl 4,6-di-*O*-acetyl-2-*O*-isobutyryl-1-thio-β-D-glucopyranoside (3.21)

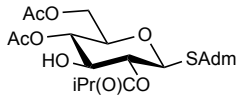

According to general procedure D, **3.20** (41 mg, 0.1 mmol), (*R*)-BTM (2.5 mg, 0.01 mmol), *i*Pr_2NEt (50 µl, 0.3 mmol), isobutyric anhydride (41 µL, 0.25 mmol) and $CHCl_3$ (1 mL) were used. The product **3.21** was isolated by column chromatography on silica gel (hexane:ethyl acetate - 1.5/1) as a colorless foam (43 mg, 90%).

^{1}H NMR (500 MHz, $CDCl_3$): δ 4.86 (t, *J* = 9.5 Hz, 1H), 4.76 (t, *J* = 9.5 Hz, 1H), 4.64 (d, *J* = 10.0 Hz, 1H), 4.17-4.09 (m, 2H), 3.73 (t, *J* = 9.5 Hz, 1H), 3.65-3.62 (m, 1H), 2.59-2.53 (m, 1H), 2.07 (s, 3H), 2.00 – 2.04 (m, 6H), 1.92-1.81 (m, 6 H), 1.70-1.63 (m, 6H). 1.18 (d, *J* = 7.5 Hz, 3H), 1.17 (d, *J* = 7.0 Hz, 3H).

^{13}C NMR (101 MHz, $CDCl_3$) δ 176.6, 170.9, 170.8, 80.0, 75.6, 75.5, 72.5, 71.4, 63.1, 46.4, 44.2 (3C), 36.3 (3C), 34.2, 29.9 (3C), 21.0, 20.9, 19.2, 18.9.

IR (neat) v: 3455, 3018, 2971, 2852, 2359, 2338, 1737, 1466, 1451, 1372, 1237, 1157, 1085, 1031, 803, 753, 666.

HRMS (ESI) m/z calculated for $C_{24}H_{36}O_8SNa$ $(M+Na)^+$ 507.2029, found 507.2012.

Preparation of **adamantyl 6-*O*-acetyl-4-*O*-benzoyl-1-thio-β-D-glucopyranoside (3.22)**

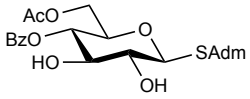

Diol **S8** (150 mg, 0.29 mmol) and pyridine (37 µL, 0.46 mmol) were dissolved in CH_2Cl_2 (3 mL). The reaction mixture was cooled to -40 ^oC. Acetyl chloride (23 µL, 0.32 mmol) in CH_2Cl_2 (1 mL) was added dropwise. The reaction mixture was allowed to warm to room temperature. After stirring for 3 hours, the reaction mixture was quenched with methanol (0.2 mL) and concentrated *in vacuo*. The residue was purified by silica gel column chromatography (hexane:ethyl acetate - 1/2) to give the intermediate (130 mg, 80%).

The above intermediate (130 mg, 0.23 mmol), DMAP (6 mg, 0.046 mmol) and Et_3N (128 µL, 0.92 mmol) were dissolved in dry CH_2Cl_2 (1 mL). BzCl (53 µL, 0.46 mmol) was added. After stirring at room temperature overnight, the reaction mixture was diluted with CH_2Cl_2, washed with saturated $NaHCO_3$ and brine. Filtration, concentration *in vacuo* and purification on silica gel column chromatography (hexane:ethyl acetate - = 1/1 to 1/2) gave the intermediate (136 mg, 90%).

The above intermediate (95 mg, 0.2 mmol) was dissolved in CH_2Cl_2 (2 mL), AcOH (0.8 mL) and pyridine (1.2 mL) were added. The reaction mixture was cooled to 0 ^oC. NH_2NH_2-H_2O (38 µL, 1.6 mmol) was added. After stirring at room temperature overnight, the reaction mixture was quenched with acetone (1 mL) and concentrated *in vacuo*. The

residue was purified by silica gel column chromatography (hexane:ethyl acetate - 1.3/1) to give the product **3.22** (57 mg, 83%) as a colorless foam.

^{1}H NMR (400 MHz, $CDCl_3$) δ 8.01 (d, *J* = 7.3 Hz, 2H), 7.56 (t, *J* = 7.4 Hz, 1H), 7.42 (t, *J* = 7.7 Hz, 2H), 5.12 (t, *J* = 9.6 Hz, 1H), 4.60 (d, *J* = 9.9 Hz, 1H), 4.23 – 4.11 (m, 2H), 3.8 – 3.9 (m, 2H), 3.55 (br s, 1H), 3.46 (t, *J* = 9.3 Hz, 1H), 3.18 (br s, 1H), 2.12 – 1.86 (m, 12H), 1.64 – 1.72 (m, 6H).

^{13}C NMR (101 MHz, $CDCl_3$) δ 170.8, 166.0, 133.5, 129.9 (2C), 129.3, 128.5 (2C), 82.0, 76.2, 75.5, 73.0, 71.5, 63.5, 46.7, 44.1 (3C), 36.2 (3C), 29.9 (3C), 20.7.

IR (neat) v: 3407, 3019, 2908, 2852, 1729, 1451, 1369, 1352, 1263, 1216, 1097, 1070, 1026, 711, 667.

HRMS (ESI) m/z calculated for $C_{25}H_{32}O_7SNa$ $(M+Na)^+$ 499.1766, found 499.1743.

---

adamantyl 6-*O*-acetyl-4-*O*-benzoyl-2-*O*-isobutyryl-1-thio-β-D-glucopyranoside (3.23)

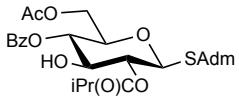

According to general procedure D, **3.22** (38 mg, 0.08 mmol), (*R*)-BTM (2.0 mg, 0.008 mmol), *i*Pr_2NEt (40 µL, 0.24 mmol), isobutyric anhydride (32 µL, 0.2 mmol) and $CHCl_3$ (0.8 mL) were used. The product **3.23** was isolated by column chromatography on silica gel (hexane:ethyl acetate - 2/1) as a colorless foam (37 mg, 86%).

^{1}H NMR (500 MHz, $CDCl_3$): δ 8.01 (d, *J* = 8.0 Hz, 2H), 7.56 (t, *J* = 7.5 Hz, 1H), 7.42 (t, *J* = 8.0 Hz, 2H), 5.12 (t, *J* = 10.0 Hz, 1H), 4.85 (t, *J* = 9.5 Hz, 1H), 4.73 (d, *J* = 10.5 Hz, 1H), 4.22-4.14 (m, 2H), 3.92 (t, *J* = 9.0 Hz, 1H), 3.85-3.81 (m, 1H), 2.60-2.52 (m, 1H), 2.03 (s, 3H), 1.96-1.83 (m, 9H), 1.71-1.65 (m, 6 H), 1.19 (d, *J* = 7.0 Hz, 3H), 1.17 (d, *J* = 7.0 Hz, 3H).

^{13}C NMR (126 MHz, $CDCl_3$) δ 176.5, 170.8, 166.3, 133.7, 130.0, 129.2, 128.7, 80.1, 75.6, 75.5, 72.5, 72.4, 63.5, 46.4, 44.2 (3C), 36.3 (3C), 34.2, 29.9 (3C), 20.8, 19.2, 18.9.

IR (neat) v: 3450, 2973, 2906, 2850, 2363, 2336, 1735, 1451, 1386, 1271, 1032, 713.

HRMS (ESI) m/z calculated for $C_{29}H_{38}O_8SNa$ $(M+Na)^+$ 569.2185, found 569.2162.

Preparation of **adamantyl 4-*O*-benzoyl-6-*O*-*tert*-butyldiphenylsilyl-1-thio-β-D-glucopyranoside (3.24)**

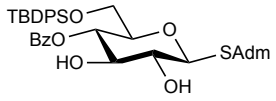

Diol **S8** (247 mg, 0.47 mmol) and imidazole (96 mg, 1.41 mmol) were dissolved in dry DMF (1 mL). The reaction mixture was cooled to 0 °C. TBDPSCl (0.14 mL, 0.52 mmol) was added dropwise. After stirring at 0 °C for 18 hours, the reaction mixture was diluted with ethyl acetate, washed with water and brine. The organic layer was dried over anhydrous Na_2SO_4, filtered and concentrated *in vacuo*. The residue was purified by silica gel column chromatography (hexane:ethyl acetate - = 1/1 to 1/1.5) to give the intermediate (324 mg, 90%).

The above intermediate (324 mg, 0.42 mmol), DMAP (11 mg, 0.084 mmol) and Et_3N (0.3 mL, 2.1 mmol) were dissolved in dry CH_2Cl_2 (1 mL). BzCl (0.1 mL, 0.85 mmol) was added. After stirring at room temperature overnight, the reaction mixture was diluted with CH_2Cl_2, washed with saturated $NaHCO_3$ and brine. The organic layer was dried over anhydrous Na_2SO_4, filtered and concentrated *in vacuo*. The residue was purified by silica gel column chromatography (hexane:ethyl acetate - 4/1 to 1/1) to give the intermediate **S9** (368 mg, 99%).

The above intermediate (200 mg, 0.23 mmol) was dissolved in dry CH_2Cl_2 (2.3 mL). AcOH (1 mL) and pyridine (1.5 mL) were added. The reaction mixture was cooled to 0 ^oC. 64% NH_2NH_2-H_2O (70 µL, 0.92 mmol) was added. After stirring at room temperature for 4 hours, the reaction mixture was quenched with acetone (1 mL) and concentrated *in vacuo*. The residue was purified by silica gel column chromatography (hexane:ethyl acetate - 1.5/1) to give the product **3.24** (133 mg, 86%) as a colorless foam.

^{1}H NMR (400 MHz, $CDCl_3$) δ 7.83 (d, *J* = 7.4 Hz, 2H), 7.56 (d, *J* = 6.7 Hz, 2H), 7.48 (dd, *J* = 11.5, 7.2 Hz, 3H), 7.31 (t, *J* = 7.7 Hz, 2H), 7.24-7.11 (m, 6H), 5.03 (t, *J* = 9.5 Hz, 1H), 4.57 (d, *J* = 9.8 Hz, 1H), 3.79-3.64 (m, 4H), 3.39 (t, *J* = 9.2 Hz, 1H), 1.97-1.87 (m, 9H), 1.61 (s, 6H), 0.90 (s, 9H).

^{13}C NMR (101 MHz, $CDCl_3$) δ 166.3, 135.7 (2C), 135.6 (2C), 133.4, 133.2, 133.1, 130.0 (2C), 129.7, 129.7, 129.5, 128.5 (2C), 127.7 (4C), 81.9, 79.2, 76.6, 73.3, 71.6, 63.6, 46.7, 44.4 (3C), 36.2 (3C), 29.9 (3C), 26.7 (3C), 19.2.

IR (neat) v: 3020, 2949, 2400, 2348, 1725, 1483, 1392, 1265, 1215, 1147, 1115, 1007, 928, 747, 668.

HRMS (ESI) m/z calculated for $C_{39}H_{48}O_6SSiNa$ $(M+Na)^+$ 695.2839, found 695.2818.

---

adamantyl 2-*O*-acetyl-4-*O*-benzoyl-6-*O*-*tert*-butyldiphenylsilyl-1-thio-β-D-glucopyranoside (3.25)

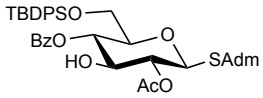

According to general procedure E, **3.24** (58 mg, 0.086 mmol), (*R*)-BTM (2.2 mg, 0.0086 mmol), *i*Pr_2NEt (29 µL, 0.17 mmol), AcOH (6 µL, 0.11 mmol), Piv_2O (19 µL, 0.11 mmol) and $CHCl_3$ (0.9 mL) were used. The product **3.25** was isolated by column chromatography on silica gel (hexane:ethyl acetate - 3/1) as a colorless foam (54 mg, 89%).

^{1}H NMR (400 MHz, $CDCl_3$) δ 7.84 (d, *J* = 7.7 Hz, 2H), 7.58 (d, *J* = 7.1 Hz, 2H), 7.50 (dd, *J* = 14.7, 7.5 Hz, 3H), 7.34 (t, *J* = 7.6 Hz, 2H), 7.30 – 7.17 (m, 4H), 7.12 (t, *J* = 7.4 Hz, 2H), 5.08 (t, *J* = 9.5 Hz, 1H), 4.83 (t, *J* = 9.5 Hz, 1H), 4.67 (d, *J* = 10.1 Hz, 1H), 3.84 (t, *J* = 9.1 Hz, 1H), 3.78 – 3.61 (m, 3H), 2.05 (s, 3H), 2.01 – 1.80 (m, 9H), 1.62 (s, 6H), 0.91 (s, 9H).

^{13}C NMR (101 MHz, $CDCl_3$) δ 170.5, 166.7, 135.7 (2C), 135.6 (2C), 133.6, 133.1, 133.0, 130.0 (2C), 129.8, 129.7, 129.4, 128.6 (2C), 127.8 (2C), 127.7 (2C), 80.0, 79.0, 75.8, 73.3, 72.3, 63.4, 46.2, 44.3 (3C), 36.3 (3C), 29.9 (3C), 26.7 (3C), 21.3, 19.2.

IR (neat) v: 3510, 3071, 2921, 2852, 1719, 1451, 1428, 1389, 1268, 1242, 1113, 1046, 970, 804, 756.

HRMS (ESI) m/z calculated for $C_{41}H_{50}O_7SSiNa$ $(M+Na)^+$ 737.2944, found 737.2924.

Preparation of **adamantyl 4-*O*-benzoyl-6-*O*-(2,3,4-tri-*O*-benzoyl-β-L-fucopyranosyl)-(1->6)-β-D-glucopyranoside (3.26)**

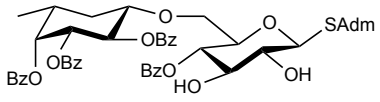

Thioglycoside **S9** (162 mg, 0.19 mmol) was dissolved in dry THF (2 mL). 70% HF-Py (146 µL, 5.6 mmol) was added. After stirring at room temperature for 12 hours, the reaction mixture was quenched with sat. aq. $NaHCO_3$ and extracted with ethyl acetate (30 mL × 3). The organic layer was washed with brine, dried over anhydrous Na_2SO_4, filtered and concentrated *in vacuo*. The residue was purified by silica gel column chromatography (hexane:ethyl acetate - 1/1) to give the intermediate (110 mg, 92%).

The above intermediate (110 mg, 0.17 mmol) and donor **S7**[15] (162 mg, 0.26 mmol) were dissolved in dry CH_2Cl_2 (1.5 mL). 4Å MS (270 mg) were added. The reaction mixture was stirred at room temperature for 30 min and then cooled to -30 ^oC. TMSOTf (24 µL, 0.13 mmol) was added dropwise. After stirring at -30 ^oC for 3 hours, the reaction mixture was quenched with Et_3N (1 mL) and concentrated *in vacuo*. The residue was purified by silica gel column chromatography (hexane:ethyl acetate - 1/1) to give the disaccharide intermediate (161 mg, 87%).

The above disaccharide intermediate (161 mg, 0.15 mmol) was dissolved in CH_2Cl_2 (1.5 mL). AcOH (0.7 mL) and pyridine (1 mL) were added. The reaction mixture was cooled to 0 ^oC. 64% NH_2NH_2-H_2O (45 µL, 0.59 mmol) was added. After stirring for 12 hours, the reaction mixture was quenched with acetone (1 mL) and concentrated *in vacuo*. The residue was purified by silica gel column chromatography (hexane:ethyl acetate - 2/1 to 1.3/1) to give the product **3.26** (107 mg, 81%) as a colorless foam.

^{1}H NMR (400 MHz, $CDCl_3$) δ 7.98 (d, *J* = 7.8 Hz, 2H), 7.91 (d, *J* = 7.7 Hz, 4H), 7.69 (d, *J* = 7.9 Hz, 2H), 7.55 – 7.46 (m, 2H), 7.45 – 7.26 (m, 8H), 7.15 (dd, *J* = 14.7, 7.3 Hz, 2H), 5.66 – 5.54 (m, 2H), 5.42 (dd, *J* = 10.2, 2.5 Hz, 1H), 4.92 (t, *J* = 9.6 Hz, 1H), 4.74 (d, *J* = 7.9 Hz, 1H), 4.42 (d, *J* = 9.8 Hz, 1H), 4.00 (dd, *J* = 11.7, 4.9 Hz, 1H), 3.88 (q, *J* = 6.4 Hz, 1H), 3.70 (d, *J* = 11.7 Hz, 1H), 3.62 (t, *J* = 8.4 Hz, 2H), 2.97 (t, *J* = 9.2 Hz, 1H), 2.02 – 2.00 (m, 3H), 1.89 – 1.83 (m, 6H), 1.64 – 1.62 (m, 6H), 1.15 (d, *J* = 6.2 Hz, 3H).

^{13}C NMR (101 MHz, $CDCl_3$) δ 166.4, 166.1, 165.9, 165.2, 133.6, 133.5, 133.3, 133.3, 130.1, 130.0, 129.9, 129.7, 129.5, 129.4, 129.0, 128.7, 128.6, 128.4, 101.7, 81.9, 76.7, 73.1, 72.3, 71.4, 71.2, 69.8, 69.8, 68.0, 46.7, 44.2 (3C), 36.3 (3C), 30.0 (3C), 16.3.

IR (neat) v: 3020, 2922, 2852, 1727, 1451, 1392, 1265, 1216, 1179, 1071, 1027, 755, 710, 669.

HRMS (ESI) m/z calculated for $C_{50}H_{52}O_{13}SNa$ $(M+Na)^+$ 915.3026, found 915.2994.

---

adamantyl 2-*O*-acetyl-4-*O*-benzoyl-6-*O*-(2,3,4-tri-*O*-benzoyl-β-L-fucopyranosyl)-(1->6)-β-D-glucopyranoside (3.27)

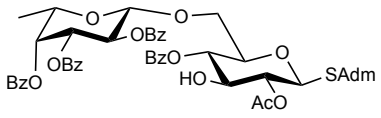

According to general procedure E, **3.26** (57 mg, 0.064 mmol), (*R*)-BTM (1.6 mg, 0.0064 mmol), *i*Pr_2NEt (21 µL, 0.13 mmol), AcOH (5 µL, 0.083 mmol), Piv_2O (17 µL, 0.083 mmol) and $CHCl_3$ (0.6 mL) were used. The product **3.27** was isolated by column chromatography on silica gel (hexane:ethyl acetate - 1.5/1) as a colorless foam (55 mg, 92%).

^{1}H NMR (400 MHz, $CDCl_3$) δ 7.98 (d, *J* = 7.4 Hz, 2H), 7.93 (d, *J* = 7.4 Hz, 2H), 7.88 (d, *J* = 7.4 Hz, 2H), 7.70 (d, *J* = 7.4 Hz, 2H), 7.55 – 7.25 (m, 10H), 7.22 – 7.13 (dd, *J* = 14.4, 6.7 Hz, 2H), 5.68 – 5.55 (m, 2H), 5.41 (dd, *J* = 10.4, 3.4 Hz, 1H), 4.93 (t, *J* = 9.6 Hz, 1H), 4.81 (d, *J* = 8.0 Hz, 1H), 4.65 – 4.52 (m, 2H), 4.00 (dd, *J* = 11.8, 5.0 Hz, 1H), 3.89 (q, *J* = 6.3 Hz, 1H), 3.81 – 3.74 (m, 1H), 3.71 (t, *J* = 8.9 Hz, 1H), 3.64 (dd, *J* = 9.9, 3.5 Hz, 1H), 2.08 – 1.92 (s, 6H), 1.93 – 1.78 (m, 6H), 1.66 – 1.62 (s, 6H), 1.16 (d, *J* = 6.4 Hz, 3H).

^{13}C NMR (101 MHz, $CDCl_3$) δ 170.1, 166.2, 166.0, 165.7, 165.1, 133.5, 133.4, 133.2, 133.2, 130.0 (2C), 129.9 (2C), 129.8 (2C), 129.8 (2C), 129.6, 129.3, 129.3, 128.9, 128.5 (4C), 128.4 (2C), 128.3 (2C), 101.3, 79.9, 77.5, 75.6, 73.1, 72.3, 71.8, 71.1, 69.7, 69.7, 67.4, 46.3, 44.0 (3C), 36.2, (3C) 29.8 (3C), 21.1, 16.2.

IR (neat) v: 3431, 3019, 2922, 2851, 1729, 1585, 1452, 1426, 1315, 1265, 1217, 1177, 1111, 1070, 1027.

HRMS (ESI) m/z calculated for $C_{52}H_{54}O_{14}SNa$ $(M+Na)^+$ 957.3132, found 957.3082.

Preparation of **adamantyl 3-*O*-benzyl-6-*O*-*tert*-butyldimethylsilyl-1-thio-β-D-galactopyranoside (3.28)**

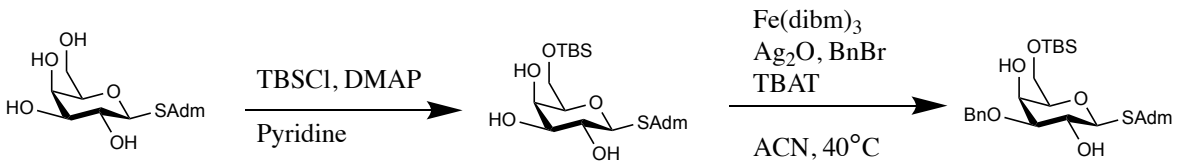

S3 **S10** **3.28**

To an oven-dried RB equipped with a magnetic stir bar, the previously mentioned **S3** (330 mg,1.0 equiv, 1 mmol) was dissolved in pyridine (3 mL) to a reaction concentration of 0.3 M. TBSCl (195.9 mg, 1.3 equiv, 1.3 mmol) and DMAP (24.4 mg, 0.2 equiv, 0.2 mmol) were added sequentially to the RB, and the RB was flushed with Argon. The RB was allowed to stir until reaction completion. The reaction was quenched with sat. aq. $NaHCO_3$, at which time the solution turned a milky color. The reaction contents were transferred to a separatory funnel, extracted with CH_2Cl_2 three times, the combined organic layers were washed with sat. aq. $NaHCO_3$ twice and dried over Na_2SO_4. After filtration and concentration *in vacuo*, the crude product was purified via column chromatography using a gradient from 100% hexane to 1:1 hexane:ethyl acetate. **S10** was obtained as a white powder (312 mg, 70%).

According to literature procedures (aka general procedure F),[56] **S10** (365 mg, 0.82 mmol), MeCN (3.5mL), Ag_2O (114 mg, 0.49 mmol), TBAB (26.4 mg, 0.0822 mmol), $Fe(dibm)_3$ (42.7 mg, 0.082 mmol), and BnBr (146 μL, 1.23 mmol) were added sequentially. **3.28** was isolated as a white/light yellow foam (311 mg, 71% yield).

^{1}H NMR (400 MHz, $CDCl_3$) δ 7.39 – 7.21 (m, 5H), 4.77 (d, *J* = 12.0 Hz, 1H), 4.70 (d, *J* = 12.0 Hz, 1H), 4.42 (d, *J* = 9.9 Hz, 1H), 3.96 (d, *J* = 3.2 Hz, 1H), 3.79 (dd, *J* = 10.3, 6.3 Hz, 1H), 3.75 – 3.69 (m, 1H), 3.67 (t, *J* = 10.6 Hz, 1H), 3.44 – 3.36 (m, 2H), 2.37 (d, *J* = 1.6 Hz, 1H), 2.35 – 2.30 (m, 1H), 2.01 – 1.97 (m, 3H), 1.96 – 1.88 (m, 3H), 1.83 (d, *J* = 12.2 Hz, 3H), 1.71 – 1.58 (m, 6H), 0.83 (s, 9H), 0.01 (s, 3H), 0.00 (s, 3H).

^{13}C NMR (101 MHz, $CDCl_3$) δ 138.1, 128.6 (2C), 128.0, 127.9 (2C), 82.6, 81.5, 78.6, 72.2, 69.7, 66.7, 62.3, 46.3, 44.2 (3C), 36.2 (3C), 29.8 (3C), 25.9 (3C), 18.3, -5.4, -5.5.

IR (neat) v: 3593, 3468, 3375, 3062, 2904, 2851, 2367, 1743, 1455, 1370, 1342, 1251, 1139, 1098, 1073, 1049, 1028.

HRMS (ESI) m/z calculated for $C_{29}H_{46}O_5SSiNa$ $(M+Na)^+$ 557.2727, found 557.2734.

---

adamantyl 2-*O*-acetyl-3-*O*-benzyl-6-*O*-*tert*-butyldimethylsilyl-1-thio-β-D-galactopyranoside (3.29)

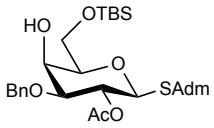

According to general procedure E, **3.28** (39.5 mg, 0.074 mmol), (*R*)-BTM (1.9 mg, 0.0074 mmol), *i*Pr_2NEt (25.8 μL, 0.15 mmol), AcOH (5.8 μL, 0.096 mmol), Piv_2O (19.5 μL, 0.096 mmol) and $CHCl_3$ (0.75 mL) were used. The product **3.29** was isolated by column chromatography on silica gel (hexane:ethyl acetate - 9/1) as an amorphous solid (39 mg, 92%).

^{1}H NMR (400 MHz, $CDCl_3$) δ 7.39 – 7.27 (m, 5H), 5.12 (t, *J* = 9.7 Hz, 1H), 4.69 (d, *J* = 12.2 Hz, 1H), 4.58 (d, *J* = 12.2 Hz, 1H), 4.53 (d, *J* = 10.2 Hz, 1H), 4.07 (d, *J* = 3.3 Hz, 1H), 3.86 (dd, *J* = 10.2, 6.5 Hz, 1H), 3.78 (dd, *J* = 10.3, 5.7 Hz, 1H), 3.52 (dd, *J* = 9.3, 3.3 Hz, 1H), 3.45 (t, *J* = 6.2 Hz, 1H), 2.43 (s, 1H), 2.07 – 1.93 (m, 6H), 1.95 – 1.87 (m, 3H), 1.87 – 1.77 (m, 3H), 1.67 (d, *J* = 6.9 Hz, 6H), 0.89 (s, 9H), 0.07 (s, 3H), 0.06 (s, 3H).

^{13}C NMR (101 MHz, $CDCl_3$) δ 169.7, 137.7, 128.5 (2C), 128.0, 127.7 (2C), 80.2, 80.0, 78.5, 71.5, 69.3, 66.0, 62.2, 45.8, 44.0 (3C), 36.2 (3C), 29.8 (3C), 25.9 (3C), 21.2, 18.3, -5.4, -5.5.

IR (neat) v: 2912, 2850, 2361, 2342, 1735, 1697, 1558, 1455, 1368, 1229, 1148, 1102, 1060, 1042.

HRMS (ESI) m/z calculated for $C_{31}H_{48}O_6SSiNa$ $(M+Na)^+$ 599.2833, found 557.2942.

Preparation of **adamantyl 3-*O*-benzyl-1-thio-β-L-arabinopyranoside (3.30)**

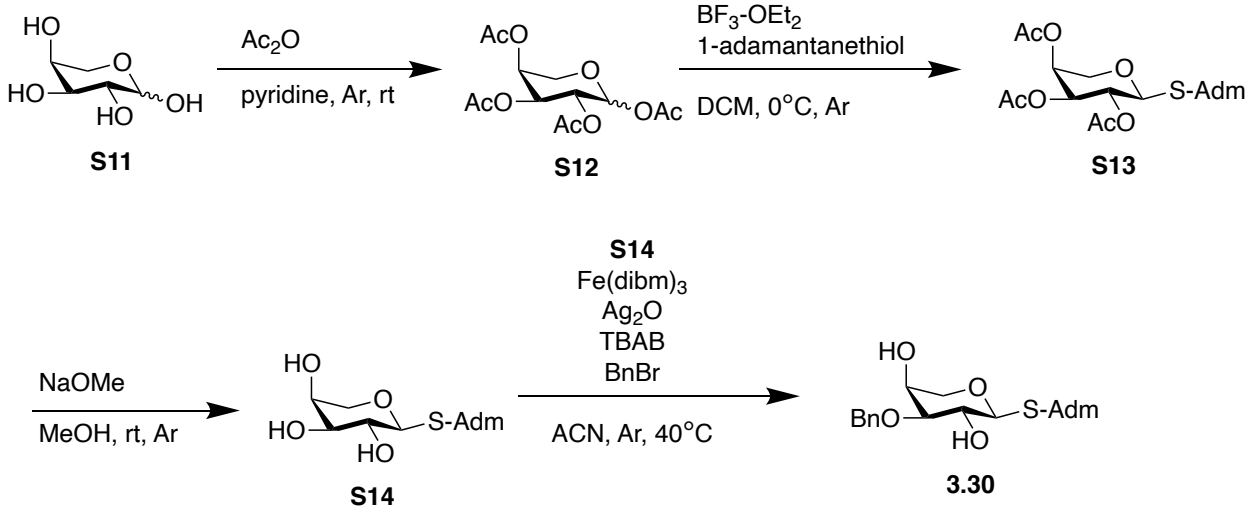

To an oven-dried RB flask, commercially available **S11** (2.0 g, 1.0 equiv, 13.3 mmol) was dissolved in pyridine (5.4 mL, 5.0 equiv, 66.5 mmol), followed by addition of acetic anhydride (11.3 mL, 9.0 equiv, 120 mmol). The flask was attached to a reflux condenser and stirred in a 140 ^{o}C oil bath overnight. Upon reaction completion, the reaction mixture was concentrated. The crude material was then purified by column chromatography using a gradient from 100% hexane to hexane:ethyl acetate = 1:1. **S12** was obtained as a white solid (3.95 g, 93%).

S13 was obtained following general procedure A and using **S11** (3.9 g, 1.0 equiv, 12.25 mmol), 1-adamantanethiol (2.47g, 1.1 equiv, 14.7 mmol), CH_2Cl_2, and BF_3-OEt_2 (5 mL, 1.4 equiv, 20.16 mmol). **S13** was obtained as an amorphous solid (1.5 g, 29%).

Following general procedure B, **S13** (1.9 g, 1.0 equiv, 2.35 mmol), NaOMe (12.9 mg, 0.1 equiv, 0.24 mmol), and MeOH were used. Upon reaction completion, quench, and concentration, the crude product **S14** was carried forward without further purification.

Following literature procedure[3] (aka general procedure F), **S14** (145 mg, 1.0 equiv, 0.48 mmol), MeCN (5.0 mL), Ag_2O (66.8mg, 0.6 equiv, 0.29 mmol), TBAB (15.4 mg, 0.1 equiv, 0.048 mmol), $Fe(dibm)_3$ (25 mg, 0.1 equiv, 0.048 mmol), and BnBr (86 μL, 1.5 equiv, 0.72 mmol) were added sequentially. **3.30** was isolated as a white foam (136 mg, 72% yield).

^{1}H NMR (400 MHz, $CDCl_3$) δ 7.46 – 7.28 (m, 5H), 4.83 (d, *J* = 11.8 Hz, 1H), 4.74 (d, *J* = 11.9 Hz, 1H), 4.45 (d, *J* = 9.3 Hz, 1H), 4.05 (dd, *J* = 12.7, 2.6 Hz, 1H), 3.96 (s, 1H), 3.75

(t, *J* = 8.9 Hz, 1H), 3.50 (dd, *J* = 10.2, 5.9 Hz, 2H), 2.50 (s, 1H), 2.49 (s, 1H), 2.06 (s, 3H), 1.97 (d, *J* = 12.3 Hz, 3H), 1.88 (d, *J* = 12.4 Hz, 3H), 1.74 – 1.65 (m, 6H).

^{13}C NMR (101 MHz, $CDCl_3$) δ 137.9, 128.6 (2C), 128.0, 127.9 (2C), 82.9, 80.5, 72.3, 69.8, 68.8, 67.0, 46.3, 44.2 (3C), 36.1 (3C), 29.8 (3C).

IR (neat) v: 3482, 3389, 2902, 2847, 2359, 2343, 1750, 1605, 1496, 1453, 1416, 1367, 1342, 1300, 1261, 1232, 1191, 1134, 1117, 1087, 1065, 1051, 1032.

HRMS (ESI) m/z calculated for $C_{22}H_{30}O_4SNa$ $(M+Na)^+$ 413.1757, found 413.1751.

---

adamantyl 3-*O*-benzyl-2-*O*-isobutyryl-1-thio-β-L-arabinopyranoside (3.31)

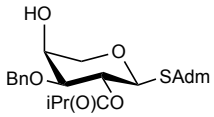

According to general procedure D, **3.30** (29 mg, 0.1 mmol), (*R*)-BTM (2.5 mg, 0.01 mmol), *i*Pr_2NEt (52.3 μL, 3.0 equiv, 0.3 mmol), isobutryric anhydride (41.5 μL, 2.5 equiv, 0.25 mmol) and $CHCl_3$ (1 mL) were used. The product **3.31** was isolated by column chromatography on silica gel (hexane:ethyl acetate - 9/1 to 2/1) as a clear oil (28 mg, 82%).

^{1}H NMR (400 MHz, $CDCl_3$) δ 7.44 – 7.28 (m, 5H), 5.22 (t, *J* = 4.9 Hz, 1H), 5.02 (d, *J* = 4.5 Hz, 1H), 4.82 (d, *J* = 11.7 Hz, 1H), 4.53 (d, *J* = 11.7 Hz, 1H), 4.07 (dd, *J* = 11.5, 7.8 Hz, 1H), 3.92 (tt, *J* = 7.9, 3.8 Hz, 1H), 3.66 (t, *J* = 4.4 Hz, 1H), 3.51 (dd, *J* = 11.6, 3.8 Hz, 1H), 2.58 (hept, *J* = 6.7 Hz, 1H), 2.35 (d, *J* = 8.2 Hz, 1H), 2.08 – 1.99 (m, 3H), 1.90 (q, *J* = 12.7 Hz, 6H), 1.74 – 1.62 (m, 6H), 1.21 (d, *J* = 6.7 Hz, 3H), 1.19 (d, *J* = 6.7 Hz, 3H).

^{13}C NMR (101 MHz, $CDCl_3$) δ 175.9, 137.3, 128.6 (2C), 128.2, 128.1 (2C), 78.0, 76.1, 72.0, 70.2, 65.0, 63.1, 46.0, 43.8 (3C), 36.2 (3C), 34.1, 29.8 (3C), 19.0, 18.9.

IR (neat) v: 3482, 3389, 2902, 2847, 2359, 2342, 1750, 1605, 1496, 1453, 1416, 1367, 1342, 1300, 1261, 1232, 1191, 1134, 1117, 1087, 1065, 1051, 1032.

HRMS (ESI) m/z calculated for $C_{26}H_{36}O_5SNa$ $(M+Na)^+$ 483.2176, found 483.2166.

Preparation of **adamantyl 3-*O*-benzyl-1-thio-β-L-fucopyranoside (3.32)**

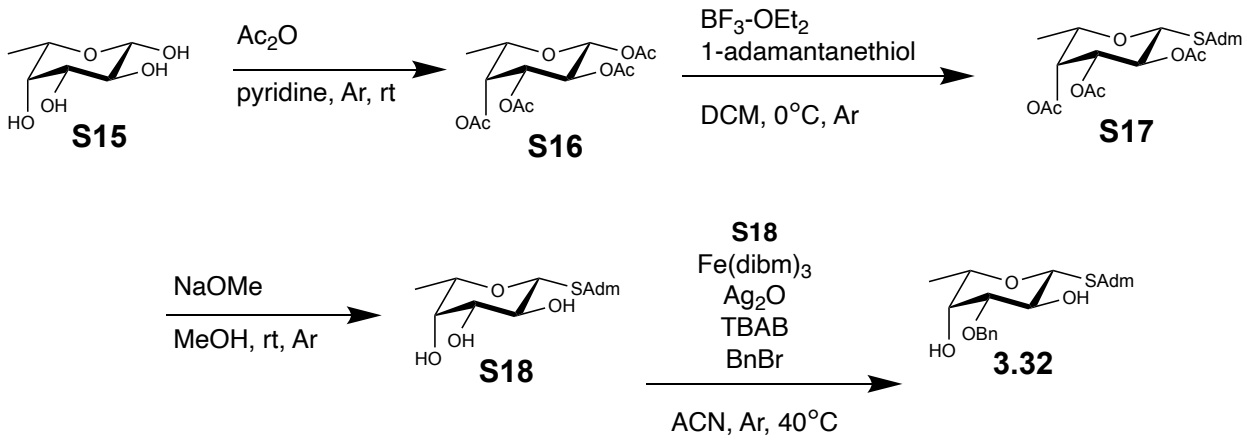

To an oven-dried RB flask, commercially available **S15** (900 mg, 1.0 equiv, 5.49 mmol) was dissolved in pyridine (16.2 mL), followed by addition of acetic anhydride (33.9 mL). The flask was attached to a reflux condenser and stirred in a 140 °C oil bath overnight. Upon reaction completion, the reaction mixture was concentrated. The crude material was then purified by column chromatography using a gradient from 100% hexane to hexane:ethyl acetate = 1:1. **S16** was obtained as a white solid (1.65 g, 91%).

S17 was obtained following general procedure A and using **S16** (1.43 g, 1.0 equiv, 4.3 mmol), 1-adamantanethiol (841 mg, 1.16 equiv, 5 mmol), CH_2Cl_2, and BF_3-OEt_2 (2.1 mL, 2.0 equiv, 8.6 mmol). **S17** was obtained as an amorphous solid (890 mg, 47%).

Following general procedure B, **S17** (810 mg, 1.0 equiv, 0.84 mmol), NaOMe (9.7 mg, 0.1 equiv, 0.18 mmol), and MeOH were used. Upon reaction completion, quench, and concentration, the crude product **S18** was carried forward without further purification.

Following literature procedure[3] (aka general procedure F), **S18** (266 mg, 1.0 equiv, 0.85 mmol), MeCN, Ag_2O (118.2 mg, 0.6 equiv, 0.51 mmol), TBAB (27.4 mg, 0.1 equiv, 0.085 mmol), $Fe(dibm)_3$ (44.33 mg, 0.1 equiv, 0.085 mmol), and BnBr (151.6 μL, 1.5 equiv, 1.28 mmol) were added sequentially. **3.32** was isolated as an amorphous solid (207 mg, 60% yield).

^{1}H NMR (400 MHz, $CDCl_3$) δ 7.29 – 7.41 (m, 5H), 4.81 (d, *J* = 12.1 Hz, 1H), 4.76 (d, *J* = 11.8 Hz, 1H), 4.44 (d, *J* = 9.8 Hz, 1H), 3.79 (t, *J* = 3.2 Hz, 1H), 3.68 (t, *J* = 9.5 Hz, 1H), 3.59 (q, *J* = 6.7 Hz, 1H), 3.45 (dd, *J* = 8.9, 3.4 Hz, 1H), 2.43 (s, 1H), 2.27 (d, *J* = 3.4 Hz, 1H), 2.06 (s, 3H), 1.98 (d, *J* = 12.5 Hz, 3H), 1.89 (d, *J* = 12.5 Hz, 3H), 1.79 – 1.63 (m, 6H), 1.33 (d, *J* = 6.4 Hz, 3H).

^{13}C NMR (101 MHz, $CDCl_3$) δ 138.0, 128.6 (2C), 127.9, 127.9 (2C), 82.3, 81.6, 74.2, 72.1, 69.7, 69.4, 46.3, 44.1 (3C), 36.2 (3C), 29.8 (3C), 16.9.

IR (neat) v: 3599, 3590, 3566, 3479, 2981, 2915, 2886, 2359, 2341, 1646, 1540, 1389, 1176, 1144, 1081, 1061.

HRMS (ESI) m/z calculated for $C_{23}H_{32}O_4SNa$ $(M+Na)^+$ 427.1914, found 427.1898.

---

adamantyl 3-*O*-benzyl-2-*O*-isobutyryl-1-thio-β-L-fucopyranoside (3.33)

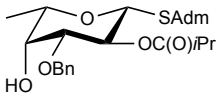

According to the procedure D, **3.32** (41 mg, 1.0 equiv, 0.1 mmol), (*R*)-BTM (2.5 mg, 10 mol %, 0.01 mmol), *i*Pr$_2$NEt (52.3 μL, 3.0 equiv, 0.3 mmol), isobutryric anhydride (41.5 μL, 2.5 equiv, 0.25 mmol) and $CHCl_3$ (1 mL) were used. The product **3.32** was isolated by column chromatography on silica gel (hexane:ethyl acetate - 9/1 to 2/1) as a clear oil (40 mg, 83%).

^{1}H NMR (400 MHz, $CDCl_3$) δ 7.37 – 7.27 (m, 5H), 5.11 (t, *J* = 9.8 Hz, 1H), 4.67 (d, *J* = 12.1 Hz, 1H), 4.61 – 4.53 (m, 2H), 3.84 (d, *J* = 3.4 Hz, 1H), 3.60 – 3.55 (m, 2H), 2.50 (hept, *J* = 7.0 Hz, 1H), 2.36 (s, 1H), 2.05 – 2.00 (m, 3H), 1.92 (d, *J* = 12.5 Hz, 3H), 1.87 – 1.78 (m, 3H), 1.69 – 1.67 (m 6H), 1.35 (d, *J* = 6.5 Hz, 3H), 1.19 (d, *J* = 7.0 Hz, 3H), 1.17 (d, *J* = 7.0 Hz, 3H).

^{13}C NMR (101 MHz, $CDCl_3$) δ 175.5, 137.5, 128.5 (2C), 128.0, 127.67 (2C), 80.3, 80.0, 73.9, 71.5, 69.1, 68.5, 45.8, 44.1 (3C), 36.2 (3C), 34.2, 29.8 (3C), 19.1, 18.9, 16.9.

IR (neat) v: 2981, 2914, 1735, 1455, 1373, 1250, 1152, 1118, 1091, 1073, 1063, 1039, 1026.

HRMS (ESI) m/z calculated for $C_{27}H_{38}O_5SNa$ $(M+Na)^+$ 497.2332, found 497.2321.

Preparation of **adamantyl 6-*O*-pivaloyl-1-thio-β-D-galactopyranoside (3.34)**

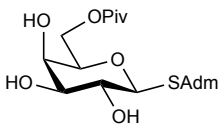

In an oven-dried RB equipped with a magnetic stir bar, adamantyl 1-thio-β-D-galactopyranoside (**S3**, 150 mg, 0.45 mmol) and DMAP (5.5 mg, 0.045 mmol, 10 mol %) were dissolved in dry pyridine (1.5 mL). While stirring in an ice-water bath, pivaloyl chloride (61 μL, 0.50 mmol, 1.1 equiv) was added dropwise. After stirring at the same temperature for 2 hours, the reaction mixture was diluted with ethyl acetate, washed successively with 1*N* HCl, sat. $NaHCO_3$ and brine, dried over Na_2SO_4, filtered and concentrated in vacuo. The crude material was purified by column chromatography (CH_2Cl_2/MeOH - 20:1) to provide **3.34** (74 mg, 39%) as a white foam.

^{1}H NMR (400 MHz, $CDCl_3$) δ 4.51 (d, *J* = 9.4 Hz, 1H), 4.36 (dd, *J* = 11.7, 5.0 Hz, 1H), 4.21 (dd, *J* = 11.7, 7.4 Hz, 1H), 3.97 – 3.91 (m, 1H), 3.73 (ddd, *J* = 7.5, 5.0, 1.1 Hz, 1H), 3.68 – 3.63 (m, 1H), 3.59 (td, *J* = 9.2, 1.7 Hz, 1H), 3.40 (d, *J* = 4.9 Hz, 1H), 2.95 (d, *J* = 4.7 Hz, 1H), 2.87 (d, *J* = 2.0 Hz, 1H), 2.09 – 2.02 (m, 3H), 2.02 – 1.94 (m, 3H), 1.94 – 1.87 (m, 3H), 1.76 – 1.65 (m, 6H), 1.20 (s, 9H).

^{13}C NMR (101 MHz, $CDCl_3$) δ 178.6, 82.2, 76.1, 74.5, 70.1, 68.8, 63.6, 46.5, 44.2 (3C), 38.8, 36.1 (3C), 29.8 (3C), 27.1 (3C).

IR (neat) v: 3391, 2970, 2905, 2851, 1724, 1480, 1450, 1395, 1365, 1343, 1285, 1230, 1167, 1145, 1098, 1059, 1025, 978, 943, 867, 829, 795, 733, 702.

HRMS (ESI) m/z calculated for $C_{21}H_{34}O_6SNa$ $(M+Na)^+$ 437.1974, found 437.1949.

---

adamantyl 2-*O*-acetyl-6-*O*-pivaloyl-1-thio-β-D-galactopyranoside (3.35)

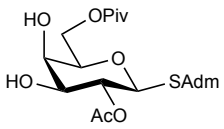

According to general procedure E, **3.34** (19 mg, 0.046 mmol), (*R*)-BTM (1.2 mg, 0.005 mmol, 10 mol %), *i*Pr_2NEt (24 μL, 0.14 mmol, 3.0 equiv), acetic acid (5.2 μL, 0.092 mmol, 2.0 equiv), Piv_2O (18.6 μL, 0.92 mmol, 2.0 equiv) and $CHCl_3$ (0.2 mL) were used. The product **3.35** was isolated by column chromatography on silica gel (CH_2Cl_2:MeOH - 20:1) as a colorless oil (13.3 mg, 64%).

^{1}H NMR (400 MHz, $CDCl_3$) δ 4.90 (t, *J* = 9.7 Hz, 1H), 4.59 (d, *J* = 10.1 Hz, 1H), 4.40 (dd, *J* = 11.7, 5.6 Hz, 1H), 4.19 (dd, *J* = 11.7, 7.0 Hz, 1H), 3.90 (br s, 1H), 3.75 – 3.63 (m, 2H), 2.95 (br s, 1H), 2.70 (br s, 1H), 2.12 (s, 3H), 2.08 – 2.01 (m, 3H), 1.98 – 1.91 (m, 3H), 1.89 – 1.82 (m, 3H), 1.75 – 1.61 (m, 6H), 1.20 (s, 9H).

^{13}C NMR (101 MHz, $CDCl_3$) δ 178.8, 171.1, 79.9, 75.82, 73.5, 71.4, 69.0, 63.1, 46.1, 44.0 (3C), 38.8, 36.1 (3C), 29.7 (3C), 27.1 (3C), 21.2.

IR (neat) v: 3490, 3458, 3413, 3389, 3375, 3348, 2972, 2906, 2850, 1726, 1480, 1450, 1396, 1369, 1343, 1285, 1233, 1168, 1147, 1100, 1058, 1040, 977, 910, 868, 825, 732, 706, 686, 657.

HRMS (ESI) m/z calculated for $C_{23}H_{36}O_7SNa$ $(M+Na)^+$ 479.2079, found 479.2056.

Acylation of **3.34** using DMAP as catalyst

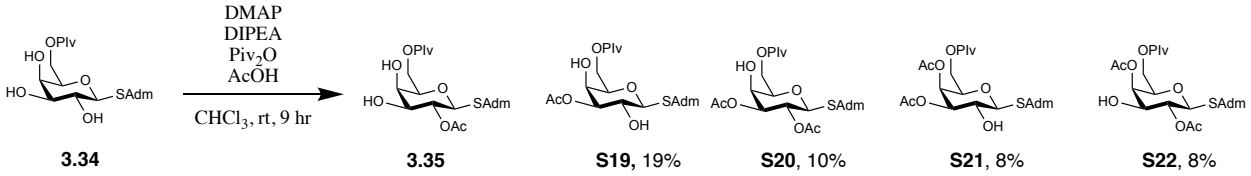

3.34 **3.35** **S19,** 19% **S20**, 10% **S21**, 8% **S22**, 8%

According to general procedure E, **3.34** (35.9 mg, 0.087 mmol), DMAP (1.1 mg, 0.009 mmol, 10 mol %), *i*Pr_2NEt (45 μL, 0.26 mmol, 3.0 equiv), acetic acid (7.4 μL, 0.13 mmol, 1.5 equiv), Piv_2O (26.4 μL, 0.13 mmol, 1.5 equiv) and $CHCl_3$ (0.3 mL) were used. The products were isolated by column chromatography on silica gel (ethyl acetate/hexanes - 15% to 50%).

---

adamantyl 3-*O*-acetyl-6-*O*-pivaloyl-1-thio-β-D-galactopyranoside (S19)

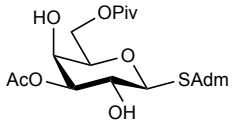

^{1}H NMR (400 MHz, $CDCl_3$) δ 4.93 (dd, *J* = 9.6, 3.2 Hz, 1H), 4.58 (d, *J* = 9.9 Hz, 1H), 4.32 (dd, *J* = 11.7, 5.3 Hz, 1H), 4.20 (dd, *J* = 11.7, 7.1 Hz, 1H), 4.02 (dd, *J* = 6.1, 3.3 Hz, 1H), 3.82 – 3.72 (m, 2H), 2.36 (d, *J* = 1.9 Hz, 1H), 2.20 (s, 1H), 2.18 (s, 3H), 2.10 – 2.03 (m, 3H), 2.02 – 1.95 (m, 3H), 1.93 – 1.86 (m, 3H), 1.77 – 1.65 (m, 6H), 1.20 (s, 9H).

^{13}C NMR (101 MHz, $CDCl_3$) δ 178.5, 170.4, 82.9, 76.0, 75.7, 67.7, 67.5, 63.1, 46.8, 44.1 (3C), 38.8, 36.1 (3C), 29.8 (3C), 27.1 (3C), 21.1.

IR (neat) v: 3517, 3447, 2961, 2904, 2849, 1717, 1480, 1450, 1397, 1367, 1342, 1276, 1240, 1169, 1147, 1085, 1058, 1042, 1020, 1000, 974, 945, 911, 829, 771, 733, 704, 683.

HRMS (ESI) m/z calculated for $C_{23}H_{36}O_7SNa$ $(M+Na)^+$ 479.2079, found 479.2053.

---

adamantyl 2,3-di-*O*-acetyl-6-*O*-pivaloyl-1-thio-β-D-galactopyranoside (S20)

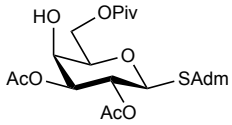

^{1}H NMR (500 MHz, $CDCl_3$) δ 5.18 (t, *J* = 10.0 Hz, 1H), 5.02 (dd, *J* = 9.8, 3.2 Hz, 1H), 4.67 (d, *J* = 10.1 Hz, 1H), 4.33 (dd, *J* = 11.7, 5.1 Hz, 1H), 4.21 (dd, *J* = 11.7, 7.2 Hz, 1H), 4.04 (ddd, *J* = 5.6, 3.3, 1.7 Hz, 1H), 3.79 (dd, *J* = 7.0, 5.4 Hz, 1H), 2.21 (d, *J* = 5.9 Hz, 1H), 2.10 (s, 3H), 2.07 – 2.02 (m, 6H), 1.97 – 1.92 (m, 3H), 1.87 – 1.81 (m, 3H), 1.75 – 1.64 (m, 6H), 1.20 (s, 9H).

^{13}C NMR (126 MHz, $CDCl_3$) δ 178.5, 170.2, 169.6, 80.3, 76.0, 74.3, 67.8, 67.7, 63.2, 46.3, 44.1 (3C), 38.8, 36.2 (3C), 29.8 (3C), 27.2 (3C), 21.02, 20.97.

IR (neat) v: 3471, 2960, 2907, 2851, 1748, 1727, 1480, 1450, 1368, 1343, 1226, 1167, 1152, 1085, 1053, 1041, 914, 850, 829, 796, 732.

HRMS (ESI) m/z calculated for $C_{25}H_{38}O_8SNa$ $(M+Na)^+$ 521.2185, found 521.2174.

---

adamantyl 3,4-di-*O*-acetyl-6-*O*-pivaloyl-1-thio-β-D-galactopyranoside (S21)

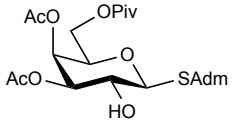

^{1}H NMR (500 MHz, $CDCl_3$) δ 5.41 (dd, *J* = 3.4, 1.1 Hz, 1H), 5.01 (dd, *J* = 9.7, 3.4 Hz, 1H), 4.63 (d, *J* = 9.9 Hz, 1H), 4.13 – 4.08 (m, 2H), 3.97 (ddd, *J* = 7.1, 6.0, 1.2 Hz, 1H), 3.74 (td, *J* = 9.7, 1.5 Hz, 1H), 2.35 (d, *J* = 1.8 Hz, 1H), 2.11 (s, 3H), 2.09 – 2.06 (m, 3H), 2.05 (s, 3H), 2.02 – 1.96 (m, 3H), 1.92 – 1.87 (m, 3H), 1.76 – 1.66 (m, 6H), 1.18 (s, 9H).

^{13}C NMR (126 MHz, $CDCl_3$) δ 178.1, 170.3, 170.2, 82.9, 74.5, 73.7, 67.7, 67.4, 62.2, 47.0, 44.2 (3C), 38.8, 36.1 (3C), 29.8 (3C), 27.1 (3C), 20.9, 20.7.

IR (neat) v: 3472, 2972, 2907, 2851, 2360, 1746, 1480, 1452, 1369, 1242, 1223, 1163, 1082, 1041, 946, 913, 825, 769, 731, 686.

HRMS (ESI) m/z calculated for $C_{25}H_{38}O_8SNa$ $(M+Na)^+$ 521.2185, found 521.2174.

---

adamantyl 2,4-di-*O*-acetyl-6-*O*-pivaloyl-1-thio-β-D-galactopyranoside (S22)

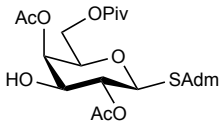

^{1}H NMR (400 MHz, $CDCl_3$) δ 5.35 (dd, *J* = 3.7, 1.1 Hz, 1H), 4.94 (t, *J* = 9.8 Hz, 1H), 4.65 (d, *J* = 10.1 Hz, 1H), 4.17 (dd, *J* = 11.5, 5.5 Hz, 1H), 4.06 (dd, *J* = 11.5, 7.4 Hz, 1H), 3.92 – 3.84 (m, 2H), 2.35 (d, *J* = 6.2 Hz, 1H), 2.16 (s, 3H), 2.12 (s, 3H), 2.08 – 2.02 (m, 3H), 1.98 – 1.92 (m, 3H), 1.89 – 1.82 (m, 3H), 1.76 – 1.64 (m, 6H), 1.19 (s, 9H).

^{13}C NMR (101 MHz, $CDCl_3$) δ 178.1, 171.0, 170.9, 79.9, 74.6, 72.6, 71.0, 70.1, 62.6, 46.2, 44.0 (3C), 38.7, 36.1 (3C), 29.7 (3C), 27.1 (3C), 21.1, 20.8.

IR (neat) v: 3453, 2962, 2907, 2851, 1729, 1480, 1451, 1371, 1227, 1165, 1100, 1056, 1041, 946, 910, 824, 731.

HRMS (ESI) m/z calculated for $C_{25}H_{38}O_8SNa$ $(M+Na)^+$ 521.2185, found 521.2176.

---

adamantyl 2,6-di-*O*-acetyl-1-thio-β-D-galactopyranoside (3.37)

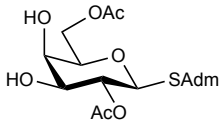

According to general procedure E, adamantyl 1-thio-β-D-galactopyranoside (**S3**, 100 mg, 0.30 mmol), (*R*)-BTM (7.6 mg, 0.03 mmol, 10 mol %), *i*Pr_2NEt (158 μL, 0.91 mmol, 3.0 equiv), acetic acid (52 μL, 0.91 mmol, 3.0 equiv), Piv_2O (184 μL, 0.91 mmol, 3.0 equiv) and $CHCl_3$ (3 mL) were used. The product **3.37** was isolated by column chromatography on silica gel (CH_2Cl_2:MeOH - 20:1) as a colorless oil (70 mg, 56%).

^{1}H NMR (400 MHz, $CDCl_3$) δ 4.92 (t, *J* = 9.7 Hz, 1H), 4.58 (d, *J* = 10.1 Hz, 1H), 4.33 (dd, *J* = 11.7, 5.6 Hz, 1H), 4.28 (dd, *J* = 11.7, 7.2 Hz, 1H), 3.97 (dd, *J* = 3.5, 1.0 Hz, 1H), 3.72 (ddd, *J* = 6.7, 5.6, 1.1 Hz, 1H), 3.68 (dd, *J* = 9.3, 3.5 Hz, 1H), 2.11 (s, 3H), 2.06 (s, 3H), 2.06 – 2.02 (m, 3H), 1.98 – 1.91 (m, 3H), 1.89 – 1.82 (m, 3H), 1.76 – 1.64 (m, 6H).
^{13}C NMR (101 MHz, $CDCl_3$) δ 171.14, 171.07, 80.0, 75.7, 73.5, 71.2, 69.0, 63.2, 46.2, 44.0 (3C), 36.2 (3C), 29.8 (3C), 21.2, 20.8.
IR (neat) v: 3433, 2904, 2850, 1738, 1449, 1370, 1228, 1148, 1099, 1041, 977, 869, 820, 760, 733, 701.
HRMS (ESI) m/z calculated for $C_{20}H_{30}O_7SNa$ $(M+Na)^+$ 437.1610, found 437.1592.

---

adamantyl 3-*O*-benzoyl-4,6-*O*-benzylidene-2-*O*-isobutyryl-1-thio-β-D-galactopyranoside (3.38)

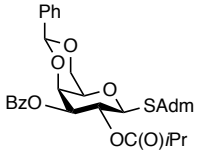

To an oven dried RB flask, **3.13g** (720 mg, 1.47 mmol) was dissolved in pyridine (7.3 mL) and BzCl (307.5 μL, 2.66 mmol) was added. The flask was purged with Argon and capped with a septum. The mixture was stirred at room temperature overnight. 0.5 mL MeOH was used to quench the reaction. The crude reaction mixture was concentrated. The residue was dissolved in 100 mL ethyl acetate, washed with 1M HCl 3 times with 30 mL each time, and then washed with 30 mL of sat. aq. $NaHCO_3$. The combined organic layers were dried over Na_2SO_4, filtered, and purified via column chromatography (pentane:ethyl acetate - 9:1 to 7:3). Product **3.38** was isolated as white/clear flake-like foam (487 mg, 62%).

^{1}H NMR ^{1}H NMR (400 MHz, $CDCl_3$) δ 8.05 – 7.98 (m, 2H), 7.59 – 7.46 (m, 3H), 7.41 (t, *J* = 7.7 Hz, 2H), 7.33 (dd, *J* = 5.1, 1.9 Hz, 3H), 5.56 (t, *J* = 10.0 Hz, 1H), 5.50 (s, 1H), 5.27 (dd, *J* = 9.9, 3.6 Hz, 1H), 4.80 (d, *J* = 10.1 Hz, 1H), 4.54 (d, *J* = 3.5 Hz, 1H), 4.35 (dd, *J* = 12.4, 1.6 Hz, 1H), 4.06 (dd, *J* = 12.4, 1.8 Hz, 1H), 3.63 (s, 1H), 2.44 (hept, *J* = 7.2 Hz, 1H), 2.05 (q, *J* = 3.2 Hz, 3H), 2.00 (d, *J* = 12.5 Hz, 3H), 1.88 (d, *J* = 12.3 Hz, 3H), 1.76 – 1.65 (m, 6H), 1.07 (d, *J* = 7.0 Hz, 3H), 0.99 (d, *J* = 7.0 Hz, 3H).

^{13}C NMR (101 MHz, $CDCl_3$) δ 175.4, 166.2, 137.6, 133.4, 130.0 (2C), 129.2, 128.9, 128.5 (2C), 128.0 (2C), 126.4 (2C), 100.9, 80.3, 74.0, 74.0, 69.5, 69.3, 66.6, 46.3, 44.1 (3C), 36.2 (3C), 34.0, 29.8 (3C), 18.9, 18.8.

IR (neat) v: 2902, 2850, 2358, 2338, 1721, 1451, 1367, 1339, 1314, 1275, 1249, 1219, 1176, 1153, 1128, 1100, 1078, 1042, 1026, 1010.

HRMS (ESI) m/z calculated for $C_{34}H_{40}O_7SNa$ $(M+Na)^+$ 615.2387, found 615.2378.

Acceptor compounds for the glycosylation reactions in Table 4, including **3.39a**, **3.39b**, and **3.39c**, were bought from commercial sources.

Acceptor **3.39d**[57], **3.39e**[58] and **3.39f**[59] were prepared according to literature procedures.

---

benzyl 3-*O*-benzoyl-4,6-*O*-benzylidene-2-*O*-isobutyryl-β-D-galactopyranoside (3.40a)

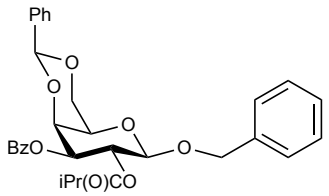

To an oven-dried reaction vessel equipped with a magnetic stir bar, glycosyl donor **3.38** (30 mg, 1.0 equiv, 0.0506 mmol), glycosyl acceptor **3.39a** benzyl alcohol (10.5 μL, 2.0 equiv, 0.1012 mmol) and NIS (22.8 mg, 2.0 equiv, 0.1012 mmol) were added sequentially to a mixture of CH_2Cl_2 and MeCN (2 : 1, v/v, 0.6 mL/0.3 mL). To this mixture, TMSOTf (10.1 μL, 1.1 equiv, 0.0557 mmol) was added at -78 °C under argon. The reaction mixture was slowly warmed up to 0 °C over 5 h and quenched with saturated $NaHCO_3$ solution. The mixture was then extracted with CH_2Cl_2, and the combined organic layers were washed successively with 10% $Na_2S_2O_3$ aqueous solution and brine, dried over anhydrous Na_2SO_4, and concentrated *in vacuo*. The anomeric ratio of the products was determined by integration of the ^1H NMR spectrum of the crude product mixture. Pure glycosylation product **3.40a** (27.1 mg, 81%) was obtained by purification with column chromatography (pentane:ethyl acetate - 3/1) as an amorphous solid.

^{1}H NMR (400 MHz,$CDCl_3$) δ 8.06 – 8.00 (m, 2H), 7.60 – 7.48 (m, 3H), 7.45 – 7.39 (m, 2H), 7.40 – 7.24 (m, 8H), 5.71 (dd, *J* = 10.4, 8.0 Hz, 1H), 5.54 (s, 1H), 5.20 (dd, *J* = 10.4, 3.6 Hz, 1H), 4.97 (d, *J* = 12.3 Hz, 1H), 4.70 (d, *J* = 12.3 Hz, 1H), 4.68 (d, *J* = 8.0 Hz, 1H), 4.52 (dd, *J* = 3.6, 1.1 Hz, 1H), 4.42 (dd, *J* = 12.4, 1.7 Hz, 1H), 4.13 (dd, *J* = 12.4, 1.8 Hz, 1H), 3.63 – 3.58 (m, 1H), 2.44 (hept, *J* = 7.0 Hz, 1H), 1.05 (d, *J* = 7.0 Hz, 3H), 0.96 (d, *J* = 7.0 Hz, 3H).

^{13}C NMR (101 MHz, $CDCl_3$) δ 175.6, 166.2, 137.5, 137.2, 133.5, 130.0 (2C), 129.1, 120.0, 128.5 (2C), 128.4 (2C), 128.1 (2C), 127.84 (2C), 127.79, 126.3 (2C), 100.9, 99.7, 73.7, 72.8, 70.1, 69.0, 68.1, 66.5, 34.0, 18.9, 18.8.

IR (neat) v: 2926, 2358, 1729, 1268, 1058, 1025.

HRMS (ESI) m/z calculated for $C_{31}H_{32}O_8K$ $(M+K)^+$ 571.1729, found 571.1722.

---

cyclohexyl 3-*O*-benzoyl-4,6-*O*-benzylidene-2-*O*-isobutyryl-β-D-galactopyranoside (3.40b)

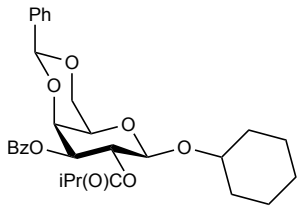

To an oven-dried reaction vessel equipped with a magnetic stir bar, glycosyl donor **3.38** (30 mg, 1.0 equiv, 0.0506 mmol), glycosyl acceptor **3.39b** (10.1 mg, 2.0 equiv, 0.1012 mmol) and NIS (22.8 mg, 2.0 equiv, 0.1012 mmol) were added sequentially to a mixture

of CH_2Cl_2 and MeCN (2 : 1, v/v). To this mixture, TMSOTf (10.1 μL, 1.1 equiv, 0.0557 mmol) was added at -78 °C under argon. The reaction mixture was slowly warmed up to 0 °C over 5 h and quenched with saturated $NaHCO_3$ solution. The mixture was then extracted with CH_2Cl_2, and the combined organic layers were washed successively with 10% $Na_2S_2O_3$ aqueous solution and brine, dried over anhydrous Na_2SO_4, and concentrated *in vacuo*. The anomeric ratio of the products was determined by integration of the ^{1}H NMR spectrum of the crude product mixture. Pure glycosylation product **3.40b** (13.4 mg, 51%) was obtained by purification with column chromatography (pentane:ethyl acetate - 3/1) as an amorphous solid.

^{1}H NMR (400 MHz, $CDCl_3$) δ 8.06 – 7.99 (m, 2H), 7.58 – 7.47 (m, 3H), 7.42 (dd, *J* = 8.4, 7.1 Hz, 2H), 7.37 – 7.30 (m, 3H), 5.57 (dd, *J* = 10.4, 8.0 Hz, 1H), 5.51 (s, 1H), 5.20 (dd, *J* = 10.4, 3.8 Hz, 1H), 4.70 (d, *J* = 8.0 Hz, 1H), 4.50 (dd, *J* = 3.8, 1.1 Hz, 1H), 4.35 (dd, *J* = 12.4, 1.7 Hz, 1H), 4.10 (dd, *J* = 12.4, 1.8 Hz, 1H), 3.74 – 3.64 (m, 1H), 3.61 – 3.55 (m, 1H), 2.46 (hept, *J* = 7.0 Hz, 1H), 1.99 – 1.88 (m, 1H), 1.84 (m, 1H), 1.79 – 1.65 (m, 2H), 1.55 – 1.40 (m, 2H), 1.40 – 1.14 (m, 4H), 1.07 (d, *J* = 7.0 Hz, 3H), 0.99 (d, *J* = 7.0 Hz, 3H).

^{13}C NMR (101 MHz, $CDCl_3$) δ 175.5, 166.3, 137.6, 133.4, 130.0 (2C), 129.2, 128.9, 128.5 (2C), 128.1 (2C), 126.3 (2C), 100.8, 99.4, 77.4, 73.8, 73.0, 69.1, 68.4, 66.3, 34.1, 33.4, 31.7, 25.6, 23.9, 23.8, 18.9 (2C).

IR (neat) v: 3567, 2361, 2359, 2343, 2341, 1943, 1919, 1890, 1869, 1844, 1829, 1811, 1792, 1772, 1749, 1734, 1717, 1699, 1684, 1670, 1653, 1558, 1541, 1520, 1507

HRMS (ESI) m/z calculated for $C_{30}H_{36}O_8Na$ $(M+Na)^+$ 547.2302, found 547.2293.

6-*O*-(3-*O*-benzoyl-4,6-*O*-benzylidene-2-*O*-isobutyryl-β-D-galactopyranosyl)-(1->6) 1,2:3,4-di-*O*-isopropylidene-α-D-galactopyranoside (3.40c)

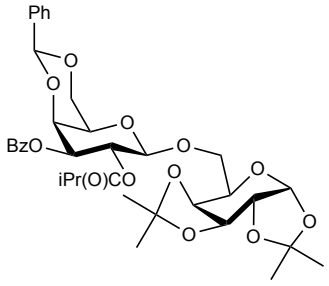

To an oven-dried reaction vessel equipped with a magnetic stir bar, glycosyl donor **3.38** (30 mg, 1.0 equiv, 0.0506 mmol), glycosyl acceptor – commercially available **3.39c** (1.3 to 2 equiv) and NIS (2 equiv) were added sequentially to a mixture of CH_2Cl_2 and MeCN (2 : 1, v/v, 0.6 mL/0.2mL). To this mixture, TMSOTf (10.2 μL,1.1 equiv) was added at -78 ^oC under argon. The reaction mixture was slowly warmed up to 0 ^oC over 5 h and quenched with saturated $NaHCO_3$ solution. The mixture was then extracted with CH_2Cl_2, and the combined organic layers were washed successively with 10% $Na_2S_2O_3$ aqueous solution and brine, dried over anhydrous Na_2SO_4, and concentrated *in vacuo*. The anomeric ratio of the products was determined by integration of the ^1H NMR spectrum of the crude product mixture. Pure glycosylation products were obtained by purification with column chromatography (pentane:ethyl acetate - 4:1). **3.40c** was obtained as an amorphous solid (20.4 mg, 58%).

^{1}H NMR (400 MHz, $CDCl_3$) δ 8.02 (d, *J* = 7.6 Hz, 2H), 7.61 – 7.46 (m, 3H), 7.41 (t, *J* = 7.7 Hz, 2H), 7.33 (dd, *J* = 5.4, 1.9 Hz, 3H), 5.63 (dd, *J* = 10.4, 8.0 Hz, 1H), 5.52 (s, 1H), 5.49 (d, *J* = 5.0 Hz, 1H), 5.20 (dd, *J* = 10.5, 3.6 Hz, 1H), 4.70 (d, *J* = 8.0 Hz, 1H), 4.58 (dd, *J* = 7.9, 2.3 Hz, 1H), 4.52 (d, *J* = 3.7 Hz, 1H), 4.37 (d, *J* = 12.4 Hz, 1H), 4.28 (dd, *J* = 5.0, 2.4 Hz, 1H), 4.23 (dd, *J* = 8.1, 1.8 Hz, 1H), 4.17 – 4.04 (m, 2H), 3.98 (d, *J* = 6.4 Hz, 1H), 3.72 (dd, *J* = 11.0, 7.0 Hz, 1H), 3.60 (s, 1H), 2.50 (hept, *J* = 7.0 Hz, 1H), 1.50 (s, 3H), 1.45 (s, 3H), 1.33 (s, 3H), 1.31 (s, 3H), 1.08 (d, *J* = 6.9 Hz, 3H), 0.98 (d, *J* = 7.0 Hz, 3H).

^{13}C NMR (101 MHz, $CDCl_3$) δ 175.7, 166.2, 137.5, 133.4, 130.0 (2C), 129.2, 128.9, 128.5 (2C), 128.1 (2C), 126.3 (2C), 109.3, 108.6, 101.4, 100.8, 96.3, 73.7, 72.8, 71.3, 70.7, 70.6, 69.0, 68.9, 68.1, 67.6, 66.5, 33.8, 26.1, 26.0, 25.1, 24.3, 18.9, 18.8.

IR (neat) v: 2985, 2925, 2854, 1724, 1457, 1374, 1254, 1210, 1167, 1066

HRMS (ESI) m/z calculated for $C_{36}H_{44}O_{13}Na$ $(M+Na)^+$ 707.2674, found 707.2678.

6-*O*-(3-*O*-benzoyl-4,6-*O*-benzylidene-2-*O*-isobutyryl-β-D-galactopyranosyl)-(1->5)-3-*O*-benzoyl-1,2-*O*-isopropylidene-α-D-xylofuranoside (3.40d)

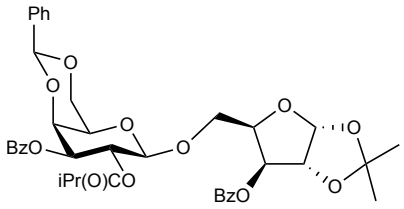

To an oven-dried reaction vessel equipped with a magnetic stir bar, glycosyl donor **3.38** (30 mg, 1.0 equiv, 0.0506 mmol), glycosyl acceptor **3.39d** (19.4 mg, 1.3 equiv, 0.0658

mmol) and NIS (22.8 mg, 2.0 equiv, 0.1012 mmol) were added sequentially to a mixture of CH_2Cl_2 and MeCN (2 : 1, v/v, 0.6 mL/0. 3 mL). To this mixture, TMSOTf (10.1 μL, 1.1 equiv, 0.0557 mmol) was added at -78 ^oC under argon. The reaction mixture was slowly warmed up to 0 ^oC over 5 h and quenched with saturated $NaHCO_3$ solution. The mixture was then extracted with CH_2Cl_2, and the combined organic layers were washed successively with 10% $Na_2S_2O_3$ aqueous solution and brine, dried over anhydrous Na_2SO_4, and concentrated *in vacuo*. The anomeric ratio of the products was determined by integration of the ^1H NMR spectrum of the crude product mixture. Glycosylation product **3.40d** was obtained as a 6.5:1 ratio of beta:alpha anomers (beta – 62.9 mg, 58% and alpha – 3.2 mg, 9%) was obtained by purification with column chromatography (pentane:ethyl acetate - 3:1) as an amorphous solid.

^{1}H NMR (400 MHz, $CDCl_3$) δ 8.12 – 8.05 (m, 2H), 8.04 – 7.97 (m, 2H), 7.60 – 7.29 (m, 11H), 5.91 (d, *J* = 3.8 Hz, 1H), 5.59 (dd, *J* = 10.4, 8.0 Hz, 1H), 5.49 (s, 1H), 5.21 (dd, *J* = 10.4, 3.6 Hz, 1H), 4.77 (d, *J* = 8.0 Hz, 1H), 4.76 – 4.71 (m, 1H), 4.63 – 4.54 (m, 3H), 4.53 – 4.47 (m, 2H), 4.30 (dd, *J* = 12.5, 1.5 Hz, 1H), 4.06 (dd, *J* = 12.5, 1.8 Hz, 1H), 3.59 – 3.55 (m, 1H), 2.47 (hept, *J* = 7.0 Hz, 1H), 1.50 (s, 3H), 1.32 (s, 3H), 1.07 (d, *J* = 7.0 Hz, 3H), 1.00 (d, *J* = 7.0 Hz, 3H).

^{13}C NMR (101 MHz, $CDCl_3$) δ 175.2, 166.3, 166.2, 137.5, 133.6, 132.9, 130.1, 130.0 (2C), 129.9 (2C), 129.01, 129.00, 128.5 (2C), 128.3 (2C), 128.2 (2C), 126.4 (2C), 112.1, 105.2, 101.1, 99.5, 82.8, 80.5, 78.0, 73.5, 72.7, 68.7, 68.1, 66.9, 62.7, 34.0, 26.8, 26.3, 18.9, 18.8.

IR (neat) v: 3530, 3458, 2984, 2875, 2853, 2369, 2354, 2342, 2323, 2312, 1734, 1730, 1720, 1463, 1454, 1402, 1373, 1363, 1344, 1312, 1270, 1232, 1221, 1197, 1183, 1163, 1143, 1096, 1085, 1067, 1030, 1023

HRMS (ESI) m/z calculated for $C_{39}H_{42}O_{13}Na$ $(M+Na)^+$ 741.2518, found 741.2520.

---

methyl 2,3,6-tri-*O*-benzyl-4-*O*-(3-*O*-benzoyl-4,6-*O*-benzylidene-2-*O*-isobutyryl-β-D-galactopyranosyl)-(1->4)-β-D-glucopyranoside (3.40e)

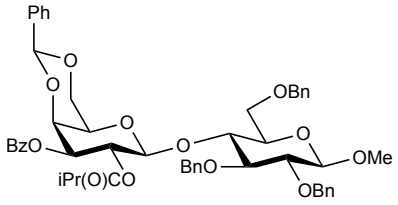

To an oven-dried reaction vessel equipped with a magnetic stir bar, glycosyl donor **3.38** (25 mg, 1.0 equiv, 0.0422 mmol), glycosyl acceptor **3.39e**[58] (25.5 mg, 1.3 equiv, 0.548 mmol) and NIS (19.0 mg, 2.0 equiv, 0.0844 mmol) were added sequentially to a mixture of CH_2Cl_2 and MeCN (2 : 1, v/v, 0.5 mL/0.25 mL). To this mixture, TMSOTf (8.4 μL, 1.1 equiv, 0.0464 mmol) was added at -78 °C under argon. The reaction mixture was slowly warmed up to 0 °C over 5 h and quenched with saturated $NaHCO_3$ solution. The mixture was then extracted with CH_2Cl_2, and the combined organic layers were washed successively with 10% $Na_2S_2O_3$ aqueous solution and brine, dried over anhydrous Na_2SO_4, and concentrated *in vacuo*. The anomeric ratio of the products was determined by integration of the ^1H NMR spectrum of the crude product mixture. Pure glycosylation

product **3.40e** (27.4 mg, 73%) was obtained by purification with column chromatography (pentane:ethyl acetate - 3:1) as an amorphous solid.

^{1}H NMR (400 MHz, $CDCl_3$) δ 8.04 – 7.98 (m, 2H), 7.58 – 7.52 (m, 1H), 7.48 – 7.23 (m, 19H), 7.20 – 7.13 (m, 3H), 5.54 (dd, *J* = 10.4, 8.1 Hz, 1H), 5.45 (s, 1H), 5.11 (d, *J* = 10.8 Hz, 1H), 4.97 (dd, *J* = 10.4, 3.6 Hz, 1H), 4.87 (d, *J* = 11.0 Hz, 1H), 4.79 (d, *J* = 10.8 Hz, 1H), 4.77 (d, *J* = 12.0 Hz, 1H), 4.72 (d, *J* = 11.0 Hz, 1H), 4.71 (d, *J* = 8.1 Hz, 1H), 4.48 (d, *J* = 12.0 Hz, 1H), 4.37 (dd, *J* = 3.6, 1.0 Hz, 1H), 4.29 (d, *J* = 7.8 Hz, 1H), 4.22 (dd, *J* = 12.4, 1.5 Hz, 1H), 4.00 (dd, *J* = 9.8, 9.2 Hz, 1H), 3.88 (dd, *J* = 12.4, 1.9 Hz, 1H), 3.82 (dd, *J* = 10.9, 3.8 Hz, 1H), 3.77 (dd, *J* = 10.9, 1.9 Hz, 1H), 3.64 (t, *J* = 9.2 Hz, 1H), 3.56 (s, 3H), 3.42 (dd, *J* = 9.2, 7.8 Hz, 1H), 3.37 (ddd, *J* = 9.8, 3.8, 1.9 Hz, 1H), 3.16 – 3.12 (m, 1H), 2.40 (hept, *J* = 7.0 Hz, 1H), 1.02 (d, *J* = 6.9 Hz, 3H), 0.93 (d, *J* = 7.0 Hz, 3H).
^{13}C NMR (101 MHz, $CDCl_3$) δ 175.4, 166.1, 138.9, 138.7, 138.2, 137.7, 133.5, 130.0 (2C), 129.1, 128.8, 128.5 (4C), 128.29 (2C), 128.26 (2C), 128.1 (2C), 128.02 (2C), 127.96 (4C), 127.9, 127.5, 127.3, 126.3 (2C), 104.7, 100.8, 100.4, 82.8, 81.9, 77.1, 75.7, 74.84, 74.82, 73.6, 73.5, 73.0, 69.0, 68.7, 68.2, 66.4, 57.1, 34.0, 19.1, 18.7.
IR (neat) v 3567, 2927, 2853, 2359, 1734, 1717, 1698, 1684, 1653, 1558, 1541, 1521, 1508, 1489, 1473, 1457, 1397, 1270, 1048
HRMS (ESI) m/z calculated for $C_{52}H_{56}O_{13}Na$ $(M+Na)^+$ 911.3613, found 911.3611.

---

methyl 2,4,6-tri-*O*-benzyl-3-*O*-(3-*O*-benzoyl-4,6-*O*-benzylidene-2-*O*-isobutyryl-β-D-galactopyranosyl)-(1->3)-α-D-glucopyranoside (3.40f)

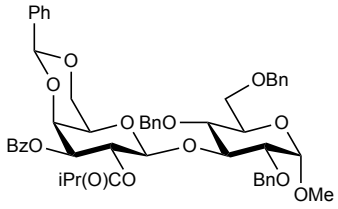

To an oven-dried reaction vessel equipped with a magnetic stir bar, glycosyl donor **3.38** (25 mg, 1.0 equiv, 0.0422 mmol), glycosyl acceptor **3.39f**[59] (25.5 mg, 1.3 equiv, 0.548 mmol) and NIS (19.0 mg, 2.0 equiv, 0.0844 mmol) were added sequentially to a mixture of CH_2Cl_2 and MeCN (2 : 1, v/v, 0.5 mL/0.25 mL). To this mixture, TMSOTf (8.4 μL, 1.1 equiv, 0.0464 mmol) was added at -78 °C under argon. The reaction mixture was slowly warmed up to 0 °C over 5 h and quenched with saturated $NaHCO_3$ solution. The mixture was then extracted with CH_2Cl_2, and the combined organic layers were washed successively with 10% $Na_2S_2O_3$ aqueous solution and brine, dried over anhydrous Na_2SO_4, and concentrated *in vacuo*. The anomeric ratio of the products was determined by integration of the ^{1}H NMR spectrum of the crude product mixture. Glycosylation products **beta-3.40e** and **alpha-3.40e**(beta – 23.1 mg, 62% and alpha – 5.0 mg, 13%) were obtained by purification with column chromatography (hexane:ethyl acetate - 3:1) both as an amorphous solid.

^{1}H NMR (400 MHz, $CDCl_3$) δ 8.07 – 8.01 (m, 2H), 7.59 – 7.52 (m, 1H), 7.48 – 7.20 (m, 19H), 7.14 – 7.02 (m, 3H), 5.69 (dd, *J* = 10.4, 8.1 Hz, 1H), 5.51 (s, 1H), 5.31 (d, *J* = 8.1 Hz, 1H), 5.21 (dd, *J* = 10.4, 3.7 Hz, 1H), 5.20 (d, *J* = 10.1 Hz, 1H), 4.76 (d, *J* = 11.4 Hz, 1H), 4.63 – 4.56 (m, 2H), 4.55 – 4.48 (m, 3H), 4.45 – 4.38 (m, 2H), 4.32 (dd, *J* = 12.4, 1.5 Hz, 1H), 4.03 (dd, *J* = 12.4, 1.9 Hz, 1H), 3.75 – 3.69 (m, 2H), 3.66 – 3.59 (m, 2H),

3.56 (dd, *J* = 9.6, 3.5 Hz, 1H), 3.54 – 3.51 (m, 1H), 3.31 (s, 3H), 2.51 (hept, *J* = 7.0 Hz, 1H), 1.13 (d, *J* = 7.0 Hz, 3H), 0.97 (d, *J* = 7.0 Hz, 3H).

^{13}C NMR (101 MHz, $CDCl_3$) δ 175.8, 166.2, 138.3, 138.0, 137.82, 137.77, 133.4, 130.0 (C2), 129.2, 129.1 (2C), 128.8, 128.6 (2C), 128.5 (2C), 128.4 (2C), 128.32 (2C), 128.28, 128.2 (2C), 128.1 (2C), 128.0 (2C), 127.8, 127.4, 126.4 (2C), 100.9, 100.5, 97.5, 81.3, 78.1, 75.7, 75.4, 73.9, 73.6, 73.5, 73.1, 69.7, 69.2, 68.8, 68.5, 66.4, 55.0, 34.1, 19.2, 18.8.

IR (neat) v: 2919, 2851, 2362, 1717, 1653, 1541, 1456, 1271, 1047

HRMS (ESI) m/z calculated for $C_{52}H_{56}O_{13}Na$ $(M+Na)^+$ 911.3613, found 911.3608.

***p*-methoxyphenyl 4,6-*O*-benzylidene-2-*O*-4-oxopentanoyl-β-D-galactopyranoside (3.48)**

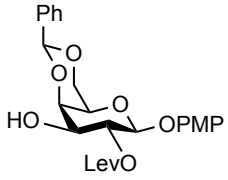

According to general procedure E, **3.47**[60] (37 mg, 0.1 mmol), (*R*)-BTM (2.5 mg, 0.01 mol), *i*Pr_2NEt (50 ul, 0.3 mmol), LevOH (25 uL, 0.25 mmol), Piv_2O (43 uL, 0.25 mmol) and $CHCl_3$ (1 mL) were used. The product **3.48** was isolated by column chromatography on silica gel (hexane:ethyl acetate - 1/4) as a colorless foam (40 mg, 85%).

^{1}H NMR (500 MHz, $CDCl_3$): δ 7.50 (m, 2H), 7.35 (m, 3H), 7.01 (d, *J* = 9.0 Hz, 2H), 6.80 (d, *J* = 9.0 Hz, 2H), 5.53 (s, 1H), 5.33 (dd, *J* = 8.5, 9.5 Hz, 1H), 4.86 (d, *J* = 8.0 Hz, 1H),

4.34 (d, *J* = 12.5 Hz, 1H), 4.23 (d, *J* = 3.5 Hz, 1H), 4.08 (d, *J* = 11.5 Hz, 1H), 3.80 (d, *J* = 10.0 Hz, 1H), 3.74 (s, 3H), 3.54 (br, 1H), 2.75-2.73 (m, 2H), 2.65-2.62 (m, 2H), 2.14 (s, 3H).

^{13}C NMR (126 MHz, $CDCl_3$) δ 206.7, 172.5, 155.7, 151.5, 137.5, 129.4, 128.4 (2C), 126.6 (2C), 119.2 (2C), 114.6 (2C), 101.6, 100.8, 75.5, 72.4, 71.6, 69.0, 66.8, 55.8, 38.2, 30.0, 28.2.

IR (neat) v: 3017, 2981, 2921, 2889, 1742, 1719, 1507, 1401, 1366, 1216, 1161, 1100, 1082, 827, 753.

HRMS (ESI) m/z calculated for $C_{25}H_{28}O_9Na$ $(M+Na)^+$ 495.1631, found 495.1629.

***p*-methoxyphenyl *3-O-*(2,3-di-*O*-benzoyl-4,6-*O*-(di-*tert*-butyl)silylene-α-D-galactopyranosyl)-(1->3)-4,6-*O*-benzylidene-2-*O*-4-oxopentanoyl-β-D-galactopyranoside (3.49)**

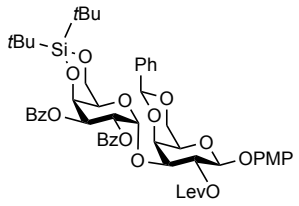

Acceptor **5** (234 mg, 0.49 mmol) and donor **8**[61] (399 mg, 0.59 mmol) were dissolved in dry dichloromethane (5 mL). 4Å MS (600 mg) were added. The reaction mixture was stirred for 30 min at room temperature and then cooled to 0 °C. TMSOTf (9 uL, 0.049 mmol) was added slowly. After stirring at 0 °C for 3 hours, the reaction mixture was quenched with Et_3N (0.2 mL), filtered and concentrated in vacuo. The residue was purified

by column chromatograph on silica gel (hexane:ethyl acetate - 2/1) to give the product **3.49** (403 mg, 83%) as a white foam.

^{1}H NMR (500 MHz, $CDCl_3$): δ 7.90 (d, *J* = 7.5 Hz, 2H), 7.72 (d, *J* = 8.0 Hz, 2H), 7.39-6.85 (m, 13H), 6.68 (d, *J* = 9.0 Hz, 2H), 5.60-5.44 (m, 4H), 5.13 (s, 1H), 4.92 (br, 1H), 4.71 (d, *J* = 7.5 Hz, 1H), 4.36 (d, *J* = 12.0 Hz, 1H), 4.19-4.12 (m, 3H), 4.04 (br, 1H), 3.88-3.82 (m, 2H), 3.61 (s, 3H), 3.27 (br, 1H), 2.89-2.82 (m, 1H), 2.66-2.60 (m, 1H), 2.53-2.47 (m, 2H), 2.11 (s, 3H), 1.06 (s, 9H), 0.90 (s, 9H).

^{13}C NMR (126 MHz, $CDCl_3$) δ 206.5, 171.3, 166.5, 165.7, 155.5, 151.4, 137.2, 133.1, 133.0, 130.0, 129.6 (4C), 129.0, 128.44, 128.36 (2C), 128.30 (2C), 127.8 (2C), 125.9 (2C), 118.9 (2C), 114.4 (2C), 101.2, 100.3, 93.9, 74.5, 71.6, 71.2, 70.8, 69.9, 68.8, 68.7, 67.6, 66.9, 66.5, 55.6, 37.7, 29.9, 28.0, 27.6 (3C), 27.3 (3C), 23.3, 20.8.

IR (neat) v: 2936, 2861, 2391, 2347, 2069, 1753, 1508, 1338, 1284, 1218, 1180, 1156, 995.

HRMS (ESI) m/z calculated for $C_{53}H_{62}O_{16}SiNa$ $(M+Na)^+$ 1005.3705, found 1005.3709.

---

methyl 2,3,6-tri-*O*-benzyl-4-*O*-(4,6-*O*-benzylidene-2-*O*-4-oxopentanoyl-3-*O*-(2,3-di-*O*-benzoyl-4,6-*O*-(di-*tert*-butyl)silylene-α-D-galactopyranosyl)-(1->3)-β-D-galactopyranosyl)-(1->4)-β-D-glucopyranoside (3.42) made via Cation-*n* directed acylation

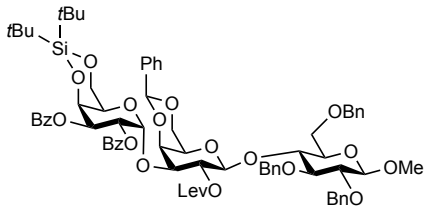

To a solution of the disaccharide **3.50** (280 mg, 0.29 mmol) in toluene/CH_3CN/H_2O (1.4 mL/2.1 mL/1.4 mL), CAN (781 mg, 1.4 mmol) was added. After being stirred at room temperature for 1 hour, the solution was poured into ice water and extracted with CH_2Cl_2. The organic layer was washed with saturated aqueous $NaHCO_3$ and brine, and dried over Na_2SO_4. Filtration, concentration in vacuo, and purification by silica gel column chromatography (hexane:ethyl acetate - 1.5/1 to 1/1.5) afforded the corresponding lactol (174 mg, 70%). The above lactol (174 mg, 0.2 mmol) was dissolved in dry CH_2Cl_2 (0.6 mL). CCl_3CN (0.1 mL, 1.0 mmol) and DBU (10 uL, 0.04 mmol) were added. After stirring overnight, the reaction mixture was concentrated in vacuo. The residue was purified by silica gel column chromatography (hexane:ethyl acetate - 2/1 + 3% Et_3N) to provide the imidate (130 mg, 64%).

The above imidate (116 mg, 0.11 mmol) and acceptor **3.39e**[58] (24 mg, 0.052 mmol) were dissolved in dry CH_2Cl_2 (1 mL). 4Å MS (140 mg) were added. The reaction mixture was stirred at room temperature for 30 min and then cooled to 0 ^oC. 0.05 M TMSOTf (0.2 mL, 0.01 mmol) in CH_2Cl_2 was added. After stirring at 0 ^oC for 2 hours, the reaction mixture was quenched with Et_3N (0.1 mL). Filtration, concentration in vacuo and purification on silica gel column chromatograph (hexane:ethyl acetate - 3/1 to 1.5/1) provided trisaccharide **3.42** (55 mg, 81%) as a white foam.

^{1}H NMR (500 MHz, $CDCl_3$) δ 8.00 – 7.95 (m, 2H), 7.89 – 7.84 (m, 2H), 7.49 (t, *J* = 7.5 Hz, 1H), 7.40 – 7.25 (m, 15H), 7.22 – 7.16 (m, 4H), 7.13 – 7.07 (m, 4H), 6.98 (t, *J* = 7.6 Hz, 2H), 5.66 (dd, *J* = 10.5, 3.7 Hz, 1H), 5.52 – 5.44 (m, 2H), 5.32 (dd, *J* = 10.1, 8.0 Hz, 1H), 5.25 (s, 1H), 5.03 (d, *J* = 10.9 Hz, 1H), 4.91 (d, *J* = 3.2 Hz, 1H), 4.86 (d, *J* = 11.1 Hz, 1H), 4.78 (d, *J* = 12.1 Hz, 1H), 4.74 – 4.68 (m, 2H), 4.54 (d, *J* = 8.1 Hz, 1H), 4.47 (d, *J* = 12.0 Hz, 1H), 4.37 (dd, *J* = 12.7, 2.1 Hz, 1H), 4.30 (d, *J* = 7.8 Hz, 1H), 4.21 (dd, *J* = 12.8, 1.7 Hz, 1H), 4.16 – 4.05 (m, 3H), 3.99 (s, 1H), 3.94 (t, *J* = 9.3 Hz, 1H), 3.88 (dd, *J* = 11.2, 3.5 Hz, 1H), 3.85 – 3.80 (m, 1H), 3.74 (dd, *J* = 12.4, 1.8 Hz, 1H), 3.60 (t, *J* = 9.0 Hz, 1H), 3.58 – 3.53 (m, 4H), 3.47 (d, *J* = 9.5 Hz, 1H), 3.39 (dd, *J* = 9.2, 7.8 Hz, 1H), 2.85 – 2.76 (m, 2H), 2.62 – 2.47 (m, 2H), 2.21 (s, 3H), 1.13 (s, 9H), 0.97 (s, 9H).

^{13}C NMR (126 MHz, $CDCl_3$) δ 206.5, 171.1, 166.5, 165.9, 138.9, 138.7, 138.4, 137.5, 133.0, 130.0, 129.7 (2C), 129.7 (2C), 129.2, 128.4 (3C), 128.4 (2C), 128.32 (2C), 128.25 (2C), 128.22 (2C), 128.02 (2C), 127.93 (3C), 127.92 (2C), 127.74 (2C), 127.70, 127.47, 127.11, 126.0 (2C), 104.6, 100.6, 100.46, 94.7, 82.9, 82.0, 75.7, 75.7, 74.8 (2C), 73.6 (2C), 72.4, 71.2, 70.9, 70.7, 68.8, 68.5, 68.3, 67.7, 66.8, 66.3, 57.1, 37.6, 30.0, 27.9, 27.6 (3C), 27.3 (3C), 23.3, 20.7.

IR (neat) v: 3411, 2980, 2886, 1738, 1726, 1379, 1287, 1216, 1160, 1071, 950, 758, 668.

HRMS (ESI) m/z calculated for $C_{74}H_{86}O_{20}SiNa$ $(M+Na)^+$ 1345.5379, found 1345.5358.

---

adamantyl 3-*O*-(2,3-di-*O*-benzoyl-4,6-*O*-(di-*tert*-butyl)silylene-α-D-galactopyranosyl)-(1->3)-4,6-*O*-benzylidene-2-*O*-4-oxopentanoyl-β-D-galactopyranoside (3.51)

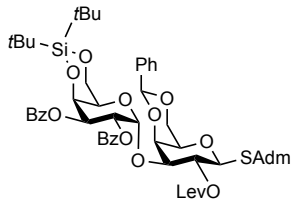

To an oven-dried vial equipped with a stir bar, trichloroimidate donor **3.45** (67 mg, 1.2 equiv, 0.1 mmol) and glycosyl acceptor **3.13f** (43 mg, 1.0 equiv, 0.083 mmol) were added followed by 1.5 mL CH_2Cl_2 and 4 Å MS. The reaction vial was allowed to stir at room temperature for ~40 minutes. The reaction vessel was then placed in a 0 ^oC ice bath for ~10 minutes, followed by the addition of TMSOTf (1.5 μL, 0.11 equiv, 0.0083 mmol). The vial was flushed with Argon, capped with a septum, and stirred in a 0 ^oC ice bath until reaction completion. Upon reaction completion, Et_3N was used to quench the reaction to pH neutral. The reaction contents were then filtered, concentrated *in vacuo*, and purified via flash chromatography using 100% hexane to hexane:ethyl acetate = 4:1. Product **3.51** was isolated as an amorphous solid (53 mg, 62%).

^{1}H NMR (400 MHz, $CDCl_3$) δ 7.86 (d, *J* = 7.1 Hz, 2H), 7.70 (dd, *J* = 8.0, 1.4 Hz, 2H), 7.37 (t, *J* = 7.5 Hz, 1H), 7.24 (td, *J* = 7.7, 2.4 Hz, 3H), 7.07 (d, *J* = 6.9 Hz, 2H), 7.01 (td, *J* = 7.6, 2.3 Hz, 3H), 6.88 (t, *J* = 7.6 Hz, 2H), 5.57 – 5.47 (m, 2H), 5.39 (dd, *J* = 10.4, 3.1 Hz, 1H), 5.23 (t, *J* = 9.7 Hz, 1H), 5.13 (s, 1H), 4.85 (d, *J* = 3.1 Hz, 1H), 4.48 (d, *J* = 10.0 Hz,

1H), 4.30 (dd, *J* = 12.6, 2.0 Hz, 1H), 4.16 – 4.07 (m, 3H), 3.97 (s, 1H), 3.83 – 3.74 (m, 2H), 3.26 (s, 1H), 2.87 (dt, *J* = 18.4, 7.2 Hz, 1H), 2.64 (dt, *J* = 18.4, 6.2 Hz, 1H), 2.51 – 2.42 (m, 2H), 2.12 (s, 3H), 1.90 (s, 3H), 1.83 (d, *J* = 12.3 Hz, 3H), 1.71 (d, *J* = 12.3 Hz, 3H), 1.62 – 1.49 (m, 6H), 1.00 (s, 9H), 0.86 (s, 9H).

^{13}C NMR (101 MHz, $CDCl_3$) δ 206.7, 171.4, 166.6, 165.7, 137.3, 133.1, 132.9, 130.1, 129.7 (2C), 129.6 (2C), 129.1, 128.4, 128.3 (4C), 127.7 (2C), 126.0 (2C), 100.5, 94.1, 80.3, 76.4, 72.2, 71.1, 70.7, 69.5, 69.2, 68.9, 68.7, 67.6, 66.9, 46.2, 44.0 (3C), 37.8, 36.2 (3C), 30.0, 29.8 (3C), 28.3, 27.6 (3C), 27.3 (3C), 23.3, 20.7.

IR (neat) v 2925, 2361, 1716, 1452, 1362, 1280, 1220, 1152, 1105, 1072, 1028

HRMS (ESI) m/z calculated for $C_{56}H_{70}O_{14}SSiNa$ $(M+Na)^+$ 1049.4148, found 1049.4119.

---

methyl 2,3,6-tri-*O*-benzyl-4-*O*-(4,6-*O*-benzylidene-2-*O*-4-oxopentanoyl-3-*O*-(2,3-di-*O*-benzoyl-4,6-*O*-(di-*tert*-butyl)silylene-α-D-galactopyranosyl)-(1->3)-β-D-galactopyranosyl)-(1->4)-β-D-glucopyranoside (3.42) made via *S*-adamantyl directed site-selective acylation

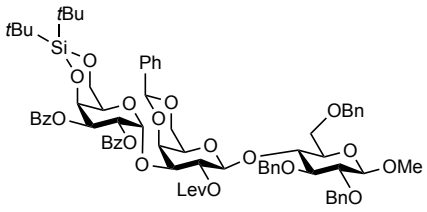

To an oven-dried reaction vessel equipped with a magnetic stir bar, glycosyl donor **3.51** (7.5 mg, 0.0073 mmol), glycosyl acceptor **3.39e** (4.4 mg, 0.0095 mmol, 1.3 equiv) and

NIS (3,3 mg, 0.0146 mmol, 2 equiv) were added sequentially to a mixture of CH_2Cl_2 and MeCN (0.15 mL, 2 : 1, v/v). To this mixture, TMSOTf (1.5 uL, 0.0080 mmol, 1.1 equiv) was added at -78°C under argon. The reaction mixture was slowly warmed up to 0°C over 5 h and quenched with saturated $NaHCO_3$ solution. The mixture was then extracted with CH_2Cl_2, and the combined organic layers were washed successively with 10% $Na_2S_2O_3$ aqueous solution and brine, dried over anhydrous Na_2SO_4, and concentrated *in vacuo*. The anomeric ratio of the products was determined by integration of the ^{1}H NMR spectrum of the crude product mixture. Pure glycosylation products were obtained by purification with flash chromatography (hexane:ethyl acetate - 3/1 to 1.5/1) provided trisaccharide **3.42** (6.7 mg, 69%) as a white foam.

^{1}H NMR (500 MHz, $CDCl_3$): δ 8.00 – 7.95 (m, 2H), 7.88 – 7.83 (m, 2H), 7.53 – 7.46 (m, 1H), 7.43 – 7.26 (m, 15H), 7.23 – 7.15 (m, 4H), 7.14 – 7.06 (m, 4H), 6.98 (t, *J* = 7.7 Hz, 2H), 5.66 (dd, *J* = 10.5, 3.7 Hz, 1H), 5.49 (t, *J* = 3.8 Hz, 2H), 5.32 (dd, *J* = 10.1, 8.0 Hz, 1H), 5.25 (s, 1H), 5.03 (d, *J* = 10.8 Hz, 1H), 4.91 (d, *J* = 3.1 Hz, 1H), 4.86 (d, *J* = 11.1 Hz, 1H), 4.77 (d, *J* = 12.1 Hz, 1H), 4.70 (dd, *J* = 10.9, 4.5 Hz, 2H), 4.54 (d, *J* = 8.0 Hz, 1H), 4.47 (d, *J* = 12.0 Hz, 1H), 4.37 (dd, *J* = 12.7, 2.0 Hz, 1H), 4.30 (d, *J* = 7.7 Hz, 1H), 4.21 (dd, *J* = 12.6, 1.7 Hz, 1H), 4.10 (dd, *J* = 12.3, 1.5 Hz, 1H), 4.06 (d, *J* = 3.5 Hz, 1H), 3.99 (s, 1H), 3.94 (t, *J* = 9.3 Hz, 1H), 3.88 (dd, *J* = 11.2, 3.5 Hz, 1H), 3.82 (dd, *J* = 11.2, 1.8 Hz, 1H), 3.74 (dd, *J* = 12.4, 1.8 Hz, 1H), 3.63 – 3.56 (m, 4H), 3.50 – 3.44 (m, 1H), 3.39 (dd, *J* = 9.2, 7.8 Hz, 1H), 2.81 (td, *J* = 6.5, 1.9 Hz, 2H), 2.62 – 2.46 (m, 2H), 2.21 (s, 3H), 1.13 (s, 9H), 0.97 (s, 9H).

^{13}C NMR (126 MHz, $CDCl_3$) δ 206.56, 171.17, 166.47, 165.88, 138.93, 138.71, 138.40, 137.46, 133.17, 133.01, 130.00, 129.71 (2C), 129.65 (2C), 129.14, 128.41 (3C), 128.38 (2C), 128.33 (2C), 128.26 (2C), 128.22 (2C), 128.03 (2C), 127.94 (3C), 127.75 (3C), 127.72, 127.47, 127.12, 125.99, 104.64, 100.55, 100.47, 94.74, 82.89, 81.95, 75.75, 75.71, 74.81, 73.56, 72.35, 71.16, 70.92, 70.72, 68.81, 68.25, 67.65, 66.80, 66.26, 57.10, 51.88, 41.66, 36.36, 29.97, 29.72, 29.44, 27.56 (3C), 27.28 (3C), 24.75, 23.28, 20.73.

IR (neat) v 3411, 2980, 2886, 1738, 1726, 1379, 1287, 1216, 1160, 1071, 950, 758, 668.

HRMS (ESI) m/z calculated for $C_{74}H_{86}O_{20}SiNa$ $(M+Na)^+$ 1345.5379, found 1345.5358.

3.7.4 Computational Details:

All DFT calculations were performed using Gaussian 09. Geometries were optimized using the M06-2X density functional with the 6-31G(d) basis set. Vibrational frequency calculations were performed for all of the stationary points to confirm if each optimized structure is a local minimum or a transition state structure. For single-point energy calculations, the ω-B97XD functional was used with the 6-311++G(d,p) basis set. The SMD solvation model[62] using Chloroform as solvent was used in the single point energy calculations. The substrate-catalyst dispersion energy ($\Delta E_{dispersion}$) in the acyl transfer transition state is calculated using:

$$\Delta E_{dispersion} = E_{disp\text{-}TS} - E_{disp\text{-}BTM} - E_{disp\text{-}substrate}$$

Where $E_{disp\text{-}TS}$, $E_{disp\text{-}BTM}$, and $E_{disp\text{-}substrate}$ are the dispersion energies of the acylation transition state (**C2-TS** and **C3-TS**), and the acylated (*R*)-BTM catalyst and the substrate (**3.12e**) in their transition state geometry, respectively. The dispersion energies were calculated from the dispersion energy corrections to the "dispersion-free" HF theory using the DFT-D3 package[63] with the zero-damping method.

Details of the C2-acylation and the C3-acylation transition states:

Other possible isomers of the C2- and C3-acylation transition states (**C2-TS2**, **C3-TS2**, **C3-TS3**) were shown in Figure S1. These isomers are all higher in energy than **C2-TS** and **C3-TS** (**Figure 3-8** in the main manuscript). **C2-TS2** involves the "C-H up" conformation, which means the carbonyl of the acylated (*R*)-BTM catalyst approaches the substrate *anti* to the C−H bond on the carbon that is being acylated. Even though the lone pair-π interaction is present in this transition state, it has been demonstrated in our

previous work that this “C-H up” conformation is generally disfavored due to greater steric repulsions about the forming O-acyl bond.[40] Similarly, the C3-acylation transition state **C3-TS3** also involves the “C-H up” conformation, and thus is disfavored. In **C3-TS2,** the adamantyl group adopts a conformation that is similar to that in conformer A of the *S*-glycocide substrate (**3.12e**) (Figure S2). While in **C3-TS** (**Figure 3-8** in the main manuscript), the adamantyl group adopts a conformation similar to that in conformer **B** of **3.12e**. Both conformers **A** and **B** are stabilized by exo-anomeric effects.[1] In **3.12e**, the stability of these conformers is comparable. While **A** is more favorable sterically, **B** is stabilized due to C-H/pi interactions with the benzylidene protecting group. Our calculations indicate conformation **B** is favored in the C3-acylation transition state, with **C3-TS** being 1.8 kcal/mol more stable than **C3-TS2**.

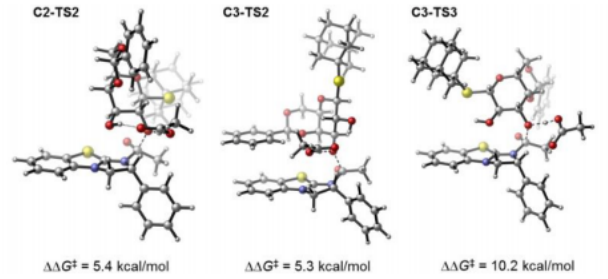

Figure S1. Other transition state isomers for the C2- and C3-acylation of *S*-glycoside **3.12e**. The relative Gibbs free energies are with respect to the **C2-TS** in **Figure 3-8** of the main manuscript.

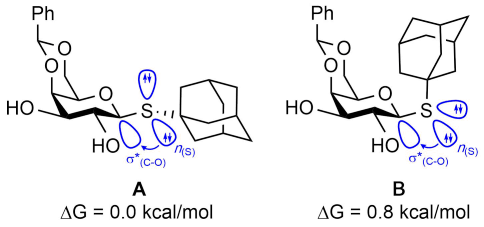

Figure S2. Depiction of the preferred *exo*-anomeric conformers of *S*-adamantyl 4,6-*O*-benzylidene-1-thio-β-D-galactopyranoside **3.12e**.

Cartesian Coordinates of the most favorable transition states for C2- and C3-Acylation

C2-TS
M06-2X/6-31G(d) SCF energy: -3136.070942 a.u.
M06-2X/6-31G(d) SCF enthalpy: -3135.169592 a.u.
M06-2X/6-31G(d) SCF free energy: -3135.296560 a.u.
ωB97X-D/6-311++G(d,p) SCF energy in solution: -3137.066805 a.u.
ωB97X-D/6-311++G(d,p) enthalpy in solution: -3136.165456 a.u.
ωB97X-D/6-311++G(d,p) free energy in solution: -3136.292423 a.u.
Three lowest frequencies (cm^{-1}): -534.3704 16.9546 19.7094
Imaginary frequency: -534.3704 cm^{-1}

Cartesian coordinates

ATOM	X	Y	Z
O	-1.46128600	-0.52730000	-2.61994200
C	-3.94113900	-3.28633600	1.34361700
O	-4.34080100	-2.11632200	1.36490700
C	-4.67660600	-4.37004200	2.11080400
H	-4.00082400	-4.81582000	2.84574300
H	-4.97605900	-5.16409500	1.42171900
H	-5.55181200	-3.95711000	2.61190600
O	-2.90677700	-3.69964700	0.69437100
H	-2.34609900	-2.74500100	0.18570300
N	-2.40618300	0.52539100	-0.87711100
C	-1.46061700	1.44540700	-0.88086000
N	-1.50567500	2.23746600	0.19207300
S	-0.25620400	1.88165300	-2.03463500
C	-0.61333400	3.30308400	0.16078400
C	0.15138600	3.27467500	-1.01469800
C	-0.45283500	4.30781600	1.10920800
C	1.09642200	4.26233900	-1.26424200
H	-1.04359500	4.31103400	2.01941500
C	0.48922400	5.29668300	0.84697200
H	1.69924800	4.23827200	-2.16614800
C	1.25140500	5.27848600	-0.32539200
H	0.63545800	6.09284200	1.56890500
H	1.98232800	6.05967700	-0.50264700
C	-3.26672800	0.66916800	0.32994500
H	-3.29081700	-0.30057100	0.83988700
C	-4.65786900	1.12540800	-0.05646100
C	-5.77379200	0.46032900	0.45122300
C	-4.82950600	2.23126400	-0.89488400
C	-7.05250800	0.91035200	0.12380100
H	-5.62965500	-0.41776300	1.07540500
C	-6.10599100	2.67389100	-1.22098400
H	-3.96097800	2.74531900	-1.30454500
C	-7.22146700	2.01287400	-0.70773600
H	-7.91967300	0.38813000	0.51594600
H	-6.23216100	3.53013700	-1.87631900
H	-8.21949600	2.35555600	-0.96304700
C	-2.36201600	-0.58745000	-1.78909200
C	-2.49111500	1.73944700	1.16342200
H	-3.14575100	2.55058200	1.48858400
H	-1.96212600	1.29303000	2.00957900
C	-0.08660200	-3.29721300	-1.17667700
C	-0.38609300	-2.07491200	-0.29413500
C	0.16209400	-2.34890600	1.11981000
C	1.91321700	-3.76385100	0.25699800
C	1.41913500	-3.51825500	-1.16777000
H	0.13562600	-1.20393900	-0.72387700
H	-0.56241900	-4.17616900	-0.71594500
H	1.54197500	-4.73834600	0.61289300
H	1.68811000	-4.37267900	-1.80933000
H	-0.46492400	-3.14200300	1.55727200
C	3.43553900	-3.74054100	0.25039700
H	3.83028500	-3.78545800	1.26743200
H	3.81477400	-4.59829300	-0.32727300
C	3.41098300	-2.31355900	-1.61133600
H	3.80420100	-3.12109700	-2.26000300
O	1.52187800	-2.72558800	1.13440200
S	-0.06114200	-0.92436000	2.26044600
O	-1.74037800	-1.81069300	-0.22222600

O	-0.59653500	-3.19073000	-2.47879700
H	-0.65023200	-2.24899500	-2.71739000
O	3.89796900	-2.52366600	-0.30717300
O	2.01580100	-2.33050200	-1.67033200
C	3.87923600	-0.94865900	-2.06382100
C	5.17837200	-0.53238700	-1.77280900
C	3.01835200	-0.09935100	-2.75923300
C	5.61553000	0.72705600	-2.17316600
H	5.83587100	-1.19187800	-1.21474800
C	3.46099600	1.15887500	-3.16213300
H	2.00600700	-0.42681400	-2.97210500
C	4.75794200	1.57543400	-2.87095000
H	6.62577000	1.04734000	-1.93756600
H	2.79061300	1.81127100	-3.71608800
H	5.10135300	2.55598000	-3.18706900
C	1.52106800	0.02740900	2.19832100
C	1.99030400	0.31675300	0.76563900
C	1.18913500	1.36504500	2.88989200
C	2.64630200	-0.65796500	2.99722400
H	1.18151500	0.82511700	0.22009500
H	2.21028500	-0.61957800	0.24500500
C	3.24190400	1.20870500	0.79538300
H	0.82666300	1.17797900	3.91001800
H	0.38309000	1.86937300	2.33870400
C	2.43424700	2.26816400	2.92281500
H	2.88080900	-1.62126100	2.54102800
H	2.29456800	-0.84648000	4.01970100
C	3.89562500	0.23954600	3.01576000
H	3.56611200	1.39431500	-0.23647600
C	2.90449300	2.53654000	1.48620600
C	4.35669000	0.49225700	1.57112200
H	2.17113900	3.21629200	3.41002700
C	3.55847300	1.57099800	3.70166900
H	4.69039300	-0.27066700	3.57373300
H	2.11557200	3.05470000	0.93030500
H	3.78336900	3.19564800	1.49734200
H	4.58873400	-0.46087300	1.08045500
H	5.26923600	1.10425900	1.56519000
H	4.44484400	2.21831900	3.73404300
H	3.24631700	1.39120400	4.73889600
C	-3.61867400	-1.38911400	-1.93804800
H	-4.12222900	-1.54217600	-0.98099800
H	-4.28449700	-0.86490100	-2.63292500
H	-3.32644000	-2.35232000	-2.35932500

C3-TS
M06-2X/6-31G(d) SCF energy: -3136.069118 a.u.
M06-2X/6-31G(d) SCF enthalpy: -3135.167049 a.u.
M06-2X/6-31G(d) SCF free energy: -3135.291572 a.u.
ωB97X-D/6-311++G(d,p) SCF energy in solution: -3137.064300 a.u.
ωB97X-D/6-311++G(d,p) enthalpy in solution: -3136.162231 a.u.
ωB97X-D/6-311++G(d,p) free energy in solution: -3136.286754 a.u.
Three lowest frequencies (cm^{-1}): -289.0763 16.9060 21.7587
Imaginary frequency: -289.0763 cm^{-1}

Cartesian coordinates

ATOM	X	Y	Z
O	2.79691800	-0.13104900	2.89925800
C	0.65118200	-1.20747700	-1.97897800
O	0.95010500	-2.36808700	-1.72038500
C	0.25368900	-0.78956000	-3.37791600
H	0.94211500	-1.23502300	-4.09971500
H	0.23068900	0.29721400	-3.47854800
H	-0.74426000	-1.18570700	-3.58782000
O	0.66180200	-0.23171600	-1.10415000
H	0.92453500	-0.62043800	-0.09378100
N	3.47554700	-0.04033500	0.71115900
C	2.93737500	1.16523900	0.55856200
N	2.92225200	1.59044600	-0.70324000
S	2.18403000	2.23177600	1.67112100
C	2.25176700	2.79164100	-0.90397300
C	1.78717400	3.30149800	0.31483700
C	2.01713900	3.44817400	-2.10715700
C	1.06458400	4.48861900	0.35226800

H	2.38054700	3.04043800	-3.04485800
C	1.29464900	4.63443900	-2.05913600
H	0.67819100	4.87592100	1.28963400
C	0.82357800	5.14955900	-0.84665800
H	1.08379900	5.16389700	-2.98226700
H	0.24247700	6.06501400	-0.84145900
C	3.66852500	-0.63684600	-0.63626600
H	2.85811900	-1.35586200	-0.79457700
C	4.99472400	-1.33346300	-0.80703600
C	5.03936200	-2.52120400	-1.53608700
C	6.17147900	-0.79458200	-0.28491700
C	6.25651100	-3.16267400	-1.75246700
H	4.11408100	-2.94454200	-1.92191500
C	7.38536200	-1.44046900	-0.49533600
H	6.12928100	0.11908000	0.30304000
C	7.42964500	-2.62282400	-1.23268900
H	6.28547400	-4.08887300	-2.31745800
H	8.29767200	-1.02418800	-0.07976500
H	8.37762300	-3.12633000	-1.39375100
C	2.97881900	-0.80965500	1.89382500
C	3.49854400	0.58592600	-1.59314000
H	4.46205600	0.93377700	-1.97775700
H	2.81548400	0.37771300	-2.41949200
C	0.29219200	-1.41623500	1.93703300
C	-0.78653600	-2.18302400	1.16148900
C	-2.00482400	-2.45104700	2.04945400
C	-1.53535300	-0.51024600	3.39171000
C	-0.31355000	-0.15910700	2.54507300
H	-1.09664500	-1.53391400	0.33371400
H	0.64979100	-2.05522100	2.76274200
H	-1.20824200	-1.05225700	4.29555200
H	0.43333800	0.36463500	3.15962500
H	-1.70858800	-3.18774600	2.81541500
C	-2.24561900	0.77909700	3.77965100
H	-3.20595700	0.56101300	4.24964300
H	-1.61362300	1.35080500	4.47839300
C	-1.36812300	1.83447800	1.88883500
H	-0.67339300	2.40335200	2.54555300
O	-2.47878000	-1.26411700	2.66321700
O	1.34237600	-1.13806700	1.06082800
O	-2.52758000	1.55228900	2.62662500
O	-0.71142800	0.67719900	1.46189000
C	-1.76729100	2.65393300	0.68505600
C	-1.35535700	2.29775300	-0.59810600
C	-2.55911800	3.78744100	0.87358600
C	-1.75063200	3.07036900	-1.68901800
H	-0.73479600	1.41808900	-0.73866800
C	-2.94057500	4.56244000	-0.21727300
H	-2.89270600	4.04336700	1.87527200
C	-2.53993600	4.20209300	-1.50349700
H	-1.43826300	2.78128500	-2.68915000
H	-3.56361100	5.43894500	-0.06616300
H	-2.84823200	4.79996200	-2.35633400
O	-0.28703700	-3.40521600	0.69531000
H	0.35173800	-3.18505700	-0.00824500
S	-3.41294600	-3.23756700	1.21844300
C	3.48576600	-2.23050100	1.93289800
H	3.35442700	-2.75281900	0.98532200
H	4.54617100	-2.21640800	2.20483000
H	2.92922100	-2.75583500	2.71058200
C	-3.80710500	-2.16441800	-0.23418100
C	-2.95594500	-2.54723800	-1.46219100
C	-5.28028000	-2.49635400	-0.56048700
C	-3.71469900	-0.65389000	0.05850600
H	-3.08093400	-3.61948200	-1.65768700
H	-1.88794700	-2.39565200	-1.26997900
C	-3.40688800	-1.72650600	-2.68226000
H	-5.90534000	-2.25173300	0.30675000
H	-5.38420900	-3.57404800	-0.74710300
C	-5.74786000	-1.70132200	-1.79179300
H	-2.69876600	-0.35119500	0.32736300
H	-4.34097900	-0.41164200	0.92484700
C	-4.16498100	0.13969300	-1.17888600
H	-2.78371100	-1.99406100	-3.54630500
C	-4.87237500	-2.05523000	-3.00184300

C	-3.26446900	-0.22828900	-2.36846700
H	-6.79325000	-1.95711300	-2.00378100
C	-5.62566700	-0.19733300	-1.50745000
H	-4.06564700	1.21071800	-0.96272400
H	-4.97057800	-3.12177900	-3.24237500
H	-5.20494500	-1.48897600	-3.88206300
H	-2.21969600	0.00397800	-2.11402900
H	-3.53117200	0.37349200	-3.24858500
H	-5.96339000	0.37689100	-2.38073900
H	-6.27017500	0.08090800	-0.66383000

3.7.5 Spectra

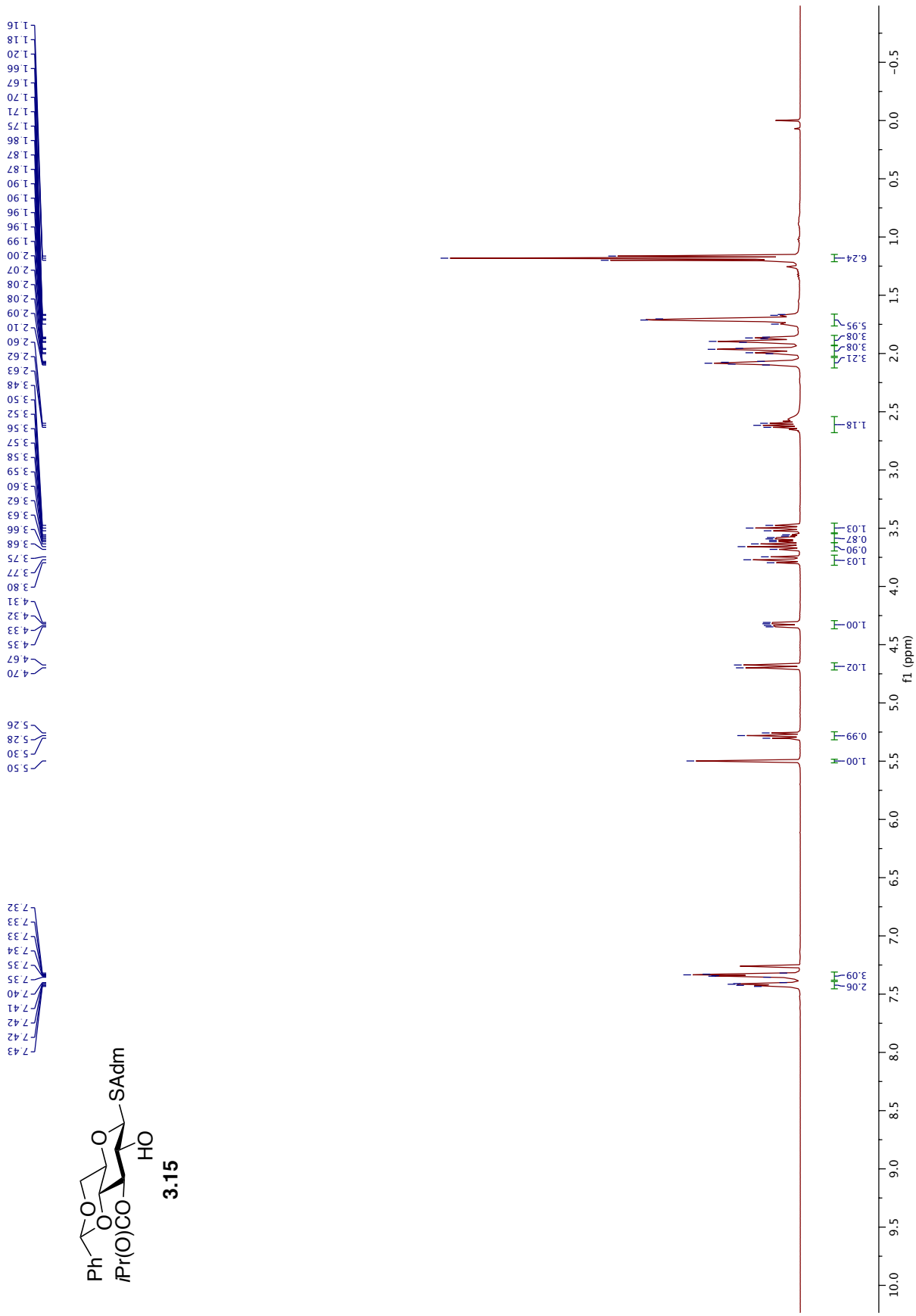
Ph
O
O
O
iPr(O)CO
HO
SAdm
3.15
f1 (ppm)

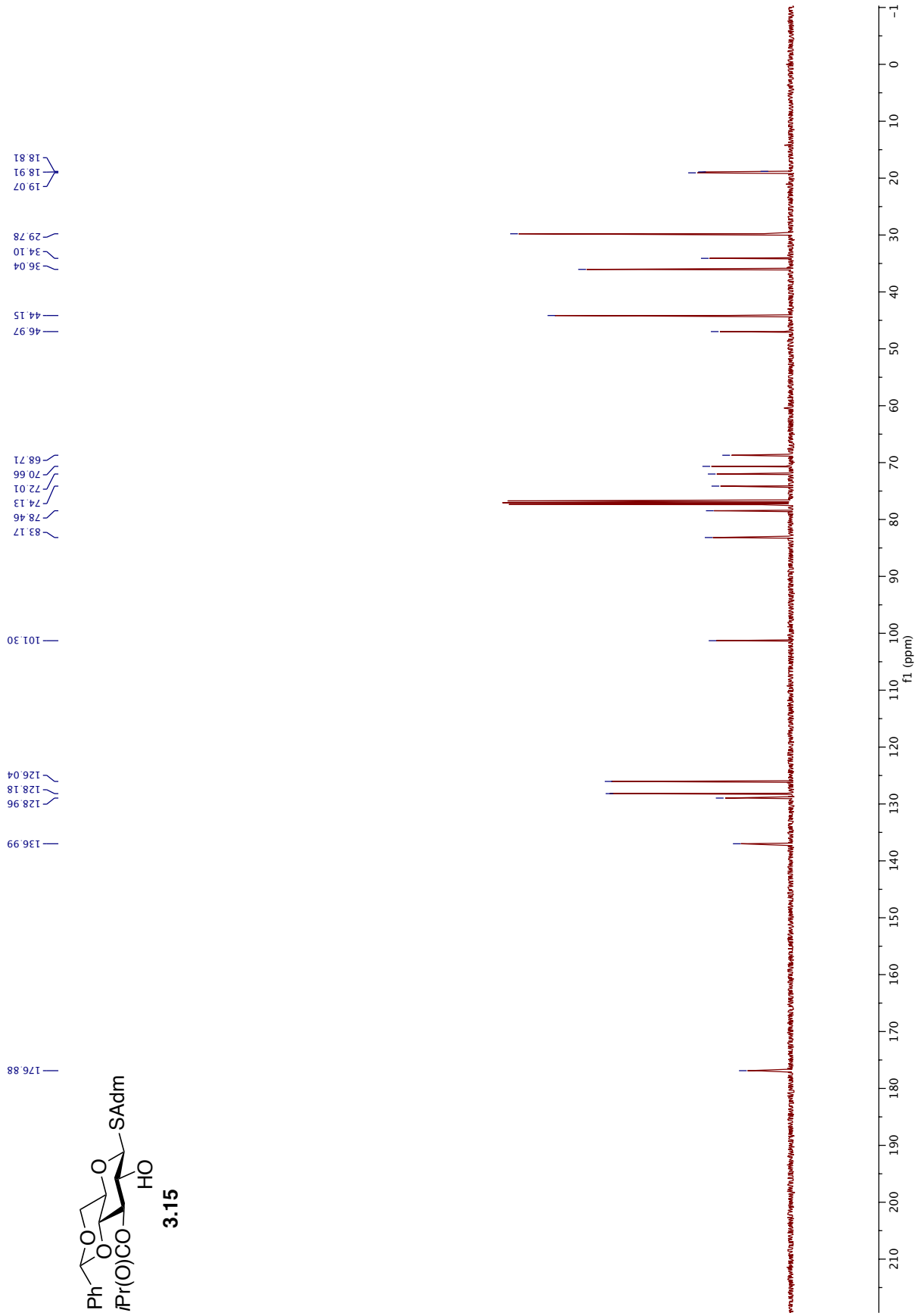
Ph
O
O
O
iPr(O)CO
O
SAdm
HO
3.15
176.88
136.99
128.96
128.18
126.04
101.30
83.17
78.46
74.13
72.01
70.66
68.71
46.97
44.15
36.04
34.10
29.78
19.07
18.91
18.81
f1 (ppm)

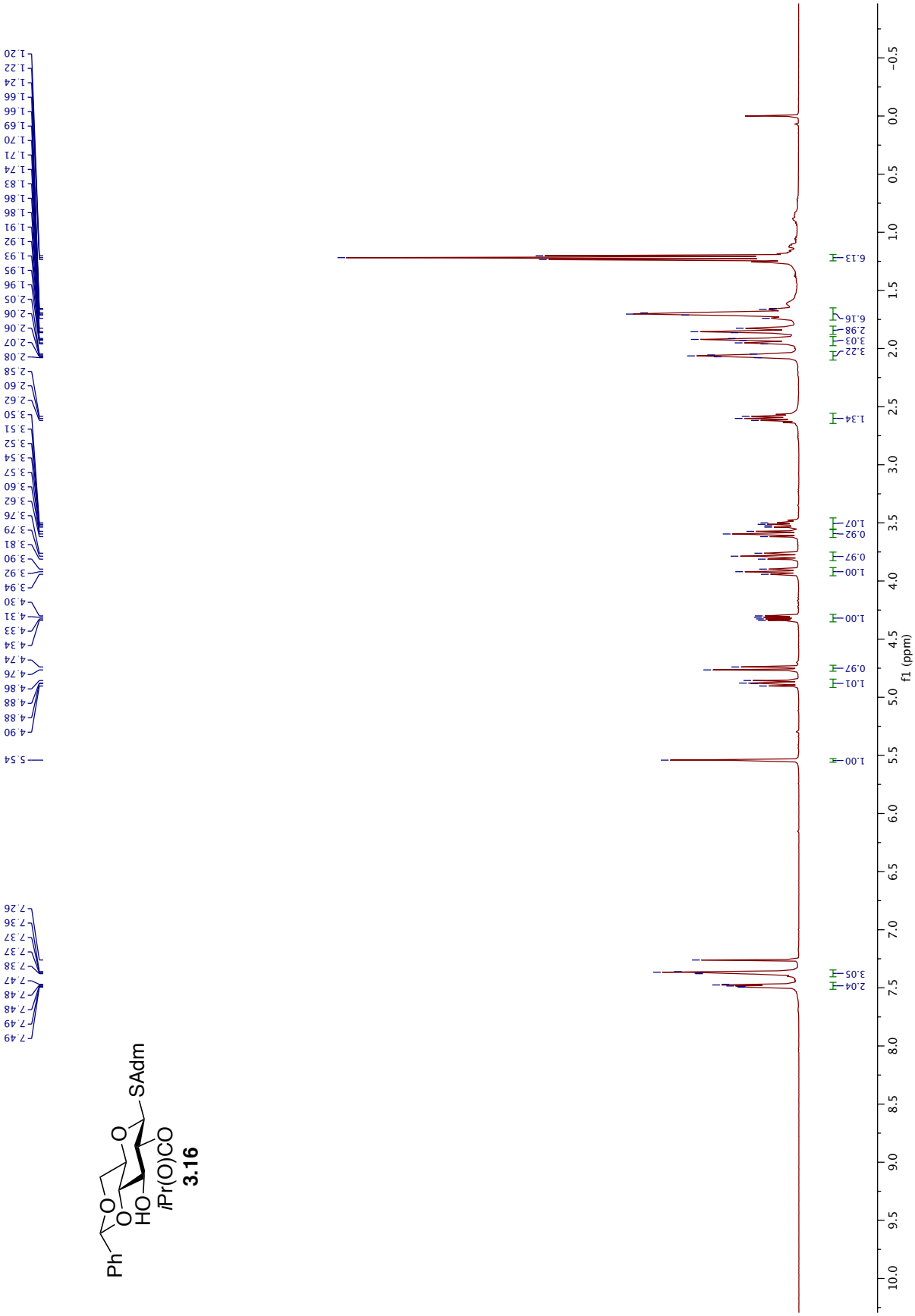
Ph
O
O
HO
O
SAdm
iPr(O)CO
3.16
f1 (ppm)

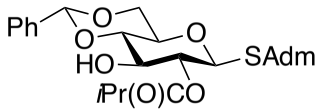
Ph
O
O
O
HO
SAdm
iPr(O)CO

3.16

176.14
136.96
129.30
128.35
126.30
101.89
80.76
80.49
73.85
72.28
70.00
68.69
46.35
44.11
36.13
34.05
29.75
19.05
18.85
210 200 190 180 170 160 150 140 130 120 110 100 90 80 70 60 50 40 30 20 10 0 -1
f1 (ppm)

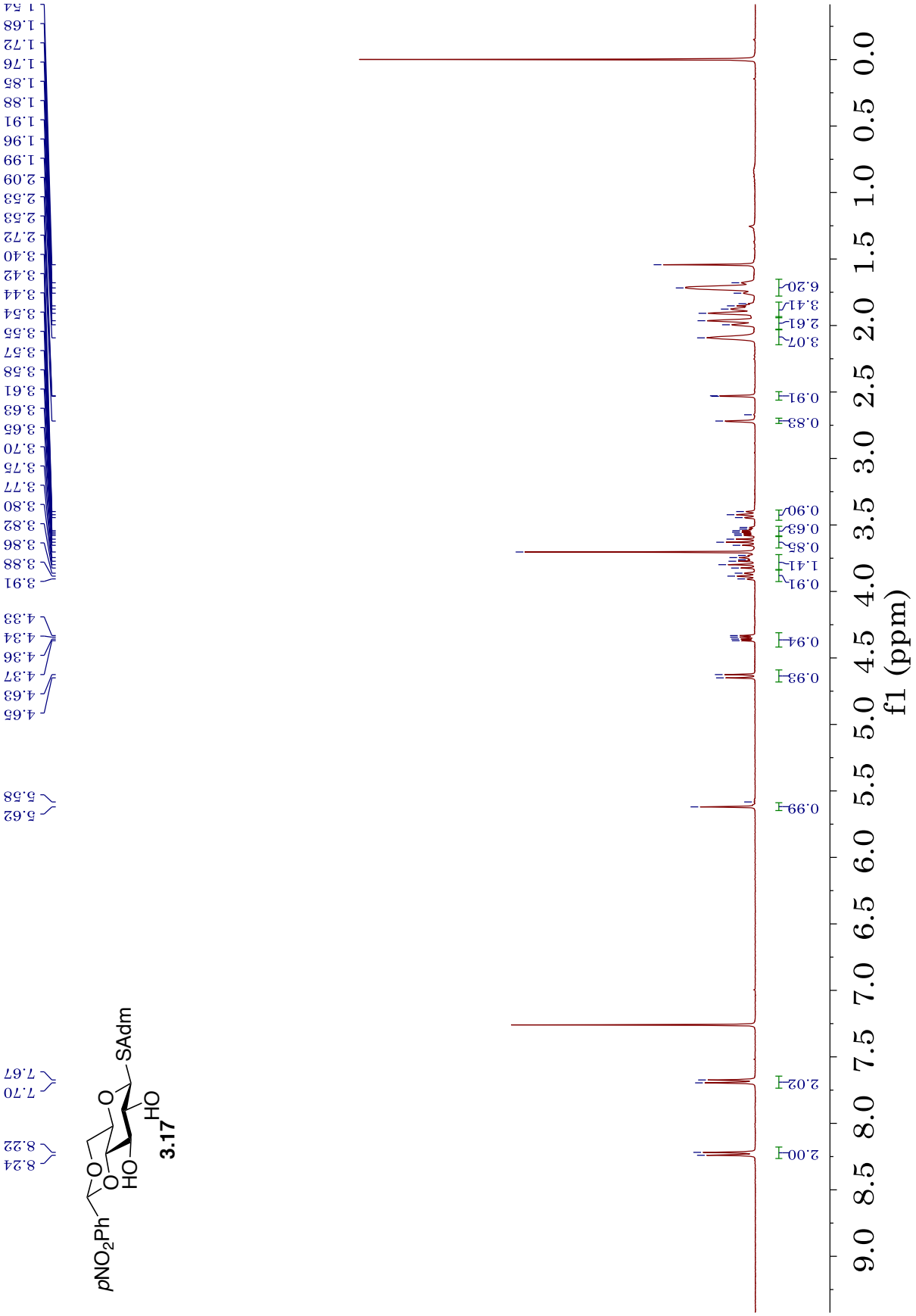
pNO2Ph
O
O
O
HO
HO
SAdm
3.17
f1 (ppm)

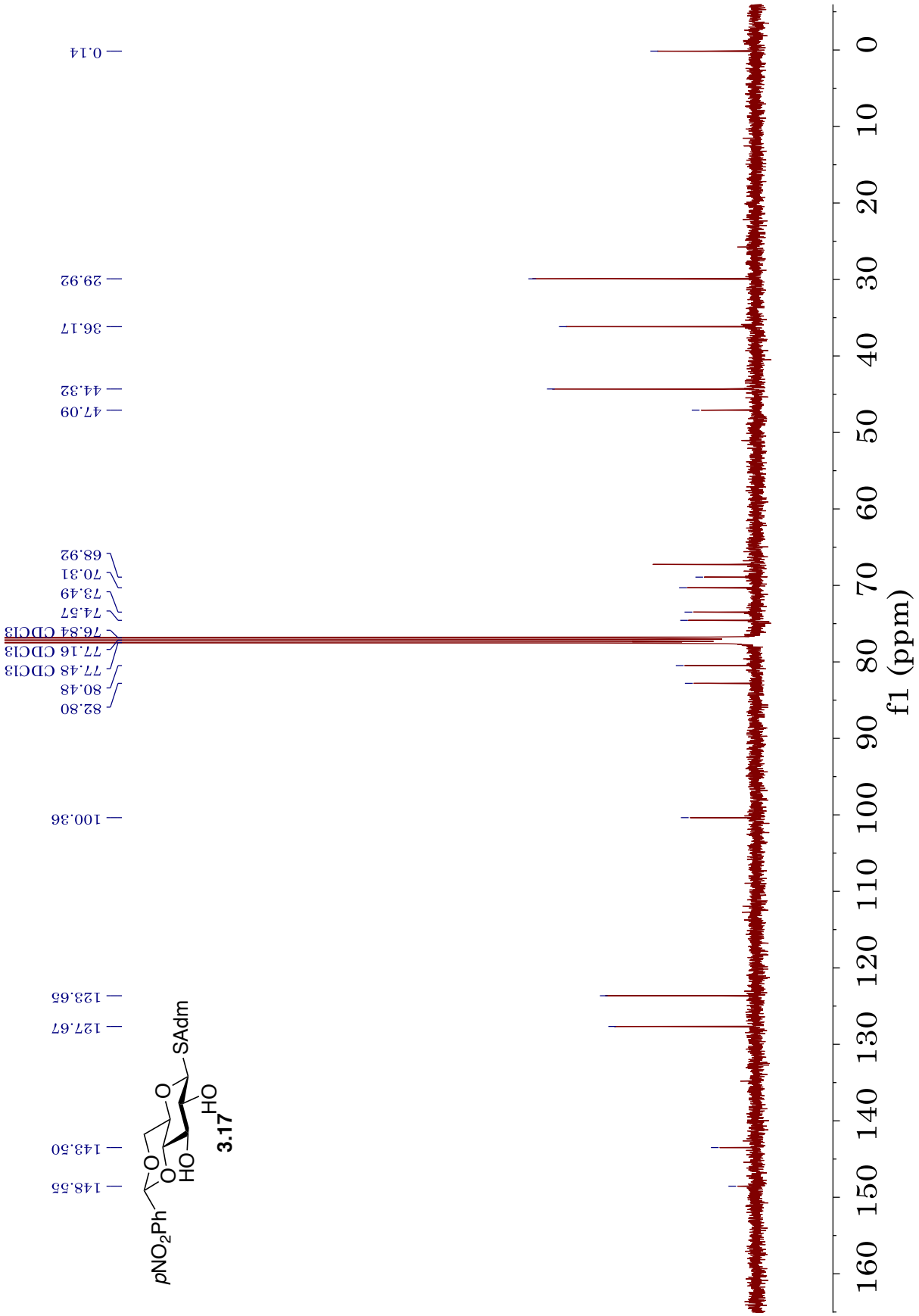
f1 (ppm)
0
10
20
30
40
50
60
70
80
90
100
110
120
130
140
150
160
0.14
29.92
36.17
44.32
47.09
68.92
70.31
73.49
74.57
76.84 CDCl3
77.16 CDCl3
77.48 CDCl3
80.48
82.80
100.36
123.65
127.67
143.50
148.55
pNO2Ph
O
O
O
HO
HO
SAdm
3.17

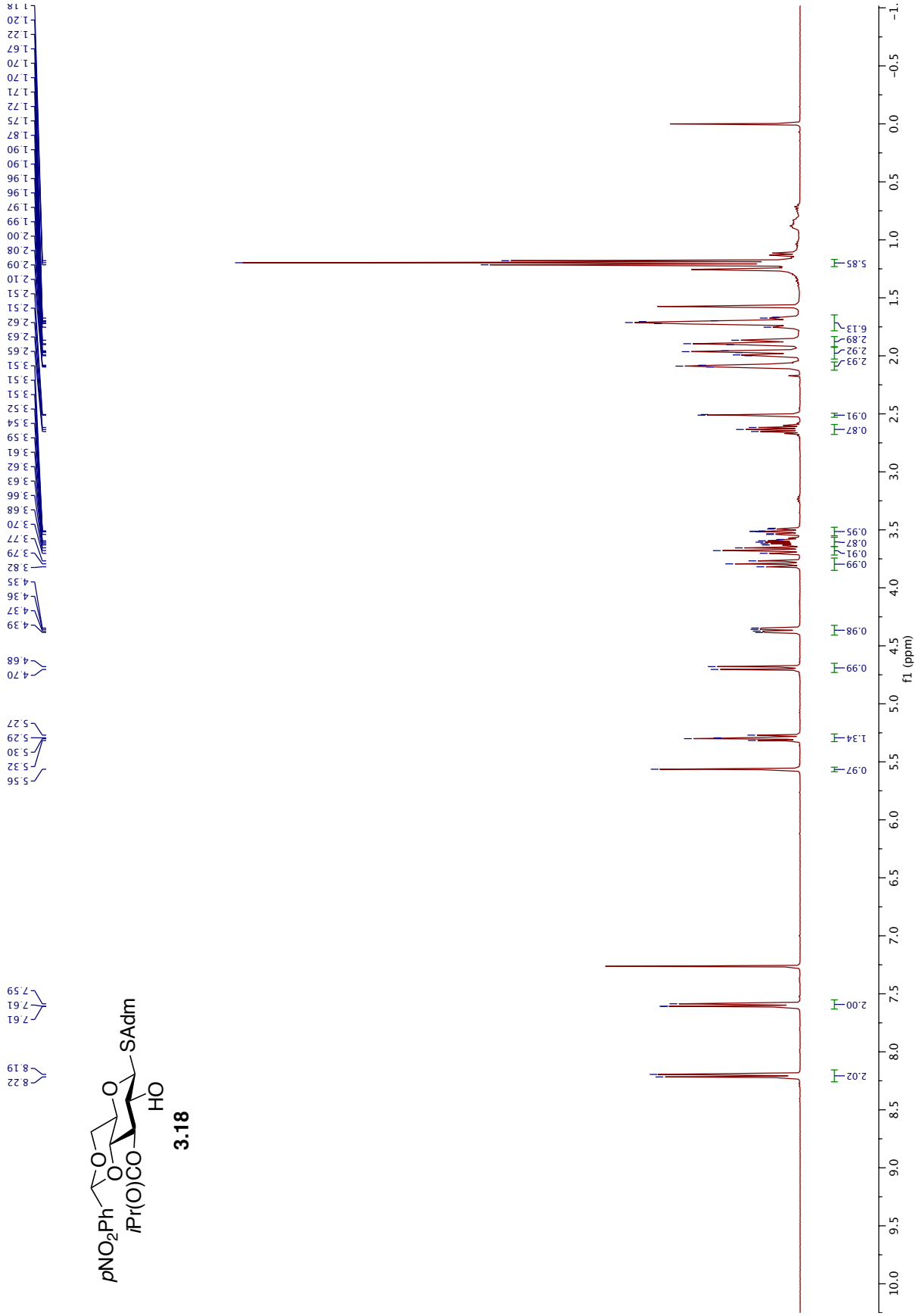
pNO2Ph
iPr(O)CO
SAdm
HO
3.18
f1 (ppm)

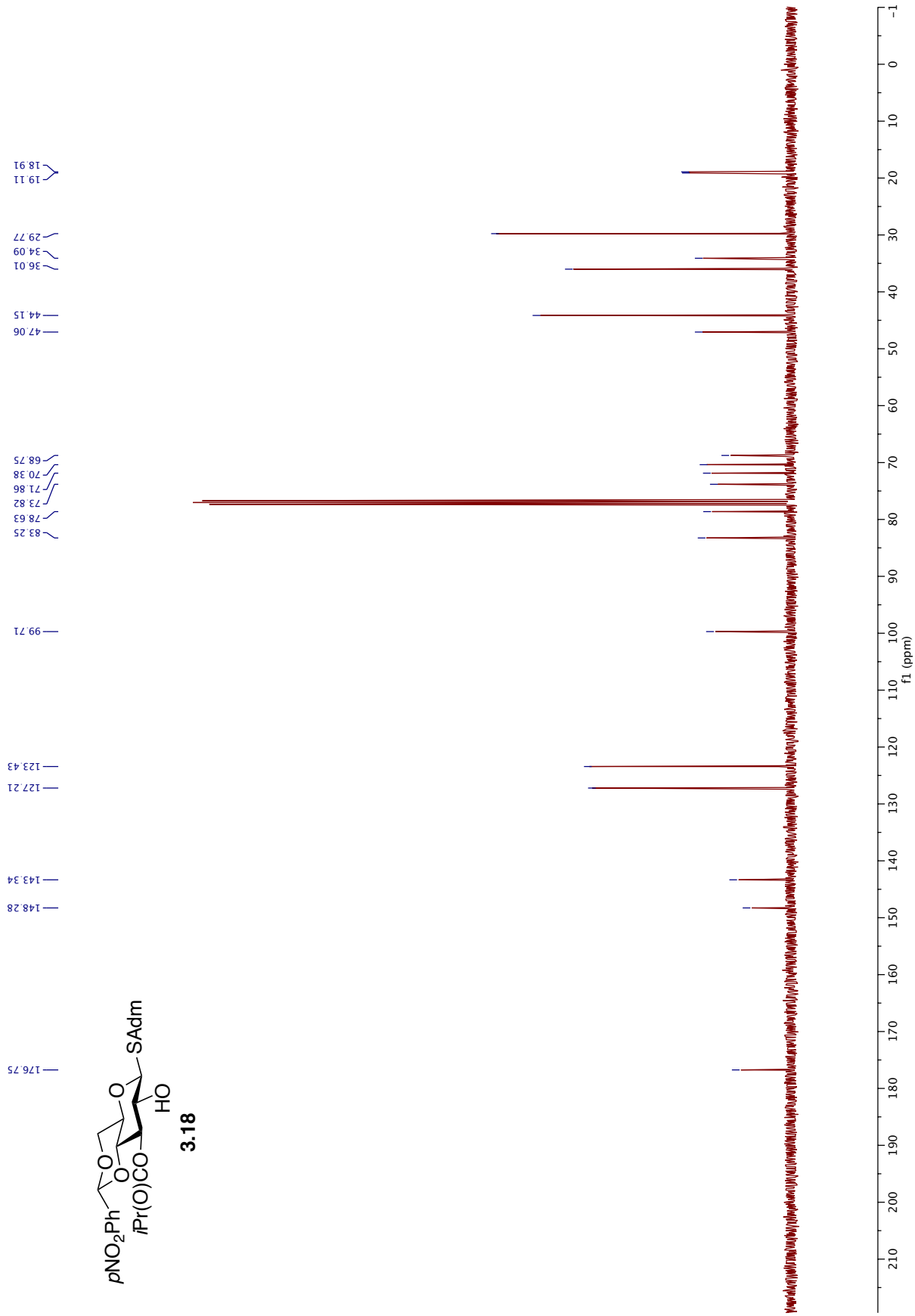
18.91
19.11
29.77
34.09
36.01
44.15
47.06
68.75
70.38
71.86
73.82
78.63
83.25
99.71
123.43
127.21
143.34
148.28
176.75
f1 (ppm)
SAdm
HO
O
O
O
O
pNO2Ph
iPr(O)CO

3.18

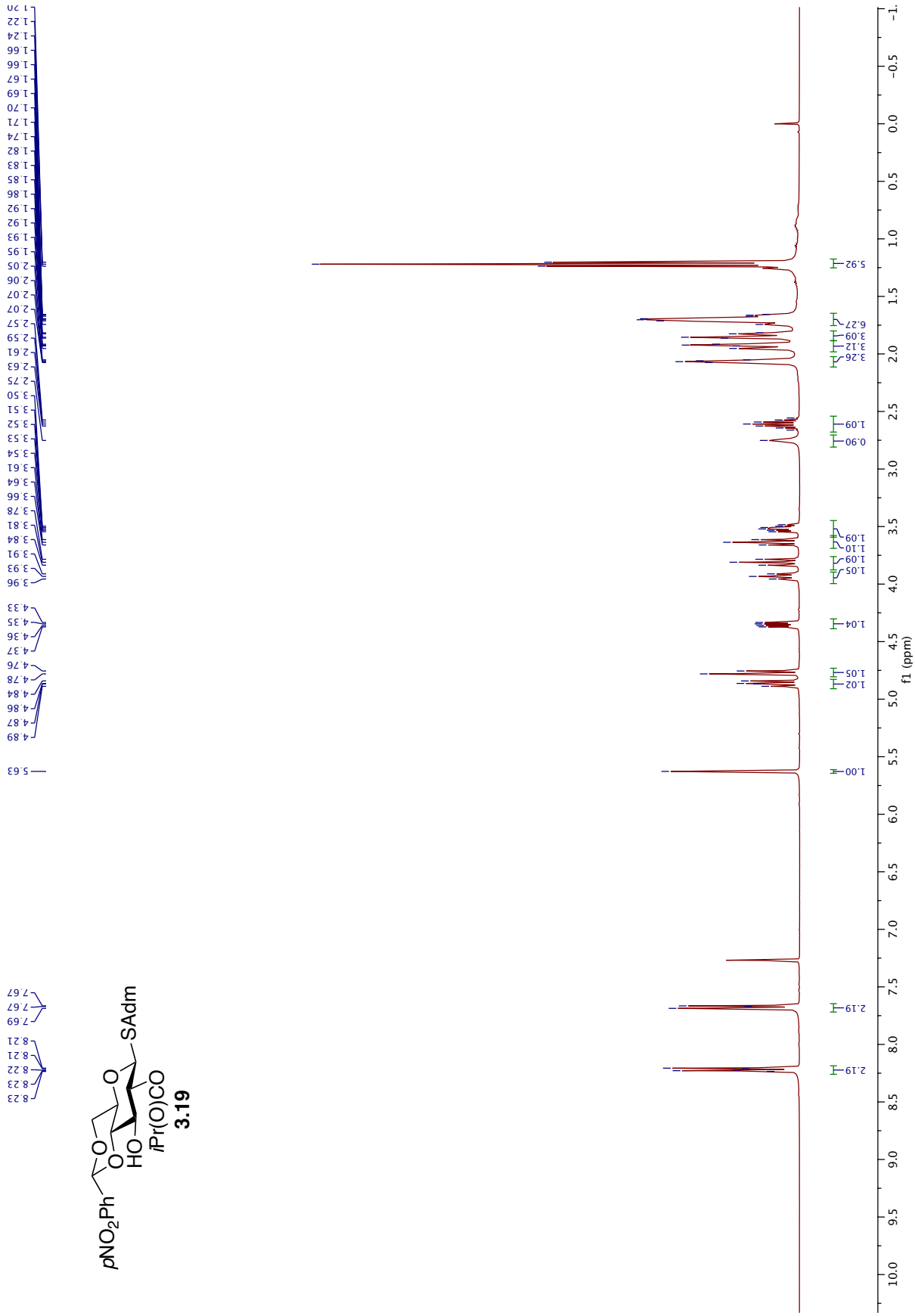
pNO2Ph
O
O
HO
O
O
SAdm
iPr(O)CO
3.19
f1 (ppm)

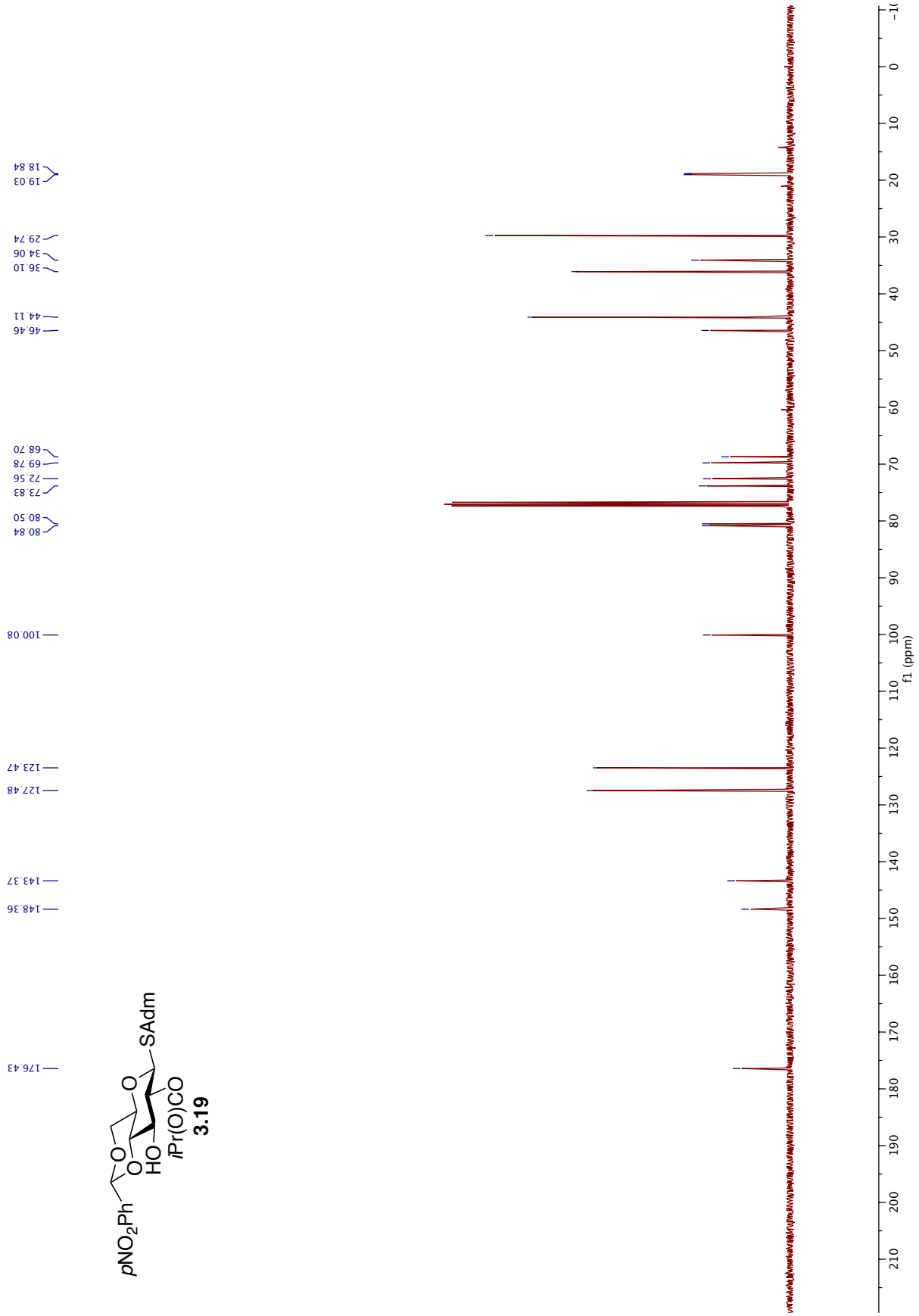
pNO2Ph
O
O
HO
O
SAdm
iPr(O)CO
3.19
176.43
148.36
143.37
127.48
123.47
100.08
80.84
80.50
73.83
72.56
69.78
68.70
46.46
44.11
36.10
34.06
29.74
19.03
18.84
f1 (ppm)

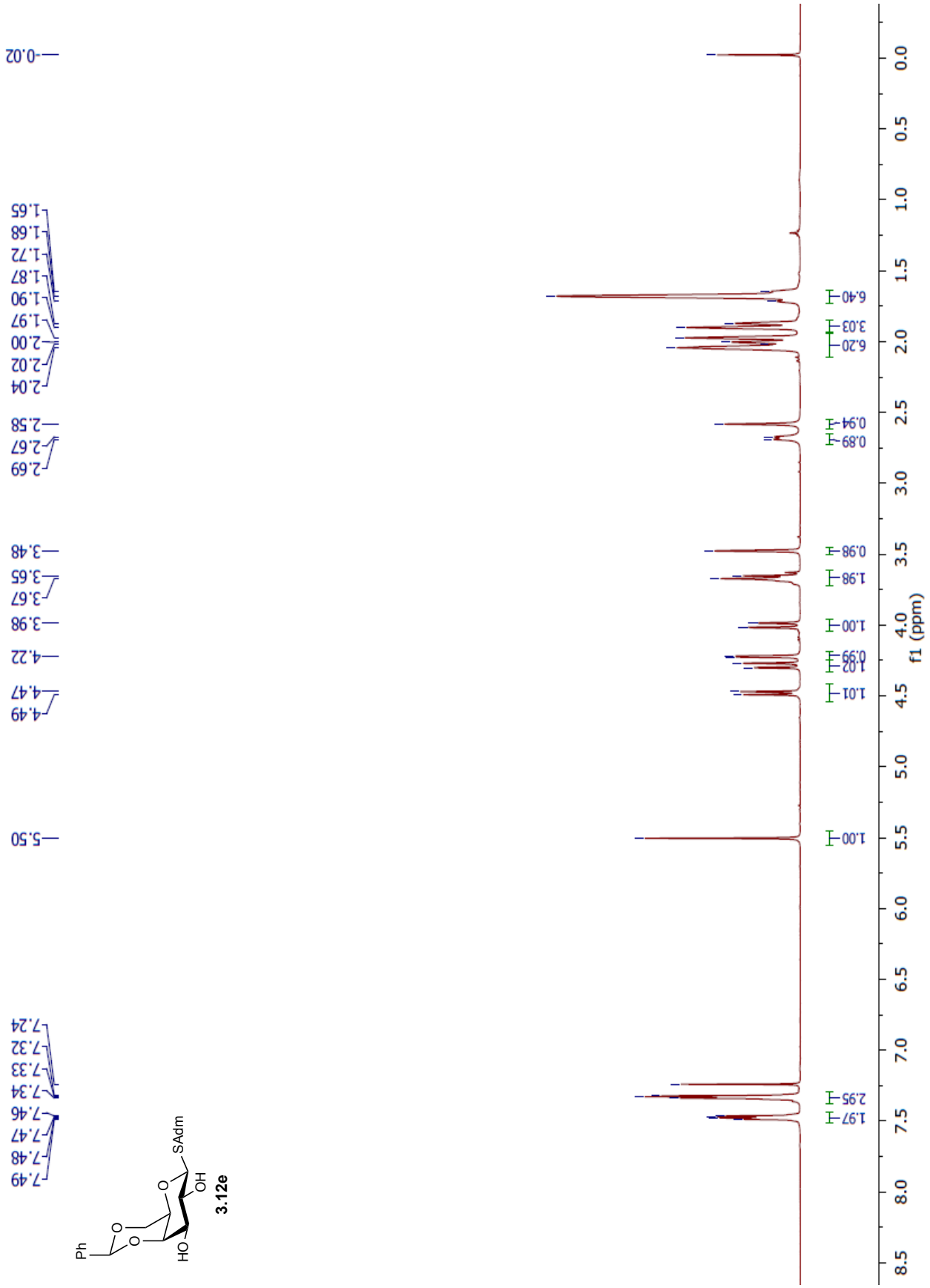
-0.02
1.65
1.68
1.72
1.87
1.90
1.97
2.00
2.02
2.04
2.58
2.67
2.69
3.48
3.65
3.67
3.98
4.22
4.47
4.49
5.50
7.24
7.32
7.33
7.34
7.46
7.47
7.48
7.49
6.40
3.03
6.20
0.94
0.89
0.98
1.98
1.00
0.99
1.02
1.01
1.00
2.95
1.97
0.0
0.5
1.0
1.5
2.0
2.5
3.0
3.5
4.0
4.5
5.0
5.5
6.0
6.5
7.0
7.5
8.0
8.5
f1 (ppm)
Ph
O
O
O
HO
OH
SAdm
3.12e

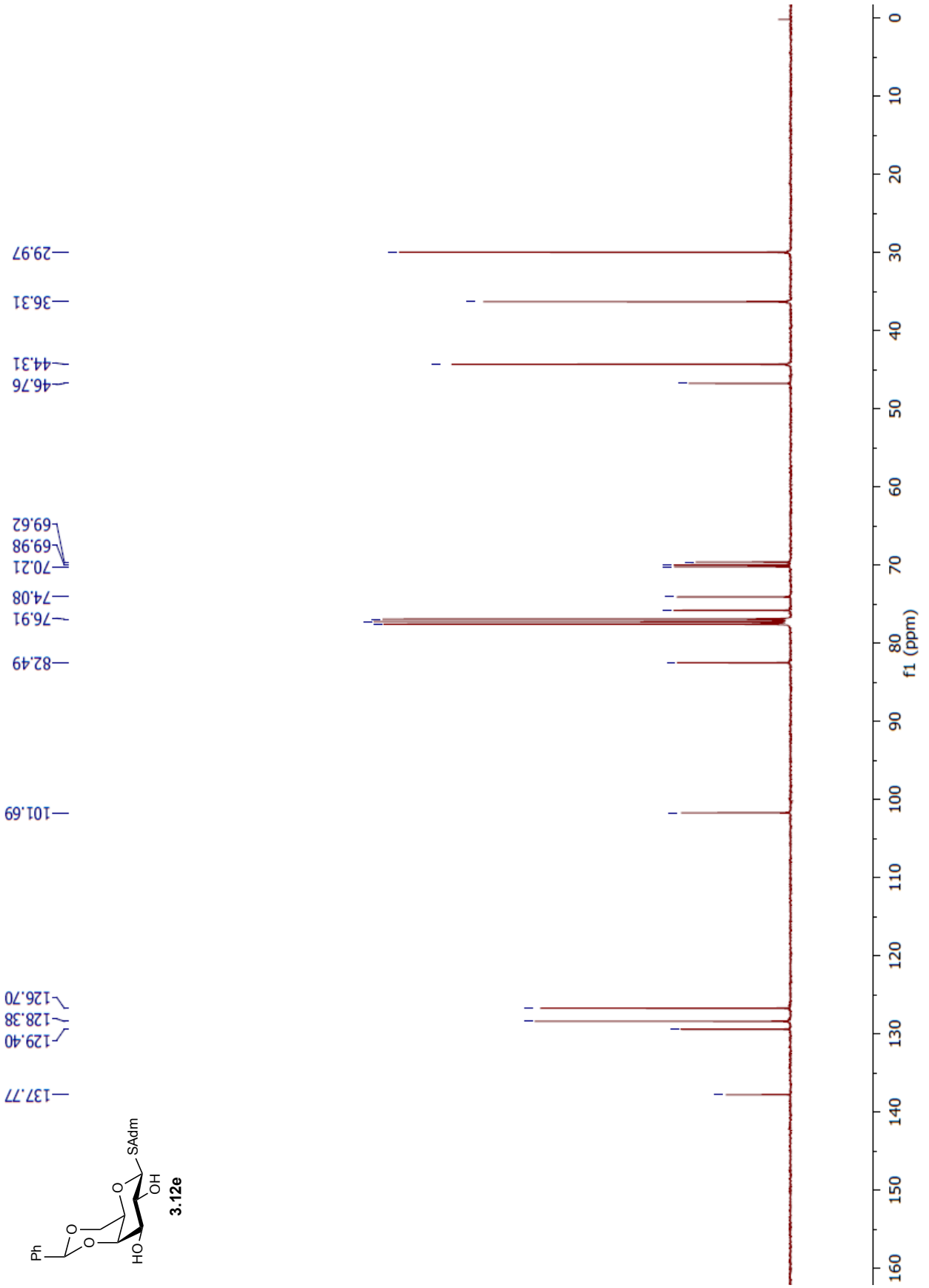
29.97
36.31
44.31
46.76
69.62
69.98
70.21
74.08
76.91
82.49
101.69
126.70
128.38
129.40
137.77
f1 (ppm)
SAdm
OH
HO
Ph
3.12e

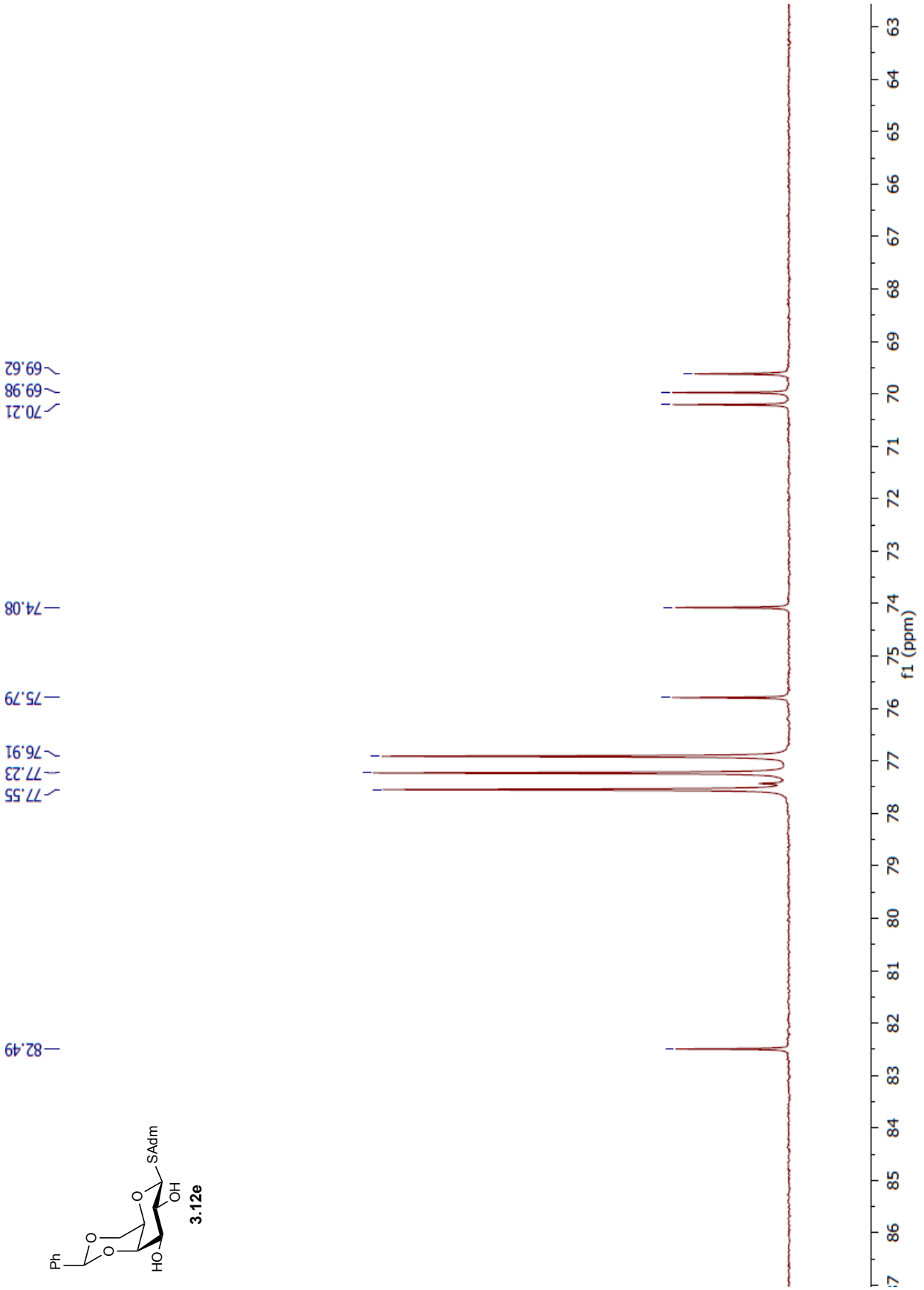
82.49
76.91
77.23
77.55
75.79
74.08
70.21
69.98
69.62
f1 (ppm)
Ph
O
O
O
HO
OH
SAdm
3.12e

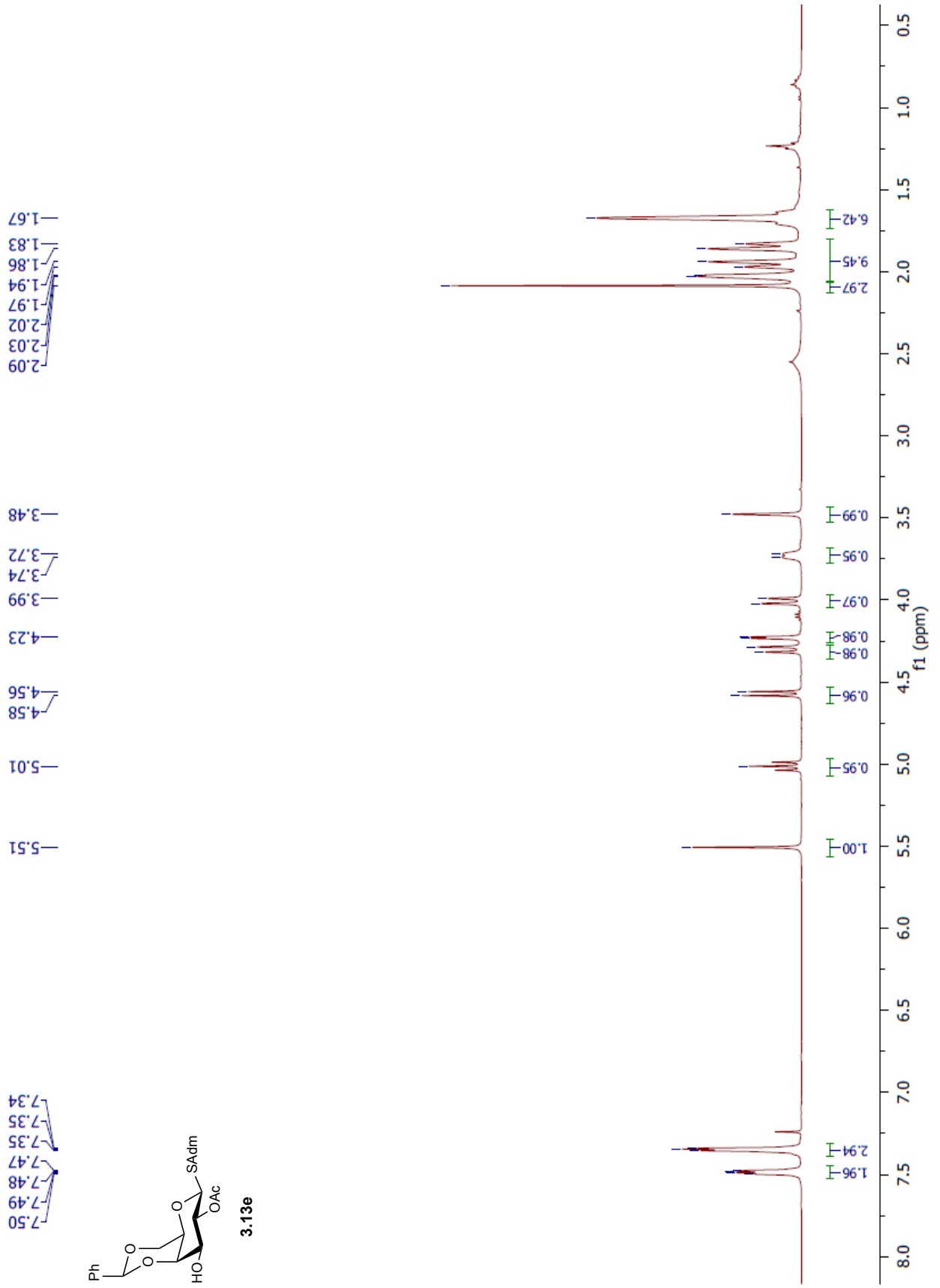
7.50
7.49
7.48
7.47
7.35
7.35
7.34
5.51
5.01
4.58
4.56
4.23
3.99
3.74
3.72
3.48
2.09
2.03
2.02
1.97
1.94
1.86
1.83
1.67
Ph
O
O
O
O
HO
SAdm
OAc
3.13e
1.00
0.95
0.96
0.98
0.98
0.97
0.95
0.99
2.97
9.45
6.42
2.94
1.96
f1 (ppm)

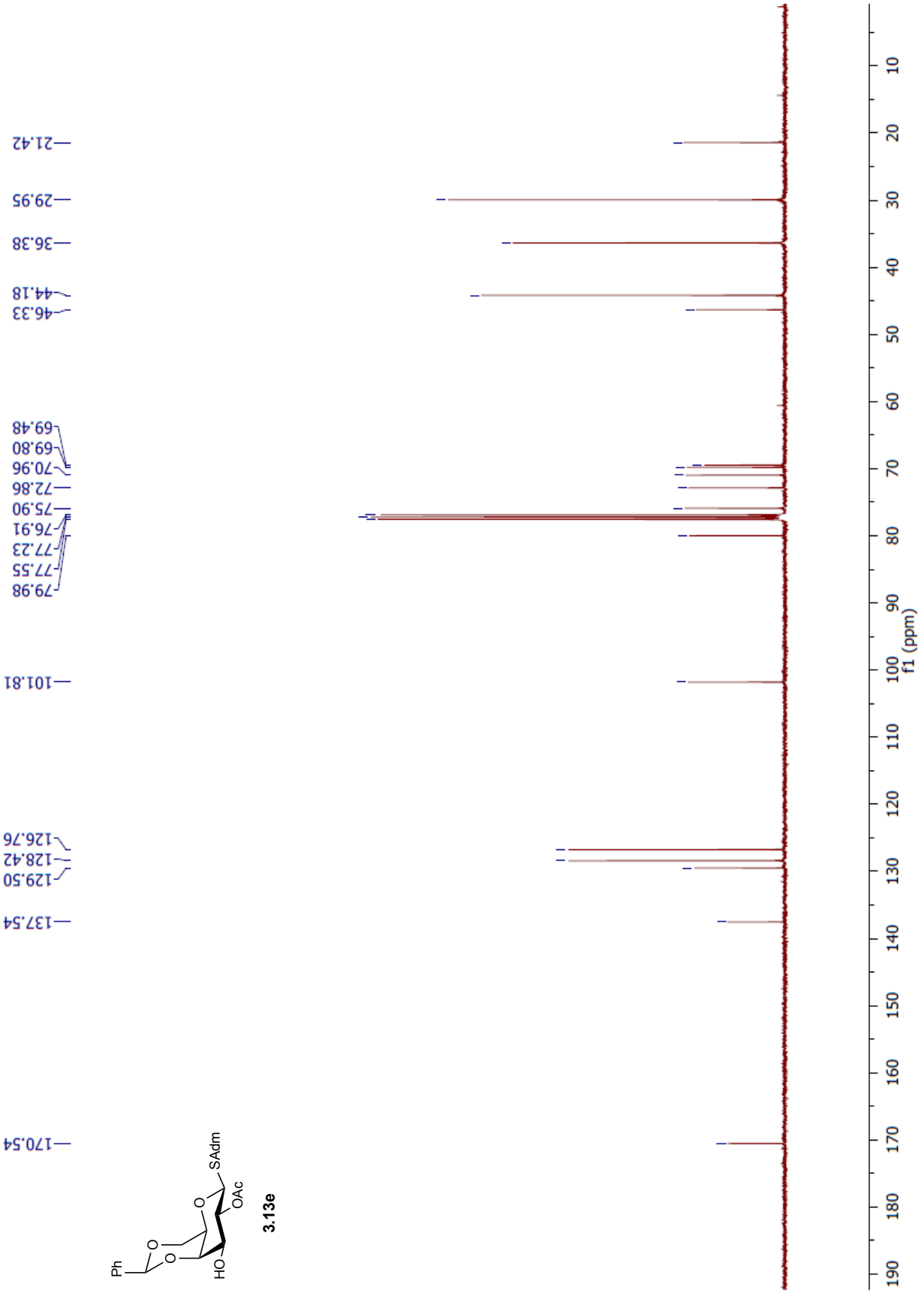
21.42
29.95
36.38
44.18
46.33
69.48
69.80
70.96
72.86
75.90
76.91
77.23
77.55
79.98
101.81
126.76
128.42
129.50
137.54
170.54
f1 (ppm)
Ph
HO
OAc
SAdm
3.13e

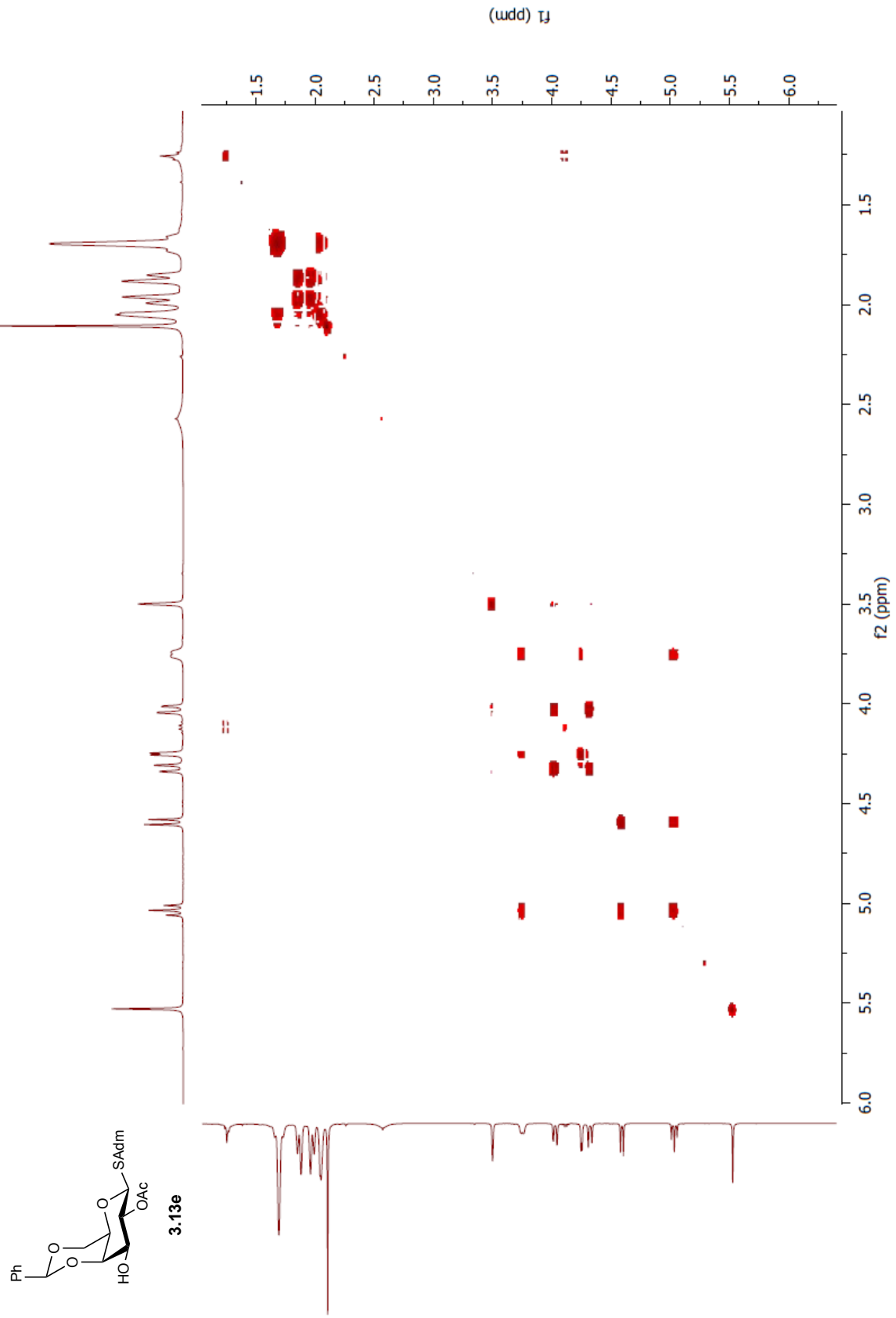
f1 (ppm)
1.5
2.0
2.5
3.0
3.5
4.0
4.5
5.0
5.5
6.0
f2 (ppm)
Ph
O
O
O
HO
OAc
SAdm
3.13e

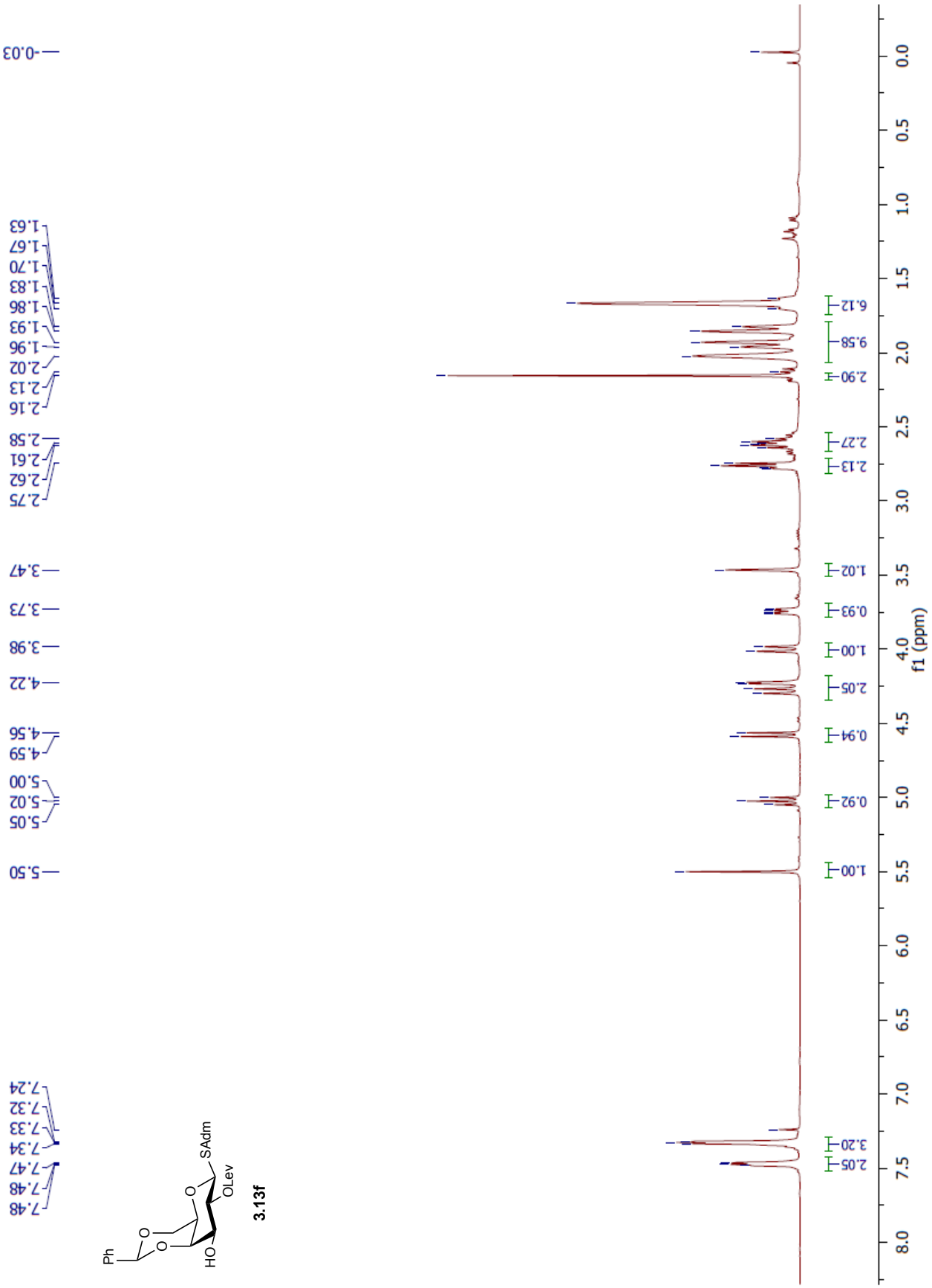
-0.03
1.63
1.67
1.70
1.83
1.86
1.93
1.96
2.02
2.13
2.16
2.58
2.61
2.62
2.75
3.47
3.73
3.98
4.22
4.56
4.59
5.00
5.02
5.05
5.50
7.24
7.32
7.33
7.34
7.47
7.48
7.48
Ph
O
O
O
HO
OLev
SAdm
3.13f
6.12
9.58
2.90
2.27
2.13
1.02
0.93
1.00
2.05
0.94
0.92
1.00
3.20
2.05
f1 (ppm)

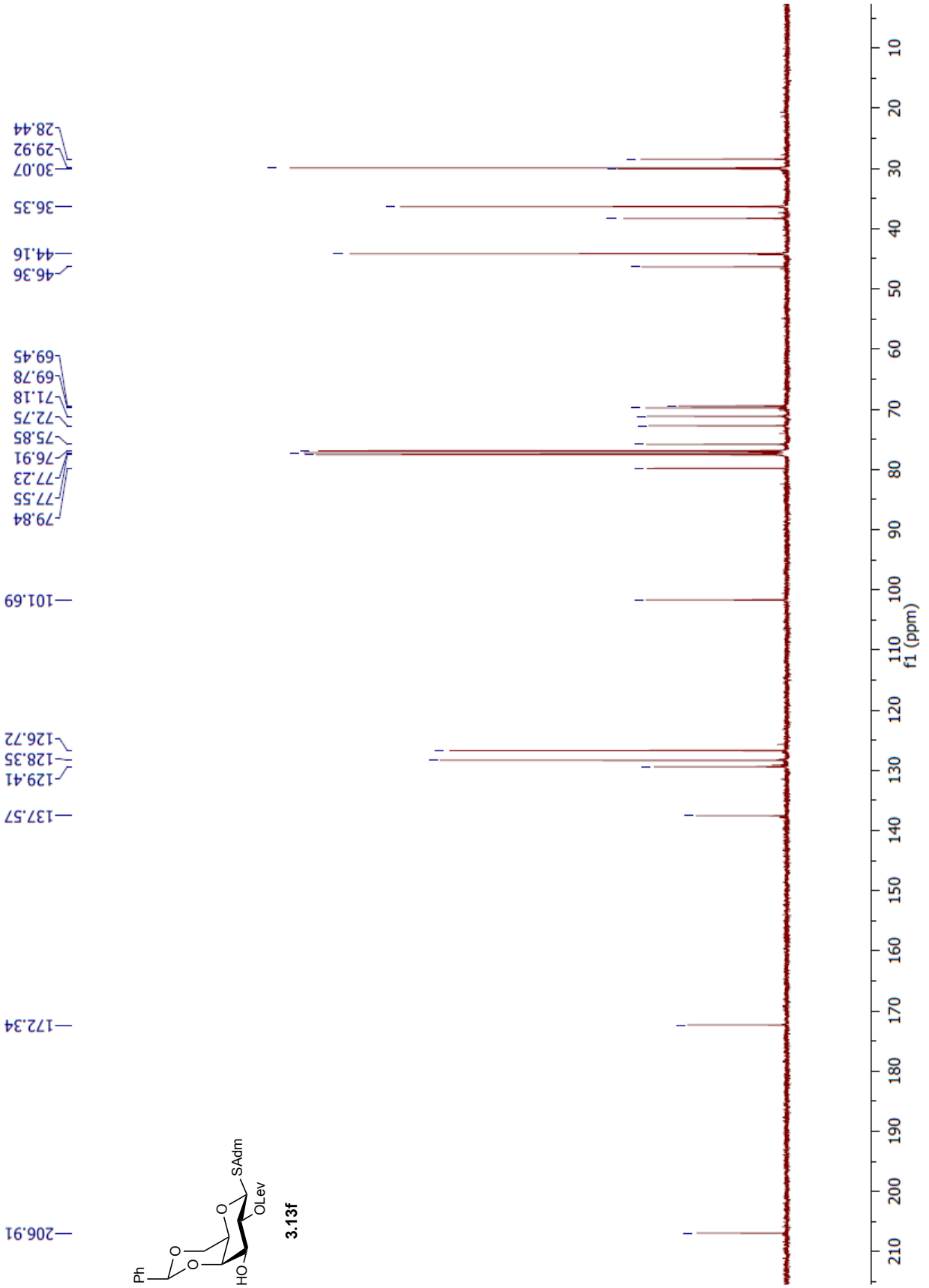
206.91
172.34
137.57
129.41
128.35
126.72
101.69
79.84
77.55
77.23
76.91
75.85
72.75
71.18
69.78
69.45
46.36
44.16
36.35
30.07
29.92
28.44
f1 (ppm)
Ph
O
O
O
HO
OLev
SAdm
3.13f

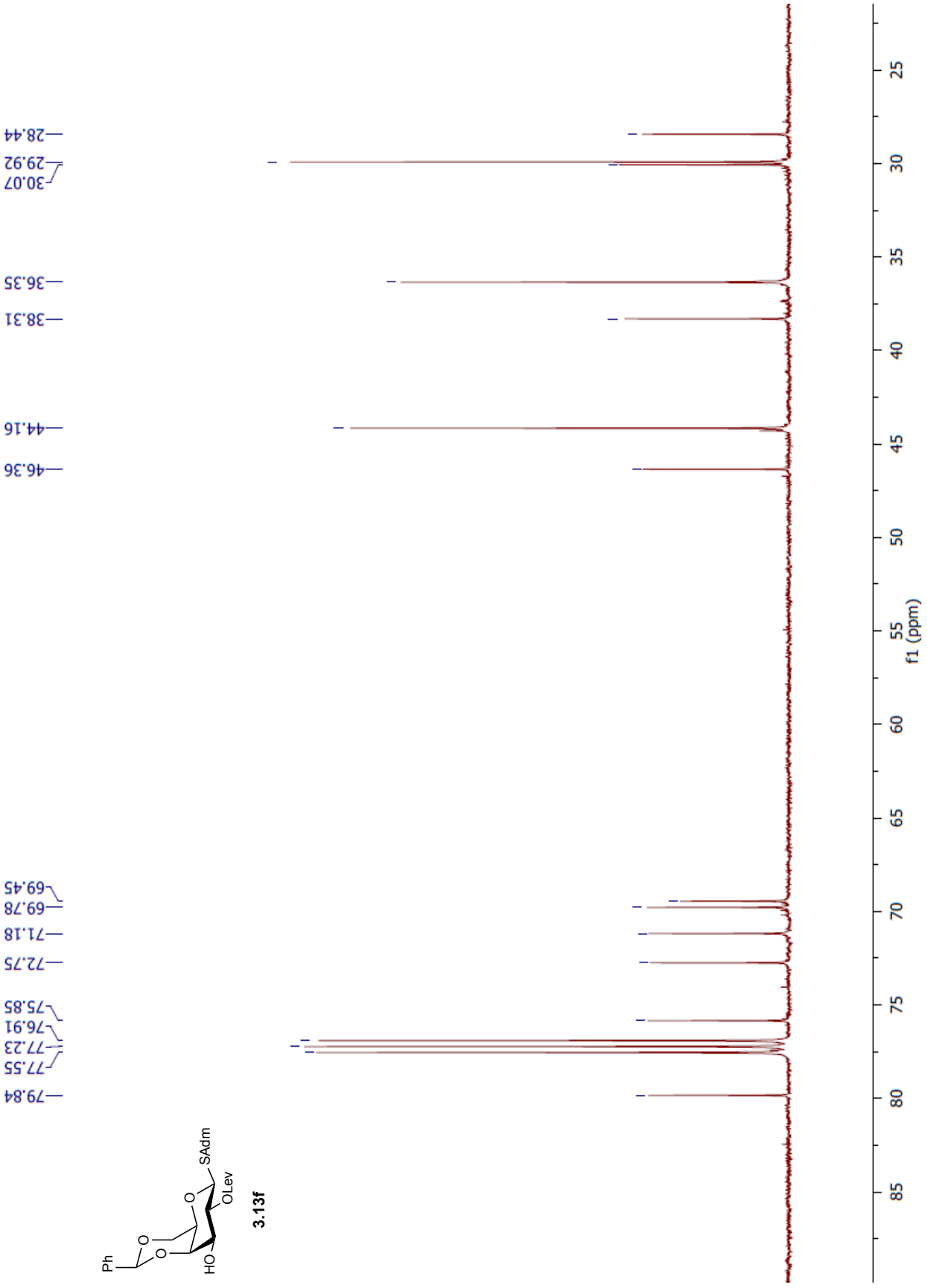
28.44
29.92
30.07
36.35
38.31
44.16
46.36
69.45
69.78
71.18
72.75
75.85
76.91
77.23
77.55
79.84
f1 (ppm)
Ph
HO
OLev
SAdm
3.13f

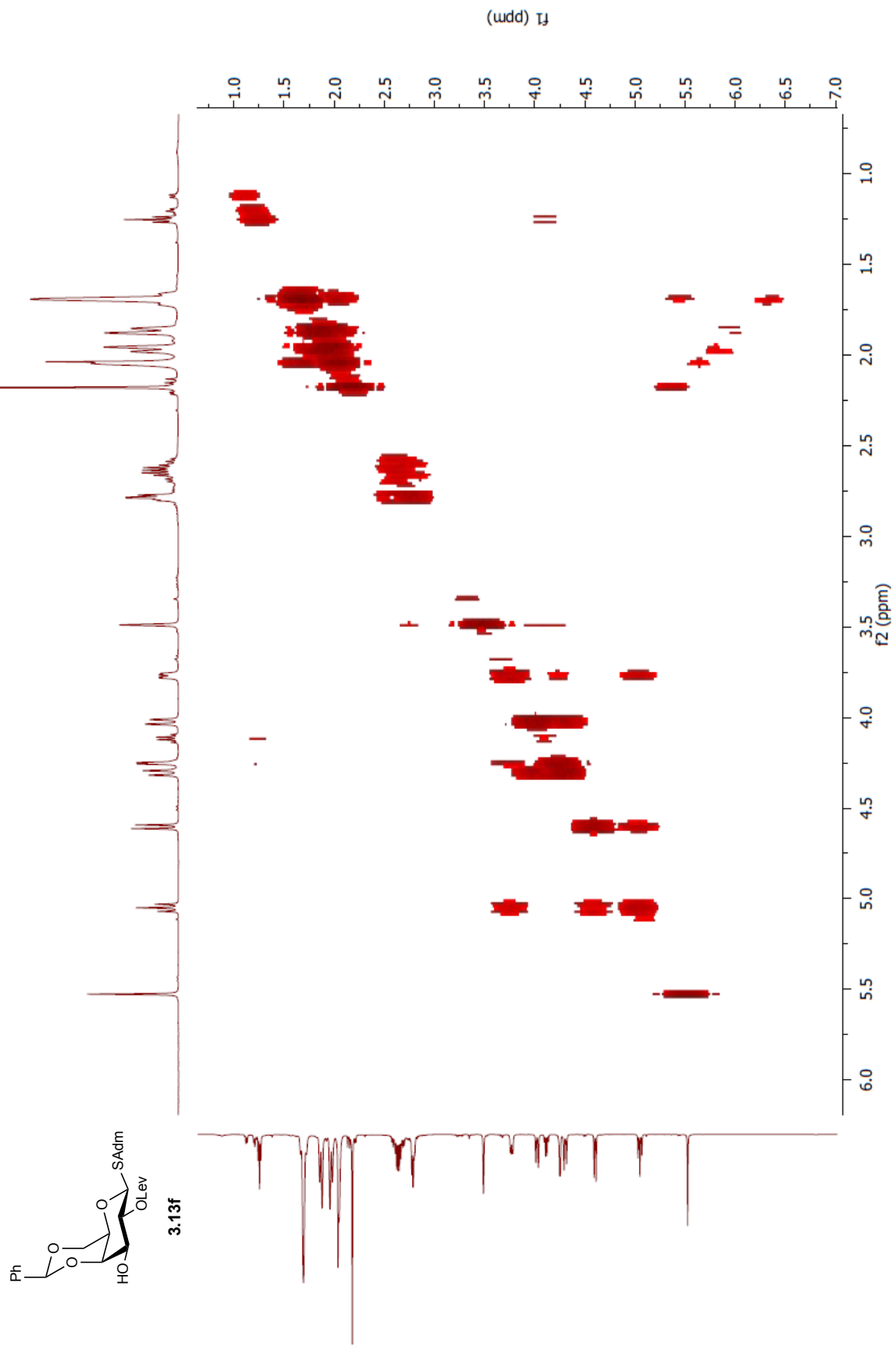
f1 (ppm)
1.0
1.5
2.0
2.5
3.0
3.5
4.0
4.5
5.0
5.5
6.0
6.5
7.0
f2 (ppm)
Ph
O
O
O
HO
OLev
SAdm
3.13f

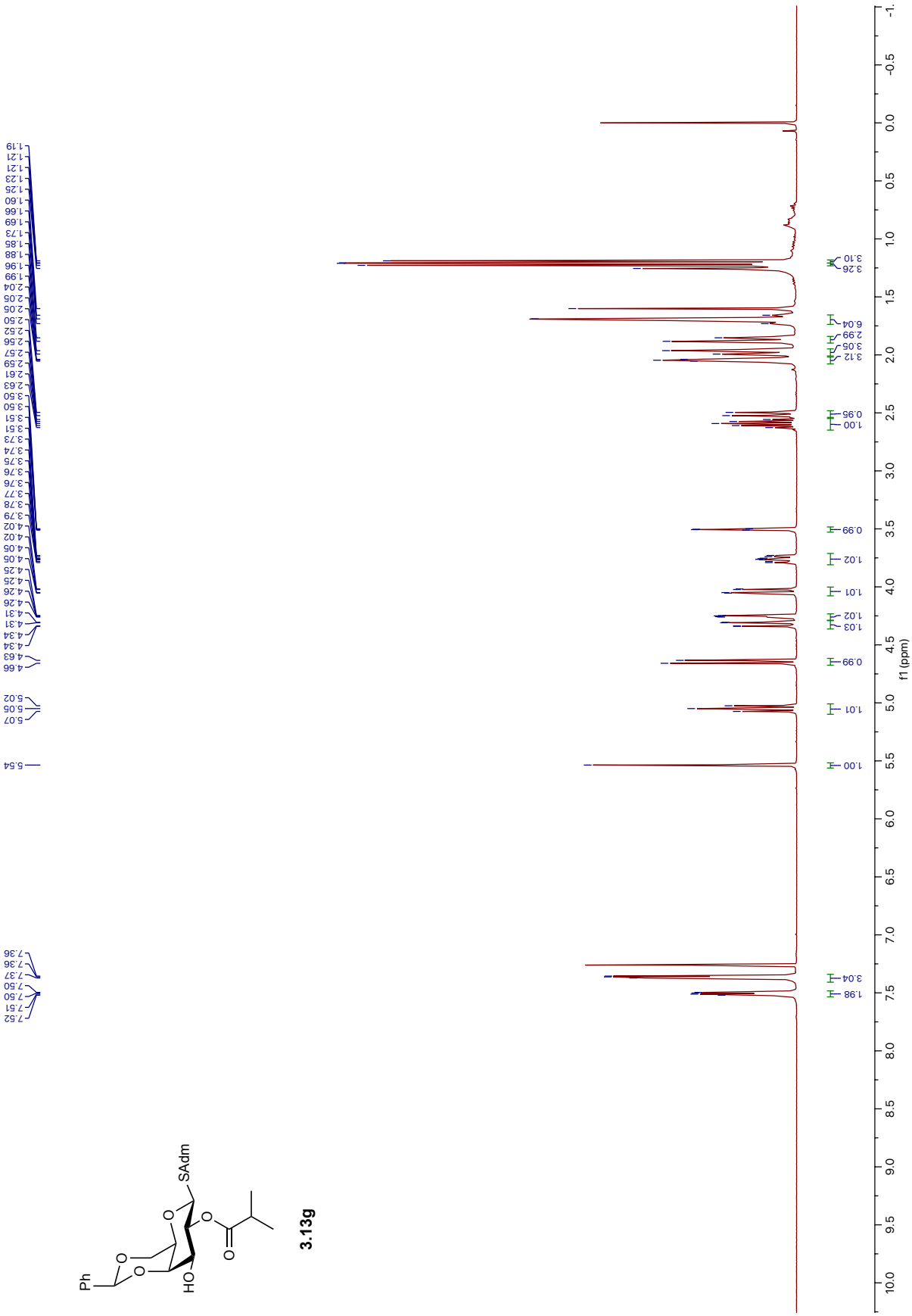
SAdm
Ph
HO
O
O
O
O
O
3.13g
f1 (ppm)

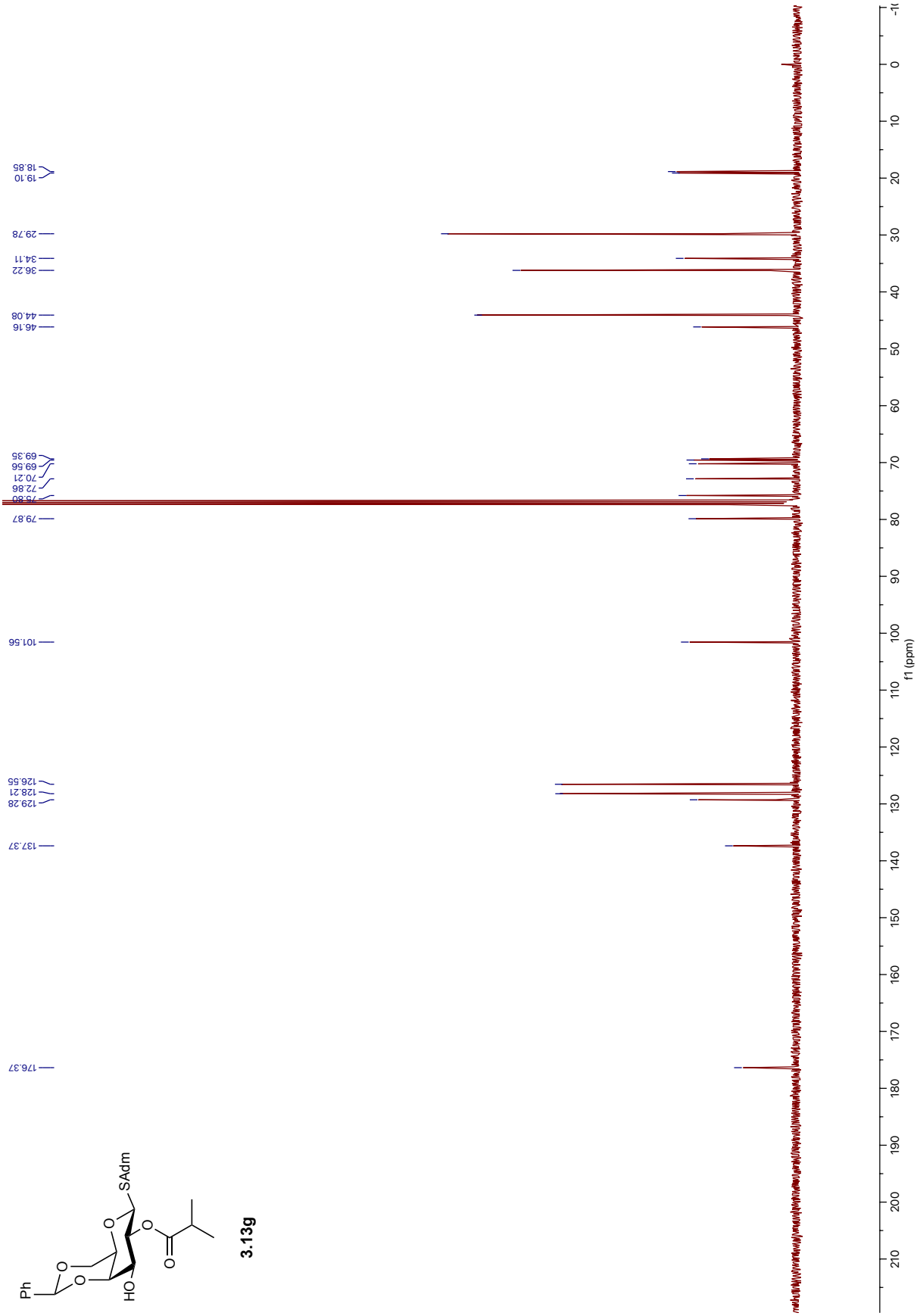
18.85
19.10
29.78
34.11
36.22
44.08
46.16
69.35
69.56
70.21
72.86
75.80
79.87
101.56
126.55
128.21
129.28
137.37
176.37
f1 (ppm)
SAdm
HO
Ph
O
O
O
O
O
3.13g

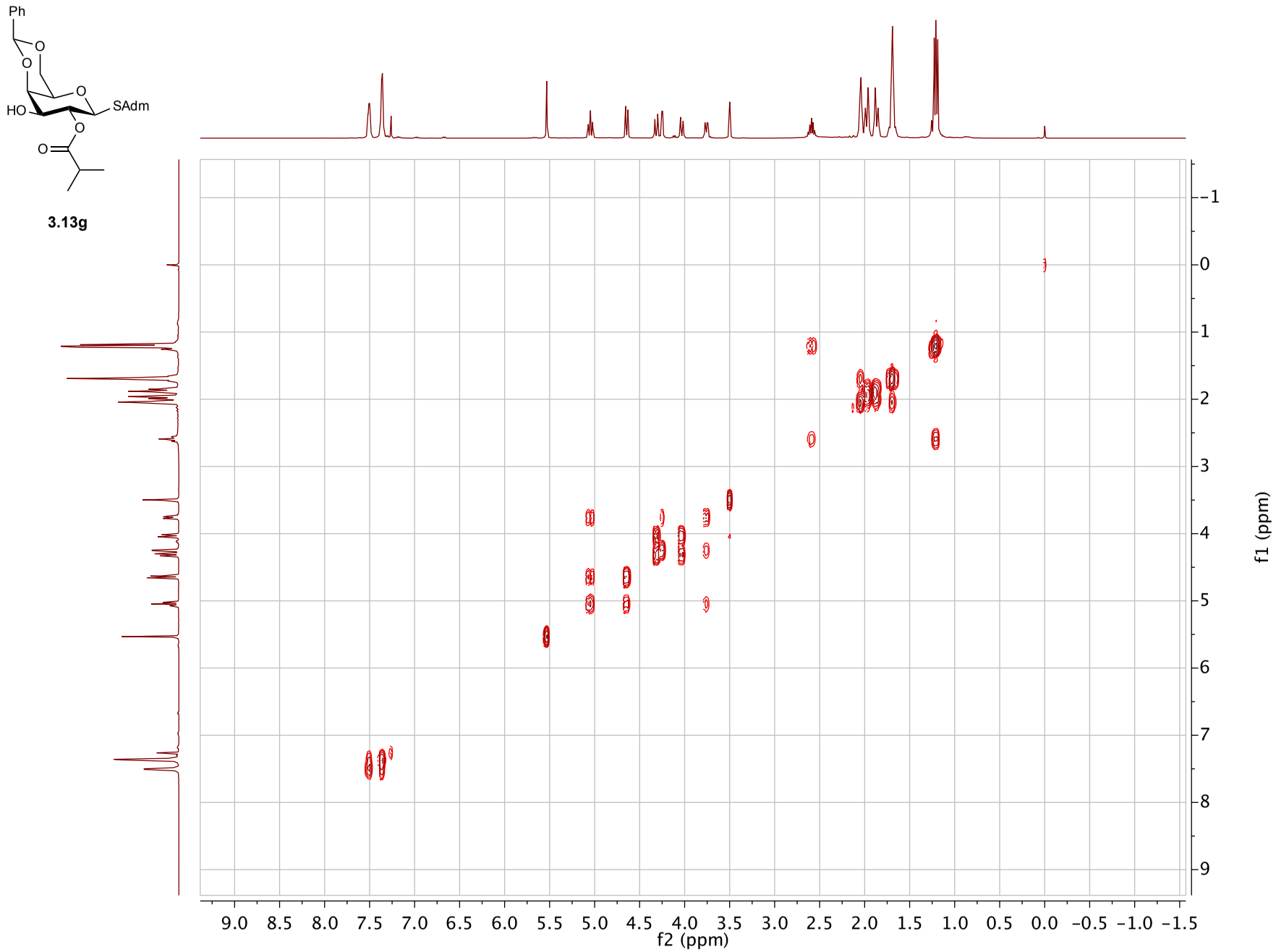
Ph
O
O
O
HO
SAdm
O
O
3.13g
9.0 8.5 8.0 7.5 7.0 6.5 6.0 5.5 5.0 4.5 4.0 3.5 3.0 2.5 2.0 1.5 1.0 0.5 0.0 −0.5 −1.0 −1.5
f2 (ppm)
−1 0 1 2 3 4 5 6 7 8 9
f1 (ppm)

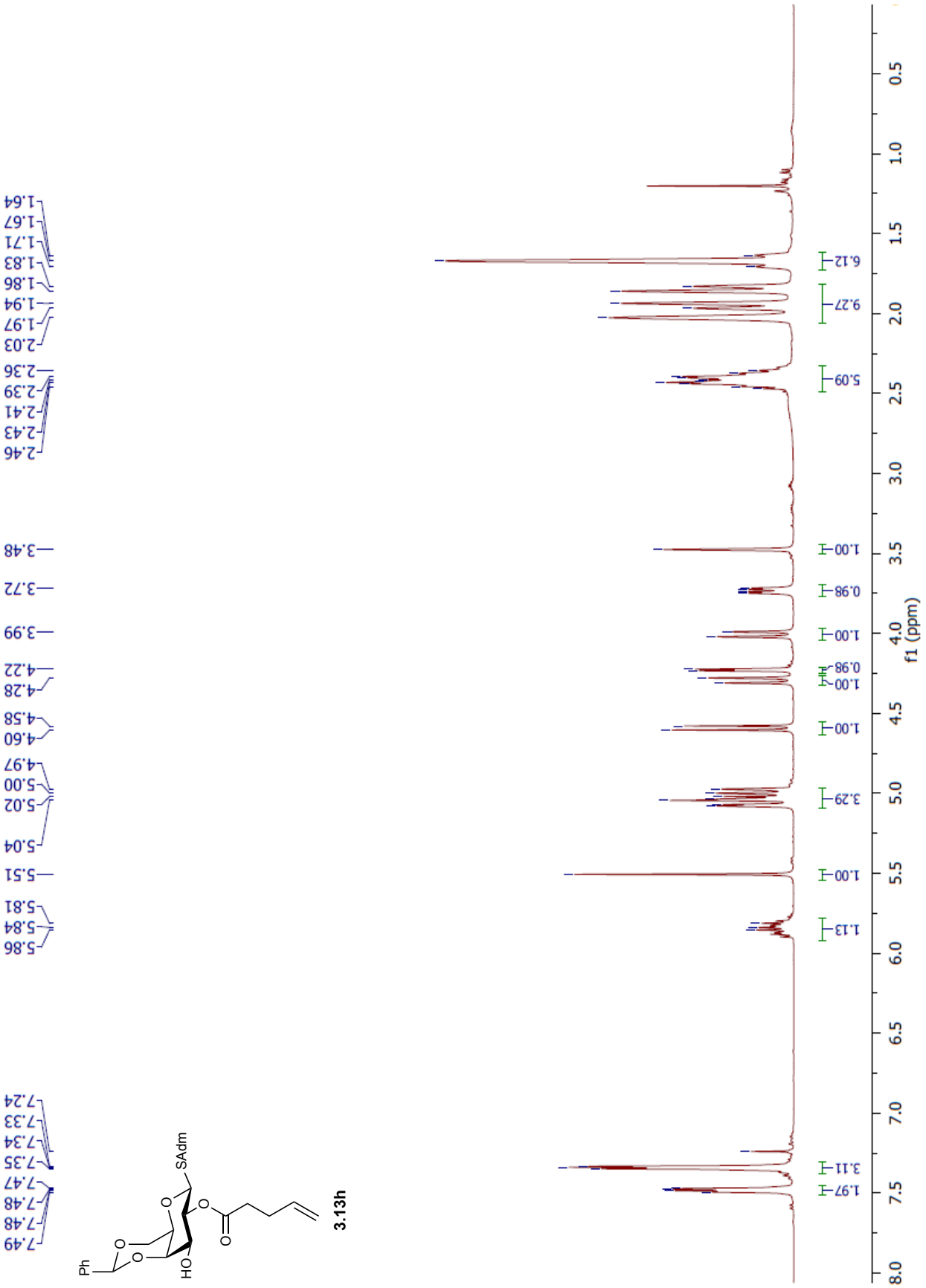
7.49
7.48
7.48
7.47
7.35
7.34
7.33
7.24
5.86
5.84
5.81
5.51
5.04
5.02
5.00
4.97
4.60
4.58
4.28
4.22
3.99
3.72
3.48
2.46
2.43
2.41
2.39
2.36
2.03
1.97
1.94
1.86
1.83
1.71
1.67
1.64
Ph
HO
SAdm
3.13h
6.12
9.27
5.09
1.00
0.98
1.00
0.98
1.00
1.00
3.29
1.00
1.13
3.11
1.97
f1 (ppm)

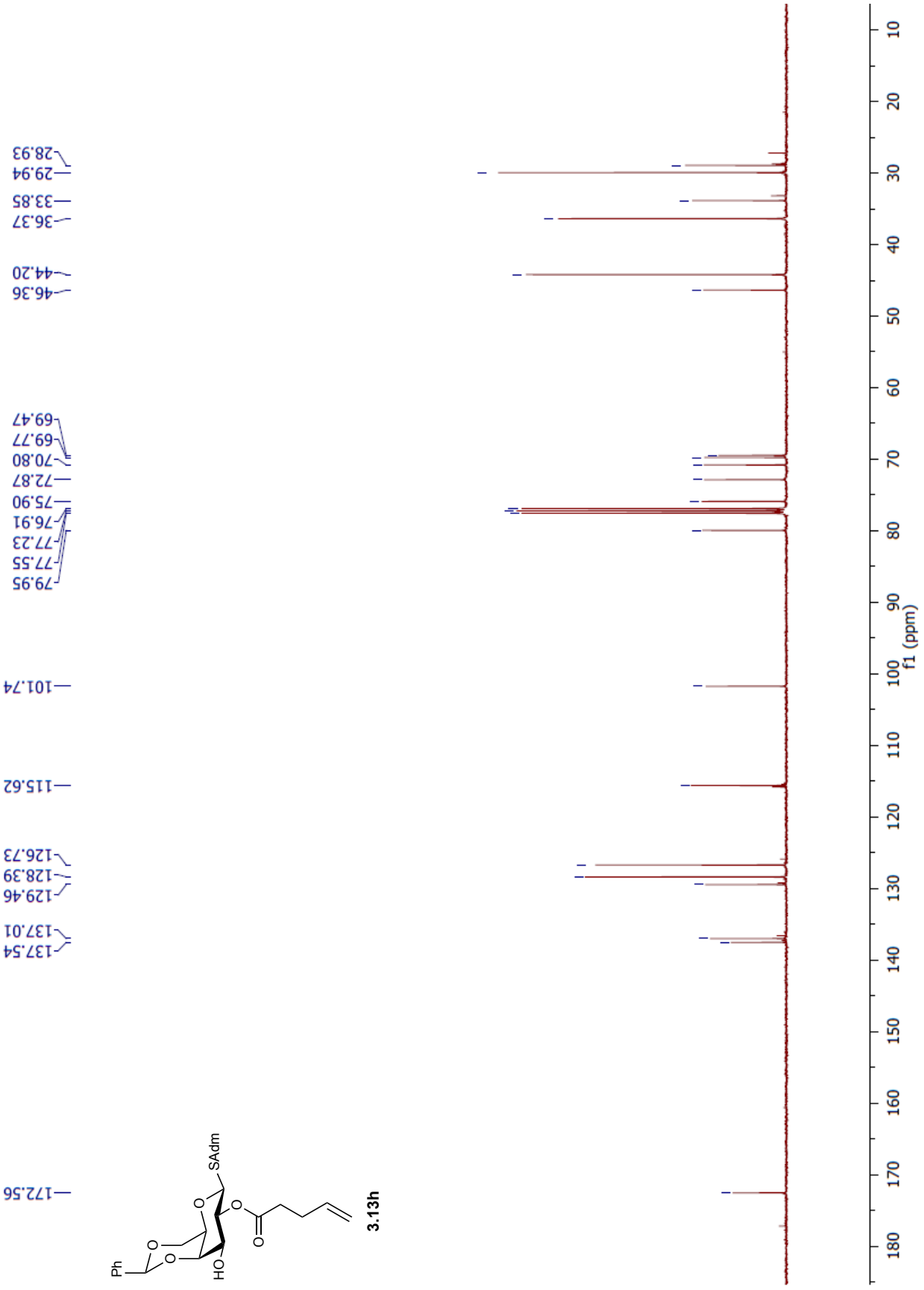
28.93
29.94
33.85
36.37
44.20
46.36
69.47
69.77
70.80
72.87
75.90
76.91
77.23
77.55
79.95
101.74
115.62
126.73
128.39
129.46
137.01
137.54
172.56
SAdm
HO
Ph
O
O
O
O
O
3.13h
f1 (ppm)
10
20
30
40
50
60
70
80
90
100
110
120
130
140
150
160
170
180

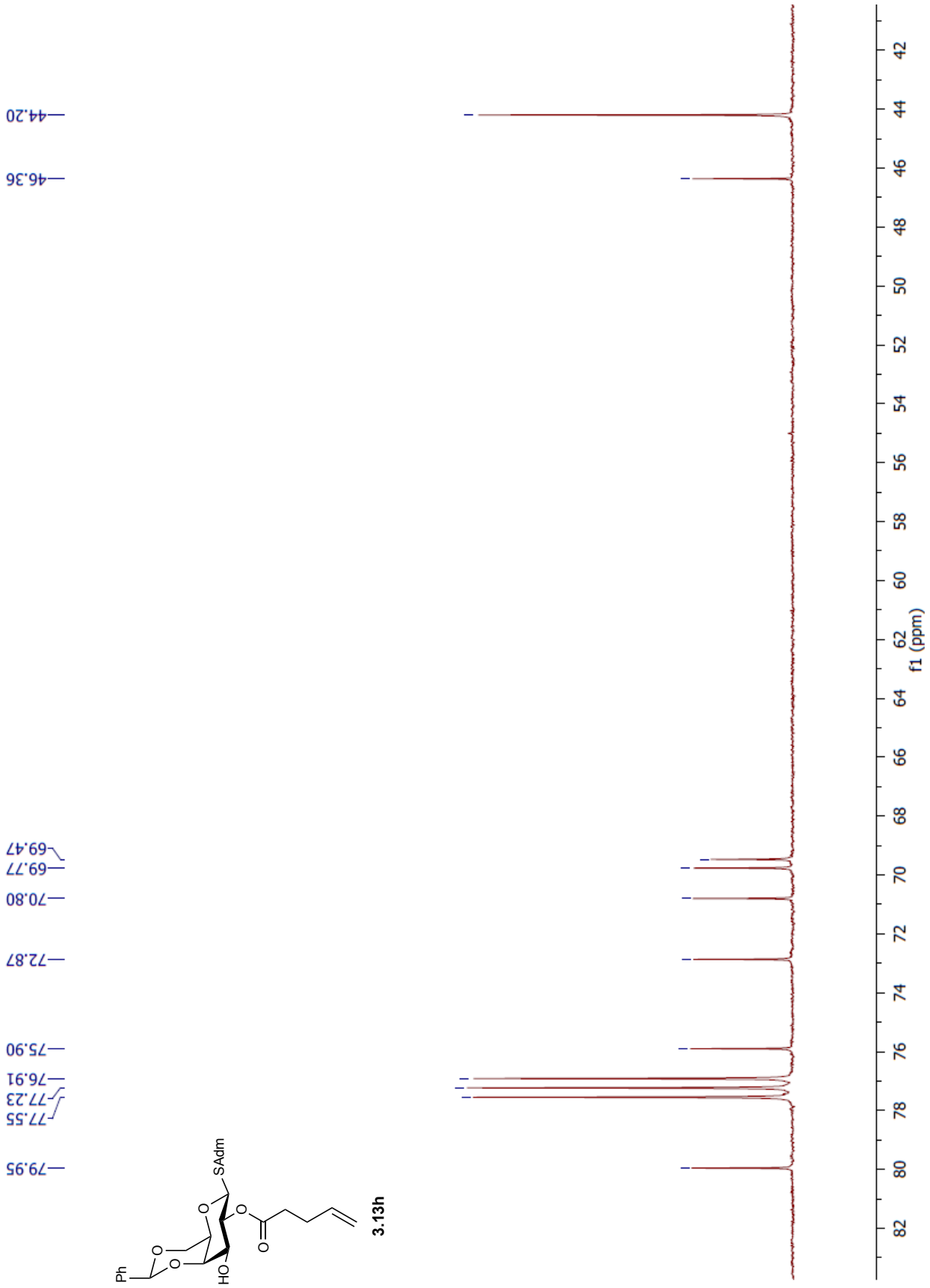
44.20
46.36
69.47
69.77
70.80
72.87
75.90
76.91
77.23
77.55
79.95
SAdm
HO
Ph
3.13h
f1 (ppm)

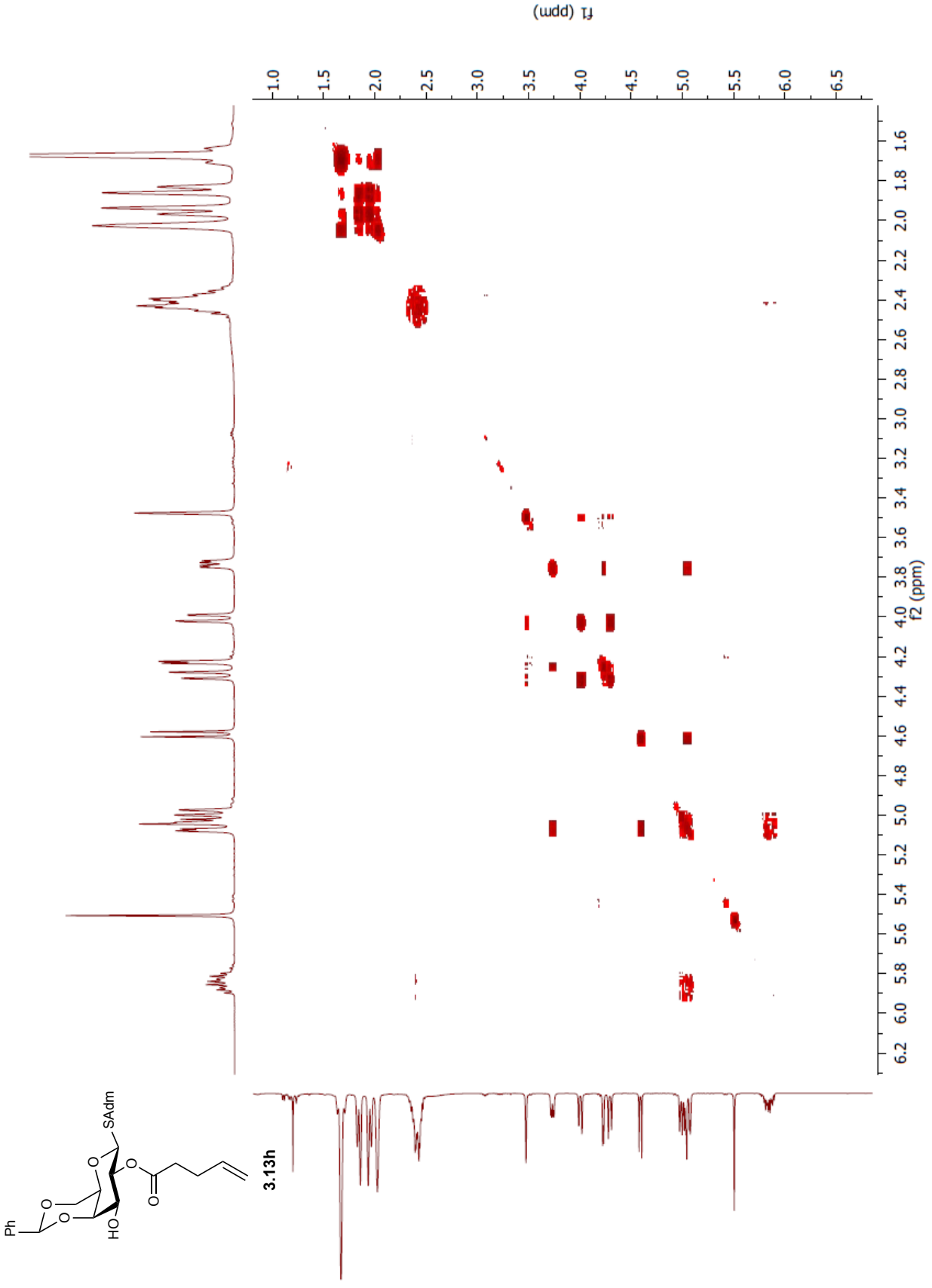
3.13h
SAdm
HO
Ph
f1 (ppm)
f2 (ppm)

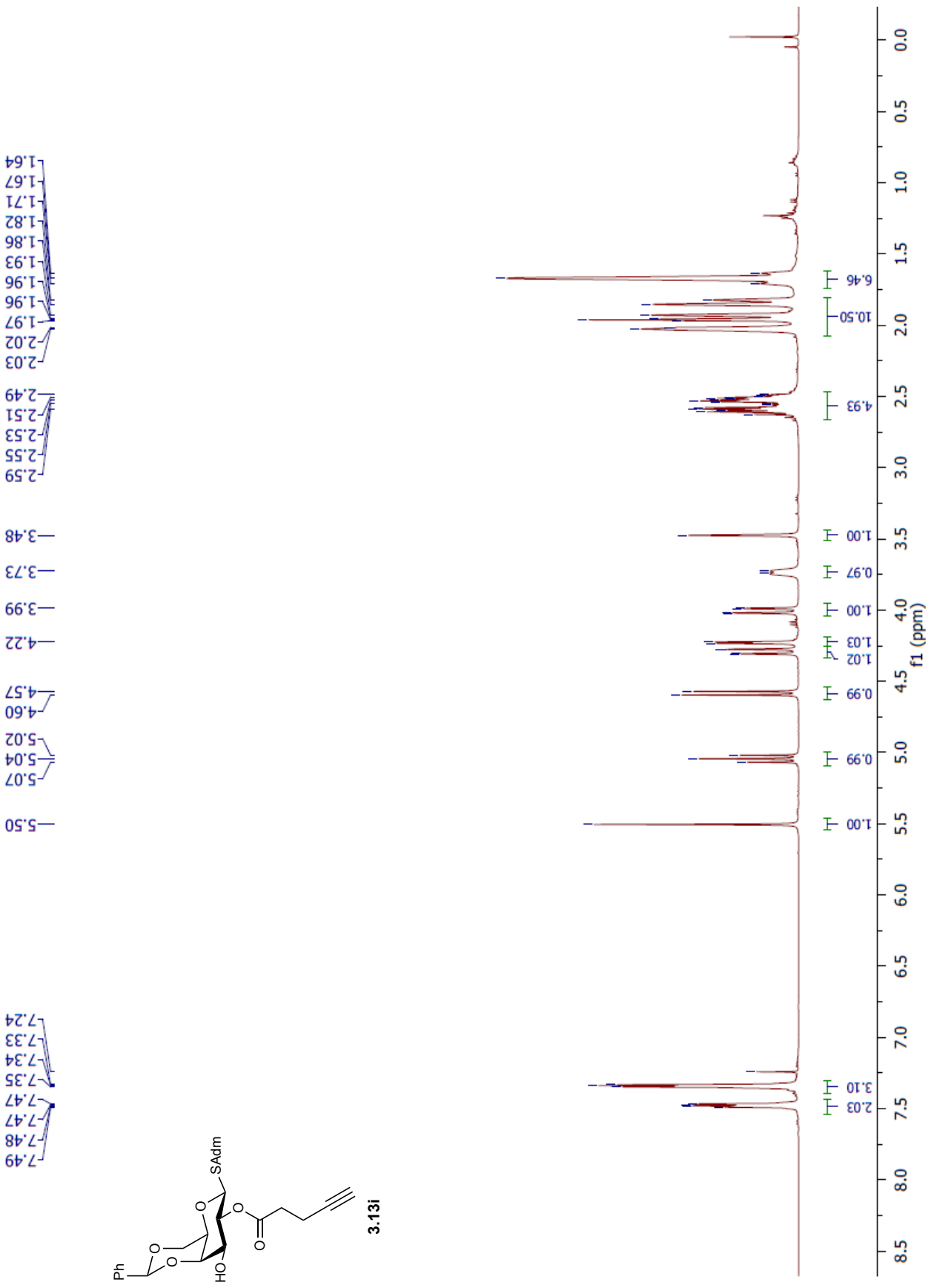
7.49
7.48
7.47
7.47
7.35
7.34
7.33
7.24
5.50
5.07
5.04
5.02
4.60
4.57
4.22
3.99
3.73
3.48
2.59
2.55
2.53
2.51
2.49
2.03
2.02
1.97
1.96
1.96
1.93
1.86
1.82
1.71
1.67
1.64
SAdm
HO
Ph
3.13i
3.10
2.03
1.00
0.99
0.99
0.99
1.02
1.03
1.00
0.97
1.00
4.93
10.50
6.46
f1 (ppm)

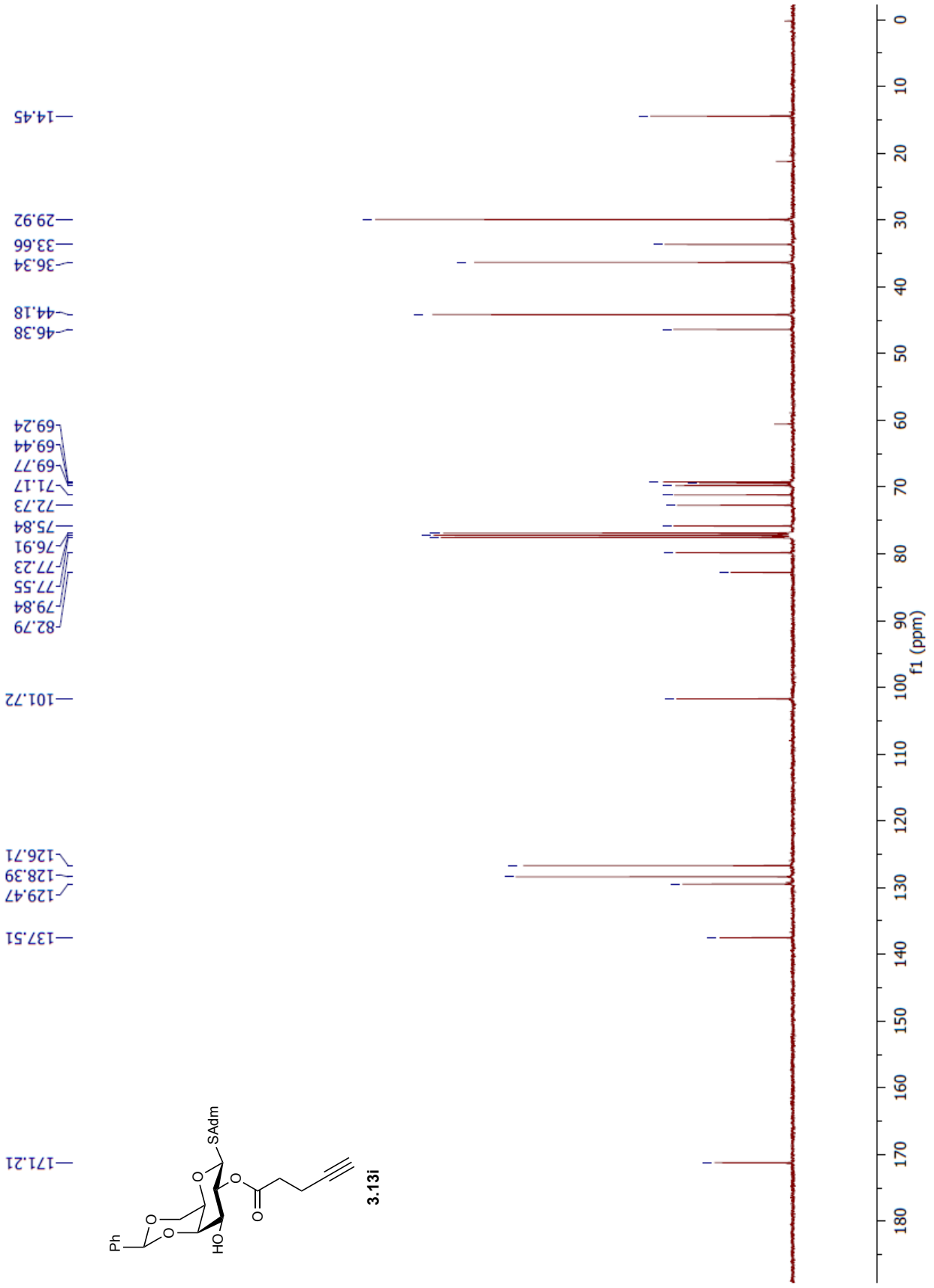
14.45
29.92
33.66
36.34
44.18
46.38
69.24
69.44
69.77
71.17
72.73
75.84
76.91
77.23
77.55
79.84
82.79
101.72
126.71
128.39
129.47
137.51
171.21
SAdm
Ph
HO
3.13i
f1 (ppm)

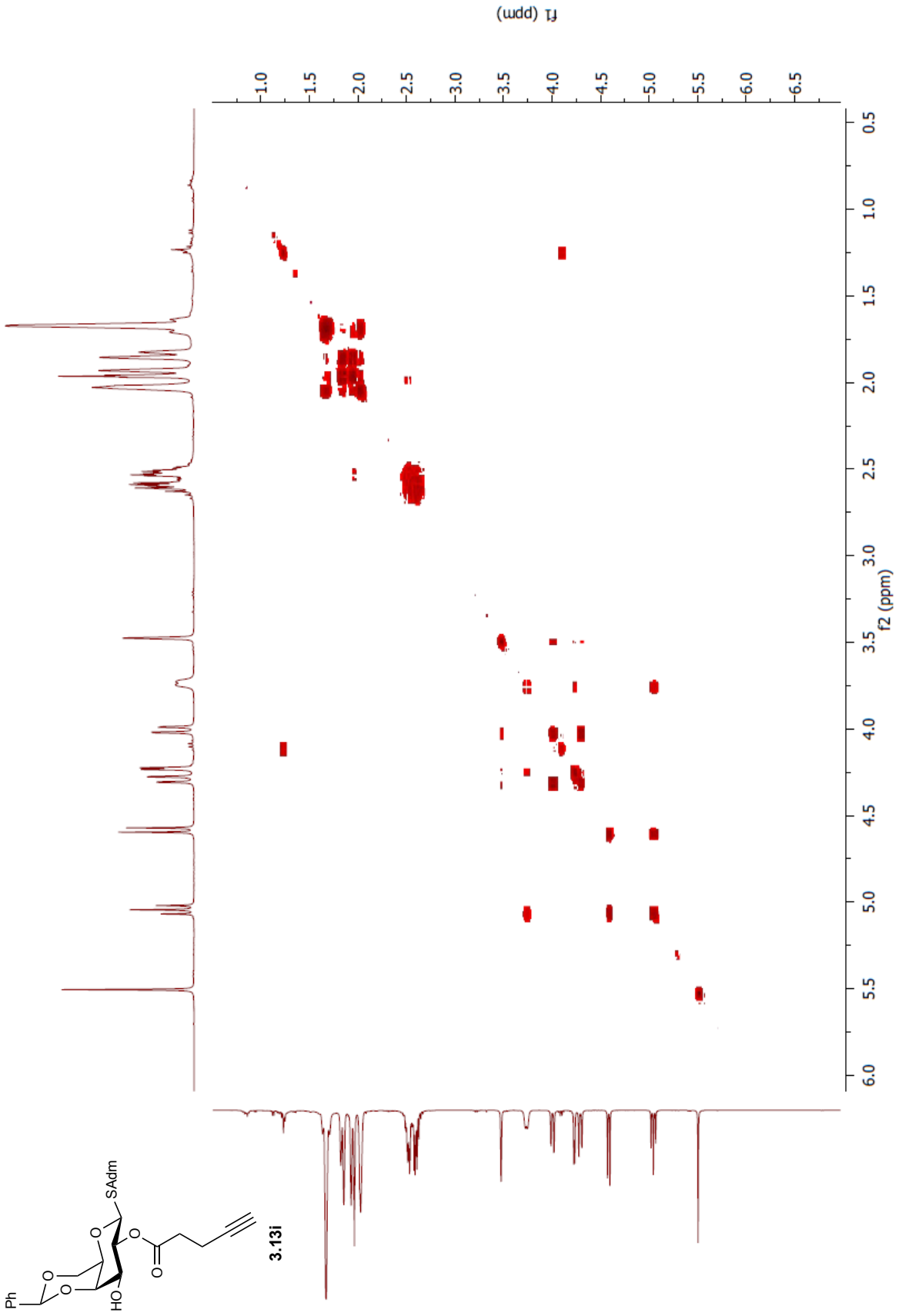
f1 (ppm)
1.0
1.5
2.0
2.5
3.0
3.5
4.0
4.5
5.0
5.5
6.0
6.5
f2 (ppm)
0.5
1.0
1.5
2.0
2.5
3.0
3.5
4.0
4.5
5.0
5.5
6.0
Ph
O
O
O
HO
O
O
SAdm
3.13i

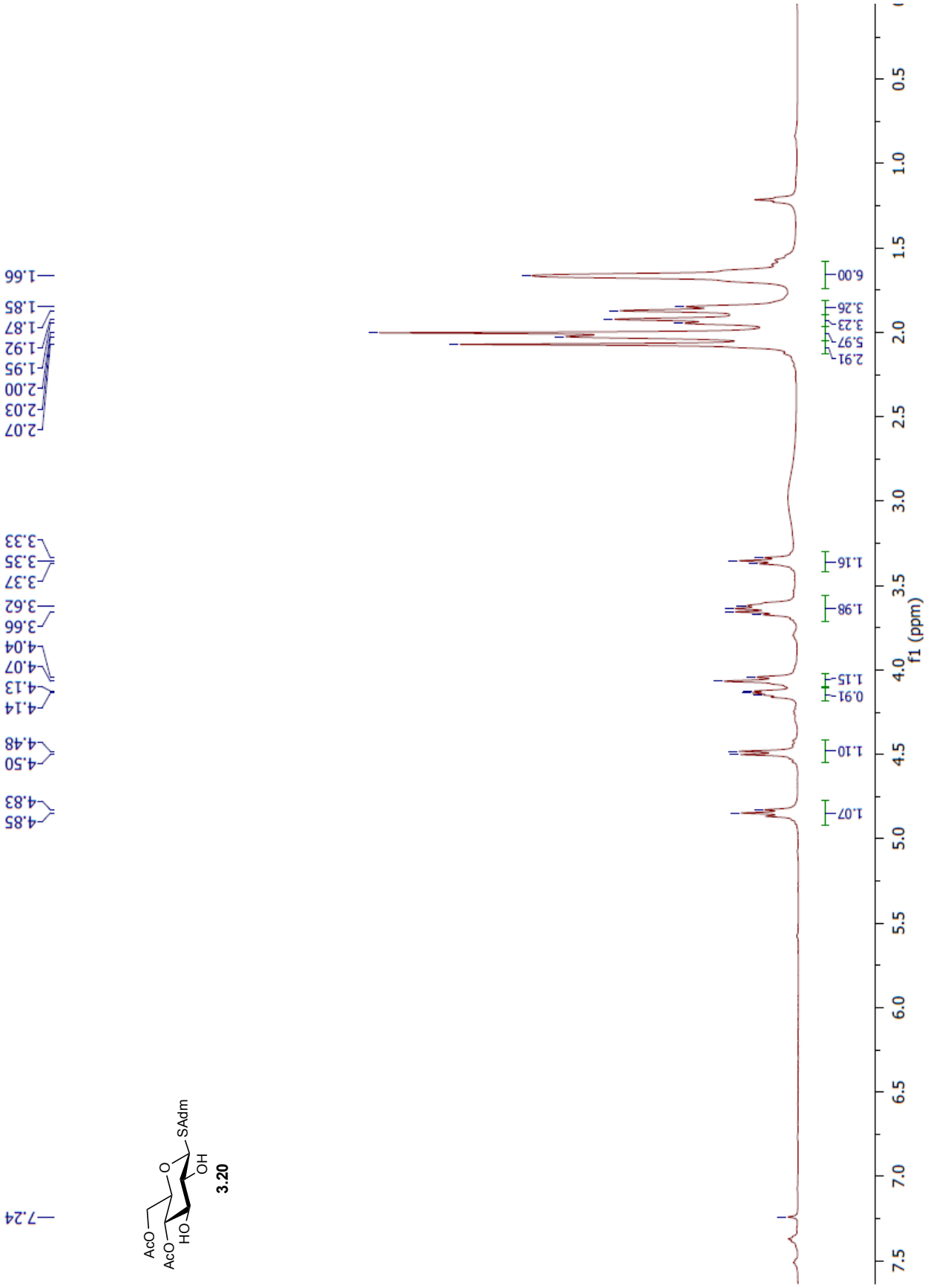
7.24
4.85
4.83
4.50
4.48
4.14
4.13
4.07
4.04
3.66
3.62
3.37
3.35
3.33
2.07
2.03
2.00
1.95
1.92
1.87
1.85
1.66
6.00
3.26
3.23
5.97
2.91
1.16
1.98
1.15
0.91
1.10
1.07
f1 (ppm)
AcO
AcO
HO
O
OH
SAdm
3.20

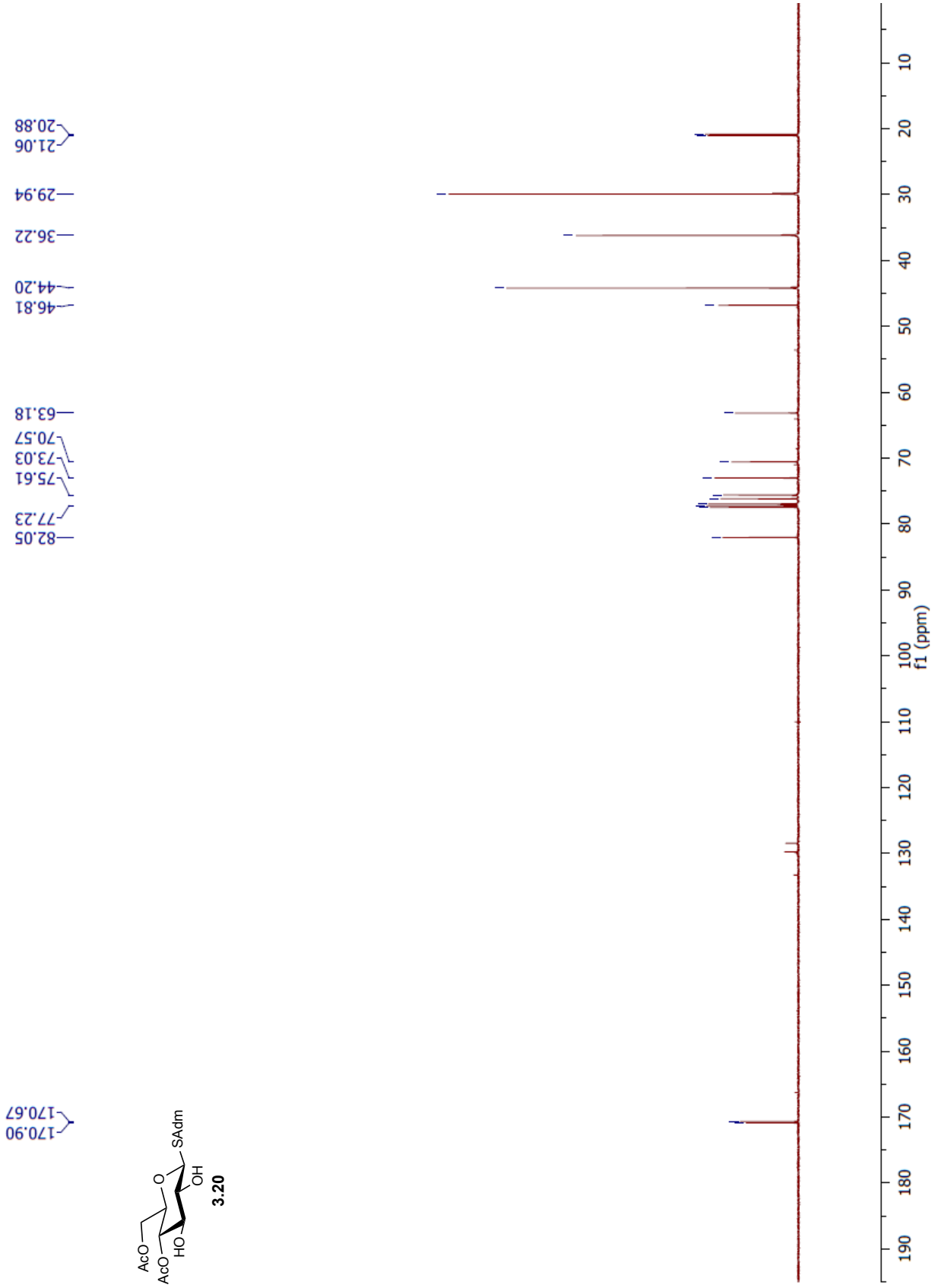
170.90
170.67
82.05
77.23
75.61
73.03
70.57
63.18
46.81
44.20
36.22
29.94
21.06
20.88
AcO
AcO
HO
O
OH
SAdm
3.20
f1 (ppm)

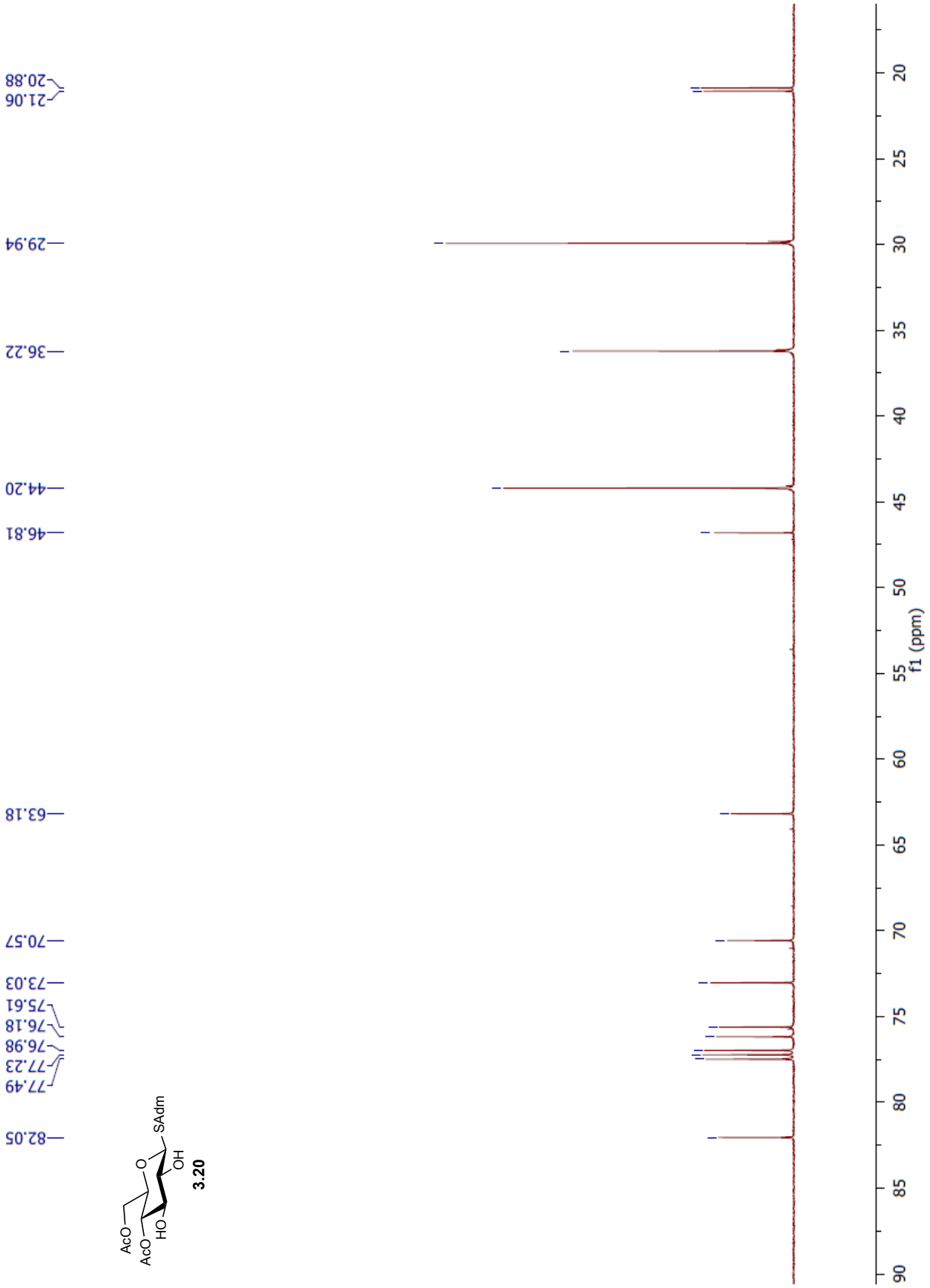
20.88
21.06
29.94
36.22
44.20
46.81
63.18
70.57
73.03
75.61
76.18
76.98
77.23
77.49
82.05
SAdm
OH
HO
AcO
AcO
O
3.20
f1 (ppm)

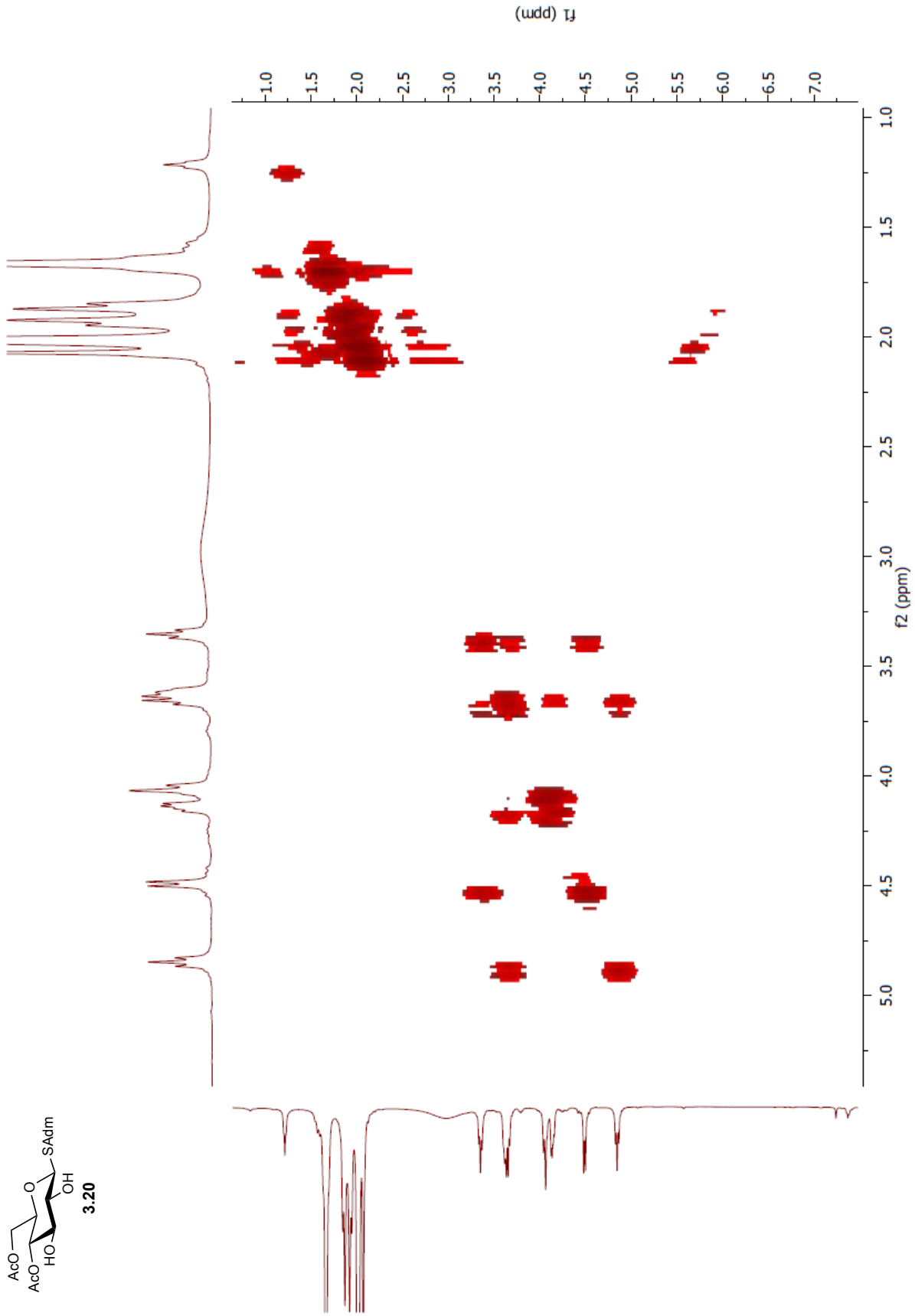
f1 (ppm)
1.0
1.5
2.0
2.5
3.0
3.5
4.0
4.5
5.0
5.5
6.0
6.5
7.0
f2 (ppm)
AcO
AcO
HO
O
OH
SAdm
3.20

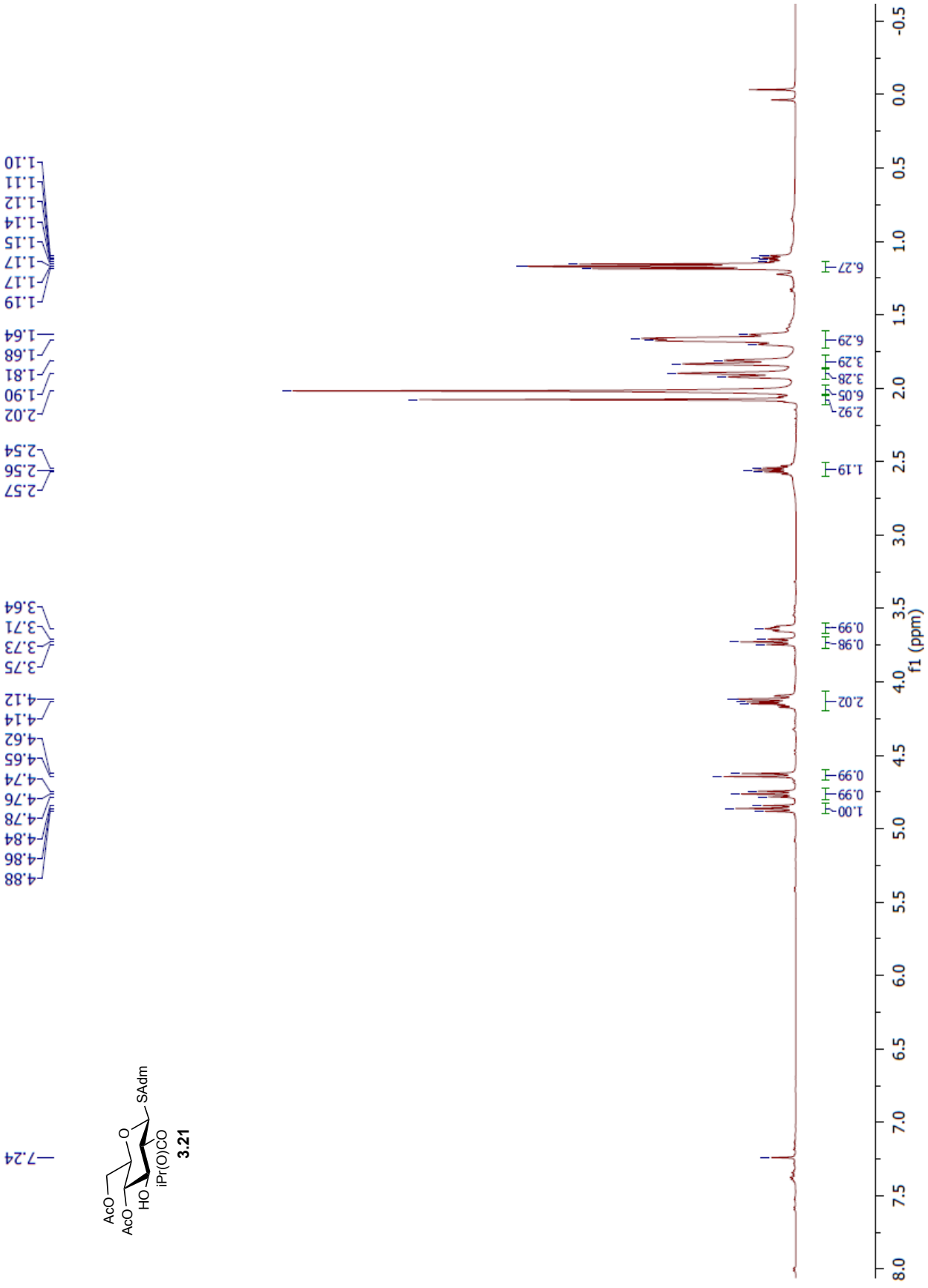
7.24
4.88
4.86
4.84
4.78
4.76
4.74
4.65
4.62
4.14
4.12
3.75
3.73
3.71
3.64
2.57
2.56
2.54
2.02
1.90
1.81
1.68
1.64
1.19
1.17
1.17
1.15
1.14
1.12
1.11
1.10
6.27
6.29
3.29
3.28
6.05
2.92
1.19
0.99
0.98
2.02
0.99
0.99
1.00
AcO
AcO
HO
iPr(O)CO
O
SAdm
3.21
f1 (ppm)

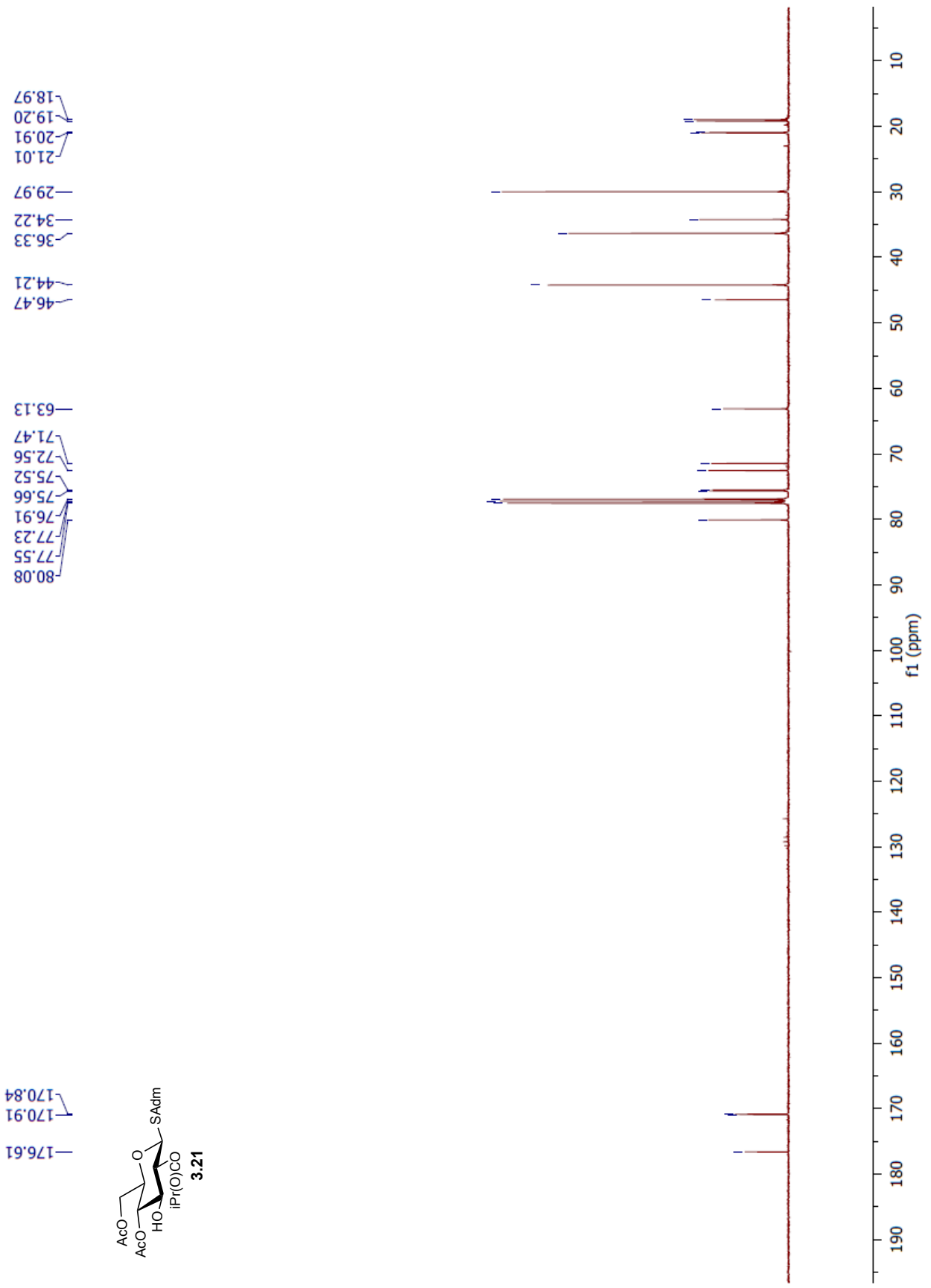
18.97
19.20
20.91
21.01
29.97
34.22
36.33
44.21
46.47
63.13
71.47
72.56
75.52
75.66
76.91
77.23
77.55
80.08
170.84
170.91
176.61
AcO
AcO
HO
O
SAdm
iPr(O)CO
3.21
f1 (ppm)

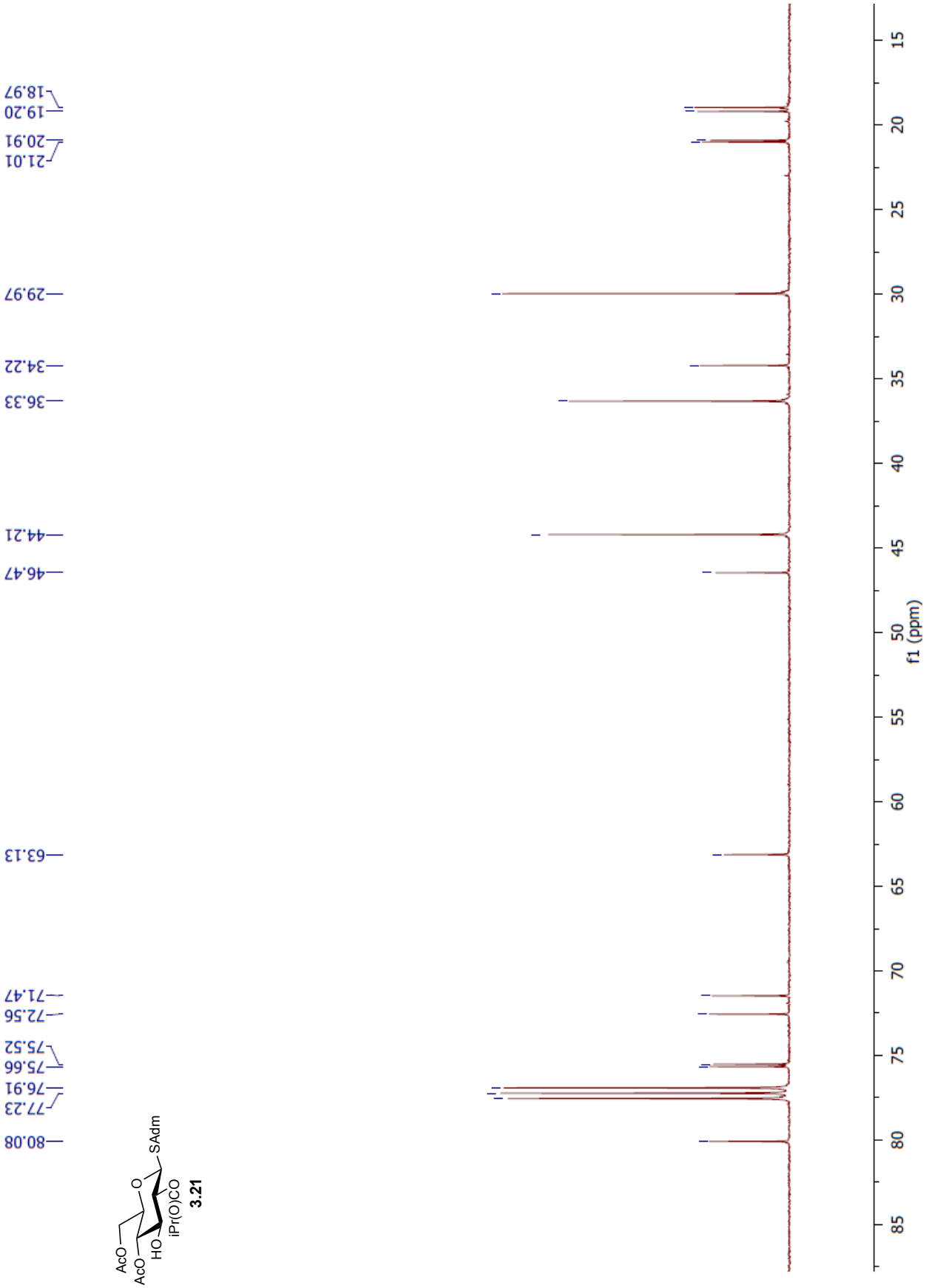
18.97
19.20
20.91
21.01
29.97
34.22
36.33
44.21
46.47
63.13
71.47
72.56
75.52
75.66
76.91
77.23
80.08
SAdm
iPr(O)CO
AcO
AcO
HO
O
3.21
f1 (ppm)

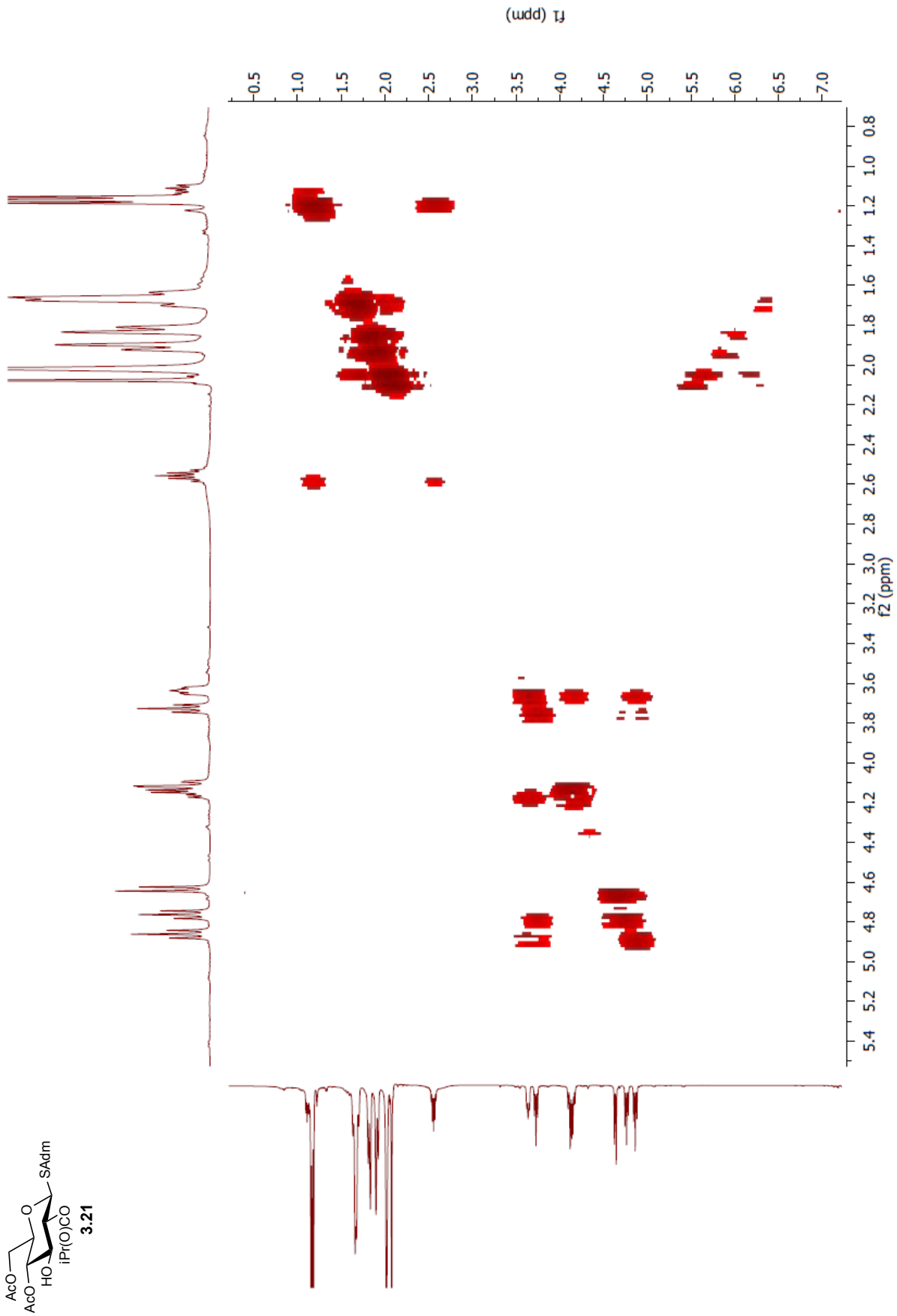
f1 (ppm)
0.5
1.0
1.5
2.0
2.5
3.0
3.5
4.0
4.5
5.0
5.5
6.0
6.5
7.0
f2 (ppm)
0.8
1.0
1.2
1.4
1.6
1.8
2.0
2.2
2.4
2.6
2.8
3.0
3.2
3.4
3.6
3.8
4.0
4.2
4.4
4.6
4.8
5.0
5.2
5.4
AcO
AcO
HO
iPr(O)CO
O
SAdm
3.21

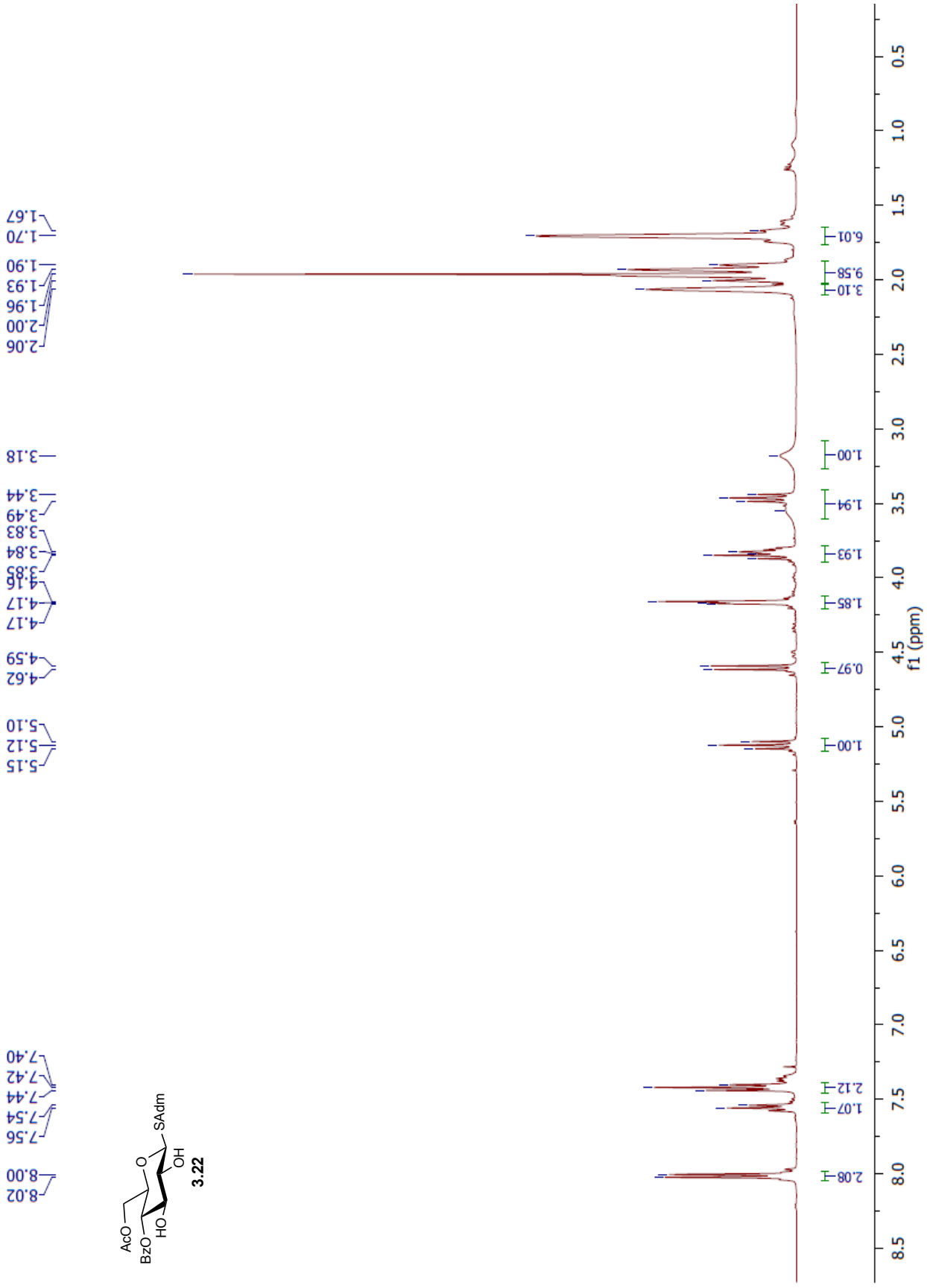
8.02
8.00
7.56
7.54
7.44
7.42
7.40
5.15
5.12
5.10
4.62
4.59
4.17
4.17
4.16
3.85
3.84
3.83
3.49
3.44
3.18
2.06
2.00
1.96
1.93
1.90
1.70
1.67
2.08
1.07
2.12
0.97
1.00
1.85
1.93
1.94
1.00
3.10
9.58
6.01
f1 (ppm)
AcO
BzO
HO
OH
SAdm
O
3.22

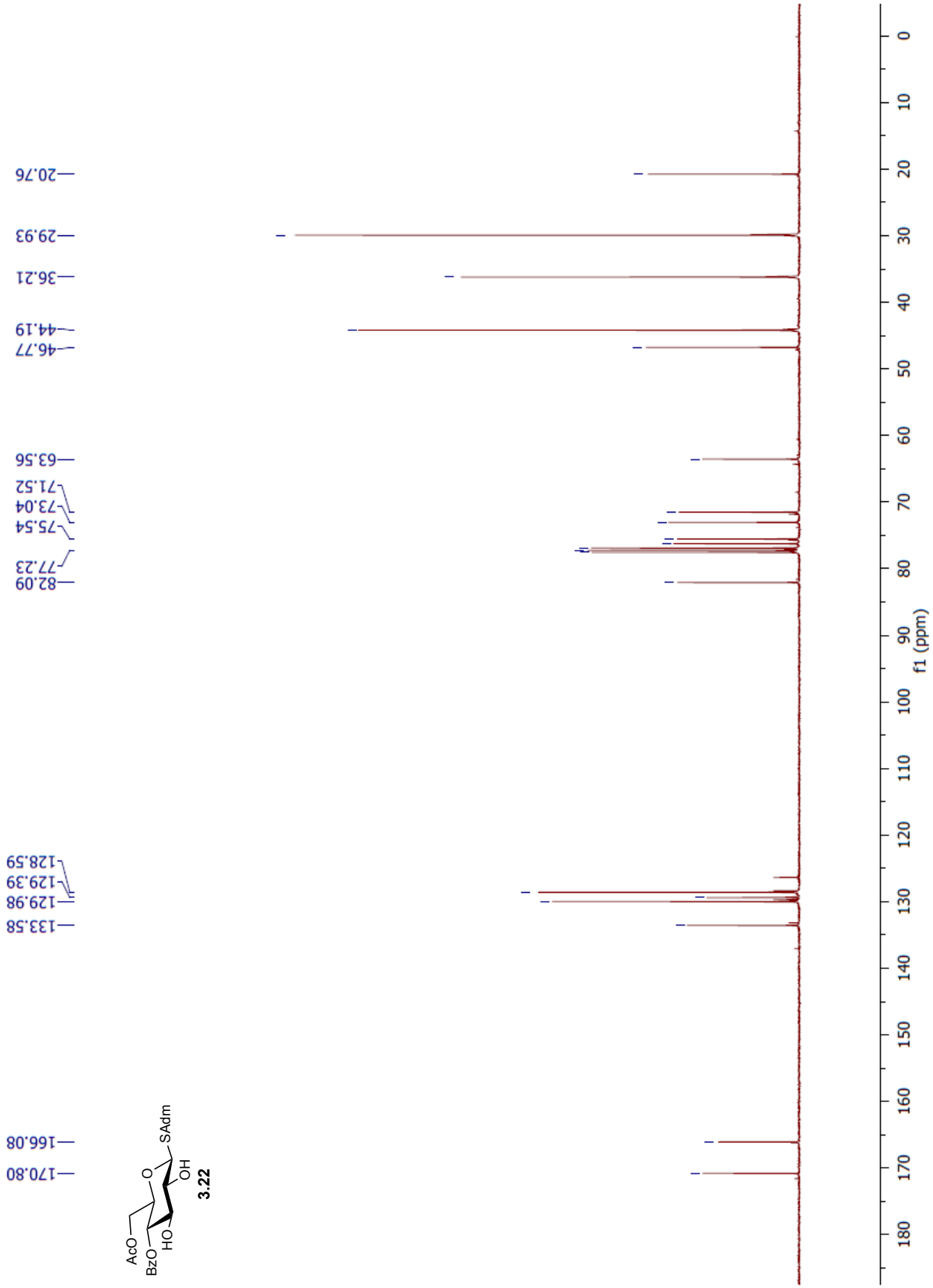
20.76
29.93
36.21
44.19
46.77
63.56
71.52
73.04
75.54
77.23
82.09
128.59
129.39
129.98
133.58
166.08
170.80
f1 (ppm)
SAdm
OH
HO
BzO
AcO
O
3.22

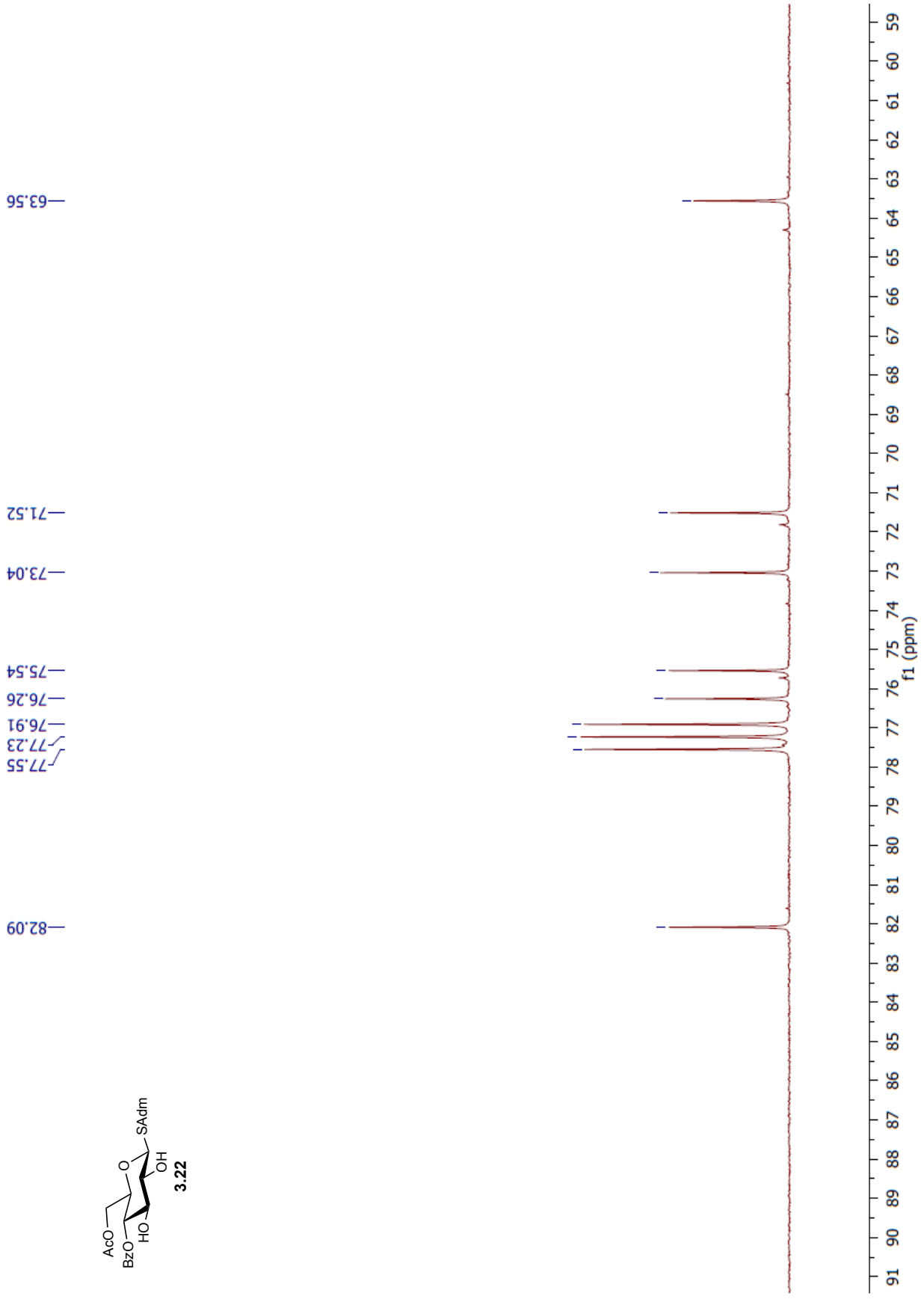
63.56
71.52
73.04
75.54
76.26
76.91
77.23
77.55
82.09
f1 (ppm)
SAdm
OH
O
HO
BzO
AcO
3.22

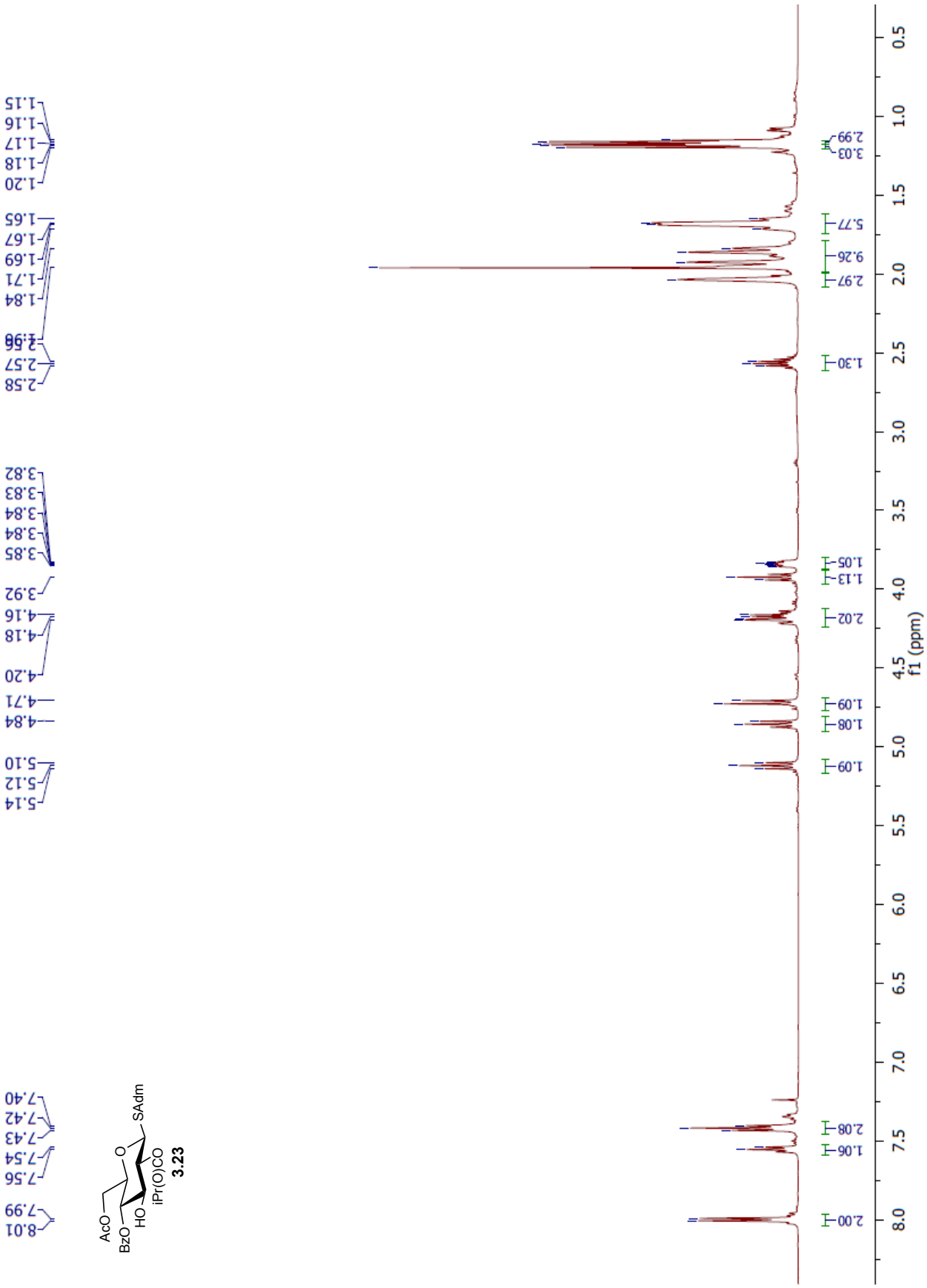
AcO
BzO
HO
O
iPr(O)CO
SAdm
3.23
f1 (ppm)

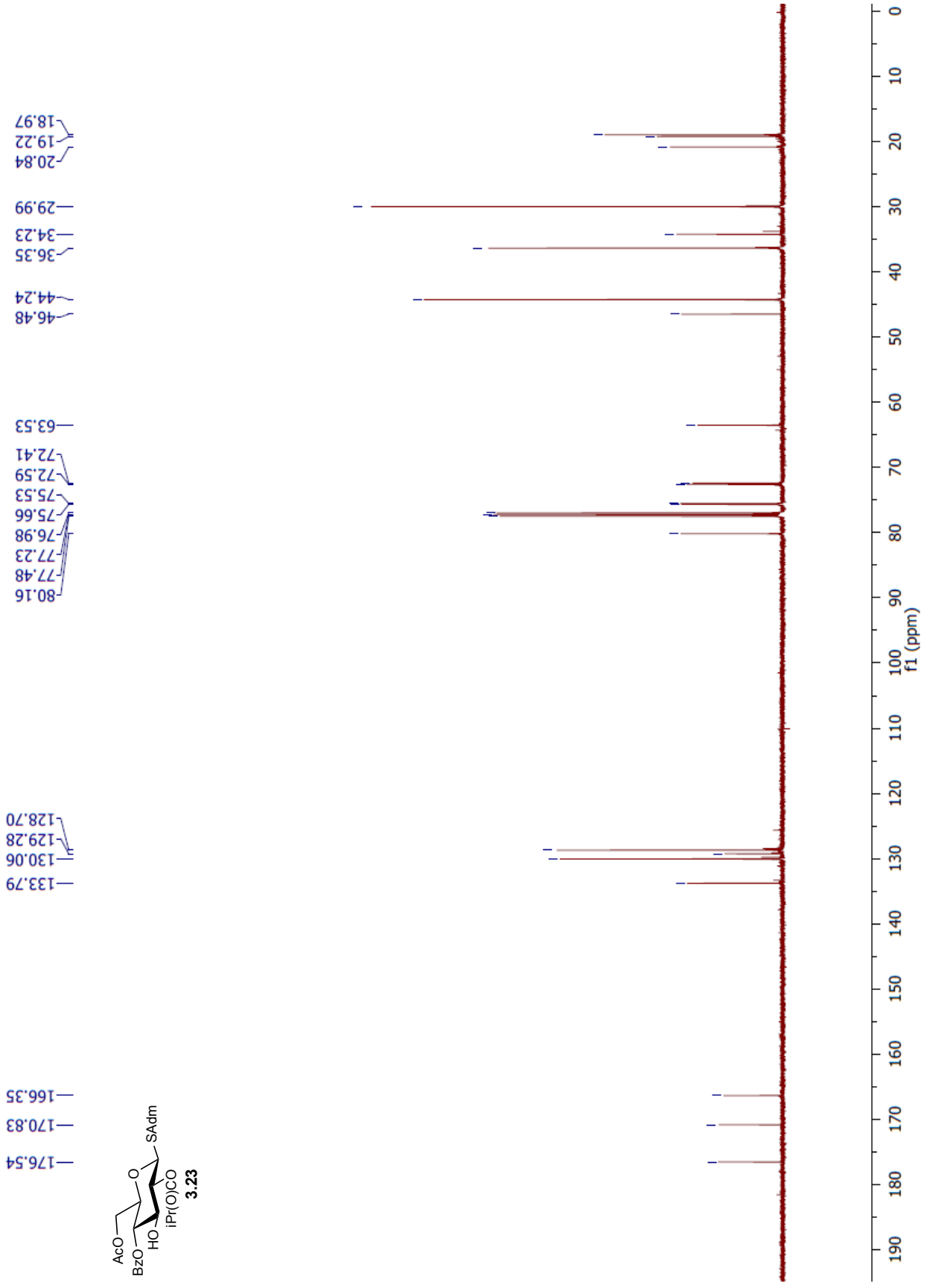
18.97
19.22
20.84
29.99
34.23
36.35
44.24
46.48
63.53
72.41
72.59
75.53
75.66
76.98
77.23
77.48
80.16
128.70
129.28
130.06
133.79
166.35
170.83
176.54
AcO
BzO
HO
iPr(O)CO
O
SAdm
3.23
f1 (ppm)

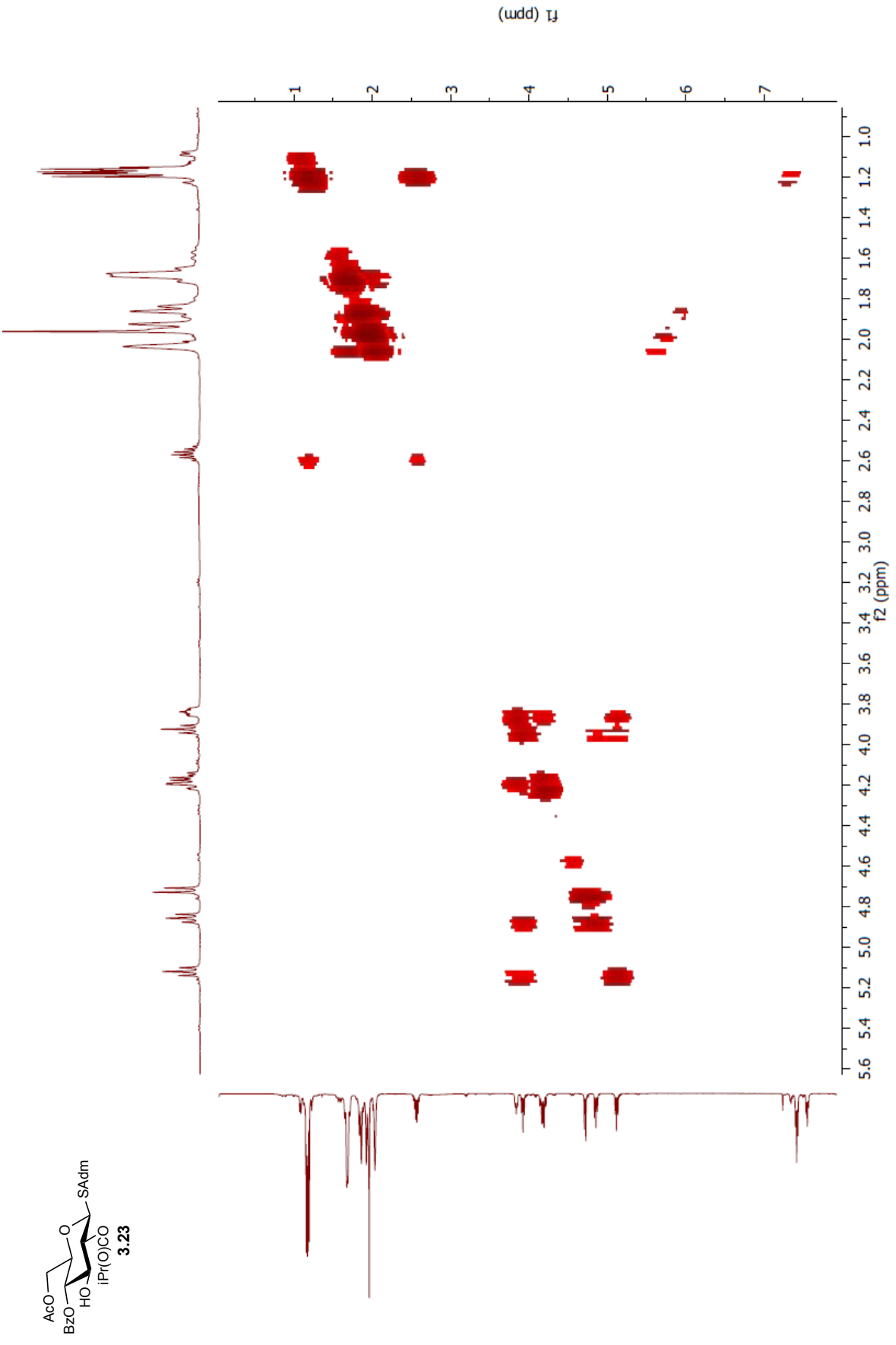
f1 (ppm)
f2 (ppm)
AcO
BzO
HO
iPr(O)CO
O
SAdm
3.23

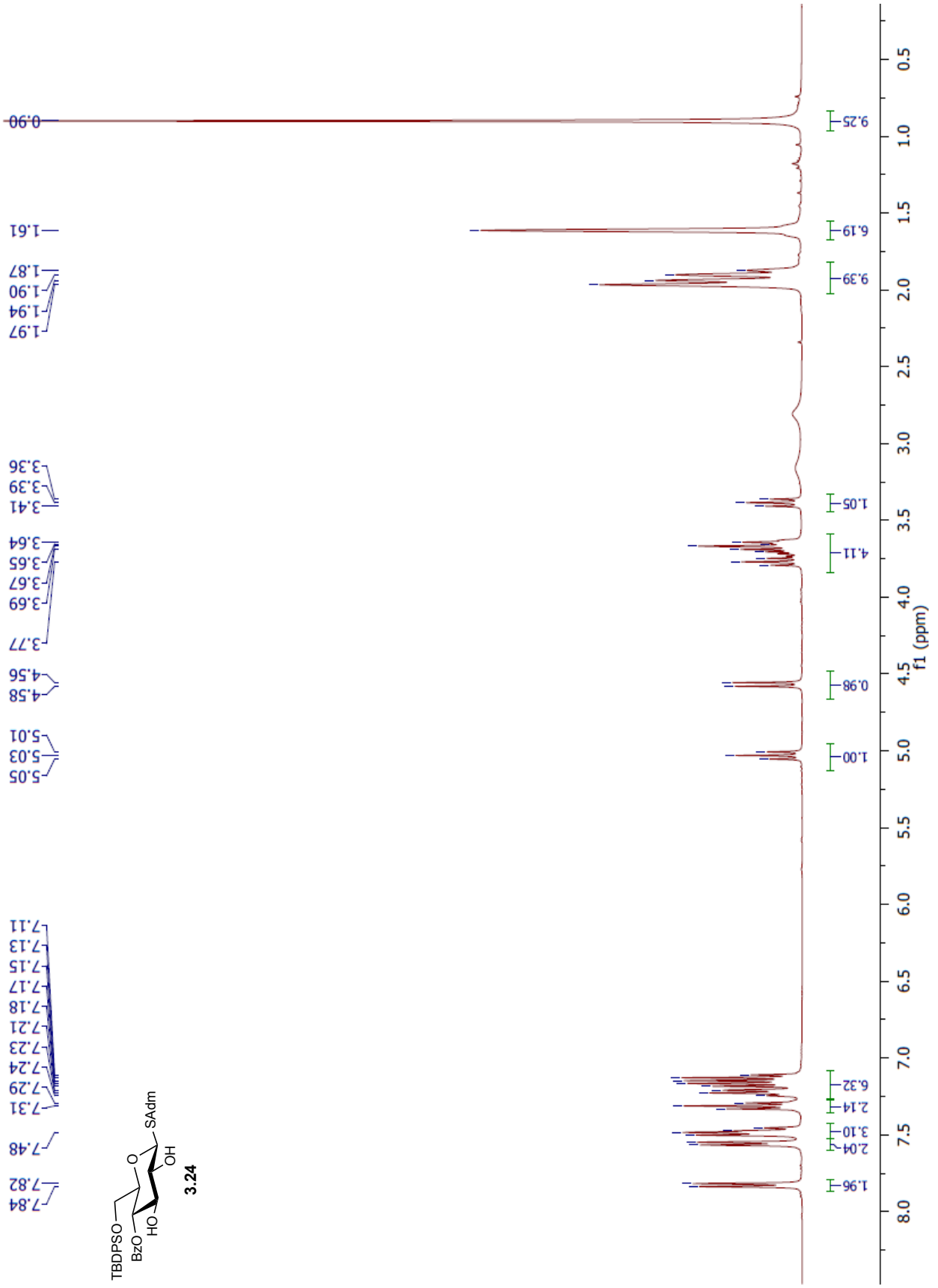
0.90
1.61
1.87
1.90
1.94
1.97
3.36
3.39
3.41
3.64
3.65
3.67
3.69
3.77
4.56
4.58
5.01
5.03
5.05
7.11
7.13
7.15
7.17
7.18
7.21
7.23
7.24
7.29
7.31
7.48
7.82
7.84
9.25
6.19
9.39
1.05
4.11
0.98
1.00
6.32
2.14
3.10
2.04
1.96
f1 (ppm)
TBDPSO
BzO
HO
O
SAdm
OH
3.24

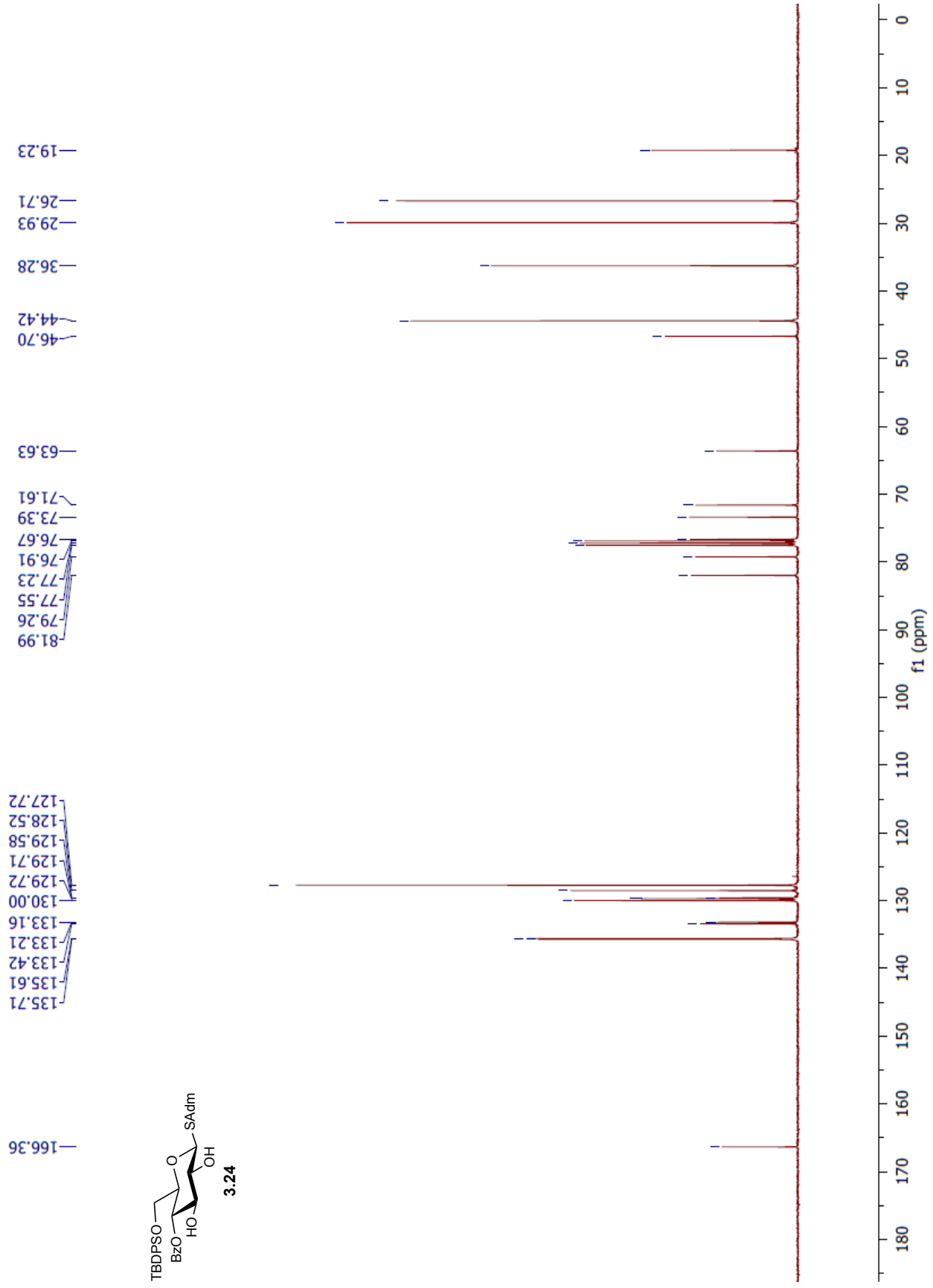
19.23
26.71
29.93
36.28
44.42
46.70
63.63
71.61
73.39
76.67
76.91
77.23
77.55
79.26
81.99
127.72
128.52
129.58
129.71
129.72
130.00
133.16
133.21
133.42
135.61
135.71
166.36
TBDPSO
BzO
HO
O
OH
SAdm
3.24
f1 (ppm)

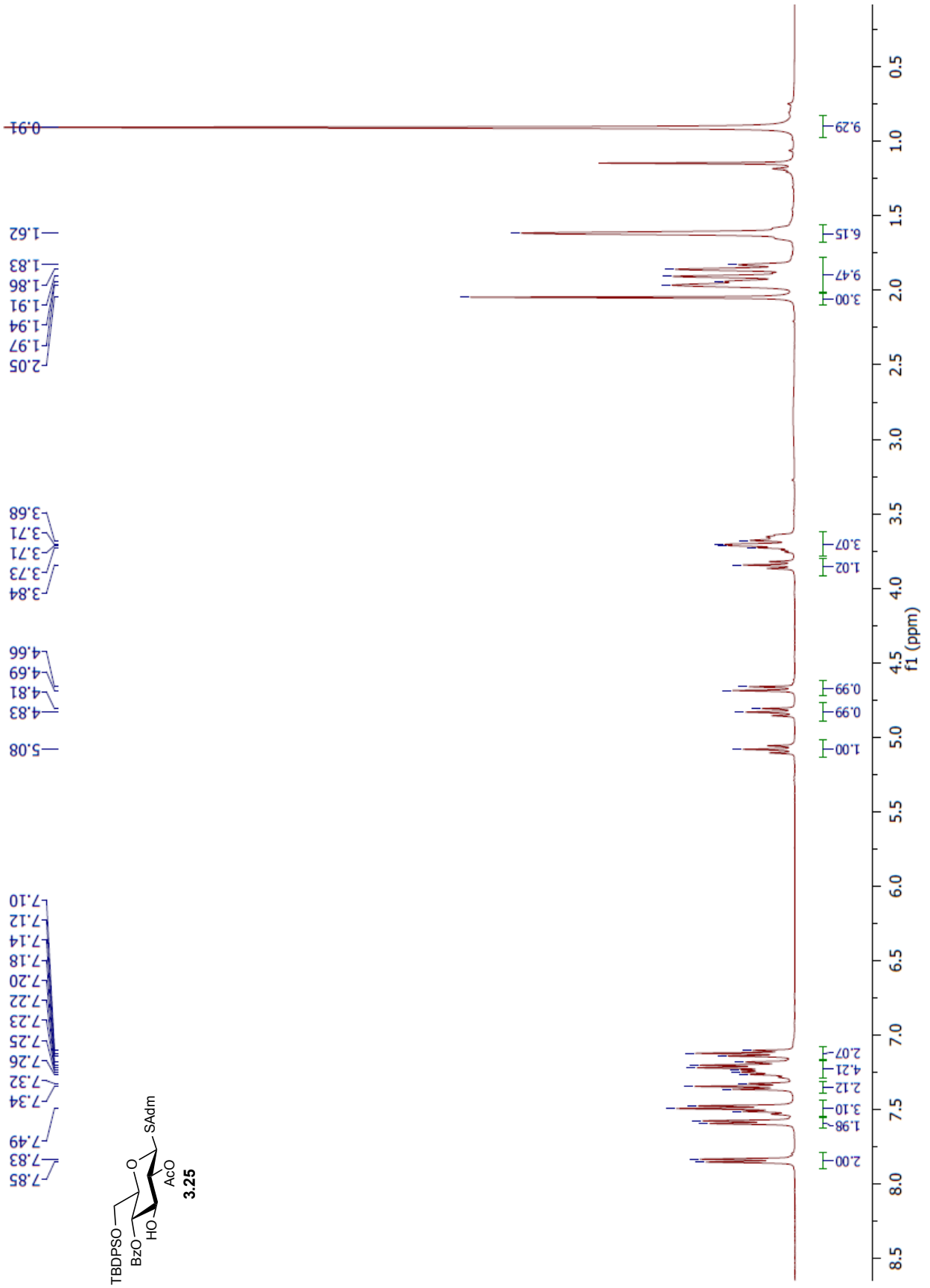
0.91
1.62
1.83
1.86
1.91
1.94
1.97
2.05
3.68
3.71
3.71
3.73
3.84
4.66
4.69
4.81
4.83
5.08
7.10
7.12
7.14
7.18
7.20
7.22
7.23
7.25
7.26
7.32
7.34
7.49
7.83
7.85
9.29
6.15
9.47
3.00
3.07
1.02
0.99
0.99
1.00
2.07
4.21
2.12
3.10
1.98
2.00
f1 (ppm)
TBDPSO
BzO
HO
O
SAdm
AcO
3.25

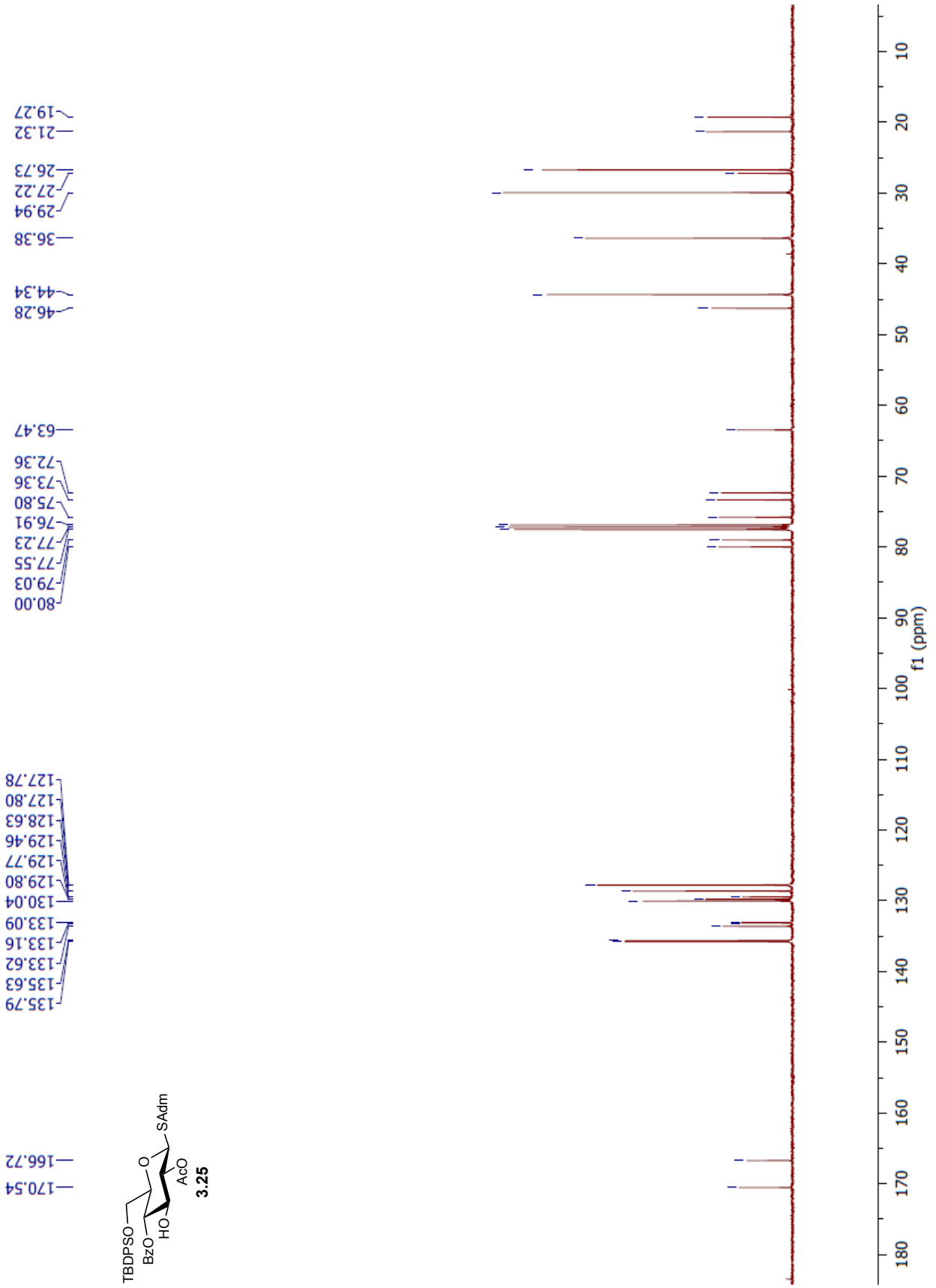
19.27
21.32
26.73
27.22
29.94
36.38
44.34
46.28
63.47
72.36
73.36
75.80
76.91
77.23
77.55
79.03
80.00
127.78
127.80
128.63
129.46
129.77
129.80
130.04
133.09
133.16
133.62
135.63
135.79
166.72
170.54
TBDPSO
BzO
HO
O
AcO
SAdm
3.25
f1 (ppm)

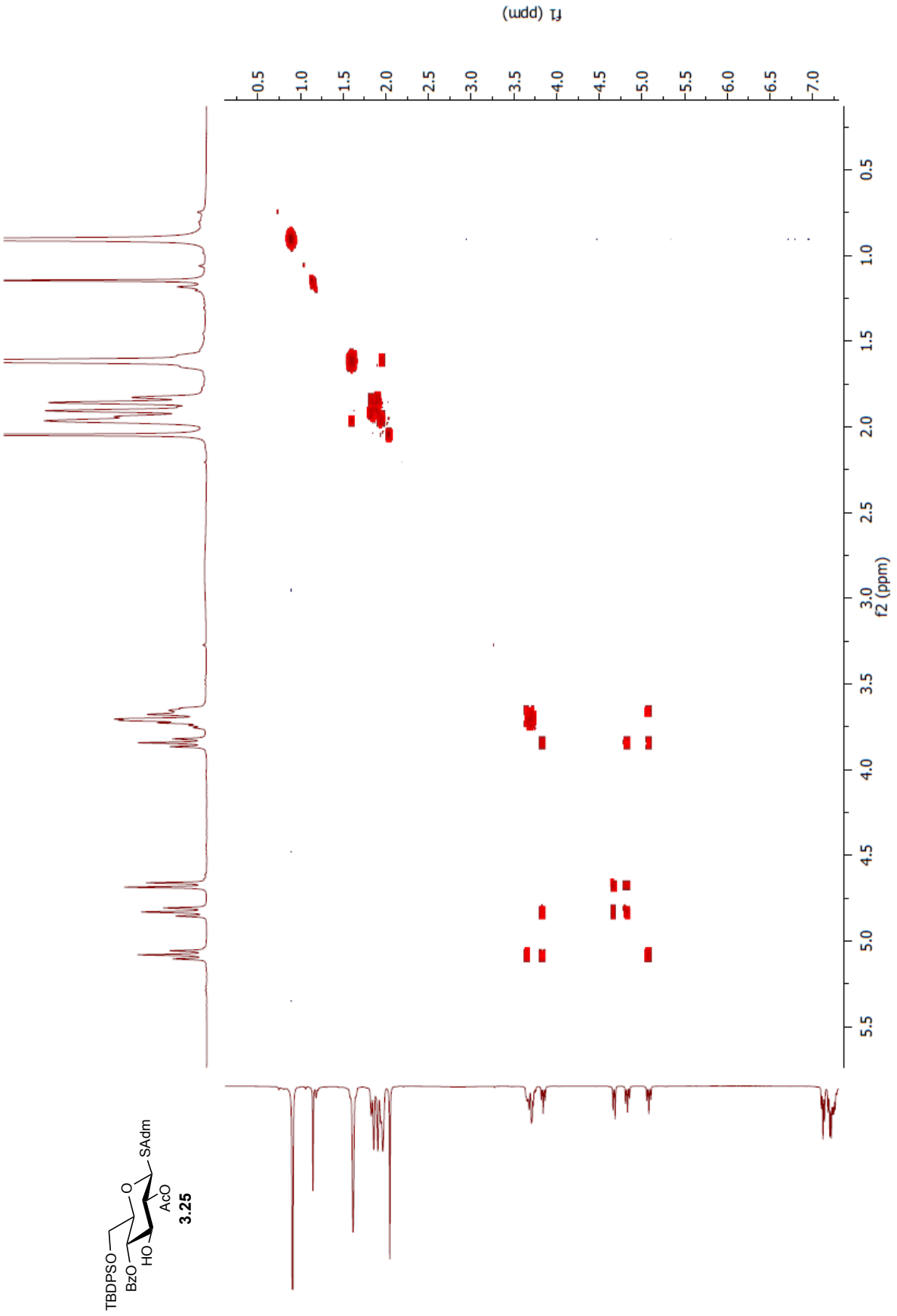
f1 (ppm)
0.5
1.0
1.5
2.0
2.5
3.0
3.5
4.0
4.5
5.0
5.5
6.0
6.5
7.0
f2 (ppm)
TBDPSO
BzO
HO
O
SAdm
AcO
3.25

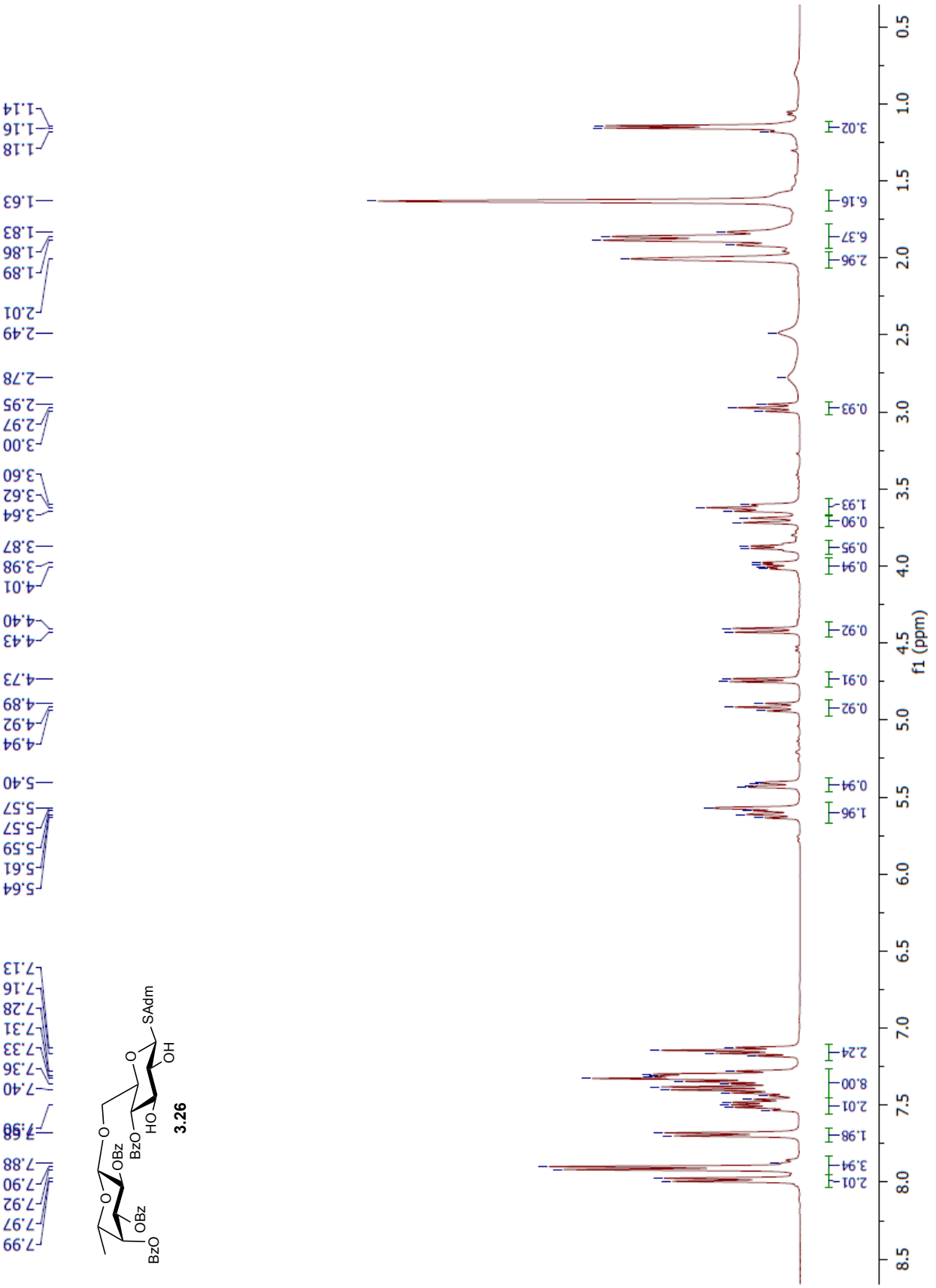
3.26
SAdm
OH
HO
BzO
OBz
OBz
BzO
f1 (ppm)

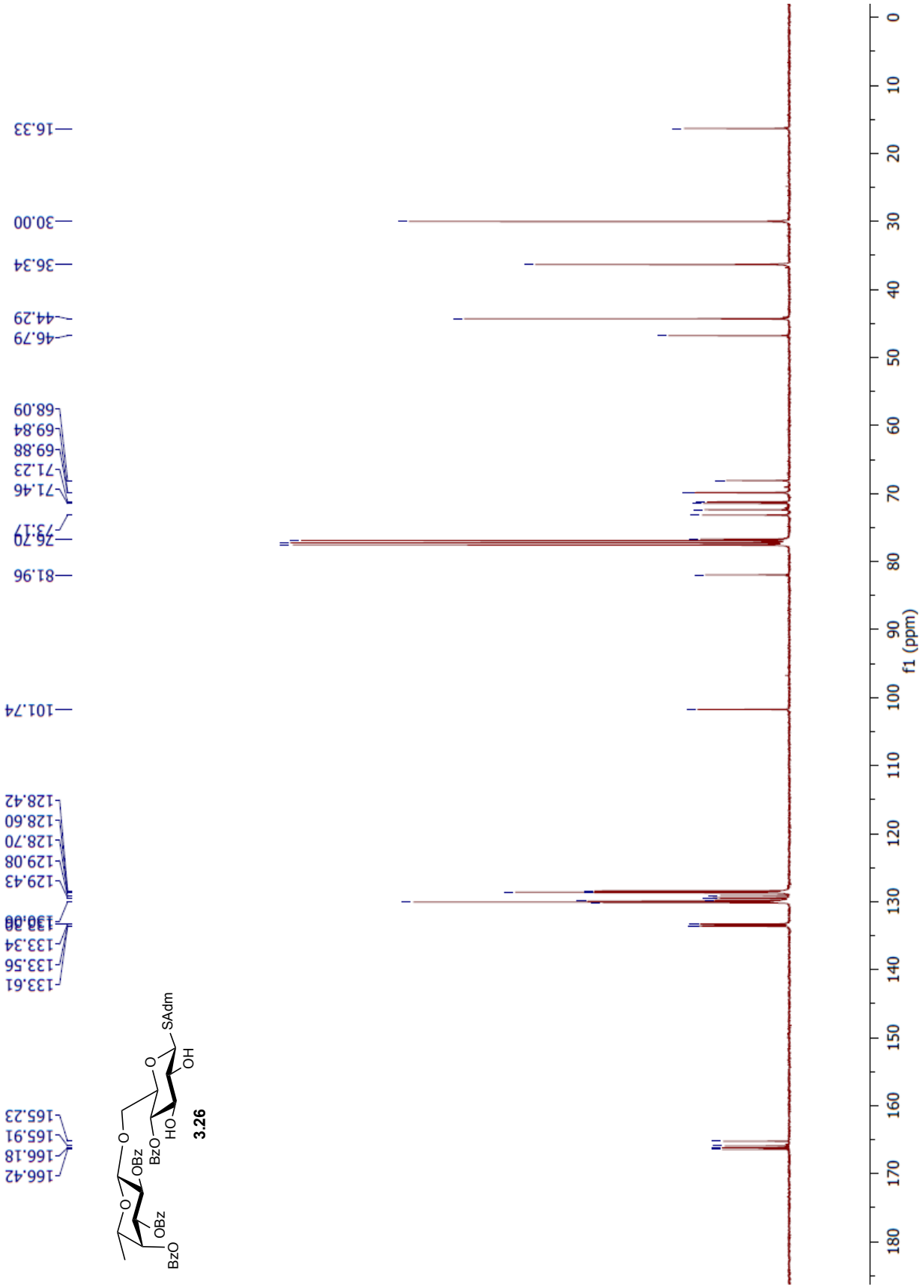
16.33
30.00
36.34
44.29
46.79
68.09
69.84
69.88
71.23
71.46
73.17
76.70
81.96
101.74
128.42
128.60
128.70
129.08
129.43
133.34
133.56
133.61
165.23
165.91
166.18
166.42
BzO
OBz
OBz
O
O
BzO
HO
O
SAdm
OH
3.26
f1 (ppm)

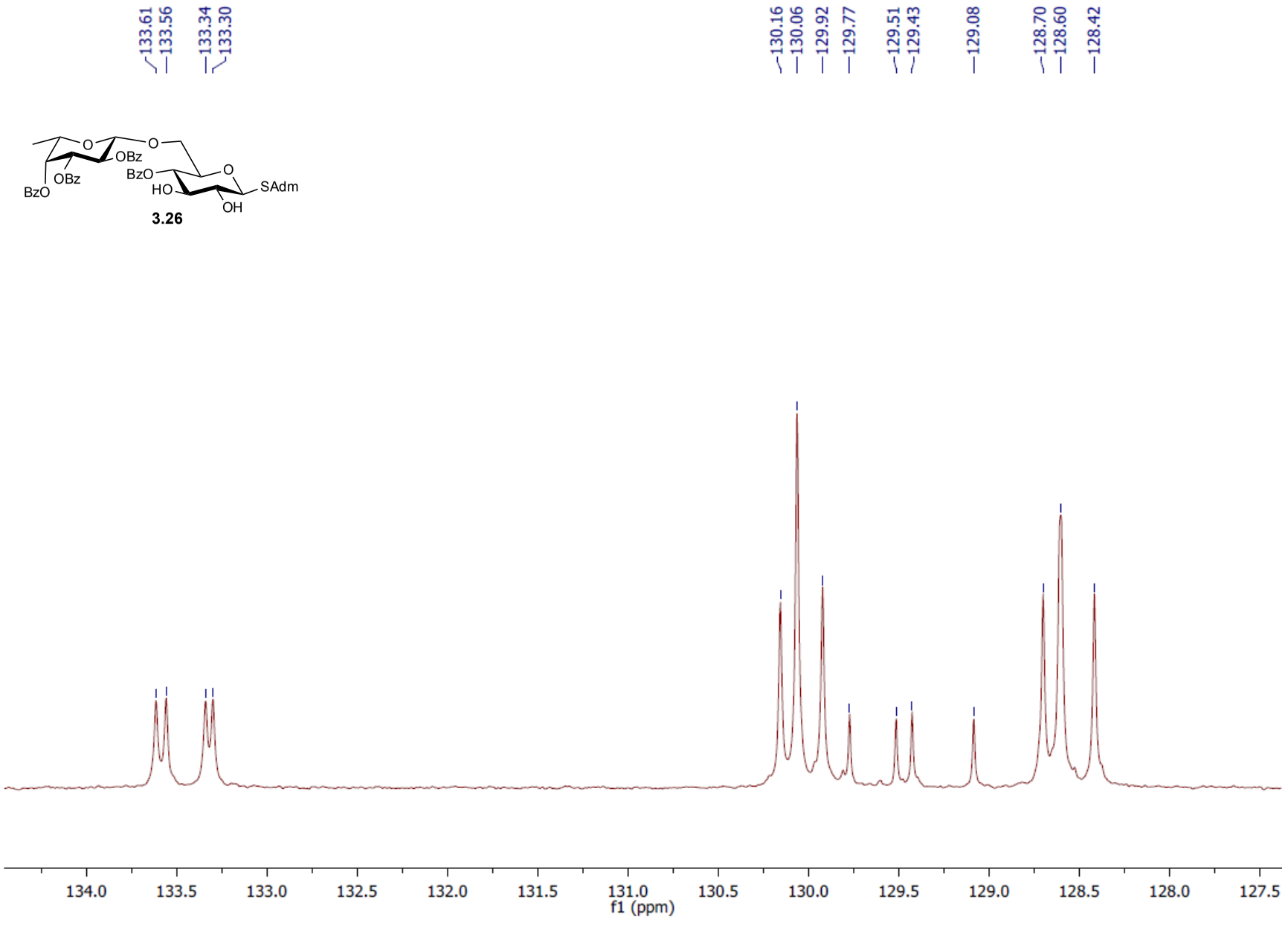
133.61
133.56
133.34
133.30
130.16
130.06
129.92
129.77
129.51
129.43
129.08
128.70
128.60
128.42
O
O
OBz
BzO
OBz
BzO
O
HO
SAdm
OH
3.26
134.0
133.5
133.0
132.5
132.0
131.5
131.0
130.5
130.0
129.5
129.0
128.5
128.0
127.5
f1 (ppm)

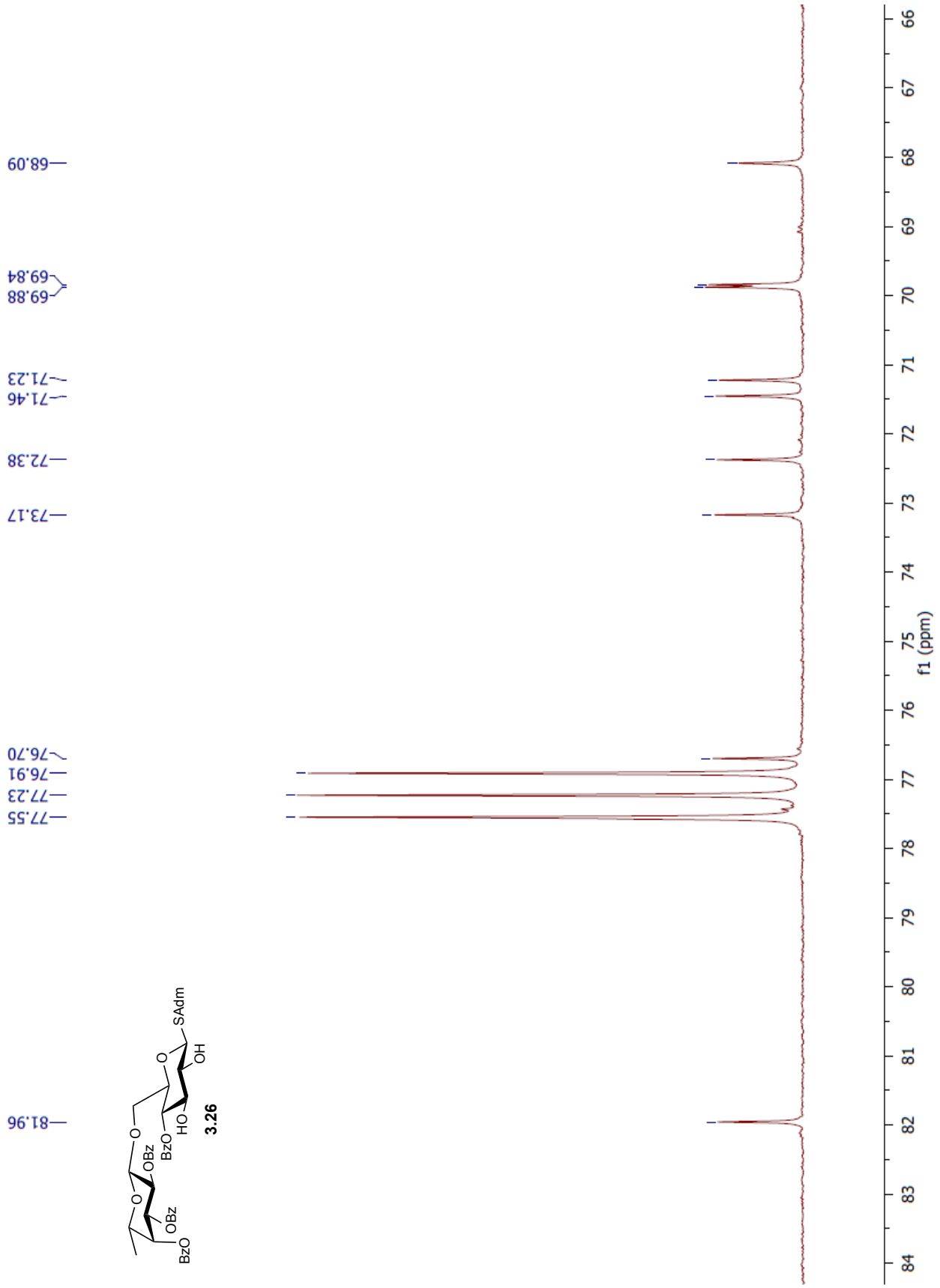
68.09
69.84
69.88
71.23
71.46
72.38
73.17
76.70
76.91
77.23
77.55
81.96
f1 (ppm)
66
67
68
69
70
71
72
73
74
75
76
77
78
79
80
81
82
83
84
SAdm
OH
HO
BzO
OBz
OBz
BzO
O
O
O
3.26

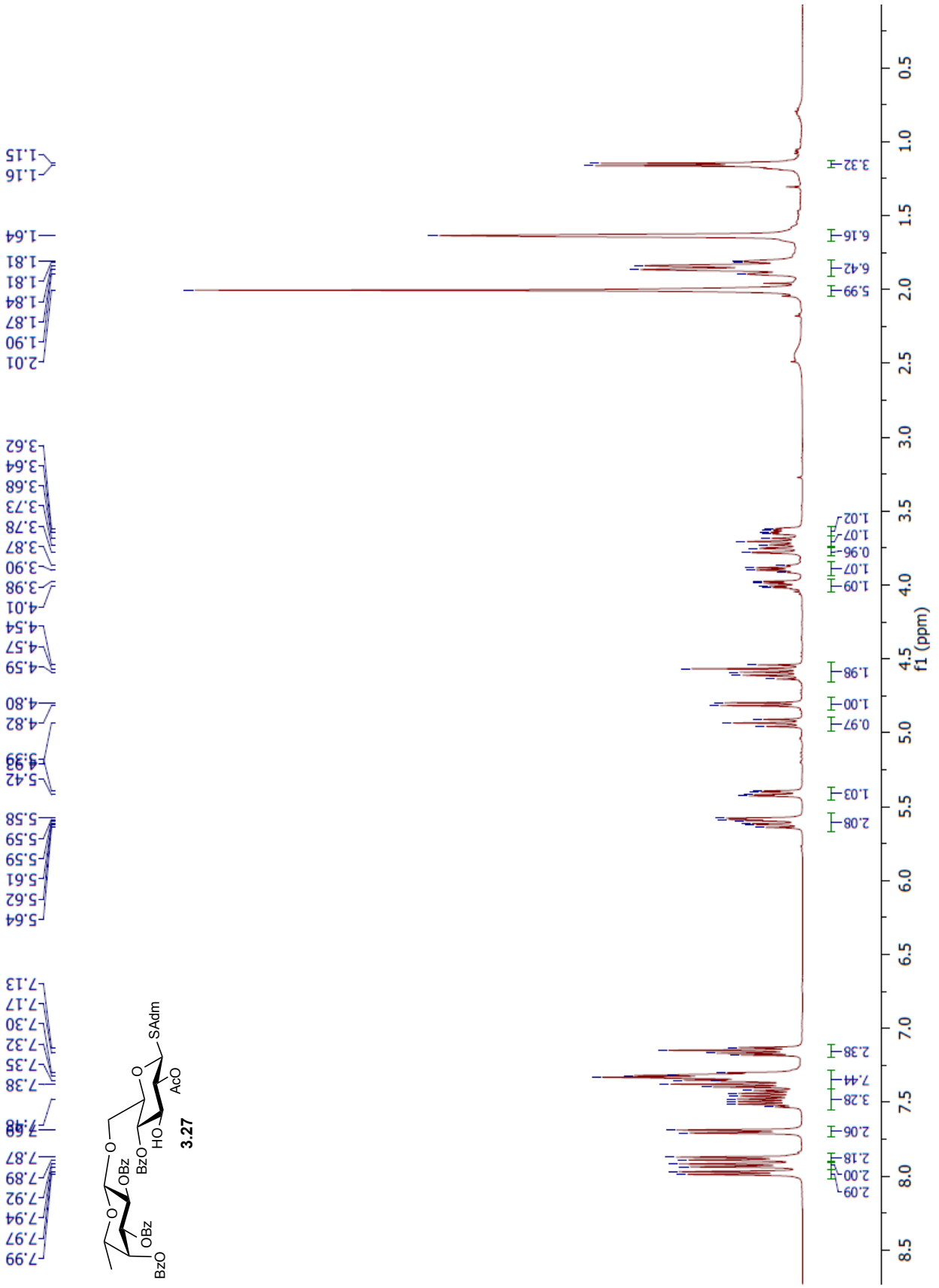
f1 (ppm)
3.27

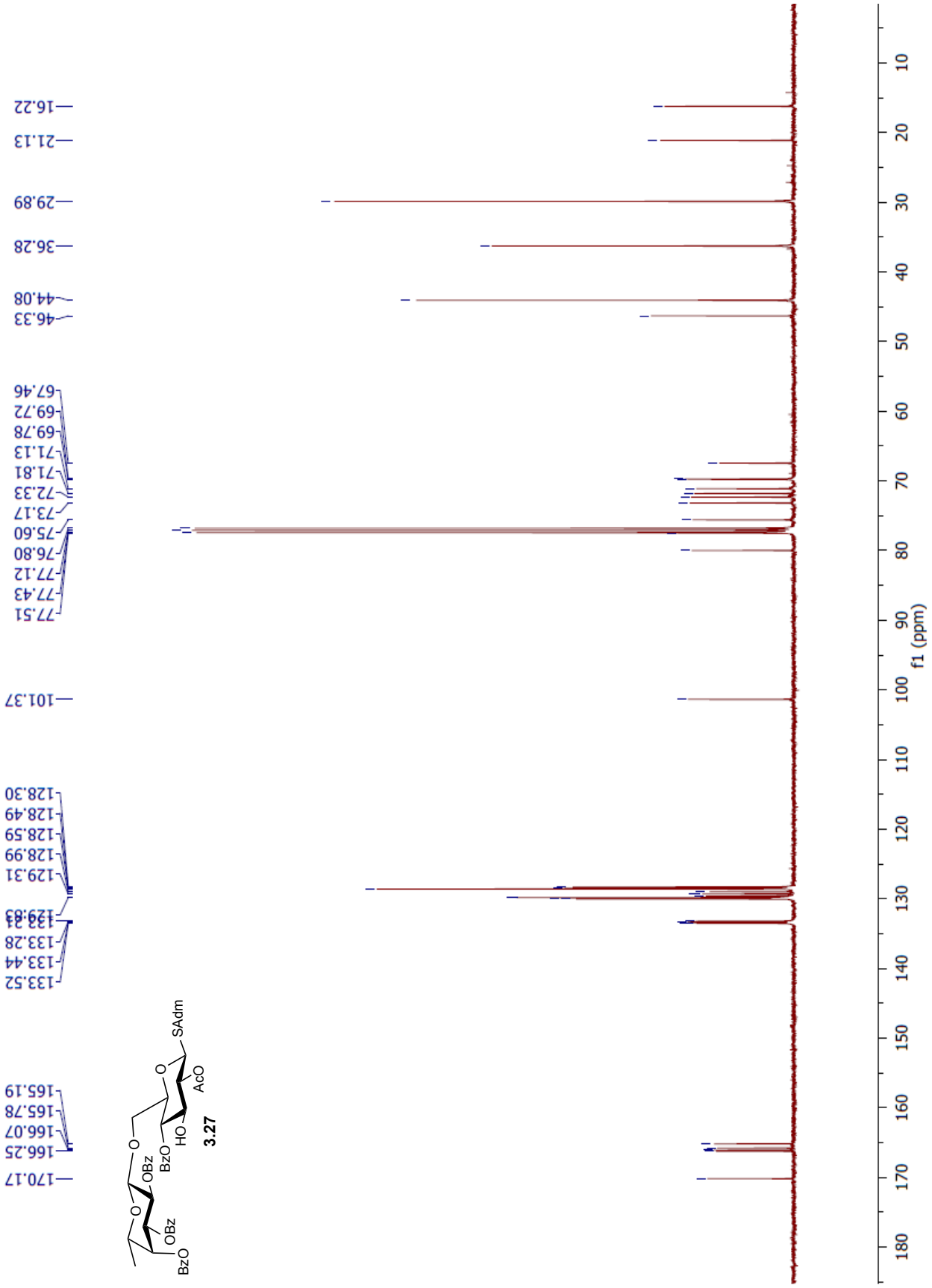
16.22
21.13
29.89
36.28
44.08
46.33
67.46
69.72
69.78
71.13
71.81
72.33
73.17
75.60
76.80
77.12
77.43
77.51
101.37
128.30
128.49
128.59
128.99
129.31
129.83
133.11
133.28
133.44
133.52
165.19
165.78
166.07
166.25
170.17
BzO
OBz
OBz
O
O
BzO
HO
AcO
O
SAdm
3.27
10
20
30
40
50
60
70
80
90
100
110
120
130
140
150
160
170
180
f1 (ppm)

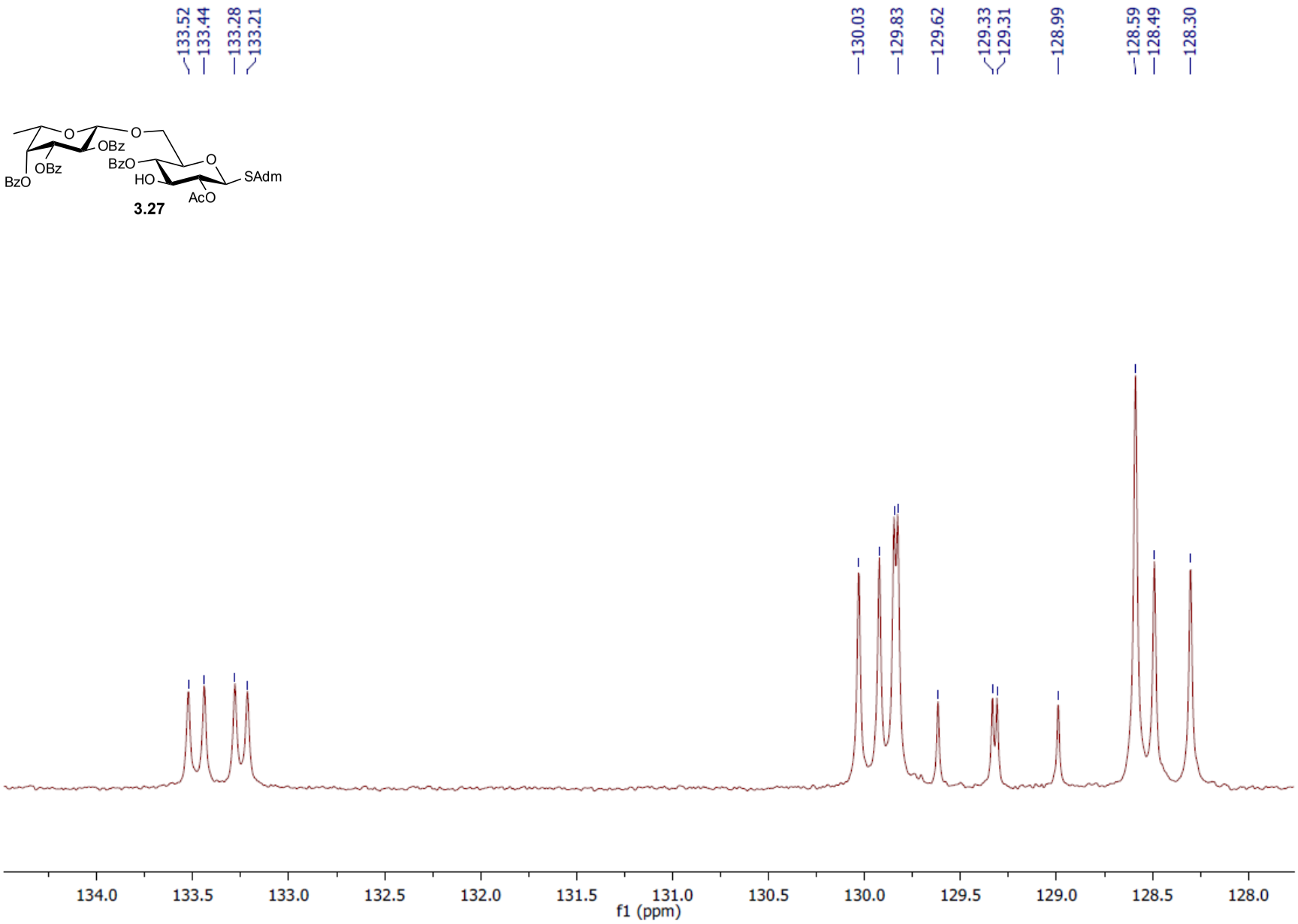
133.52
133.44
133.28
133.21
130.03
129.83
129.62
129.33
129.31
128.99
128.59
128.49
128.30
BzO
OBz
OBz
BzO
HO
AcO
O
O
O
SAdm
3.27
134.0
133.5
133.0
132.5
132.0
131.5
131.0
130.5
130.0
129.5
129.0
128.5
128.0
f1 (ppm)

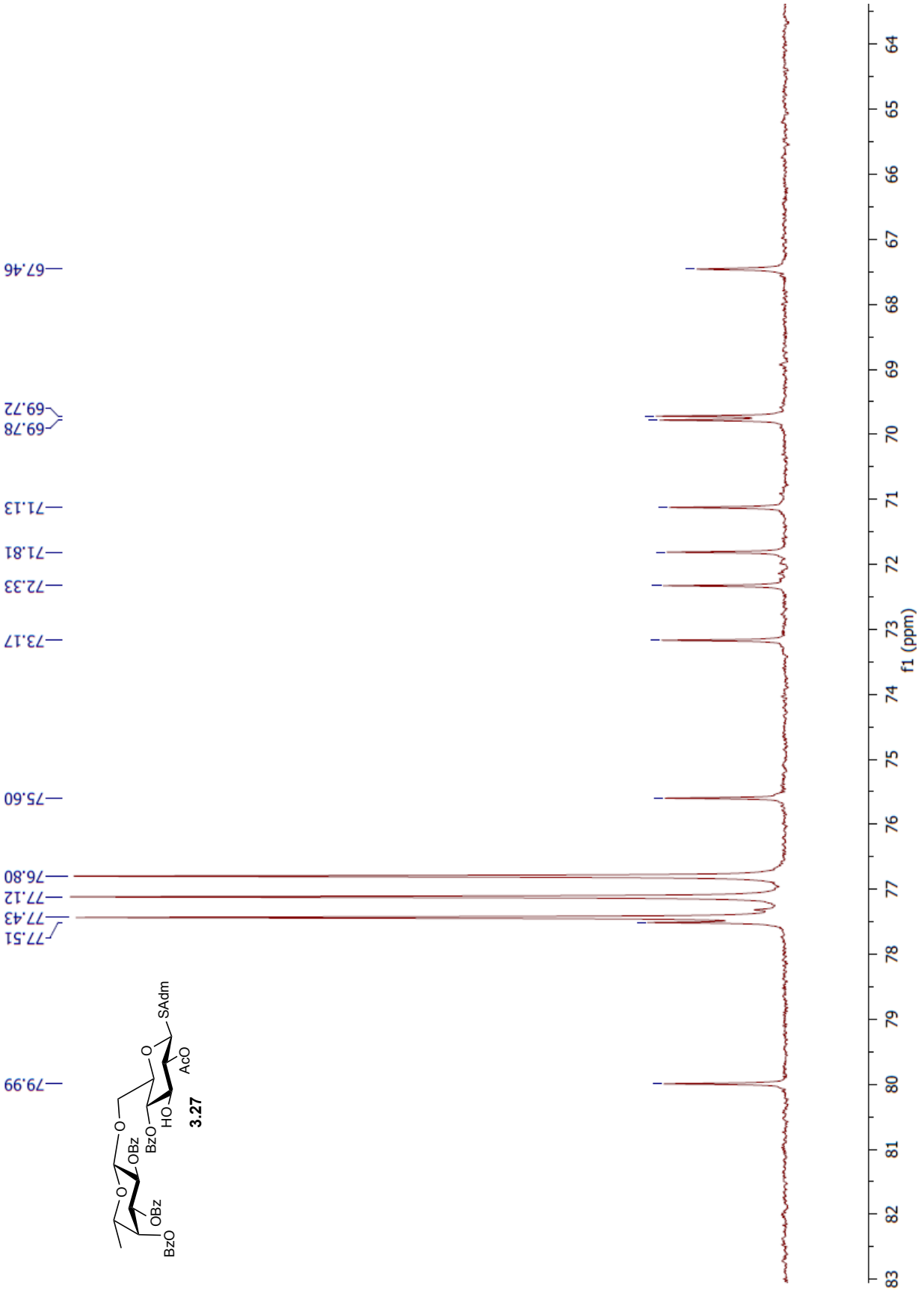
67.46
69.72
69.78
71.13
71.81
72.33
73.17
75.60
76.80
77.12
77.43
77.51
79.99
SAdm
AcO
HO
BzO
OBz
OBz
BzO
O
O
O
3.27
64
65
66
67
68
69
70
71
72
73
74
75
76
77
78
79
80
81
82
83
f1 (ppm)

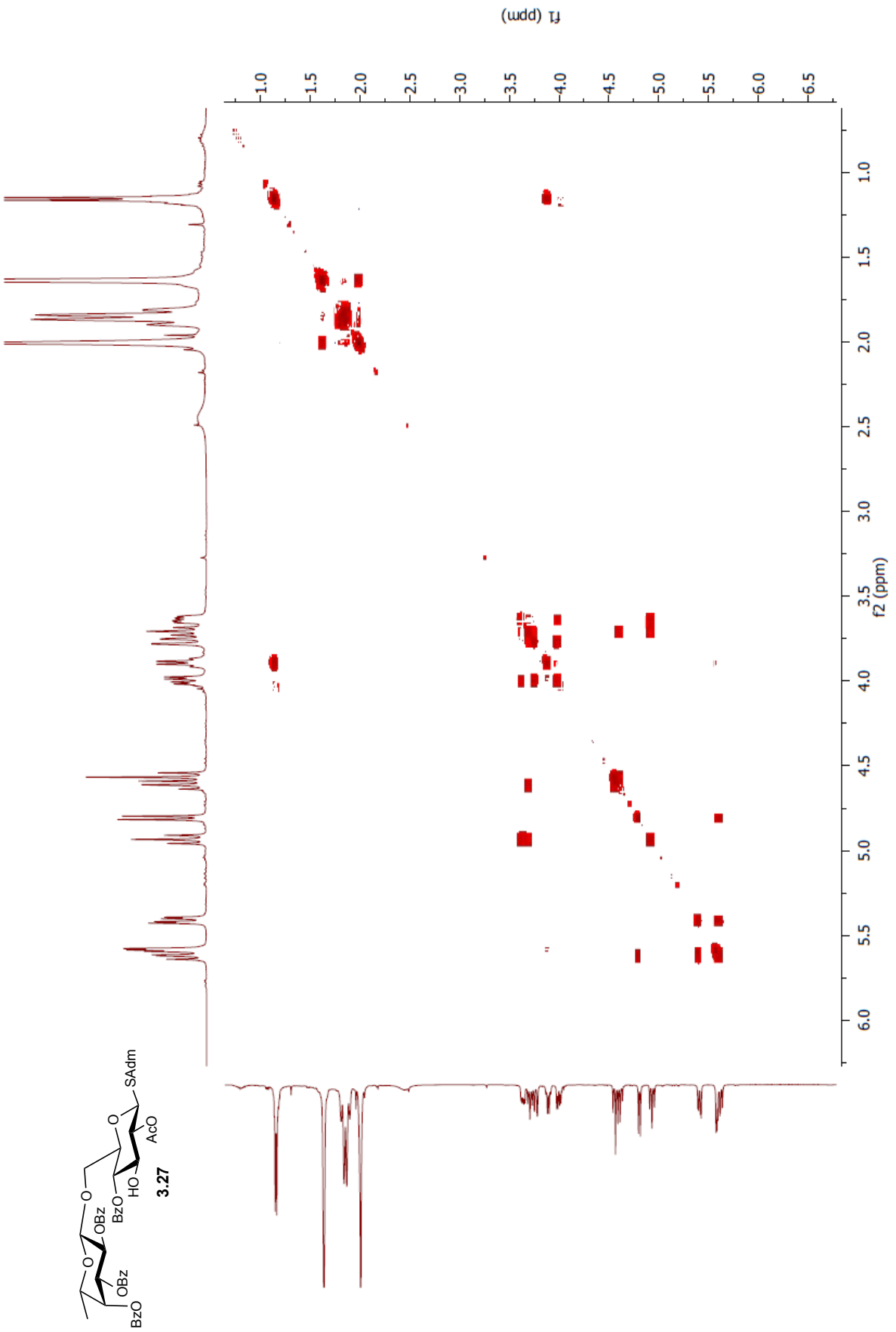
f1 (ppm)
1.0
1.5
2.0
2.5
3.0
3.5
4.0
4.5
5.0
5.5
6.0
6.5
f2 (ppm)
BzO
OBz
O
OBz
BzO
HO
AcO
SAdm
3.27

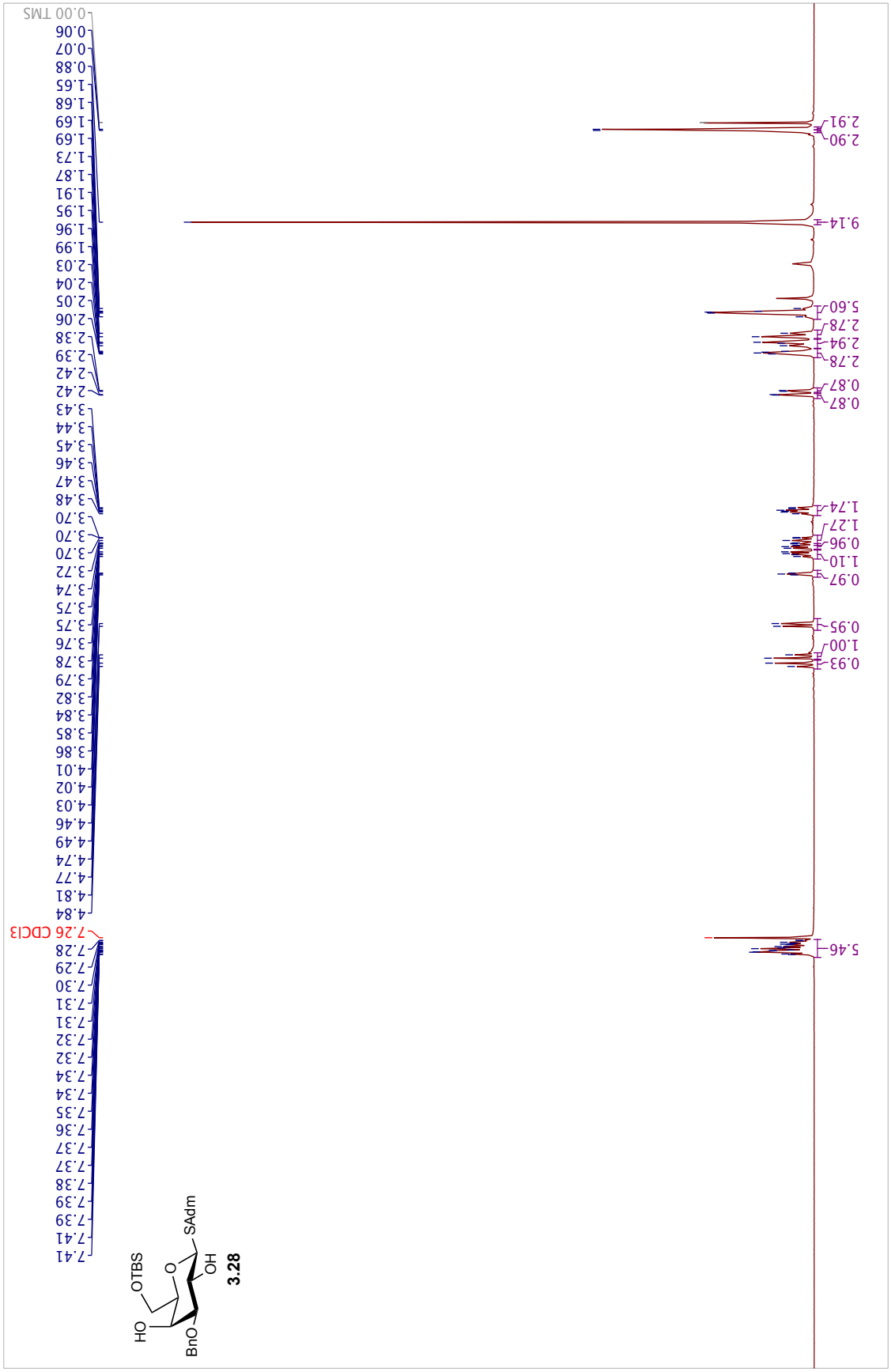
f1 (ppm)
HO
OTBS
O
SAdm
OH
BnO
3.28

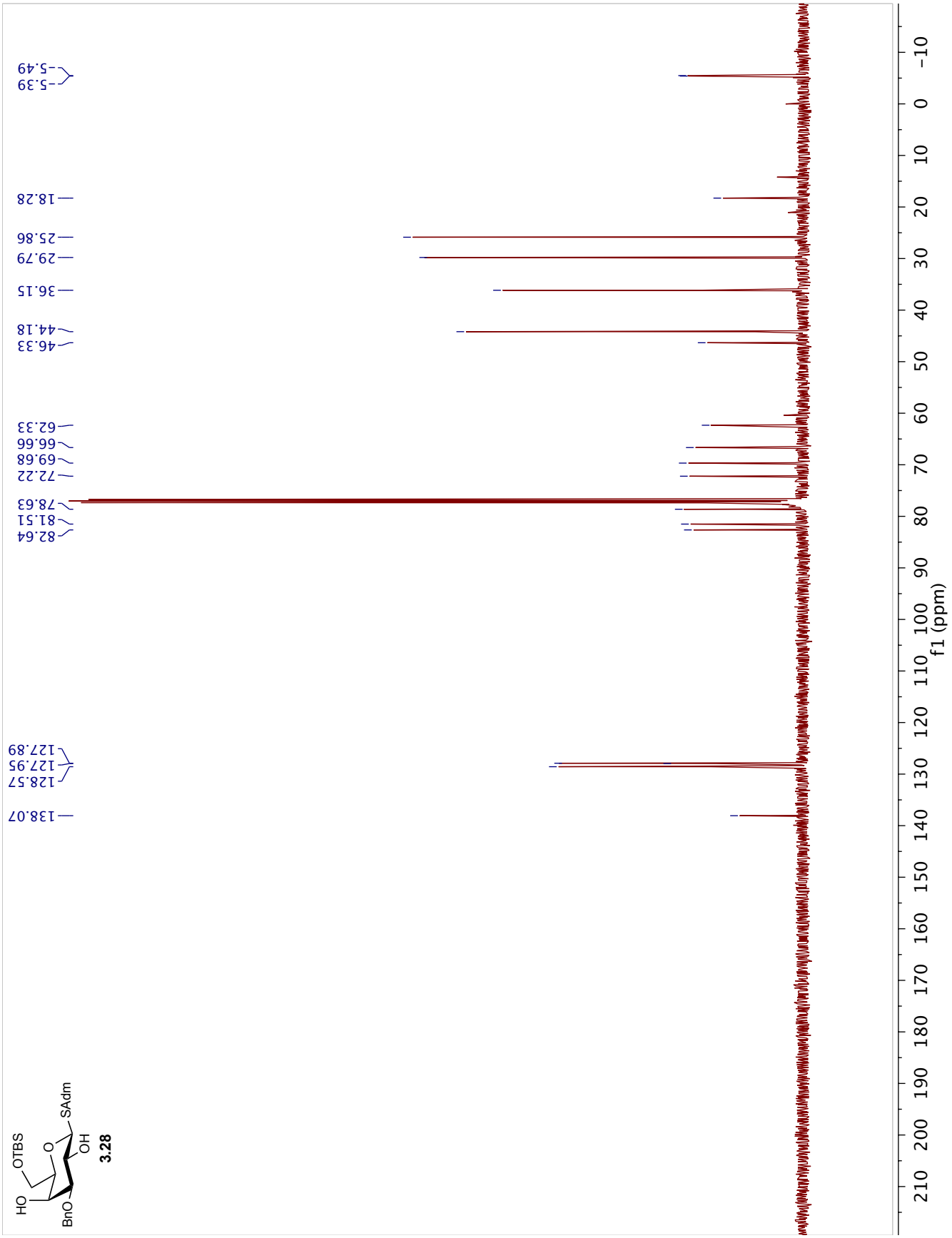
-5.49
-5.39
18.28
25.86
29.79
36.15
44.18
46.33
62.33
66.66
69.68
72.22
78.63
81.51
82.64
127.89
127.95
128.57
138.07
210 200 190 180 170 160 150 140 130 120 110 100 90 80 70 60 50 40 30 20 10 0 -10
f1 (ppm)
HO
OTBS
O
SAdm
OH
BnO
3.28

HO
OTBS
O
SAdm
OH
BnO
3.28
f2 (ppm)
f1 (ppm)

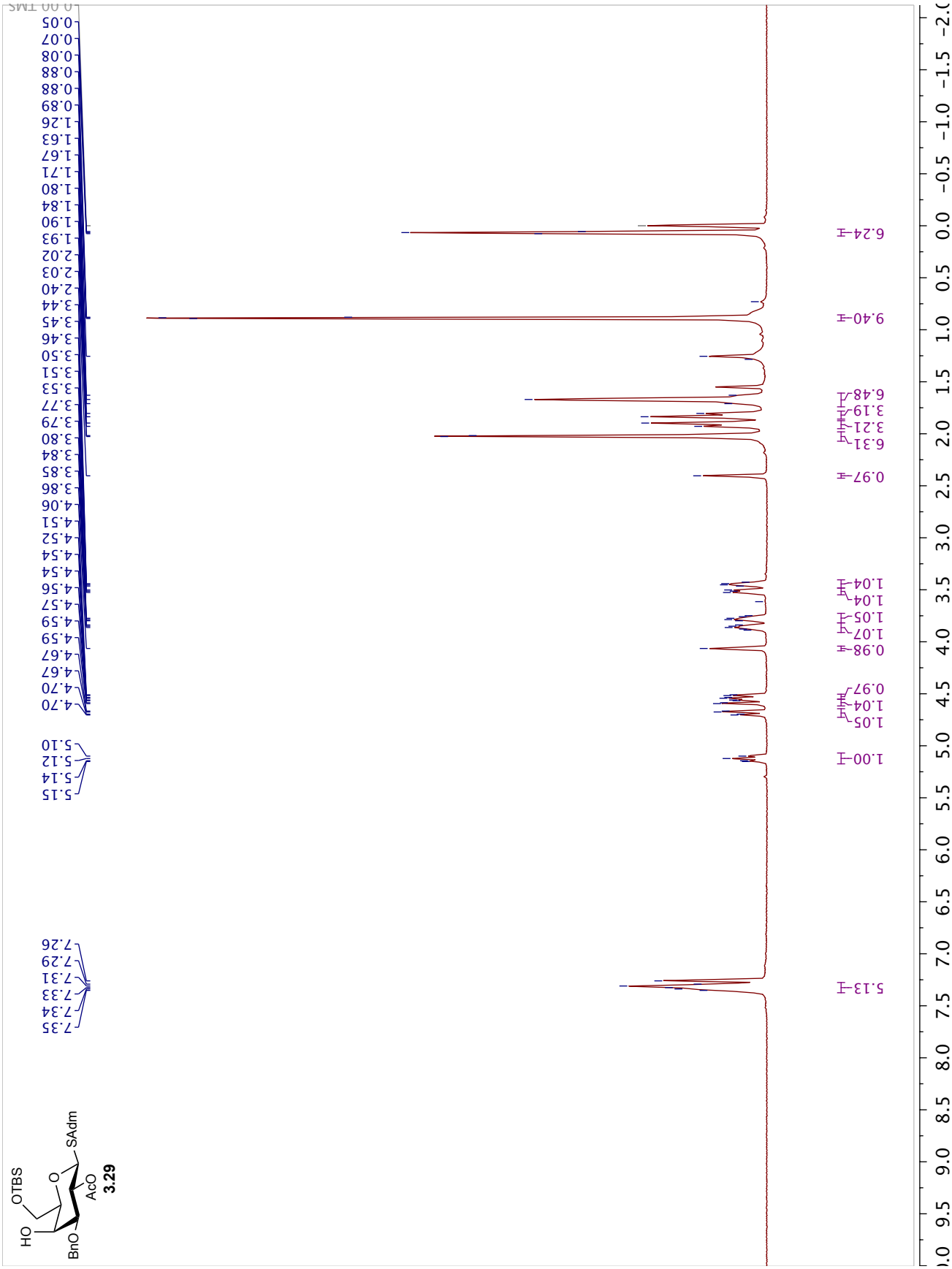
OTBS
O
SAdm
AcO
HO
BnO
3.29
f1 (ppm)

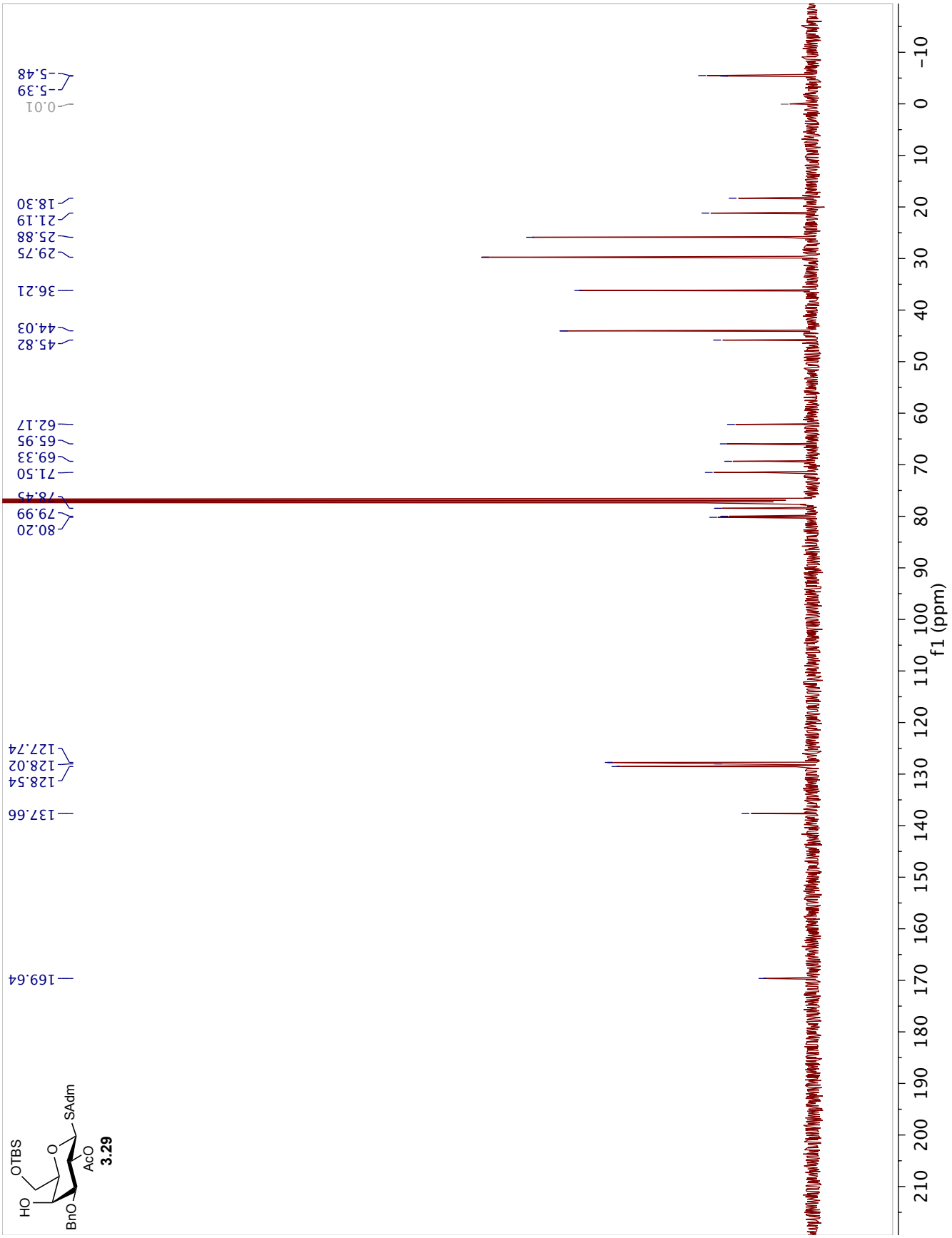
-5.48
-5.39
0.01
18.30
21.19
25.88
29.75
36.21
44.03
45.82
62.17
65.95
69.33
71.50
78.45
79.99
80.20
127.74
128.02
128.54
137.66
169.64
f1 (ppm)
OTBS
HO
BnO
O
AcO
SAdm
3.29

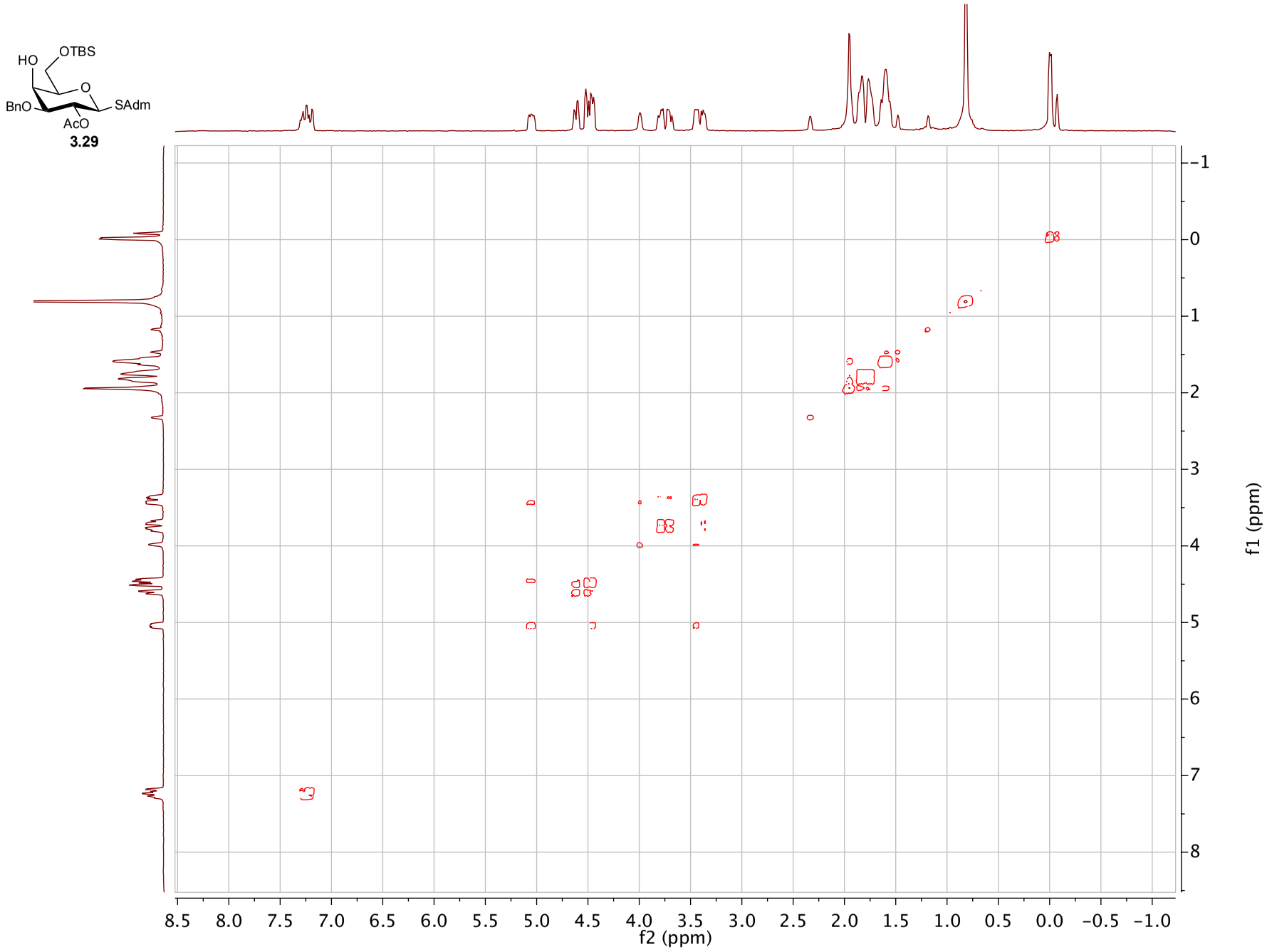
HO
OTBS
O
BnO
SAdm
AcO
3.29
f2 (ppm)
f1 (ppm)

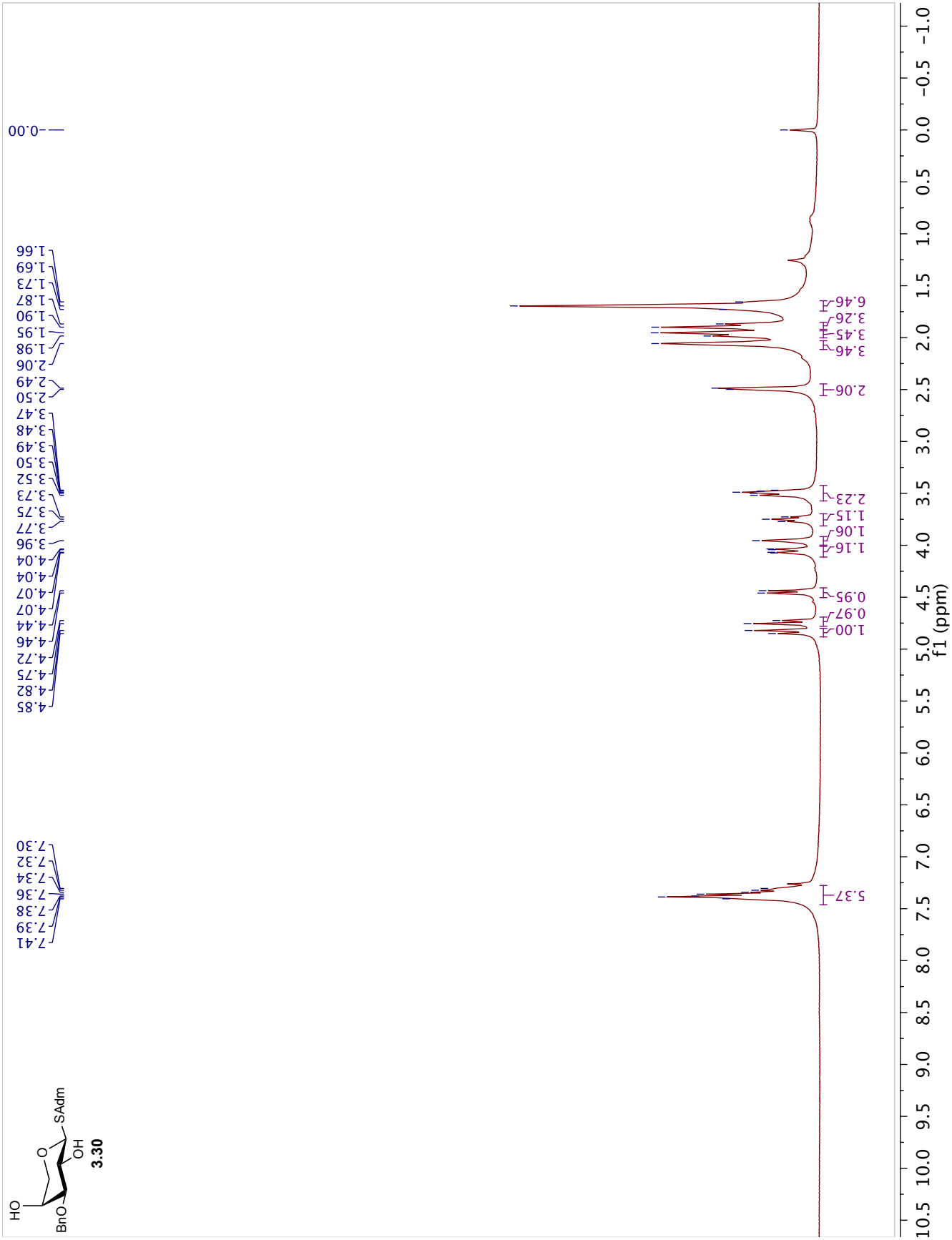
HO
BnO
O
SAdm
OH
3.30
f1 (ppm)

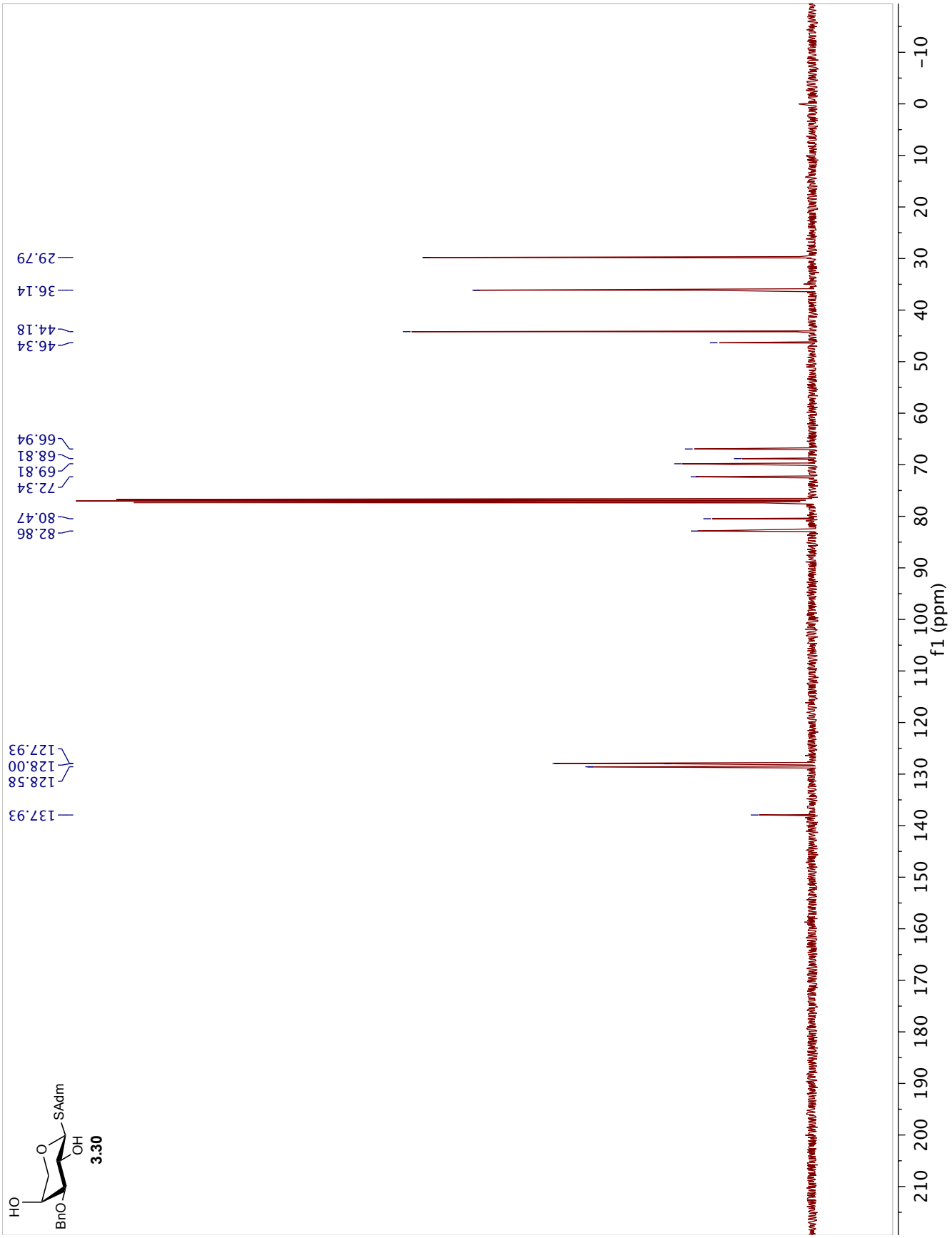
29.79
36.14
44.18
46.34
66.94
68.81
69.81
72.34
80.47
82.86
127.93
128.00
128.58
137.93
f1 (ppm)
HO
BnO
O
OH
SAdm
3.30

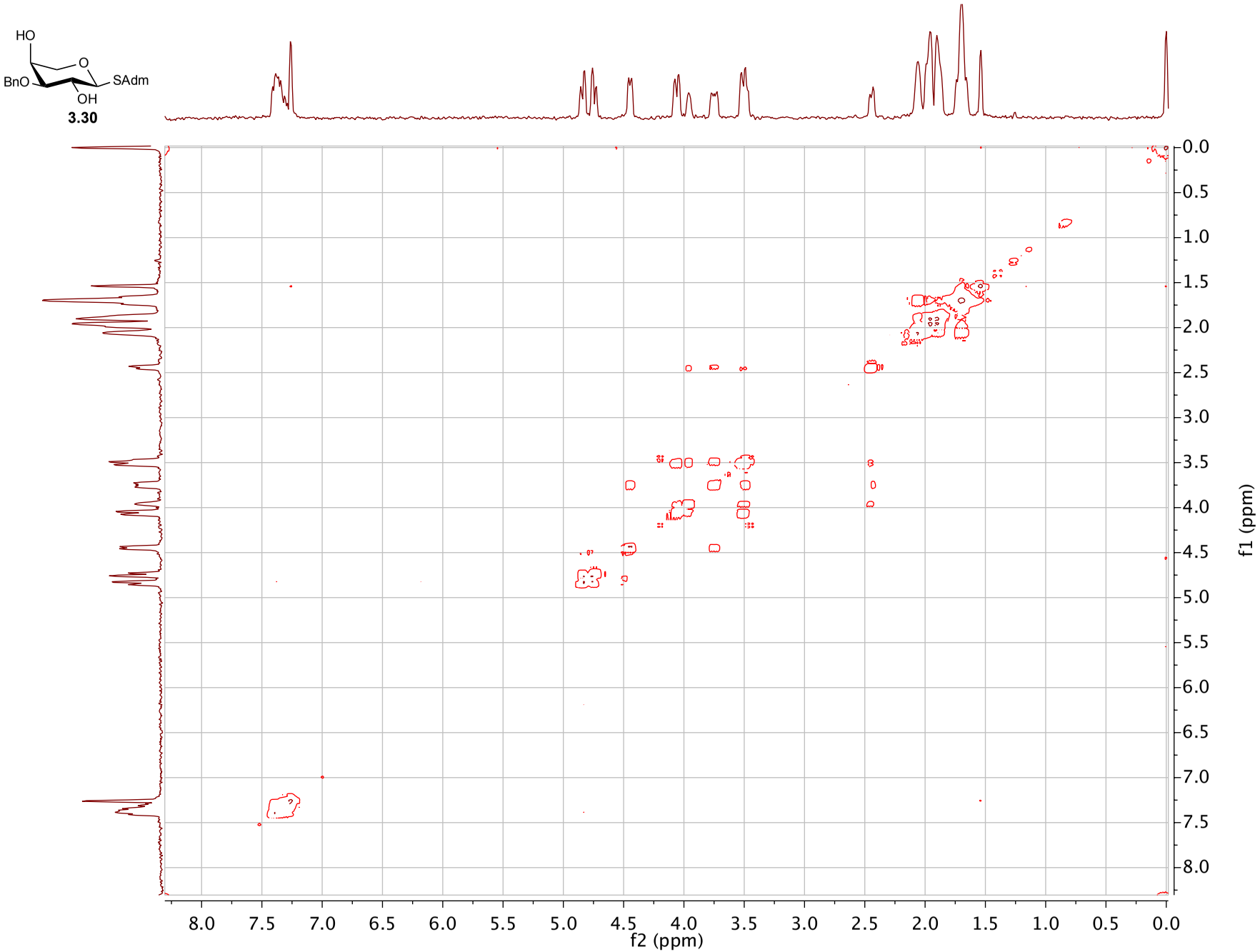
HO
O
BnO
SAdm
OH
3.30
f2 (ppm)
f1 (ppm)

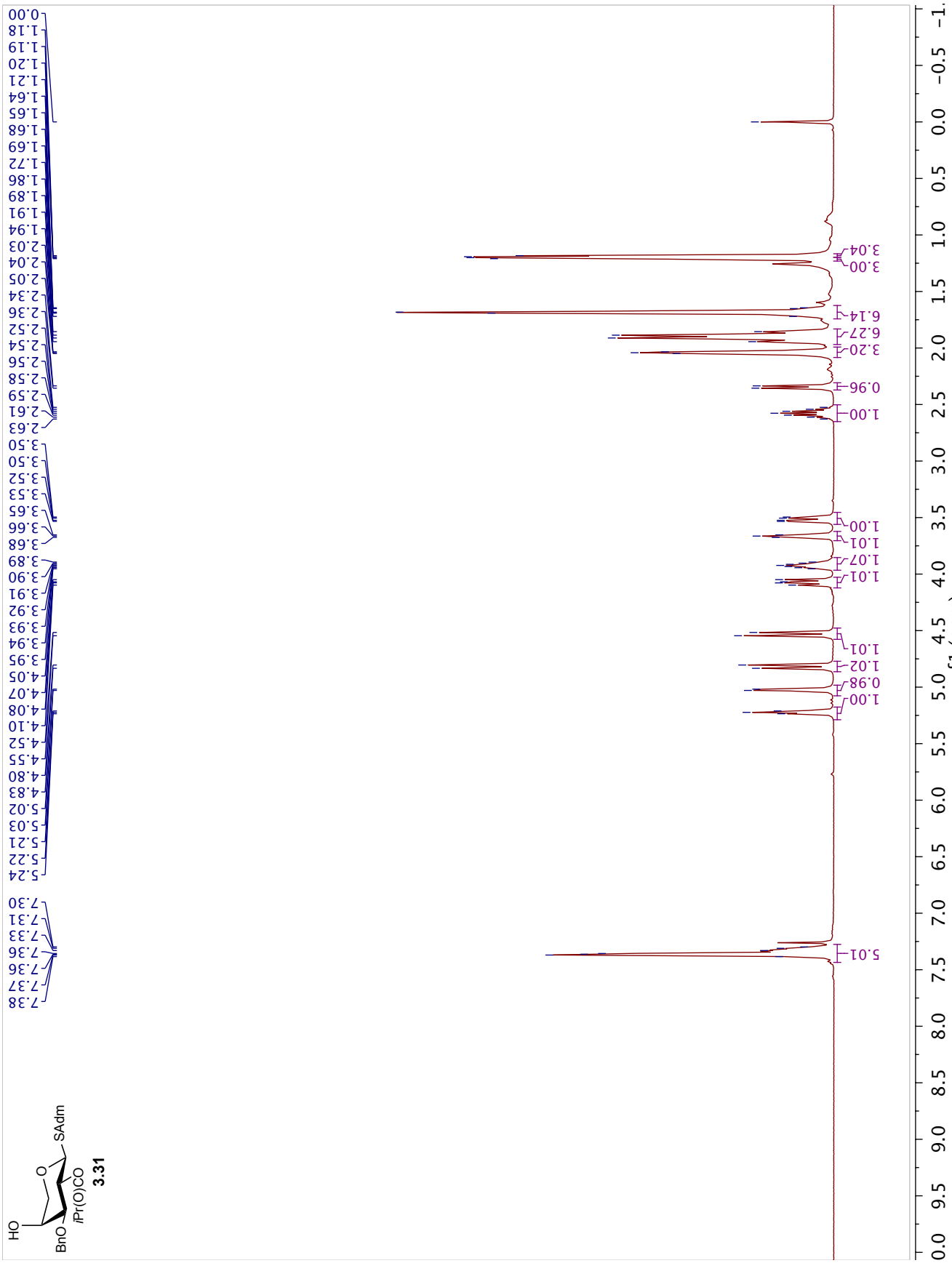
HO
BnO
O
SAdm
iPr(O)CO
3.31
f1 (ppm)

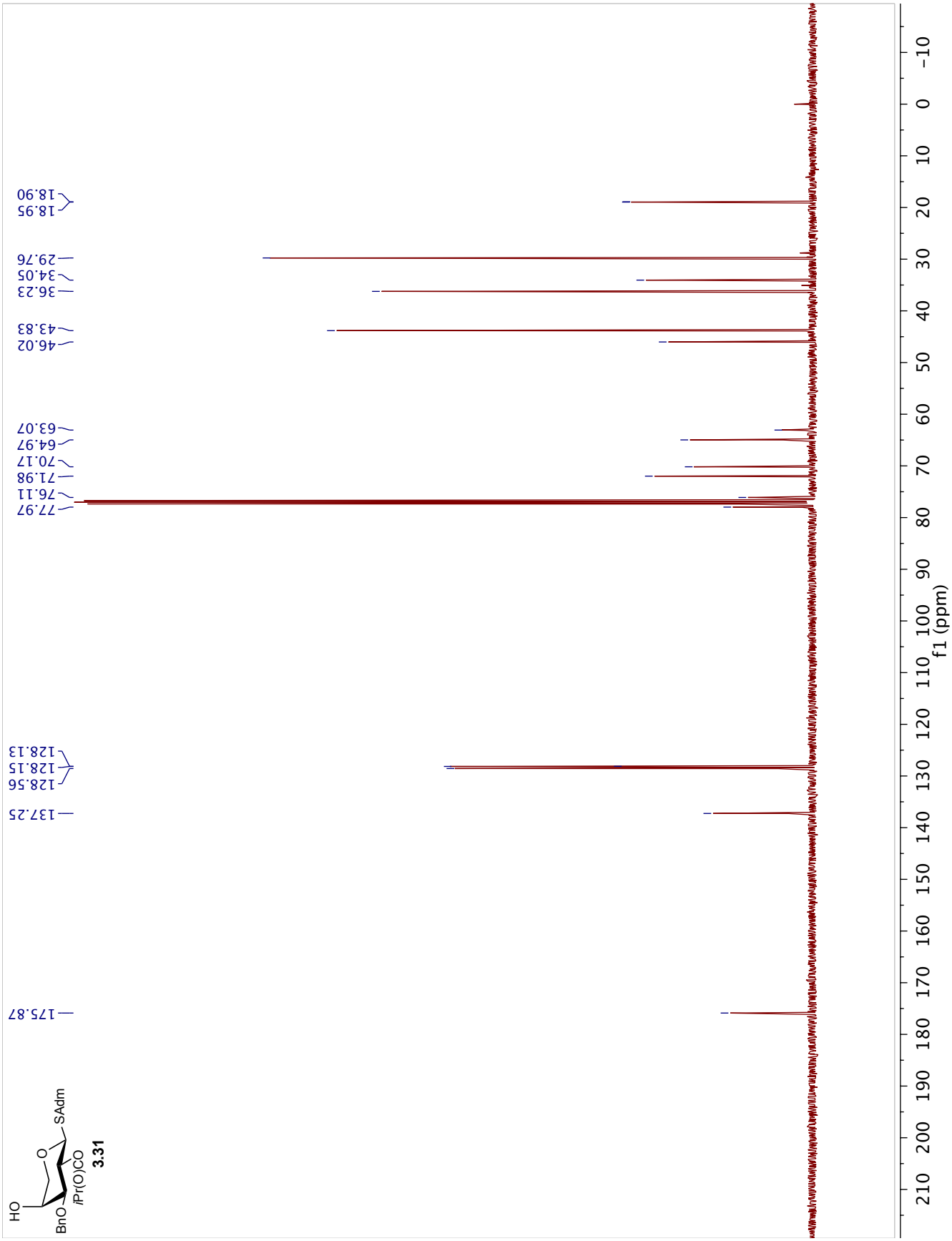
HO
BnO
iPr(O)CO
O
SAdm
3.31
175.87
137.25
128.56
128.15
128.13
77.97
76.11
71.98
70.17
64.97
63.07
46.02
43.83
36.23
34.05
29.76
18.95
18.90
f1 (ppm)

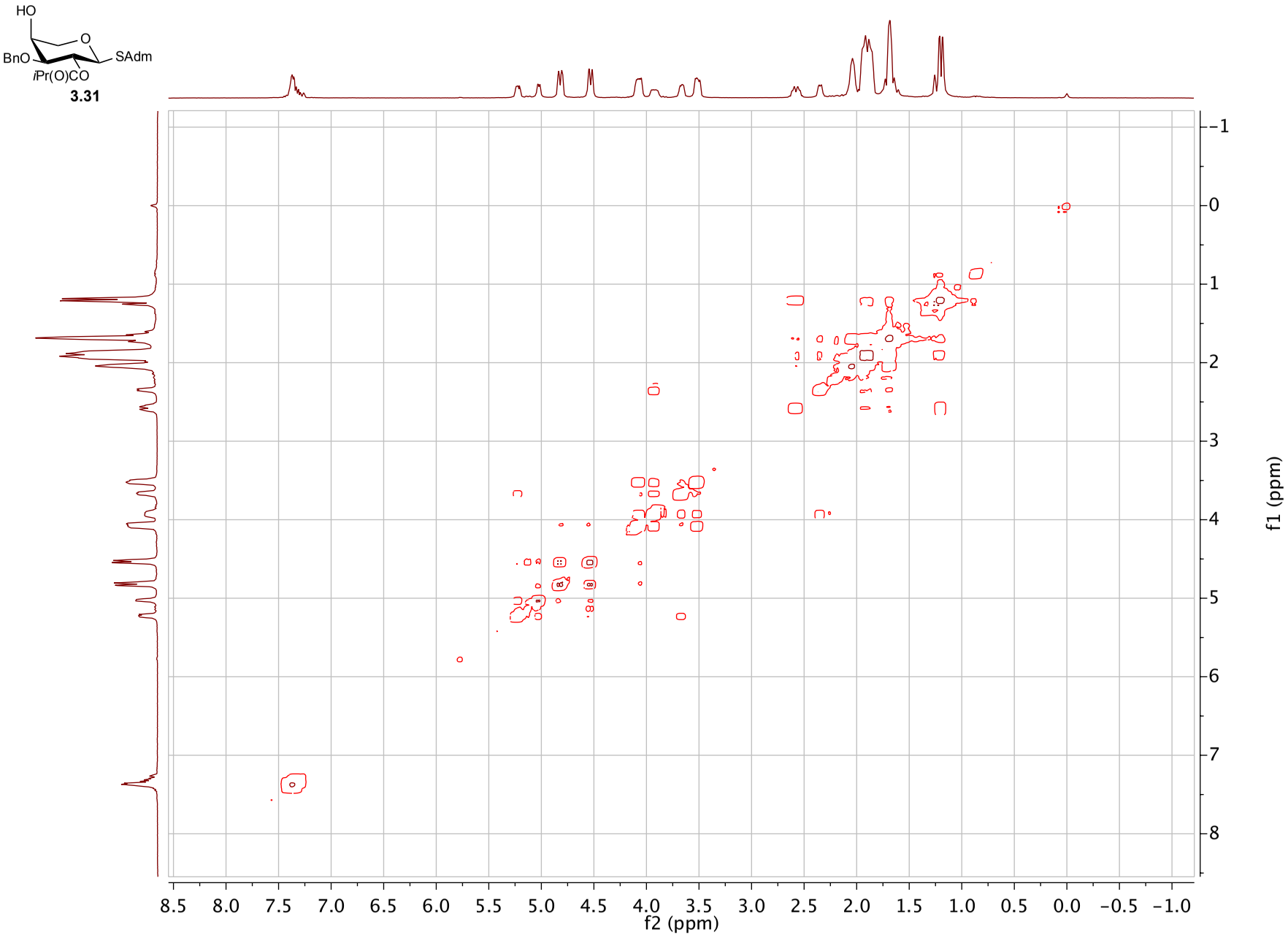
HO
O
BnO
SAdm
iPr(O)CO
3.31
8.5 8.0 7.5 7.0 6.5 6.0 5.5 5.0 4.5 4.0 3.5 3.0 2.5 2.0 1.5 1.0 0.5 0.0 -0.5 -1.0
f2 (ppm)
-1 0 1 2 3 4 5 6 7 8
f1 (ppm)

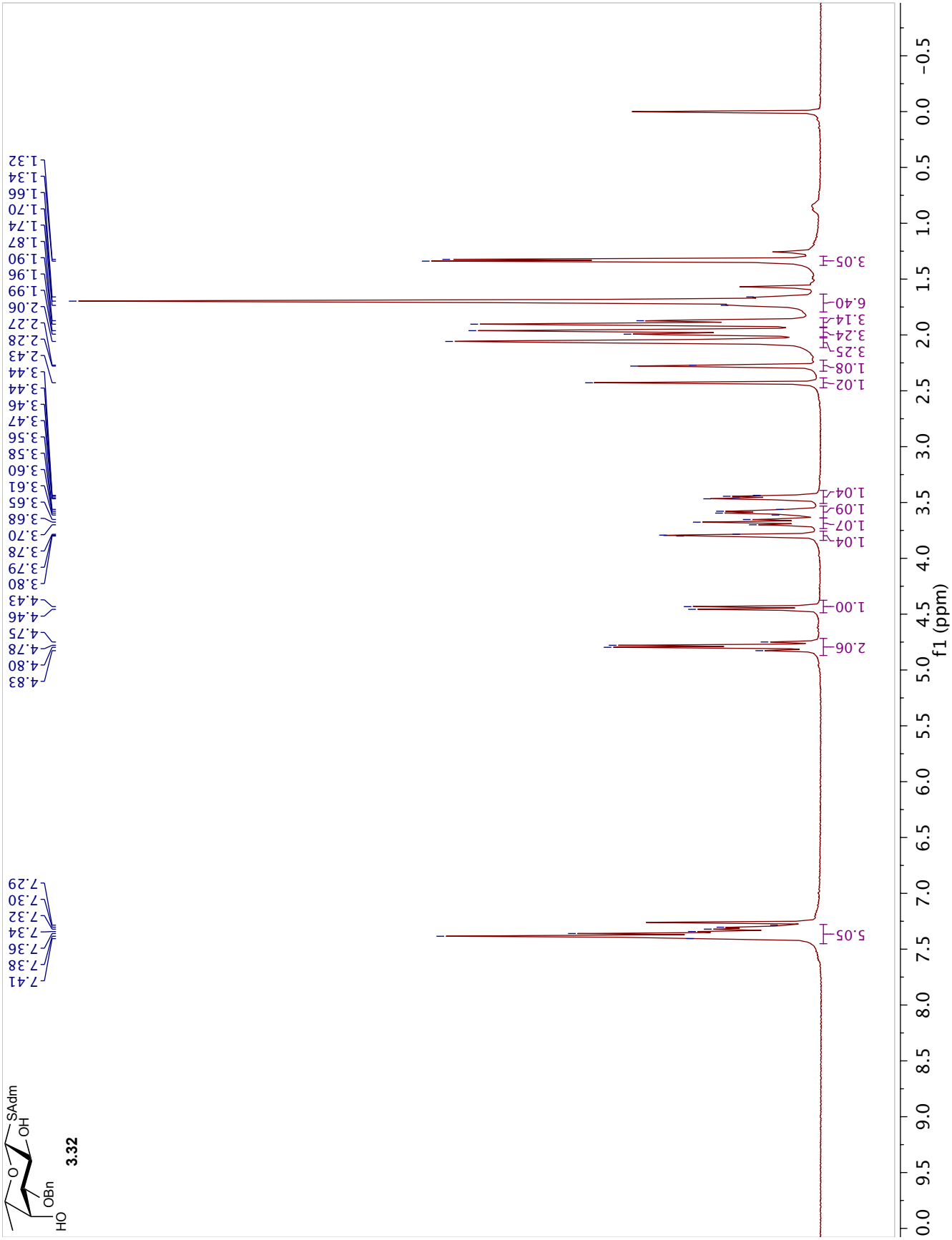
SAdm
OH
O
OBn
HO
3.32
f1 (ppm)

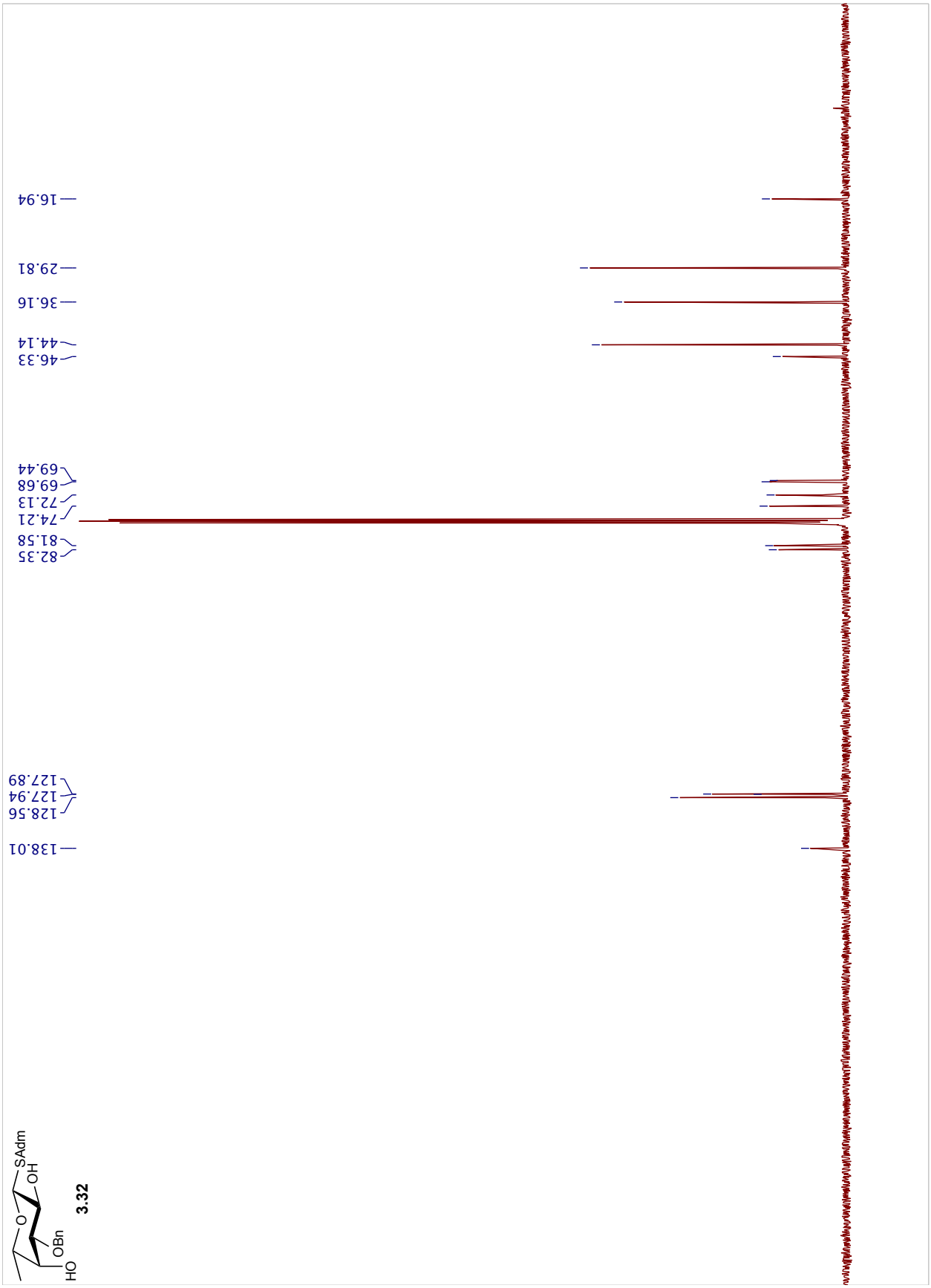
16.94
29.81
36.16
44.14
46.33
69.44
69.68
72.13
74.21
81.58
82.35
127.89
127.94
128.56
138.01
SAdm
OH
O
OBn
HO
3.32
f1 (ppm)

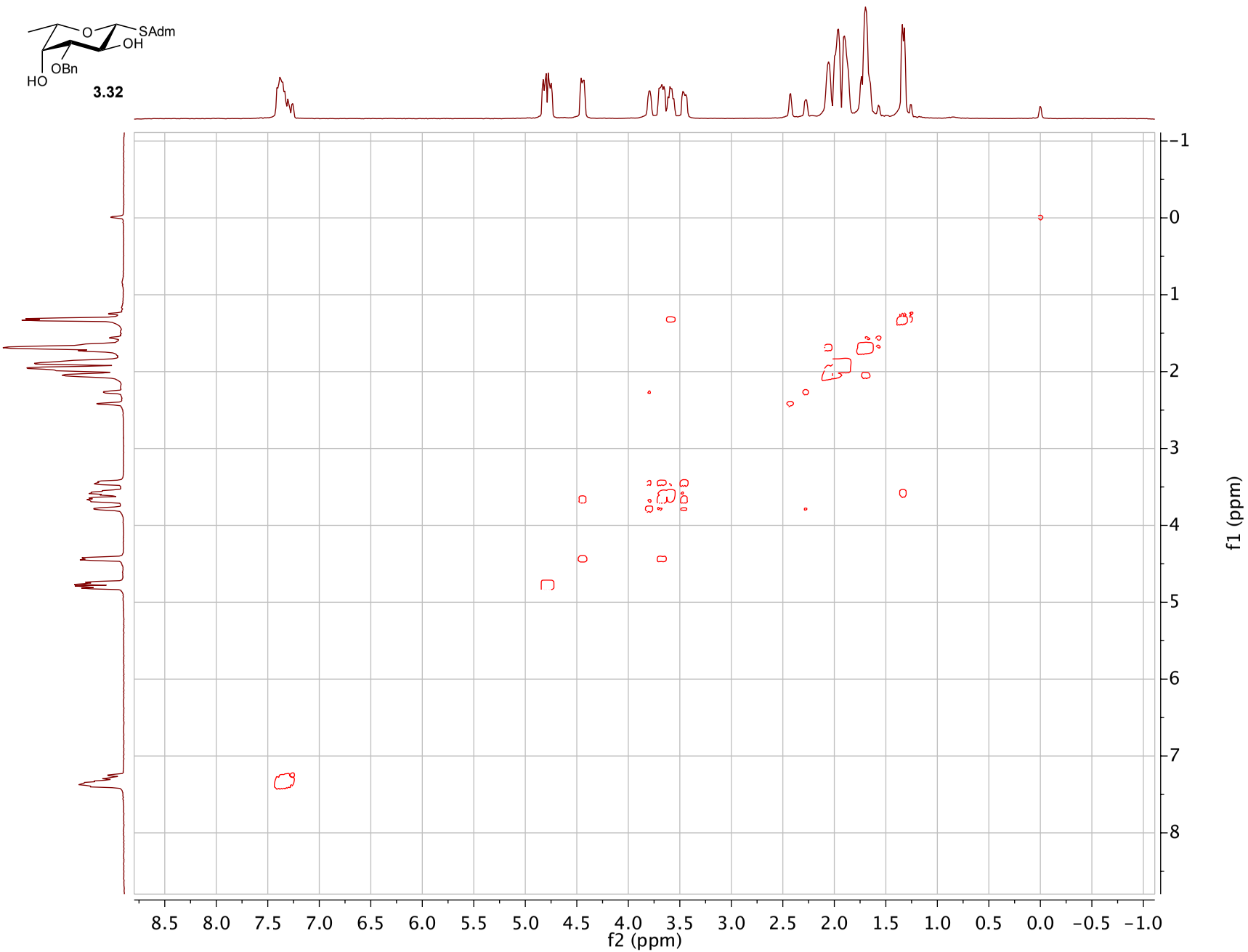
O
SAdm
OH
OBn
HO
3.32
8.5 8.0 7.5 7.0 6.5 6.0 5.5 5.0 4.5 4.0 3.5 3.0 2.5 2.0 1.5 1.0 0.5 0.0 −0.5 −1.0
f2 (ppm)
−1 0 1 2 3 4 5 6 7 8
f1 (ppm)

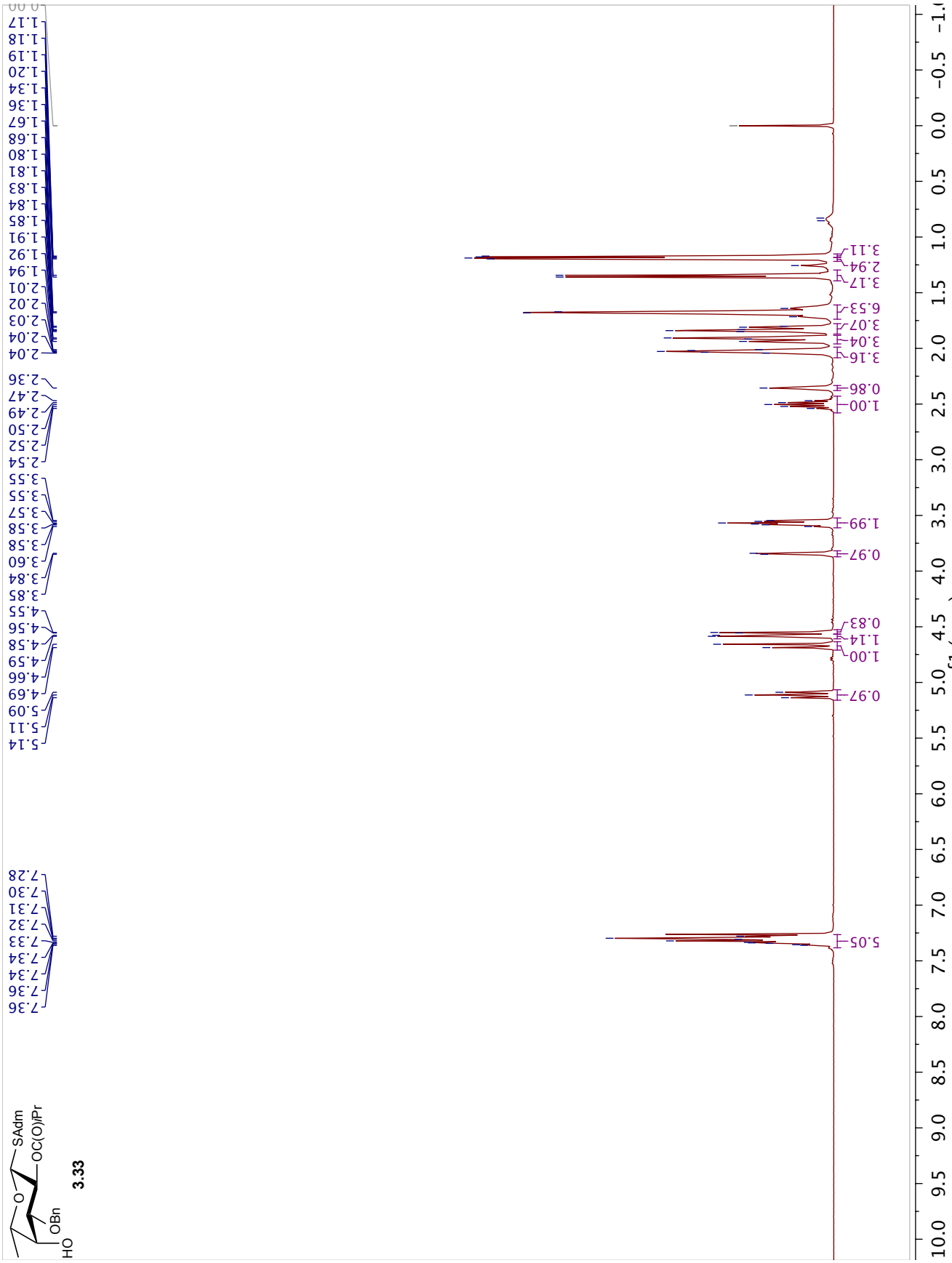
SAdm
OC(O)iPr
O
OBn
HO
3.33
f1 (ppm)

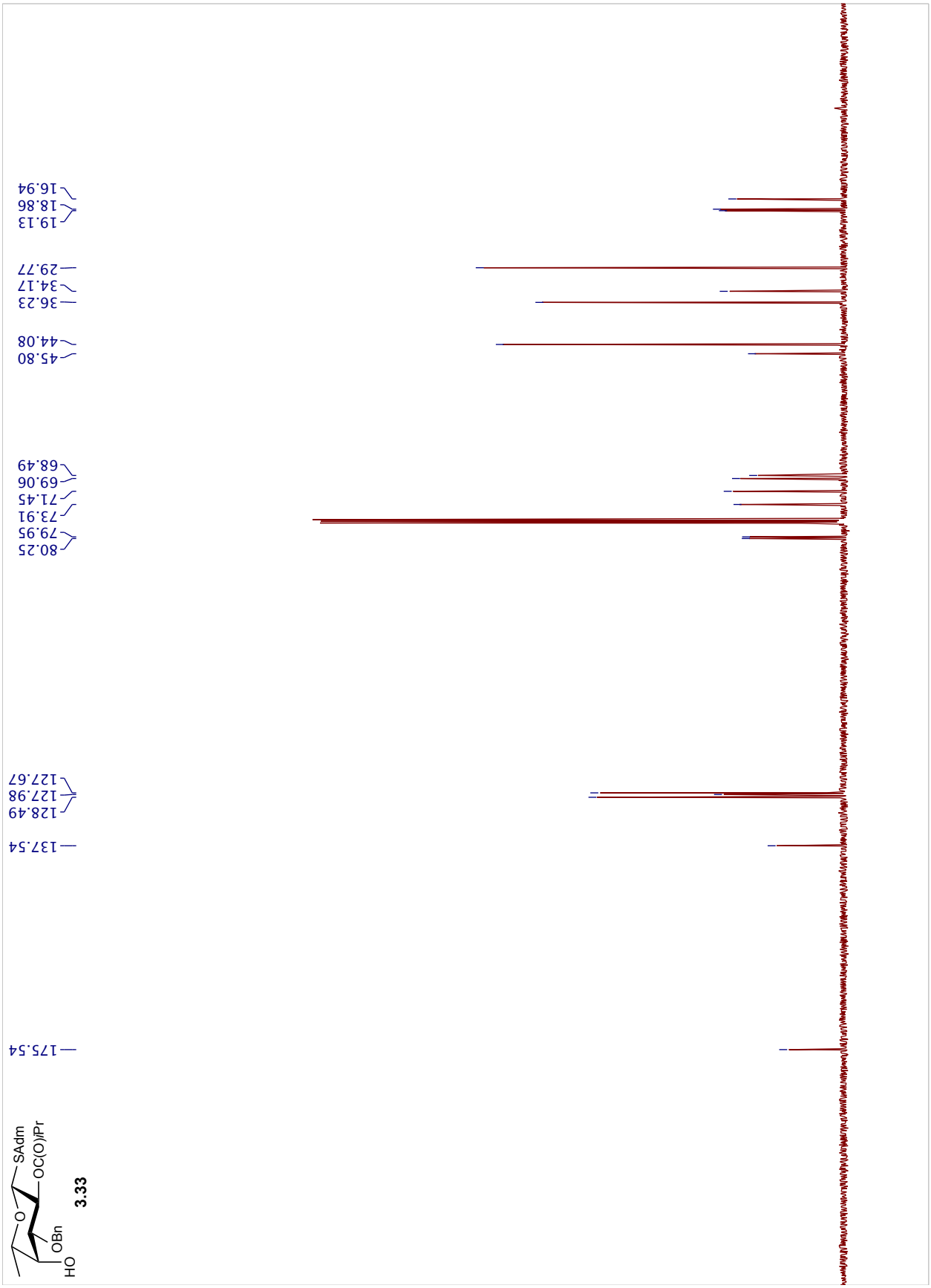
175.54
137.54
128.49
127.98
127.67
80.25
79.95
73.91
71.45
69.06
68.49
45.80
44.08
36.23
34.17
29.77
19.13
18.86
16.94
f1 (ppm)
SAdm
OC(O)iPr
OBn
HO
O
3.33

SAdm
OC(O)iPr
O
OBn
HO
3.33
f1 (ppm)
f2 (ppm)

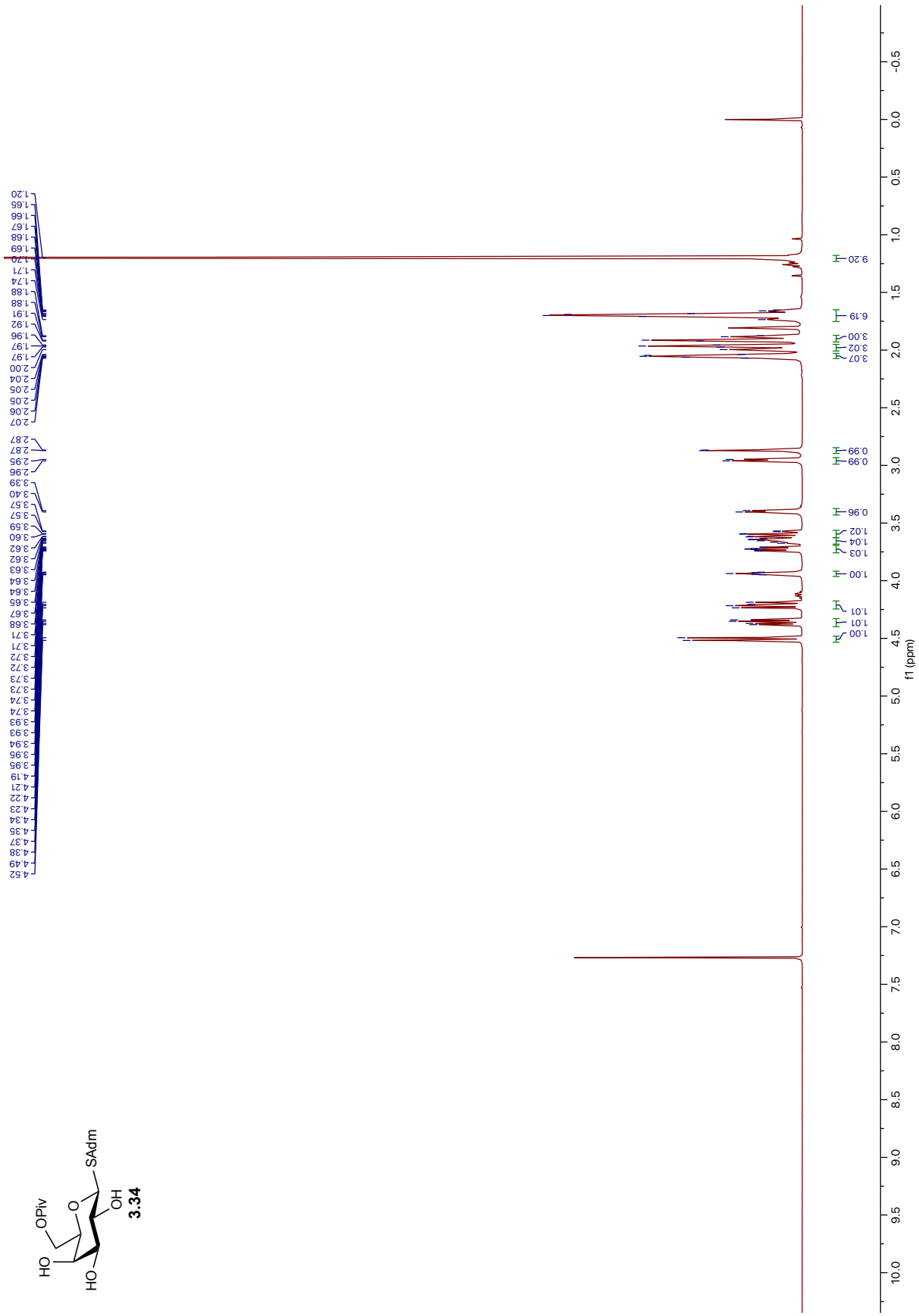
HO
OPiv
O
SAdm
OH
HO
3.34
f1 (ppm)

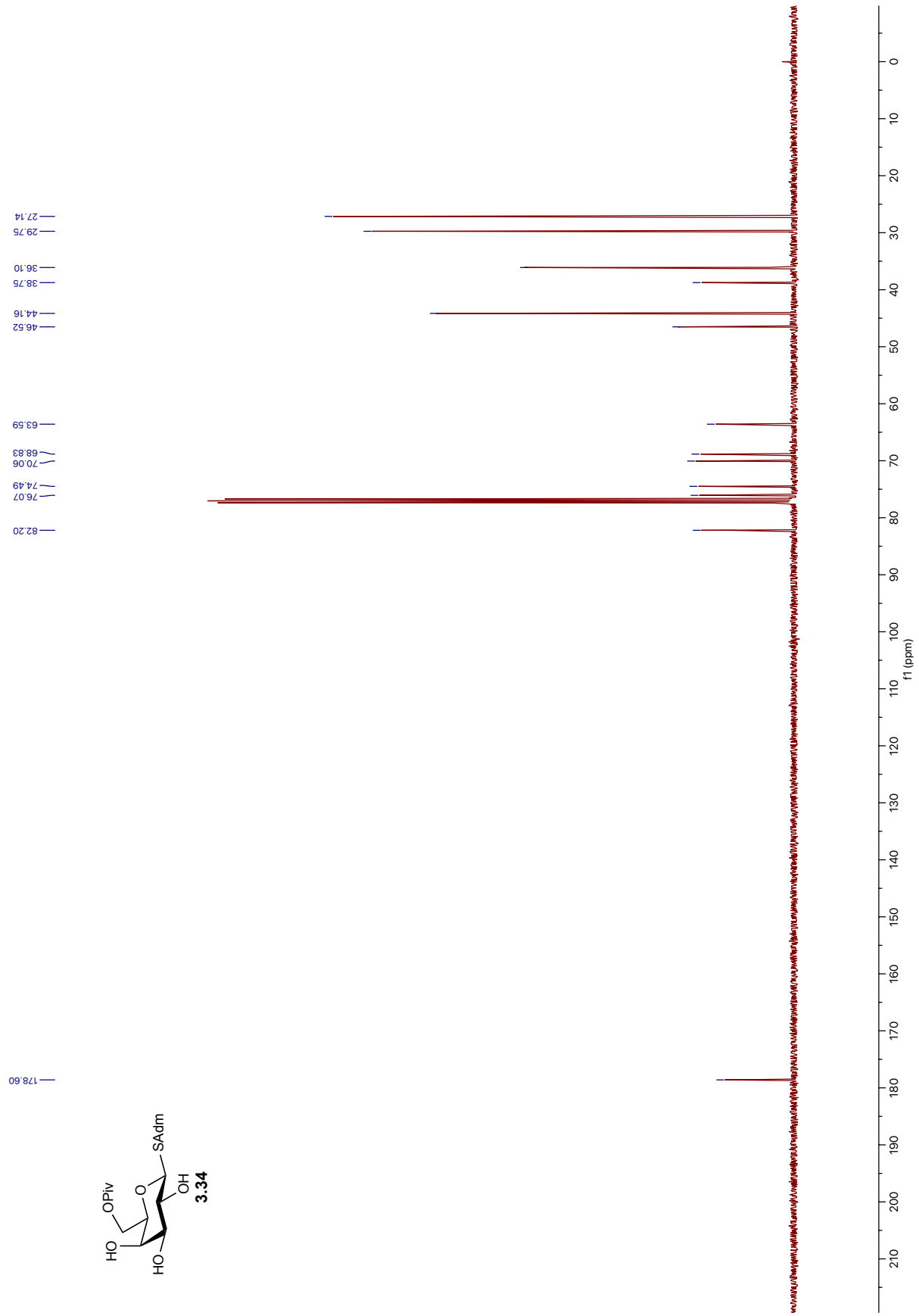
27.14
29.75
36.10
38.75
44.16
46.52
63.59
68.83
70.06
74.49
76.07
82.20
178.60
f1 (ppm)
HO
OPiv
O
SAdm
OH
HO
3.34

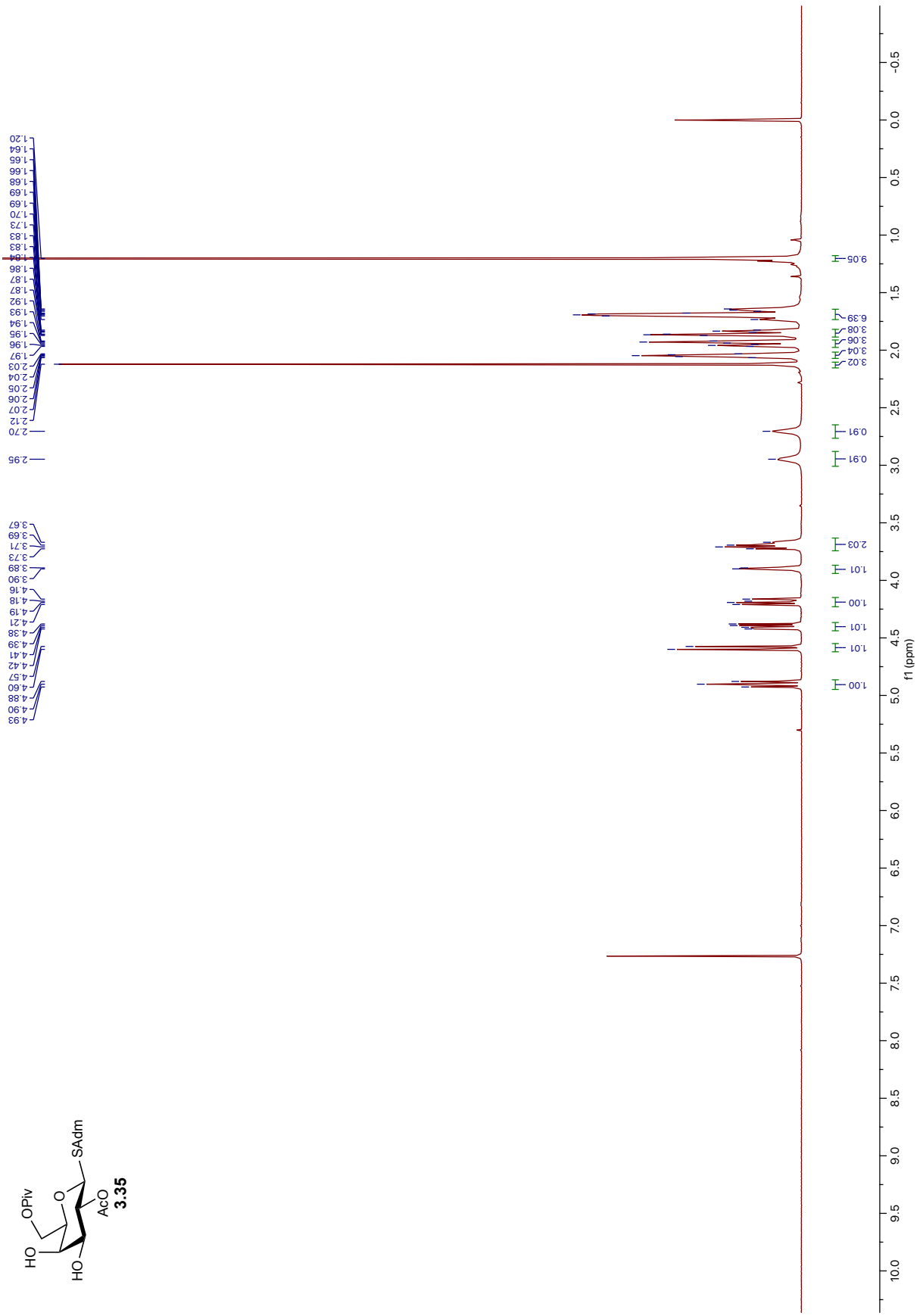
HO
OPiv
O
SAdm
AcO
HO
3.35
f1 (ppm)

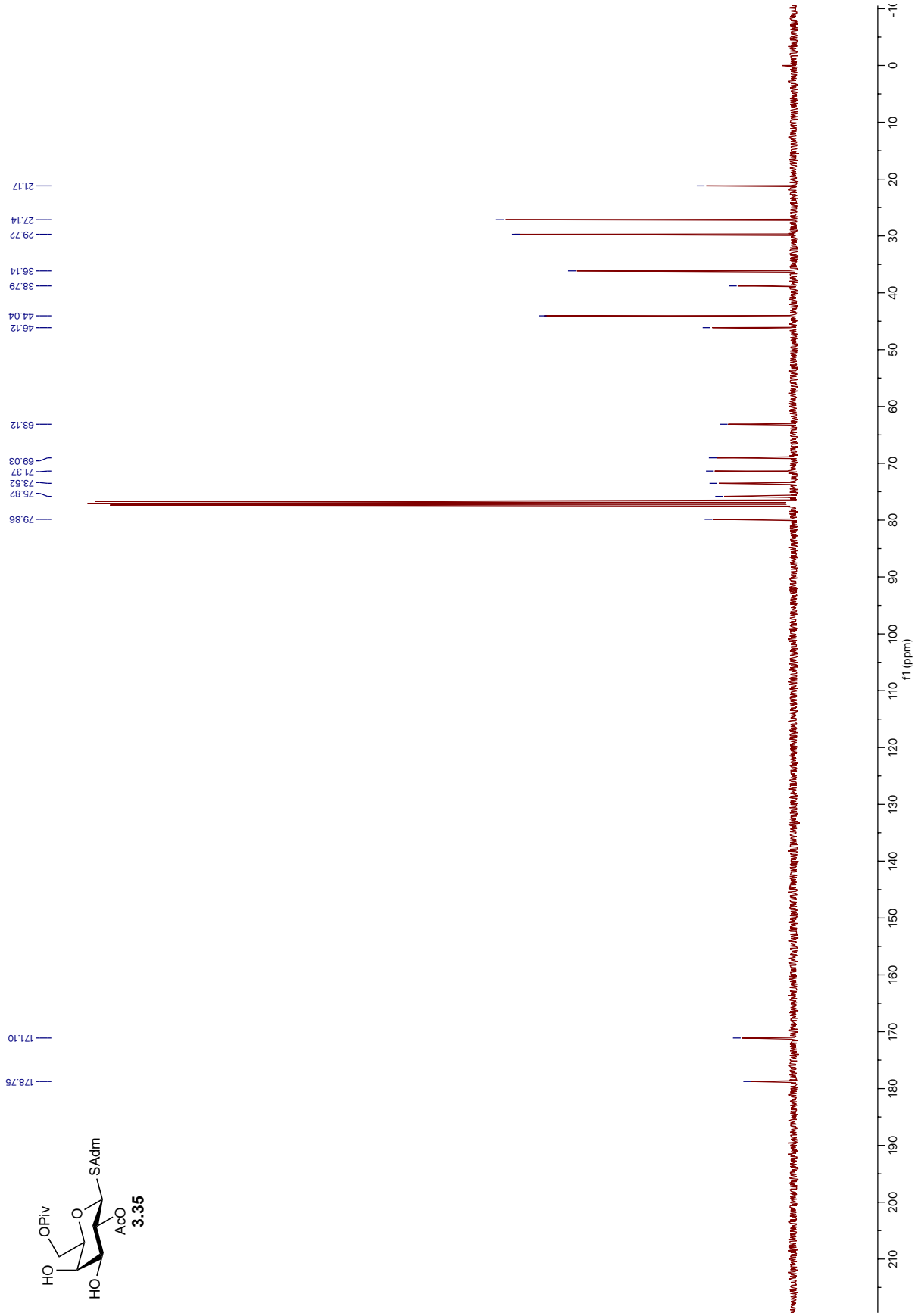
21.17
27.14
29.72
36.14
38.79
44.04
46.12
63.12
69.03
71.37
73.52
75.82
79.86
171.10
178.75
f1 (ppm)
HO
OPiv
O
SAdm
AcO
HO
3.35

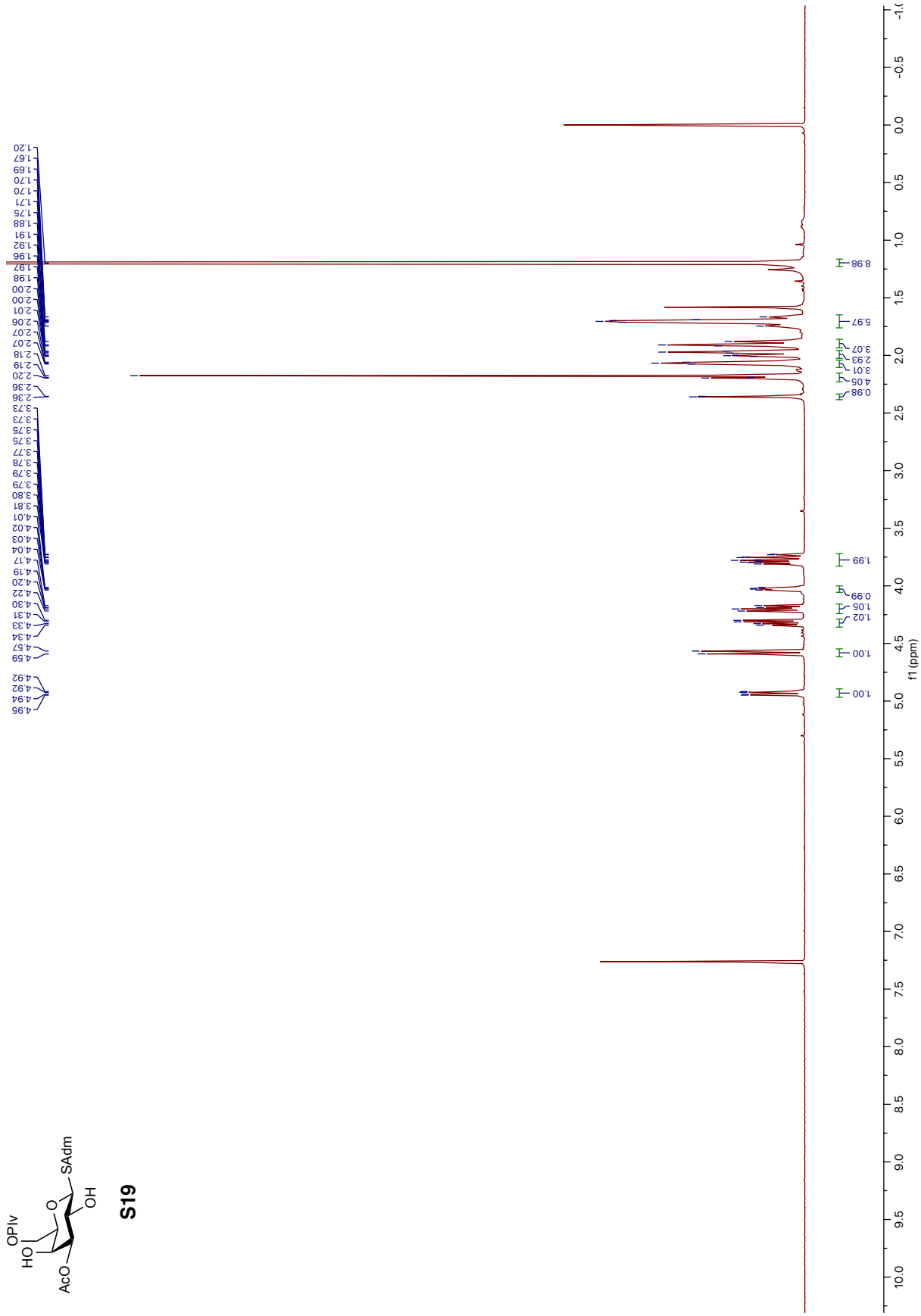

S19

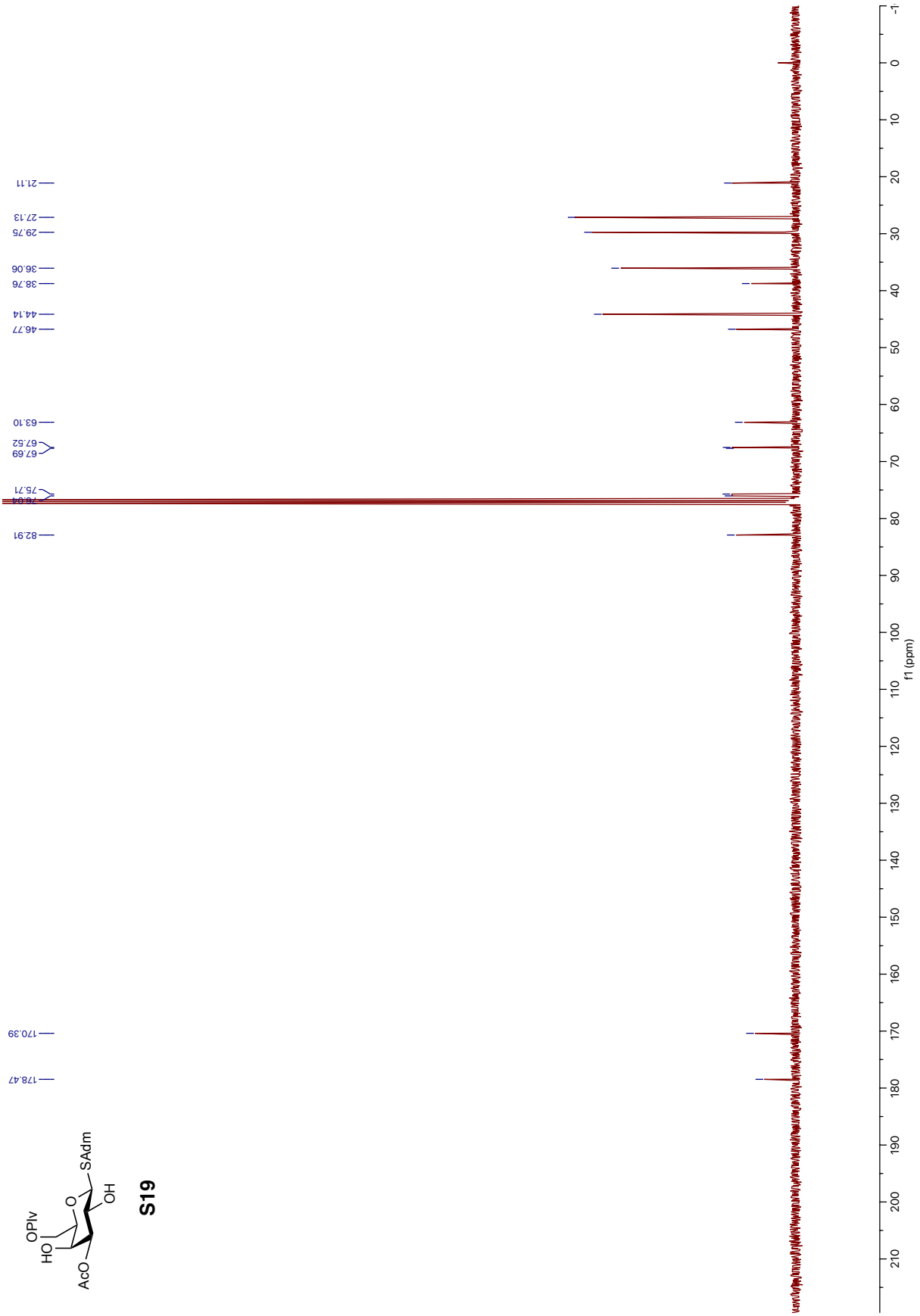
21.11
27.13
29.75
36.06
38.76
44.14
46.77
63.10
67.69
67.52
75.71
76.01
82.91
170.39
178.47
f1 (ppm)
OPiv
HO
AcO
O
SAdm
OH

S19

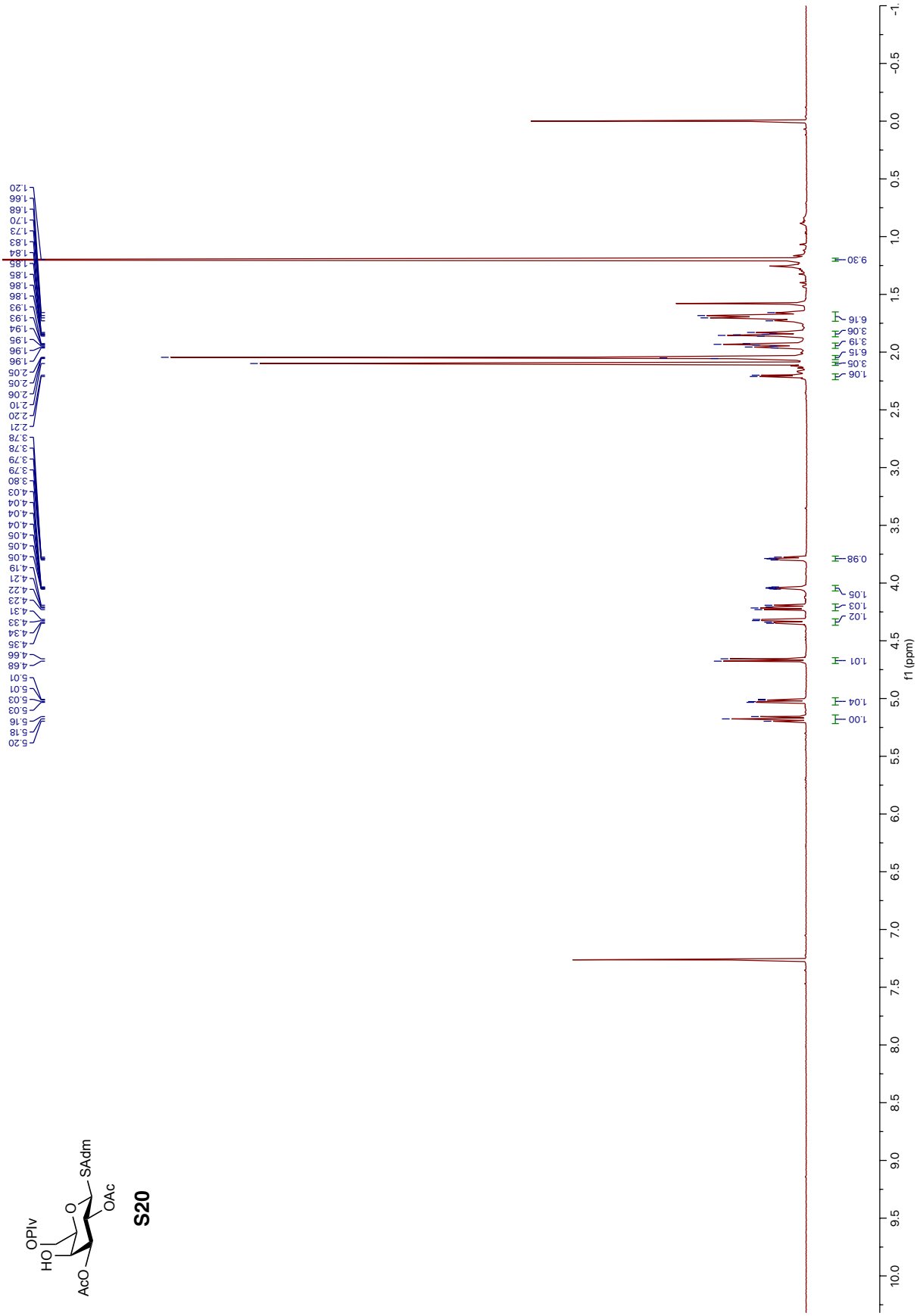

S20

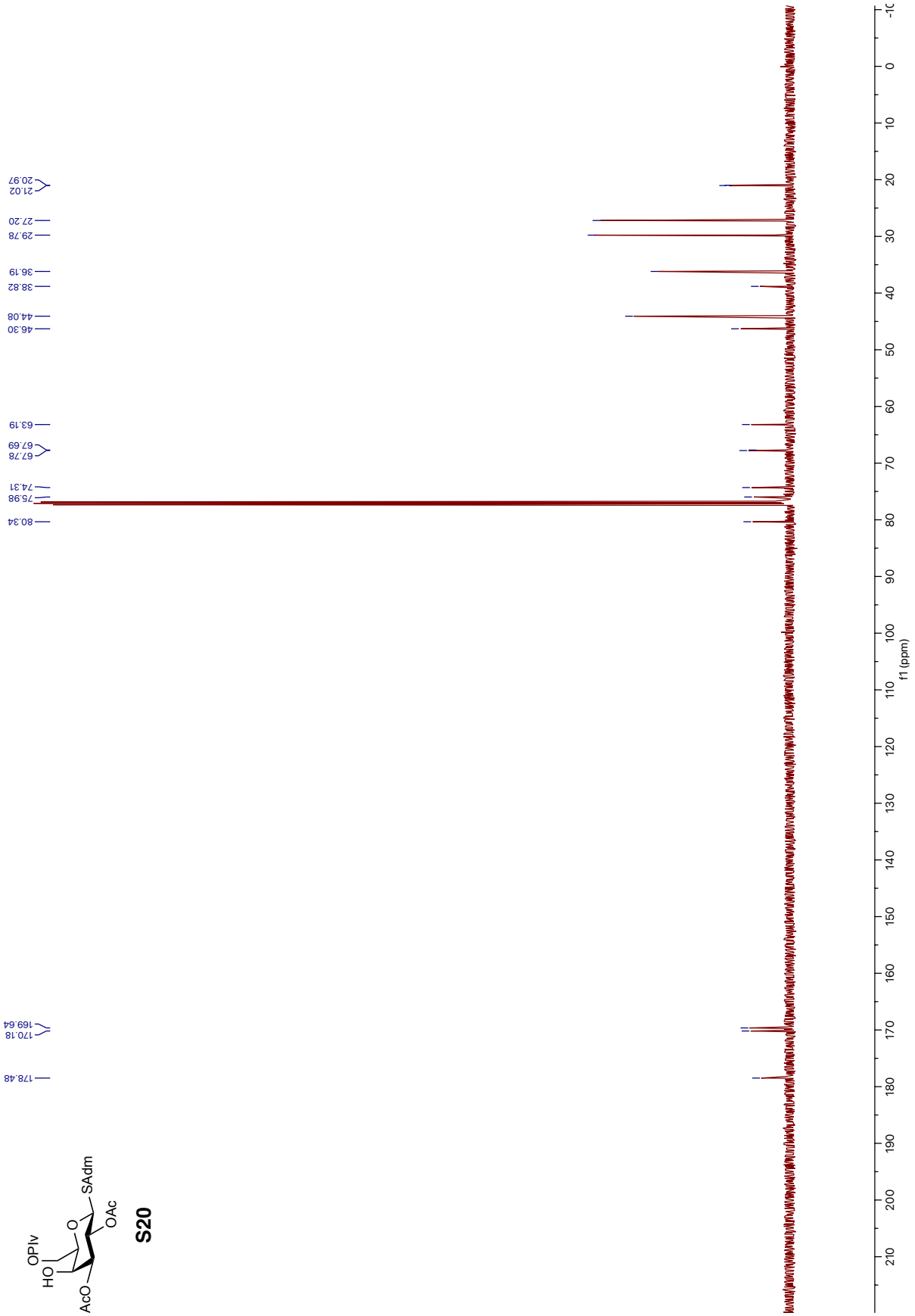
20.97
21.02
27.20
29.78
36.19
38.82
44.08
46.30
63.19
67.69
67.78
74.31
75.98
80.34
169.64
170.18
178.48
f1 (ppm)
OPIv
HO
AcO
O
SAdm
OAc

S20

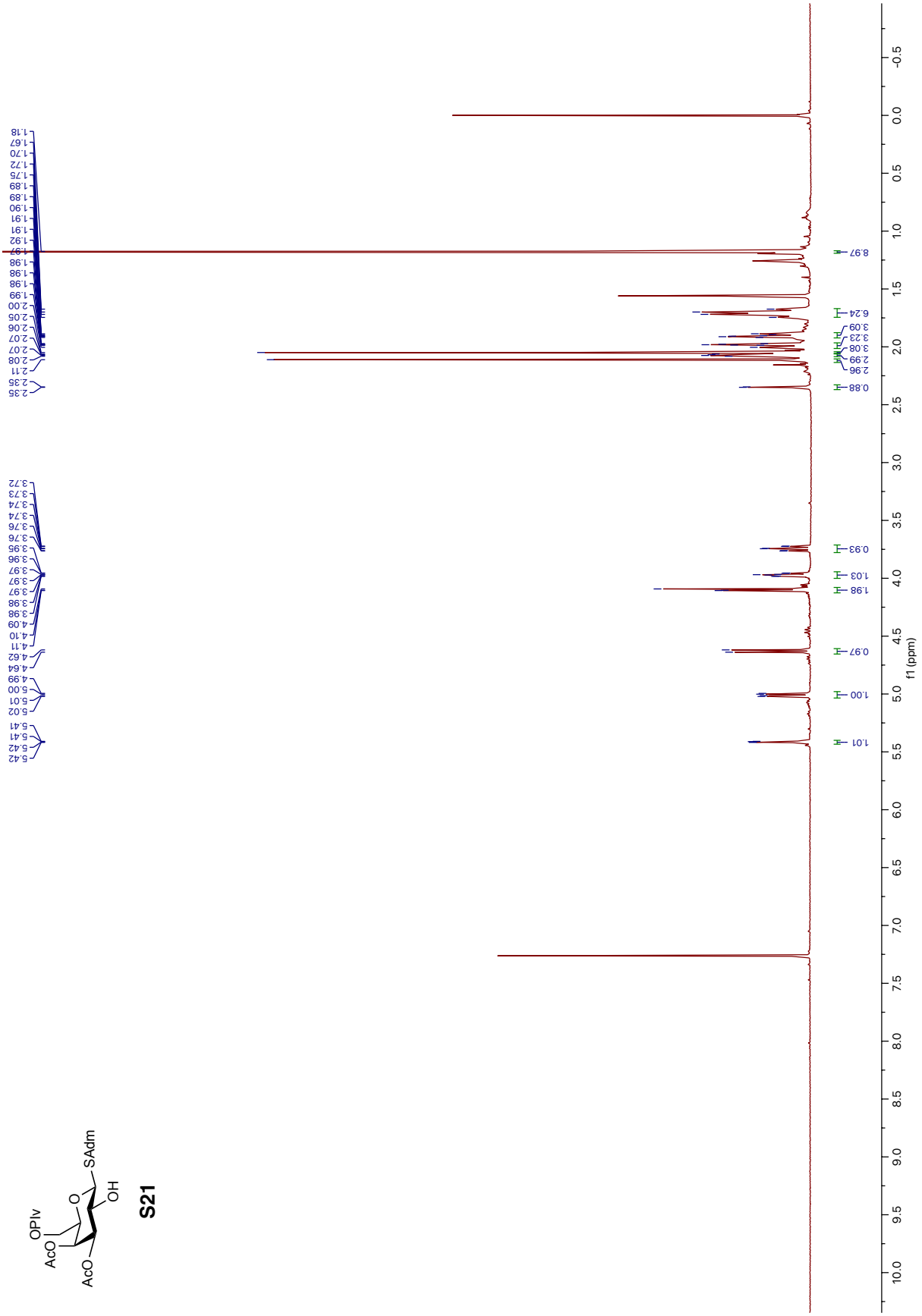

S21

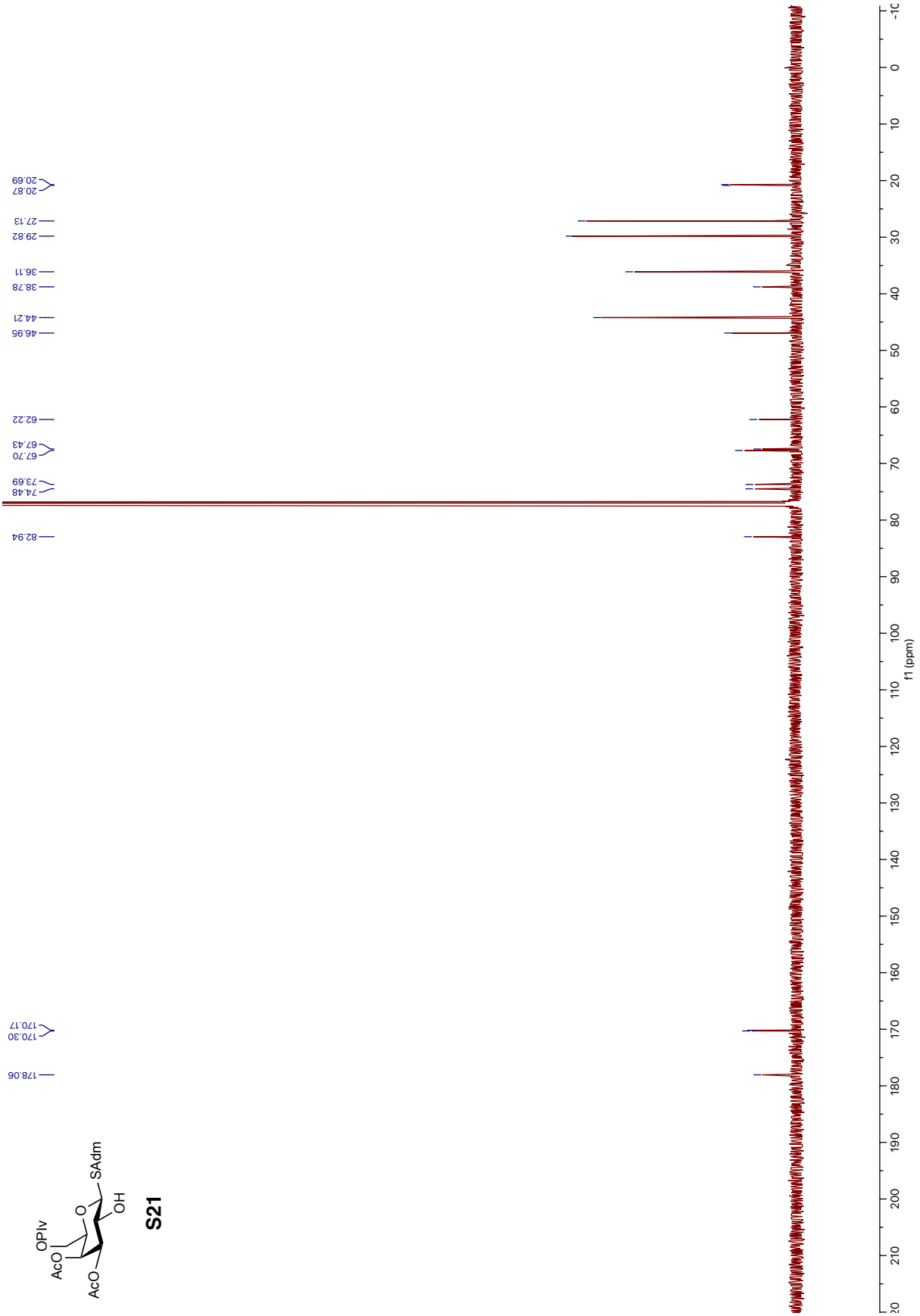
178.06
170.30
170.17
82.94
74.48
73.69
67.70
67.43
62.22
46.95
44.21
38.78
36.11
29.82
27.13
20.87
20.69
f1 (ppm)
OPiv
AcO
AcO
O
SAdm
OH

S21

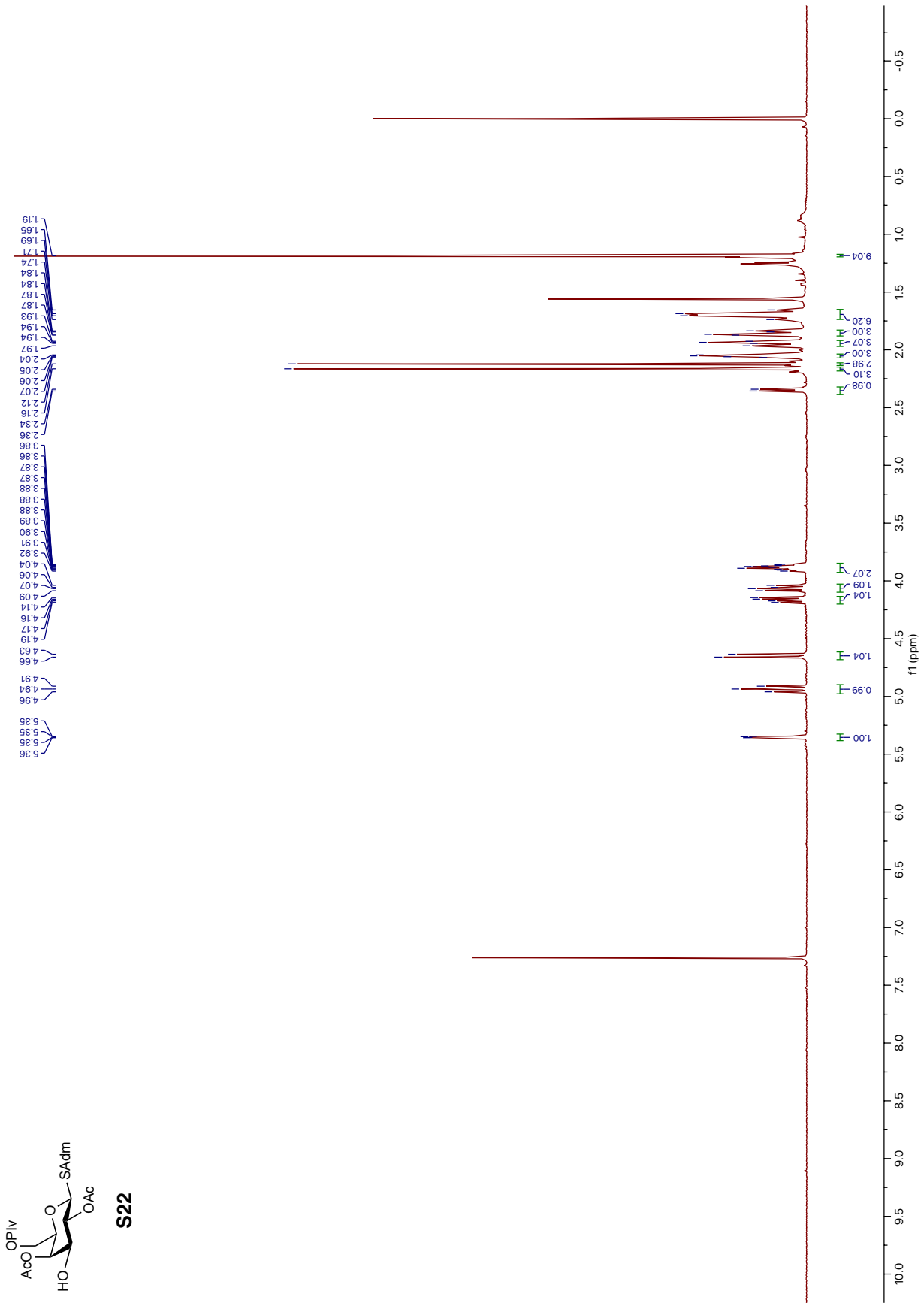

S22

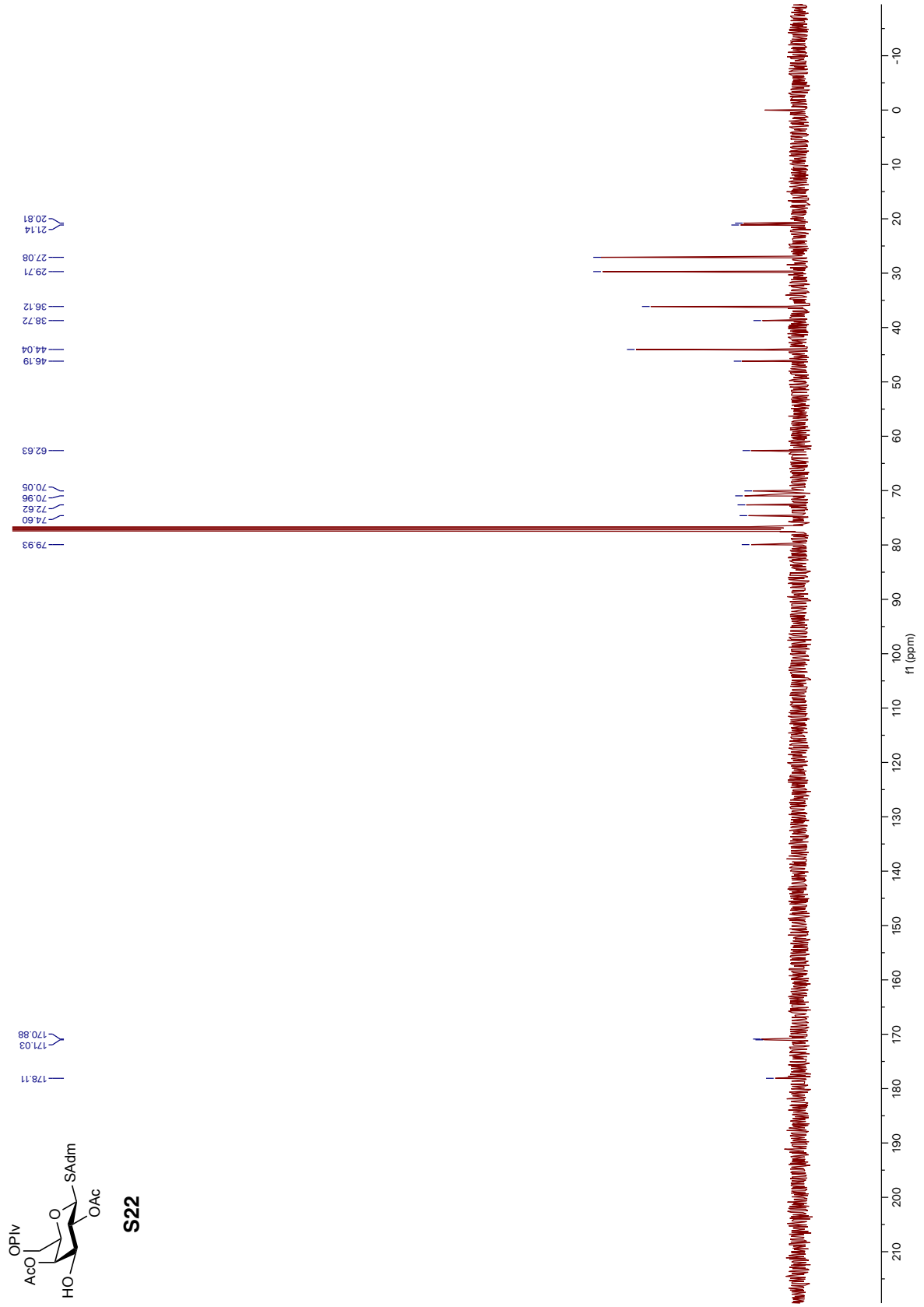
20.81
21.14
27.08
29.71
36.12
38.72
44.04
46.19
62.63
70.05
70.96
72.62
74.60
79.93
170.88
171.03
178.11
f1 (ppm)
OPiv
AcO
HO
O
OAc
SAdm
S22

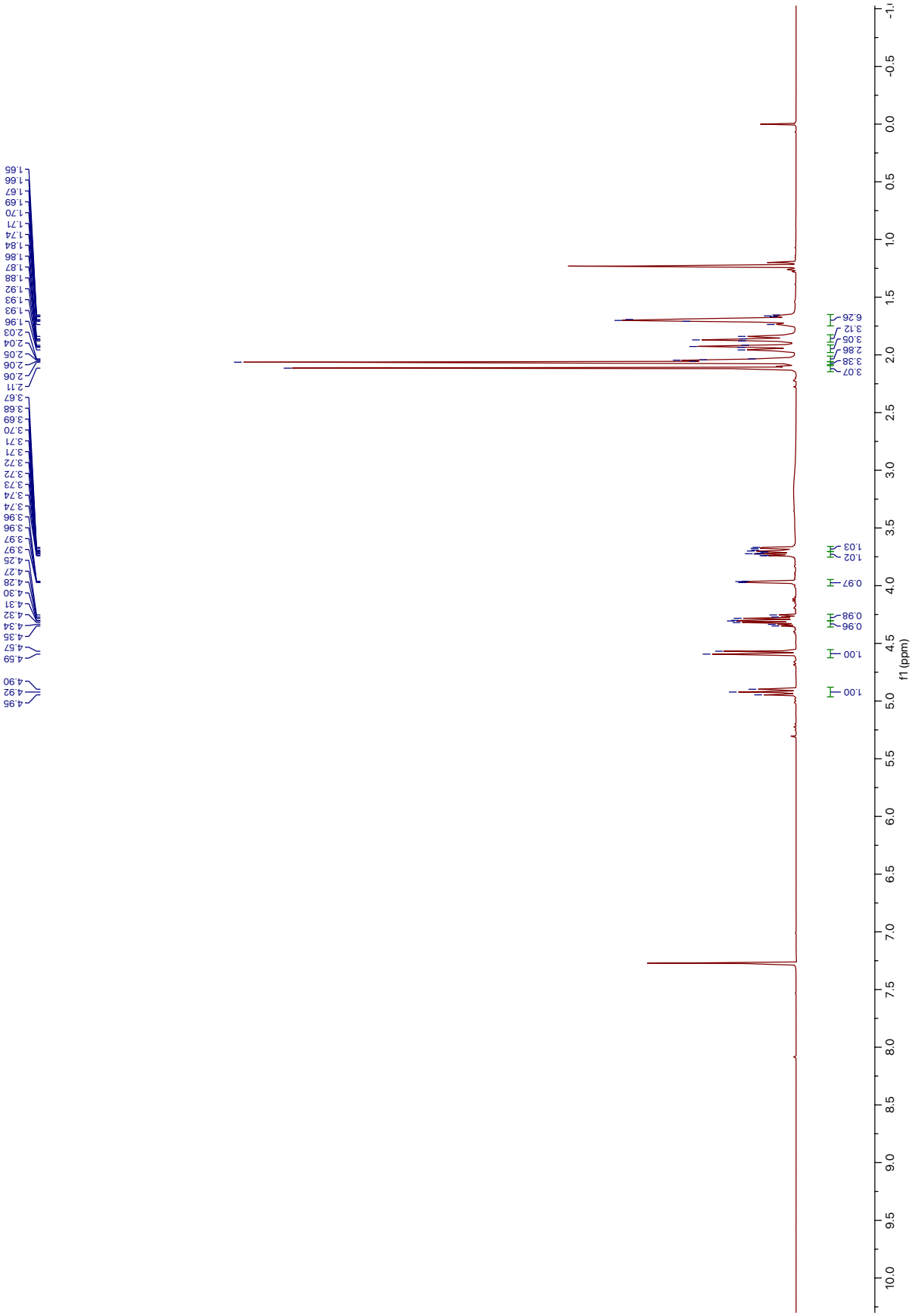
f1 (ppm)

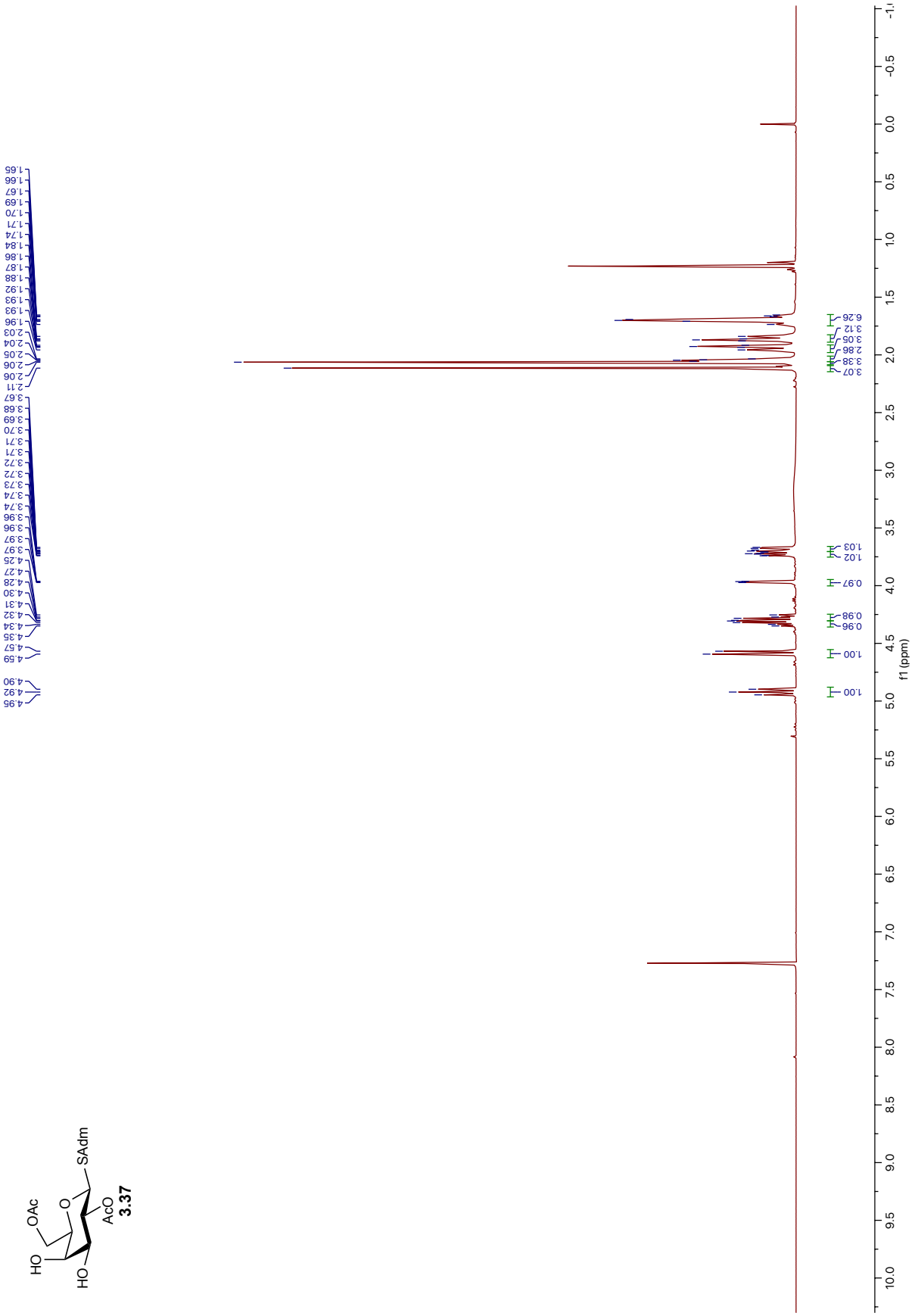
HO
OAc
O
SAdm
AcO
HO
3.37
f1 (ppm)

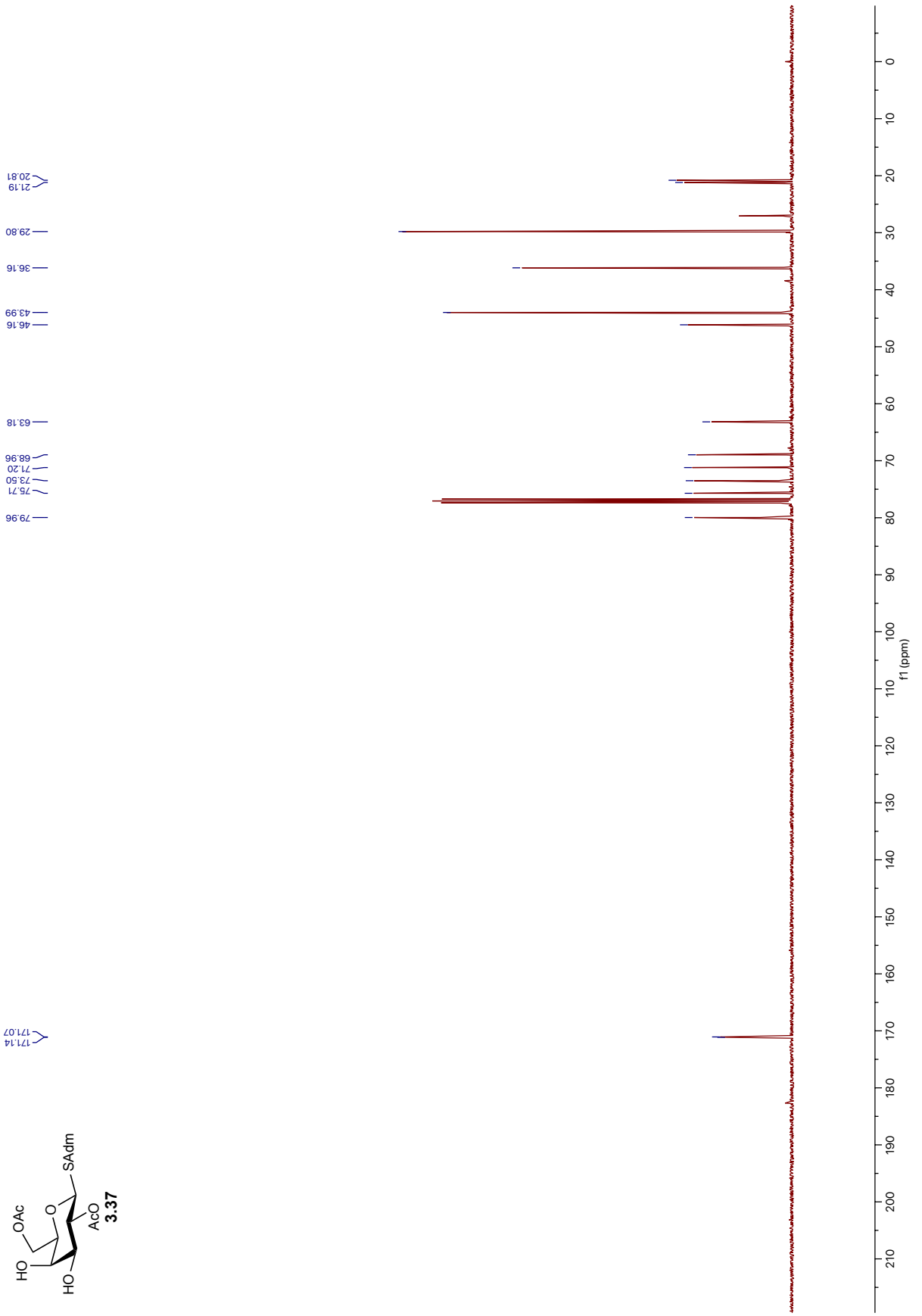
171.14
171.07
79.96
76.71
73.50
71.20
68.96
63.18
46.16
43.99
36.16
29.80
21.19
20.81
f1 (ppm)
HO
OAc
O
SAdm
AcO
HO
3.37

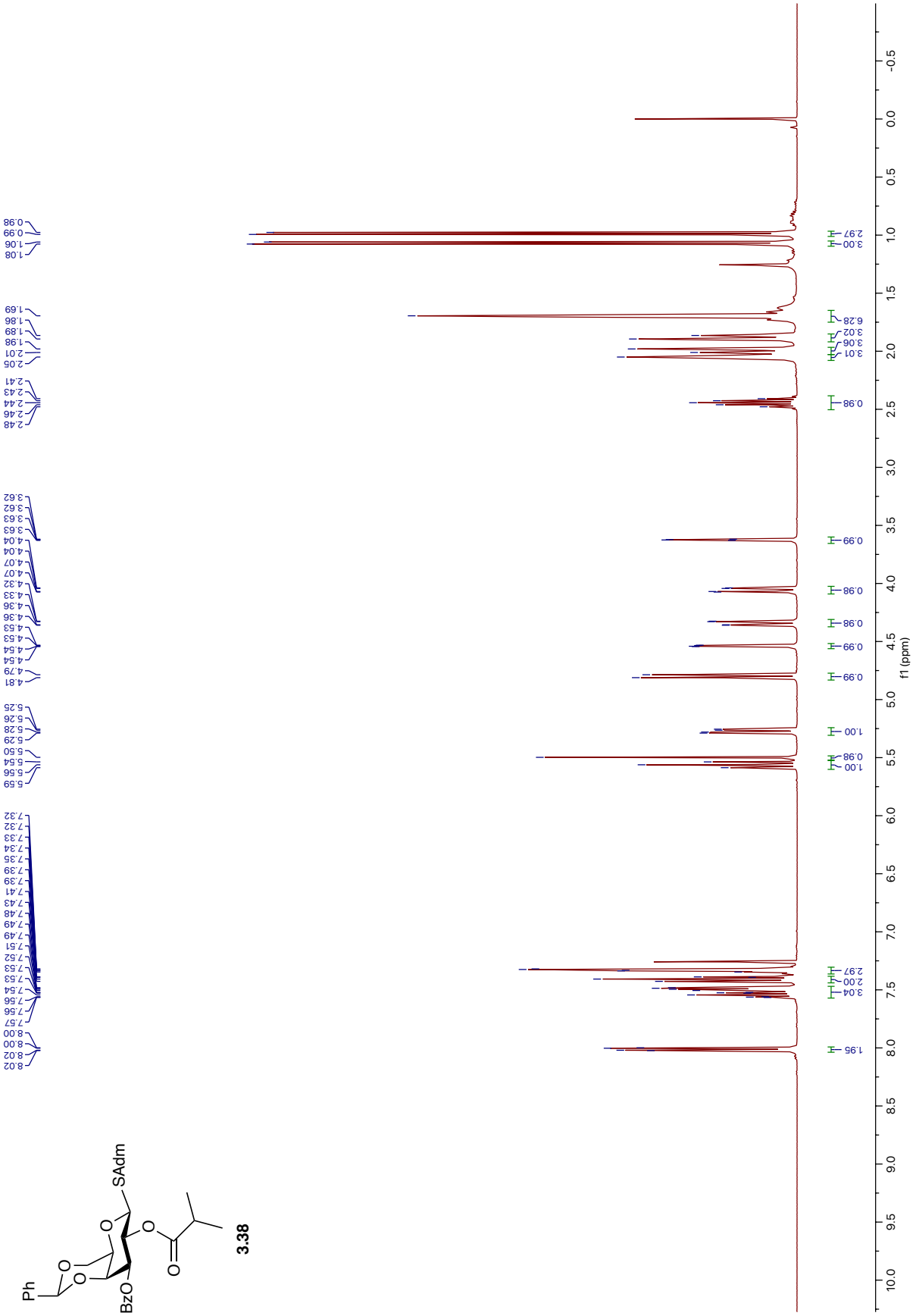
SAdm
BzO
Ph
O
O
O
O
O
O
3.38
f1 (ppm)

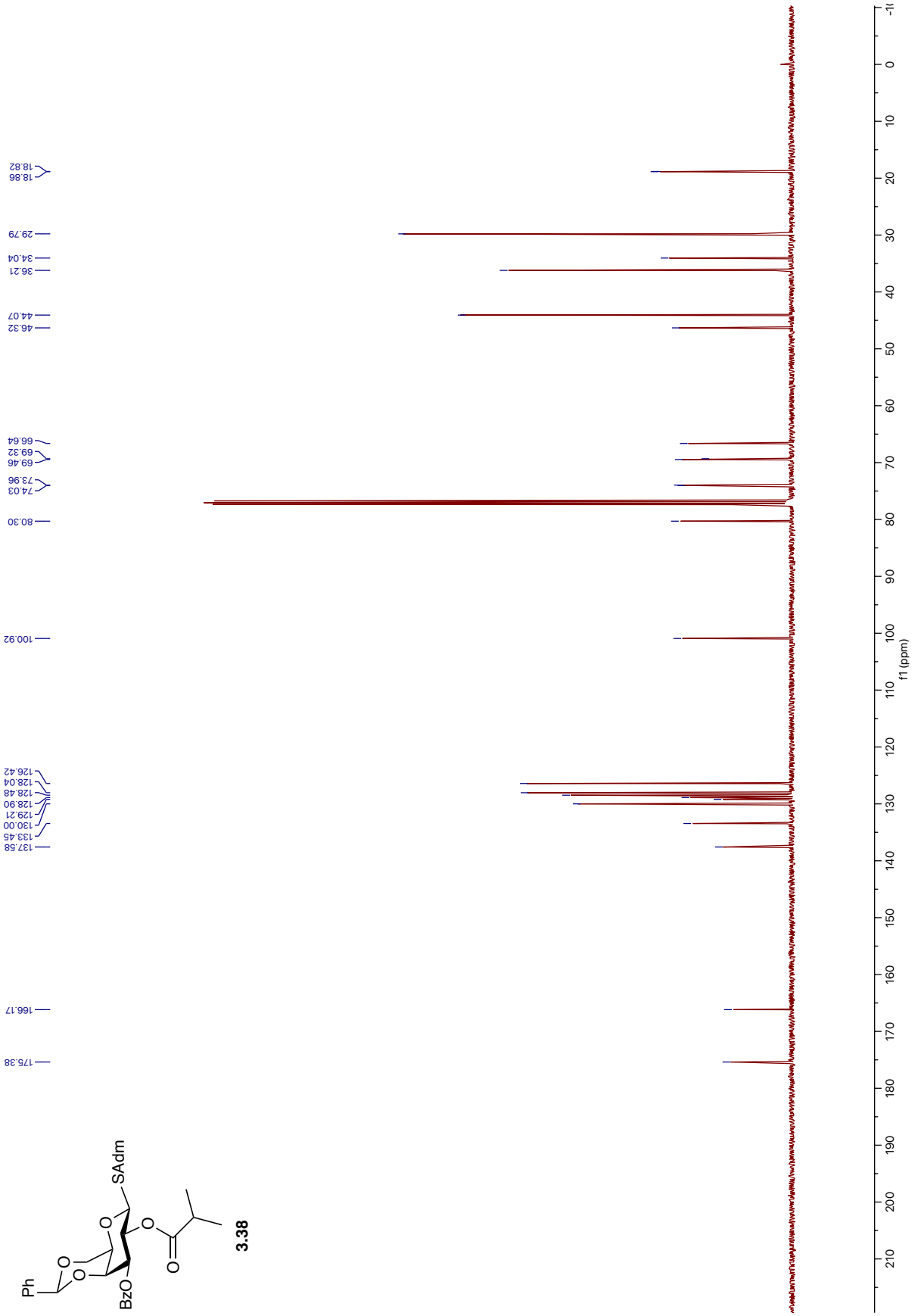
18.82
18.86
29.79
34.04
36.21
44.07
46.32
66.64
69.32
69.46
73.96
74.03
80.30
100.92
126.42
128.04
128.48
128.90
129.21
130.00
133.45
137.58
166.17
175.38
Ph
BzO
SAdm
O
O
O
O
O
3.38
f1 (ppm)

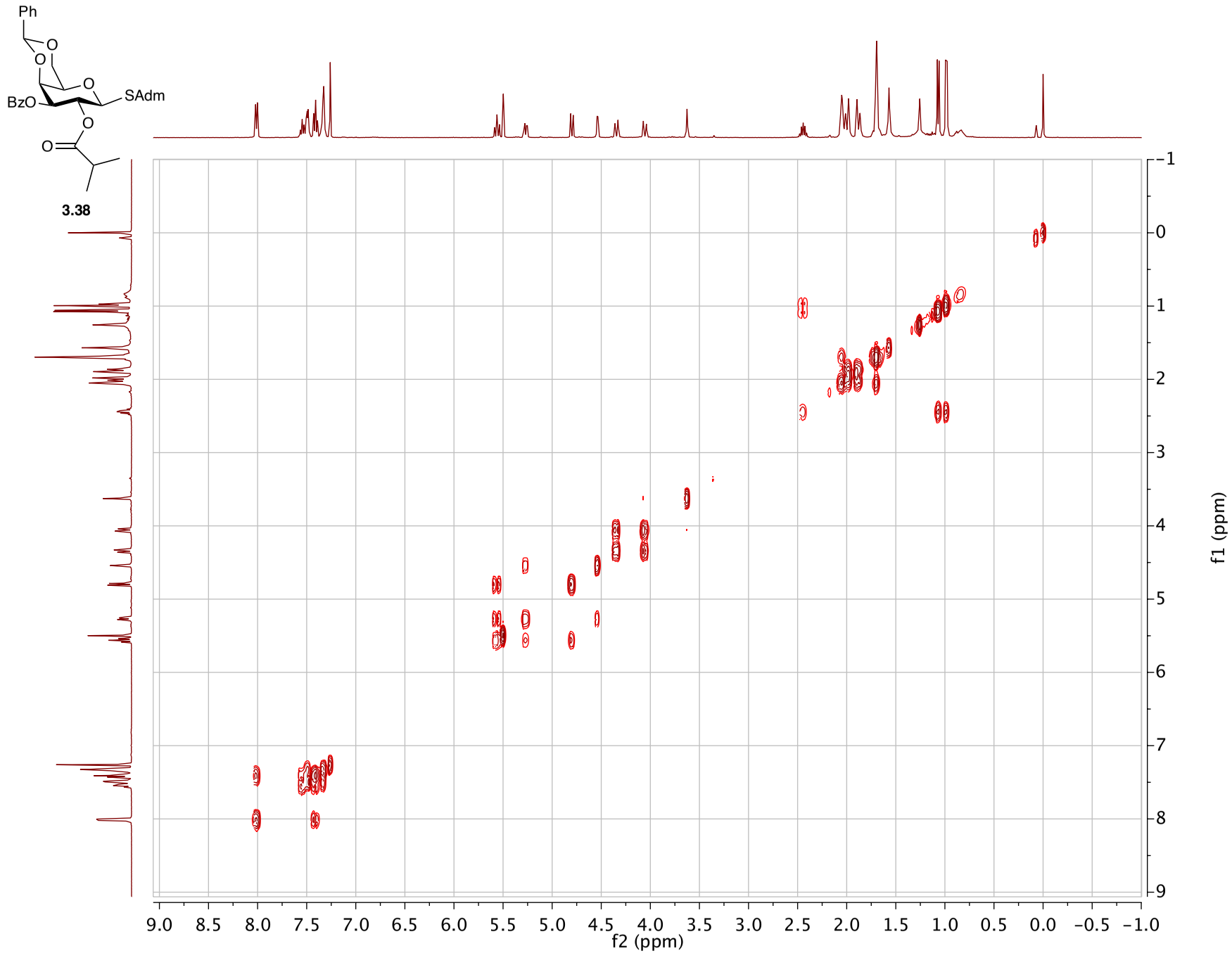
Ph
O
O
O
BzO
SAdm
O
O
3.38
f2 (ppm)
f1 (ppm)
9.0
8.5
8.0
7.5
7.0
6.5
6.0
5.5
5.0
4.5
4.0
3.5
3.0
2.5
2.0
1.5
1.0
0.5
0.0
-0.5
-1.0
-1
0
1
2
3
4
5
6
7
8
9

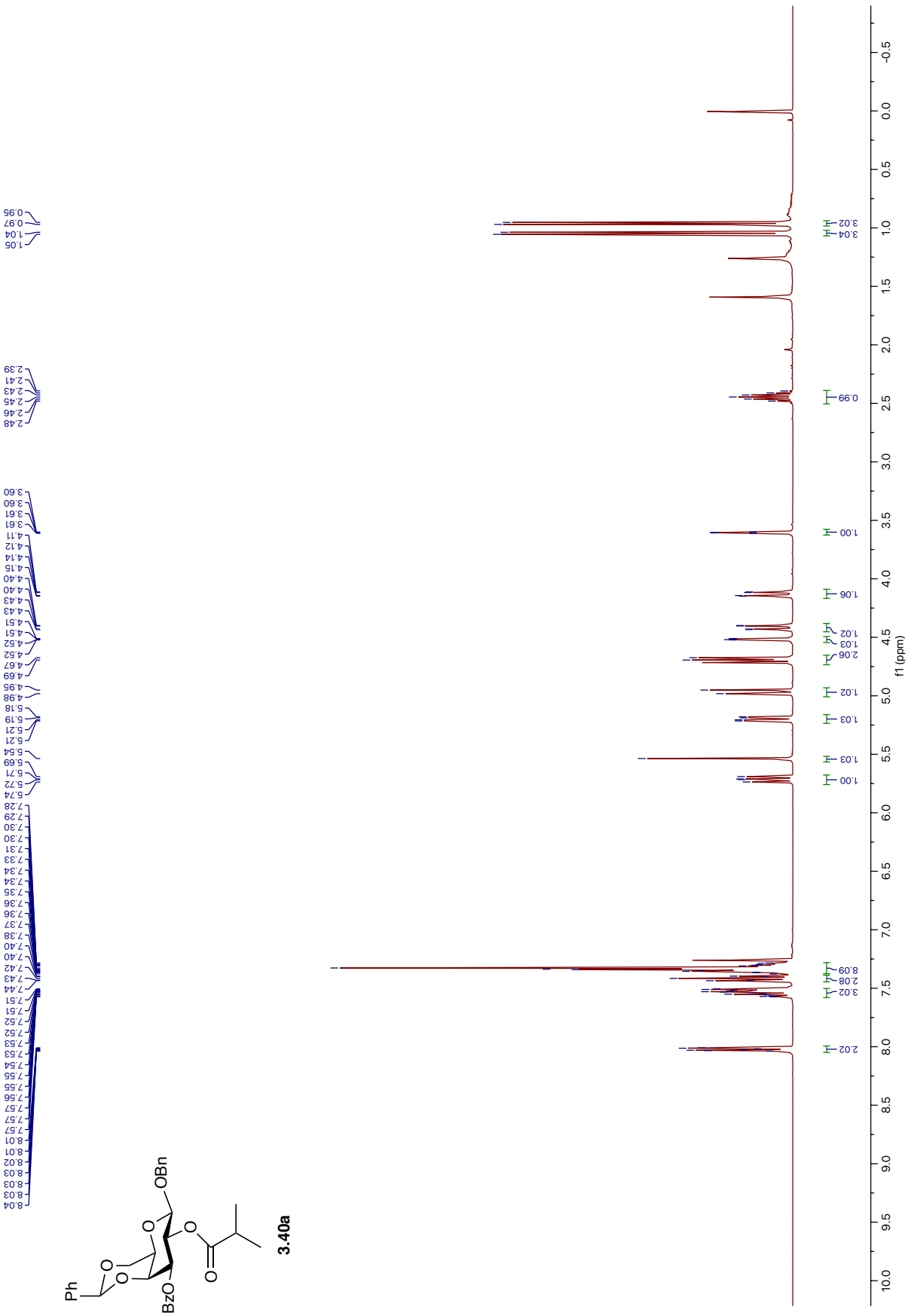
Ph
BzO
OBn
3.40a
f1 (ppm)

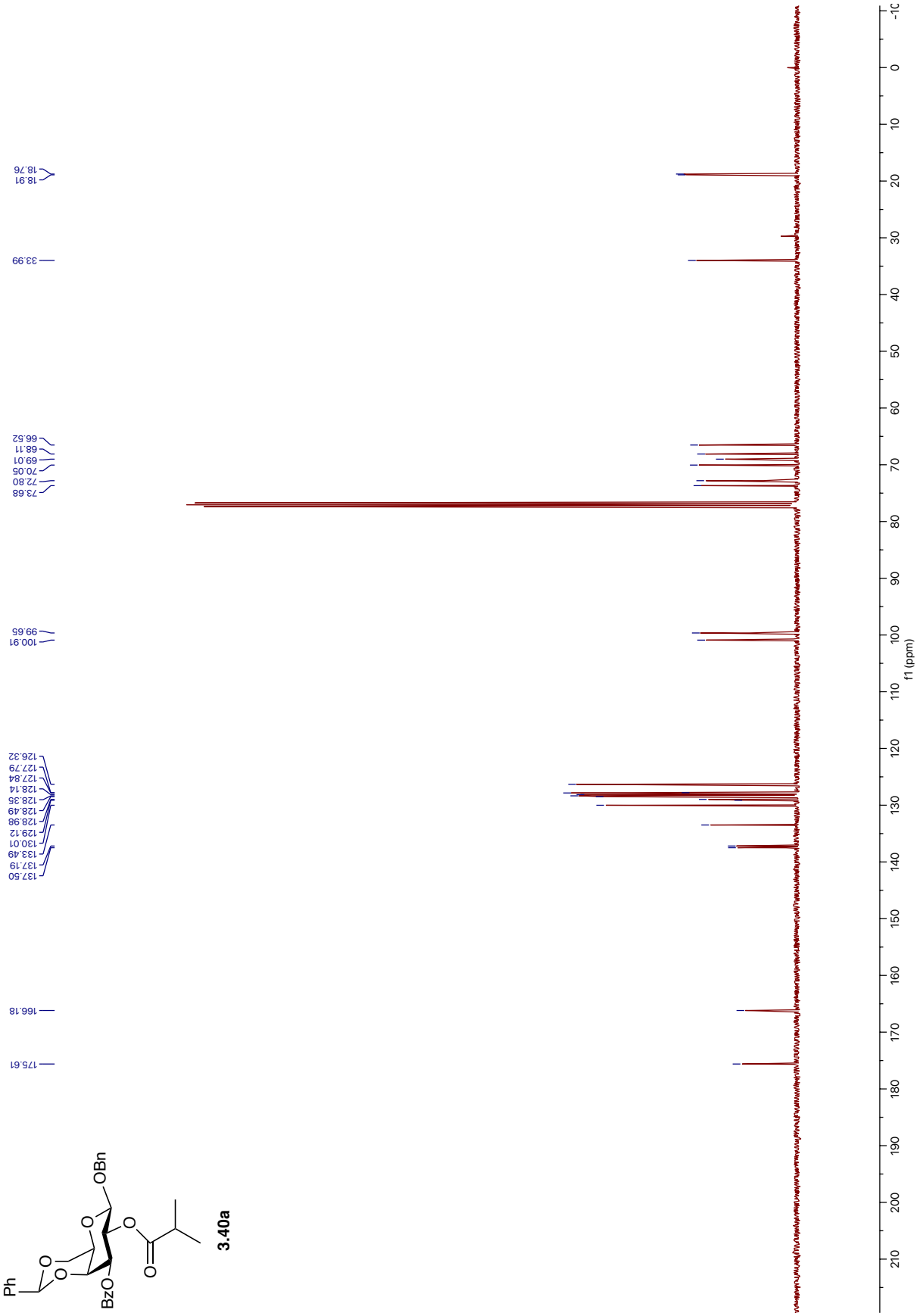
18.76
18.91
33.99
66.52
68.11
69.01
70.05
72.80
73.68
99.65
100.91
126.32
127.79
127.84
128.14
128.35
128.49
128.98
129.12
130.01
133.49
137.19
137.50
166.18
175.61
f1 (ppm)
Ph
OBn
BzO
O
3.40a

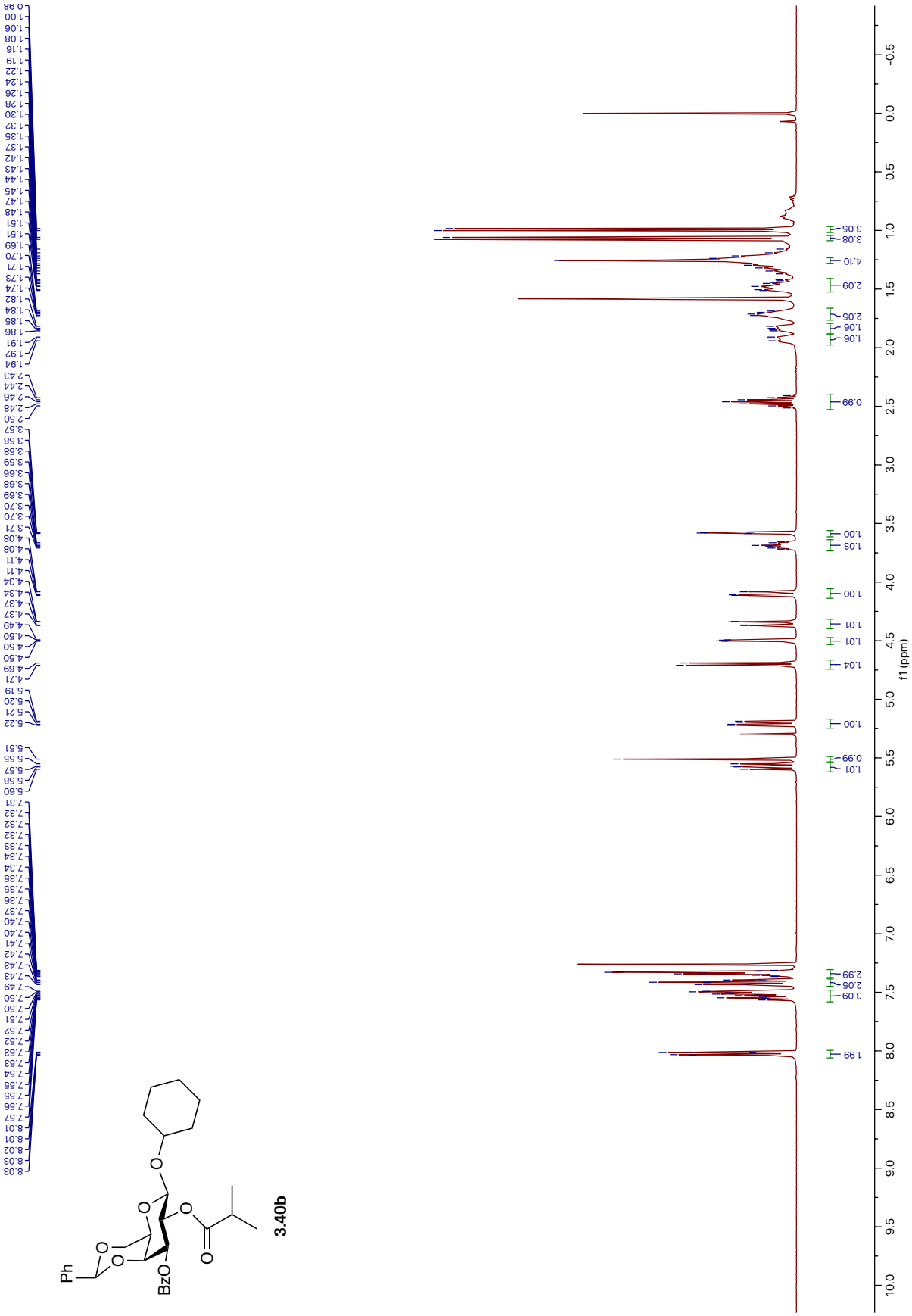
3.40b
Ph
BzO
O
f1 (ppm)

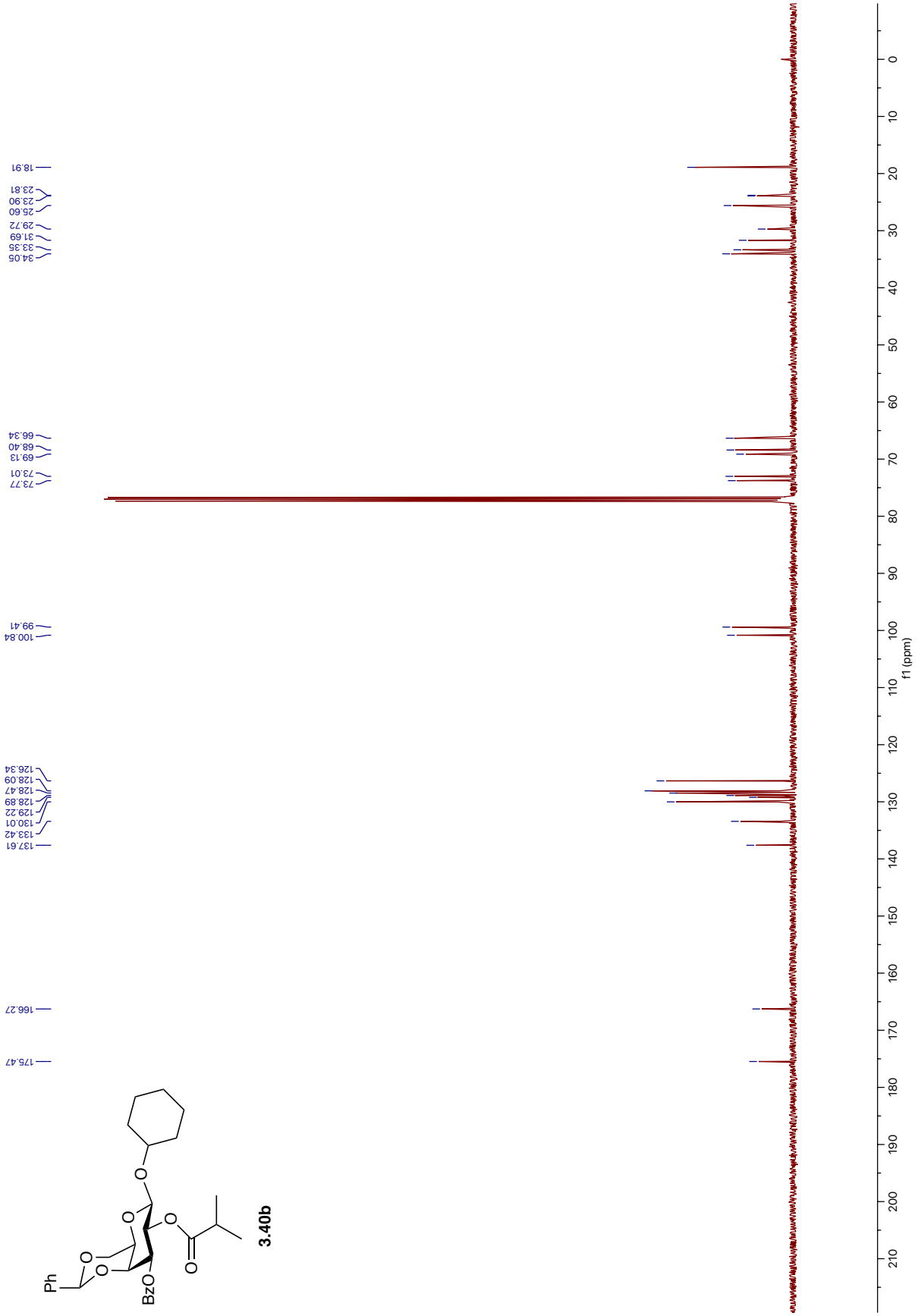
18.91
23.81
23.90
25.60
29.72
31.69
33.35
34.05
66.34
68.40
69.13
73.01
73.77
99.41
100.84
126.34
128.09
128.47
128.89
129.22
130.01
133.42
137.61
166.27
175.47
f1 (ppm)
Ph
BzO
O
3.40b

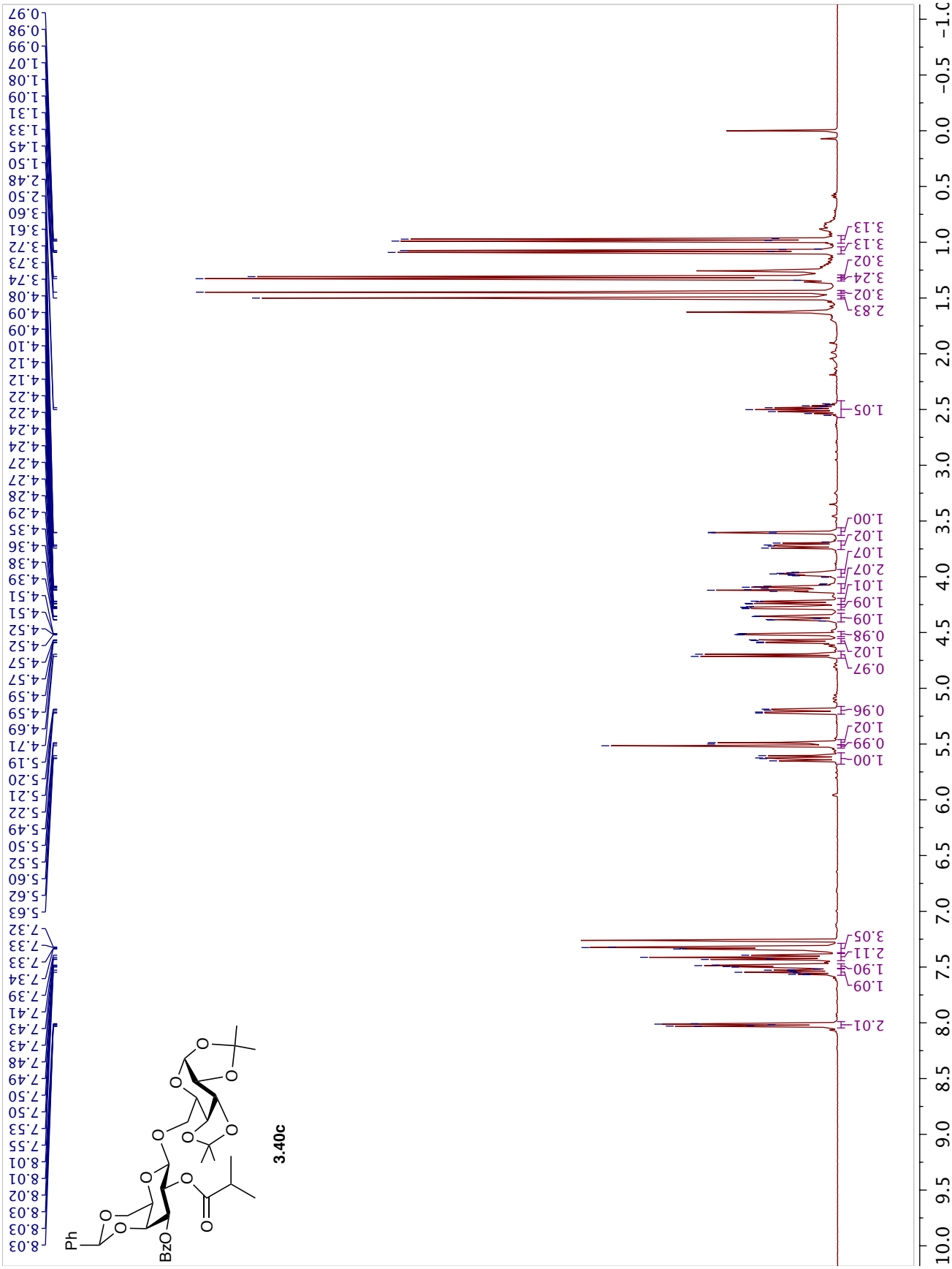
3.40c
Ph
BzO
f1 (ppm)

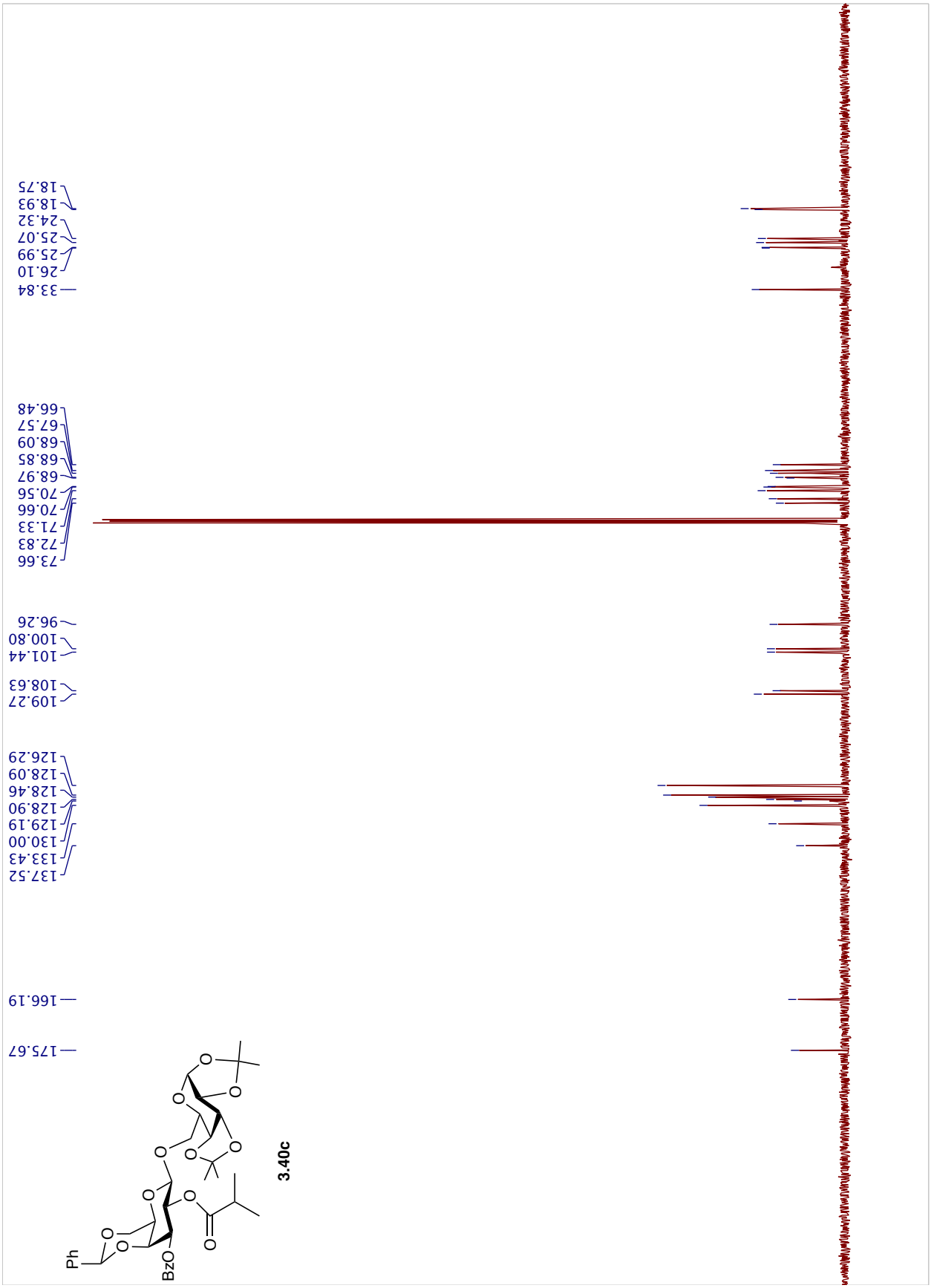
175.67
166.19
137.52
133.43
130.00
129.19
128.90
128.46
128.09
126.29
109.27
108.63
101.44
100.80
96.26
73.66
72.83
71.33
70.66
70.56
68.97
68.85
68.09
67.57
66.48
33.84
26.10
25.99
25.07
24.32
18.93
18.75
Ph
BzO
3.40c
f1 (ppm)

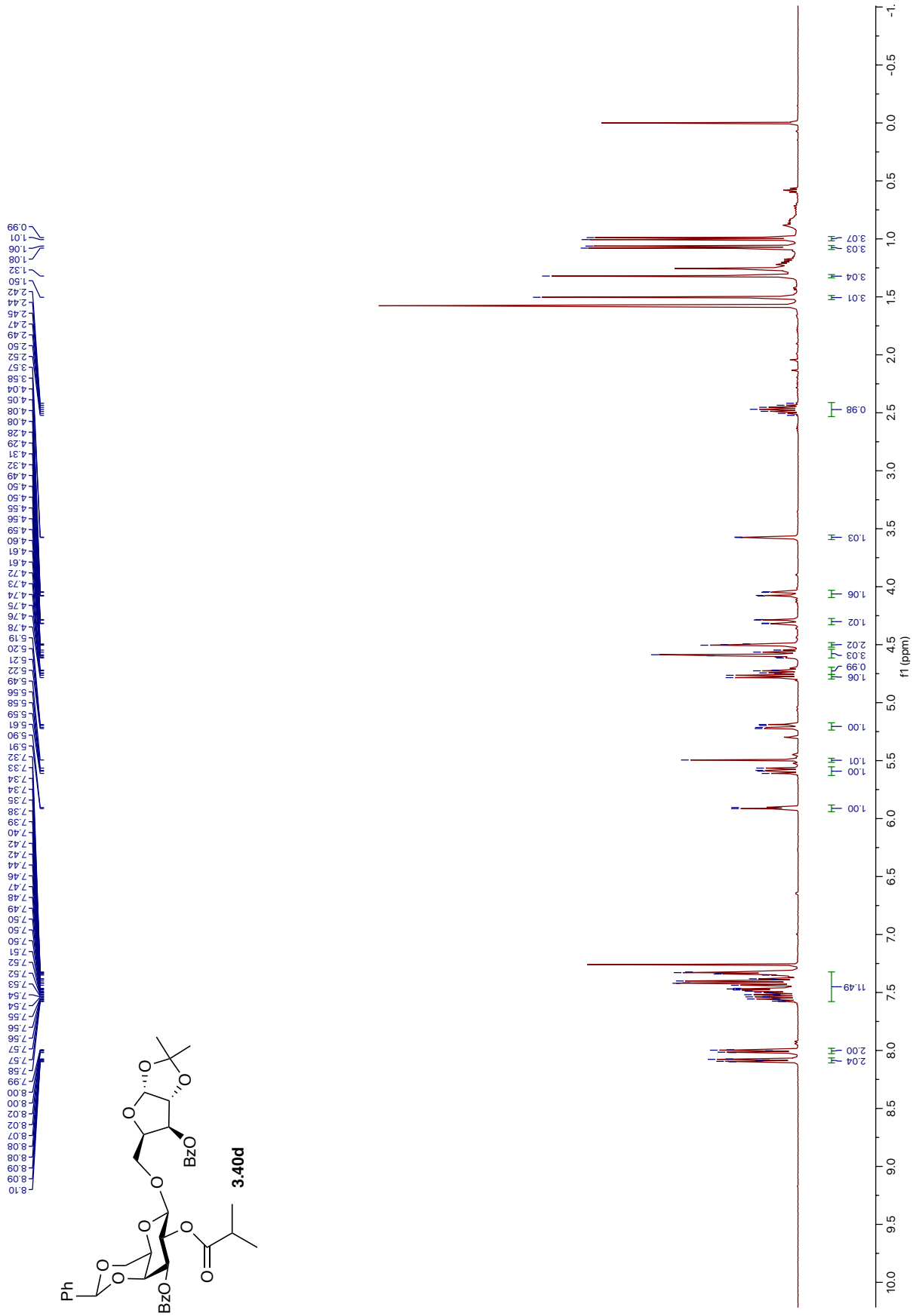
3.40d
Ph
BzO
BzO
f1 (ppm)

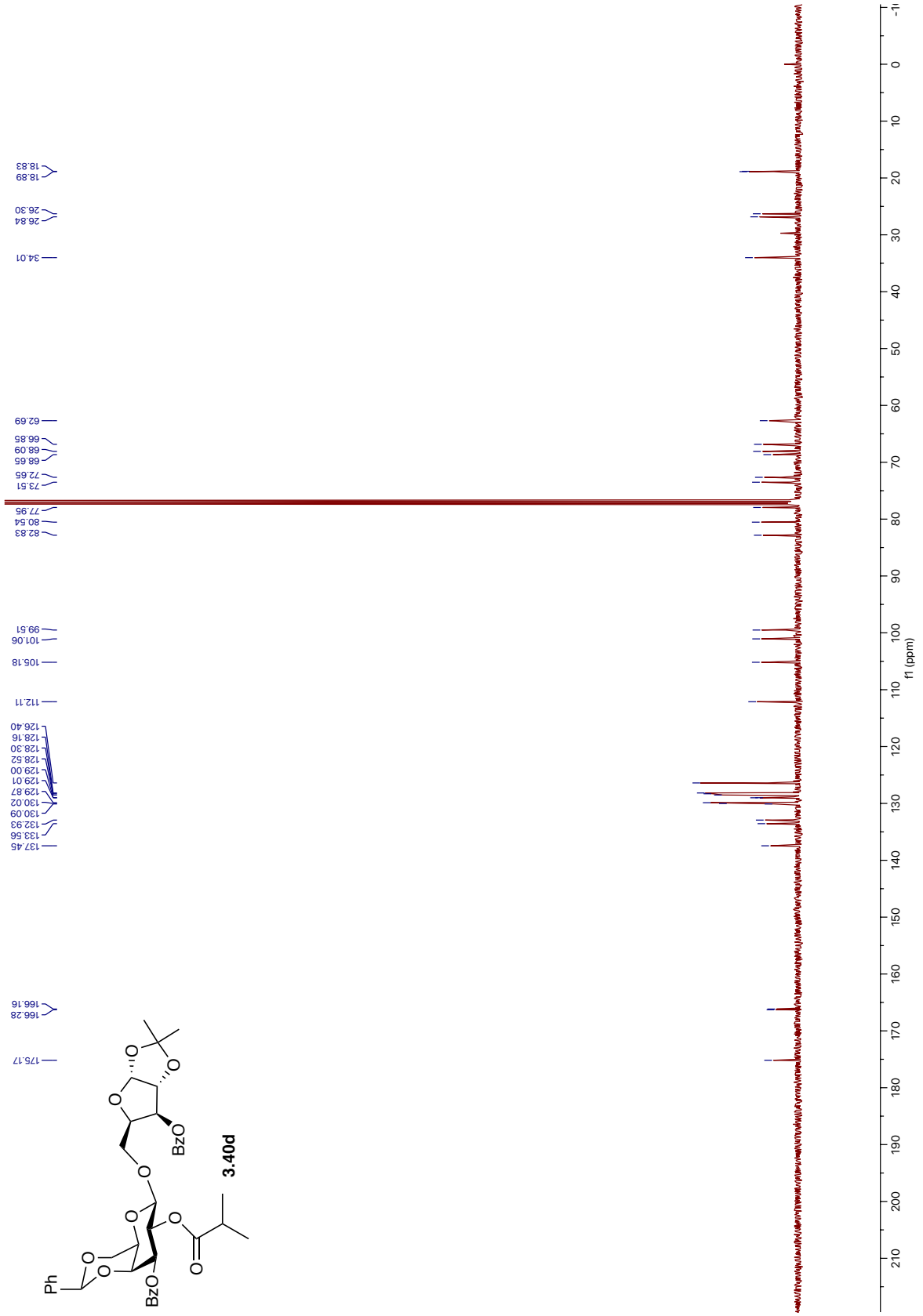
3.40d
BzO
BzO
Ph
175.17
166.28
166.16
137.45
133.56
132.93
130.09
130.02
129.87
129.01
129.00
128.52
128.30
128.16
126.40
112.11
105.18
101.06
99.51
82.83
80.54
77.95
73.51
72.65
68.65
68.09
66.85
62.69
34.01
26.84
26.30
18.89
18.83
f1 (ppm)

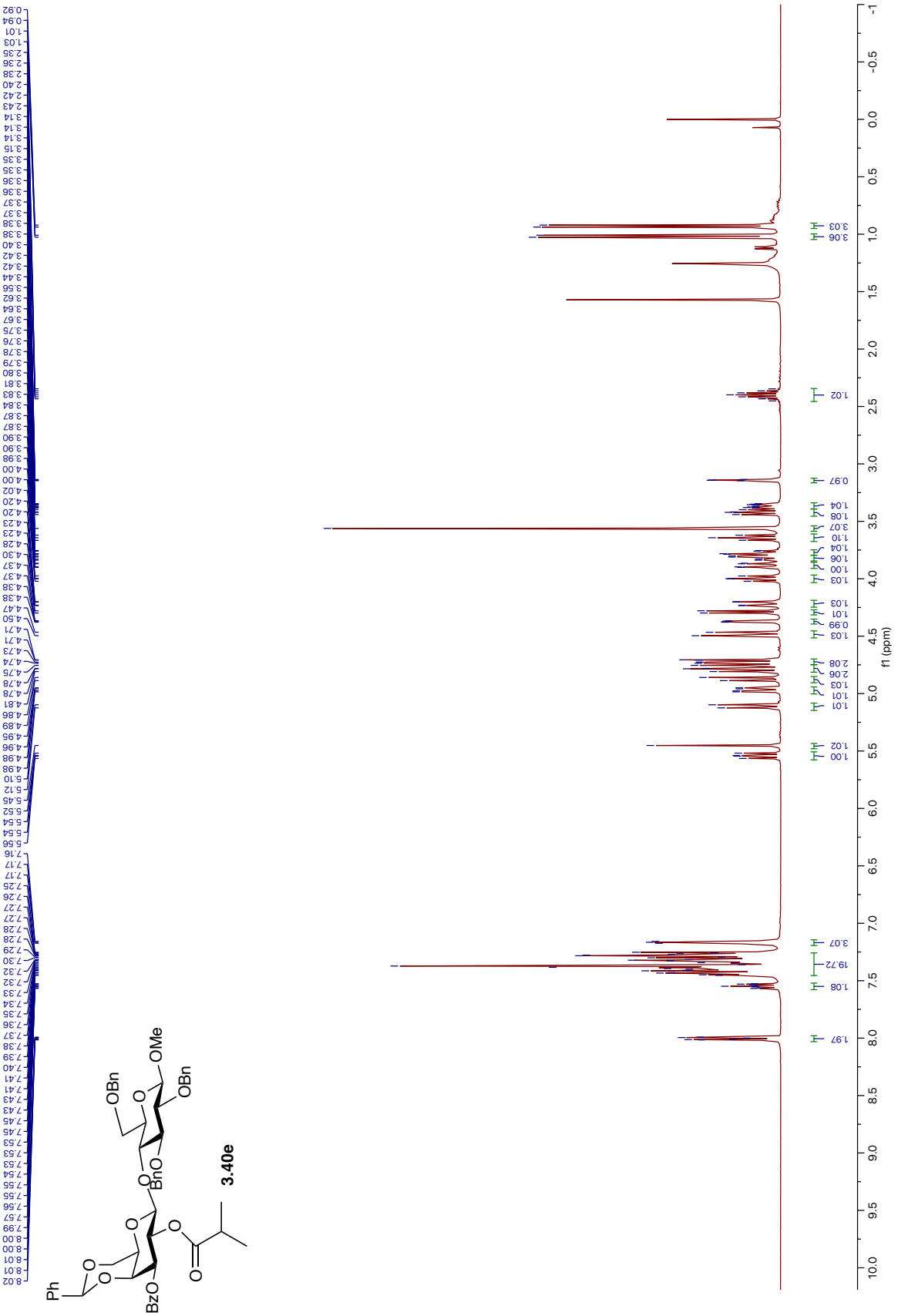
Ph
BzO
BnO
OBn
OBn
OMe
O
3.40e
f1 (ppm)

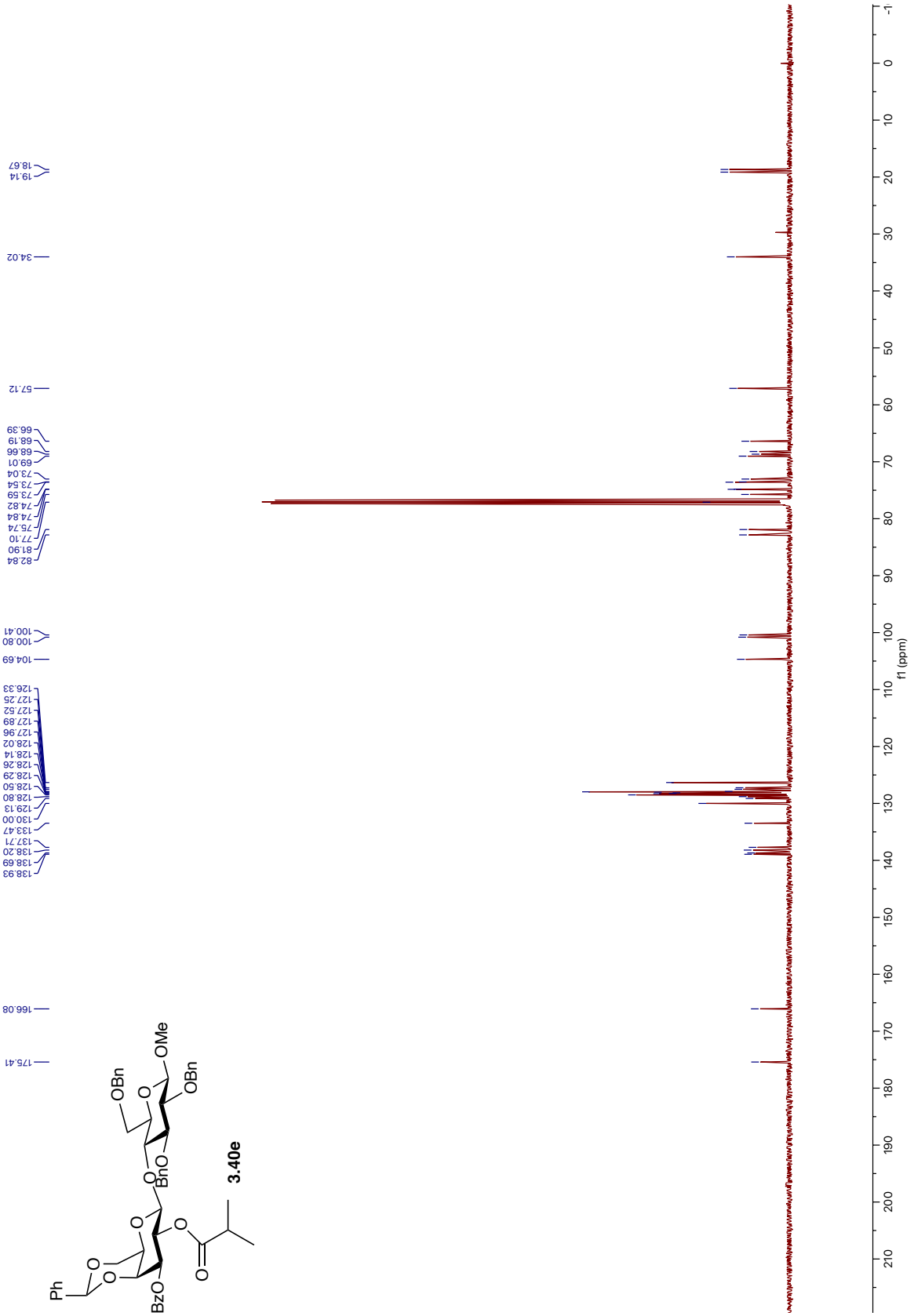
3.40e
f1 (ppm)

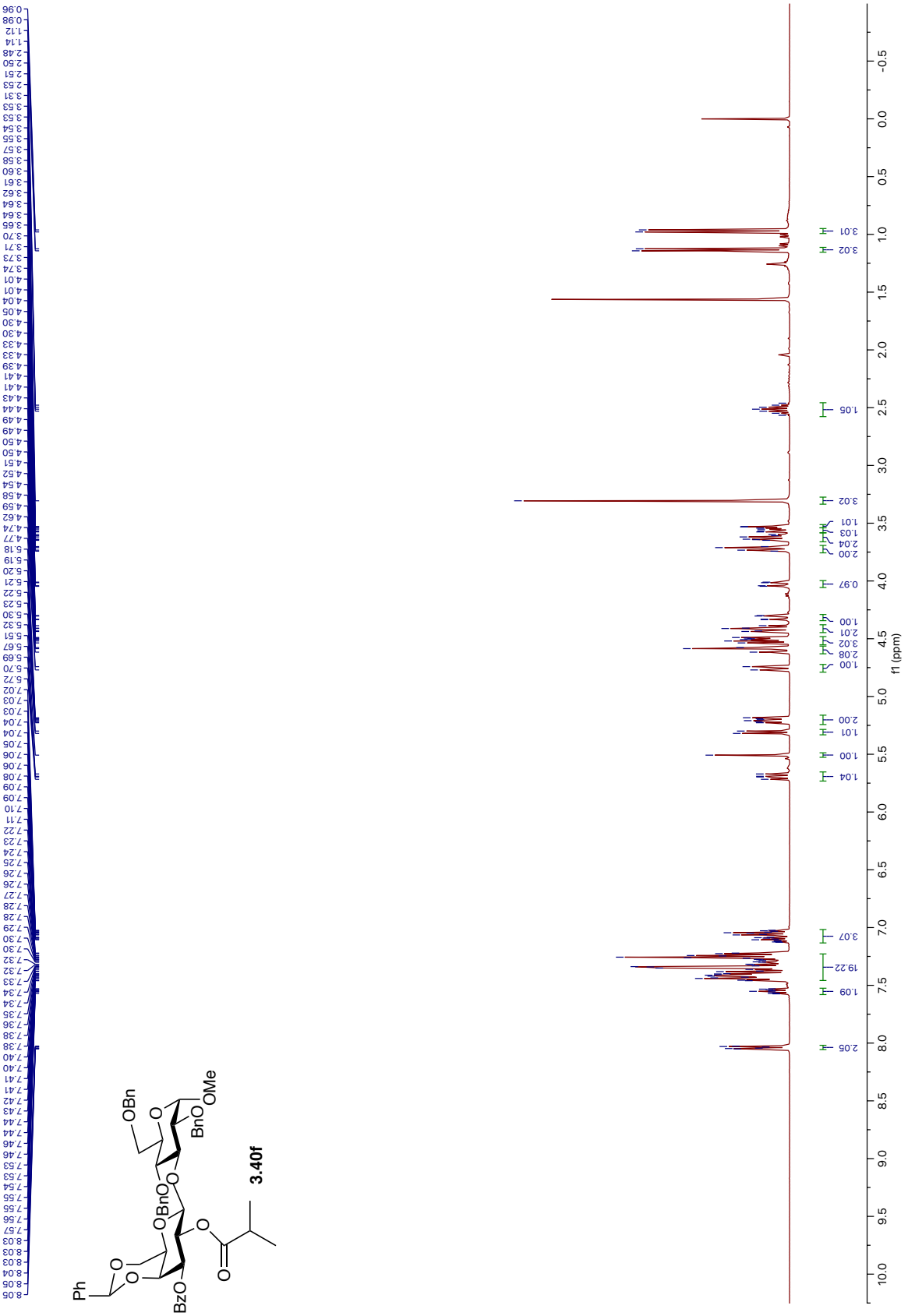
Ph
BzO
OBn
BnO
OMe
3.40f
f1 (ppm)

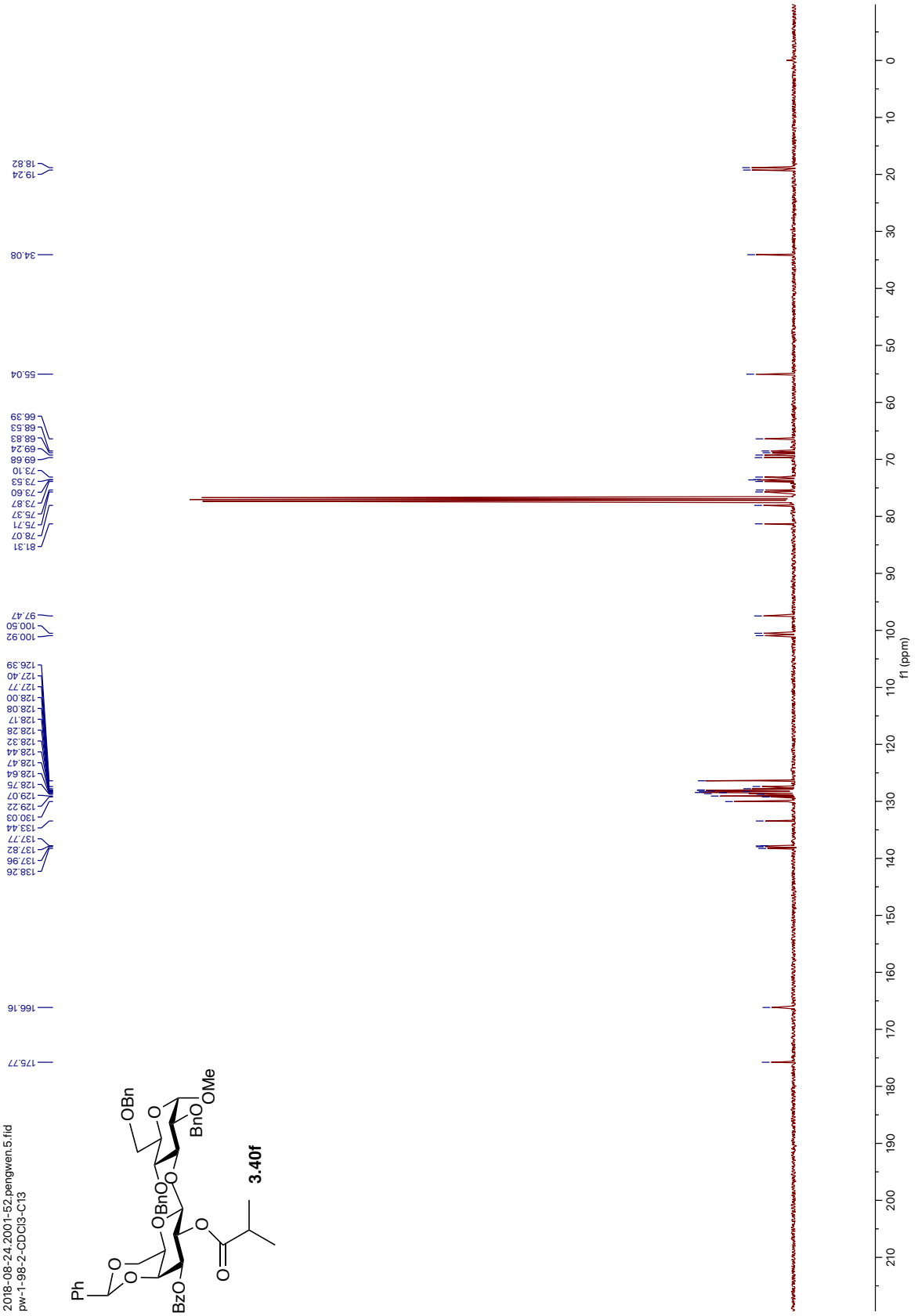
2018-08-24.2001-52.pengwen.5.fid
pw-1-98-2-CDCl3-C13
3.40f
Ph
BzO
BnO
BnO
OBn
OMe
O
f1 (ppm)

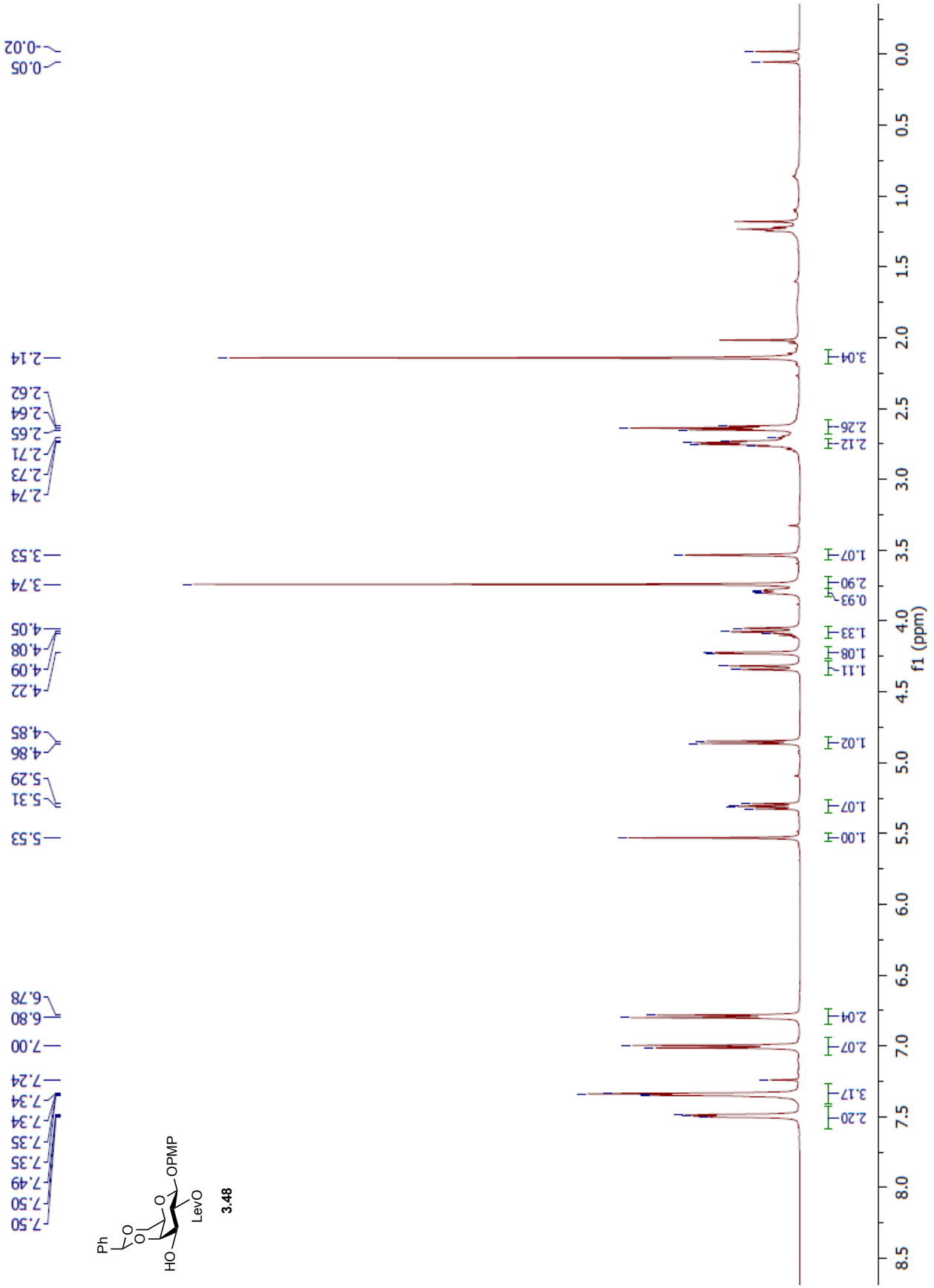
-0.02
0.05
2.14
2.62
2.64
2.65
2.71
2.73
2.74
3.53
3.74
4.05
4.08
4.09
4.22
4.85
4.86
5.29
5.31
5.53
6.78
6.80
7.00
7.24
7.34
7.34
7.35
7.35
7.49
7.50
7.50
3.04
2.26
2.12
1.07
2.90
0.93
1.33
1.08
1.11
1.02
1.07
1.00
2.04
2.07
3.17
2.20
f1 (ppm)
Ph
O
O
HO
O
LevO
OPMP
3.48

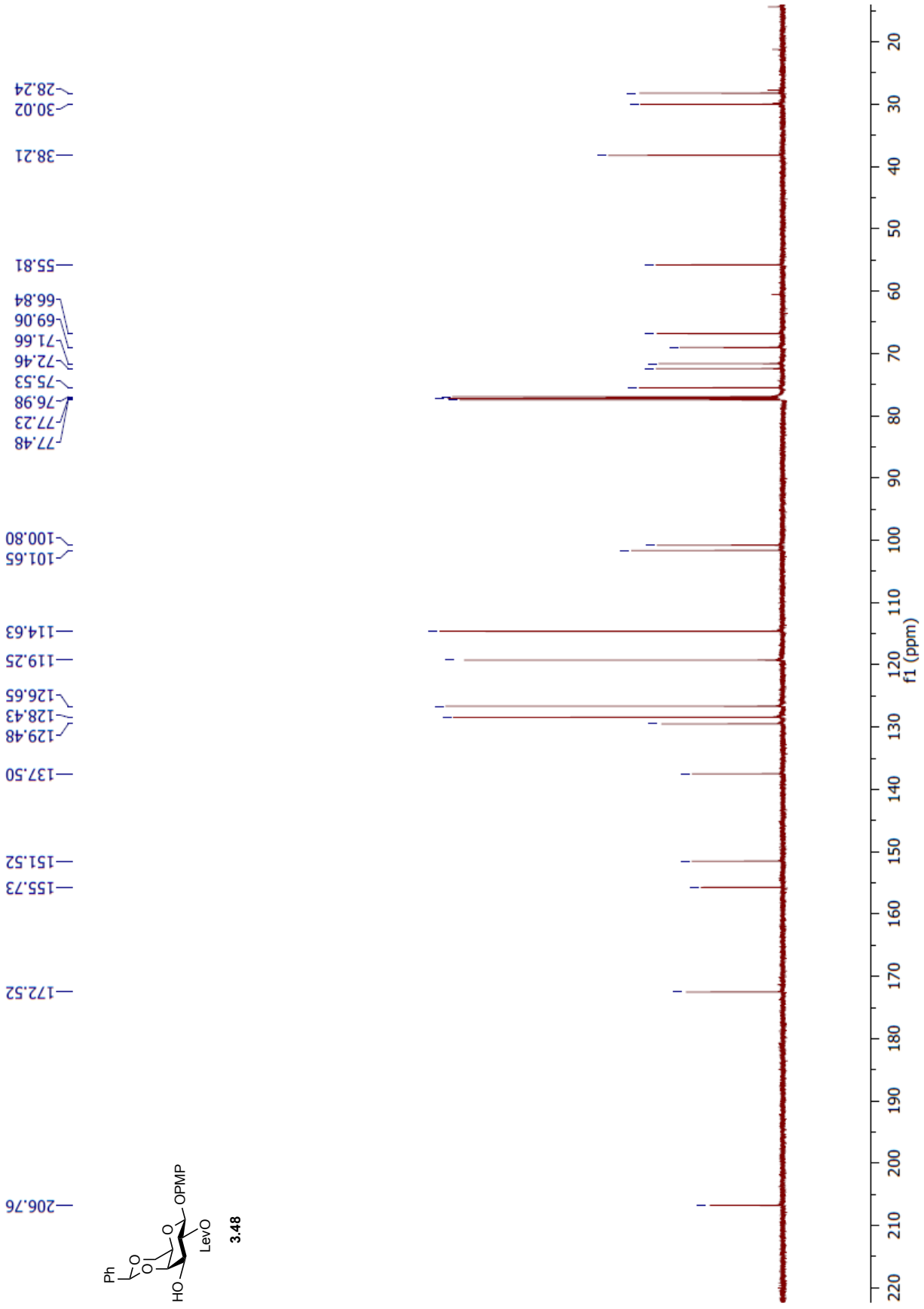
28.24
30.02
38.21
55.81
66.84
69.06
71.66
72.46
75.53
76.98
77.23
77.48
100.80
101.65
114.63
119.25
126.65
128.43
129.48
137.50
151.52
155.73
172.52
206.76
f1 (ppm)
Ph
HO
LevO
OPMP
3.48

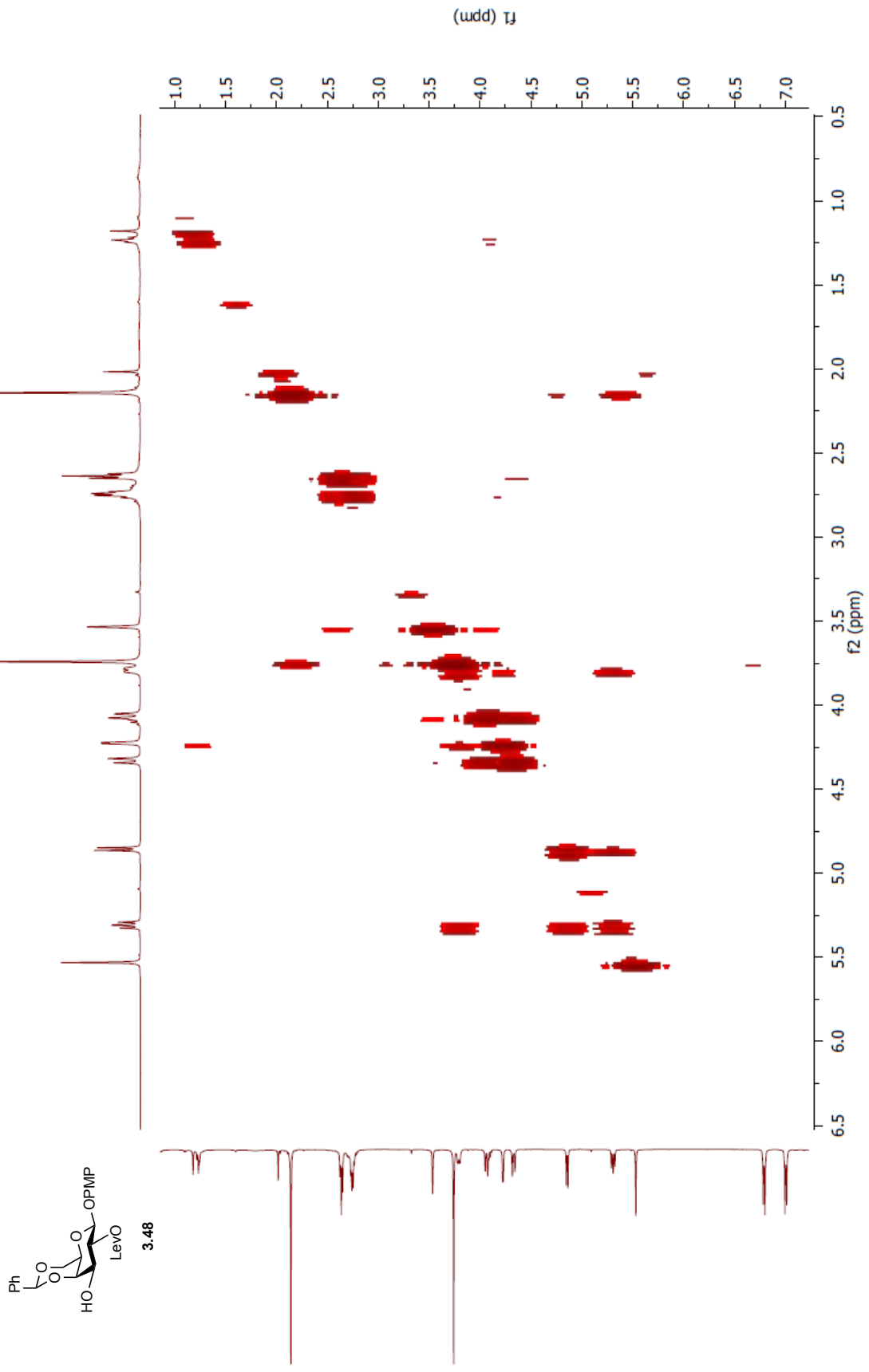
f1 (ppm)
1.0
1.5
2.0
2.5
3.0
3.5
4.0
4.5
5.0
5.5
6.0
6.5
7.0
f2 (ppm)
0.5
1.0
1.5
2.0
2.5
3.0
3.5
4.0
4.5
5.0
5.5
6.0
6.5
Ph
O
O
O
HO
LevO
OPMP
3.48

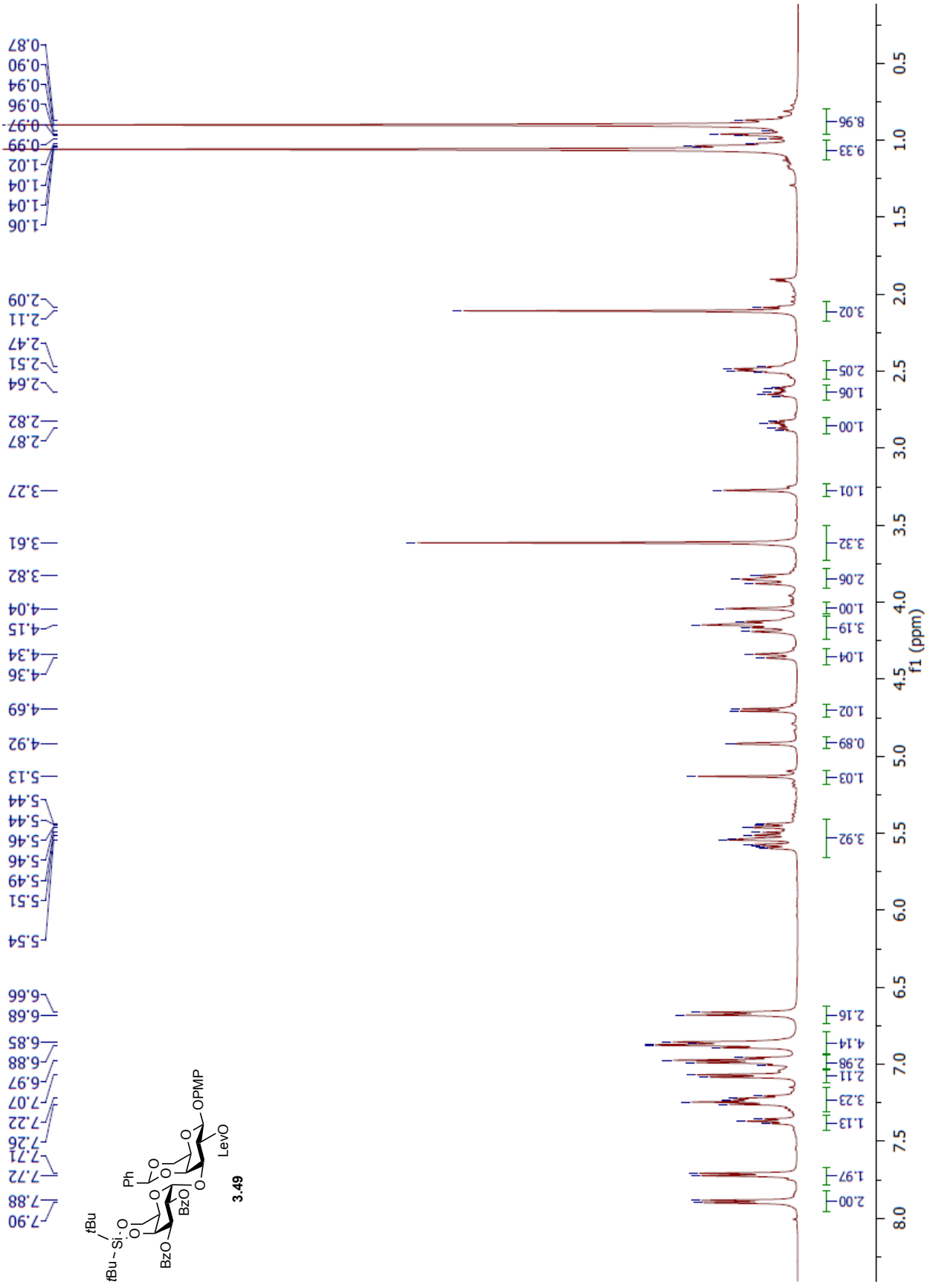
f1 (ppm)
3.49

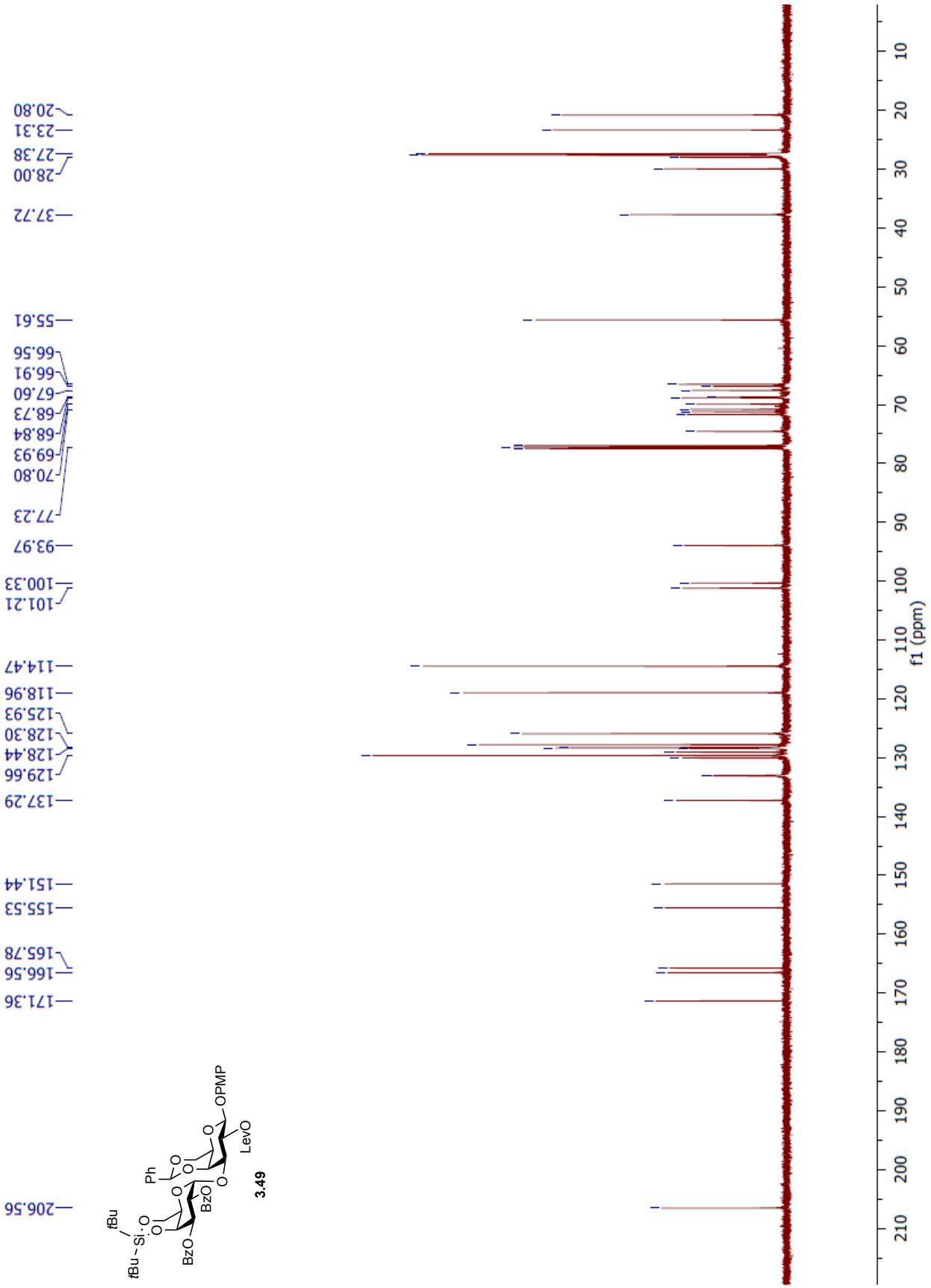
20.80
23.31
27.38
28.00
37.72
55.61
66.56
66.91
67.60
68.73
68.84
69.93
70.80
77.23
93.97
100.33
101.21
114.47
118.96
125.93
128.30
128.44
129.66
137.29
151.44
155.53
165.78
166.56
171.36
206.56
f1 (ppm)
3.49

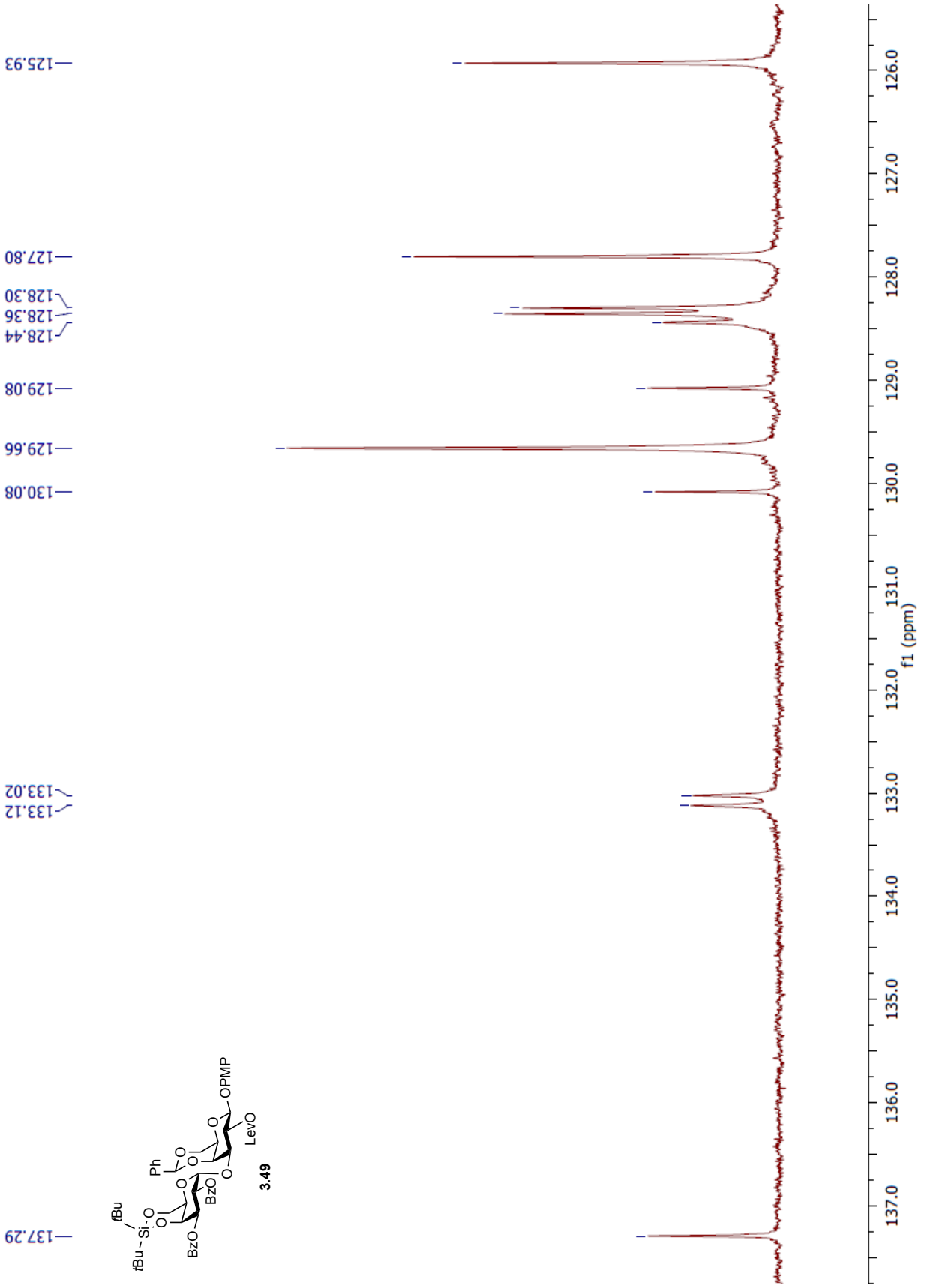
137.29
133.12
133.02
130.08
129.66
129.08
128.44
128.36
128.30
127.80
125.93
fBu
fBu
Si
O
O
BzO
O
O
Ph
O
O
BzO
O
O
LevO
OPMP
3.49
137.0
136.0
135.0
134.0
133.0
132.0
131.0
130.0
129.0
128.0
127.0
126.0
f1 (ppm)

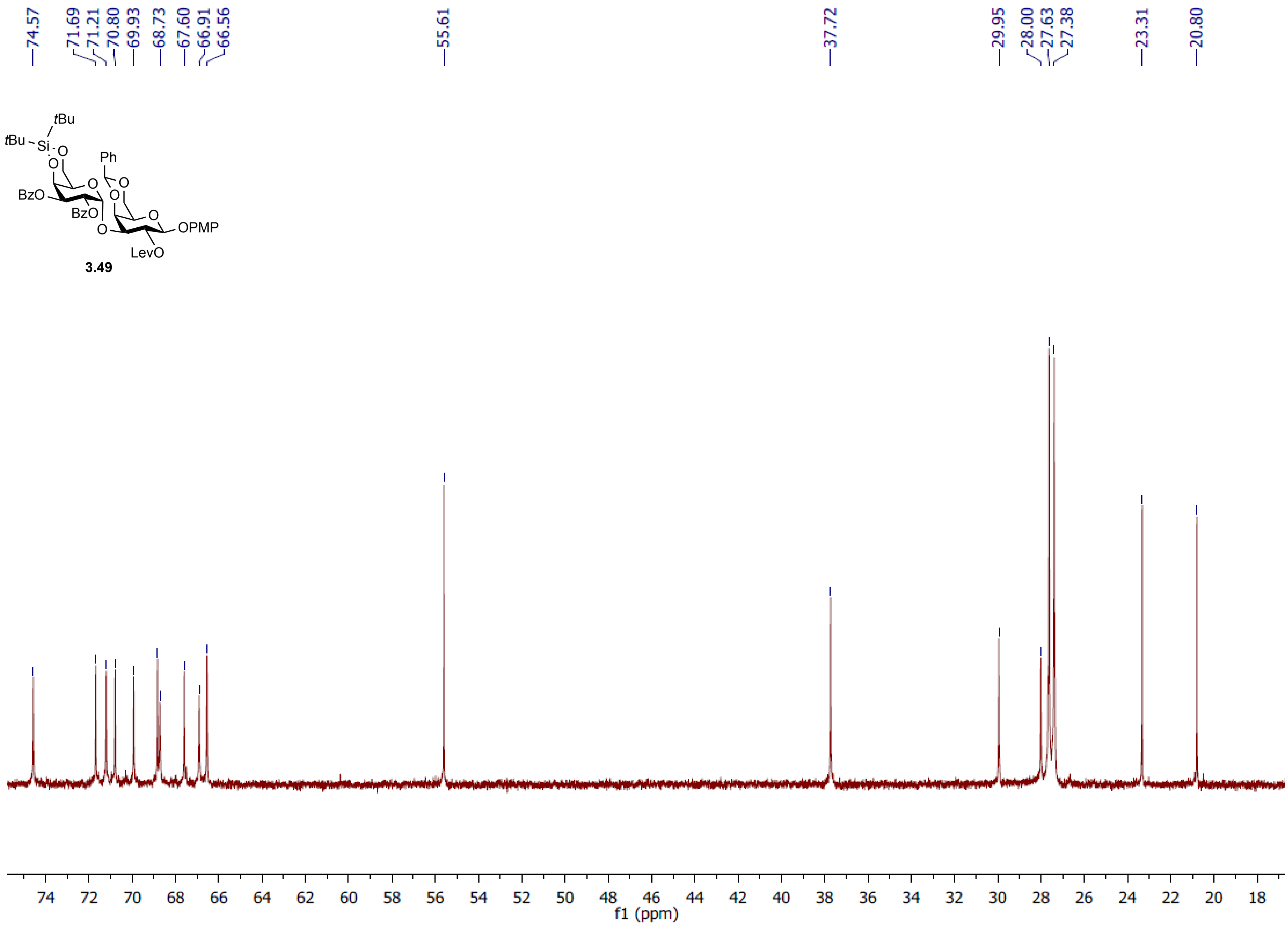
74.57
71.69
71.21
70.80
69.93
68.73
67.60
66.91
66.56
55.61
37.72
29.95
28.00
27.63
27.38
23.31
20.80
tBu
tBu
Si
O
O
BzO
BzO
O
O
Ph
O
O
O
OPMP
LevO
3.49
74
72
70
68
66
64
62
60
58
56
54
52
50
48
46
44
42
40
38
36
34
32
30
28
26
24
22
20
18
f1 (ppm)

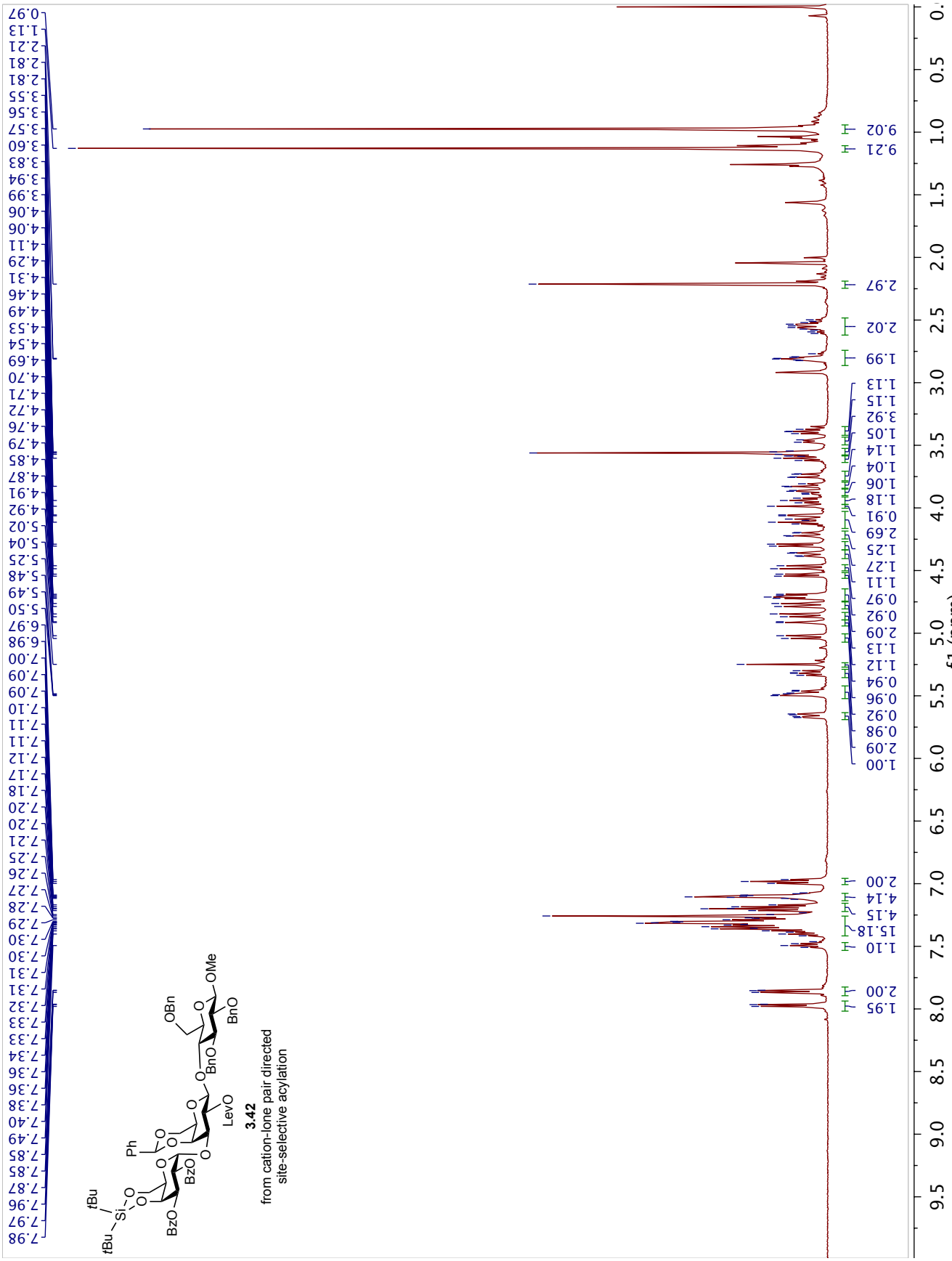
f1 (ppm)
3.42
from cation-lone pair directed
site-selective acylation

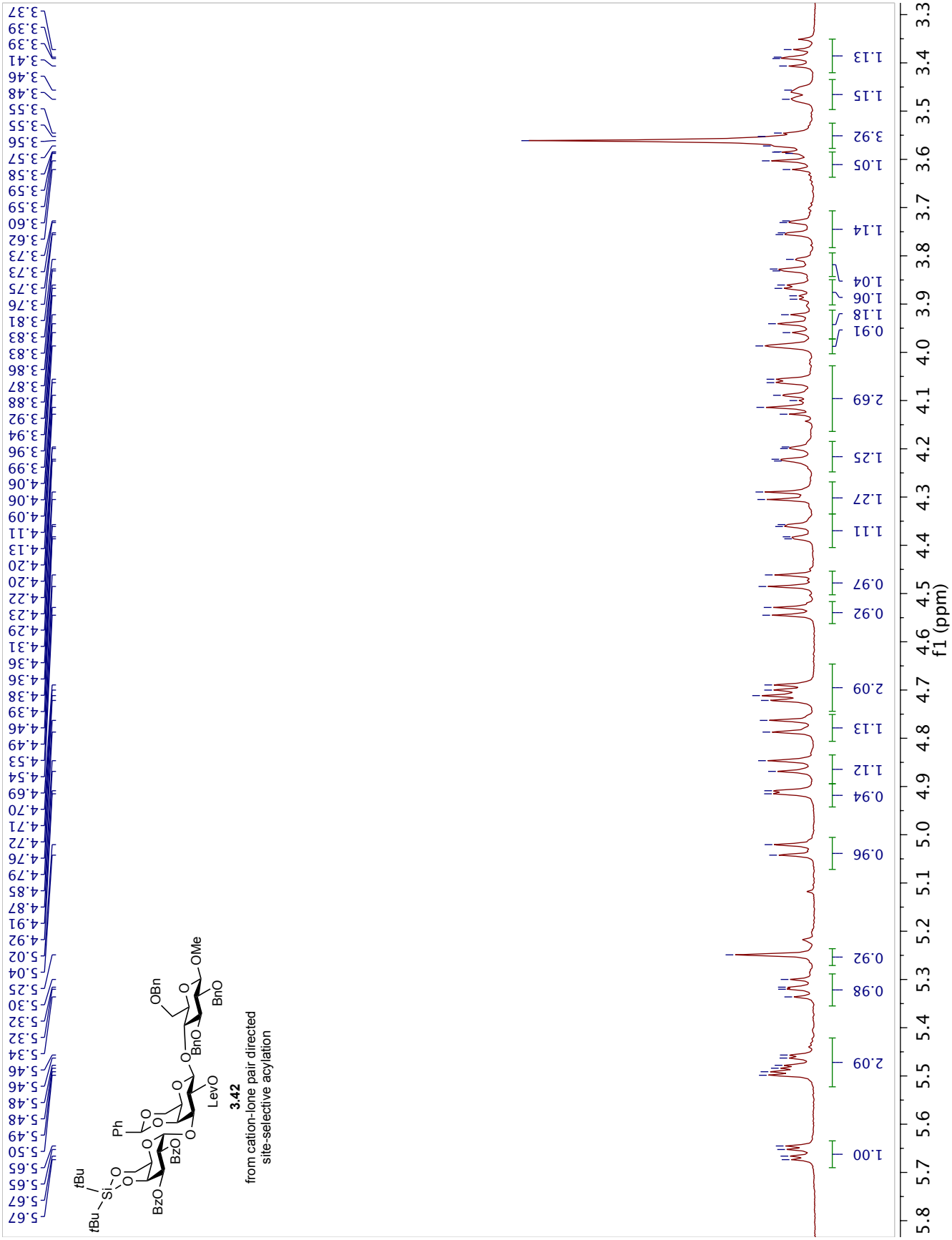
tBu
tBu
Si
O
O
Ph
O
O
BzO
BzO
O
O
O
LevO
O
BnO
OBn
O
OMe
BnO
3.42
from cation-lone pair directed
site-selective acylation
f1 (ppm)

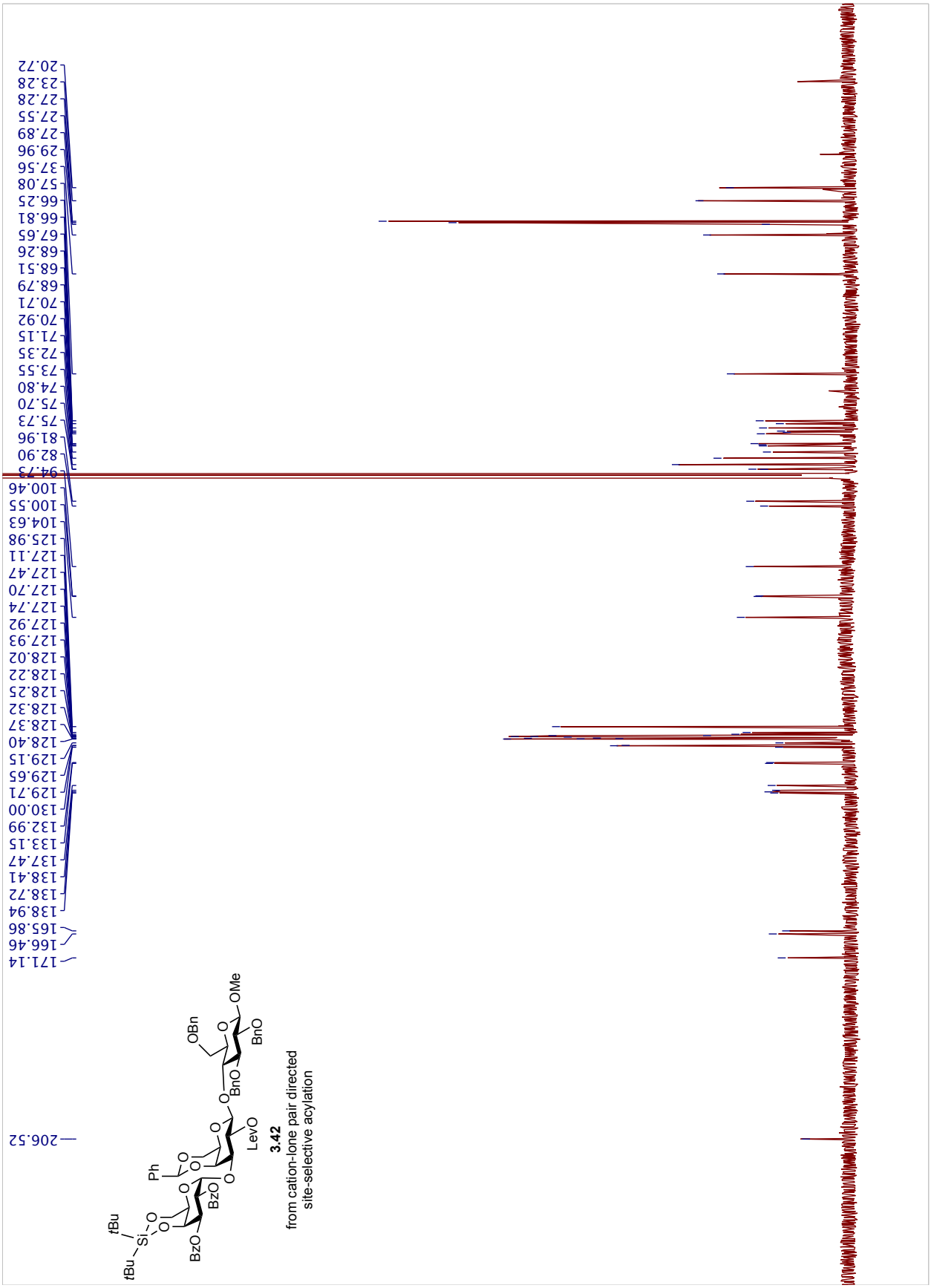
20.72
23.28
27.28
27.55
27.89
29.96
37.56
57.08
66.25
66.81
67.65
68.26
68.51
68.79
70.71
70.92
71.15
72.35
73.55
74.80
75.70
75.73
81.96
82.90
94.73
100.46
100.55
104.63
125.98
127.11
127.47
127.70
127.74
127.92
127.93
128.02
128.22
128.25
128.32
128.37
128.40
129.15
129.65
129.71
130.00
132.99
133.15
137.47
138.41
138.72
138.94
165.86
166.46
171.14
206.52
f1 (ppm)
3.42
from cation-lone pair directed
site-selective acylation

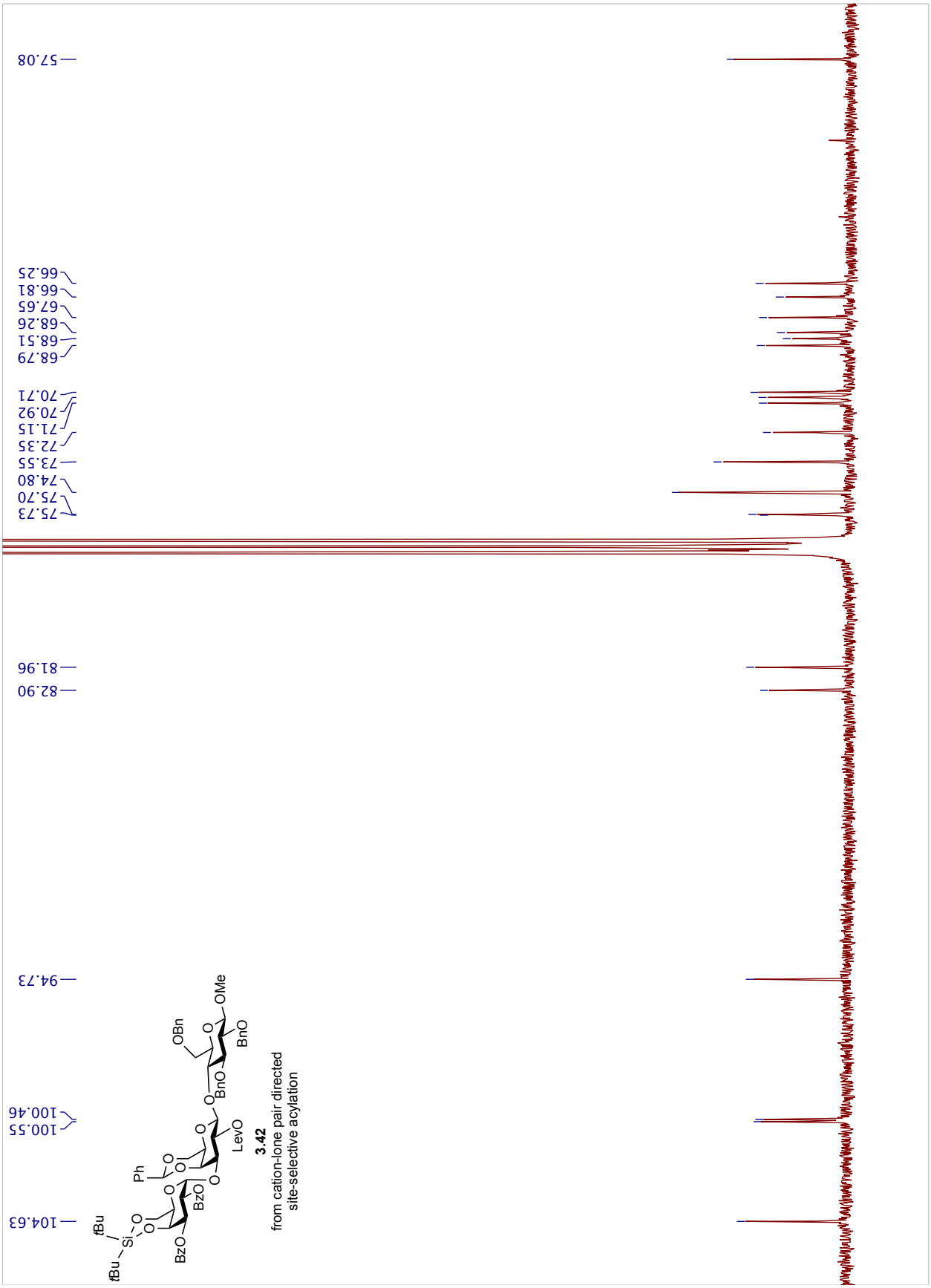
57.08
66.25
66.81
67.65
68.26
68.51
68.79
70.71
70.92
71.15
72.35
73.55
74.80
75.70
75.73
81.96
82.90
94.73
100.46
100.55
104.63
f1 (ppm)
3.42
from cation-lone pair directed
site-selective acylation

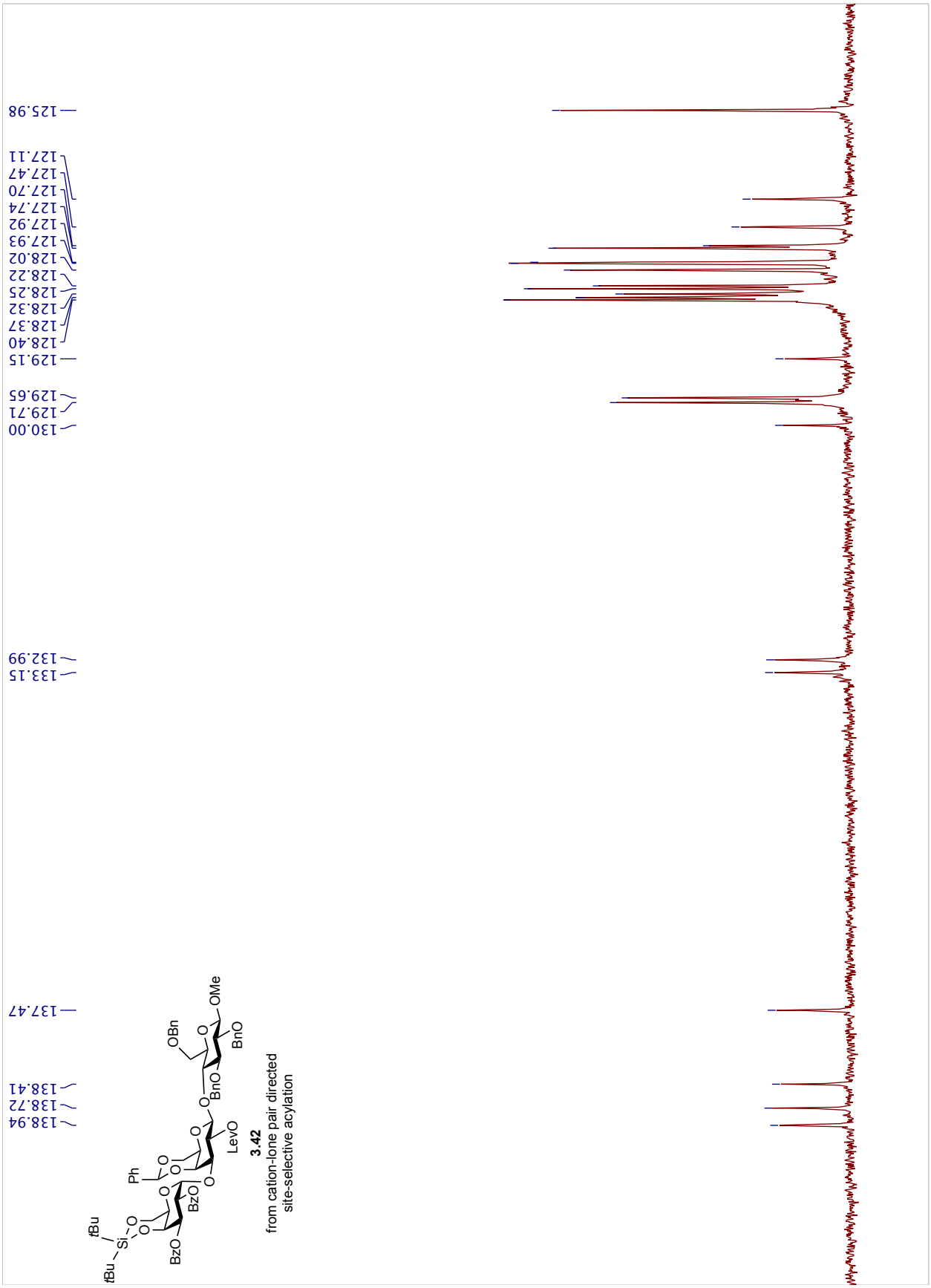
125.98
127.11
127.47
127.70
127.74
127.92
127.93
128.02
128.22
128.25
128.32
128.37
128.40
129.15
129.65
129.71
130.00
132.99
133.15
137.47
138.41
138.72
138.94
fBu
fBu
Si
O
O
Ph
O
O
O
BzO
BzO
O
O
O
O
LevO
O
BnO
OBn
O
OMe
BnO
3.42
from cation-lone pair directed
site-selective acylation
140
139
138
137
136
135
134
133
132
131
130
129
128
127
126
125
f1 (ppm)

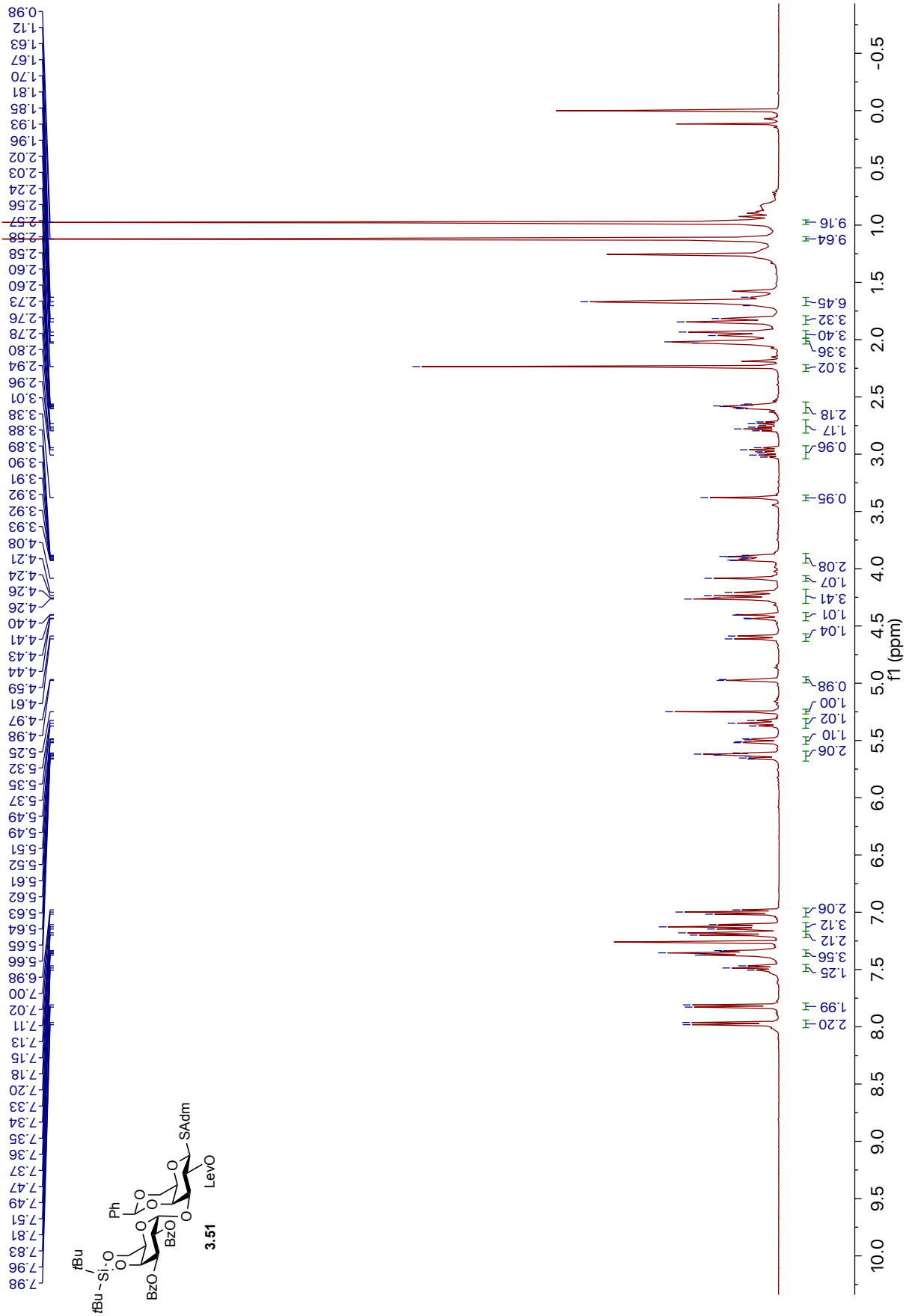
tBu
tBu - Si - O
O
BzO
O
O
Ph
O
O
BzO
O
O
SAdm
LevO
3.51
f1 (ppm)

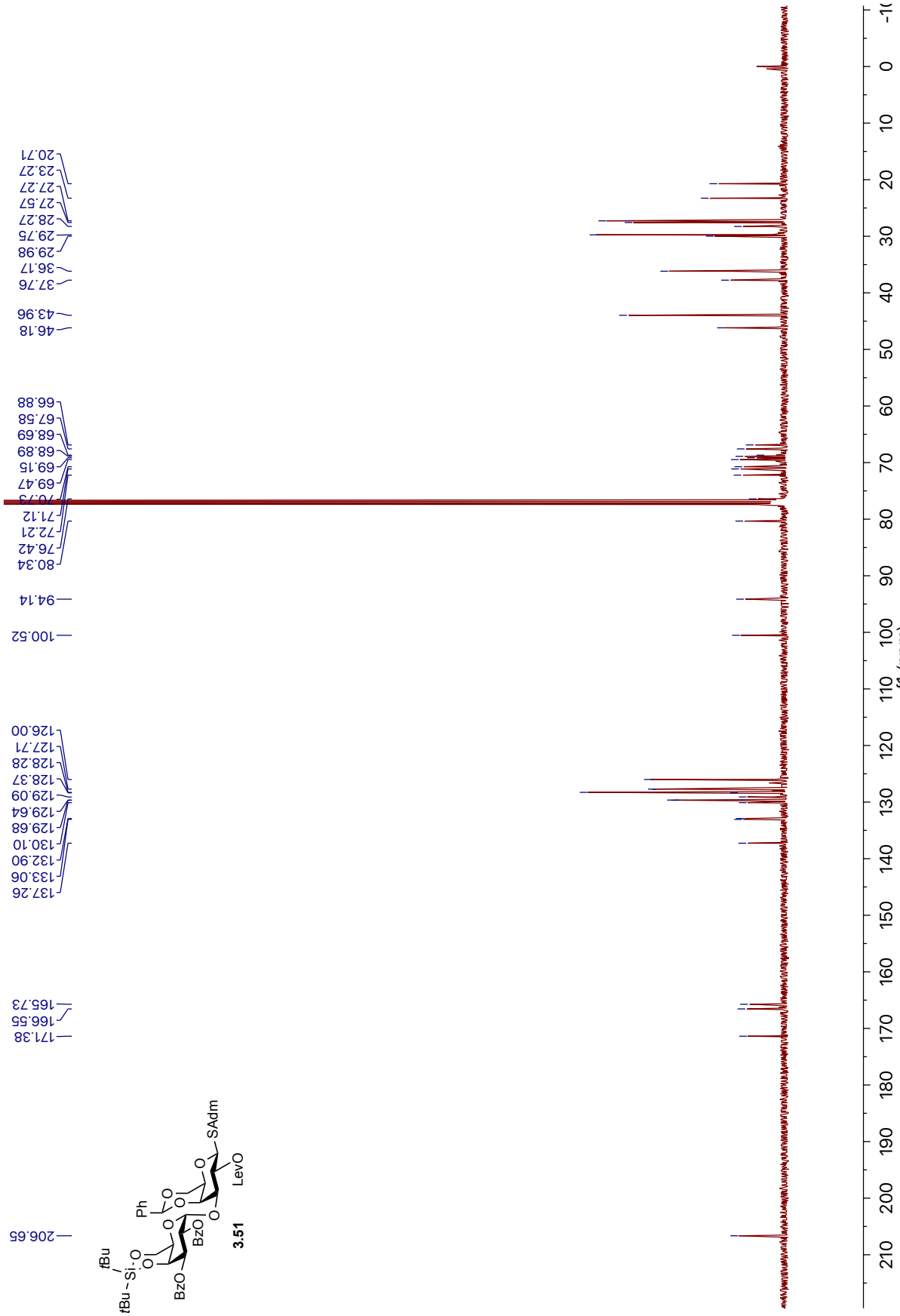
206.65
171.38
166.55
165.73
137.26
133.06
132.90
130.10
129.68
129.64
129.09
128.37
128.28
127.71
126.00
100.52
94.14
80.34
76.42
72.21
71.12
70.73
69.47
69.15
68.89
68.69
67.58
66.88
46.18
43.96
37.76
36.17
29.98
29.75
28.27
27.57
27.27
23.27
20.71
f1 (ppm)
tBu
tBu
Si
O
O
O
BzO
BzO
O
O
O
Ph
O
O
O
O
O
LevO
SAdm
3.51

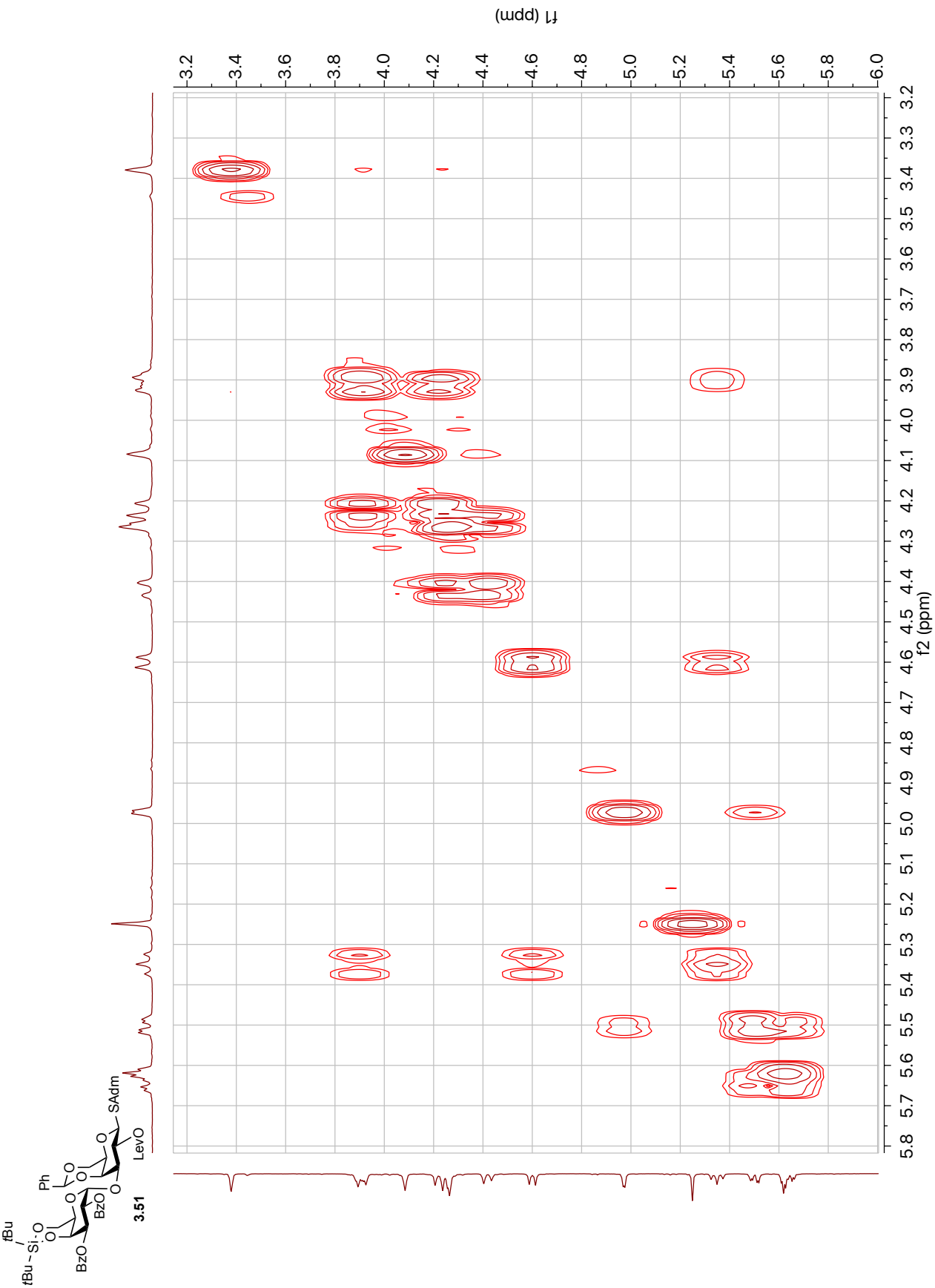
tBu
tBu
Si
O
O
BzO
O
O
Ph
O
O
BzO
O
O
SAdm
LevO
3.51
f1 (ppm)
f2 (ppm)

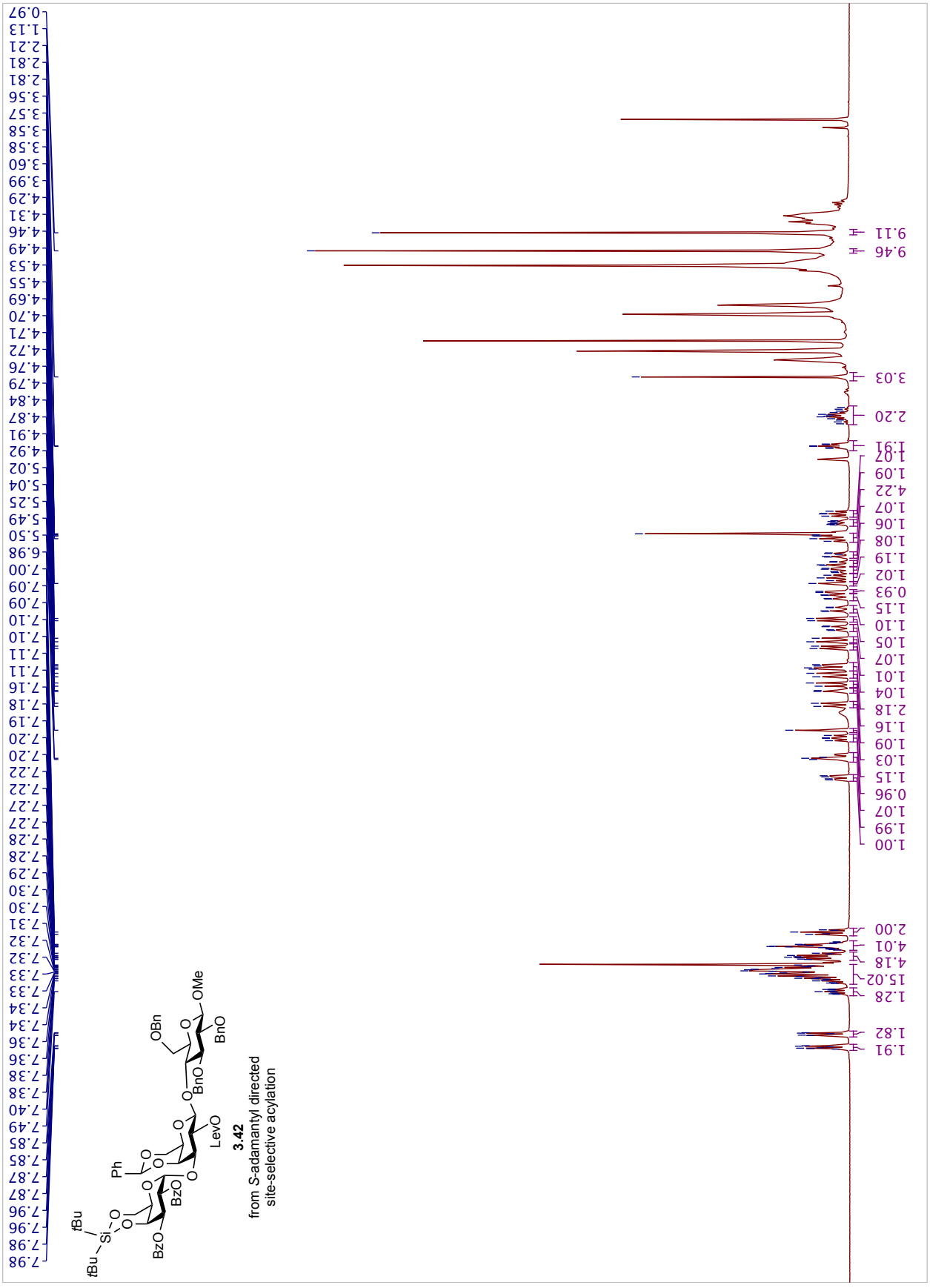
3.42
from S-adamantyl directed
site-selective acylation
f1 (ppm)

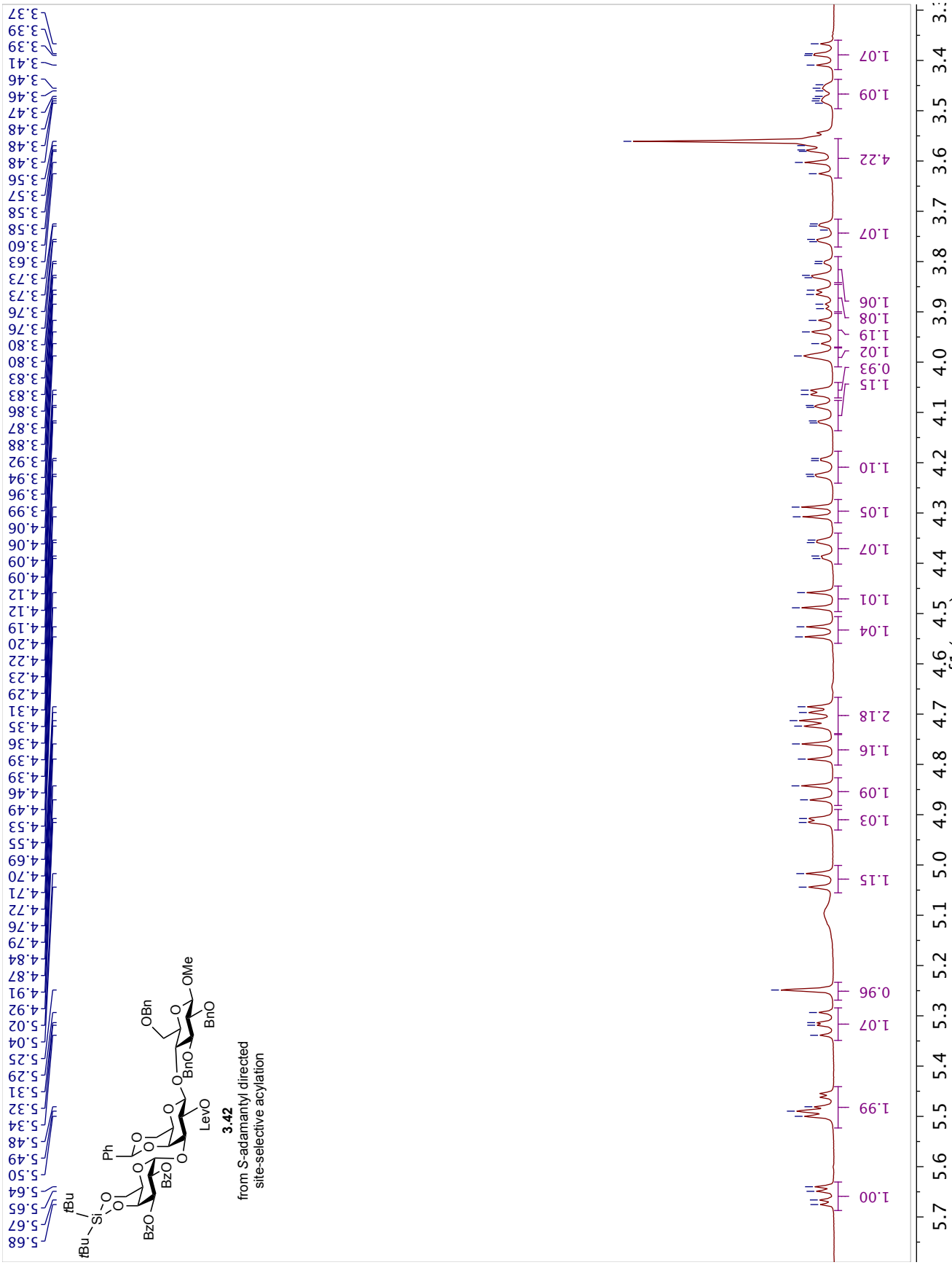
3.42
from S-adamantyl directed
site-selective acylation
f1 (ppm)

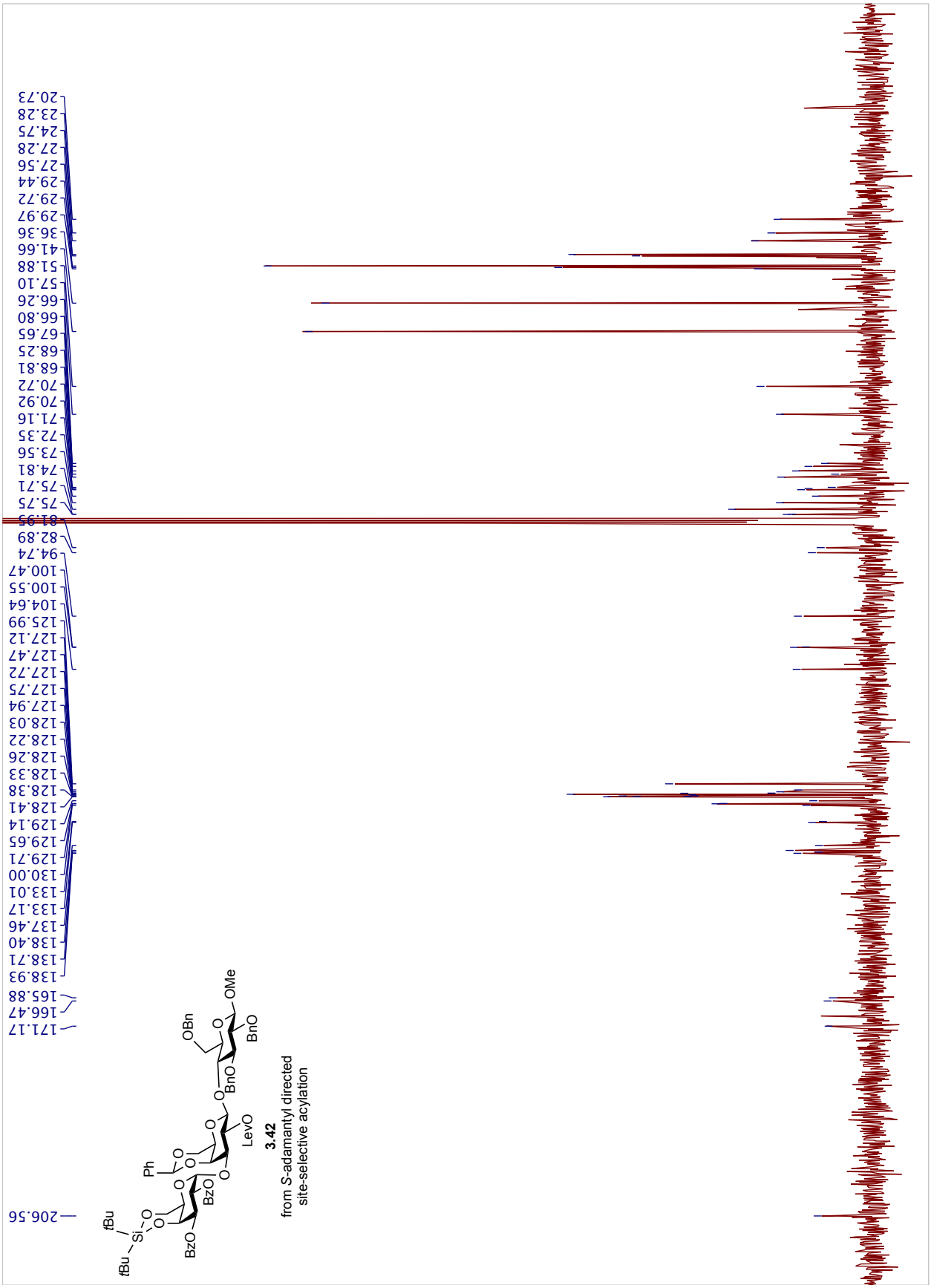
206.56
171.17
166.47
165.88
138.93
138.71
138.40
137.46
133.17
133.01
130.00
129.71
129.65
129.14
128.41
128.38
128.33
128.26
128.22
128.03
127.94
127.75
127.72
127.47
127.12
125.99
104.64
100.55
100.47
94.74
82.89
81.95
75.75
75.71
74.81
73.56
72.35
71.16
70.92
70.72
68.81
68.25
67.65
66.80
66.26
57.10
51.88
41.66
36.36
29.97
29.72
29.44
27.56
27.28
24.75
23.28
20.73
tBu
tBu
Si
O
O
BzO
BzO
O
O
O
Ph
O
O
O
O
LevO
O
O
BnO
OBn
O
OMe
BnO
3.42
from S-adamantyl directed
site-selective acylation
f1 (ppm)

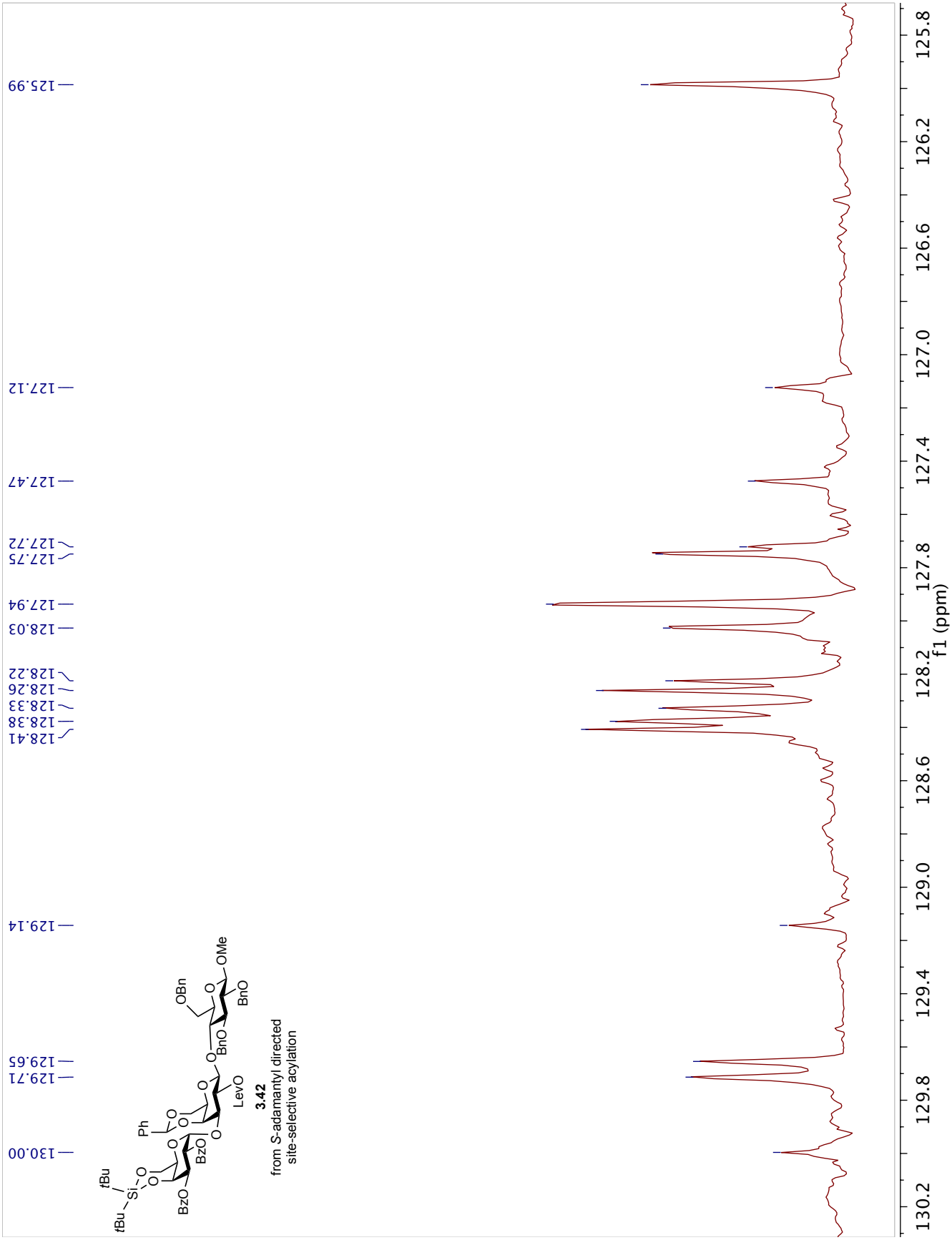
125.99
127.12
127.47
127.72
127.75
127.94
128.03
128.22
128.26
128.33
128.38
128.41
129.14
129.65
129.71
130.00
3.42
from S-adamantyl directed
site-selective acylation
f1 (ppm)

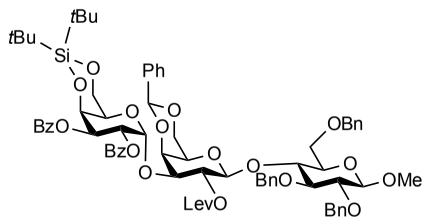

3.42
from *S*-adamantyl directed site-selective acylation

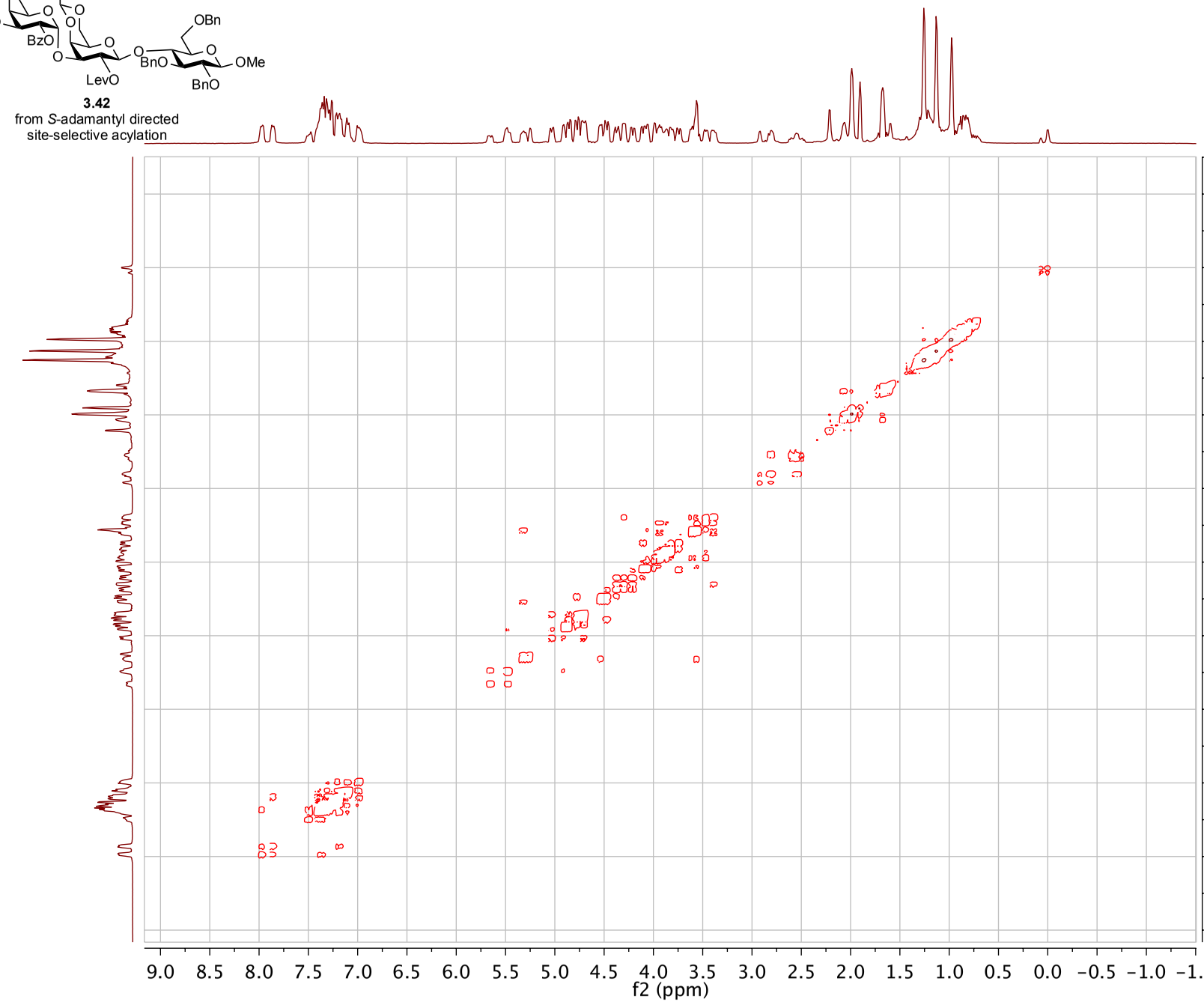

3.8 References

1. Moremen, K. W.; Tienmeyer, M.; Nairn, A. V., Vertebrate protein glycosylation: Diversity, synthesis and function . *Nat. Rev. Mol. Cell Biol.* **2012,** *13*, 448–462.

2. Bertozzi, C. R.; Kiessling, L. L., Chemical glycobiology. *Science* **2001,** *291* (5512), 2537-2364.

3. Gijsen, H. J. M.; Qiao, L.; Fitz, W.; Wong, C. H., Recent advances in the chemoenzymatic synthesis of carbohydrates and carbohydrate mimetics. *Chemical Reviews* **1996,** *96*, 443-473.

4. Varki, A., Biological roles of oligosaccharides: All of the theories are correct. *Glycobiology* **1993,** *3* (2), 97-130.

5. Parodi, A. J., Protein glucosylation and its role in protein folding. *Annu. Rev. Biochem.* **2000,** *69*, 69–93.

6. Stencel-Baerenwald, J. E.; Reiss, K.; Reiter, D. M.; Stehle, T.; Dermody, T. S., "The sweet spot: Defining virus-sialic acid interactions. *Nat. Rev. Microbiol.* **2014,** *12*, 739–749.

7. Apweiler, R.; Hermjakob, H.; Sharon, N., On the frequency of protein glycosylation, as deduced from analysis of the swiss-prot database. *Biochim. Biophys. Acta.* **1999,** *1473*, 4–8.

8. Wang, H. Y.; Blaszczyk, S. A.; Xiao, G.; Tang, W., Chiral reagents in glycosylation and modification of carbohydrates. *Chem. Soc. Rev.* **2018,** *47* (3), 681-701.

9. Guo, Z.; Boons, G. J., *Carbohydrate-based vaccines and immunotherapies*. John Wiley & Sons:: Hoboken, NJ,, 2009.

10. Craft, K. M.; Townsend, S. D., Mother knows best: Deciphering the antibacterial properties of human milk oligosaccharides. *Acc Chem Res* **2019,** *52* (3), 760-768.

11. Guerrini, M.; Zhang, Z.; Shriver, A.; Naggi, S.; Masuko, R.; Langer, B.; Casu, B.; Linhardt, R. J.; Torri, G.; Sasisekharan, R., Orthogonal approaches to detect potential contaminants in heparin. *Proc. Natl. Acad. Sci.* **2009,** *106*, 16956–16961.

12. Transforming glycoscience: A roadmap for the future. Council, N. R., Ed. The National Academies Press: Washington, DC, 2012; p 191.

13. Huang, Z.; Dong, G., Site-selectivity control in organic reactions: A quest to differentiate reactivity among the same kind of functional groups. *Acc. Chem. Res.* **2017,** *50*, 465-471.

14. Hartwig, J. F., Catalyst-controlled site-selective bond activation. *Acc. Chem. Res.* **2017,** *50*, 549-555.

15. Toste, F. D.; Sigman, M. S.; Miller, S. J., Pursuit of non-covalent interactions for strategic site-selective catalysis. *Acc. Chem. Res.* **2017,** *50*, 609-615.

16. Blaszczyk, S. A.; Tang, W., Addressing the challenge of carbohydrate site selectivity by synergistic catalysis. *Chem* **2017,** *3* (5), 722-723.

17. Lawandi, J.; Rocheleau, S.; Moitessier, N., Regioselective acylation, alkylation, silylation and glycosylation of monosaccharides. *Tetrahedron* **2016,** *72* (41), 6283-6319.

18. Giuliano, M. W.; Miller, S. J., Topics in current chemistry. Kawabata, T., Ed. Springer International Publishing AG: Gewerbestrasse, 2016; Vol. 372, p 157.

19. Ueda, Y.; Kawabata, T., Topics in current chemistry. Kawabata, T., Ed. Springer International Publishing AG: Gewerbestrasse, 2016; Vol. 372, p 203.

20. Lee, D.; Taylor, M. S., Borinic acid-catalyzed regioselective acylation of carbohydrate derivatives. *J. Am. Chem. Soc.* **2011,** *133* (11), 3724-7.

21. Mancini, R. S.; Lee, J. B.; Taylor, M. S., Boronic esters as protective groups in carbohydrate chemistry: Processes for acylation, silylation and alkylation of glycoside-derived boronates. *Org. Biomol. Chem.* **2017,** *15* (1), 132-143.

22. Gouliaras, C.; Lee, D.; Chan, L.; Taylor, M. S., Regioselective activation of glycosyl acceptors by a diarylborinic acid-derived catalyst. *J. Am. Chem. Soc.* **2011,** *133* (35), 13926-13929.

23. Mancini, R. S.; Lee, J. B.; Taylor, M. S., Sequential functionalizations of carbohydrates enabled by boronic esters as switchable protective/activating groups. *Journal of Organic Chemistry* **2017,** *82*, 8777-8791.

24. Fukuhara, K.; Shimada, N.; Nishino, T.; Kaji, E.; Makino, K., Regioselective, tin-free sulfation of unprotected hexopyranosides by using phenylboronic acid. *Eur. J. Org. Chem.* **2016,** *2016* (5), 902-905.

25. Oshima, K.; Kitzazona, E.; Aoyama, Y., Complexation-induced activation of sugar oh groups. Regioselective alkylation of methyl fucopyranoside via cyclic phenylboronate in the presence of amine. *Tetrahedron Letters* **1997,** *38* (28), 5001-5004.

26. Grindley, T. B., Applications of tin-containing intermediates to carbohydrate chemistry. *Adv. Carbohydr. Chem. Biochem.* **1998,** *53*, 17-142.

27. David, S.; Hanessian, S., Regioselective manipulation of hydroxyl groups via organotin derivatives. *Tetrahedron* **1985,** *41* (4), 643-663.

28. Ren, B.; Ramström, O.; Zhang, Q.; Ge, J.; Dong, H., An iron(iii) catalyst with unusually broad substrate scope in regioselective alkylation of diols and polyols. *Chem. Eur. J.* **2016,** *22*, 2481-2486.

29. Ren, B.; Lv, J.; Zhang, Y.; Tian, J.; Dong, H., Highly efficient selective benzylation of carbohydrates catalyzed by iron (iii) with silver oxide and bromide anion as co-catalysts. *ChemCatChem* **2017,** *9*, 950-953.

30. Peng, P.; Linseis, M.; Winter, R. F.; Schmidt, R. R., Regioselective acylation of diols and triols: The cyanide effect. *J. Am. Chem. Soc.* **2016,** *138* (18), 6002-9.

31. Sun, X.; Lee, H.; Lee, S.; Tan, K. L., Catalyst recognition of cis-1,2-diols enables site-selective functionalization of complex molecules. *Nat. Chem.* **2013,** *5* (9).

32. Tong, M. L.; Huber, F.; Taghuo Kaptouom, E. S.; Cellnik, T.; Kirsch, S. F., Enhanced site-selectivity in acylation reactions with substrate-optimized catalysts on solid supports. *Chem Commun* **2017,** *53* (21), 3086-3089.

33. Allen, C. L.; Miller, S. J., Chiral copper(ii) complex-catalyzed reactions of partially protected carbohydrates. *Org. Lett.* **2013,** *15* (24), 6178-6181.

34. Griswold, K. S.; Miller, S. J., A peptide-based catalyst approach to regioselective functionalization of carbohydrates. *Tetrahedron* **2003,** *59*, 8869-8875.

35. Sánchez-Roselló, M.; Puchlopek, A. L. A.; Morgan, A. J.; Miller, S. J., Site-selective catalysis of phenyl thionoformate transfer as a tool for regioselective deoxygenation of polyols. *J. Org. Chem* **2008,** *73* (5), 1774-1782.

36. Yanagi, M.; Imayoshi, A.; Ueda, Y.; Furuta, T.; Kawabata, T., Carboxylate anions accelerate pyrrolidinopyridine (ppy)-catalyzed acylation: Catalytic site-selective acylation of a carbohydrate by in situ counteranion exchange. *Org. Lett.* **2017,** *19* (12), 3099-3102.

37. Rocheleau, S.; Pottel, J.; Huskić, I.; Moitessier, N., Highly regioselective monoacylation of unprotected glucopyranoside using transient directing-protecting groups. *Eur. J. Org. Chem.* **2017,** *2017* (3), 646-656.

38. Wang, H. Y.; Yang, K.; Yin, D.; Liu, C.; Glazier, D. A.; Tang, W., Chiral catalyst-directed dynamic kinetic diastereoselective acylation of lactols for de novo synthesis of carbohydrate. *Org. Lett.* **2015,** *17* (21), 5272-5.

39. Li, X.; Liu, P.; Houk, K. N.; Birman, V. B., Origin of enantioselectivity in cf3−pip-catalyzed kinetic resolution of secondary benzylic alcohols. *J. Am. Chem. Soc.* **2008,** *130*, 13836-13837.

40. Xiao, G.; Cintron-Rosado, G. A.; Glazier, D. A.; Xi, B. M.; Liu, C.; Liu, P.; Tang, W., Catalytic site-selective acylation of carbohydrates directed by cation-n interaction. *J. Am. Chem. Soc.* **2017,** *139* (12), 4346-4349.

41. LIan, G.; Zhang, X.; Biao, Y., Thioglycosides in carbohydrate research. *Carbohydr. Res.* **2015,** *403*, 13-22.

42. Stick, R. V.; Williams, S. J., *Carbohydrates: The essential molecules of life*. Elsevier: Oxford, 2009.

43. Blaszczyk, S. A.; Xiao, G.; Wen, P.; Hao, H.; Wu, J.; Wang, B.; Carattino, F.; Li, Z.; Glazier, D. A.; McCarty, B. J.; Liu, P.; Tang, W., S-adamantyl group directed site-selective acylation: Applications in streamlined assembly of oligosaccharides. *Angew. Chem. Int. Ed.* **2019,** *58* (28), 9542-9546.

44. Moya-Lopez, J. F.; Elhalem, E.; Recio, R.; Alvarez, E.; Fernandez, I.; Khiar, N., Studies on the diastereoselective oxidation of 1-thio-beta-d-glucopyranosides: Synthesis of the usually less favoured r(s) sulfoxide as a single diastereoisomer. *Org. Biomol. Chem.* **2015,** *13* (6), 1904-14.

45. Shiina, I.; Nakata, N., The first asymmetric esterification of free carboxylic acids with racemic alcohols using benzoic anhydrides and tetramisole derivatives: An application to the kinetic resolution of secondary benzylic alcohols. *Tetrahedron Lett.* **2007,** *48* (47), 8314—8317.

46. Nakata, K.; Gotoh, K.; Ono, K.; Futami, K.; Shiina, I., Kinetic resolution of racemic 2-hydroxy-γ-butyrolactones by asymmetric esterification using diphenylacetic acid with pivalic anhydride and a chiral acyl-transfer catalyst. *Org. Lett.* **2013,** *15* (6), 1170-1173.

47. Shiina, I.; Nakata, K.; Ono, K.; Onda, Y.; Itagaki, M., Kinetic resolution of racemic α-arylalkanoic acids with achiral alcohols via the asymmetric esterification using carboxylic anhydrides and acyl-transfer catalysts. *J. Am. Chem. Soc.* **2010,** *132* (33), 11629-11641.

48. Dohi, H.; Nishida, Y., Utilization of thioglycosides without unpleasant odors for sugar chain synthesis: Advances in molecular design and thioglycosidation methods. *Trends in Glycoscience and Glycotechnology* **2014,** *26* (151), 119-130.

49. Li, Z. T.; Gildersleeve, J. C., Mechanistic studies and methods to prevent aglycon transfer of thioglycosides. *J. Am. Chem. Soc.* **2006,** *128*, 11612-.

50. Crich, D.; Li, W., A-selective sialylations at −78 °c in nitrile solvents with a 1-adamantanyl thiosialoside. *Org. Lett.* **2007,** *72* (20), 7794-7797.

51. Lahmann, M.; Oscarson, S., Investigation of the reactivity difference between thioglycoside donors with variant aglycon parts. *Canadian Journal of Chemistry* **2002,** *80* (8), 889-893.

52. Bendelac, A.; Savage, P. B.; Teyton, L., The biology of nkt cells. *Annual Review of Immunology* **2007,** *25*, 297-336.

53. Matsuda, J. L.; Mallevaey, T.; Scott-Browne, J.; Gapin, L., Cd1d-restricted inkt cells, the 'swiss-army knife' of the immune system. *Current Opinion in Immunology* **2008,** *20* (3), 358-368.

54. Zhou, D.; Mattner, J.; Cantu III, V.; Schrantz, N.; Yin, N.; Gao, Y.; Sagiv, Y.; Hudspeth, K.; Wu, Y.-P.; Yamashita, T.; Teneberg, S.; Wang, D.; Proia, R. L.; Levery, S. B.; Savage, P. B.; Teyton, L.; Bendelac, A., Lysosomal glycosphingolipid recognition by nkt cells. *Science* **2004,** *306*, 1786-1789.

55. Mandal, S. S.; Liao, G.; Guo, Z., Chemical synthesis of the tumor-associated globo h antigen. *RSC Adv.* **2015,** *5*, 23311-23319.

56. Ren, B.; Lv, J.; Zhang, Y.; Tian, J.; Dong, H., *ChemCatChem.* **2017,** *9*, 950-953.

57. Chevallier, O. P.; Migaud, M. E., *Nucleosides, Nucleotides & Nucleic Acids* **2008,** *27* (10-11), 1127-1143.

58. Yondea, Y.; Kawada, T.; Rosenau, T.; Kosma, P., *Carb. Res.* **2005,** *340*, 2428-2435.

59. Kalikanda, J.; Li, Z., *Carb. Res.* **2011,** *346* (15), 2380-2383.

60. Li, J.; Li, W.; Yu, B., *Org. Biomol. Chem.* **2013,** *11*, 4971–4974.

61. Kimura, A.; Imamura, A.; Ando, H.; Ishida, H.; Kiso, M., A novel synthetic route to α-galactosyl ceramides and igb3 using dtbs-directed α-selective galactosylation. *Synlett.* **2006,** *15*, 2379-2382.

62. Marenich, A. V.; Cramer, C. J.; Truhlar, D. G., *J. Phys. Chem. B* **2009,** *113*, 6378-6396.

63. Grimme, S.; Antony, J.; Ehrlich, S.; Krieg, H., *J. Chem. Phys.* **2010,** *132*, 154104-154107.

To all of those who struggled with mental health at any point in their lives, this is for you.